

CONTROL OF QUANTUM SYSTEMS

CONTROL OF QUANTUM SYSTEMS

THEORY AND METHODS

Shuang Cong

University of Science and Technology of China

WILEY

This edition first published 2014
© 2014 John Wiley & Sons Singapore Pte. Ltd.

Registered office

John Wiley & Sons Singapore Pte. Ltd., 1 Fusionopolis Walk, #07-01 Solaris South Tower, Singapore 138628.

For details of our global editorial offices, for customer services and for information about how to apply for permission to reuse the copyright material in this book please see our website at www.wiley.com.

All Rights Reserved. No part of this publication may be reproduced, stored in a retrieval system or transmitted, in any form or by any means, electronic, mechanical, photocopying, recording, scanning, or otherwise, except as expressly permitted by law, without either the prior written permission of the Publisher, or authorization through payment of the appropriate photocopy fee to the Copyright Clearance Center. Requests for permission should be addressed to the Publisher, John Wiley & Sons Singapore Pte. Ltd., 1 Fusionopolis Walk, #07-01 Solaris South Tower, Singapore 138628, tel: 65-66438000, fax: 65-66438008, email: enquiry@wiley.com.

Wiley also publishes its books in a variety of electronic formats. Some content that appears in print may not be available in electronic books.

Designations used by companies to distinguish their products are often claimed as trademarks. All brand names and product names used in this book are trade names, service marks, trademarks or registered trademarks of their respective owners. The Publisher is not associated with any product or vendor mentioned in this book. This publication is designed to provide accurate and authoritative information in regard to the subject matter covered. It is sold on the understanding that the Publisher is not engaged in rendering professional services. If professional advice or other expert assistance is required, the services of a competent professional should be sought.

Limit of Liability/Disclaimer of Warranty: While the publisher and author have used their best efforts in preparing this book, they make no representations or warranties with respect to the accuracy or completeness of the contents of this book and specifically disclaim any implied warranties of merchantability or fitness for a particular purpose. It is sold on the understanding that the publisher is not engaged in rendering professional services and neither the publisher nor the author shall be liable for damages arising herefrom. If professional advice or other expert assistance is required, the services of a competent professional should be sought.

Library of Congress Cataloging-in-Publication Data

Cong, Shuang.

Control of quantum systems : theory and methods / Shuang Cong.

pages cm

Includes bibliographical references and index.

ISBN 978-1-118-60812-8 (hardback)

1. Quantum systems – Automatic control. 2. Control theory. I. Title.

TK7874.885.C66 2014

530.1201'1 – dc23

2013037723

A catalogue record for this book is available from the British Library.

ISBN: 978-1-118-60812-8

Typeset in 10/12pt TimesLTStd by Laserwords Private Limited, Chennai, India

Contents

About the Author	xiii
Preface	xv
1 Introduction	1
1.1 Quantum States	2
1.2 Quantum Systems Control Models	3
1.2.1 Schrödinger Equation	4
1.2.2 Liouville Equation	4
1.2.3 Markovian Master Equations	5
1.2.4 Non-Markovian Master Equations	5
1.3 Structures of Quantum Control Systems	6
1.4 Control Tasks and Objectives	8
1.5 System Characteristics Analyses	9
1.5.1 Controllability	9
1.5.2 Reachability	9
1.5.3 Observability	10
1.5.4 Stability	10
1.5.5 Convergence	10
1.5.6 Robustness	10
1.6 Performance of Control Systems	11
1.6.1 Probability	11
1.6.2 Fidelity	11
1.6.3 Purity	12
1.7 Quantum Systems Control	13
1.7.1 Description of Control Problems	13
1.7.2 Quantum Control Theory and Methods	13
1.8 Overview of the Book	16
References	18
2 State Transfer and Analysis of Quantum Systems on the Bloch Sphere	21
2.1 Analysis of a Two-level Quantum System State	21
2.1.1 Pure State Expression on the Bloch Sphere	21
2.1.2 Mixed States in the Bloch Sphere	24

2.1.3	<i>Control Trajectory on the Bloch Sphere</i>	26
2.2	State Transfer of Quantum Systems on the Bloch Sphere	27
2.2.1	<i>Control of a Single Spin-1/2 Particle</i>	28
2.2.2	<i>Situation with the Minimum Qt of Control Fields</i>	30
2.2.3	<i>Situation with a Fixed Time T</i>	31
2.2.4	<i>Numerical Simulations and Results Analyses</i>	33
	References	37
3	Control Methods of Closed Quantum Systems	39
3.1	Improved Optimal Control Strategies Applied in Quantum Systems	39
3.1.1	<i>Optimal Control of Quantum Systems</i>	40
3.1.2	<i>Improved Quantum Optimal Control Method</i>	42
3.1.3	<i>Krotov-Based Method of Optimal Control</i>	43
3.1.4	<i>Numerical Simulation and Performance Analysis</i>	45
3.2	Control Design of High-Dimensional Spin-1/2 Quantum Systems	48
3.2.1	<i>Coherent Population Transfer Approaches</i>	48
3.2.2	<i>Relationships between the Hamiltonian of Spin-1/2 Quantum Systems under Control and the Sequence of Pulses</i>	49
3.2.3	<i>Design of the Control Sequence of Pulses</i>	52
3.2.4	<i>Simulation Experiments of Population Transfer</i>	53
3.3	Comparison of Time Optimal Control for Two-Level Quantum Systems	57
3.3.1	<i>Description of System Model</i>	58
3.3.2	<i>Geometric Control</i>	59
3.3.3	<i>Bang-Bang Control</i>	61
3.3.4	<i>Time Comparisons of Two Control Strategies</i>	64
3.3.5	<i>Numerical Simulation Experiments and Results Analyses</i>	66
	References	71
4	Manipulation of Eigenstates – Based on Lyapunov Method	73
4.1	Principle of the Lyapunov Stability Theorem	74
4.2	Quantum Control Strategy Based on State Distance	75
4.2.1	<i>Selection of the Lyapunov Function</i>	76
4.2.2	<i>Design of the Feedback Control Law</i>	77
4.2.3	<i>Analysis and Proof of the Stability</i>	78
4.2.4	<i>Application to a Spin-1/2 Particle System</i>	80
4.3	Optimal Quantum Control Based on the Lyapunov Stability Theorem	81
4.3.1	<i>Description of the System Model</i>	82
4.3.2	<i>Optimal Control Law Design and Property Analysis</i>	84
4.3.3	<i>Simulation Experiments and the Results Comparisons</i>	86
4.4	Realization of the Quantum Hadamard Gate Based on the Lyapunov Method	88
4.4.1	<i>Mathematical Model</i>	89
4.4.2	<i>Realization of the Quantum Hadamard Gate</i>	90
4.4.3	<i>Design of Control Fields</i>	92
4.4.4	<i>Numerical Simulations and Comparison Results Analyses</i>	94
	References	96

5	Population Control Based on the Lyapunov Method	99
5.1	Population Control of Equilibrium State	99
5.1.1	<i>Preliminary Notions</i>	99
5.1.2	<i>Control Laws Design</i>	100
5.1.3	<i>Analysis of the Largest Invariant Set</i>	101
5.1.4	<i>Considerations on the Determination of P</i>	104
5.1.5	<i>Illustrative Example</i>	105
5.1.6	<i>Appendix: Proof of Theorem 5.1</i>	107
5.2	Generalized Control of Quantum Systems in the Frame of Vector Treatment	110
5.2.1	<i>Design of Control Law</i>	110
5.2.2	<i>Convergence Analysis</i>	113
5.2.3	<i>Numerical Simulation on a Spin-1/2 System</i>	114
5.3	Population Control of Eigenstates	117
5.3.1	<i>System Model and Control Laws</i>	117
5.3.2	<i>Largest Invariant Set of Control Systems</i>	118
5.3.3	<i>Analysis of the Eigenstate Control</i>	118
5.3.4	<i>Simulation Experiments</i>	119
	References	123
6	Quantum General State Control Based on Lyapunov Method	125
6.1	Pure State Manipulation	125
6.1.1	<i>Design of Control Law and Discussion</i>	125
6.1.2	<i>Control System Simulations and Results Analyses</i>	129
6.2	Optimal Control Strategy of the Superposition State	131
6.2.1	<i>Preliminary Knowledge</i>	132
6.2.2	<i>Control Law Design</i>	133
6.2.3	<i>Numerical Simulations</i>	134
6.3	Optimal Control of Mixed-State Quantum Systems	135
6.3.1	<i>Model of the System to be Controlled</i>	136
6.3.2	<i>Control Law Design</i>	137
6.3.3	<i>Numerical Simulations and Results Analyses</i>	142
6.4	Arbitrary Pure State to a Mixed-State Manipulation	145
6.4.1	<i>Transfer from an Arbitrary Pure State to an Eigenstate</i>	146
6.4.2	<i>Transfer from an Eigenstate to a Mixed State by Interaction Control</i>	147
6.4.3	<i>Control Design for a Mixed-State Transfer</i>	149
6.4.4	<i>Numerical Simulation Experiments</i>	151
	References	154
7	Convergence Analysis Based on the Lyapunov Stability Theorem	155
7.1	Population Control of Quantum States Based on Invariant Subsets with the Diagonal Lyapunov Function	155
7.1.1	<i>System Model and Control Design</i>	155
7.1.2	<i>Correspondence between any Target Eigenstate and the Value of the Lyapunov Function</i>	156
7.1.3	<i>Invariant Set of Control Systems</i>	157

7.1.4	<i>Numerical Simulations</i>	161
7.1.5	<i>Summary and Discussion</i>	164
7.2	A Convergent Control Strategy of Quantum Systems	165
7.2.1	<i>Problem Description</i>	165
7.2.2	<i>Construction Method of the Observable Operator</i>	166
7.2.3	<i>Proof of Convergence</i>	168
7.2.4	<i>Route Extension Strategy</i>	173
7.2.5	<i>Numerical Simulations</i>	174
7.3	Path Programming Control Strategy of Quantum State Transfer	176
7.3.1	<i>Control Law Design Based on the Lyapunov Method in the Interaction Picture</i>	177
7.3.2	<i>Transition Path Programming Control Strategy</i>	178
7.3.3	<i>Numerical Simulations and Results Analyses</i>	182
	References	186
8	Control Theory and Methods in Degenerate Cases	187
8.1	Implicit Lyapunov Control of Multi-Control Hamiltonian Systems Based on State Error	187
8.1.1	<i>Control Design</i>	188
8.1.2	<i>Convergence Proof</i>	192
8.1.3	<i>Relation between Two Lyapunov Functions</i>	193
8.1.4	<i>Numerical Simulation and Result Analysis</i>	193
8.2	Quantum Lyapunov Control Based on the Average Value of an Imaginary Mechanical Quantity	195
8.2.1	<i>Control Law Design and Convergence Proof</i>	195
8.2.2	<i>Numerical Simulation and Result Analysis</i>	199
8.3	Implicit Lyapunov Control for the Quantum Liouville Equation	200
8.3.1	<i>Description of Problem</i>	201
8.3.2	<i>Derivation of Control Laws</i>	202
8.3.3	<i>Convergence Analysis</i>	205
8.3.4	<i>Numerical Simulations</i>	209
	References	211
9	Manipulation Methods of the General State	213
9.1	Quantum System Schmidt Decomposition and its Geometric Analysis	213
9.1.1	<i>Schmidt Decomposition of Quantum States</i>	214
9.1.2	<i>Definition of Entanglement Degree Based on the Schmidt Decomposition</i>	215
9.1.3	<i>Application of the Schmidt Decomposition</i>	216
9.2	Preparation of Entanglement States in a Two-Spin System	220
9.2.1	<i>Construction of the Two-Spin Systems Model in the Interaction Picture</i>	220
9.2.2	<i>Design of the Control Field Based on the Lyapunov Method</i>	223
9.2.3	<i>Proof of Convergence for the Bell States</i>	226
9.2.4	<i>Numerical Simulations</i>	227
9.3	Purification of the Mixed State for Two-Dimensional Systems	230

9.3.1	<i>Purification by Means of a Probe</i>	230
9.3.2	<i>Purification by Interaction Control</i>	232
9.3.3	<i>Numerical Experiments and Results Comparisons</i>	233
9.3.4	<i>Discussion</i>	234
	References	235
10	State Control of Open Quantum Systems	237
10.1	State Transfer of Open Quantum Systems with a Single Control Field	237
10.1.1	<i>Dynamical Model of Open Quantum Systems</i>	237
10.1.2	<i>Derivation of Optimal Control Law</i>	238
10.1.3	<i>Control System Design</i>	241
10.1.4	<i>Numerical Simulations and Results Analyses</i>	242
10.2	Purity and Coherence Compensation through the Interaction between Particles	246
10.2.1	<i>Method of Compensation for Purity and Coherence</i>	247
10.2.2	<i>Analysis of System Evolution</i>	250
10.2.3	<i>Numerical Simulations</i>	253
10.2.4	<i>Discussion</i>	255
	Appendix 10.A Proof of Equation 10.59	257
	References	258
11	State Estimation, Measurement, and Control of Quantum Systems	261
11.1	State Estimation Methods in Quantum Systems	261
11.1.1	<i>Background of State Estimation of Quantum Systems</i>	262
11.1.2	<i>Quantum State Estimation Methods Based on the Measurement of Identical Copies</i>	262
11.1.3	<i>Quantum State Reconstruction Methods Based on System Theory</i>	267
11.2	Entanglement Detection and Measurement of Quantum Systems	268
11.2.1	<i>Entanglement States</i>	269
11.2.2	<i>Entanglement Witnesses</i>	271
11.2.3	<i>Entanglement Measures</i>	273
11.2.4	<i>Non-linear Separability Criteria</i>	277
11.3	Decoherence Control Based on Weak Measurement	278
11.3.1	<i>Construction of a Weak Measurement Operator</i>	279
11.3.2	<i>Applicability of Weak Measurement</i>	280
11.3.3	<i>Effects on States</i>	282
	Appendix 11.A Proof of Normed Linear Space ($A, \ \bullet\ $)	286
	References	287
12	State Preservation of Open Quantum Systems	291
12.1	Coherence Preservation in a Λ -Type Three-Level Atom	291
12.1.1	<i>Models and Objectives</i>	292
12.1.2	<i>Design of Control Field</i>	294
12.1.3	<i>Analysis of Singularities Issues</i>	297
12.1.4	<i>Numerical Simulations</i>	299
12.2	Purity Preservation of Quantum Systems by a Resonant Field	301
12.2.1	<i>Problem Description</i>	302

12.2.2	<i>Purity Property Preservation</i>	303
12.2.3	<i>Discussion</i>	306
12.3	Coherence Preservation in Markovian Open Quantum Systems	307
12.3.1	<i>Problem Formulation</i>	308
12.3.2	<i>Design of Control Variables</i>	311
12.3.3	<i>Numerical Simulations</i>	313
12.3.4	<i>Discussion</i>	315
	Appendix 12.A Derivation of H_C	316
	References	317
13	State Manipulation in Decoherence-Free Subspace	321
13.1	State Transfer and Coherence Maintenance Based on DFS for a Four-Level Energy Open Quantum System	321
13.1.1	<i>Construction of DFS and the Desired Target State</i>	322
13.1.2	<i>Design of the Lyapunov-Based Control Law for State Transfer</i>	325
13.1.3	<i>Numerical Simulations</i>	326
13.2	State Transfer Based on a Decoherence-Free Target State for a Λ -Type N -Level Atomic System	328
13.2.1	<i>Construction of the Decoherence-Free Target State</i>	328
13.2.2	<i>Design of the Lyapunov-Based Control Law for State Transfer</i>	331
13.2.3	<i>Numerical Simulations and Results Analyses</i>	332
13.3	Control of Quantum States Based on the Lyapunov Method in Decoherence-Free Subspaces	336
13.3.1	<i>Problem Description</i>	336
13.3.2	<i>Control Design in the Interaction Picture</i>	338
13.3.3	<i>Construction of P and Convergence Analysis</i>	339
13.3.4	<i>Numerical Simulation Examples and Discussion</i>	345
	References	348
14	Dynamic Decoupling Quantum Control Methods	351
14.1	Phase Decoherence Suppression of an n -Level Atom in Ξ -Configuration with Bang-Bang Controls	351
14.1.1	<i>Dynamical Decoupling Mechanism</i>	352
14.1.2	<i>Design of the Bang–Bang Operations Group in Phase Decoherence</i>	355
14.1.3	<i>Examples of Design</i>	357
14.2	Optimized Dynamical Decoupling in Ξ -Type n -Level Atom	360
14.2.1	<i>Periodic Dynamical Decoupling</i>	361
14.2.2	<i>Uhrig Dynamical Decoupling</i>	361
14.2.3	<i>Behaviors of Quantum Coherence under Various Dynamical Decoupling Schemes</i>	362
14.2.4	<i>Examples</i>	365
14.2.5	<i>Discussion</i>	366
14.3	An Optimized Dynamical Decoupling Strategy to Suppress Decoherence	366
14.3.1	<i>Universal Dynamical Decoupling for a Qubit</i>	367
14.3.2	<i>An Optimized Dynamical Decoupling Scheme</i>	369

14.3.3	<i>Simulation and Comparison</i>	369
14.3.4	<i>Discussion</i>	375
	References	378
15	Trajectory Tracking of Quantum Systems	381
15.1	Orbit Tracking of Quantum States Based on the Lyapunov Method	382
15.1.1	<i>Description of the System Model</i>	382
15.1.2	<i>Design of Control Law</i>	384
15.1.3	<i>Numerical Simulation Experiments and Results Analysis</i>	385
15.2	Orbit Tracking Control of Quantum Systems	389
15.2.1	<i>System Model and Control Law Design</i>	390
15.2.2	<i>Numerical Simulation Experiments</i>	391
15.3	Adaptive Trajectory Tracking of Quantum Systems	394
15.3.1	<i>Description of the System Model</i>	396
15.3.2	<i>Control System Design and Characteristic Analysis</i>	398
15.3.3	<i>Numerical Simulation and Result Analysis</i>	400
15.4	Convergence of Orbit Tracking for Quantum Systems	402
15.4.1	<i>Description of the Control System Model</i>	403
15.4.2	<i>Control Law Derivation</i>	404
15.4.3	<i>Convergence Analysis</i>	404
15.4.4	<i>Applications and Experimental Results Analyses</i>	411
	References	416
Index		419

About the Author



Shuang Cong was born in Hefei, China. She obtained her Bachelor's degree from the Department of Automatic Control, Beijing University of Aeronautics and Astronautics, in 1982, and her PhD degree in systems engineering from the University of Rome "La Sapienza", Italy, in 1995. She is currently Professor of Automation at the University of Science and Technology of China (USTC). Professor Cong has authored more than 340 research papers and invited papers published in academic journals at home and abroad or presented to international academic conferences. She has published one textbook in Chinese, entitled *Neural Network Theory and Applications towards to the MATLAB Toolbox* (third edition, 2009; the second edition was published in 2003 and the first edition in 1998), and five Chinese monographs:

graphs: *Neural Networks, Fuzzy System and the Application in Motion Control* (2001), *Vision-based Network Remote Control Systems* (2013), *Introduction to Quantum Mechanical Systems Control* (2006), *Applied Motion Control Technologies* (first author, 2006), and *Parallel Robots-Modeling, Control Optimization and Applications* (first author, 2010). She has also edited an English book entitled *Frontiers in Adaptive Control* (2009). *Control of Quantum Systems: Theory and Methods* is her second monograph about quantum systems control.

Preface

Quantum control theory and methods are gaining increased attention and importance in the world. This area involves many fields of science, and there are many issues to be addressed so it is a continually developing research field. Until recently it has been difficult to find an integrated treatment of the relevant topics in one source, partly because of their rapidly changing nature. However, quantum control theory and methods are now sufficiently mature to warrant a reference book that extends the classical treatment of control theory and methods to the quantum domain. This book aims to provide a self-contained survey of these topics for graduate students and researchers in quantum engineering and quantum information sciences. The contents include the newest research achievements obtained in recent years. They are the result of a combination of macro-control theory and microscopic quantum system features.

The quantum control theory and methods in this book may have the potential to solve existing problems that cannot be solved by quantum physics, quantum chemistry, quantum computing, quantum communication, and quantum information. The progress of quantum control theory and methods will promote the progress and development of quantum information, quantum computing, and quantum communication. This book may open the door for researchers, academics, and engineers in relevant research fields to solve existing problems and provide them with new theories and methods for controlling quantum systems.

My previous book on quantum system control, *Introduction to Quantum Mechanical Systems Control* (Scientific Press. 2006, ISBN 7-03-016474-1, in Chinese), covered the theoretical basis and modeling of quantum mechanical systems, the Lie group and Lie algebra and its applications, unitary evolution operator decomposition and its implementation, bilinear systems and their control, the controllability and reachability of quantum systems, feedback control of quantum systems, mixed and entangled states and their analysis, the geometric algebra of quantum systems, optimal control of quantum systems, quantum measurement, feedback coherent control of quantum systems, and the application of quantum systems. This book is my second book on quantum system control and is a research reference book.

There are many issues to be addressed in quantum information, quantum computing, and quantum communication. All of these issues are essentially quantum system control problems, and quantum control theory and methods are used to solve them. This book can be a research reference book for graduate students, researchers, academics, and engineers in quantum physics, chemistry, information, communication, electrical and mechanical engineering, applied mathematics, and computer science whose research interests involve quantum systems control. The only prerequisite is an introductory course in quantum mechanics at first-year graduate level, as typically taught in physics departments. One of the book's primary goals

is to give the graduate student with a limited background in control theory, but a familiarity with quantum dynamical systems, the tools to engineer those systems. A second objective is to offer a convenient reference for active and experienced researchers in quantum engineering and quantum information theory. The first chapter introduces the basic concepts of quantum states and quantum control models, including Schrödinger equations, the Liouville equation, Markovian master equations, and non-Markovian master equations. For control systems we introduce structures of quantum control systems, control tasks and objectives, system characteristic analysis, performance of control systems, description of control problems, and quantum control theories and methods. However, this requires readers who are undergraduate students to have some knowledge of advanced mathematics and advanced algebra.

The book focuses on control theory and methods in quantum systems, divided into two parts: control theory and methods for closed and open quantum systems. The control theory and methods for closed quantum systems include geometric control, bang-bang control, improved optimal control strategy, and the Krotov-based method of optimal control. Because optimal quantum control is the most popular quantum method and it was introduced in my earliest book, *Introduction to Quantum Mechanical Systems Control*, it has not been repeated in this book. However, throughout the book there are references to the concept of optimal control.

The Lyapunov-based quantum control method is a highlight of this book. Five chapters are used to introduce this control method, of which three cover the control method used for state-to-state transfer and population control, the transfer of states includes eigenstates, superposition states, and mixed states, and the convergence of this control method. A further chapter deals with the issues of degenerate cases. Other types of state manipulation, such as the preparation of entanglement states, the purification of mixed states, and Schmidt decomposition of quantum states, are also covered.

Five chapters cover the control methods of open quantum systems. For general cases, the control methods of state transfer with a single control field, purity and coherence compensation through the interaction between particles, and decoherence control based on weak measurement are introduced. One chapter investigates the state preservation of open quantum systems, which concerns the purity preservation of quantum systems through the resonant field and coherence preservation in Markovian open quantum systems. The decoherence-free subspace is a special control method for the control of open quantum systems, and this is covered in a separate chapter, as is the dynamic decoupling quantum control method, which is another important control method for open quantum systems.

Finally, as with control in system engineering, systems control should be classified in two categories: state transfer (or state regulation) and trajectory tracking. Trajectory tracking of quantum systems is presented in the last chapter of this book.

This book required the cooperation of many people, including Dr Sen Kuang, Dr Yuesheng Lou, Dr Jie Yang, Dr Fangfang Meng, Ms Yuanyuan Zhang, Dr Fei Yang, Ms Jianxiu Liu, Mr Jie Wen, Mr Linping Chan, and Ms Yaping Zhu.

In writing this book I have benefited from interactions with many people. In particular, I would like to thank Professor Herschel Rabitz for his kind hospitality at the Princeton University for 5 months from January through June 2012, during which time I learnt many points of interest. My thanks also go to the Frick Chemistry Laboratory at Princeton University for its hospitality. Doctoral students and researchers at the laboratory have been very kind and I learnt a lot from discussions with them.

I would like to thank John Wiley & Sons for its assistance and for agreeing to publish this book and the National Science Foundation for financial support during the research work.

Shuang Cong

June 29, 2013

University of Science and Technology of China,

Hefei, P. R. China

1

Introduction

The theory of quantum mechanics was one of the major discoveries of the history of science in the twentieth century. It is very important to study the properties of quantum mechanical systems and their control. As quantum technologies have matured, a lot of practical applications of quantum control have been realized in quantum optics, cavity quantum electro-dynamics (QED), atomic spin ensembles, ion trapping, and Bose–Einstein condensation, and so on, which means that the manipulation of quantum phenomena is a rapidly growing research field. The improvements in nanotechnology and its manufacture process as well as increasing interests in new applications of quantum effects, including quantum information process, mean the control of quantum phenomena is becoming a growing concern all over the world in areas such as quantum computation, quantum chemistry, nano-material, and quantum physics. In the past three decades, researchers have been trying to expand the control theories that are obtained from the macroscopic world to the microscopic world, and this has gradually become a new system control theory in interdisciplinary fields: quantum control theory. The methods and technologies of quantum control have become one of the leading research areas in the world. The main topics of quantum control theory are, from the control system perspective, to investigate how to manipulate a system state trajectory and its evolution. For this purpose, quantum control theory is used to design an external realizable control law to achieve a desired control goal by combining control theory and the characteristics of quantum systems. Developing a special control theory and methods for quantum systems has been a challenging task. This task requires interdisciplinary researchers with interest in the development and applications of novel quantum control methodologies to fundamental physical, chemical, and biological problems from the quantum physics, chemistry, quantum information, mathematical and computer sciences, and control engineering communities. On the other hand, the field of quantum information involves the complex task of designing and effectively manipulating multi-qubit systems. However, this problem is beset by significant difficulties, such as the corruption of quantum information caused by decoherence. Finding solutions to the problem of decoherence, resulting from the unavoidable interaction of a quantum system with its environment, is one of the most critical challenges impeding practical realization of a quantum information processor (QIP). Current strategies for decoherence management are being developed by researchers from three distinct communities within quantum information science (QIS), namely, dynamical decoupling (DD), optimal control (OC), and quantum error correction (QEC). All of the

problems to be solved in these areas are in fact control problems, which should be solved by means of control theory and methods. The aim of a control theory is to find a method of transforming a system by means of controlling action in order to achieve its prescribed behavior. A control theory can be used effectively only when it is executed in the whole process of control systems design because control theory is one part of the whole process of control systems design.

The whole process of control system design and implementation, which can also be called control system engineering, in the order in which it is done is (i) modeling, including identification, estimation, and filter; (ii) system synthesis, including controllability, observability, and/or reachability; (iii) control laws design; (iv) control systems analysis, including stability and/or convergence; (v) the numerical simulation of the control system; and (vi) actual system experimental implementation. A designer could do every part of the process if necessary, but because it is a huge control engineering process in fact it is better for one person to study only one or two parts of the design. The problems that exist in each part of the process may be solved by several available theories, methods, or tools, so in practice no one person can do all the control system design and implementation. In most cases the focus is on the study of control methods for a system in which the model of a system to be controlled does not need to be built because it is given. The controllability does not be studied because it is known that the system to be controlled is controllable. If it is not the case, controllability analysis has to be done. No-one can design a control law for an uncontrollable system. In other words, no control method can be used to achieve the desired behavior for an uncontrollable system. Not doing some work in a control system design does not mean that it is not important, but that it is known or the requirement has been satisfied. This book is mainly concerned with steps (iii) to (v) of the process of control system design. Because the quantum control system concerns interdisciplinary knowledge, let us start with quantum states.

1.1 Quantum States

A quantum system can be completely described by its state vector $|\psi\rangle$ in a complex vector space with an inner product known as Hilbert space. $|\psi\rangle$ is a unit vector in the system's state space and is called the wave function. In physics, bra-ket notation is often used to denote such vectors. The notation $|\bullet\rangle$ is represented by a single vector known as a ket, while $\langle\bullet|$ is a bra. This notation is known as Dirac representation in a complex Hilbert space H . A quantum state is also called as a qubit. The wave function $|\psi\rangle$ represents a pure state. This "state" in quantum mechanics is different from that in classical systems. For a classical system, the state usually describes some real physical properties such as the position or the momentum, which are generally observable. However, a quantum state $|\psi\rangle$ cannot be directly observed and also does not directly correspond to the physical quantity of the quantum system. Since the global phase of a quantum state $|\psi\rangle$ has no observable physical effect, we often say that the vectors $|\psi\rangle$ and $e^{i\alpha}|\psi\rangle$, in which $i = \sqrt{-1}$ and $\alpha \in \mathbb{R}$, describe the same physical state. For example, in quantum information theory the information is coded by a two-level (two-state) quantum system and the state $|\psi\rangle$ of a qubit can be written as

$$|\psi\rangle = \cos \frac{\theta}{2} |0\rangle + e^{i\alpha} \sin \frac{\theta}{2} |1\rangle \quad (1.1)$$

where $\theta \in [0, \pi]$ and $\alpha \in [0, 2\pi]$. Then $|0\rangle$ and $|1\rangle$ correspond to the states 0 and 1 for a classical bit.

A quantum system can be closed or open according to whether or not the system is isolated from the external environment. The closed quantum system is under conditions of absolute zero temperature or does not interact with the external environment, and its state evolution is unitary. However, quantum systems usually cannot meet these ideal conditions in practical quantum information processing and quantum computing, and have interactions with the external environment, and are therefore treated as open quantum systems. In practical applications, the quantum systems to be controlled are usually not simple closed systems. They may be quantum ensembles or open quantum systems and their states cannot be written in the form of unit vectors $|\psi\rangle$. In this case, it is necessary to introduce the density operator or density matrix $\rho : H \rightarrow H$ to describe quantum states of quantum ensembles or open quantum systems. A density operator ρ is positive and has a trace equal to one. Suppose that a quantum system is in an ensemble $\{p_j, |\psi_j\rangle\}$ of pure states; that is, in a mixture of a number of pure states $|\psi_j\rangle$ with respective probabilities p_j . The density matrix for the system is defined as

$$\rho = \sum_j p_j |\psi_j\rangle\langle\psi_j| \quad (1.2)$$

where $|\psi_j| = (|\psi_j\rangle)^{\dagger}$ and $\sum_j p_j = 1$. Here, the operation $(\bullet)^{\dagger}$ refers to the conjugate transpose.

For a pure state $|\psi\rangle$, there is $\rho = |\psi\rangle\langle\psi|$ and $tr(\rho^2) = 1$. If the state ρ of a quantum system satisfies $tr(\rho^2) < 1$, we call the quantum state a mixed state.

A composite quantum system assumed to be made up of two subsystems A and B is defined on a Hilbert space $H = H_A \otimes H_B$, which is the tensor product of the Hilbert spaces H_A and H_B . For the composite quantum system, its state ρ_{AB} can be described by the tensor product of the states of its subsystems: $\rho_{AB} = \rho_A \otimes \rho_B$. Consider any bipartite pure state $|\psi\rangle_{AB}$. If it can be written as a tensor product of pure states $|\varphi\rangle_A \in H_A$ and $|\vartheta\rangle_B \in H_B$,

$$|\psi\rangle_{AB} = |\varphi\rangle_A \otimes |\vartheta\rangle_B \quad (1.3)$$

we call it a separable state; otherwise, we call it an entangled state. Quantum entanglement is a uniquely quantum mechanical phenomenon that plays a key role in many interesting applications of quantum communication and quantum computation.

When performing a particular measurement on a quantum state, the result is usually described by a probability distribution, and the distribution is completely determined by the quantum state and the observable describing the measurement. These probability distributions are necessary for both mixed states and pure states.

1.2 Quantum Systems Control Models

There are some different descriptions of a system model to be controlled. If the system to be controlled is a closed quantum system, its model is generally described by the Schrödinger or quantum Liouville equations, both of which are bilinear models. Bilinear models are widely used to describe closed quantum control systems such as molecular systems in physical chemistry and spin systems in nuclear magnetic resonance (NMR). For example, consider a spin-1/2 system in a constant magnetic field along the z -axis and controlled by magnetic fields along the x -axis and y -axis.

1.2.1 Schrödinger Equation

The Schrödinger equation, describing states of quantum particles, has analytical solutions that determine precisely how the state changes with time. The state $|\psi(t)\rangle$ of a closed quantum system evolves according to the Schrödinger equation

$$i\hbar \frac{\partial}{\partial t} |\psi(t)\rangle = H_0 |\psi(t)\rangle, |\psi(t=0)\rangle = |\psi_0\rangle \quad (1.4)$$

where H_0 is the free Hamiltonian of the system and a Hermitian operator on H , and \hbar is the reduced Planck's constant. For convenience, we usually assume $\hbar = 1$. For simplicity, we consider finite dimensional quantum systems, which are appropriate approximations in many practical situations.

The control of the system may be realized by a set of control functions $u_k(t) \in \mathbb{R}$ coupled to the system via time-independent interaction Hamiltonians $H_k (k = 1, 2, \dots)$. Then the total Hamiltonian $H(t) = H_0 + \sum_k u_k(t) H_k$ determines the controlled evolution

$$i \frac{\partial}{\partial t} |\psi(t)\rangle = \left(H_0 + \sum_k u_k(t) H_k \right) |\psi(t)\rangle \quad (1.5)$$

Equation 1.5 is a bilinear quantum system control model.

1.2.2 Liouville Equation

If we use the density matrix $\rho(t)$ to describe the state of a closed quantum system, the evolution equation of the density matrix $\rho(t)$ can be described by the quantum Liouville equation

$$i\dot{\rho}(t) = [H(t), \rho(t)] \quad (1.6)$$

where $[H, \rho] = H\rho - \rho H$ is the commutation operator.

A control system with density matrix $\rho(t)$ as its state has the control system model

$$i \frac{\partial}{\partial t} \rho(t) = \left[H_0 + \sum_k u_k(t) H_k, \rho(t) \right] \quad (1.7)$$

where $\rho(t)$ is the variable to be controlled, H_0 is the free (or internal) Hamiltonian, and H_k is the control (or external) Hamiltonian. Usually we can assume that H_0 and H_k are all independent of time; $u_k(t)$ is an external control field, which is a real value.

Generally, the evolution of a Hamiltonian system is unitary in a closed quantum system. Unitary evolution preserves the spectrum of the quantum state, that is, the eigenvalues of the density matrix. All density matrices that have the same eigenvalues form a set of unitarily equivalent states, for example the set of all pure states. The control problem involving pure states is always expected to be described by the wave function $|\psi\rangle$ and its Schrödinger equation in Hilbert space. Equation 1.7 can also be used to control a mixed state. In practice, the system equation chosen depends on the problem to be solved. Compared to the Liouville equation, the Schrödinger equation in which the wave function is a variable is simple. However, the wave function can be used only in the pure states systems and not in the systems of mixed

states. There is no such a limitation for the Liouville equation with density matrix $\rho(t)$ as its variable. When pure states are manipulated, Equation 1.5 is equivalent to the expression of density operator as $\rho(t) = |\psi\rangle\langle\psi|$. But Equation 1.7 is valid for mixed states manipulations. It is to be noted that although we can regard the model in Equation 1.5 as a particular case of Equation 1.7, the case in Equation 1.5 for pure states always gives more straightforward results and provides some inspiring ideas for studying Equation 1.7.

1.2.3 Markovian Master Equations

In many practical applications, the quantum systems to be controlled are open quantum systems. In fact, this is the case for most quantum control systems since such systems unavoidably interact with their external environments, including control inputs and measurement devices. For an open quantum system, a quantum master equation with the density matrix $\rho(t)$ is suitable for describing the characteristics of the state. One of the simplest cases is when a Markovian approximation can be applied where a short environmental correlation time is supposed and memory effects may be neglected. For an N -dimensional open quantum system with Markovian dynamics, the state $\rho(t)$ can be described by the following Markovian master equation:

$$\dot{\rho}(t) = -\frac{i}{\hbar}[H, \rho] + \mathcal{L}\rho \quad (1.8)$$

where the generator \mathcal{L} of the semigroup represents a super-operator. The explicit form of this matrix can be derived using rigorous master equation formalism. The first term of Equation 1.8 describes the standard dynamics and the last term accounts for the gain and the damping mechanism, which has the form of the Liouville super-operator and can be written in the Lindblad form (Dacies, 1976):

$$\mathcal{L}\rho = \sum \left[F_i^\dagger F_i \rho + \rho F_i^\dagger F_i - 2F_i \rho F_i^\dagger \right] \quad (1.9)$$

where F_i and F_i^\dagger form a collection of generalized atomic creation and annihilation operators characteristic for a particular problem.

The Lindblad form of the master equation guarantees that the interaction with the damping reservoir preserves the positivity of the density operator.

1.2.4 Non-Markovian Master Equations

In the case of weak coupling, assuming the form of the interaction Hamiltonians between the system and the environment is bilinear, the two-level reduced system model described by the non-Markovian time-convolution-less master equation can be written as follows:

$$\dot{\rho}_s = -\frac{i}{\hbar}[H, \rho_s] + \mathcal{L}_t(\rho_s) \quad (1.10)$$

$$\mathcal{L}_t(\rho_s) = \frac{\Delta(t) + \gamma(t)}{2} \left([\sigma_- \rho_s, \sigma_-^\dagger] + [\sigma_-, \rho_s \sigma_-^\dagger] \right) + \frac{\Delta(t) - \gamma(t)}{2} \left([\sigma_+ \rho_s, \sigma_+^\dagger] + [\sigma_+, \rho_s \sigma_+^\dagger] \right) \quad (1.11)$$

where $H = H_0 + \sum_k u_k(t)H_k$ is the total Hamiltonian, $H_0 = \frac{1}{2}\omega_0\sigma_z$ and H_m are the system and control Hamiltonian, respectively, ω_0 is the transition frequency of the two-level system, and

$f_m(t)$ is the modulation by the time-dependent external control field. The control Hamiltonians can be described by $H_m = \sigma_i$ ($i = x, y, z$), where $\sigma_x, \sigma_y, \sigma_z$ are the Pauli matrices σ and $\sigma_{\pm} = \frac{\sigma_x \pm i\sigma_y}{2}$ are the rising and lowering operators, respectively. $\mathcal{L}_t(\rho_s)$ describes the interaction between the system and the environment. In the Ohmic environment, the analytic expression for the dissipation coefficient $\gamma(t)$ appearing in Equation 1.11 is

$$\gamma(t) = \frac{\alpha^2 \omega_0 r^2}{1 + r^2} \{ 1 - e^{-r\omega_0 t} [\cos(\omega_0 t) + r \sin(\omega_0 t)] \} \quad (1.12)$$

and the diffusion coefficient $\Delta(t)$ is (Maniscalco *et al.*, 2004):

$$\begin{aligned} \Delta(t) = & \alpha^2 \omega_0 \frac{r^2}{1 + r^2} \{ \coth(\pi r_0) - \cot(\pi r_c) e^{-\omega_c t} [r \cos(\omega_0 t) - \sin(\omega_0 t)] \\ & + \frac{1}{\pi r_0} \cos(\omega_0 t) [\bar{F}(-r_c, t) + \bar{F}(r_c, t) - \bar{F}(ir_0, t) - \bar{F}(-ir_0, t)] \\ & - \frac{1}{\pi} \sin(\omega_0 t) [\frac{e^{-v_1 t}}{2r_0(1+r_0^2)} [(r_0 - i)\bar{G}(-r_0, t) + (r_0 + i)\bar{G}(r_0, t)] \\ & + \frac{1}{2r_c} [\bar{F}(-r_c, t) - \bar{F}(r_c, t)]] \} \end{aligned} \quad (1.13)$$

where α is the coupling constant, $r_0 = \omega_0/2\pi kT$, $r_c = \omega_c/2\pi kT$, $r = \omega_c/\omega_0$ (kT is the environment temperature), ω_c is the high-frequency cutoff, $\bar{F}(x, t) \equiv {}_2F_1(x, 1+x, e^{-v_1 t})$, $\bar{G}(x, t) \equiv {}_2F_1(2, 1+x, 2+x, e^{-v_1 t})$ and ${}_2F_1(a, b, c, z)$ is the Gauss hypergeometric function (Gradshteyn and Ryzhik, 1994).

Under conditions of high temperature, one has

$$\Delta(t)^{HT} = 2\alpha^2 kT \frac{r^2}{1 + r^2} \left\{ 1 - e^{-r\omega_0 t} \left[\cos(\omega_0 t) - \frac{1}{r} \sin(\omega_0 t) \right] \right\} \quad (1.14)$$

From Equations 1.12 and 1.14, at high temperature both $\gamma(t) \approx 0$ and $|\Delta(t)| \gg \gamma(t)$ hold. In such a case, the diffusion coefficient $\Delta(t)$ plays a dominant role in the non-unitary dynamics of the system. The essential difference between Markovian systems and non-Markovian systems is the existence of the environment memory effect. If the decay rate is defined as $\beta_{1,2}(t) = \frac{\Delta(t) \pm \gamma(t)}{2}$, then the difference is distinguished by the sign of $\beta_i(t)$, that is, when $\beta_i(t) \geq 0$, the system mainly presents Markovian characteristics; when $\beta_i(t) < 0$, non-Markovian characteristics are predominant. In the case of high temperature, one can easily get $\beta_1(t) \approx \beta_2(t) = \frac{\Delta(t)}{2} = \beta(t)$ since $\gamma(t) \approx 0$. Note that at medium and low temperatures the approximation conditions in the Gauss hypergeometric function used to derive Equation 1.14 are not available, and $\gamma(t)$ can no longer be negligible, so $\beta_i(t)$ is related to both $\Delta(t)$ and $\gamma(t)$.

1.3 Structures of Quantum Control Systems

Systems, in one sense, are devices that take input and produce an output. A system can be thought to operate on the input to produce the output. The output is related to the input by a

relationship known as the system response. The system response usually can be modeled by a mathematical relationship between the system input and the system output. A control system is a device, or a set of devices, that manages, commands, directs, or regulates the behavior of other devices or systems.

Control systems are broadly classified as either closed-loop or open-loop control systems. From the system control point of view, whether or not a system is feedback (or closed-loop) control depends on the expression of its control law: it is feedback when control law is a function of the output variable of the system. An open-loop control system is controlled directly and runs only in pre-arranged ways, or only by an input signal. Open-loop control systems do not make use of feedback. The benefit of an open-loop system is often the low cost associated with running the processes. In this case, there is no need for feedback to be taken into consideration. The drawbacks of the open-loop system are less accuracy of control and less robustness of the disturbance and uncertainty because no measurement of the system output is used to alter the control. The open-loop control has been very successful in the control of some simple quantum systems. However, it has had some difficulties in more complex quantum control tasks such as suppressing the decoherence and dealing with the disturbances in quantum systems. A natural solution to this problem is to explore closed-loop control strategies.

In closed-loop control the system is self-adjusting. Data do not flow one way. They may pass back from a specific device to the start of the control system, telling it to adjust itself accordingly. Feedback loops take the system output into consideration, which enables the system to adjust its performance to meet a desired output response. Figure 1.1 is a basic feedback control system structure in which the output value of the system y is used to help prepare the next output value. In this way, one can create a system that correct error e . Figure 1.1 shows a feedback loop with the value 1. We call this a unity feedback control system.

A feedback control has many advantages: (i) it can increase the robustness of the system; (ii) it can increase the stability of the control system; (iii) it can automatically implement the control; and (iv) it can increase the performance of a control system. It is not an exaggeration to say that the outstanding achievements of control theory in engineering, including aeronautics and astronautics, in the last 50 years have become possible owing to the development of efficient feedback design methods.

As we know, feedback is an effective strategy in classical control theory and the aim of feedback is to compensate for the effects of unpredictable disturbances on a system under control or to make automatic control possible when the initial state of the system is unknown. In classical control, many results have shown that feedback control is superior to open-loop control. In feedback control, it is usually necessary to obtain information about the state of the system through measurement. However, the measurements of a quantum system will unavoidably destroy the state of the measured quantum system, which makes the situation more complex

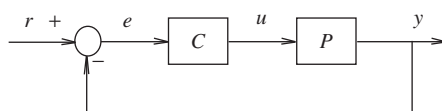


Figure 1.1 Basic feedback control system structure

when applying feedback to quantum systems. In spite of this difficulty, important progress has been made and feedback has been used to improve the control performance for squeezed states (Chen and Elliott, 1990; Misawa and Kobayashi, 2000), quantum entanglement (Malkmus *et al.*, 2005), and quantum state reduction (Muller *et al.*, 1990; Assion *et al.*, 1996) in many areas such as quantum optics (Herek, Materny, and Zewail, 1994), superconducting quantum systems (Assion *et al.*, 1996), Bose–Einstein condensate (Cerullo *et al.*, 1996), and nanomechanical systems (Bardeen *et al.*, 1998).

In quantum feedback control, the two main approaches to information acquisition are projective measurement and continuous weak measurement. The system to be controlled is a quantum system. However, the controller may be quantum, classical, or a quantum/classical hybrid. Several paradigms of quantum feedback have been proposed, such as Markovian quantum feedback (Brixner, Damrauer, and Gerber, 2001), Bayesian quantum feedback (Dupont *et al.*, 1995), and coherent quantum feedback (Brown and Rabitz, 2002). In Markovian quantum feedback, any time delay is ignored and a memory-less controller is assumed, that is, the measurement record is immediately fed back into the system to alter the system dynamics and may then be forgotten (Knutsen *et al.*, 2004). Hence, the equation describing the resulting evolution is a Markovian master equation. In Bayesian quantum feedback, the process is divided into two steps involving state estimation and feedback control. The best estimates of the dynamical variables are obtained continuously from the measurement record and feed back to control the system dynamics (Dupont *et al.*, 1995). In coherent quantum feedback, the feedback controller itself is a quantum system and it processes quantum information. Feedback control is typically a closed-loop control system. In fact, a feedback control system with the output state obtained from mathematical models can also be designed. The premise of state feedback based on mathematical models is that the state of the system rightly evolves according to the mathematical model, which requires a closed quantum system due to the requirement of consistency between states from the model and from the real system.

1.4 Control Tasks and Objectives

In contrast to the states controlled in macroscopic systems, the states in quantum systems and their applications involve the manipulation and tracking of some particular states, such as active control in the molecular dynamics of the chemical reaction to selectively obtain the resultant, using the laser intensity and phase to manipulate the system's population, which transfers the molecular system from a initial base state to an excited state with high probability. In quantum computation, population transfer to the target state by radiation-induced excitation of atoms and molecules is in fact a kind of computing operation, and population transfer is used to prepare initial pure states. Fast parallel computing in a quantum system depends on its particular coherence, which is the computation of the superposition states. In quantum application of secret communication, the most important quantum states used are entangled states. The preparation, manipulation, and preservation of quantum states are the aims of using quantum control methods.

Generally, the objective in a control system, according to Figure 1.1, is to make some output, say y , behave in a desired way by manipulating some input, say u . The simplest objective might be to keep y small (or close to some equilibrium point), a regulation or manipulation problem, or to keep $y - r$ small for r , a reference or command signal, in some set, the trajectory tracking

problem. From the control system perspective, the control tasks and objectives of a quantum system can be itemized as follows:

1. The state preparation: to obtain the prescribed state from the arbitrary initial state.
2. The state-to-state transition: to transfer a given initial state to a desired target state. The state-to-state transition is also called state-transition control. There is also a special state-transition control called population transfer control or population control. The control goal of this type of control task is to drive a quantum system from an initial given state (or population) to a pre-determined target state (or population).
3. The gate control and evolution control.
4. The trajectory tracking: to track the trajectory of a reference system.
5. The state preservation: to maintain the state unchanged.

The first four tasks can be for both closed and open quantum systems, while the fifth is the control goal specifically for open quantum systems.

1.5 System Characteristics Analyses

1.5.1 Controllability

Controllability is a major issue in system analysis before a control strategy is applied, and is used to judge whether it is possible to control or stabilize the system. The controllability relates to the possibility of controlling a particular system by using an appropriate control signal. If the system is not controllable, then no control signal will be able to manipulate its state. The controllability of quantum systems is a fundamental theoretical notion in quantum control as well as having practical importance because of its close connection with the universality of quantum computation and the possibility of attaining atomic- or molecular-scale transformations. We can more precisely define the concept of controllability: A state x_0 is controllable at time t_0 if for some finite time t_1 there exists an input $u(t)$ that transfers the state $x(t)$ from x_0 to the origin at time t_1 . In this book, we assume that the systems to be controlled are all controllable.

Generally, the results on the controllability of quantum systems only show if the system is controllable, but do not provide constructive methods to design a control law for manipulating a quantum system from an initial state to a predetermined target state. If a quantum system is controllable, the design of a proper control law to realize desired control goals is another important task, and one that this book will consider. Hence, it is desirable to develop useful methods to design such a control law, and these will be provided in this book.

1.5.2 Reachability

The reachability is also an important essential characteristic of a system. We can write the definition of reachability more precisely: A state x_1 is called reachable at time t_1 if for some finite initial time t_0 there exists an input $u(t)$ that transfers the state $x(t)$ from the origin at t_0 to x_1 . A system is reachable at time t_1 if every state x_1 in the state space is reachable at time t_1 . Similar to the controllability, if a system is reachable then one can design a control law to manipulate its state to reach the target state.

The difference between the controllability and the reachability is that the former refers to the possibility of transferring a system state to the origin, while the latter refers to the possibility of transferring a system state from an initial state to the target state. So in a quantum control system, the controllability in fact refers to the reachability.

1.5.3 Observability

The term observability describes whether or not the internal state variables of the system can be externally measured. If a state is not observable, the controller will not be able to determine the behavior of an unobservable state and hence cannot use it to stabilize the system directly. If a system is said to be observable at time t_0 with the system in state $x(t_0)$, it is possible to determine this state from the observation of the output over a finite time interval.

Controllability (reachability) and observability play an important role in the design of control systems in state space. In fact, the conditions of controllability and observability may govern the existence of a complete solution to the control system design problem. The solution to this problem may not exist if the system considered is not controllable. Although most physical systems are controllable and observable, the corresponding mathematical model may not possess the properties of controllability and observability. In this case it is necessary to know the conditions for a system to be controllable and observable.

1.5.4 Stability

Stability is a very important concept in system control theory, that is, under what conditions will a system become unstable? If it is unstable, how should we stabilize the system? Whether or not a system is stable is a property of the system itself and does not depend on the input or driving function of the system.

Stability is also one of the hardest function properties to prove. There are several different criteria for system stability, but the most common requirement is that the system must produce a finite output when it is subjected to a finite input.

1.5.5 Convergence

Convergence refers to the notion that some functions and sequences approach a limit under certain conditions.

There is a difference between classical control theory and quantum control theory: probability is the control objective of quantum systems, which means the control goal is not achievable completely for a stable control system with non-zero error. For this reason, a convergent control with zero error is required in quantum control systems. In summary, a mature quantum control theory is able to not only manipulate various states of particular needs, but also to design a convergent control law.

1.5.6 Robustness

A control system must always have some robustness. A robust control system is one in which the performance does not change much if the actual system is slightly different from the

mathematical model used for the synthesis and controller design. This specification is important: no real physical system truly behaves like the series of differential equations used to represent it mathematically. Typically, a simpler mathematical model is chosen in order to simplify the calculation because the true system dynamics can be so complicated that a complete model is impossible.

1.6 Performance of Control Systems

1.6.1 Probability

A quantum system can be in two possible states, for example the polarization of a photon. When the polarization is measured, it could be horizontal, labeled as state $|H\rangle$, or vertical, labeled state $|V\rangle$. Until its polarization is measured, the photon can be in a superposition of both these states, so its wave function $|\psi\rangle$ would be written:

$$|\psi\rangle = \alpha|H\rangle + \beta|V\rangle$$

The probability amplitudes of states $|H\rangle$ and $|V\rangle$ are α and β , respectively. When the photon's polarization is measured, the system is horizontally polarized with probability $|\alpha|^2$ and vertically polarized with probability $|\beta|^2$. Therefore, a photon with the wave function $|\psi\rangle = \sqrt{\frac{1}{3}}|H\rangle + i\sqrt{\frac{2}{3}}|V\rangle$, whose polarization is measured, would have a probability of $\frac{1}{3}$ to be horizontally polarized and a probability of $2/3$ to be vertically polarized. The measurement must give either $|H\rangle$ or $|V\rangle$, so the total probability of measuring $|H\rangle$ and $|V\rangle$ must be 1. This leads to a constraint that $|\alpha|^2 + |\beta|^2 = 1$; more generally, the sum of the squared moduli of the probability amplitudes of all the possible states is equal to 1. The wave function that fulfills this constraint is called the normalized wave function.

The probability amplitude interprets the physical meaning of the wave function. In quantum mechanics, a probability amplitude is a complex number whose modulus squared represents a probability or probability density. For example, if the probability amplitude of a quantum state is α , the probability of measuring that state is $|\alpha|^2$. The values taken by a normalized wave function ψ at each point x are probability amplitudes, since $|\psi(x)|^2$ gives the probability density at position x .

1.6.2 Fidelity

In quantum information theory, the fidelity is a measure of the “closeness” of two quantum states. It is not a metric on the space of density matrices, but it can be used to define the Bures metric on this space.

Definition 1.1 Given two density matrices ρ and σ , the fidelity is defined by

$$F(\rho, \sigma) = \text{Tr} \left[\sqrt{\sqrt{\rho}\sigma\sqrt{\rho}} \right]$$

By $M^{1/2}$ of a positive $\rho = |\phi\rangle\langle\phi|$ semi-definite matrix M we mean its unique positive square root given by the spectral theorem. The Euclidean inner product from the classical definition

is replaced by the Hilbert–Schmidt inner product. When the states are classical, that is, when ρ and σ commute, the definition coincides with that for probability distributions.

An equivalent definition is given by

$$F(\rho, \sigma) = \|\sqrt{\rho}\sqrt{\sigma}\|_{tr}$$

where the norm is the trace norm (sum of the singular values). This definition has the advantage that it clearly shows that the fidelity is symmetric in its two arguments.

Some examples follow.

1. Suppose that one of the states is pure: Then $\sqrt{\rho} = \rho = |\phi\rangle\langle\phi|$ and the fidelity is

$$F(\rho, \sigma) = \text{Tr} \left[\sqrt{|\phi\rangle\langle\phi| \sigma |\phi\rangle\langle\phi|} \right] = \sqrt{\langle\phi|\sigma|\phi\rangle} \text{Tr} \left[\sqrt{|\phi\rangle\langle\phi|} \right] = \sqrt{\langle\phi|\sigma|\phi\rangle}$$

If the other state is also pure, $\sigma = |\psi\rangle\langle\psi|$, then the fidelity is

$$F(\rho, \sigma) = \sqrt{\langle\phi|\psi\rangle\langle\psi|\phi\rangle} = |\langle\phi|\psi\rangle|.$$

This is sometimes called the overlap between two states. If, say, $|\phi\rangle$ is an eigenstate of an observable, and the system is prepared in $|\psi\rangle$, then $F(\rho, \sigma)^2$ is the probability of the system being in state $|\phi\rangle$ after the measurement.

2. Let ρ and σ be two density matrices that commute with each other. They can therefore be simultaneously diagonalized by unitary matrices, and we can write

$$\rho = \sum_i p_i |i\rangle\langle i| \text{ and } \sigma = \sum_i q_i |i\rangle\langle i|$$

for some orthonormal basis $\{|i\rangle\}$. Direct calculation shows the fidelity is

$$F(\rho, \sigma) = \sum_i \sqrt{p_i q_i}$$

This shows that, heuristically, the fidelity of quantum states is a genuine extension of the notion from probability theory.

1.6.3 Purity

In quantum mechanics, and especially quantum information theory, the purity of a state is a scalar defined as

$$\gamma = \text{Tr}(\rho^2)$$

where ρ is the density matrix of the state.

For the closed quantum system, the purity of a pure state is always equal to 1, that is, $\text{Tr}(\rho^2) = 1$, while the purity of a mixed state is less than 1, that is, $\text{Tr}(\rho^2) < 1$.

The purity is trivially related to the linear entropy S_L of a state by

$$\gamma = 1 - S_L$$

1.7 Quantum Systems Control

1.7.1 Description of Control Problems

The greatest advantage of a control law designed according to system control theory is that one can design a better or OC law and determine its parameters by the control theory instead of by tentative experiments. The control law derived from theory will lead an experiment to its desired results. In this sense, the design of the control law is the task of finding the best parameters according to some control theory, which results in many challenges for quantum control engineering:

1. It is not always a convex optimization problem.
2. The space to be searched for optimization is always infinite: it can be defined in either a finite $[0, t_f]$ or an infinite $[0, \infty)$ interval. In practice, one way to reduce optimization space is to obtain a finite-dimensional solution with control parameters that is the most common one and can be realized by means of smoothing constant function approximation.
3. To solve partial differential equations, a time-consuming computation is needed.
4. It is difficult to solve the equation of a controlled system in a non-standard form.
5. The model of a controlled system is less accurate.

The parameterized control field in a general form is $u(t) = \sum_{m=1}^M a_m \cos(\omega_m t + \phi_m)$, where a_m , ω_m , and ϕ_m are parameters to be optimized according to the control theory. The most typical problem in a quantum system is to design a set of control functions $u_m(t)$, $m = 1, \dots, M$, to steer the system from its initial state to a desired target one. For unitary evolution in a Hamiltonian system, the frequency spectrum of $\rho(t)$ is time-independent or $Tr[\rho^n(t)] = Tr[\rho_0^n(t)]$, $\forall n \in 1, \dots, N$. That is to say, to make sure the target state ρ_f is achievable, the same frequency spectrum (or entropy) is used for both ρ_0 and ρ_f . The system is controllable for its density matrix. If the entropies of ρ_0 and ρ_f are different from each other, one can minimize the distance index $\|\rho(t) - \rho_f(t)\|$ to accomplish the control task.

It can be shown that ρ_f is stationary under the condition that ρ_f and H_0 are commutable, viz. $[H_0, \rho_f(0)] = 0$. Thus, quantum state control for most target states is a problem of the transfer. For a non-stationary target, it is a trajectory tracking problem: find a function $u(t)$ to make a trajectory of $\rho(t)$ with initial state ρ_0 track the target trajectory of $\rho_f(t)$. In the latter case, the problem may need to distinguish trajectory tracking. Both orbit tracking and functional tracking exist in quantum systems. It is considered that $\rho(t)$ itself is a trajectory and the target state ρ_f evolves according to its own orbit. The orbit is expressed as the globe phase of the quantum state, which does not influence the states' amplitude and does not need to be considered. In both orbit and functional tracking, the trajectory of $\rho(t)$ is a time-dependent function and can be decided by the control value.

1.7.2 Quantum Control Theory and Methods

Quantum control theory is a rapidly developing research area. Controlling quantum phenomena has been an implicit goal in much quantum physics and chemistry research since the establishment of quantum mechanics (Warren, Rabitz, and Dahleh, 1993; Chu, 2002). One of

the main goals in quantum control theory is to establish a firm theoretical footing and develop a series of systematic methods for the active manipulation and control of quantum systems (Mabuchi and Khaneja, 2005). This goal is non-trivial since microscopic quantum systems have many unique characteristics (e.g., entanglement and coherence) which do not occur in classical mechanical systems and the dynamics of quantum systems must be described by quantum theory. In recent years, the development of the general principles of quantum control theory has been recognized as an essential requirement for the future application of quantum technologies (Dowling and Milburn, 2003).

Similar to macroscopic control systems, we can divide quantum control systems into two classes: state transfer and trajectory tracking. The former can be subdivided into control of pure states and general states. Many kinds of control methods have been proposed for every control problem. Each control method has its own characteristics and a range of suitable applications. Among the different control methods there are certain differences in the amount of computation, the performance of the solution and the degree of difficulty of the realization. A complete control process of quantum systems involves choosing the proper system model to be controlled and designing a control strategy to reach the desired control goal, which requires knowledge of various mathematical models and related control theories.

Generally, the premise to design a controller for a system is the system's controllability, otherwise the desired output state cannot be achieved by any control input. The controllability of the controlled system must therefore be studied before designing a controller. The controllability conditions themselves only provide the criterion to determine whether or not a system is controllable and do not take a part in the controller design. The basic condition required so that the controller designed by a control theory can be used is stability of the whole control system. If the controlled system is not only stable but also convergent, the error between the reference and the controlled system will be zero. The stability can only guarantee an allowable error range, not the convergence. However, a convergent system must be stable. So far controllability in quantum control theory has received much attention and great progress has been made, especially for finite-dimensional closed quantum systems.

It is worth noting that automatic control systems have been widely used in physical experiments for a long time. Between the late 1980s and the early 1990s, ultrafast lasers, so-called femtosecond lasers, appeared along with the rapid development of laser industry. This new generation of lasers has the ability to generate pulses with durations of a few femtoseconds ($1\text{ fs} = 10^{-15}\text{ seconds}$) and even less. The duration of such a pulse is comparable with the period of a molecule's natural oscillation, therefore a femtosecond laser can, in principle, be used as a means of controlling a single molecule or atom. A consequence of such an application is the possibility of realizing the chemist's dream of changing the natural course of chemical reactions. In addition, control is an important part of many recent nanoscale applications: nanomotors, nanowires, nano chips, nano robots, and so on. Using the apparatus of modern control theory, new horizons in studying the interactions of atoms and molecules may bring new ways and possible limits for the intervention in intimate processes of the micro-world.

Many control methods and technologies for systems have been proposed. The easiest one is π pulses dynamics, different pulse areas of which in resonant single-photo transition or resonant double-photos Raman transition are used to build coherent states. This can realize the complete population overturn of a two-level system but comes with the difficulties of accurate control of pulse intensity and duration time. Based on adiabatic theory, some manipulation technologies have been proposed and realized, such as Chirped Adiabatic Passage (CHIRAP)

and Stimulated Raman Adiabatic Passage (STIRAP). In both of these the adjustment of pulse parameters such as frequency, amplitude envelope, and so on is extremely slow to make the transition go along adiabatic defined dressed states. The strategy is expected to achieve complete population transfer of the target state. In view of the facts mentioned above, it is very difficult to apply these theories to more general needs such as the control of a superposition state or a mixed state. Furthermore, control law is based on the feedback of measure, where measurement is described by measure operators. In general, the reliability of measure operators is a serious problem that feedback control has to face.

Among the control methods based on control theories, quantum OC based on optimal control theory (OCT) is the most successful, and turns the problem of state manipulation into the one of global optimization. In the OC approach, the quantum control problem can be formulated as a problem of seeking a set of admissible controls satisfying the system dynamic equations and simultaneously minimizing a cost functional. The cost functional may be different according to the practical requirements of the quantum control problems, such as minimizing the control time and the control energy, the error between the initial state and target state, or a combination of these requirements. Many useful tools in traditional OC, such as the variational method, the Pontryagin minimum principle, and convergent iterative algorithms, can be adapted to quantum systems and applied to search for OCs. OC techniques have been widely applied to control quantum phenomena in physical chemistry and NMR experiments. In such a control method, time-independent performance functions are more flexible and suitable for diverse optimal problems, but the main weakness of these is that the optimal problem is a two-point boundary value problem, and the evolution of system dynamical equations and their states depend on the initial control field. One has to guess an initial value to start the design process of the control field and to optimize by continuous iterations. This requires a large amount of computing, which limits its application to quantum physics, where a rapid response is needed.

Lyapunov-based control methods are powerful tools for feedback controller design in classical control theory (Dong and Petersen, 2010). In quantum control, the acquisition of feedback information through measurements usually destroys the state being measured, which makes it difficult to directly apply Lyapunov approaches to quantum feedback controller design. However, one may first complete the feedback control design by simulation on a computer, which will give a sequence of controls, then apply the control sequence to the quantum system to be controlled in an open-loop form (Mirrahimi, Rouchon, and Turinici, 2005; Kuang and Cong, 2008). This is a feedback design and open-loop control strategy at the current level of technology. This strategy is especially useful for some difficult quantum control tasks (Altafini, 2007). The most important aspects of Lyapunov-based control design are the construction of the Lyapunov function, the determination of the control law, and the analysis of the convergence.

The advantage of the Lyapunov-based method is that control law can be obtained directly from the Lyapunov indirect stability theorem without iterations from the solution of partial differential equations, which makes it possible to realize rapid quantum control. The main shortcoming of the Lyapunov-based method is that it is usually only a stable control method, not a convergent control method. A given target state requires the control system to be convergent to guarantee that the system achieves the desired target state. To achieve this goal the convergence of the Lyapunov-based method has been studied intensely in recent years.

Bang-bang control and geometry control are alternative control methods often used in quantum systems. Geometry control is suitable for lower level systems, especially when combined with the Bloch sphere, which can help the physical meaning of the quantum state in a two-level

system to be understood. The trajectory of geometry control of a pure state in two-level systems is just the trajectory on a Bloch sphere, while the trajectory of the mixed state is the points inside the Bloch sphere. The bang-bang control in control theory is a type of simple switch control, which corresponds to the pulse control in quantum systems. Because of its simple realization, bang-bang control was used earlier in quantum systems. In open quantum systems several special control theories and methods have been developed, such as the decoherence-free subspace (DFS) method and the dynamic decoupling quantum control method.

All of the quantum control theories and methods mentioned above are covered in this book.

There are important differences between quantum control theory and its experimental implementation. Control solutions obtained from theoretical studies strongly depend on the employed model Hamiltonian. However, for real systems controlled in the laboratory, the Hamiltonians usually are not well known (except for the simplest cases) and the Hamiltonians for the system-environment coupling are known to an even lesser degree. An additional difficulty is the computational complexity of accurately solving the OC equations for realistic polyatomic molecules. Another important difference between control theory and experiment arises from the difficulty of reliably implementing theoretical control designs in the laboratory because of instrumental noise and other limitations. As a result, optimal theoretical control designs generally will not be optimal in the laboratory. Notwithstanding these comments, control simulations continue to be very valuable and they even set forth the logic leading to practical laboratory control.

1.8 Overview of the Book

This book presents the latest developments and achievements in control theories and methods in both closed and open quantum systems. The contents are suitable for both active researchers and non-experts who wish to enter the field. Each chapter discusses how to use and design the particular control method or theory, which types of systems can use it, and what information can be learned from the control system. Some possible further developments and extensions of the methods that may be expected in the near future are also mentioned. The book places an emphasis on ideas and concepts, with a fair to moderate amount of mathematical rigor. The simulation experiments and results display all essential information about the quantum state under the control methods used and will greatly enhance the reader's understanding of quantum mechanics and the effectiveness of control theories.

The book can be divided into two parts: control theory and methods for closed and open quantum systems. Chapter 1 is provides an introduction to the subject. Chapters 2–9 cover control methods for closed quantum systems, and Chapters 10–14 cover control methods for open quantum systems. Chapter 15 discusses the trajectory tracking of quantum systems. In the control theory and methods for the closed quantum systems section, Chapters 4–8 concentrate on quantum control theory based on the Lyapunov method.

The book is organized as follows.

We begin the basic analysis of system states in a simple two-level quantum system on the Bloch sphere in Chapter 2. We also introduce the state transfer of quantum systems on the Bloch sphere by means of geometric control. The Bloch sphere is a suitable tool used to present a qubit because it gives us an intuitive vision to understand the physical meanings of quantum bits or variables. We first present the descriptions of pure states, superposition states, and mixes states. Then we propose the control methods of a single spin-1/2 particle in a Bloch

sphere in which we focus on the situations of a minimum control field and a fixed time T , respectively.

Chapter 3 is about the general control methods of closed quantum systems. Two improved OC strategies applied to quantum systems are presented first. After that the design of the control sequence of pulses for a high-dimensional spin-1/2 quantum system is used to prepare the entangled state. Chapter 3 also provides a comparison study between geometric control and bang-bang control, which are the two earliest control methods used in quantum systems.

Chapters 4–8 introduce quantum control theory based on the Lyapunov method. The first three chapters are the Lyapunov methods that are used in state transfer between diverse quantum states. They are the manipulation of eigenstates, population control, and general state control, respectively. Chapter 7 covers the convergence analysis of the Lyapunov method. The Lyapunov method is discussed in so many chapters because this method is an increasingly interesting method used in quantum control systems. It will be applied in quantum systems as it is in control engineering applications. From the convergence conditions obtained in Chapter 7, it can be seen that the convergence conditions are so strong that most practical systems are not able to satisfy them. In order to relax the convergence conditions to comply with actual cases, we specifically introduce control theory and method in degenerate cases in Chapter 8.

Chapter 4 introduces the eigenstates transfer control law design process for the selected Lyapunov function based on the state distance according to the Lyapunov stability theorem. We also present an optimal quantum control based on the Lyapunov stability theorem, and the realization of the quantum Hadamard gate based on the Lyapunov method.

There are three parts in Chapter 5: the population control of equilibrium states, the generalized control of quantum systems in the frame of vector treatment, and the population control of eigenstate and its simulation.

Chapter 6 covers the general state control method in quantum systems, including superposition state manipulation, pure state control strategy, and the OC of the mixed state, and from any pure state to mixed state manipulation.

Chapter 7 focuses on the convergence analysis of the Lyapunov-based method. This chapter starts with the mathematical expressions of invariant set and then gives the analysis of invariant set based on the connectivity graph of energy levels. For the diagonal Lyapunov function, the construction and adjustment principles of diagonal elements are presented. The initial state is also considered. A necessary and sufficient convergence condition is introduced and strict proof of convergence will be presented. For the case where the convergence condition is not satisfied, a path programming the control strategy of the quantum state transfer is presented to solve the problem.

Quantum control systems that do not satisfy the necessary and sufficient convergence conditions are called non-degenerate cases. Chapter 8 deals with these kinds of control systems. For this purpose, an implicit Lyapunov function is introduced, and an implicit Lyapunov control approach to multi-control Hamiltonians systems based on state error and an implicit Lyapunov control approach based on the average value are presented.

Chapter 9 covers the manipulation methods of the general state and studies three alternative situations: quantum system Schmidt decomposition and its geometric analysis, the preparation of entanglement states in a two-spin system, and the purification of a mixed state for two-dimensional systems.

Chapters 10–14 present the control methods of open quantum systems, with Chapter 10 concentrating on the presentation of general control methods. Chapter 11 covers state estimation,

measurement, and control of quantum systems, and Chapter 12 covers the control method of state preservation. Chapter 13 explains state manipulation in the DFS and Chapter 14 covers dynamic decoupling quantum control methods. The specific contents of these five chapters are as follows.

The states transfer of open quantum systems with a single control field is presented in Chapter 10. In the simulations, the free evolution of the system without the external control and system behavior under the control action are compared. Two cases are studies: in one the target states are equilibrium states of the system to be controlled and in the other some mixed states are examined. Chapter 10 also introduces purity and coherence compensation by the interactions between particles.

The state estimation methods in quantum systems are presented in Chapter 11. The state estimation methods introduced include the quantum state estimation method based on measuring the identical copy of the system, state topography, the maximum entropy estimation method, the maximum likelihood (ML) estimation method, the Bayesian method, the minimum variance (least square-variance, LS) estimation method, and the quantum state reconstruction method. We also introduce entanglement detection and measurement of quantum systems, which include entangled state representation, separation criterion, entanglement witnesses in experiments, entanglement quantization, entanglement degree of a multi-body system, the estimation of entanglement degree, and non-linear separation criteria. Finally in Chapter 11 we present decoherence control based on weak measurement.

Chapter 12 highlights state preservation of open quantum systems. The coherence preservation in a Λ -type three-level atom, the purity preservation of quantum systems by resonant field, and the coherence preservation in Markovian open quantum systems are studied.

In the study of state manipulation in the DFSs in Chapter 13, the construction of DFS which contains the desired target state is presented first, then the Lyapunov-based method in the interaction picture is designed. Three simulation experiments are implemented in a three-level Λ -type quantum system, a four-level energy open quantum system, and a Λ -type N -level atomic system.

Dynamic decoupling is a special control method in open quantum systems. In Chapter 14 we present the phase decoherence suppression in an arbitrary n -level atom in ξ -configuration with bang-bang controls, the optimized DD in an ξ -type n -level atom, and an optimized DD strategy to suppress decoherence. This chapter should help the reader to have a better understanding of the dynamic decoupling quantum control method.

Chapter 15 covers the trajectory tracking of quantum systems, which is another type of control relative to state transfer (regulation) control. We focus on orbit tracking control of closed quantum systems. In the numerical simulation experiments and results analyses, we explain tracking control between eigenstates, between superposition states, between eigenstates and superposition states, and between superposition states and eigenstates. We propose an adaptive trajectory tracking of quantum systems. We also study the convergence of orbit tracking for quantum systems in which several cases and problems, including diagonal target states and non-diagonal target density matrices, are considered and solved.

References

- Altafini, C. (2006) Feedback control of spin systems. *Quantum Information Processing*, **6**(1), 9–36.
Assion, A., Baumert, T., Helbing, J. et al. (1996) Coherent control by a single phase shaped femtosecond laser pulse. *Chemical Physics Letters*, **259**(5–6), 488–494.

- Bardeen, C.J., Yakovlev, V.V., Squier, J.A. *et al.* (1998) Quantum control of population transfer in green fluorescent protein by using chirped femtosecond pulses. *Journal of the American Chemical Society*, **120**, 13023–13027.
- Brixner, T., Damrauer, N. and Gerber, G. (2001) Femtosecond quantum control. *Advances in Atomic, Molecular, and Optical Physics*, **46**, 1–54.
- Brown, C. and Rabitz, H. (2002) Some mathematical and algorithmic challenges in the control of quantum dynamics phenomena. *Journal of Mathematical Chemistry*, **31**(1), 17–63.
- Cerullo, G., Bardeen, C.J., Wang, Q. *et al.* (1996) High-power femtosecond chirped pulse excitation of molecules in solution. *Chemical Physics Letters*, **262**(3–4), 362–368.
- Chen, C. and Elliott, D.S. (1990) Measurements of optical phase variations using interfering multiphoton ionization processes. *Physical Review Letters*, **65**(14), 1737–1740.
- Chu, S. (2002) Cold atoms and quantum control. *Nature*, **416**, 206–210.
- Dacies, E.B. (1976) Markovian master equations II. *Mathematical Annals*, **219**, 147–158.
- Dong, D. and Petersen, I.R. (2010) Quantum control theory and applications: a survey. *IET Control Theory and Applications*, **4**(12), 2651–2671.
- Dowling, J.P. and Milburn, G.J. (2003) Quantum technology: the second quantum revolution. *Philosophical Transactions of the Royal Society A*, **361**(1809), 1655–1674.
- Dupont, E., Corkum, P.B., Liu, H.C. *et al.* (1995) Phase-controlled currents in semiconductors. *Physics Review Letters*, **74**(18), 3596–3599.
- Gradshteyn, I.S. and Ryzhik, I.M. (1994) *Table of Integrals, Series and Products*, (7th edn), Elsevier, London.
- Herek, J.L., Materny, A. and Zewail, A.H. (1994) Femtosecond control of an elementary unimolecular reaction from the transition-state region. *Chemical Physics Letters*, **228**(1–3), 15–25.
- Knutsen, K.P., Johnson, J.C., Miller, A.E. *et al.* (2004) High spectral resolution multiplex CARS spectroscopy using chirped pulses. *Chemical Physics Letters*, **387**(4–6), 436–441.
- Kuang, S. and Cong, S. (2008) Lyapunov control methods of closed quantum systems. *Automatica*, **44**(1), 98–108.
- Mabuchi, H. and Khaneja, N. (2005) Principles and applications of control in quantum systems. *International Journal of Robust and Nonlinear Control*, **15**(15), 647–667.
- Malkmus, S., Durr, R., Sobotta, C. *et al.* (2005) Chirp dependence of wave packet motion in oxazine 1. *Journal of Physical Chemistry A*, **109**(46), 10488–10492.
- Maniscalco, S., Piilo, J., Intravaia, F. *et al.* (2004) Lindblad- and non-Lindblad-type dynamics of a quantum Brownian particle. *Physical Review A*, **70**(3), 032113.
- Mirrahimi, M., Rouchon, P. and Turinici, G. (2005) Lyapunov control of bilinear Schrödinger equations. *Automatica*, **41**(11), 1987–1994.
- Misawa, K. and Kobayashi, T. (2000) Wave-packet dynamics in a cyanine dye molecule excited with femtosecond chirped pulses. *Journal of Chemical Physics*, **113**(17), 7546–7553.
- Muller, H.G., Bucksbaum, P.H., Schumacher, D.W. *et al.* (1990) Above-threshold ionisation with a two-colour laser field. *Journal of Physics B: Atomic, Molecular and Optical Physics*, **23**(16), 2761–2769.
- Warren, W.S., Rabitz, H. and Dahleh, M. (1993) Coherent control of quantum dynamics: the dream is alive. *Science*, **259**, 1581–1589.

2

State Transfer and Analysis of Quantum Systems on the Bloch Sphere

There is a one-to-one correspondence between the state of a single qubit and the point on the Bloch sphere, based on which the action of a control field can be analyzed clearly. The transfer between arbitrary states can be decomposed on the Bloch sphere into three rotations around the x -axis, y -axis, and z -axis.

2.1 Analysis of a Two-level Quantum System State

The Bloch vector (Bloch, 1946) provides the representation of the quantum state of a two-level system in terms of real observables, and allows the identification of quantum states with points in a closed ball in three-dimensional Euclidean space. In quantum information theory, for instance, the states of a single qubit can be identified with points on the surface of the Bloch sphere (when the state is pure) or points inside the sphere (when the state is mixed). The unitary operations can be interpreted as rotations of the Bloch sphere. The decoherence processes as the linear or affine contractions of the Bloch sphere (Bloch, 1946; Lindblad, 1976). In this section, we focus on the description of the different states of a qubit and the trajectories of the control actions on/in the Bloch sphere.

2.1.1 Pure State Expression on the Bloch Sphere

The simplest quantum mechanical system is the quantum-bit, or qubit. A qubit system is a two-state system that can be described by a vector in two-dimensional complex Hilbert space. The favorite qubit models are the spin of a spin-1/2 particle, nucleus spin in magnetic fields, the horizontal and vertical polarizations of a photon, or the ground and the first excited states of an electron in an atom. In general, qubits are denoted in Dirac's bra-ket notation. $|0\rangle$ represents a qubit in the zero state, pronounced "ket zero." The two basis vectors $|0\rangle$ and $|1\rangle$ correspond to the possible states a classical bit can take. However, in contrast to the state 0 or 1 of a

classical bit, the state of a single qubit is $|0\rangle$ or $|1\rangle$ or their superposition. According to quantum mechanics, the evolution of the closed system obeys the Schrödinger equation:

$$i\hbar|\psi\rangle = H|\psi\rangle \quad (2.1)$$

where H is the system Hamiltonian.

According to the superposition principle of quantum states, the pure state of a single qubit can be presented as:

$$|\psi\rangle = \alpha|0\rangle + \beta|1\rangle \quad (2.2)$$

where α and β are complex coefficients of eigenstates.

The qubit described by $|\psi\rangle$ in Equation 2.2 is in a coherent superposition of $|0\rangle$ and $|1\rangle$. The values $|\alpha|^2$ and $|\beta|^2$ give the probabilities of measuring $|0\rangle$ and $|1\rangle$ states, respectively. They satisfy the probability completeness:

$$\alpha^2 + \beta^2 = 1 \quad (2.3)$$

which is the fundamental difference distinguishing quantum bits from classical ones. Using Equation 2.3, the qubit description can be rewritten as:

$$|\psi(\theta, \phi)\rangle = e^{i\gamma} \left(\cos \frac{\theta}{2} |0\rangle + e^{i\phi} \sin \frac{\theta}{2} |1\rangle \right) \quad (2.4)$$

Since $e^{i\gamma}$ is just an arbitrary phase factor that does not have any observable effect, Equation 2.4 has an equivalent form:

$$|\psi(\theta, \phi)\rangle = \cos \frac{\theta}{2} |0\rangle + e^{i\phi} \sin \frac{\theta}{2} |1\rangle = U(t)|\psi(0)\rangle \quad (2.5)$$

where θ and ϕ are $0 \leq \theta \leq \pi$ and $0 \leq \phi \leq 2\pi$, $U(t)$ is the state transfer matrix (or evolution operator) of the system and $|\psi(0)\rangle$ is the initial state of the system.

The parameters θ and ϕ in Equation 2.5 define a point on a three-dimensional sphere. When it is used to represent a qubit, this sphere is known as the Bloch sphere, as shown in Figure 2.1.

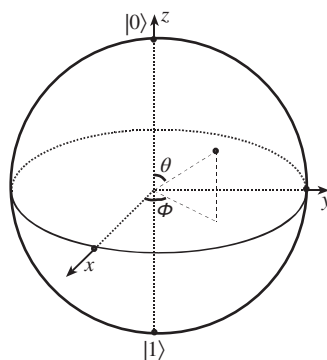


Figure 2.1 Presentation of qubit on the Bloch sphere

A qubit can be any point on the surface of this sphere. It can therefore hold an infinite amount of information. However, this actually is not the case because a qubit collapses to either $|0\rangle$ or $|1\rangle$ after being measured. Measurements are possible in something other than the computational basis. In terms of the Bloch sphere, the usual measurement operator described really measures zero for “up” and one for “down,” but it could just as easily measure “left” and “right” (along the y -axis). Usually, though, such a measurement is made by rotating the y -axis to the z -axis. The measuring in the up–down direction is equivalent to measure the Z operator, and the measuring in the left–right direction is equivalent to measure the Y operator. It is also possible to measure a more complicated operator by using a basis with multiple qubits.

The standard observables for a qubit are the Pauli operators (or matrices). They are Hermitian and thus represent observables. Defining $|0\rangle = (1 \ 0)^T$ and $|1\rangle = (0 \ 1)^T$, we can write the Pauli matrices as:

$$X \equiv \sigma_x = \begin{pmatrix} 0 & 1 \\ 1 & 0 \end{pmatrix} = |1\rangle\langle 0| + |0\rangle\langle 1| \quad (2.6a)$$

$$Y \equiv \sigma_y = \begin{pmatrix} 0 & -i \\ i & 0 \end{pmatrix} = i|1\rangle\langle 0| - i|0\rangle\langle 1| \quad (2.6b)$$

$$Z \equiv \sigma_z = \begin{pmatrix} 1 & 0 \\ 0 & -i \end{pmatrix} = |0\rangle\langle 0| - |1\rangle\langle 1| \quad (2.6c)$$

The eigenvalues of each Pauli operator are $+1$ and -1 . The standard basis ket $|0\rangle$ and $|1\rangle$ are the eigenvectors of Z operator. To emphasize the connection with the Z operator, one sometimes denotes $|0\rangle$ by $|\uparrow\rangle$ and $|1\rangle$ by $|\downarrow\rangle$. Basis vectors span the space and therefore one may write the eigenvectors of X and Y as linear combinations of $|0\rangle$ and $|1\rangle$. For example, the eigenvectors of X are $|x_+\rangle = (1/\sqrt{2})(|0\rangle + |1\rangle)$ and $|x_-\rangle = (1/\sqrt{2})(|0\rangle - |1\rangle)$; the subscripts of $+$ and $-$ denote the eigenvalue signature. Similarly, the eigenvectors of Y may be written as $|y_+\rangle = (1/\sqrt{2})(|0\rangle + i|1\rangle)$ and $|y_-\rangle = (1/\sqrt{2})(|0\rangle - i|1\rangle)$. They are shown in the Bloch sphere in Figure 2.2.

The X , Y , and Z bases have the property that if a qubit is in an eigenstate of one basis and is projected onto another basis, the probability of finding it to be either up or down is $1/2$. Such

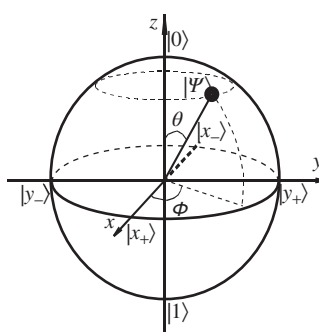


Figure 2.2 The Bloch sphere representation of a qubit. The angle θ is measured from the z -axis and the angle ϕ from the x - y plane

a set of basis is termed mutually unbiased. X is also called the bit flip operator as it turns a $|0\rangle$ into a $|1\rangle$ and vice versa. Z is called the phase flip operator as it switches between the states $\alpha|0\rangle + \beta|1\rangle$ and $\alpha|0\rangle - \beta|1\rangle$.

2.1.2 Mixed States in the Bloch Sphere

In the pure state case we think of the state as being isolated and not affected by the entire universe. In a more realistic situation we do not have total knowledge about the physical system. Maybe we have restricted access to the information, such that the best we can say about the system is that it may be in the pure state A or B with certain probabilities. What we can do in this situation is to represent the state with a statistical ensemble that gives us probabilistic information. We say that the system is in a mixed state and we call the representation of it in the quantum mechanics a density operator.

In the density operator formalism, we describe quantum states by operators on the system's Hilbert space instead of unit vectors on it. For any quantum state vector $|\psi\rangle$, the corresponding density operator ρ is the projection operator $|\psi\rangle\langle\psi|$. As linear operators may be, and often are, represented by matrices, density operators are also called density matrices.

A mixed state has the definite probabilities of being in some mixture of pure states $|\psi_i\rangle$, with corresponding probabilities p_i that sum to unity, therefore one may write the density operator in more general terms, which incorporate both mixed and pure states, as a weighted sum of pure states $|\psi_i\rangle$ with probabilities p_i as their weighting factors:

$$\rho = \sum_{i=1}^n p_i |\psi_i\rangle\langle\psi_i| \quad (2.7)$$

The density matrix ρ of a two-state system is a positive semi-definite Hermitian 2×2 matrix having unit trace. It can always be a given expression in terms of the three trace-free Pauli matrices σ_i , ($i = x, y, z$), which are generators of $su(2)$, and $I/\sqrt{2}$ (Mandilara and Clark1, 2005):

$$\rho = (1/2)(1 + \sigma \cdot r) \quad (2.8)$$

in which $\sigma = (\sigma_x, \sigma_y, \sigma_z)$ is the standard Pauli vector and $r = (r_x, r_y, r_z)$ is the Bloch vector with $|r| = 1$ if and only if ρ is a pure state, and $|r| < 1$ for mixed states.

Because $1/2 \leq Tr(\rho^2) \leq 1$, two limiting values $1/2$ and 1 correspond to maximally mixed states and pure states, respectively. In matrix form with respect to $|0\rangle$, the $|1\rangle$ basis density matrix ρ reads (Mosseri and Dandoloff, 2001):

$$\rho = \frac{1}{2} \begin{pmatrix} 1 + r_z & r_x - ir_y \\ r_x + ir_y & 1 - r_z \end{pmatrix} \quad (2.9)$$

To find out the range of values for (r_x, r_y, r_z) one can use the fact that $r_x^2 + r_y^2 + r_z^2 = Tr(\rho^2) \leq 1$, where the equation holds for pure states only. Consequently, one can identify the density operator through the points in the position of the radius of the Bloch sphere, in which pure states are points on the surface while non-pure states are points inside the sphere, as shown in Figure 2.3.

A projection measurement of the system described by a mixed state will generate a pure state, defined by a point on the Bloch sphere. When $|r| = 0$ the system is said to be maximally mixed and we have minimal information about it. Performing a measurement on such a state

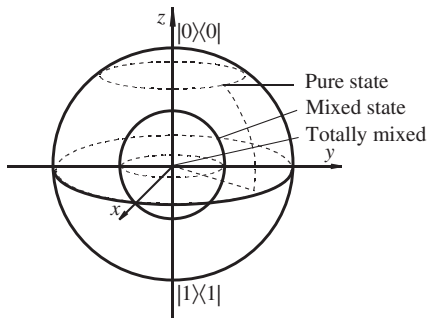


Figure 2.3 Pure states and mixed states of the Bloch sphere, in which the state $|0\rangle\langle 0|$ is found at the north pole and $|1\rangle\langle 1|$ at the south pole. The totally mixed state is in the center of the Bloch sphere

will generate a pure state, defined by any point on the Bloch sphere with probability 1/2. A maximally mixed state is symmetric under the rotation.

For one qubit system, a general qubit is described by:

$$\rho = \begin{pmatrix} |\alpha|^2 & \alpha^* \beta \\ \alpha \beta^* & |\beta|^2 \end{pmatrix} \quad (2.10)$$

A general qubit may have a point anywhere on the Bloch sphere, with uniform probability. The diagonal elements of the density operator determine the populations of the energy eigenstates, while the off-diagonal elements determine the coherences between energy eigenstates. However, the presentation of a density operator does not tell us exactly what kind of pure state is. For example, we can have a superposition state of $|0\rangle$ and $|1\rangle$, and each has probability 1/2. The density operator is then $(1/2)(|0\rangle\langle 0| + |1\rangle\langle 1|) = I/2$ (I is the unit matrix) or:

$$\rho = \begin{pmatrix} 1/2 & 0 \\ 0 & 1/2 \end{pmatrix} \quad (2.11)$$

In this case the information is zero, which represents the fact that we know nothing about where a general qubit point is on the Bloch sphere. Because the same density operator can be made by mixing the states $|+\rangle = (1/\sqrt{2})(|0\rangle + |1\rangle)$ and $|-\rangle = (1/\sqrt{2})(|0\rangle - |1\rangle)$ in equal amounts, or the three states $|0\rangle$, $|+\rangle$, and $(1/2)|0\rangle - (\sqrt{3}/2)|1\rangle$ in amounts $p_1 = (1/2) - \sqrt{3}/6$, $p_2 = \sqrt{3}/(3 + \sqrt{3})$, and $p_3 = 1 - \sqrt{3}/3$, respectively, we call these different collections of pure states with corresponding probabilities $\{p_i, |\psi_i\rangle\}$ ensembles. Sometimes they are also called realizations and we say that an ensemble realizes a mixed state. Hence, when we describe a state of an ensemble by its density operator, we discard the information about which ensemble the mixed state is made from. The density operator still describes the mixed state as well as can be done, as states from different ensembles having the same density operator are experimentally indistinguishable. This inability to distinguish them makes the density operator a perhaps more intuitive representation of a state than the state vector. As shown above, two vectors differing by a phase factor represent the same state, but when the vector is put together with its dual vector to form a pure state density operator, the phase factor vanishes because of the complex conjugation. Hence, all state vectors representing the same state are represented by the same density operator.

The evolution of a closed quantum system is always the unitary evolution. Unitary evolution preserves the spectrum of the quantum state (i.e., the eigenvalues of the density matrix). All density matrices that have the same eigenvalues form a set of unitarily equivalent states (e.g., the set of all pure states).

2.1.3 Control Trajectory on the Bloch Sphere

A given physical system is characterized by a state vector $|\psi(t)\rangle$ whose dynamics are governed by the Schrodinger equation as:

$$i\hbar \frac{\partial |\psi(t)\rangle}{\partial t} = H|\psi(t)\rangle \quad (2.12)$$

It can be shown from the Schrodinger equation (Equation 2.12) that the density operator satisfies the following differential equation:

$$\dot{\rho}(t) = -\frac{i}{\hbar}[H, \rho] \quad (2.13)$$

which is called the quantum Liouville equation.

A master equation is a differential equation that describes a quantum system in contact with its surroundings. Under certain conditions, one can derive the Lindblad equation, which is a master equation, as:

$$\dot{\rho}(t) = -\frac{i}{\hbar}[H, \rho] + \mathcal{L}\rho \quad (2.14)$$

where the generator \mathcal{L} of the semigroup represents a super-operator. The explicit form of this matrix can be derived using rigorous master equation formalism. The first term of the time evolution describes the standard coherent two-level dynamics and the last term accounts for the gain and the damping mechanism. This term has the form of the Liouville super-operator, which can be written in the Lindblad form (Lindblad, 1976):

$$\mathcal{L}\rho = \sum [F_i^\dagger F_i \rho + \rho F_i^\dagger F_i - 2F_i \rho F_i^\dagger] \quad (2.15)$$

where F_i and F_i^\dagger form a collection of generalized atomic creation and annihilation operators characteristic for a particular problem. The Lindblad form of the master equation guarantees that the interaction with the damping reservoir preserves the positivity of the density operator.

In realistic setups, the qubit is usually exposed to a noisy channel leading to the decoherence of quantum information. Because of the decoherence there is no such thing as a perfect qubit or a perfect quantum logical gate (Mahler and Weburu, 1998). If a qubit is exposed to a noisy channel one can observe a loss of coherence and it is still an open question whether or not there is an intrinsic lower limit to the decoherence rate for an arbitrary qubit. The quantum or the stochastic noise is an undesirable but unavoidable property of quantum logical gates. The issue that the stochastic noise of a qubit can dramatically change logical operations has become one of the central themes of error correction and noise stabilization in quantum computational schemes. The control of the decoherence of a qubit is a central problem of various models of quantum computation, where an incoming qubit is transmitted through a noisy channel. Because of the noise the statistical properties of such a qubit can be changed, for example pure states become mixed states. For a class of such noisy channels, one could ask the question of a possible optimization or minimization of the decoherence effect of a qubit. One fundamental

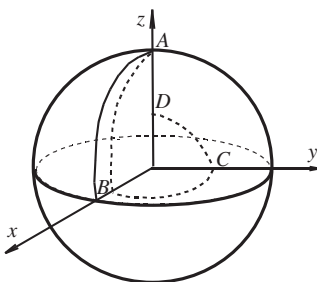


Figure 2.4 The evolution of a state in the case of three magnetic fields

goal is to seek those noises that minimize a fidelity or an entropy of such a channel. In order to perform such a task, a general understanding of a wide class of noises acting on the qubit is required. This problem has attracted a lot of attention and has been studied in the framework of quantum information theory. For this system, unitary evolution is on a spherical shell within the Bloch sphere. The dissipation causes more general motion within the Bloch sphere. This motion corresponds to the action of a certain semi-group (Alicki and Lendi, 1987). When two magnetic external control fields act on the system, this control will let the coordinate system be chosen so that the Bloch vector of the qubit points along the positive z -axis with unit length at time $t = 0$. Then we switch on a magnetic field directed along the y -axis until the Bloch vector has rotated $\pi/2$ radians. The vector is now found in the equatorial plane of the Bloch sphere, pointing in the x -direction. In the same manner, switch on the magnetic field in the z -direction and rotate the vector by $\pi/2$ radians. The magnetic field is assumed to be equal to the strength in the two directions.

For three control magnetic fields acting on the system, the procedure is analogous to the former case with two magnetic fields. We first operate with a magnetic field in the y -direction and then in the z -direction. What differs is that we also operate with a third magnetic field in the direction of the positive x -axis. This last field forces the Bloch vector to rotate to a final position, on the positive z -axis, which is the same direction as we started with.

In the pure and unitary cases this evolution describes a closed path on the Bloch sphere. In the decoherence case the evolution is non-cyclic: we end up with a Bloch vector in the same direction as we started with, but shorter. The trajectories of system under action of control are as shown in Figure 2.4, in which the thick line represents the evolution in the pure case and the dashed line is the decoherence case (note that the unitary case is a cyclic, while the decoherence case is a non-cyclic).

In conclusion, we have presented the pure and mixed states of a two-level system in detail from the aspect of the Bloch sphere in this section. The trajectories of the control action with two and three magnetic field actions in the Bloch sphere have been also analyzed. This should help in understanding the properties that exist in the states of quantum systems.

2.2 State Transfer of Quantum Systems on the Bloch Sphere

We know from Section 2.1 that the Bloch sphere provides a significant geometric description (Nielsen and Chuang, 2000) for spin-1/2 quantum systems, and gives an intuitionistic understanding to quantum states and their evolutions. It maps the state of a single qubit as a point

on a three-dimensional sphere, and a unitary evolution of the state as a rotation operation of the point around an axis. The coherent vector representation or the Bloch equation (Allen and Eberly, 1987; Alicki and Lendi, 1987) is under this comprehension. In mathematics, the unitary state transfer matrices of an N -level quantum system are made up of a unitary group $SU(N)$, whose generator, namely Lie algebra $g = su(N)$, forms the orthogonal basis set of the system density matrices. The coherent vectors are the adjoint representation of $su(2)$ elements on a $so(3)$ basis (Altafini, 2003). The Bloch sphere description takes an important role in the domains of quantum information, quantum computation, and quantum control. A lot of investigations are carried out under this description, such as the study of the stochastic decoherence of qubits (Wodkiewicz, 2001), the decomposition of the unitary operator (Cong, 2006), the analysis of the controllability of coherent control (Altafini, 2003), and the problem of preserving the coherence of quantum systems (Lidar and Schneider, 2005). Initially the Bloch sphere representation is restricted to a single qubit; how the geometric notions of the Bloch description can be extended to two qubits (Fano, 1957) and even higher dimensions (Byrd and Khaneja, 2003; Kimura, 2003; Kimura and Kossakowski, 2004) are attractive issues. Rossen Dandoloff *et al.* developed the Bloch sphere representation of entangled states of two qubits (Mosseri and Dandoloff, 2001) and Mandilara *et al.* discussed the evolution tracking of a system induced by local operation on one of two qubits (Mandilara, Clark, and Byrd, 2005).

In a single qubit situation, as will be shown in this section, it is feasible to design control fields to steer an initial state to a specific target state under the Bloch sphere description of a quantum system. In such a way a clear understanding can be made of the relation between the actual action of control fields and its mathematical representation, for example the invariable magnetic field along the z -axis corresponds to the rotation operator around the z -axis σ_z , and the rotation magnetic field in the $x-y$ plane corresponds to the rotation operator around the x -axis σ_x .

From the Bloch sphere shown in Figure 2.1 one can see that the sphere coordinates of a point on the Bloch sphere can be presented with right-angle coordinates as follows:

$$\begin{cases} x = \sin \theta \cos \varphi \\ y = \sin \theta \sin \varphi \\ z = \cos \theta \end{cases} \quad (2.16)$$

The states of a single qubit could have an intuitionistic illustration using the Bloch sphere, and any unitary evolution of the state of a single qubit can be decomposed as rotations of a point on the Bloch sphere. Based on this intuitionistic representation of a quantum state, the state evolution trajectory can be observed on the Bloch sphere, the effect of parameters can be illustrated, and control fields can be designed to steer states to the arbitrary target states of a single qubit under different conditions.

2.2.1 Control of a Single Spin-1/2 Particle

Taking a spin-1/2 particle in an invariable magnetic field B_0 along the z -axis as the controlled system, the control magnetic fields on the $x-y$ plane are:

$$\begin{cases} B_x = A \cos(\omega t + \varphi) \\ B_y = -A \sin(\omega t + \varphi) \end{cases} \quad (2.17)$$

In Equation 2.1, the system Hamiltonian H is composed of the free Hamiltonian H_0 and the control Hamiltonian H_c :

$$H = H_0 + H_c \quad (2.18)$$

and:

$$H_0 = -\frac{\hbar}{2}\omega_0\sigma_z, H_c = -\frac{\hbar\Omega}{2}(e^{-i(\omega t+\phi)}I^- + e^{i(\omega t+\phi)}I^+) \quad (2.19)$$

in which $\omega_0 = \gamma B_0$ is the eigenfrequency of the qubit in the outside magnetic field, γ is the magnetic ratio of spin particle, and $\Omega = \gamma A$ is the Rabi frequency of the particle, which is a real number: $\sigma_z = \begin{pmatrix} 1 & 0 \\ 0 & -1 \end{pmatrix}$, $I^- = \begin{pmatrix} 0 & 0 \\ 1 & 0 \end{pmatrix}$, $I^+ = \begin{pmatrix} 0 & 1 \\ 0 & 0 \end{pmatrix}$.

Hereby the matrix form of the control system Hamiltonian H is:

$$H = H_0 + H_c = -\frac{\hbar}{2} \begin{pmatrix} \omega_0 & \Omega e^{i(\omega t+\phi)} \\ \Omega e^{-i(\omega t+\phi)} & -\omega_0 \end{pmatrix} \quad (2.20)$$

In a resonant situation therefore, namely the frequency of the control fields is equal to the eigen-frequency of the system, $\omega = \omega_0$, the state transfer matrix of system $U(t)$ can be deduced according to the Schrödinger equation as:

$$U(t) = \begin{pmatrix} e^{i\omega_0 t/2} & 0 \\ 0 & e^{-i(\omega_0 t+2\phi)/2} \end{pmatrix} \begin{pmatrix} \cos\left(\frac{\Omega t}{2}\right) & i \sin\left(\frac{\Omega t}{2}\right) \\ i \sin\left(\frac{\Omega t}{2}\right) & \cos\left(\frac{\Omega t}{2}\right) \end{pmatrix} \begin{pmatrix} 1 & 0 \\ 0 & e^{i\phi} \end{pmatrix} \quad (2.21)$$

It can be seen from Equation 2.21 that the state transfer matrix $U(t)$ comprises three matrices: the first matrix is $\begin{pmatrix} e^{i\omega_0 t/2} & 0 \\ 0 & e^{-i(\omega_0 t+2\phi)/2} \end{pmatrix}$, the second term is $\begin{pmatrix} \cos\left(\frac{\Omega t}{2}\right) & i \sin\left(\frac{\Omega t}{2}\right) \\ i \sin\left(\frac{\Omega t}{2}\right) & \cos\left(\frac{\Omega t}{2}\right) \end{pmatrix}$, and the third item is $\begin{pmatrix} 1 & 0 \\ 0 & e^{i\phi} \end{pmatrix}$. The first matrix makes the point rotate around the z -axis by an angle of $(\omega_0 t + \phi)$, and an additional global phase factor; the third matrix makes a rotation around the z axis by an angle of ϕ , while the second matrix makes the point on the Bloch sphere rotate around the x -axis by an angle of Ωt .

It can be also seen from Equation 2.21 that to steer the state transfer is equivalent to controlling the three parameters Ω , ϕ , and t . The different selection of the parameters leads to different state transfer matrices, although from the same initial state to the same given target state. For example, the two trajectories on the Bloch sphere shown in Figure 2.5 have the same initial state a and the same target state d . In Figure 2.5a, the control fields make the state rotate an initial phase of ϕ from a to b around the z -axis under the action of the third matrix in Equation 2.21. Then the second matrix of the control makes the state rotate an angle of Ωt from b to c around the x -axis, and c is rotated to d under the action of the first matrix. In Figure 2.5b the initial phase of the control field is 0, so the action of the third matrix can be ignored, and a is rotated to e around the x -axis by the second matrix and the first matrix rotates e to d . The thick lines in Figure 2.5b are the actual trajectories of the compound actions of three parts of control field while the thin lines denote the states transfer trajectories decomposed according to Equation 2.21.

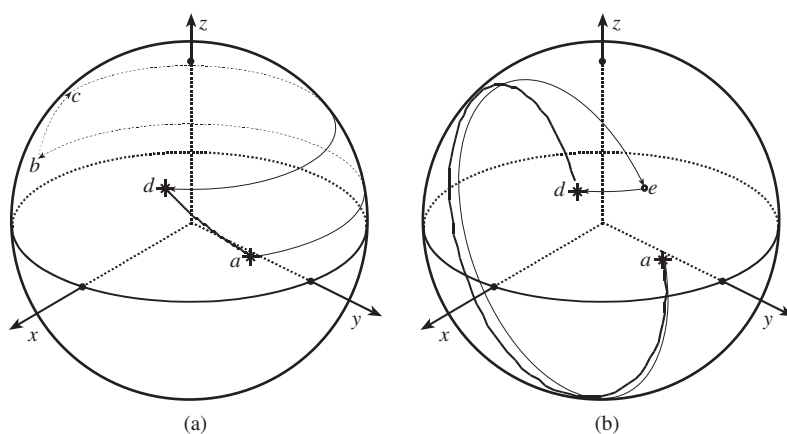


Figure 2.5 Different trajectories of states transfer on the Bloch sphere: (a) state transfer with an initial phase of ϕ and (b) state transfer with zero initial phase

For a given initial state and prescribed target state, one always desires the transfer trajectory to be optimal under the action of control, which means the control either makes the shortest time or the minimal trajectory. We will investigate these two different situations in the following subsections.

2.2.2 Situation with the Minimum Ωt of Control Fields

In this situation the minimum rotation angle around the x -axis Ωt is desired. For a given initial point $a(\theta_1, \phi_1, 1)$ and a prescribed target point $d(\theta_2, \phi_2, 1)$ on the Bloch sphere, the minimum value of Ωt is equal to $\Delta\theta = |\theta_2 - \theta_1|$ when points a and d are rotated to points a' and d' on the plane $x=0$, as shown in Figure 2.6, and the minimum rotation angle from point a' to point d' is $\Delta\theta$, which occurs when $\theta_1 > \theta_2$. If $\theta_1 \leq \theta_2$, then points a' and d' should be on the right side with positive y -coordinates. In order to get the minimum Ωt , the rotation of ϕ should be from a to a' , and the rotation of $\omega_0 t + \phi$ should be from d' to d . In the other case in which the control field has the opposite direction, the rotation around the z -axis should be in the opposite direction. In this way the required time of steering for the state transfer can be decreased.

The parameters of a control field with a minimum Ωt must satisfy the following conditions:

$$\begin{cases} \Omega t = \Delta\theta \\ \phi = \frac{3\pi}{2} - \phi_1, \theta_1 > \theta_2; \quad \phi = \frac{\pi}{2} - \phi_1, \theta_1 \leq \theta_2 \\ \omega_0 t = \text{mod}(\phi_1 - \phi_2, 2\pi) \end{cases} \quad (2.22)$$

If there is upper limit on Ω , for example, $\Omega \leq \Omega_{\max}$, then one has $t \geq t_{\min} = \Delta\theta / \Omega_{\max}$ according to Equation 2.22, thus we get:

$$t = \frac{\text{mod}(\phi_1 - \phi_2, 2\pi) + 2k\pi}{\omega_0} \quad (2.23)$$

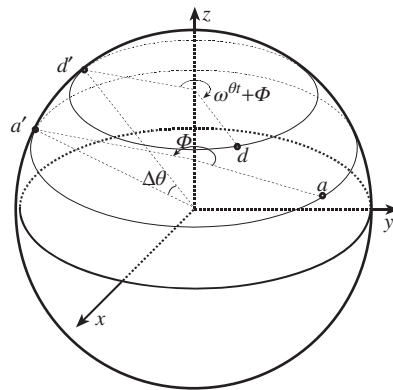


Figure 2.6 The parameters with a minimum Ωt

where k can be determined by the following equation:

$$k = \text{ceil}\left(\frac{\omega_0 t_{\min} - \text{mod}(\phi_1 - \phi_2, 2\pi)}{2\pi}\right) \quad (2.24)$$

in which the function $\text{ceil}(\bullet)$ takes the integer of (\bullet) toward positive infinitude; it is 0 only when $\omega_0 t_{\min} \leq \text{mod}(\phi_1 - \phi_2, 2\pi)$.

If there is a restriction on finish time, for example $t \leq t_{\max}$, it can also be shown that:

$$\Omega \geq \Omega_{\min} = \Delta\theta/t_{\max} \quad (2.25)$$

In general situations there are restrictions on both Ω and t , so the following equations must be satisfied according to the analysis above:

$$\begin{cases} t_{\min} \leq t \leq t_{\max} \\ \Omega_{\min} \leq \Omega \leq \Omega_{\max} \end{cases} \quad (2.26)$$

Hence in the situation with the minimum Ωt , Equations 2.22 and 2.26 should be satisfied in general.

It should be emphasized that neither the time nor the length of the trajectory on the Bloch sphere is optimized in this situation, although the control field has the minimum Ωt . In addition, the uniqueness of the trajectory under the control design is determined by the uniqueness of the coordinates of the initial state and the target state. If the point is on the pole of the Bloch sphere, viz. on the z -axis, the trajectory will not be unique for the arbitrary value of ϕ_1 or ϕ_2 , which is a special case.

2.2.3 Situation with a Fixed Time T

Usually the control operations to quantum systems should be fast enough because of the existence of the decoherence of systems in actually applications, for example the control action

should be finished in a fixed time T , but without the request of minimum Ωt . Now we will study how to obtain the parameters Ω and ϕ in such a situation.

Because the eigen-frequency ω_0 is a constant when the control field is invariable, the point on the Bloch sphere is rotated by an angle of $\omega_0 T$ for a given T . If d is rotated toward the opposite direction to the point d' , it is equivalent to the problem of obtaining the control parameters Ω and ϕ to make a transfer from the point a to the point d' but without considering the action of ω_0 . The action of the initial phase ϕ is to rotate the state from points a and d' by an angle of ϕ around the z -axis to the points a' and d'' on the same $y-z$ plane, so the point a will be rotated to the point a' under the action of the third matrix of Equation 2.21 and the point d'' will be rotated to d' after the rotation around the x -axis under the action of the first matrix (without considering ω_0). So Ω can be obtained if the angle on the $y-z$ plane $\psi = \text{mod}(\arg(y_{at} + iz_{at}) - \arg(y_{d''} + iz_{d''}), 2\pi)$ is known. The decomposition of state transfer is shown in Figure 2.7.

Thus the initial phase ϕ must satisfy the following equation:

$$\tan \phi = \frac{\sin \theta_1 \cos \phi_1 - \sin \theta_2 \cos(\phi_2 + \omega_0 T)}{\sin \theta_1 \sin \phi_1 - \sin \theta_2 \sin(\phi_2 + \omega_0 T)} \quad (2.27)$$

therefore we can obtain the initial phase ϕ from Equation 2.27 and Ω can be determined by the angle ψ of points a' and d'' on the $y-z$ plane:

$$\Omega = \psi / T \quad (2.28)$$

According to the connection of the sphere coordinates and the right-hand coordinates, one can get:

$$\tan(\psi) = \tan(\Omega T) = \frac{\cos \theta_1 \sin \theta_2 \sin(\phi_2 + \omega_0 T + \phi) - \sin \theta_1 \cos \theta_2 \sin(\phi_1 + \phi)}{\sin \theta_1 \sin \theta_2 \sin(\phi_1 + \phi) \sin(\phi_2 + \omega_0 T + \phi) + \cos \theta_1 \cos \theta_2} \quad (2.29)$$

In the situation that the initial state or the target state is an eigenstate of the Hamiltonian, one has $\psi = \Delta\theta$. If $(\theta_1 + \theta_2)/2 = \pi/2$, then $\psi = \pi$. Ω is in inverse proportion to T according

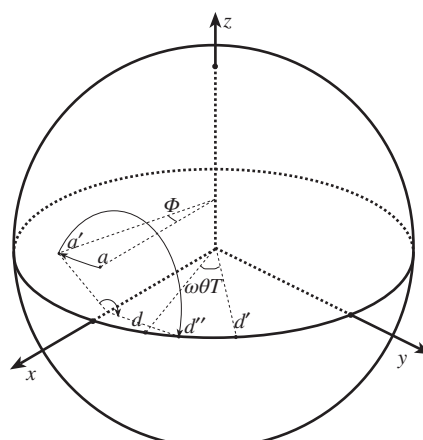


Figure 2.7 Decomposition of state transfer for a given time T

to Equation 2.28. For general situations the relation of Ω and T can be found according to Equations 2.27–2.29 to be:

$$\Omega = \begin{cases} \arctan(f(T))/T, & \psi \in (0, \frac{\pi}{2}] \\ (\pi - \arctan(f(T)))/T, & \psi \in (\frac{\pi}{2}, \pi] \\ (\pi + \arctan(f(T)))/T, & \psi \in (\pi, \frac{3\pi}{2}] \\ (2\pi - \arctan(f(T)))/T, & \psi \in (\frac{3\pi}{2}, 2\pi] \end{cases} \quad (2.30)$$

where $f(T)$ is defined as:

$$f(T) = \frac{\sqrt{\sin^2\theta_1 + \sin^2\theta_2 - 2\sin\theta_1\sin\theta_2\cos(\phi_2 - \phi_1 + \omega_0 T)}}{\cos^2(\phi_2 - \phi_1 + \omega_0 T) + \left(2\cot\theta_1\cot\theta_2 - \frac{\sin^2\theta_1 + \sin^2\theta_2}{\sin\theta_1\sin\theta_2}\right)} \left[(-\cot\theta_1 - \cot\theta_2)\cos(\phi_2 - \phi_1 + \omega_0 T) + \frac{\cos\theta_1}{\sin^2\theta_1} + \frac{\cos\theta_2}{\sin^2\theta_2} \right] \quad (2.31)$$

Equations 2.27, 2.30, and 2.31 give the conditions that the parameters need to satisfy for a given T . If there is a restriction on Ω , then the valid range of T can be obtained by Equations 2.30 and 2.31.

The following numerical simulations verify the effectiveness of the control fields designed for both situations discussed above.

2.2.4 Numerical Simulations and Results Analyses

Numerical system simulation experiments are done based on the previous analysis. The constant ω_0 is set to be a relatively small value 5 in the simulations in order to observe the trajectory of the state transfer on the Bloch sphere more clearly. Because γ is a constant related to the individual spin particle, only $\gamma B_x = \Omega \cos(\omega_0 t + \phi)$ will be given in figures below for convenience.

1) Numerical simulations for the minimum Ωt

The example used in the numerical simulation is to steer a state transfer from initial state $|0\rangle$ to target state $|1\rangle$. In this case $\Delta\theta = \pi$, and the values of ϕ_1 and ϕ_2 are arbitrary because the projections of the two states on the x - y plane are both in the origin. In the simulation experiments, $\phi_1 = \phi_2 = \pi/2$. Then one can get $t = 1.2566$ and $k = 1$ according to the third condition of Equations 2.22 and 2.24, respectively. Hence $\Omega = 2.5$ and $\phi = 0$ can be obtained according to the first condition of Equation 2.22. The control field and the trajectory of state transfer on the Bloch sphere are shown in Figure 2.8, from which one can see that the transfer from state $|0\rangle$ to $|1\rangle$ is successful under the action of the control field, but the trajectory of the state transfer goes a circuit around the z -axis, which is mostly caused by the values of ϕ_1 and ϕ_2 . In fact, in the present case, the state transfer will always be successful as long as $\Omega t = \pi$, and when Ω tends to ∞ , t tends to 0, and the length of the trajectory will tend to the minimum, which is the situation with semicircle.

The situation of a state transfer from the superposition state $(|0\rangle + |1\rangle)/\sqrt{2}$ to the state $0.8|0\rangle + 0.6|1\rangle$ is different from that in the case from $|0\rangle$ to $|1\rangle$, as shown in Figure 2.9, in which $\Delta\theta \approx 0.284$, and ϕ_1 and ϕ_2 are unique values: $\phi_1 = \phi_2 = 0$. In such a case the trajectory of the state transfer is also unique, and it goes a circuit around the z -axis so that makes

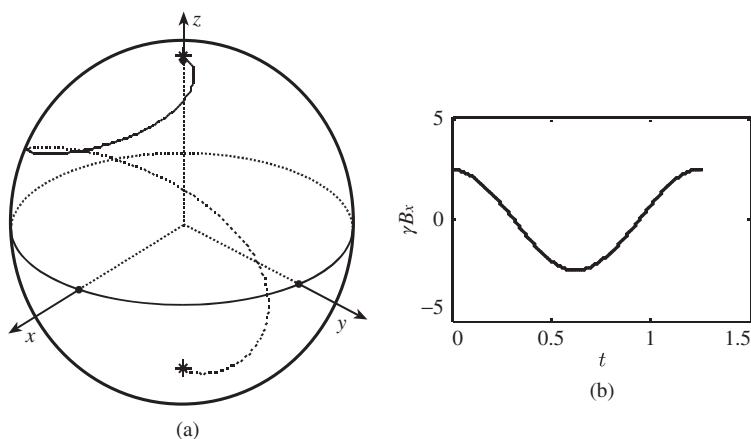


Figure 2.8 State transfer trajectory with a minimum $\Omega t = \pi$: (a) state transfer trajectory from $|0\rangle$ to $|1\rangle$ on the Bloch sphere and (b) control field

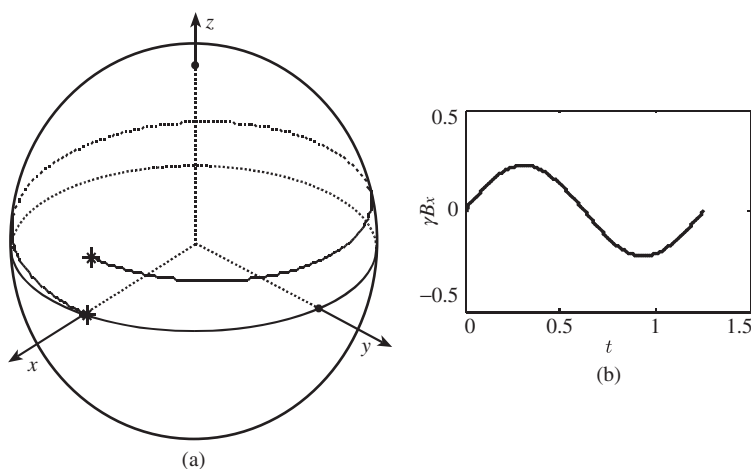


Figure 2.9 State transfer trajectory with a minimum $\Omega t \approx 0.284$: (a) state transfer trajectory from $(|0\rangle + |1\rangle)/\sqrt{2}$ to $0.8|0\rangle + 0.6|1\rangle$ and (b) control field

the trajectory and the time longer, which is caused by the conditions of $\phi_1 = \phi_2$ and $k = 1$ according to Equation 2.24, and is inescapable under the request of a minimum Ωt , viz. the trajectory has to go a circuit around the z -axis under a small value of $\Omega t_{\min} = \Delta\theta \approx 0.284$.

2) Numerical simulations for a given T

We will use the same example of steering a state transfer from $|0\rangle$ to $|1\rangle$. It is unrealistic to obtain the control parameters according to Equations 2.27, 2.30, and 2.31 for $\sin \theta_1 = \sin \theta_2 = 0$. It can be shown by the analysis from which Equations 2.27, 2.30, and

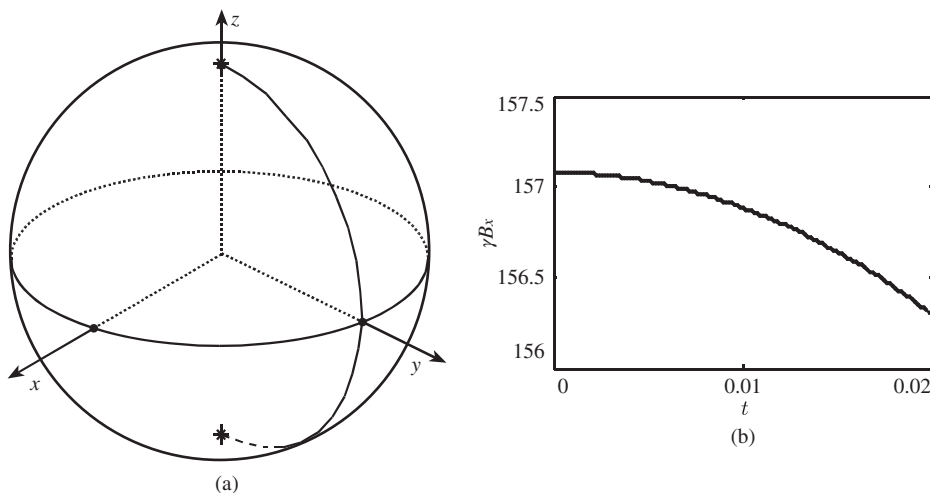


Figure 2.10 State transfer trajectory with a given time $T = 0.02$: (a) state transfer trajectory from $|0\rangle$ to $|1\rangle$ on the Bloch sphere and (b) control field

2.31 are derived that the time T determines the point d' obtained by a rotation of the target state around the z -axis by an angle of $\omega_0 T$ toward the opposite direction, and the points a and d' should be rotated by an angle of ϕ to points a' and d'' on the same $y-z$ plane. Because the rotations around the z -axis do not change the position of the initial or target states on the Bloch sphere, which are already on the same $y-z$ plane in this situation, the value of ϕ can be arbitrary. Here we set $\phi = 0$. Furthermore, the angle of rotation around the x -axis, viz. ψ , is equal to the difference between θ_1 and θ_2 , $\psi = \Omega T = \pi$. Then $\Omega = 50\pi = 157.08$ can be obtained for a given $T = 0.02$. The control field and the trajectory of the state transfer are shown in Figure 2.10. In such a case, the trajectory is also the shortest and needs a larger control value.

For the state evolution from $(|0\rangle + |1\rangle)/\sqrt{2}$ to $0.8|0\rangle + 0.6|1\rangle$ when $T = 0.02$, we can get $\theta_1 = \pi/2$, $\theta_2 \approx 1.287$, and $\phi_1 = \phi_2 = 0$ according to Equation 2.5, and we can obtain $\phi = -0.4372$ after substituting the values of θ_1 , θ_2 , ϕ_1 , and ϕ_2 in Equation 2.27, and $\Omega = 36.125$ in Equations 2.30 and 2.31. The control field and the track of the state evolution are shown in Figure 2.11. The trajectories in Figures 2.10 and 2.11 are much shorter compared with those in Figures 2.8 and 2.9. Because the state transfer under the control field design can be finished at a given time T , the trajectory will go around the z -axis by an angle of $\omega_0 T = \gamma B_0 T$. If the time T is small, then the trajectory will be short, and does not need to go a circuit around the z -axis, as shown in Figures 2.8 and 2.9, despite $\phi_1 = \phi_2$. On the other hand, the values of control fields $A = \Omega/\gamma$ will be larger according to Equation 2.28 as T becomes smaller, and Equation 2.31 is a limit function with periods $\tau = 1/\omega_0$, thus T determines mostly the values of the control field.

In fact there is usually a restriction on Ω , and the minimum time T_{\min} needed to complete the operation can be determined by Equation 2.30 for given initial and target states. The value of T_{\min} can be estimated by graphics since it is difficult to calculate precisely. Figure 2.12 shows

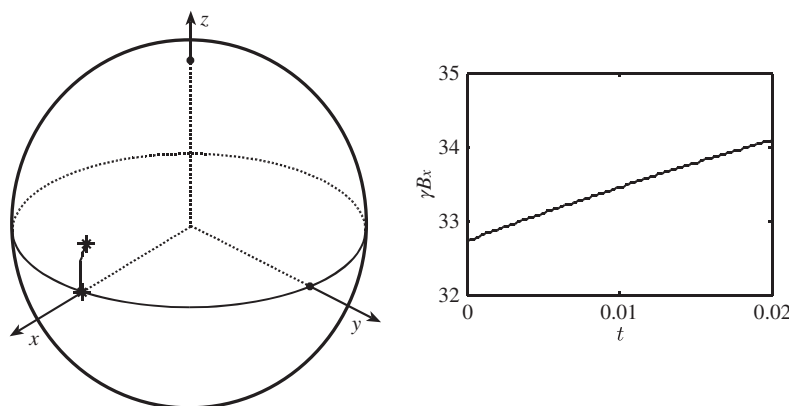


Figure 2.11 State transfer trajectory with a given time $T = 0.02$: (a) state transfer trajectory from $(|0\rangle + |1\rangle)/\sqrt{2}$ to $0.8|0\rangle + 0.6|1\rangle$ and (b) control field

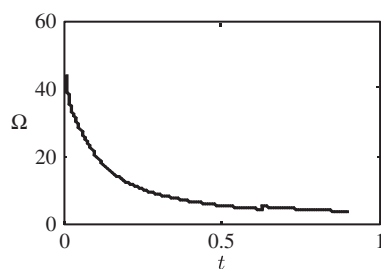


Figure 2.12 Values of Ω with T change

the variation of Ω with T in the situation with the initial state $(|0\rangle + |1\rangle)/\sqrt{2}$ and the target state $0.8|0\rangle + 0.6|1\rangle$, in which $\phi_1 = \phi_2 = 0$, $\theta_1 = \pi/2$, $\sin \theta_2 = 0.92$ and $\cos \theta_2 = 0.28$.

In fact it can be seen from Figure 2.11a that the intensities of the magnetic fields can be smaller than $A = \Omega/\gamma$ in practice because of the initial phase. For instance, in Figure 2.10 the initial phase of the control field is $\phi = \pi/4 - \omega_0 T/2 = 0.7354$ and the intensities of the magnetic fields during the whole evolution are $|A'| \leq A \cos(\phi)$ or $|A'| \leq 0.7416A$.

The numerical simulations demonstrate that control fields designed under different requirements can complete various kinds of transfer tasks between specific states, and the trajectory of a particular state transfer on the Bloch sphere is not unique. In practice the parameter Ω should be relatively small, and the operation should be fast enough to weaken the effect of decoherence. However, small control amplitude and fast operation time requirements are the parameters Ω and T , and should be selected carefully when designing the control fields. In general situations, for example, there is only the restriction on the maximum Ω , and the parameters can be selected according to Equations 2.22 and 2.26. If there is a requirement on finish time T , it is convenient to obtain parameters from Equations 2.27 and 2.30.

References

- Alicki, R. and Lendi, K. (1987) *Quantum Dynamical Semigroups and Applications*, Springer, Berlin.
- Allen, L. and Eberly, J.H. (2002) *Optical Resonance and Two-Level Atoms*, John Wiley & Sons, Inc., New York.
- Altafini, C. (2003) Controllability properties for finite dimensional quantum Markovian master equations. *Journal of Mathematical Physics*, **44**(6), 2357–2372.
- Bloch, F. (1946) Nuclear induction. *Physical Review*, **70**(7–8), 460–474.
- Byrd, M.S. and Khaneja, N. (2003) Characterization of the positivity of the density matrix in terms of the coherence vector representation. *Physical Review A*, **68**, 062322.
- Cong, S. (2006) *An Introduction to Quantum Mechanical Systems Control*, Science Press, Beijing.
- Fano, U. (1957) Description of states in quantum mechanics by density matrix and operator techniques. *Reviews of Modern Physics*, **29**, 74–93.
- Kimura, G. (2003) The Bloch vector for N-level systems. *Physics Letters A*, **314**(5–6), 339–349.
- Kimura, G. and Kossakowski, A. (2005) The Bloch-vector space for N -level systems – the spherical-coordinate point of view. *Open System Information Dynamics*, **12**, 207.
- Lidar, D.A. and Schneider, S. (2005) Stabilizing qubit coherence via tracking-control. *Quantum Information and Computation*, **5**(415), 350–363.
- Lindblad, G. (1976) On the generators of quantum dynamical semigroups. *Communications in Mathematical Physics*, **48**(2), 119–130.
- Mahler, G. and Weberru, V.A. (1998) *Quantum Networks*, Springer, Berlin.
- Mandilara, A., Clark, J.W. and Byrd, M.S. (2005) Elliptical orbits in the Bloch sphere. *Journal of Optics B: Quantum and Semiclassical Optics*, **7**(10), S277–S282.
- Mosseri, R. and Dandoloff, R. (2001) Geometry of entangled states, Bloch spheres and Hopf fibrations. *Journal of Physics A: Mathematical and General*, **34**(47), 10243–10252.
- Nielsen, M.A. and Chuang, I.L. (2000) *Quantum Computation and Quantum Information*, Cambridge University Press, Cambridge.
- Wodkiewicz, K. (2001) Stochastic decoherence of qubits. *Optics Express*, **8**(2), 145–152.

3

Control Methods of Closed Quantum Systems

3.1 Improved Optimal Control Strategies Applied in Quantum Systems

Optimal control is a very important strategy in control theory, and in recent years optimal control theory for quantum systems has received considerable attention (Rice and Zhao, 2000; Khaneja, Brockett, and Glaser, 2001; D'Alessandro, 2002). The key concept of optimal control is that the control law will be obtained by means of minimizing a cost function. As a result, choosing an appropriate cost function is one of the central tasks in the process of optimal control. Unlike the optimal control in macroscopic systems, the choice of the cost function in microcosmic systems must be considered according to the properties of quantum systems. Upon to now, the cost functions of quantum systems have mainly been of the following types:

1. Select the time optimal as the cost function (Khaneja, Brockett, and Glaser, 2001; D'Alessandro, 2002). The aim of system control is to steer a quantum system from its initial state to a given final state or a set of final states in the shortest possible time T . The cost function in such a case is:

$$J_{time} = \int_0^T 1 dt \quad (3.1)$$

Although the optimal control with the shortest time cannot be obtained directly from the function of J_{time} in Equation 3.1, the optimal control can be obtained by using appropriate decomposition of the desired unitary evolution operators (Khaneja, Brockett, and Glaser, 2001; Schirmer, 2001).

2. Select the optimal energy as the cost function (Grivopoulos and Bamieh, 2004; Boscain, Chambrion, and Gauthier, 2002; Shen, Shi, and Rabitz, 1993). In this case, the aim of system control is to steer a quantum system from its initial state to a given final state or a set of final states under the minimum control energy. The cost function is:

$$J_{energy} = \int_0^T \sum_{j=1}^m u_j^2(t) dt \quad (3.2)$$

3. Select the optimal unitary transformation as the cost function (Palao and Kosloff, 2002, 2003). In such a case, the system dynamics are fully specified by the evolution operator $U(t)$, and the desired unitary operator is U_d . One must endeavor to control the quantum system to satisfy the equation $U(T) = e^{i\varphi} U_d$. Thus the cost function is:

$$J_{\text{unitary}} = -\text{Re}(\langle \psi_0 | U_d^* U(T) | \psi_0 \rangle) \quad (3.3)$$

The cost functions summarized above have been already studied by many researchers. In practical applications, these cost functions can be used singly or in an appropriate mixture to design and implement different optimal control strategies.

In this section we will analysis the characteristics of the optimal quantum control methods, especially the solvability of the optimal quantum system control by applying general optimal control theory and the Krotov method to transfer the pure states of quantum systems, and use examples to illustrate numerical simulations.

3.1.1 Optimal Control of Quantum Systems

To facilitate the consideration of the problem, we derive the optimal control law of quantum systems in the case of with a single control law. What we derive can be extend to multiple control laws in most cases.

The equation that describes the evolution of the state is the Schrödinger equation (for simplicity, Plank's constant is taken to be $\hbar = 1$):

$$i|\dot{\psi}\rangle = H(u)|\psi\rangle = (H_0 + H_1 u)|\psi\rangle \quad (3.4)$$

in which H_0 is the internal Hamiltonian of the system, and H_1 is the control Hamiltonian, which is externally effected. $|\psi\rangle$ represents the system's state vector, the initial state is $|\psi(0)\rangle = |\psi_0\rangle$, and the desired final state at time T is $|\psi(T)\rangle = |\psi_d\rangle$.

The question we are interested in is: what is the minimum cost function to drive Equation 3.4 from $|\psi_0\rangle$ to the desired $|\psi_d\rangle$?

There are many methods for designing the optimal controller in quantum systems. The major differences between them are the choice of cost function, the construction of the Hamiltonian function, and the solving process. Here, we investigate the general optimal control method and the Krotov method. Specific derivations of these two different optimal control methods according to Equation 3.4 will be discussed below, in which the design process of general optimal control in quantum systems is the direct application of classical optimal control in quantum systems.

From the optimal control criteria point of view, we assert first that the control sequence steers the system state at time T to the desired state. The cost function can be defined as:

$$J_1 = -\langle \psi(T) | P | \psi(T) \rangle + \frac{r}{2} \int_0^T u^2(t) dt \quad (3.5)$$

where $P = |\psi_d\rangle\langle\psi_d|$ is a projective operator and the parameter r is a weighting factor that allows the relative importance of the various items to be varied. The control field $u(t)$ in J_1 is a real value. The first term of J_1 is:

$$-\langle \psi(T) | P | \psi(T) \rangle = -\| \langle \psi_d | \psi(T) \rangle \|^2 = -\| \langle \psi_0 | U_d^* U(T) | \psi_0 \rangle \|^2 \quad (3.6)$$

We find that the first term of J_1 is materially the same as the cost function J_{unitary} mentioned in Equation 3.3. The control field $u(t)$ in the second part of the cost function J_1 is a real value. The control aim is to design the control field $u(t)$ to be as small as possible. The parameter r reflects the weight of the control field.

Unlike the cost function J_1 , the cost function for normal conditions can be defined as:

$$J_2 = \frac{1}{2} \|\psi(T) - |\psi_d\rangle\|^2 + \frac{r}{2} \|u(t)\|_{L^2(C,[0,T])}^2 \quad (3.7)$$

where the control $u(t)$ of J_2 may be complex. The relation between the first term of J_2 and J_{unitary} is:

$$\frac{1}{2} \|\psi(T) - |\psi_d\rangle\|^2 = 1 - \text{Re}(\langle\psi_d|\psi(T)\rangle) = 1 - \text{Re}(\langle\psi_0|U_d^* U(T)|\psi_0\rangle) = 1 - J_{\text{unitary}} \quad (3.8)$$

Thus the first term of J_2 is also the same as the cost function J_{unitary} .

From the theory proposed by Borzi *et al.*, we find that the problem of optimal control under normal conditions gives a solution:

$$(|\bar{\psi}\rangle, \bar{u}) \in H^1(C^n, [0, T]) \times L^2(C, [0, T])$$

Now we use the method of Lagrange multipliers to change this constrained minimization problem: the minimization of J_1 under the constraint of Equation 3.4 would be changed into an unconstrained minimization. For the cost function J_1 , the Lagrange function can be defined as:

$$L_1(|\psi\rangle, |\lambda\rangle, u) = \frac{r}{2} u^2 + \text{Re} \left(|\lambda\rangle^\dagger (i|\dot{\psi}\rangle - (H_0 + H_1 u)|\psi\rangle) \right) \quad (3.9)$$

where $|\lambda\rangle^\dagger$ is complex conjugate of $|\lambda\rangle$ and $|\lambda\rangle = [\lambda_1, \lambda_2, \dots, \lambda_N]^T$ is the co-state vector.

For the cost function J_2 , the Lagrange function can be defined as:

$$L_2(|\psi\rangle, |\lambda\rangle, u) = \frac{1}{2} \|\psi(T) - |\psi_d\rangle\|^2 + \frac{r}{2} \|u(t)\|_{L^2(C,[0,T])}^2 + |\lambda\rangle^\dagger (i|\dot{\psi}\rangle - (H_0 + H_1 u)|\psi\rangle) \quad (3.10)$$

The optimal solution of J_1 can be obtained by the variation principle. Because the time T and the final state $\psi(T)$ are given, the necessary conditions for the minimum are obtained by making the Frechet derivatives of L_1 with respect to the triple $(|\psi\rangle, |\lambda\rangle, u)$ equal to zero:

$$|\dot{\psi}\rangle = \frac{\partial L_1}{\partial |\lambda\rangle}, |\dot{\lambda}\rangle = -\frac{\partial L_1}{\partial |\psi\rangle}, \frac{\partial L_1}{\partial u} = 0 \quad (3.11)$$

The following optimality can be obtained by Equations 3.6 and 3.11:

$$|\dot{\psi}\rangle = -i(H_0 + H_1 u)|\psi\rangle, |\psi(0)\rangle = |\psi_0\rangle \quad (3.12)$$

$$|\dot{\lambda}\rangle = -i(H_0 + H_1 u)|\lambda\rangle, |\lambda(T)\rangle = P|\psi(T)\rangle \quad (3.13)$$

$$ru(t) = -\text{Im}(|\lambda\rangle^\dagger H_1 |\psi\rangle) \quad (3.14)$$

where $\text{Im}(|\lambda\rangle^\dagger H_1 |\psi\rangle)$ is the imaginary part of $|\lambda\rangle^\dagger H_1 |\psi\rangle$.

The optimality of J_2 can also be obtained. The results show that the necessary conditions for the Hamiltonian function constructed to satisfy $L_2(|\hat{\psi}\rangle, |\hat{\lambda}\rangle, \hat{u}) = \min(L_2(|\psi\rangle, |\lambda\rangle, u))$ are (Borzi, Stadler, and Hohenester, 2002):

$$|\psi\rangle = -i(H_0 + H_1 u(t))|\psi\rangle, |\psi(0)\rangle = |\psi_0\rangle \quad (3.15)$$

$$|\dot{\lambda}\rangle = -i(H_0 + H_1 u(t))|\lambda\rangle, |\lambda(T)\rangle = -i(|\psi(T)\rangle - |\psi_d\rangle) \quad (3.16)$$

$$u = \frac{1}{r} \operatorname{Re} \left[p \cdot \left(\frac{\partial (H_0 + H_1 u)}{\partial u_r} |\psi\rangle \right)^* \right] + i * \frac{1}{r} \operatorname{Re} \left[p \cdot \left(\frac{\partial (H_0 + H_1 u)}{\partial u_i} |\psi\rangle \right)^* \right] \quad (3.17)$$

where u_r is the real part of the control field u and u_i is the imaginary part of u .

After establishing the optimal control schemes, one can formulate a numerical algorithm that solves the optimality Equations 3.12–3.14 or Equations 3.15–3.17 for a given initial state $|\psi_0\rangle$ and the final state $|\psi_d\rangle$, respectively, but the direct iterative algorithm cannot determine the convergence. It is therefore necessary to improve the iterative methods derived above.

3.1.2 Improved Quantum Optimal Control Method

We propose an improved method here. The main idea of improvement is to change the fixed iterative step size to make it variable. First, the initial step size is selected, then the gradient of J on the change of the control field u is calculated and the iterative step size for the next step is chosen using all the gradient changes obtained. The improved optimal control algorithm of J_2 is specified as follows:

1. Initialize, randomly choose $u^{(0)}(t)$ and $t \in [0, T]$, choose step size s and $\beta \geq 1, c \ll 1$.
2. Solve Equation 3.9, obtain the state $|\psi^{(0)}(t)\rangle$, then solve Equation 3.15 using $|\psi^{(0)}(t)\rangle$, obtain $|\lambda^{(0)}(t)\rangle$. Determine a search direction: $\begin{bmatrix} dr & di \end{bmatrix}^T = -G \begin{bmatrix} \nabla J_r & \nabla J_i \end{bmatrix}^T$, where G is a positive definite matrix, and

$$\nabla J_r = r u_r^{(0)} - \operatorname{Re} \left[p^{(0)} \left(\frac{\partial (H_0 + H_1 u)}{\partial u_r} \psi^{(0)} \right)^\dagger \right] \quad (3.18a)$$

$$\nabla J_i = r u_i^{(0)} - \operatorname{Re} \left[p^{(0)} \left(\frac{\partial (H_0 + H_1 u)}{\partial u_i} \psi^{(0)} \right)^\dagger \right] \quad (3.18b)$$

3. Determine a step size s such that:

$$J(u^{(0)} + s(dr + idi)) < J(u^{(0)}) + cs[\nabla J_r, \nabla J_i] \begin{bmatrix} dr \\ di \end{bmatrix} \quad (3.19)$$

if $s = \beta$ fulfils the equation above, set $s = \beta s$ and $u^{(0)}(t) = u^{(0)} + s(dr + idi)$, and repeat step 2; otherwise set $s = -0.5$ and go to step 3. Steps 2 and 3 are repeated until the desired convergence is achieved.

3.1.3 Krotov-Based Method of Optimal Control

In 1983, a numerical iterative method was put forward by Krotov, Fel'dman, and Engrg. Here we propose a new optimal control method based on the Krotov method. The specific design steps are as follows:

1. Choose the cost function:

$$J_3[w] = F(|\psi(T)\rangle) + \int_0^T g(t, u(t), |\psi(t)\rangle) dt \quad (3.20)$$

where w is a variable in the evolution process of systems: $w = (t, u, |\psi\rangle)$.

2. Construct an expression that is equivalent to the cost function:

$$L_3[w, \phi] = G(|\psi(T)\rangle) - \int_0^T R(t, |\psi(t)\rangle, u(t)) dt - \phi(0, |\psi_0\rangle) \quad (3.21)$$

in which $G(|\psi(T)\rangle) = F(|\psi(T)\rangle) + \phi(T, |\psi(T)\rangle)$. $\phi(t, |\psi\rangle)$ is a function that needs to be constructed, and:

$$R(t, |\psi(t)\rangle, u(t)) = \frac{\partial \phi}{\partial \psi} \cdot (-i(H_0 + H_1 u)|\psi\rangle) - g(t, u(t), |\psi(t)\rangle) + \frac{\partial}{\partial t} \phi(t, |\psi\rangle) \quad (3.22)$$

Substitute $G(|\psi(T)\rangle)$ and $R(t, |\psi(t)\rangle, u(t))$ into $L_3[w, \phi]$ will give $L_3[w, \phi] = J_3[w]$.

3. Complete the design of the optimal controller by iterative algorithm. There are three steps in iterative algorithm:

- a. Choose $u^{(0)}$, then construct a function $\varphi(t, |\psi\rangle)$ such that $L_3[w^{(0)}, \varphi]$ is a maximum with respect to $|\psi(t)\rangle$ at the point $w^{(0)}$. This is equivalent to the following two conditions:

$$R(t, |\psi^{(0)}(t)\rangle, u^{(0)}(t)) = \min_{|\psi\rangle} R(t, |\psi\rangle, u^{(0)}(t)) \quad (3.23)$$

$$G(|\psi^{(0)}(T)\rangle) = \max_{\psi} G(|\psi(T)\rangle) \quad (3.24)$$

- b. For $\varphi(t, |\psi\rangle)$, we seek a new control $u^{(1)}$ that maximizes $R(t, |\psi(t)\rangle, u(t))$ and denote it by $u^{(1)} = \arg \max_u R(t, |\psi\rangle, u)$, where the control $u^{(1)}$ is still a function of $|\psi\rangle$. Thus $u^{(1)}$ and $|\psi\rangle$ need to be solved together. The equation of the quantum system (Equation 3.1) together with the equation of control $u^{(1)}$ provide two equations for the two unknowns $u^{(1)}$ and $|\psi\rangle$. These equations may be solved self-consistently for $u^{(1)}$ and $|\psi\rangle$.
- c. It is now guaranteed that the minimization of the objective has been improved so that $L[w^{(1)}, \varphi] < L[w^{(0)}, \varphi]$. Set $u^{(0)} = u^{(1)}$, and repeat the steps above until the desired convergence is achieved.

For the quantum system given in Equation 3.1, the functions $F(|\psi(T)\rangle)$ and $g(t, |\psi(t)\rangle, u(t))$ can be defined as:

$$F(|\psi(T)\rangle) = -\langle \psi(T) | P | \psi(T) \rangle \quad (3.25)$$

$$g(t, u(t), |\psi(t)\rangle) = r(u(t) - \tilde{u}(t))^2 \quad (3.26)$$

where $P = |\psi_d\rangle \langle \psi_d|$ and $\tilde{u}(t)$ is the reference control field.

As a result, the cost function is defined as:

$$J_3[w] = -\langle \psi(T) | P | \psi(T) \rangle + \int_0^T r(u(t) - \tilde{u}(t))^2 dt \quad (3.27)$$

Construct the function $\varphi(t, |\psi\rangle)$ as

$$\varphi(t, |\psi\rangle) = \langle x|\psi\rangle + \langle \psi|x\rangle \quad (3.28)$$

where $|x\rangle = \frac{\partial}{\partial\psi}\varphi(t, |\psi^{(0)}\rangle)$ and $|x\rangle$ also satisfies the following equation:

$$\begin{aligned} |\dot{x}\rangle &= -\frac{\partial}{\partial\psi} \left(R \left(t, |\psi^{(0)}\rangle, u^{(0)}, x \right) - \frac{\partial}{\partial t} \phi(t, |\psi^{(0)}\rangle) \right) \\ &= -i(H_0 + H_1 u^{(0)})|x\rangle \\ |x(T)\rangle &= |\psi_d\rangle \end{aligned} \quad (3.29)$$

The state $|\psi\rangle$ must also satisfy the following system's equation and initial condition:

$$|\dot{\psi}\rangle = -i(H_0 + H_1 u(t))|\psi\rangle, |\psi(0)\rangle = |\psi_0\rangle \quad (3.30)$$

Substituting $L_3[w^{(0)}, \varphi]$ for $L_3[w^{(1)}, \varphi]$ gives the following equation:

$$\begin{aligned} L_3[w^{(1)}, \varphi] - L_3[w^{(0)}, \varphi] &= G(\psi^{(1)}(T)) - G(\psi^{(0)}(T)) \\ &+ \int_0^T \{R(t, \psi^{(0)}(t), u^{(0)}(t)) - R(t, \psi^{(1)}(t), u^{(1)}(t)\} dt = \Delta_1 + \Delta_2 \end{aligned} \quad (3.31)$$

where $\Delta_1 = G(|\psi^{(1)}(T)\rangle) - G(|\psi^{(0)}(T)\rangle) = (\langle \psi^{(1)}(T) | - \langle \psi^{(0)}(T) |)P(|\psi^{(1)}(T)\rangle - |\psi^{(0)}(T)\rangle \leq 0$ and $\Delta_2 = \int_0^T \{R(t, |\psi^{(0)}(t)\rangle, u^{(0)}(t)) - R(t, |\psi^{(1)}(t)\rangle, u^{(1)}(t)\} dt$.

The choice of a new control ensures $L[w^{(1)}, \varphi] - L[w^{(0)}, \varphi] \leq 0$. For any new control, the non-negativeness of Δ_1 is always right. Δ_2 is calculated as follows:

$$\Delta_2 = \int_0^T \{2\text{Im}(\langle x^{(0)} | H_1(u^{(1)} - u^{(0)}) | \psi^{(1)} \rangle - r(u^{(1)} - u^{(0)})(u^{(1)} + u^{(0)} - \tilde{u})\} dt$$

If $\Delta_2 \leq 0$ is guaranteed, the new control $u^{(1)}(t)$ is obtained:

$$u^{(1)}(t) = \tilde{u}(t) + r^{-1} \text{Im} \langle x^{(0)} | H_1 | \psi^{(1)} \rangle \quad (3.32)$$

in which $|x^{(0)}\rangle$ and $|\psi^{(1)}\rangle$ are obtained by Equations 3.29 and 3.30. Two possible choices of the control field $\tilde{u}(t)$ are analyzed. The first choice, $\tilde{u}(t) = 0$, is the one commonly used in the general optimal control method. In such a case, the additional constraint in cost function means that the total energy of the field in the time interval $[0, T]$ is limited. However, this presents a problem when the iterative procedure reaches the optimal field. The iterative method is found to reduce the total objective by reducing the total control energy, slowing and even spoiling the convergence toward the original objective. The usual remedy is to stop the iterative algorithm before this difficulty appears, but such a procedure could prevent the optimization algorithm from achieving high fidelity. A different possibility is $\tilde{u}(t) = u^{(0)}(t)$, which can avoid this problem. In this iterative algorithm the convergence to the original objective is guaranteed. In the rest of the study $\tilde{u}(t) = u^{(0)}(t)$ is chosen. The above steps are repeated until the desired convergence is achieved.

3.1.4 Numerical Simulation and Performance Analysis

To elaborate on the ideas developed above, we apply them to controlling spin-1/2 nuclei in a magnetic field. The unitary evolution of the single-spin system is given by:

$$i\hbar|\psi\rangle = (\sigma_z + \sigma_x \cdot u(t))|\psi\rangle \quad (3.33)$$

where $\sigma_z = \begin{bmatrix} 0.5 & 0 \\ 0 & -0.5 \end{bmatrix}$, $\sigma_x = \begin{bmatrix} 0 & 0.5 \\ 0.5 & 0 \end{bmatrix}$, $u(t)$ is the control field, and, for simplicity, we set Plank's constant \hbar to 1.

The initial state is set as $|\psi(0)\rangle = [1, 0]^T$, and the desired state at time T is $|\psi(T)\rangle = |\psi_d\rangle = [0, 1]^T$. We hope to seek a control field $u(t)$ that minimizes the cost function and drives the system from the initial state $|\psi_0\rangle$ to the desired state $|\psi_d\rangle$.

Two optimal control schemes are applied in the quantum system (Equation 3.33).

1) Improved optimal control method

The gradient-type minimization algorithm of Section 3.1.2 is first applied in the quantum system (Equation 3.33) and the simulation experiment is done. In the simulation, we choose the initial control field to be $u^{(0)}(t) = 0.1 \cos(t) + i^*0.1 \sin(t)$, and set $s = 0.1$, $\beta = 1.5$, $c = 0.0001$, and $r = 0.01$. The final time is $T = 10$ seconds and the subinterval size is 0.01. We stop the iteration when $\Delta J_2 \leq 10^{-4}$.

The system simulation experiment gives the number of iterations to be 7. The real parts of the optimal control field vary between -0.47 and 0.47 , and the imaginary parts vary between -0.3 and 0.3 . The state transfer error is $\| |\psi(T)\rangle - |\psi_d\rangle \|^2 = 1.2488 \times 10^{-4}$. The final cost function value is $J_2 = 7.0775 \times 10^{-3}$. Figure 3.1 shows the results of the control field, in which the solid line represents the real parts of the optimal control field and the dashed line represents the imaginary parts. Figure 3.2 shows the control procedure of the quantum-state population, in which the solid line represents a population of level 1 and the dashed line represents a population of level 0. Changing the initial control field, initial step s and β appears to have little effect on the results.

Table 3.1 shows the influence of control system performances under different values of r ($r = 1, 0.1, 0.01, 0.001$), where $\| |\psi(T)\rangle - |\psi_d\rangle \|^2$ is the state transfer error, J_2 is the value of the

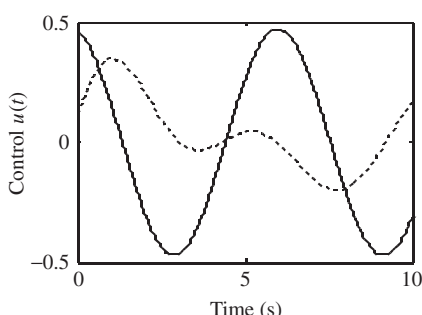


Figure 3.1 Control field under the general optimal method

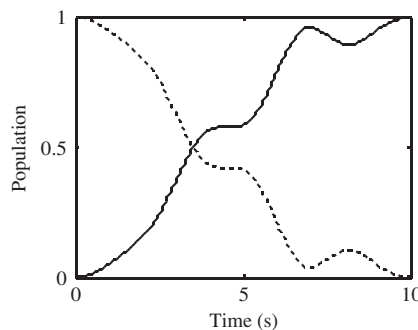


Figure 3.2 Quantum-state population under the general optimal method

Table 3.1 System performance under different values of r

r	$\ \psi(T)\rangle - \psi_d\ ^2$	J_2	K	$\text{Re}(u)$
1	8.6613×10^{-1}	6.0867×10^{-1}	2	$ 0.20 $
0.1	2.9816×10^{-3}	6.8417×10^{-2}	6	$ 0.43 $
0.01	1.2488×10^{-4}	7.0775×10^{-3}	7	$ 0.47 $
0.001	4.1309×10^{-5}	7.3018×10^{-4}	7	$ 0.48 $

Table 3.2 System performance under different values of T

T	$\ \psi(T)\rangle - \psi_d\ ^2$	J	k	$\text{Re}(u)$
1	1.3258×10^{-1}	1.4910×10^{-1}	17	-5.7 to 0.34
5	1.1852×10^{-4}	1.3640×10^{-2}	12	-0.84 to 0.96
10	1.2488×10^{-4}	7.0775×10^{-3}	7	-0.47 to 0.47
20	8.1652×10^{-6}	3.9907×10^{-3}	7	-0.27 to 0.27

cost function, k is the number of required minimization steps, and $\text{Re}(u)$ is the real part of the optimal control field.

From Table 3.1 it can be seen that when r becomes smaller, the state transfer error gets smaller, the cost function J_2 also gets smaller, but the control field gets stronger. When r becomes bigger, so does the state transfer error and the cost function J_2 , but the control field becomes weaker. Iteration steps differ little in the experimental process, thus it can be seen that smaller r values should be adopted when the intensity of the control field allows this.

Table 3.2 gives the effect of control system performance under different values of time T ($T = 1, 5, 10, 20$ seconds) while $r = 0.01$ and the other parameters are fixed.

From Table 3.2, one can see that when the final time T becomes shorter, the state transfer error gradually gets bigger, but when time T gets to a certain value, the error suddenly becomes very big. This value is about $T = 3$ seconds. Conversely, as T gets longer, the state transfer error gradually gets smaller and so does the cost function.

2) Krotov-based design method

The Krotov algorithm is also applied to the quantum system (Equation 3.33). In the system simulation experiment, we choose the initial control field: $u^{(0)}(t) = 0.5 \cos(t)$, $T = 10$ seconds, subinterval size 0.01, and $r = 1$. The iteration will stop if $\Delta J_3 \leq 10^{-4}$.

The simulation experiment results gives the number of iterations as 33. The optimal control field varies between -0.8 and 0.6 . The state transfer error is $\|\langle \psi(T) \rangle - |\psi_d\rangle\|^2 = 1.0830 \times 10^{-9}$. The cost function is $J_3 = 1.1289 \times 10^{-1}$. Figure 3.3 shows the results for the control field and Figure 3.4 show the quantum-state population, in which the solid line is the population evolution curve, where the initial state is the excited state $|1\rangle$, and the dashed line is the population evolution curve, where the initial state is the ground state $|0\rangle$.

From the simulation experiments we can conclude that the smaller the parameter r , the smaller the state transfer error and the cost function J_3 , but the bigger the control field. On the other hand, as the final time T becomes shorter, the state transfer error slowly gets bigger. As λ decreases, the error decreases and the amplitude of the control field increases. However, the oscillation will happen to the system population evolution if λ reduces to a certain degree because the control field is too big.

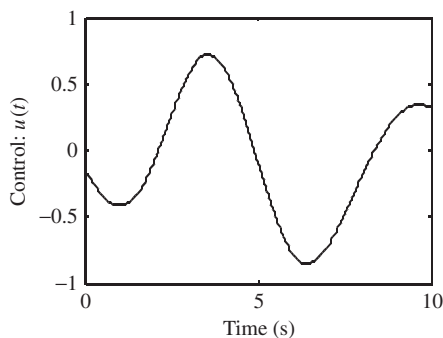


Figure 3.3 Control field under the Krotov method

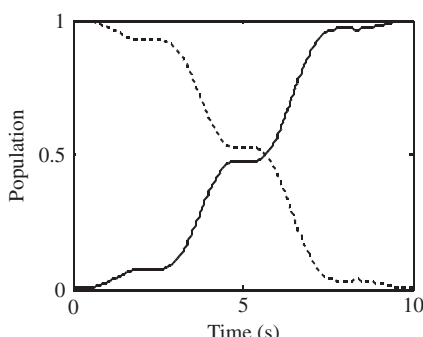


Figure 3.4 Quantum-state population under the Krotov method. The solid line represents the population of level 1 and the dashed line represents the population of level 0

3.2 Control Design of High-Dimensional Spin-1/2 Quantum Systems

Quantum theory reveals the mysterious quality of quantum systems called wave-particle duality. In quantum mechanics any state of particle can be represented by a wave function, which is a superposition of eigenstates corresponding to eigenvalues of an observable. The probability of the eigenstate under the measurement, namely the population, is denoted by the square of the module of its complex coefficient. In these various fields, the coherent state preparation or the control of quantum states is an interesting task, that is, to steer the quantum system from a specific initial state, through the interaction with the laser or radio frequency pulses, to a specific target state. The coherent preparation of the quantum state is equivalent to the problem of population transfer from a given initial state to a specific target state, that is, the coherent control problem of the population transfer. Research on the control of the population transfer is mostly concerned with some relatively simple systems or those with a few energy levels in the present literature, and in this section the design methods of pulse sequence, which are used to control the population transfer of quantum systems with a more complex energy level structure, are studied based on the strategies of π pulse dynamics and stimulated Raman adiabatic passage (STIRAP) dynamics. Our aim is to design the sequence of pulses to control the population transfer coherently for spin-1/2 quantum systems. The design of the sequence is based on the intuitive understanding of the physical model and the control parameters are obtained by simulation methods.

3.2.1 Coherent Population Transfer Approaches

In general, there are two distinct approaches to coherent population transfer using transform-limited pulses: π -pulse dynamics and adiabatic passage dynamics. Both methods can be used to create the coherent superposition starting from a particular pure state. The mostly frequently used method in adiabatic passage dynamics is STIRAP. The STIRAP procedure makes use of a so-called dark state: an adiabatic state constructed from two stable or meta-stable states that do not fluoresce (Vitanov *et al.*, 2001). The π -pulse approach uses a resonant one-photon transition between non-degenerate states or a resonant two-photon Raman transition. The coherent superposition is created by controlling the pulse area, and the complete population inversion can be achieved when the pulse area is an odd integer of π . In the adiabatic passage regime, the complete population transfer is usually to the target state as long as the adiabatic condition is satisfied. Partial population transfer can be achieved only for small values of the adiabatic parameter or, in some cases, by controlling the ratio between different Rabi frequencies. The latter method is used more frequently, for example in population transfer using stokes pulse and probe pulse with the time delay in a system of three energy levels (Wang *et al.*, 2004; Zhou *et al.*, 2005), in coherent control using a spatial phase of one single-mode laser pulse to achieve the Hadamard transformation (Mishima, Hayashi, and Lina, 2003), and in the entanglement preparation using a counterintuitive sequence of pulses in a four-level system (Malinovsky and Sola, 2004).

The π -pulse approach is usually used to create a superposition of two states: $|\psi_a\rangle$ and $|\psi_b\rangle$,

$$\Phi(\theta, \varphi) = \cos \theta \cdot |\psi_a\rangle + e^{i\varphi} \sin \theta \cdot |\psi_b\rangle \quad (3.34)$$

with prescribing mixed angle θ and superposition phase ϕ . The mixed angle θ is the direct ratio of the temporal pulse area a :

$$\theta = \frac{a}{2} \equiv \frac{1}{2} \int_{-\infty}^{\infty} \Omega(t) dt \quad (3.35)$$

where a is the product of a peak Rabi frequency and the pulse temporal width T . To produce the desired 50% : 50% superposition it is only necessary to adjust the pulse area to $\pi/2$. Such a method is obviously sensitive to variations of both peak intensity (i.e., the square of the Rabi frequency) and pulse duration T . After the Lie-group decomposition, one can get at last a sequence of π pulse, every pulse of different frequency corresponding to a transition between two particular energy levels. These pulses take the effect in a specific order, and the population is transferred from one state to another. Such a sequence of pulses is known as an intuitive sequence because of its intuitiveness.

Compared to the π -pulse regime, the STIRAP regime is more robust and the population change is not directly proportional to the temporal area, but depends on the temporal delay and the phase difference between pulses or the ratio between different Rabi frequencies. In order to have a good understanding of the STIRAP regime, the simplest case of a multilevel quantum system, a Λ atom, is illustrated. The Λ atom has two ground states and coupling (Raman coupling) with a common excited state, denoted by $|\psi_a\rangle \leftrightarrow |\psi_c\rangle \leftrightarrow |\psi_b\rangle$, and what is required is a complete (or partial) population transfer from $|\psi_a\rangle$ to $|\psi_b\rangle$. The STIRAP regime uses two pulses offset from each other in time: first the $c-b$ pulse will take effect, then after a while the $a-c$ pulse. The sequence of pulses is called a half counterintuitive sequence if the two pulses turn off simultaneously, which creates the coherent superposition of $|\psi_a\rangle$ and $|\psi_b\rangle$. If the end of the $c-b$ pulse overlaps with the beginning of the $a-c$ pulse the sequence will be called a counterintuitive sequence and this makes the complete population transfer $|\psi_a\rangle \rightarrow |\psi_b\rangle$. Adjusting the time delay of the two pulses can control the population transfer. With this method the population of the excited state can even be as low as zero, so the atomic population is transferred from one ground state to the other one without excitation of the atom.

3.2.2 Relationships between the Hamiltonian of Spin-1/2 Quantum Systems under Control and the Sequence of Pulses

The two-level quantum system is the simplest one that has important applications. A quantum system can be considered as a two-level system if there are two energy levels close to each other but far from other energy levels. A spin-1/2 particle is the most common one with two levels, for instance an electron, hence the problem of designing pulses for population transfer will be illustrated with spin-1/2 particles.

A spin-1/2 quantum system is placed in an invariable magnetic field B_0 in the z -direction, and control radio frequency pulses on the $x-y$ plane with the form:

$$B_c = B \cos(\omega t + \phi) \quad (3.36)$$

According to quantum mechanics theory, the evolution of states of a closed quantum system follows the Schrödinger equation:

$$i\hbar|\dot{\psi}\rangle = H|\psi\rangle \quad (3.37)$$

where the Hamiltonian H is composed of the free Hamiltonian H_0 and the control Hamiltonian H_c :

$$H = H_0 + H_c \quad (3.38)$$

Considering the Ising interaction model, that is, there are interactions with the z -direction only between neighboring qubits, then the Hamiltonian of the system becomes:

$$H_0 = \sum_i -\hbar(\omega_i I_i^z + 2J_{i,i+1} I_i^z I_{i+1}^z - 2J_{n,n+1} I_n^z I_{n+1}^z) \quad (3.39)$$

The control Hamiltonian of the system under the action of the control pulses is:

$$H_c = \sum_j -\frac{\hbar}{2}[\Omega_j(e^{-i\omega_{pq}t}I^- + e^{i\omega_{pq}t}I^+)] \quad (3.40)$$

where $\omega_i = \gamma_i B_0$, which is the resonant frequency of the i th qubit on the right-hand side of Equation 3.39, ω_{pq} is the frequency of the pulse coupling energy levels p and q corresponding to Ω_j , J is the interaction intensity between the i th and $(i+1)$ th qubits, $I^z = \frac{1}{2} \begin{pmatrix} 1 & 0 \\ 0 & -1 \end{pmatrix}$, $I^- = \begin{pmatrix} 0 & 0 \\ 1 & 0 \end{pmatrix}$, $I^+ = \begin{pmatrix} 0 & 1 \\ 0 & 0 \end{pmatrix}$, and $\Omega_i = \gamma_i B$ is a real number and the Rabi frequency of the i th qubit. Its physical significance is the frequency of population transfer. When B is a constant and under the condition of resonance, that is, the frequency of the control pulse is equal to the resonant frequency, the frequency of the inversion, which is defined by the population difference between the ground state and the existed state, is Ω .

Now consider the situation of two qubits. According to the quantum superposition principle, the wave function of the system is:

$$|\psi\rangle = \alpha_1|00\rangle + \alpha_2|11\rangle + \alpha_3|01\rangle + \alpha_4|10\rangle \quad (3.41)$$

where $|nm\rangle$ is the eigenstates and α_i is their complex coefficients, and $|\alpha_i|^2$ is the populations of the eigenstates satisfying the completeness condition $\sum_i |\alpha_i|^2 = 1$.

Then the Hamiltonian H of the system can be obtained according to the Ising model:

$$H = -\frac{\hbar}{2} \begin{pmatrix} \omega_1 + \omega_2 + J & 0 & \Omega_2 e^{i\omega_{13}t} & \Omega_1 e^{i\omega_{14}t} \\ 0 & -\omega_1 - \omega_2 + J & \Omega_1 e^{-i\omega_{23}t} & \Omega_2 e^{-i\omega_{24}t} \\ \Omega_2 e^{-i\omega_{13}t} & \Omega_1 e^{i\omega_{23}t} & \omega_1 - \omega_2 - J & 0 \\ \Omega_1 e^{-i\omega_{14}t} & \Omega_2 e^{i\omega_{24}t} & 0 & -\omega_1 + \omega_2 - J \end{pmatrix} \quad (3.42)$$

Substituting H and $|\psi\rangle$ in Equation 3.37 with Equations 3.41 and 3.42, gives differential equations with α_i as the variable:

$$\begin{cases} \dot{\alpha}_1 = \frac{i}{2} [(\omega_1 + \omega_2 + J)\alpha_1 + \Omega_2 e^{i\omega_{13}t}\alpha_3 + \Omega_1 e^{i\omega_{14}t}\alpha_4] \\ \dot{\alpha}_2 = \frac{i}{2} [(-\omega_1 - \omega_2 + J)\alpha_2 + \Omega_1 e^{-i\omega_{23}t}\alpha_3 + \Omega_2 e^{-i\omega_{24}t}\alpha_4] \\ \dot{\alpha}_3 = \frac{i}{2} [(\omega_1 - \omega_2 - J)\alpha_3 + \Omega_2 e^{-i\omega_{13}t}\alpha_1 + \Omega_1 e^{i\omega_{23}t}\alpha_2] \\ \dot{\alpha}_4 = \frac{i}{2} [(-\omega_1 + \omega_2 - J)\alpha_4 + \Omega_1 e^{-i\omega_{14}t}\alpha_1 + \Omega_2 e^{i\omega_{24}t}\alpha_2] \end{cases} \quad (3.43)$$

Transform the coefficients of eigenstates α_j :

$$\begin{cases} \alpha_1 = \alpha'_1 e^{i(\omega_1 + \omega_2 + J)t/2} \\ \alpha_2 = \alpha'_2 e^{i(-\omega_1 - \omega_2 + J)t/2} \\ \alpha_3 = \alpha'_3 e^{i(\omega_1 - \omega_2 - J)t/2} \\ \alpha_4 = \alpha'_4 e^{i(-\omega_1 + \omega_2 - J)t/2} \end{cases} \quad (3.44)$$

and then apply Equation 3.44 to Equation 3.43:

$$\begin{cases} \dot{\alpha}'_1 = \frac{i}{2} [\Omega_2 e^{i(\omega_{13} - \omega_2 - J)t} \alpha'_3 + \Omega_1 e^{i(\omega_{14} - \omega_1 - J)t} \alpha'_4] \\ \dot{\alpha}'_2 = \frac{i}{2} [\Omega_1 e^{-i(\omega_{23} - \omega_1 + J)t} \alpha'_3 + \Omega_2 e^{-i(\omega_{24} - \omega_2 + J)t} \alpha'_4] \\ \dot{\alpha}'_3 = \frac{i}{2} [\Omega_2 e^{-i(\omega_{13} - \omega_2 - J)t} \alpha'_1 + \Omega_1 e^{i(\omega_{23} - \omega_1 + J)t} \alpha'_2] \\ \dot{\alpha}'_4 = \frac{i}{2} [\Omega_1 e^{-i(\omega_{14} - \omega_1 - J)t} \alpha'_1 + \Omega_2 e^{i(\omega_{24} - \omega_2 + J)t} \alpha'_2] \end{cases} \quad (3.45)$$

Make use of the resonant condition, that is:

$$\omega_{13} = \omega_2 + J, \quad \omega_{14} = \omega_1 + J, \quad \omega_{23} = \omega_1 - J, \quad \omega_{24} = \omega_2 - J, \quad (3.46)$$

and denote Ω_k corresponding to ω_{pq} as Ω_{pq} . Then Equation 3.45 becomes:

$$\begin{pmatrix} \dot{\alpha}_1 \\ \dot{\alpha}_2 \\ \dot{\alpha}_3 \\ \dot{\alpha}_4 \end{pmatrix} = \frac{i}{2} \begin{pmatrix} 0 & 0 & \Omega_{13} & \Omega_{14} \\ 0 & 0 & \Omega_{23} & \Omega_{24} \\ \Omega_{13} & \Omega_{23} & 0 & 0 \\ \Omega_{14} & \Omega_{24} & 0 & 0 \end{pmatrix} \begin{pmatrix} \alpha_1 \\ \alpha_2 \\ \alpha_3 \\ \alpha_4 \end{pmatrix} \quad (3.47)$$

where we omit the “ $'$ ” on the coefficients for convenience. State $|\psi\rangle$ at any time can be obtained by solving Equation 3.47 and substituting α_i into Equation 3.44. We focus on the populations of eigenstates here, thus the local phases of the final state can be ignored, and so is Equation 3.44.

The physical meanings of Equation 3.47 can be understood through the relation between the Hamiltonian and the energy level structure and transitions of the system, as illustrated in Figure 3.5, in which Ω_{ij} are Rabi frequencies between energy levels.

According to the relation between the coefficients α_i and eigenstates defined in Equation 3.41, and considering the subscripts, we know that Ω_{14} and Ω_{23} are Rabi frequencies coupling the two states $|00\rangle$, $|10\rangle$ and $|01\rangle$, $|11\rangle$, respectively, and similarly Ω_{13} and

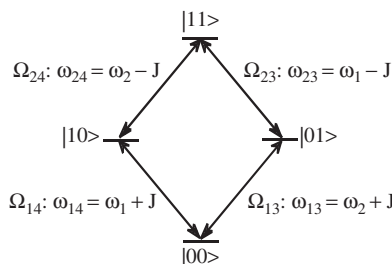


Figure 3.5 Energy-level structure and transitions of a two-qubit system

Ω_{24} are Rabi frequencies coupling the two states $|00\rangle, |01\rangle$ and $|10\rangle, |11\rangle$, respectively. In other words, the element of the Hamiltonian on position (i,j) denoted Ω_{ij} is the Rabi frequency between states i and j , and the number of transitions equals to the non-zero elements of H . For example, H_{14} and H_{23} (include their transpose position) associate with four different transitions:

$$|00\rangle \leftrightarrow |10\rangle, |01\rangle \leftrightarrow |11\rangle \quad (3.48)$$

Based on the relationship between the energy level structure and transitions of the system, we can write out directly the Hamiltonian according to a given Hamiltonian H : find all the transitions allowed that couple two energy levels p and q , and then fill the matrix on (p,q) and its transpose position with Ω_{pq} , then multiply a constant coefficient $-\hbar/2$ to get the Hamiltonian of the system. Note that the coefficients of the states have a transformation similar to Equation 3.44.

3.2.3 Design of the Control Sequence of Pulses

In the adiabatic passage approach, the state of the system will be a time-dependent eigenstate of the Hamiltonian at any time, that is, if:

$$|\psi(0)\rangle = \sum_j c_j |\phi_j(0)\rangle \quad (3.49)$$

then:

$$|\psi(t)\rangle = \sum_j c_j e^{i\beta_j(t)} |\phi_j(t)\rangle \quad (3.50)$$

where $|\phi_j(t)\rangle$ is the eigenstates of the Hamiltonian at time t and $\beta_j(t)$ is the Berry adiabatic phase. We can therefore get the populations of the system eigenstates at time t if we can ascertain c_i and the eigenstates $|\phi_j(t)\rangle$ of the Hamiltonian of the system at time t .

The analysis is quite difficult because we need to know the general forms of the system Hamiltonian eigenstates. As the dimension of the system increases, it will be very difficult to design the control pulses using Equation 3.50. In order to overcome this difficulty, we need to start from the physical meanings of the system model, analyze the population distribution of the target state, and ascertain the path of population transfer, thus control pulses can be designed by making use of an intuitive and half counterintuitive sequence. Some parameters should be fixed during the simulation. Control pulses can be designed for a multi-qubit system without solving the eigenstates of the Hamiltonian. This process will be illustrated with a three-qubits system.

The energy level structure and transitions of a three-qubits system are shown in Figure 3.6, which is only a rough diagram because the energy levels of states $|001\rangle, |010\rangle, |100\rangle$ and $|011\rangle, |110\rangle, |101\rangle$ may not be degenerate. Ω_{ij} is the Rabi frequency between two energy levels $|i\rangle$ and $|j\rangle$.

The state of the system at any time t can be denoted as follows:

$$\begin{aligned} |\psi(t)\rangle &= \alpha_1 |000\rangle + \alpha_2 |111\rangle + \alpha_3 |001\rangle + \alpha_4 |010\rangle + \alpha_5 |011\rangle \\ &\quad + \alpha_6 |100\rangle + \alpha_7 |101\rangle + \alpha_8 |110\rangle \end{aligned} \quad (3.51)$$

where α_i values are the complex coefficients of eigenstates.

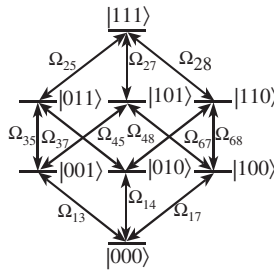


Figure 3.6 Energy-level structure and transitions of a three-qubit system

The model of a three-qubit system is as follows:

$$\dot{\alpha} = \frac{i}{2} \begin{bmatrix} \dot{\alpha}_1 \\ \dot{\alpha}_2 \\ \dot{\alpha}_3 \\ \dot{\alpha}_4 \\ \dot{\alpha}_5 \\ \dot{\alpha}_6 \\ \dot{\alpha}_7 \\ \dot{\alpha}_8 \end{bmatrix} = \begin{bmatrix} 0 & 0 & \Omega_{13} & \Omega_{14} & 0 & \Omega_{16} & 0 & 0 \\ 0 & 0 & 0 & 0 & \Omega_{25} & 0 & \Omega_{27} & \Omega_{28} \\ \Omega_{13} & 0 & 0 & 0 & \Omega_{35} & 0 & \Omega_{37} & 0 \\ \Omega_{14} & 0 & 0 & 0 & \Omega_{45} & 0 & 0 & \Omega_{48} \\ 0 & \Omega_{25} & \Omega_{35} & \Omega_{45} & 0 & 0 & 0 & 0 \\ \Omega_{16} & 0 & 0 & 0 & 0 & 0 & \Omega_{67} & \Omega_{68} \\ 0 & \Omega_{27} & \Omega_{37} & 0 & 0 & \Omega_{67} & 0 & 0 \\ 0 & \Omega_{28} & 0 & \Omega_{48} & 0 & \Omega_{68} & 0 & 0 \end{bmatrix} \begin{bmatrix} \alpha_1 \\ \alpha_2 \\ \alpha_3 \\ \alpha_4 \\ \alpha_5 \\ \alpha_6 \\ \alpha_7 \\ \alpha_8 \end{bmatrix} \quad (3.52)$$

We assume that $\Omega_{13} = \Omega_{14} = \Omega_{16} = \Omega_p$, $\Omega_{25} = \Omega_{27} = \Omega_{28} = \Omega_s$, and $\Omega_{35} = \Omega_{37} = \Omega_{45} = \Omega_{48} = \Omega_{67} = \Omega_{68} = \Omega_m$ for convenience, and call the initial state $|000\rangle$ the first grade, the states $|001\rangle, |010\rangle, |100\rangle$ the second, the states $|011\rangle, |110\rangle, |101\rangle$ the third, and the excited state $|111\rangle$ the fourth. We can see from Figure 3.6 that the second grade denotes the situation of one different qubit from the initial state, the third denotes the situation of two, and the fourth denotes the situation of three. Ω_p, Ω_m and Ω_s are the Rabi frequencies associated with population transfer between grades 1 and 2, grades 2 and 3, and grades 3 and 4, respectively. For an n -qubit system, there will be $n+1$ grades and n pulses. Our goal is to prepare the entangled state $|000\rangle + e^{i\phi}|111\rangle$, namely a half population transfer from grade 1 to grade 4.

There are two methods of doing this. First, the pulses Ω_p, Ω_m and Ω_s act on the system in turn. Ω_p applies a half population transfer from grade 1 to grade 2, then Ω_m and Ω_s make a complete population transfer from grade 2 to grade 3, and from grade 3 to grade 4, respectively. This is called an intuitive sequence. The second method applies a half counterintuitive of Ω_p and Ω_m first, that is, Ω_m precedes Ω_p and they turn off simultaneously, which makes a half population transfer from grade 1 to grade 3, and then a complete population transfer from grade 3 to grade 4 is made by Ω_s .

3.2.4 Simulation Experiments of Population Transfer

1) Entanglement preparation using intuitive and half intuitive sequences

the simulation on a three-qubit system is made based on the control pulses proposed for entanglement preparation. In simulation, time is cut into small pieces, each of length Δt . The Hamiltonian can be regarded as a constant in this small period, in other words the pulses

$\Omega_p, \Omega_m, \Omega_s$ remain fixed. According to Equation 3.52:

$$\alpha(t + \Delta t) = \exp \left\{ \frac{i}{2} \begin{bmatrix} 0 & 0 & \Omega_p(t) & \Omega_p(t) & 0 & \Omega_p(t) & 0 & 0 \\ 0 & 0 & 0 & 0 & \Omega_s(t) & 0 & \Omega_s(t) & \Omega_s(t) \\ \Omega_p(t) & 0 & 0 & 0 & \Omega_m(t) & 0 & \Omega_m(t) & 0 \\ \Omega_p(t) & 0 & 0 & 0 & \Omega_m(t) & 0 & 0 & \Omega_m(t) \\ 0 & \Omega_s(t) & \Omega_m(t) & \Omega_m(t) & 0 & 0 & 0 & 0 \\ \Omega_p(t) & 0 & 0 & 0 & 0 & 0 & \Omega_m(t) & \Omega_m(t) \\ 0 & \Omega_s(t) & \Omega_m(t) & 0 & 0 & \Omega_m(t) & 0 & 0 \\ 0 & \Omega_s(t) & 0 & \Omega_m(t) & 0 & \Omega_m(t) & 0 & 0 \end{bmatrix} \cdot \Delta t \alpha(t) \right\} \quad (3.53)$$

$$\alpha(0) = [1 \ 0 \ 0 \ 0 \ 0 \ 0 \ 0 \ 0]^T \quad (3.54)$$

The state of the system at any time t can be obtained by applying Equation 3.53 iteratively with the initial Equation 3.54, which is equivalent to $|\psi(0)\rangle = |000\rangle$, and can be easily obtained by projective measurement.

We have chosen pulses with $\sin^2 t$ and $\cos^2 t$ shapes at the beginning and the end, respectively. Some parameters, such as the intensities of the pulses, are adjusted during the simulation. Figure 3.7a shows the intuitive sequence of pulses Ω_p, Ω_m and Ω_s ; the peak values are 1.21, 2.05, and 2.35, respectively. Figure 3.7b is the population evolution during the action of the pulse sequence.

It is shown in Figure 3.7b that at the time $t = 2$, when Ω_p finishes, the population of grade 1 which includes the eigenstate $|000\rangle$ is 0.5, and the eigenstates $|001\rangle, |010\rangle$, and $|100\rangle$ have an average population of 1/6, namely the population of grade 2 is 0.5. At time $t = 4$, when Ω_m finishes, the population of grade 2 is transferred to the eigenstates $|011\rangle, |110\rangle$, and $|101\rangle$ on average and the population of grade 3 is 0.5. The effect of Ω_s is a complete population transfer from grade 3 to grade 4, namely eigenstate $|111\rangle$. The sequence gives an average population distribution for the states $|000\rangle$ and $|111\rangle$. It can be seen from the simulations that the state of system finally is $(|000\rangle - i|111\rangle)/\sqrt{2}$.

It is also shown in Figure 3.7b that the populations of eigenstates remain fixed during the times 1.5–2.5 and 3.5–4.5, thus the pulses Ω_m and Ω_s can be pre-acted at times $t = 1$ and

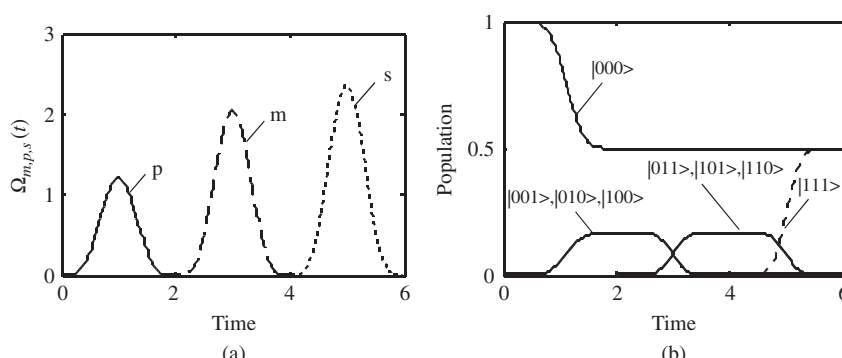


Figure 3.7 Simulation results of an intuitive sequence of control: (a) intuitive pulse sequence and (b) population dynamical evolution

$t = 2$, respectively. Figure 3.8a shows the advanced pulse sequence and Figure 3.8b shows the population dynamics, from which we can see that the target state is prepared at time $t = 3.5$.

The relation between the time area of the pulse and the effect is also studied during the simulations and the results are shown in Figure 3.9a,b. The peak values of Ω_p , Ω_m , and Ω_s in Figure 3.9a are 1.21, 1.21, and 2.35, respectively. The temporal pulse area of Ω_m in Figure 3.9a is equal to that in Figure 3.8a, approximately.

According to Equation 3.35 the angle θ is the direct ratio of temporal pulse area a and the final states of the two situation are the same, which is verified in the simulation; the only difference is that the process time of population transfer in Figure 3.9b is 0.5 slower than for the process in Figure 3.8b.

2) Entanglement preparation using a half counterintuitive sequence

The entanglement state is prepared by using the half counterintuitive pulse sequence in this simulation. The pulses are shown in Figure 3.10a, in which Ω_m works first, then Ω_p works at

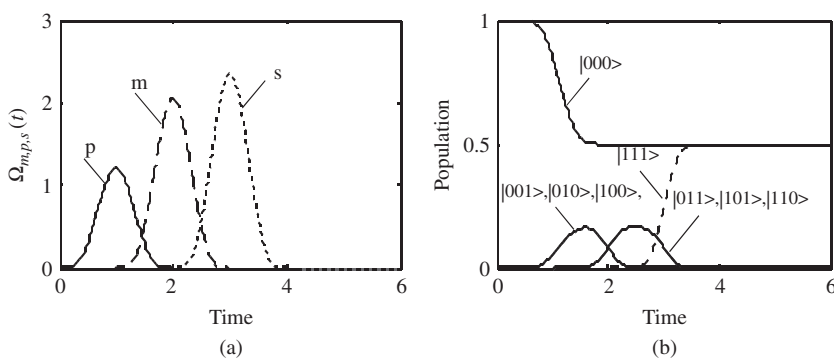


Figure 3.8 Half intuitive pulse sequence of control: (a) advanced pulse sequence and (b) population dynamical evolution

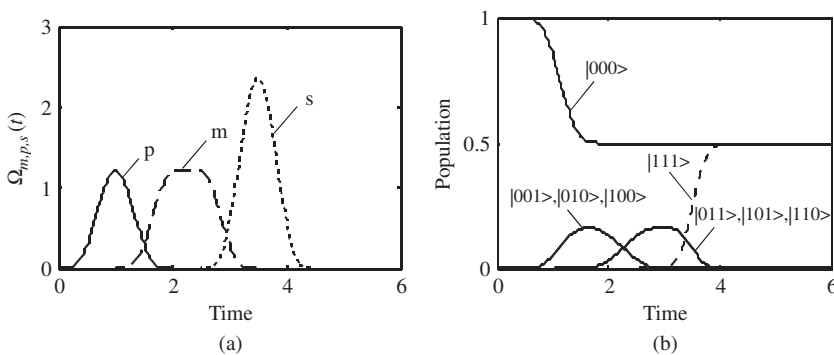


Figure 3.9 Half intuitive pulse sequence of control: (a) half intuitive pulse sequence and (b) population dynamical evolution

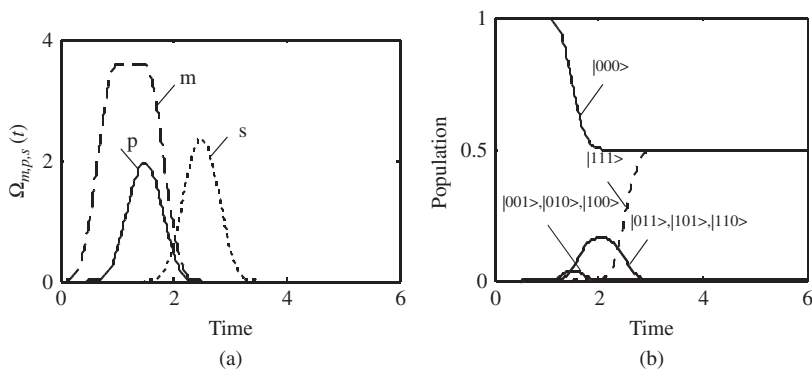


Figure 3.10 Half counterintuitive pulse sequence of control: (a) half counterintuitive pulse sequence and (b) population dynamical evolution

time $t=1$, and Ω_s is last; the peak values are 3.58, 1.94, and 2.35, respectively. Figure 3.10b shows the population dynamics of eigenstates of the system and it can be seen that peak values of the populations of states $|001\rangle$, $|010\rangle$, and $|100\rangle$ are a quarter of the ones obtained using the intuitive and half intuitive sequence. In addition, the whole process time is 0.5 a.u. faster than that shown in Figure 3.8b.

From the simulation experiments, one can see that the pulses designed based on physical meanings can control the process effectively and prepare the entanglement $(|000\rangle - i|111\rangle)/\sqrt{2}$ successfully. The experiment results demonstrate the effectiveness of pulses methods. Although it is only illustrated by a three-qubit system, the method is easily extended to the higher dimension system. For example, the energy level structure and transitions of a four-qubit system according to the Ising interaction model are shown in Figure 3.11.

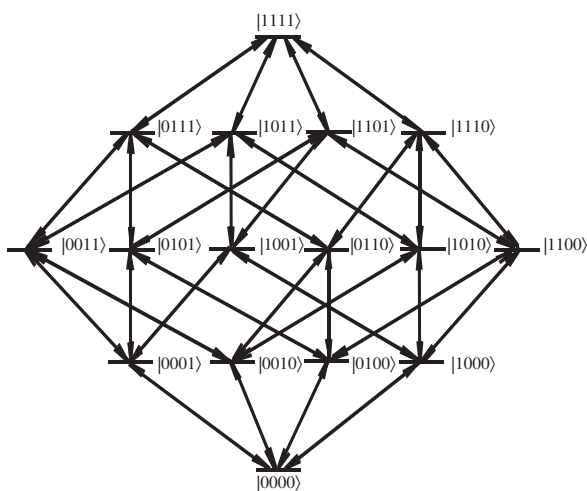


Figure 3.11 Energy-level structure and transitions of a four-qubit system

The system state at time t can be written as:

$$\begin{aligned}
 |\psi\rangle = & \alpha_1|0000\rangle + \alpha_2|1111\rangle + \alpha_3|0001\rangle + \alpha_4|0010\rangle \\
 & + \alpha_5|0011\rangle + \alpha_6|0100\rangle + \alpha_7|0101\rangle + \alpha_8|0110\rangle \\
 & + \alpha_9|0111\rangle + \alpha_{10}|1000\rangle + \alpha_{11}|1001\rangle + \alpha_{12}|1010\rangle \\
 & + \alpha_{13}|1011\rangle + \alpha_{14}|1100\rangle + \alpha_{15}|1101\rangle + \alpha_{16}|1110\rangle
 \end{aligned} \quad (3.55)$$

We can write out the Hamiltonian of the system directly according to the method proposed in this section as:

$$H = -\frac{\hbar}{2} \begin{pmatrix} 0 & 0 & \Omega_{1,3} & \Omega_{1,4} & 0 & \Omega_{1,6} & 0 & 0 & 0 & \Omega_{1,10} & 0 & 0 & 0 & 0 & 0 & 0 \\ 0 & 0 & 0 & 0 & 0 & 0 & 0 & 0 & \Omega_{2,9} & 0 & 0 & 0 & 0 & \Omega_{2,13} & 0 & \Omega_{2,15} & \Omega_{2,16} \\ \Omega_{1,3} & 0 & 0 & 0 & \Omega_{3,5} & 0 & \Omega_{3,7} & 0 & 0 & 0 & \Omega_{3,11} & 0 & 0 & 0 & 0 & 0 & 0 \\ \Omega_{1,4} & 0 & 0 & 0 & 0 & \Omega_{4,5} & 0 & 0 & \Omega_{4,8} & 0 & 0 & 0 & \Omega_{4,12} & 0 & 0 & 0 & 0 \\ 0 & 0 & \Omega_{3,5} & \Omega_{4,5} & 0 & 0 & 0 & 0 & 0 & \Omega_{5,9} & 0 & 0 & 0 & \Omega_{5,13} & 0 & 0 & 0 \\ \Omega_{1,6} & 0 & 0 & 0 & 0 & 0 & \Omega_{6,7} & \Omega_{6,8} & 0 & 0 & 0 & 0 & 0 & 0 & \Omega_{6,14} & 0 & 0 \\ 0 & 0 & \Omega_{3,7} & 0 & 0 & 0 & 0 & 0 & 0 & \Omega_{7,9} & 0 & 0 & 0 & 0 & 0 & 0 & \Omega_{7,15} & 0 \\ 0 & 0 & 0 & \Omega_{4,8} & 0 & \Omega_{6,8} & 0 & 0 & \Omega_{8,9} & 0 & 0 & 0 & 0 & 0 & 0 & 0 & \Omega_{8,16} \\ 0 & \Omega_{2,9} & 0 & 0 & \Omega_{5,9} & 0 & \Omega_{7,9} & \Omega_{8,9} & 0 & 0 & 0 & 0 & 0 & 0 & 0 & 0 & 0 \\ \Omega_{1,10} & 0 & 0 & 0 & 0 & 0 & 0 & 0 & 0 & 0 & \Omega_{10,11} & \Omega_{10,12} & 0 & \Omega_{10,14} & 0 & 0 & 0 \\ 0 & 0 & \Omega_{3,11} & 0 & 0 & 0 & 0 & 0 & 0 & \Omega_{10,11} & 0 & 0 & \Omega_{11,13} & 0 & 0 & \Omega_{11,15} & 0 \\ 0 & 0 & 0 & \Omega_{4,12} & 0 & 0 & 0 & 0 & 0 & \Omega_{10,12} & 0 & 0 & \Omega_{12,13} & 0 & 0 & 0 & \Omega_{12,16} \\ 0 & \Omega_{2,13} & 0 & 0 & \Omega_{5,13} & 0 & 0 & 0 & 0 & 0 & \Omega_{11,13} & \Omega_{12,13} & 0 & 0 & 0 & 0 & 0 \\ 0 & 0 & 0 & 0 & \Omega_{6,14} & 0 & 0 & 0 & \Omega_{10,14} & 0 & 0 & 0 & 0 & 0 & \Omega_{14,15} & \Omega_{14,16} \\ 0 & \Omega_{2,15} & 0 & 0 & 0 & \Omega_{7,15} & 0 & 0 & 0 & \Omega_{11,15} & 0 & 0 & \Omega_{14,15} & 0 & 0 & 0 & 0 \\ 0 & \Omega_{2,16} & 0 & 0 & 0 & 0 & \Omega_{8,16} & 0 & 0 & 0 & \Omega_{12,16} & 0 & \Omega_{14,16} & 0 & 0 & 0 & 0 \end{pmatrix} \quad (3.56)$$

The subsequent calculations are similar to the three-qubit situation and will not be repeated here.

The control pulses can be designed by utilizing intuitive and half counterintuitive sequences. Because of the intuitiveness of the designing method, complex deduction can be avoided. By analyzing the population distribution of the target state, the path of population transfer can be determined.

3.3 Comparison of Time Optimal Control for Two-Level Quantum Systems

Two-level quantum systems are the simplest quantum systems with important applications (Allen and Eberly, 1975; Tannoudji, Diu, and Laloe, 1977) in which the state transfer is of primary importance. Some researchers have studied the state transfer problem by using external controls (Boscain and Charlot, 2004; Boscain, Chambrion, and Gauthier, 2002; Boscain *et al.*, 2002, 2003; Brockett, 2001; D'Alessandro and Dahleh, 2001; Raginsky, 2003; Khaneja, Glaser, and Brockett, 2002). The time of quantum operation is in the nanosecond range. It is essential to achieve the transfer of quantum states in the shortest possible time for many applications. In general, for a given control objective, the amplitude of control is inversely proportional to the control time. If one only needs to achieve the state transfer as soon as possible, the amplitude of control should be very large, but in practice it is not possible for the amplitude of control to be infinite.

The geometric control theory and optimal control have been used in the state transfer of quantum systems recently (D'Alessandro and Dahleh, 2001; Khaneja, Brockett, and Glaser, 2001; Altafin, 2002; Daleh, Peirce, and Rabitz, 1988; Ramakrishna *et al.*, 2000; Boscain and Piccoli, 2004). For a two-level quantum system, the trajectories of state transfer from the north pole to the south pole on the Bloch sphere can be displayed explicitly. Boscain and Mason studied the time optimal transfer of state with bounded bang-bang control (Boscain and Mason, 2005). We also studied the state transfer problem for two-level systems using the geometric control in the x - y plane (Lou and Cong, 2011). Although the two control strategies are for the same state transfer problem, their design principles are quite different, which leads to different characteristics, so the purpose of this section is to compare the time characteristics of steering the state from the north pole to the south pole on the Bloch sphere by means of the control strategies proposed by Boscain and Mason (2005) with bounded control.

3.3.1 Description of System Model

A n -level closed quantum system can be described by the following time-dependent Schrodinger equation (the Planck constant is assumed to be $\hbar = 1$) (Boscain and Mason, 2006):

$$i\frac{d|\psi(t)\rangle}{dt} = \left(H_0 + \sum_{j=1}^m u_j(t) H_j \right) |\psi(t)\rangle \quad (3.57)$$

where, $|\psi(t)\rangle$ is a wave function that takes values on the state-space S^{2n-1} . $H_0 = \text{diag}(E_1, \dots, E_n)$ is a Hermitian matrix known as a free Hamiltonian in which E_1, \dots, E_n are real numbers representing the energy levels. It can be assumed that $\sum_{j=1}^n E_j = 0$ without loss of generality. u_1, \dots, u_m are real values representing the external controls. H_j ($j = 1, \dots, m$) values are Hermitian matrices describing the coupling between the controls and the system. The Hamiltonian $H(t) = H_0 + \sum_{j=1}^m u_j(t) H_j$ is the total Hamiltonian.

For the transfer of two fixed states in the state-space, it is necessary to consider the controllability problem first, that is, whether it is possible to steer the system from one state to another one for each pair of states. The evolution operator $U(t)$ of the system (Equation 3.57) satisfies the following equation:

$$i\frac{dU(t)}{dt} = \left(H_0 + \sum_{j=1}^m u_j(t) H_j \right) U(t) \quad (3.58)$$

On the compact Lie group $su(n)$, Equation 3.58 is a right invariant control system and satisfies

$$\text{Lie}\{iH_0, iH_1, \dots, iH_m\} = su(n) \quad (3.59)$$

which is a necessary and sufficient condition for the system in Equation 3.58 to be controllable (Boothby and Wilson, 1979). If a right invariant system is controllable, then the bilinear system is controllable (Sachkov, 1997). Thus if Equation 3.58 is controllable, then Equation 3.57 is also controllable. It is therefore possible to design controls to steer the system in Equation 3.57 from one state to another one in the state-space.

Here, we study the simplest system model of Equation 3.57, which describe a two-level quantum system, that is, set $n = 2$. The dynamics equation then becomes

$$i \frac{d|\psi(t)\rangle}{dt} = H(t)|\psi(t)\rangle \quad (3.60)$$

where $|\psi(t)\rangle = (\phi_1(t), \phi_2(t))^T$ and the squares of absolute values of $\phi_1(t)$ and $\phi_2(t)$ denote the probabilities of the eigenstates $|0\rangle$ and $|1\rangle$ under measurements, respectively, which satisfy the probability completeness

$$\sum_{j=1}^2 |\phi_j(t)|^2 = 1 \quad (3.61)$$

The total Hamiltonian $H(t)$ in Equation 3.60 is

$$H(t) = H_0 + H_c(t) \quad (3.62)$$

where $H_0 = \text{diag}(-E, E)$ is the free Hamiltonian in which $E > 0$ and H_c is the control Hamiltonian. Because the external controls in geometric and bang-bang control are different, H_c is different and the specific forms are given in Sections 3.3.2 and 3.3.3, respectively.

3.3.2 Geometric Control

The geometric control in the $x-y$ plane can be decomposed as

$$\begin{cases} \Omega_x(t) = M \cos(2Et + \varphi) \\ \Omega_y(t) = -M \sin(2Et + \varphi) \end{cases} \quad (3.63)$$

where M and $\varphi \in [0, 2\pi)$ are the amplitude and the initial phase of the controls, respectively. The control Hamiltonian $H_c(t)$ in Equation 3.62 is

$$H_c(t) = u_x(t)\sigma_x + u_y(t)\sigma_y \quad (3.64)$$

where σ_x and σ_y are the Pauli matrices.

According to Equation 3.62, the total Hamiltonian $H(t)$ is

$$H(t) = H_0 + u_x(t)\sigma_x + u_y(t)\sigma_y = \begin{pmatrix} -E & Me^{i(2Et+\varphi)} \\ Me^{-i(2Et+\varphi)} & E \end{pmatrix} \quad (3.65)$$

Placing Equation 3.65 into Equation 3.60 and rewriting it gives

$$i \frac{d|\psi(t)\rangle}{dt} = (H_0 + u_x(t)\sigma_x + u_y(t)\sigma_y)|\psi(t)\rangle \quad (3.66)$$

Comparing Equations 3.66 with Equation 3.57, one can see that $H_1 = \sigma_x$ and $H_2 = \sigma_y$. H_0 , H_1 , and H_2 satisfy the controllability (Equation 3.59), so the system in Equation 3.66 is controllable.

The state evolution operator $U(t)$ can be deduced from the Schrodinger equation (Equation 3.66):

$$U(t) = \begin{pmatrix} e^{iEt} & 0 \\ 0 & e^{-i(Et+\varphi)} \end{pmatrix} \begin{pmatrix} \cos(Mt) & i \sin(Mt) \\ i \sin(Mt) & \cos(Mt) \end{pmatrix} \begin{pmatrix} 1 & 0 \\ 0 & e^{i\varphi} \end{pmatrix} \quad (3.67)$$

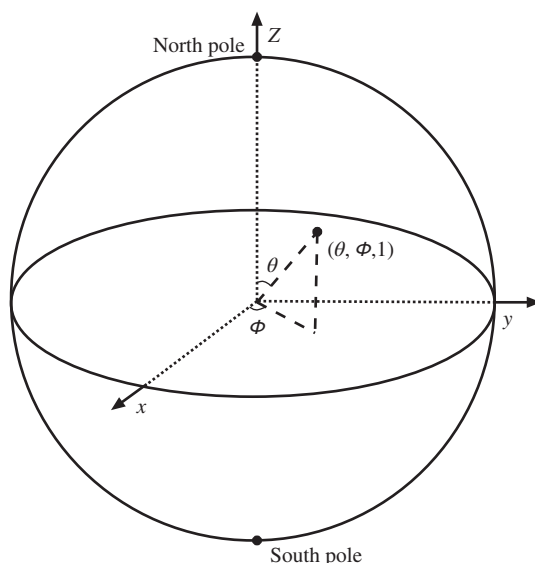


Figure 3.12 Description of a state on the Bloch sphere

From the right side of Equation 3.67 one can see that the state evolution operator $U(t)$ is composed of three matrices. The behaviors on the Bloch sphere that are shown by the three matrices are as follows: the first matrix is to make the state on the Bloch sphere rotate by $2Et + \varphi$ around the z -axis; the third matrix is to make the state rotate by φ around the z -axis and add a global phase factor to the state; the second matrix is to make the state rotate by $2Mt$ around the x -axis. The description of a state on the Bloch sphere is shown in Figure 3.12, which explains the meanings of θ and ϕ .

In the light of Equation 3.67, for two known points $a : (\theta_1, \varphi_1, 1)$ and $d : (\theta_2, \varphi_2, 1)$ on the Bloch sphere, the minimum time from a to d under geometric control is

$$t_{\min} = \frac{\Delta\theta}{2u_{\max}} \quad (3.68)$$

where $\Delta\theta = |\theta_1 - \theta_2|$ and u_{\max} is the maximum amplitude of the controls.

According to Equation 3.68, the minimum time t_{\min} relies on the different angle $\Delta\theta$ between the initial point and the target point on the Bloch sphere, and the maximum amplitude of bounded control u_{\max} . The parameter φ in Equation 3.63 can be determined by

$$\varphi = \begin{cases} \frac{3\pi}{2} - \phi_1, & \theta_1 > \theta_2 \\ \frac{\pi}{2} - \phi_1, & \theta_1 \leq \theta_2 \end{cases} \quad (3.69)$$

From Equations 3.67 and 3.69, one can get the procedure of the geometric control: based on the coordinates of the initial and target states, one can determine the parameters φ of the controls first, and then the controls in Equation 3.63 can be determined. Because the control task here is to steer the state from the north pole $(0, \phi_N, 1)$ to the south pole $(\pi, \phi_S, 1)$ on the Bloch sphere, namely to steer the state to rotate by π around the x -axis, while the angle

around the z -axis is not restrictive, the minimum time t_{\min} only relates to the second matrix in Equation 3.67. Because $\Delta\theta = |0 - \pi| = \pi$ and $u_{\max} = M$, the minimum time from the north pole to the south pole under the geometric control becomes

$$t_{\min} = \frac{\pi}{2M} \quad (3.70)$$

3.3.3 Bang-Bang Control

1) Control system model

When using bang-bang control, the control Hamiltonian $H_c(t)$ in Equation 3.62 becomes

$$H_c(t) = \begin{pmatrix} 0 & u(t) \\ u(t) & 0 \end{pmatrix} = u(t)\sigma_x \quad (3.71)$$

in which $u(t)$ is control along the x -axis and has the following form

$$\underbrace{u_{s_i}u_s \dots u_s}_{n-1} \underbrace{u_s u_{s_f}}_{n-1} \quad (3.72)$$

where s_i , s_f , and s are the times of the first bang control u_{s_i} , the last bang control u_{s_f} , and the interior bang control u_s , respectively. $n - 1$ is the number of the interior bang control. u_s represents a bang control defined on a time interval of length s .

According to Equation 3.62, the total Hamiltonian $H(t)$ is

$$H(t) = H_0 + u(t)\sigma_x = \begin{pmatrix} -E & u(t) \\ u(t) & E \end{pmatrix} \quad (3.73)$$

Placing Equation 3.73 into Equation 3.60 and rewriting gives

$$i\frac{d|\psi(t)\rangle}{dt} = (H_0 + u(t)\sigma_x)|\psi(t)\rangle \quad (3.74)$$

Comparing Equation 3.74 with Equation 3.57, one can show that $H_1 = \sigma_x \cdot H_0$ and H_1 satisfy the controllability (Equation 3.59), so the system in Equation 3.74 is controllable.

2) State transfer from north pole to south pole

The procedure of bang-bang control is as follows: for the initial state and target state, one needs to determine a set of parameters (s_i, n, s_f) first, and then the control in Equation 3.72 can be determined. There is no fixed method to determine the parameters (s_i, n, s_f) . For a same pair of states, there may be different parameters, so appropriate parameters have to be chosen so that the control time is minimized. For the same reason, a situation in which the parameters are different but the control time is the same can occur. For the situation from the north pole to the south pole there is a fixed method to determine parameters, which will be described in this subsection. When the relationship between M and E is different, the determinations of parameters are also different. In this subsection we will describe the method of determining parameters in the $M \geq E$ case and the $M < E$ case.

1. The $M \geq E$ case

In the $M \geq E$ case, the time optimal control of the system (Equation 3.74) is bang-bang control with $n = 1$ and $s_i = S_A$ or S_B , where

$$S_A = \pi - \arccos(\cot^2(\alpha)) \quad (3.75)$$

$$S_B = \pi + \arccos(\cot^2(\alpha)) \quad (3.76)$$

where $\alpha \in (0, \frac{\pi}{2})$ and

$$\alpha = \arctan\left(\frac{M}{E}\right) \quad (3.77)$$

The first bang control u_{s_i} can take $-M$ or $+M$, thus there are four time optimal controls:

$$u_1(t) = \begin{cases} M, & t \in [0, S_A] \\ -M, & t \in (S_A, T] \end{cases}, u_2(t) = \begin{cases} M, & t \in [0, S_B] \\ -M, & t \in (S_B, T] \end{cases} \quad (3.78)$$

$$u_1(t) = \begin{cases} -M, & t \in [0, S_A] \\ M, & t \in (S_A, T] \end{cases}, u_2(t) = \begin{cases} -M, & t \in [0, S_B] \\ M, & t \in (S_B, T] \end{cases} \quad (3.79)$$

in which T is the time from the north pole to the south pole under bang-bang control, namely the minimum time T_{BB1} is (Boscain and Mason, 2005)

$$T_{BB1} = T = \frac{\pi}{\sqrt{M^2 + E^2}} \quad (3.80)$$

2. The $M < E$ case

In the $M < E$ case, the time optimal control of the system (Equation 3.74) from the north pole to the south pole takes the following form (Agrachev and Gamkrelidze, 1990; Boscain and Chitour, 2005):

$$\underbrace{u_{s_i} u_{v(s_i)} \cdots u_{v(s_i)} u_{s_f}}_{n-1} \quad (3.81)$$

where $s_i \in [0, \pi]$ and $s_f \in [0, v(s_i)]$ for the time of the first bang control u_{s_i} and the last bang control u_{s_f} , respectively. The time $v(s_i)$ of the interior bang control $u_{v(s_i)}$ is decided by s_i , which is given by Boscain and Chitour (2005) as

$$v(s_i) = \pi + 2 \arctan\left(\frac{\sin(s_i)}{\cos(s_i) + \cot^2(\alpha)}\right) \quad (3.82)$$

In order to obtain the bang-bang control in Equation 3.81, the parameters (s_i, n, s_f) , s_i , and s_f need to satisfy (Boscain and Mason, 2005)

$$v(s_i) = v(s_f), s_i \in [0, \pi], s_f \in [0, v(s_i)] \quad (3.83)$$

Because $v(\cdot)$ is not a monotonic function, as shown in Figure 3.13 (for $M = 2$, $E = 2.5$), there are two solutions of s_f which satisfy Equation 3.83 for a fixed s_i : (i) $s_f = s'$, called Type-1, and (ii) $s_f = s_i$, called Type-2.

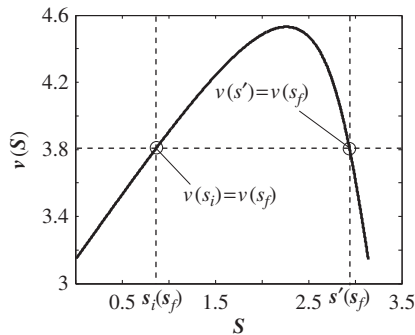


Figure 3.13 Values of $v(s)$ with $M = 2$ and $E = 2.5$

In the case of Type-1 with fixed α , the value of n in bang-bang control is

$$n(s) = \frac{2\pi}{\theta(s)} \quad (3.84)$$

where $\theta(s) = 2 \arccos \left(\sin^2 \left(\frac{v(s)}{2} \right) \cos(2\alpha) - \cos^2 \left(\frac{v(s)}{2} \right) \right)$

s_i takes the value when $n(s)$ is positive integer and s_f can be obtained from Equation 3.83. The candidate time optimal controls are

$$\underbrace{u_{s_i} u_{v(s_i)} \cdots u_{v(s_i)} u_{s_f}}_{n(s_i)-1} \quad (3.85)$$

$$\underbrace{u_{s_f} u_{v(s_i)} \cdots u_{v(s_i)} u_{s_i}}_{n(s_i)-1} \quad (3.86)$$

In the case of Type-2 with fixed α , the value of n in bang-bang control is

$$n(s) = \frac{2\beta(s)}{\theta(s)} + 1 \quad (3.87)$$

where $\beta(s) = 2 \arccos(\sin(\alpha) \cos(\alpha)(1 - \cos(s)))$.

There are two solutions s_1 and s_2 that make $n(s)$ a positive integer. s_i and s_f are the same, and equal to s_1 or s_2 . The candidate time optimal control is

$$\underbrace{u_{s_1} u_{v(s_1)} \cdots u_{v(s_1)} u_{s_1}}_{n(s_1)-1} (s_i = s_f = s_1) \quad (3.88)$$

or

$$\underbrace{u_{s_2} u_{v(s_2)} \cdots u_{v(s_2)} u_{s_2}}_{n(s_2)-1} (s_i = s_f = s_2) \quad (3.89)$$

For Type-1 and Type-2 notice that the first bang control can be M or $-M$, and there are a total of eight candidate time optimal controls in the $M < E$ case. The time T_{BB2} from the north

pole to the south pole under bang-bang control satisfies

$$T_{BB2} = s_i + (n(s_i) - 1)v(s_i) + s_f \quad (3.90)$$

$$T_{\min} < T_{BB2} < T_{\max} \quad (3.91)$$

where

$$T_{\min} = \frac{1}{2\sqrt{M^2 + E^2}} \left(\frac{\pi^2}{2\alpha} - 2\pi \right), T_{\max} = \frac{1}{2\sqrt{M^2 + E^2}} \left(\frac{\pi^2}{2\alpha} + \pi \right)$$

In other words, the minimum time T_{BB2} for steering the state from the north pole to the south pole under bang-bang control is no shorter than T_{\min} and no longer than T_{\max} .

3.3.4 Time Comparisons of Two Control Strategies

1. The $M \geq E$ case

In the case of $M \geq E$, the minimum times for steering the state from the north pole to the south pole under the geometric control and bang-bang control are shown in Equations 3.70 and 3.80, respectively,

$$t_{\min} = \frac{\pi}{2M}, T_{BB1} = \frac{\pi}{\sqrt{M^2 + E^2}} \quad (3.92)$$

Comparing times t_{\min} and T_{BB1} in Equation 3.92, gives $2M > \sqrt{M^2 + E^2}$ for $M \geq E$. The numerators are the same and equal to π , so the result is

$$t_{\min} < T_{BB1} \quad (3.93)$$

which indicates that the minimum time for steering the state from the north pole to the south pole under bang-bang control is longer than that under the geometric control, namely the geometric control is better in the $M \geq E$ case.

2. The $M < E$ case

In the $M < E$ case, the minimum times for steering the state from the north pole to the south pole under geometric control and bang-bang control are shown in Equations 3.70 and 3.91, respectively,

$$t_{\min} = \frac{\pi}{2M}, T_{\min} < T_{BB2} < T_{\max} \quad (3.94)$$

In this case, the minimum time under bang-bang control is only obtained as an interval, not as a determined value, so it is different from the $M \geq E$ case, where the minimum times can be compared directly. According to the relationship between t_{\min} and T_{\min} , there are three cases for T_{\max} which are the boundaries of the minimum time interval,:
 1. $t_{\min} > T_{\max}$

If $t_{\min} > T_{\max}$ holds, namely $\frac{\pi}{2M} > \frac{\pi^2/2\alpha+\pi}{2\sqrt{M^2+E^2}}$, the following condition needs to be satisfied:

$$E > M \sqrt{\left(\frac{\pi}{2\alpha}\right)^2 + \frac{\pi}{\alpha}} \quad (3.95)$$

Since $M < E$, another additional condition is

$$\sqrt{\left(\frac{\pi}{2\alpha}\right)^2 + \frac{\pi}{\alpha}} \geq 1 \quad (3.96)$$

Solve Equation 3.96 and notice $\alpha \in \left(0, \frac{\pi}{2}\right)$ to find:

$$0 < \alpha < \frac{\pi}{4} \quad (3.97)$$

from which one can see that Equation 3.96 holds in the $M < E$ case. The minimum time for steering the system state from the north pole to the south pole under geometric control is longer than the upper bound of the minimum time under bang-bang control when M and E satisfy Equation 3.95, therefore bang-bang control is better.

2. $T_{\min} < t_{\min} < T_{\max}$

If $T_{\min} < t_{\min} < T_{\max}$ holds, namely

$$\frac{1}{2\sqrt{M^2+E^2}} \left(\frac{\pi^2}{2\alpha} - 2\pi \right) < \frac{\pi}{2M} < \frac{1}{2\sqrt{M^2+E^2}} \left(\frac{\pi^2}{2\alpha} + \pi \right) \quad (3.98)$$

then the following inequality is satisfied

$$M \sqrt{\left(\frac{\pi}{2\alpha}\right)^2 + 3 - \frac{2\pi}{\alpha}} < E < M \sqrt{\left(\frac{\pi}{2\alpha}\right)^2 + \frac{\pi}{\alpha}}$$

In the $M < E$ case, when $\alpha \in \left(0, \frac{2-\sqrt{2}}{4}\pi\right)$, the condition that makes Equation 3.98 hold is

$$M < E < M \sqrt{\left(\frac{\pi}{2\alpha}\right)^2 + \frac{\pi}{\alpha}} \quad (3.99)$$

and when $\alpha \in \left(\frac{2-\sqrt{2}}{4}\pi, \frac{\pi}{4}\right)$, the condition that makes Equation 3.98 hold is

$$M \sqrt{\left(\frac{\pi}{2\alpha}\right)^2 + 3 - \frac{2\pi}{\alpha}} < E < M \sqrt{\left(\frac{\pi}{2\alpha}\right)^2 + \frac{\pi}{\alpha}} \quad (3.100)$$

When Equation 3.99 or Equation 3.100 is satisfied, the minimum time for steering the state from the north pole to the south pole under bang-bang control is a time interval, so the pros and cons of the two control strategies need to be determined based on the choice of parameter.

3. $t_{\min} < T_{\min}$

If $t_{\min} < T_{\min}$ holds, namely $\frac{\pi}{2M} < \frac{\pi^2/2\alpha-2\pi}{2\sqrt{M^2+E^2}}$, then $E < M \sqrt{\left(\frac{\pi}{2\alpha}\right)^2 + 3 - \frac{2\pi}{\alpha}}$ should be satisfied. Considering $M < E$, one can obtain the following conditions:

$$M < E < M \sqrt{\left(\frac{\pi}{2\alpha}\right)^2 + 3 - \frac{2\pi}{\alpha}} \quad (3.101)$$

$$\sqrt{\left(\frac{\pi}{2\alpha}\right)^2 + 3 - \frac{2\pi}{\alpha}} \geq 1 \quad (3.102)$$

Solve Equation 3.102 and notice $\alpha \in \left(0, \frac{\pi}{2}\right)$ to find:

$$0 < \alpha < \frac{2 - \sqrt{2}}{4}\pi \quad (3.103)$$

On the premise of Equations 3.103, 3.101, and 3.102 holding, the minimum time for steering the system state from the north pole to the south pole under geometric control is shorter than the lower bound of the minimum time under bang-bang control, in other words geometric control is better. This also indicates that Equation 3.99 in the second case will not occur.

3.3.5 Numerical Simulation Experiments and Results Analyses

Using the relationship of M and E , in this subsection we will give several groups of numerical experiments and verify the conclusions that were obtained in Section 3.3.4.

1) The $M \geq E$ case

1. The $M > E$ case

The experimental results for $M = 3$ and $E = 2.5$ are given in Figure 3.14, which shows the controls for steering the state from the north pole to the south pole under geometric control (Figure 3.14a) and bang-bang control (Figure 3.14b) when $M = 3$ and $E = 2.5$. The corresponding evolution trajectories are shown in Figure 3.14c and Figure 3.14d. It can be seen from Figure 3.14b that bang-bang control only needs one switch to achieve the control objective. According to Equations 3.70 and 3.80, the minimum times under geometric control and bang-bang control are $t_{\min} = 0.5236$ and $T_{BB1} = 0.8045$, respectively. One can obtain $t_{\min} < T_{BB1}$, which indicates that the minimum time for steering the system state from the north pole to the south pole under geometric control is shorter than that under bang-bang control in the $M > E$ case, verifying the conclusion in Equation 3.93.

The control shown in Figure 3.14b is the control $u_1(t)$ in Equation 3.78. Each control in Equation 3.78 or 3.79 can steer the state from the north pole to the south pole at the same time. The difference between Equations 3.78 and 3.79 is the plus-minus of controls. It is also verified that if u can steer the state from the north pole to the south pole, then $-\Omega$ can also achieve the same objective. The difference is that the rotation directions of state evolution trajectories are contrary, which is tenable not only in the $M > E$ case but also in the $M = E$ and $M < E$ cases.

2. The $M = E$ case

The experimental results for $M = 2.5$ and $E = 2.5$ are given in Figure 3.15, which shows the controls for steering the state from the north pole to the south pole under geometric control (Figure 3.15a) and bang-bang control (Figure 3.15b) when $M = E = 2.5$. The corresponding evolution trajectories are shown in Figure 3.15c and Figure 3.15d. As shown in Figure 3.15b, bang-bang control only needs one switch in the $M = E$ case. According to Equations 3.70 and 3.80, the minimum times under geometric control and bang-bang control are $t_{\min} = 0.6283$ and $T_{BB1} = 0.8886$, respectively. One can obtain $t_{\min} < T_{BB1}$, which indicates that the minimum time for steering the system state from the north pole to the south pole under geometric control is shorter than that under bang-bang control in the $M = E$ case, verifying the conclusion in Equation 3.93.

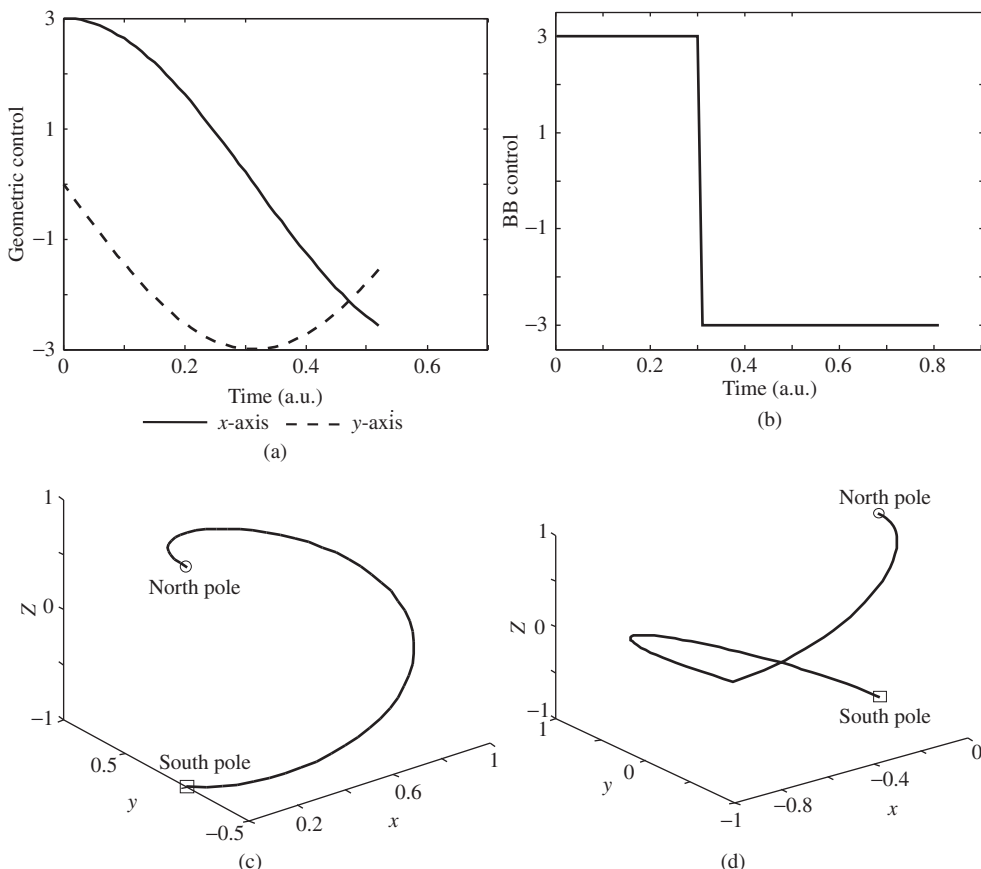


Figure 3.14 Controls and evolution trajectories when $M = 3$ and $E = 2.5$: (a) geometric control, (b) bang-bang control, (c) trajectory under geometric control, and (d) trajectory under bang-bang control

Table 3.3 shows several groups of experimental results for different (M, E) . It can be seen from the comparison of groups 1 and 5 in Table 3.3 that the values of E do not affect time under geometric control while E becomes smaller, but the minimum time becomes longer under bang-bang control from the comparison of groups 3 and 6 where M is the same. Comparing groups 5, 6, 7, and 8, the time becomes longer when M and E decrease at the same time under geometric control and bang-bang control in the $M = E$ case. Comparing groups 1 and 2 with groups 3 and 4 one can see that the time becomes longer when M becomes smaller under geometric control and bang-bang control when E is the same, which is also tenable in the $M < E$ case and can be verified by calculating Equations 3.70 and 3.80.

2) The $M < E$ case

1. $t_{\min} > T_{\max}$

If $E = 2.5$ is fixed and $M \in (0, 2.5)$ is the variable, the values of t_{\min} , T_{\min} , and T_{\max} are shown in Figure 3.16, from which one can see that in the $M < E$ case, the group

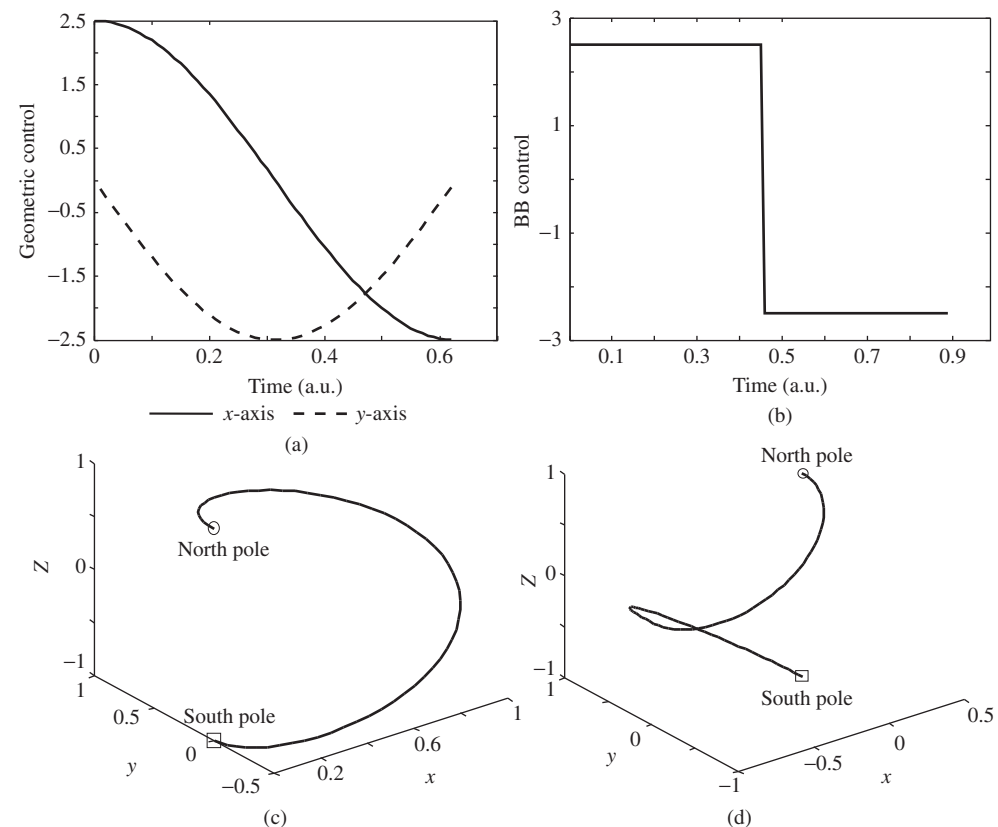


Figure 3.15 Controls and evolution trajectories when $M = 2.5$ and $E = 2.5$: (a) geometric control, (b) bang-bang control, (c) trajectory under geometric control, and (d) trajectory under bang-bang control

Table 3.3 Experimental result for different values of M and E

Group no.	Control method	M	E	Time
1	Geometric control	3	2.5	0.5236
2	Geometric control	2.5	2.5	0.6283
3	Bang-bang control	3	2.5	0.8045
4	Bang-bang control	2.5	2.5	0.8886
5	Geometric control	3	1	0.5236
6	Bang-bang control	3	1	0.9935
7	Geometric control	1	1	1.5708
8	Bang-bang control	1	1	2.2214

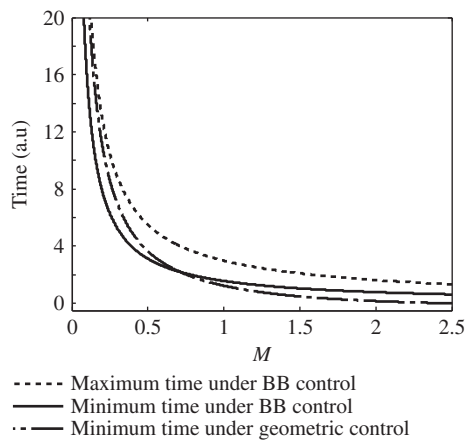


Figure 3.16 Time curves with $E = 2.5$ and $M \in (0, 2.5)$

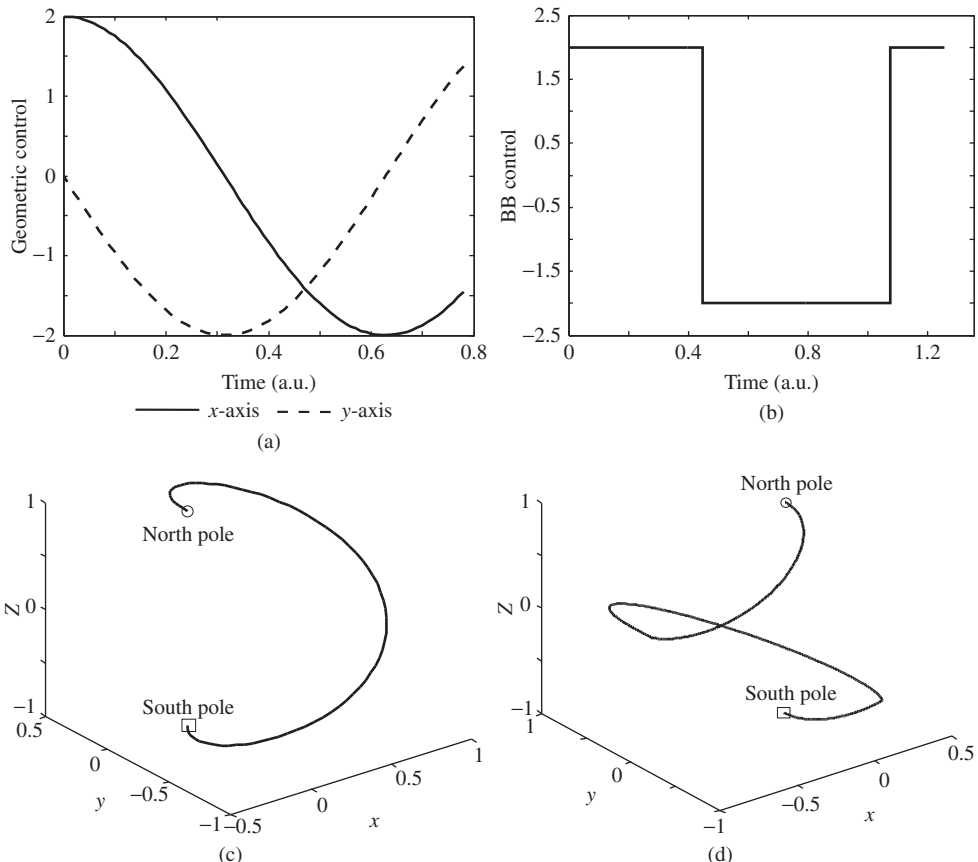


Figure 3.17 Controls and evolution trajectories when $M = 2$ and $E = 2.5$: (a) geometric control, (b) bang-bang control, (c) trajectory under geometric control, and (d) trajectory under bang-bang control

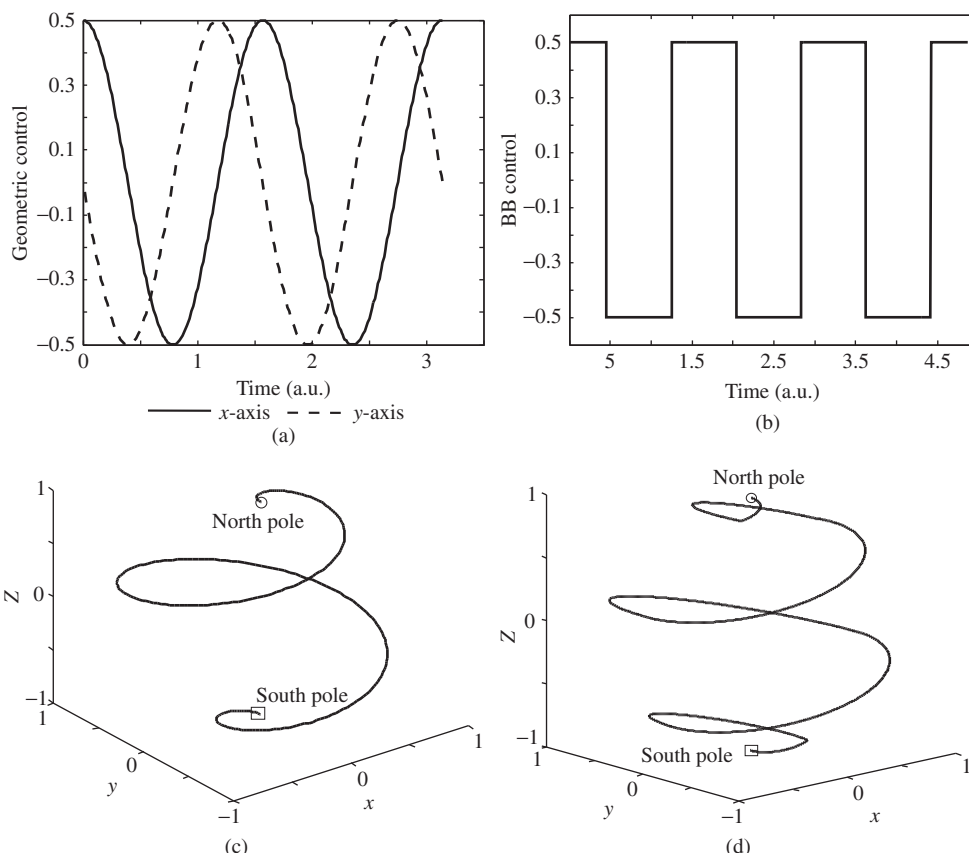


Figure 3.18 Controls and evolution trajectories when $M = 0.5$ and $E = 2.5$: (a) geometric control, (b) bang-bang control, (c) trajectory under geometric control, and (d) trajectory under bang-bang control

(M, E) in which $t_{\min} > T_{\max}$ does not exist, namely there is no group (M, E) that satisfies Equation 3.95. The $t_{\min} > T_{\max}$ case is non-existent and verified by experiments.

2. $T_{\min} < t_{\min} < T_{\max}$

If $M = 2$ and $E = 2.5$, which satisfies Equation 3.100, the experimental results are given in Figure 3.17, which shows the controls of steering the state from the north pole to the south pole under geometric control (Figure 3.17a) and bang-bang control (Figure 3.17b) when $M = 2$ and $E = 2.5$. The corresponding evolution trajectories are shown in Figure 3.17c and Figure 3.17d.

As shown in Figure 3.17b, bang-bang control needs more than one switch in the $M < E$ case. According to Equations 3.70 and 3.90, the minimum times under geometric control and bang-bang control are $t_{\min} = 0.7854$ and $T_{BB2} = 1.2558$, respectively, which indicates that $t_{\min} < T_{BB2}$.

In the case of $T_{\min} < t_{\min} < T_{\max}$, t_{\min} is always shorter than T_{BB2} for several groups of (M, E) , in other words the minimum time for steering the state from the north pole to the south pole under geometric control is shorter than that under bang-bang control.

3. $t_{\min} < T_{\min}$

If $M = 0.5$ and $E = 2.5$, which satisfies Equation 3.103, the experimental results are given in Figure 3.18, which shows the control of steering the state from the north pole to the south pole under the geometric control (Figure 3.17a) and bang-bang control (Figure 3.17b) when $M = 0.5$ and $E = 2.5$. The corresponding evolution trajectories are shown in Figure 3.18c and Figure 3.18d. According to Equations 3.70 and 3.90, the minimum times under geometric control and bang-bang control are $t_{\min} = 3.1416$ and $T_{BB2} = 4.8651$, respectively, which indicates $t_{\min} < T_{BB2}$. Because $t_{\min} < T_{\min}$, the result is as expected. The minimum time for steering the state from the north pole to the south pole under geometric control is shorter than that under bang-bang control.

All the experimental results can be summarized by saying that there exists $t_{\min} < T_{BB1}$ or $t_{\min} < T_{BB2}$, in other words the minimum time for steering the state from the north pole to the south pole under geometric control is shorter than that under bang-bang control.

References

- Agrachev, A.A. and Gamkrelidze, R.V. (1990) *Monographs and Textbooks in Pure and Applied Mathematics*, Marcel Dekker, New York.
- Allen, L. and Eberly, J.H. (1975) *Optical Resonance and Two-Level Atoms*, John Wiley & Sons, Inc., New York.
- Altafin, C. (2002) Controllability of quantum mechanical systems by root space decomposition of $\text{su}(N)$. *Journal of Mathematical Physics*, **43**(5), 2051–2062.
- Boothby, W.M. and Wilson, E.N. (1979) Determination of transitivity of bilinear systems. *SIMA Journal on Control and Optimization*, **17**(2), 212–221.
- Borzi, A., Stadler, X. and Hohenester, U. (2002) Optimal quantum control in nanostructures: theory and application to a generic three-level system. *Physical Review A*, **66**(5), 053811.
- Boscain, U., Chambrion, T. and Gauthier, J.P. (2002) On the K + P problem for a three-level quantum systems: optimality implies resonance. *Journal of Dynamical Control Systems*, **8**(4), 547–572.
- Boscain, U., Charlot, G. and Gauthier, J.P. (2003) Optimal control of the Schrodinger equation with two or three levels. *Nonlinear and Adaptive Control*, **281**, 33–43.
- Boscain, U., Charlot, G., Gauthier, J.P. et al. (2002) Optimal control in laser-induced population transfer for two- and three-level quantum systems. *Journal of Mathematical Physics*, **43**(5), 2107–2132.
- Boscain, U. and Chitour, Y. (2005) Time optimal synthesis for left-invariant control systems on $\text{SO}(3)$. *Siam Journal on Control and Optimization*, **44**(1), 111–139.
- Boscain, U. and Mason, P. (2005) Time minimal trajectories for two-level quantum systemss with drift. Proceedings of the 44th IEEE Conference on Decision and Control, and the European Control Conference, Seville, Spain, pp. 3188–3193.
- Boscain, U. and Mason, P. (2006) Time minimal trajectories for a spin 1/2 particle in a magnetic field. *Journal of Mathematical Physics*, **47**(6), 062101.
- Boscain, U. and Piccoli, B. (2004) *Optimal Synthesis for Control Systems on 2-D Manifolds*, Springer, New York.
- Brockett, R. (2001) New issues in the mathematics of control. *Mathematics unlimited – 2001*, 189–219.
- D’Alessandro, D. (2002) The optimal control problem on $\text{so}(4)$ and its applications to quantum control. *IEEE Transaction on Automatic Control*, **47**(1), 87–92.
- D’Alessandro, D. and Dahleh, M. (2001) Optimal control of two-level quantum systems. *IEEE Transaction on Automatic Control*, **46**(6), 866–876.
- Daleh, M.A., Peirce, A.M. and Rabitz, H. (1988) Optimal control of quantum mechanical systems: existence, numerical approximation, and applications. *Physical Review A*, **37**(12), 4950–4964.

- Grivopoulos, S. and Bamieh, B. (2004) Optimal population transfers for a quantum system in the limit of large transfer time. *American Control Conference*, **3**, 2481–2486.
- Khaneja, N., Brockett, R. and Glaser, S.J. (2001) Time optimal control in spin systems. *Physical Review A*, **63**(3), 032308.
- Khaneja, N., Glaser, S. and Brockett, R. (2002) Sub-Riemannian geometry and time optimal control of three spin systems: quantum gates and coherence transfer. *Physical Review A*, **65**(3), 032301.
- Lou, Y.S. and Cong, S. (2011) State transfer control of quantum systems on the Bloch sphere. *Journal of Systems Science and Complexity*, **24**(3).
- Malinovsky, V.S. and Sola, I.R. (2004) Quantum control of entanglement by phase manipulation of time-delayed pulse sequences. *Physical Review A*, **70**(4), 042304.
- Mishima, K., Hayashi, M. and Lina, S.H. (2003) Coherence control between two quantum systems using spatial phase. *Physics Letters A*, **315**(1–2), 16–22.
- Palao, J.P. and Kosloff, R. (2002) Quantum computing by an optimal control algorithm for unitary transformations. *Physical Review Letters*, **89**(18), 188301.
- Palao, J.P. and Kosloff, R. (2003) Optimal control theory for unitary transformations. *Physical Review A*, **68**(6), 062308.
- Raginsky, M. (2003) Quantum system identification. Proceedings of International Conference on Physics and Control, St. Petersburg, Russia, pp. 792–796.
- Ramakrishna, V., Flores, K.L., Rabitz, H. et al. (2000) Quantum control by decomposition of su(2). *Physical Review A*, **62**(5), 053409.
- Rice, S.A. and Zhao, M. (2000) *Optimal Control of Molecular Dynamics*, John Wiley & Sons, Inc., New York.
- Sachkov, Y.L. (1997) Controllability of affine right-invariant systems on solvable lie groups. *Discrete Mathematics and Theoretical Computer Science*, **1**, 239–246.
- Schirmer, S.G. (2001) Quantum control using lie group decompositions. *IEEE Conference on Decision and Control*, **12**, 298–303.
- Shen, L., Shi, S. and Rabitz, H. (1993) Control of coherent wave function: a linearized molecular dynamics view. *Physical Chemistry*, **97**, 8874–8881.
- Tannoudji, C.C., Diu, B. and Laloe, F. (1977) *Quantum Mechanics*, Hermann, New York.
- Vitanov, N.V., Fleischhauer, M., Shore, B.W. et al. (2001) Coherent manipulation of atoms and molecules by sequential laser pulses. *Advances in Atomic Molecular and Optical Physics*, **46**, 55–190.
- Wang, L.Q., Li, Y.F., Cao, D.M. et al. (2004) Study on coherent phase modulation of coherent population trapping in V-type atomic system. *Acta Physica Sinica*, **53**(9), 2937–2945.
- Zhou, Y.W., Ye, C.Y., Lin, Q. et al. (2005) Control of population and atomic coherence by adiabatic rapid passage. *Acta Physica Sinica*, **54**(6), 2799–2803.

4

Manipulation of Eigenstates – Based on Lyapunov Method

In recent decades, the Lyapunov-based method has been used in quantum systems control because of its simple design and without iterations. Research on the Lyapunov-based method has been in two stages. The first stage involved its applications in physics and chemistry, where it is called local optimal control (Sugawara, 2002, 2003). The method has been successfully used to solve regulation problems such as pump–dump reaction control, isomerization, and splitting reaction controls. The control goals of these problems focused on the effective excitation of eigenstate population distribution, path transfer, and wave packet shaping of quantum systems by means of experiments or simulations. The research focused on the external control field design, but the desired control goal usually cannot be guaranteed due to the lack of theoretical analysis for the final state and the control effect. In fact, in simulation experiments it is easy to see that the Lyapunov-based control law doesn't always guarantee the realization of the control goal. This is because the stable Lyapunov-based control method may not be convergent. To achieve this convergence, the second stage is used. Scientists in the fields of control systems and mathematics led the research on quantum control based on the Lyapunov method (Ferrante, Pavon, and Raccanelli, 2002a, 2002b; Paolo, 2002; Grivopoulos and Bamieh, 2003; Mirrahimi and Rouchon, 2004; Mirrahimi, Rouchon, and Turinici, 2005; Mirrahimi, Turinici, and Rouchon, 2005; Altafini, 2007; Wang and Schirmer, 2010a; Cong and Kuang, 2007; Kuang and Cong, 2008; Zhang and Cong, 2008; Cong and Zhang, 2008). They focused on analyzing theoretically the convergence of state evolution, which provides the theoretical foundation for the reachability of the Lyapunov method applied to the fields of physics and chemistry. For the Lyapunov functions selected, Mirrahimi, Rouchon, and Turinici (2005) assumed the eigenstate to be the target state for a pure state model. By means of the invariance principle, they proved the equivalence between the asymptotic stability of the target state and the controllability of the linear system of eigenstates. They also proposed adiabatic evolution to asymptotically track the target eigenstate in a unreachable linearized system. For a closed-loop system model with the density operator as its variable, Altafini and Schirmer

separately analyzed the convergence problem of the arbitrary state by dynamical system theory and the invariance principle (Altafini, 2007; Wang and Schirmer, 2010b). The authors not only designed the control law based on the completely deterministic Lyapunov function to realize the population transfer between two eigenstates, but also proposed the Lyapunov method with additional freedom. For the Lyapunov functions selected for pure states systems, we proved and compared the effect of stabilization of several Lyapunov-based methods (Kuang and Cong, 2008). Furthermore, the Lyapunov-based method was used to design the optimal control without iterations (Zhang and Cong, 2008), the preparation of the superposition state (Cong and Zhang, 2008), and the optimal control strategy to pure states. For the diagonal Lyapunov function, the convergence was guaranteed by the invariance principle (Cong and Zhang, 2009).

The advantage of the Lyapunov-based method is that it enables the control law to be obtained by means of the Lyapunov indirect stability theorem without iterations resulting from the solution of the partial differential equation, which makes it possible to realize rapid quantum control. Generally, the premise of designing a controller for a system is the system's controllability, otherwise the desired output state will not be achieved by any control input. The controllability of the controlled system must therefore be studied before designing a controller. The controllability conditions themselves only allow the determination of whether or not a system is controllable and do not take a part in the controller design. On the other hand, the basic condition that the controller designed by some control theory can be used is the stability of the whole control system. The stability can only guarantee an allowable error range but not the convergence. If the controlled system is not only stable but also convergent, the error will be zero. A convergent system must be stable. From the system control point of view, whether or not a system involves feedback (or closed-loop) control depends on the expression of its control law: it does involve feedback control when the control law is a function of the output variable of the system. In fact, we can design a feedback control system with an output state obtained from mathematical models. The premise of state feedback based on mathematical models is that the state of the system evolves according to the mathematical model, which means it is a closed quantum system because of the requirement of consistency between the state obtained from the model and that obtained from the real system. A closed quantum system refers to one without any interaction with its surroundings. Although all real quantum systems are open, many experiments on quantum system can be regarded as closed because the control is accomplished in an extremely short time that is negligible compared to the system's decoherence time. In this case, the dynamic system satisfies the Schrödinger equation or the Liouville equation. That is why it is so important to study closed quantum systems – they are the basis of open quantum systems. The role of closed quantum systems is just like the role of the ideal system in the macroscopic world: the systems are linear, constant, time-independent; they are the basis of actual systems. Only closed quantum systems are considered in this chapter.

4.1 Principle of the Lyapunov Stability Theorem

The prerequisite for any control system is that it must be stable under the action of a design control law. Generally, a system is stable if for any given boundary input of the system the error between the input and output of the system is small. One usually needs to check whether the control system is stable after it has been designed. This is often difficult. In 1892 Lyapunov proposed a method to check if a control system is stable without calculating the output of

the system for the given input. This method is known as the second (or indirect) method of Lyapunov for stability. Before we discuss Lyapunov-based control methods in quantum systems, we should introduce the principle of the Lyapunov stability theorem and its properties. First we recall the following theorem.

Consider a non-linear system

$$\dot{x}(t) = f(x) \quad (4.1)$$

in which $x(t)$ is the state vector of a system and $f(x)$ is either a linear or a non-linear function. Let us assume that $x_{eq} = 0$ is an equilibrium point of Equation 4.1.

Definition 4.1 The equilibrium point of Equation 4.1 is:

1. stable, if for each $\epsilon > 0$, there is $\delta = \delta(\epsilon) > 0$ such that $\|x(0)\| < \delta \Rightarrow \|x(t)\| < \epsilon, \forall t \geq 0$
2. unstable, if not stable
3. asymptotically stable, if it is stable and δ can be chosen such that $\|x(0)\| < \delta \Rightarrow \|x(t)\| = 0$
4. marginally stable, if it is stable but not asymptotically stable.

Theorem 4.1 Let $x = 0$ be an equilibrium point of the system Equation 4.1 $\dot{x}(t) = f(x)$, where $f : D \rightarrow \mathbb{R}^n$ and $D \subset \mathbb{R}^n$ is a domain containing $x = 0$. Let $V : D \rightarrow \mathbb{R}$ be a continuously differentiable function on a neighborhood D of $x = 0$, such that $V(0) = 0$ and $V(x) > 0$ in $D - \{0\}$, $\dot{V}(x) \leq 0$ in D . Then, $x = 0$ is stable. Moreover, if $\dot{V}(x) < 0$ in $D - \{0\}$, then $x = 0$ is asymptotically stable.

The Lyapunov stability theorem was originally used to examine the stability of a control system. Later it was also used as a method of control law design. One can design the control laws according to the conditions given in the theorem so that no further check on whether the control system is stable or not is required. It was also found that the Lyapunov-based method is a simple and easy way of obtaining the control law by means of the equation $\dot{V}(x, u) = 0$. If the control system is only required to be stable, the Lyapunov-based method is a popular method of designing a control system in control engineering.

Remark 4.1 You may have noticed that the key point of the theorem is to find a proper $V(x)$, which is called a Lyapunov function and must satisfy the following requirements: (i) $V(x)$ is continuous, (ii) $V(x)$ has a unique minimum at x_{eq} with respect to all other points in D , and (iii) along any trajectory of system contained in D the value of $V(x)$ never increases.

Remark 4.2 The advantage of the (indirect) Lyapunov stability theorem is that the stability of the system can be determined without actually solving its differential equation. The theorem can be used for both linear and non-linear control systems. The stability conditions are sufficient, but not necessary. There is no systematic method for finding Lyapunov functions, so trial and error has to be used.

4.2 Quantum Control Strategy Based on State Distance

The state transfer of quantum systems is an important objective in quantum control. When an initial state and a final state are given, the control task is how to find some realizable

control fields to drive the initial state to the final state. Many design methods may achieve this aim, such as the optimal control technique, decoupling techniques, the factorization techniques of the unitary group, and the Lyapunov-based techniques. This section is devoted to the Lyapunov-based method. A Lyapunov function is selected by the distance between two states. Based on distance concept and the Lyapunov stability theorem, although a similar feedback controller has been designed (Paolo, 2002), this section will develop the case that an initial state is orthogonal to a final state. Moreover, a simulation experiment on a spin-1/2 particle system is given and the influence of different parameters on control results determined. The procedure of controller design is also given.

4.2.1 Selection of the Lyapunov Function

In physics, if all the physical quantities representing a system are given, one will know its states (Jing, 2004). The development of quantum theory shows that the wave functions of a quantum system are its states. By expanding all the states in the Hilbert space of a quantum system as the linear combination of the eigen-functions of a mechanical quantity, one can get the same dimensional coordinate vectors. Let the dimension be n . Evidently, the n -dimensional vector space C^n is isomorphic to the Hilbert space. Correspondingly, all the quantum mechanical objects, such as quantum operators, evolution equations, and so on, are described in terms of their coordinate vectors or matrices.

If two state vectors $|\psi_1\rangle$ and $|\psi_2\rangle$ satisfy $|\psi_1\rangle = e^{i\theta}|\psi_2\rangle$, then they are equivalent. In physics, one cannot distinguish between two equivalent states. Apparently they will not satisfy the same Schrödinger equation if the phase factor $e^{i\theta}$ is time-dependent. Furthermore, every pure state of a quantum mechanical system corresponds to the equivalence class of a unitary state vector.

In this section, the distance between the actual state and the desired state is taken as a Lyapunov function. Thus the distance decreases continuously when the first-order derivative with respect to time of the Lyapunov function is kept non-positive. There are many notions of the distance between states, but the meaning of Bures distance is intuition and represents the Euclidean distance between two equivalence classes. The Bures distance is therefore adopted and defined as (Paolo, 2002):

$$d_B(|\psi_1\rangle, |\psi_2\rangle) = \min_{\theta} \| |\psi_1\rangle - e^{i\theta}|\psi_2\rangle \| \quad (4.2)$$

where $\theta \in R$ represents an arbitrary phase. One can prove:

$$d_B^2(|\psi_1\rangle, |\psi_2\rangle) = 2(1 - |\langle\psi_1|\psi_2\rangle|) \quad (4.3)$$

Considering the inconvenience in normal calculation and conventional processing, the following function may be chosen as the Lyapunov function:

$$V = \frac{1}{2}(1 - |\langle\psi_f|\psi\rangle|^2) \quad (4.4)$$

Comparing Equation 4.3 with Equation 4.4, V can represent the distance between the final state $|\psi_f\rangle$ and the actual state $|\psi\rangle$ at any given time. The physical meaning of Equation 4.4 is also evident: $|\langle\psi_f|\psi\rangle|^2$ represents the transition probability from $|\psi\rangle$ into $|\psi_f\rangle$, and when state $|\psi\rangle$ is driven entirely into the state $|\psi_f\rangle$, $V = 0$, correspondingly $d_B(|\psi_f\rangle, |\psi\rangle) = 0$.

4.2.2 Design of the Feedback Control Law

In the Schrödinger equation

$$i\hbar|\dot{\psi}(t)\rangle = H|\psi(t)\rangle, \quad H = H_0 + H_c, \quad H_c = \sum_{k=1}^r H_k u_k(t) \quad (4.5)$$

where H_0 is the internal Hamiltonian and H_c is the interaction Hamiltonian generated by the interaction between the external controls and the system. Both H_0 and H_c are independent of time. $u_k(t)$ is a realizable, scalar, real-valued control function.

For simplicity and considering the practical requirement, for example in quantum chemistry an eigenstate of the inner Hamiltonian often needs to be reached, it is assumed that the final state $|\psi_f\rangle$ is an eigenstate of the system, that is,

$$H_0|\psi_f\rangle = \lambda_0|\psi_f\rangle \quad (4.6)$$

For $V = \frac{1}{2}(1 - \langle\psi_f|\psi\rangle\langle\psi|\psi_f\rangle)$, the first-order time derivative of V is:

$$\begin{aligned} \dot{V} &= \frac{1}{2}(-\langle\psi_f|\dot{\psi}\rangle\langle\psi|\psi_f\rangle - \langle\psi_f|\psi\rangle\langle\dot{\psi}|\psi_f\rangle) \\ &= -\text{Re} \left[\langle\psi|\psi_f\rangle\langle\psi_f| \left(-\frac{i}{\hbar} \right) \left(H_0 + \sum_{k=1}^r u_k H_k \right) |\psi\rangle \right] \\ &= -\frac{1}{\hbar} \sum_{k=1}^r u_k \cdot \text{Im}[\langle\psi|\psi_f\rangle\langle\psi_f|H_k|\psi\rangle] \end{aligned} \quad (4.7)$$

From Equation 4.7, it can be seen that the most reliable method is to let each item of the summation sign be non-positive so that $\dot{V} \leq 0$. Consequently, the function form of u_k may be of the following characteristics: $K_k f_k(x_k)x_k \geq 0$, where $K_k > 0$, $x_k = \text{Im}[\langle\psi|\psi_f\rangle\langle\psi_f|H_k|\psi\rangle]$, $u_k = K_k f_k(x_k)$. Evidently, when the image of function $y_k = f_k(x_k)$ passes the origin of plane $x_k - y_k$ monotonically and lies in quadrant I or III, the above requirement will be satisfied. At the same time, $f_k(x_k) = 0$ and iff $x_k = 0$.

Analyzing Equation 4.7, one can find that feedback control u_k cannot be used in the cases where an initial state is orthogonal to a final state and the final state $|\psi_f\rangle$ is an eigenstate of every $H_k(k = 1, \dots, r)$. To solve the problem in the first case, a simple approach can be used to add a suitable measurement to change the state of the system. However, this will bring an extra disturbance to the system. To solve this problem, we take the following steps.

Writing the complex number $\langle\psi|\psi_f\rangle$ in terms of its complex exponential number $\langle\psi|\psi_f\rangle = |\langle\psi|\psi_f\rangle|e^{i\angle\langle\psi|\psi_f\rangle}$ and substituting it into Equation 4.7 gives:

$$\dot{V} = -\frac{1}{\hbar} \sum_{k=1}^r u_k \cdot |\langle\psi|\psi_f\rangle| \cdot \text{Im}[e^{i\angle\langle\psi|\psi_f\rangle}\langle\psi_f|H_k|\psi\rangle] \quad (4.8)$$

Evidently, when the actual state $|\psi\rangle$ is not orthogonal to desired final state $|\psi_f\rangle$, which makes $\langle\psi|\psi_f\rangle \neq 0$, the following u_k can also ensure $\dot{V} \leq 0$:

$$u_k = K_k f_k \{ \text{Im}[e^{i\angle\langle\psi|\psi_f\rangle}\langle\psi_f|H_k|\psi\rangle] \}, \quad (k = 1, \dots, r) \quad (4.9)$$

Although the actual state $|\psi\rangle$ is orthogonal to the desired final state $|\psi_f\rangle$, which makes $\langle\psi|\psi_f\rangle = 0$, the angle of the complex $\langle\psi|\psi_f\rangle$ in Equation 4.9 is unknown. In view of this, one can say:

$$\text{If } \langle\psi|\psi_f\rangle = 0, \text{ then } \angle\langle\psi|\psi_f\rangle = 0^\circ \quad (4.10)$$

Thus u_k in Equation 4.9 does not need to be zero and $\dot{V} = 0$ in Equation 4.8. This means that the actual state here is *turning* around the final state $|\psi_f\rangle$ and while $\langle\psi|\psi_f\rangle \neq 0$ is satisfied because of the turn, the case that $\dot{V} < 0$ will appear. The actual state will then be driven toward the final state $|\psi_f\rangle$. Equation 4.9 is therefore selected as the final control field. Note that when $|\psi\rangle = |\psi_f\rangle$ is satisfied, $u_k = 0$ holds. This means that the control field will disappear automatically when the final state is reached.

4.2.3 Analysis and Proof of the Stability

According to the function form of u_k , one can obtain $\dot{V} \leq 0$ and the whole system is stable in the Lyapunov sense at least. The conditions of asymptotic stability will be analyzed and proven as follows. Above all, several lemmas are given.

Lemma 4.1 Paolo, 2002 Given two arbitrary complex numbers z_1 and z_2 , for $z_1 \neq 0$, $\text{Im}(z_1 z_2) = 0$ iff $z_2 = \lambda z_1^*$, $\lambda \in R$.

Lemma 4.2 With the control functions of Equation 4.9, if $\langle\psi(0)|\psi_f\rangle \neq 0$, for every $t > 0$, $\langle\psi(t)|\psi_f\rangle \neq 0$ will hold.

Equation 4.4, conditions $\dot{V} \leq 0$ and $\langle\psi(0)|\psi_f\rangle \neq 0$, may be used to prove the results.

Lemma 4.3 Suppose that $\langle\psi(0)|\psi_f\rangle = 0$ holds. If $\sum_{k=1}^r K_k f_k (\text{Im}\langle\psi_f|H_k|\psi(0)\rangle) \langle\psi_f|H_k|\psi(0)\rangle \neq 0$ is satisfied, for $t > 0$, $\langle\psi(t)|\psi_f\rangle \neq 0$ will hold.

Proof When the system runs for an infinitesimal time interval, that is, $t = dt$, one has

$$|\psi(dt)\rangle \approx e^{-iH dt/\hbar} |\psi(0)\rangle \approx \left(1 - \frac{H}{\hbar} dt\right) |\psi(0)\rangle.$$

Furthermore, one can prove $\langle\psi_f|\psi(dt)\rangle \neq 0 \iff \sum_{k=1}^r u_k \langle\psi_f|H_k|\psi(0)\rangle \neq 0$. Here, $u_k = \lim_{dt \rightarrow 0} K_k f_k \left\{ \text{Im} \left[e^{i\angle\langle\psi|\psi_f\rangle} \langle\psi_f|H_k|\psi\rangle \right] \right\} = K_k f_k (\text{Im}\langle\psi_f|H_k|\psi(0)\rangle)$.

According to Lemma 4.2, one can obtain the conclusion in Lemma 4.3.

Note that the condition in Lemma 4.3 is easily satisfied in practice since both K_k and H_k have an optional degree of freedom.

In the following, the stability will be analyzed. The set of states in the case $\dot{V} = 0$ is defined as Ω . Under the action of the control functions $u_k = K_k f_k \{\text{Im}[e^{i\angle\langle\psi|\psi_f\rangle} \langle\psi_f|H_k|\psi\rangle]\}$, ($k = 1, \dots, r$), one can prove: the following three conditions are equivalent in the case that an initial state isn't orthogonal to the final state, or an initial state is orthogonal to the final state, and for $t > 0$, the condition in Lemma 4.3 is satisfied.

$$(I) \dot{V} = 0 \quad (4.11)$$

$$(II) i\hbar|\psi(t)\rangle = H_0|\psi(t)\rangle \quad (4.12)$$

$$(III) \langle\psi_f|\lambda_k I - H_k|\psi\rangle = 0, (k = 1, \dots, r, \lambda_k \in R) \quad (4.13)$$

■

Proof One can see from Equation 4.9 that

$$\begin{aligned} \dot{V} = 0 &\iff |\langle\psi|\psi_f\rangle| = 0 \text{ or } \text{Im}[e^{i\angle\langle\psi|\psi_f\rangle}\langle\psi_f|H_k|\psi\rangle] = 0 \\ &\iff |\langle\psi|\psi_f\rangle| \cdot \text{Im}[e^{i\angle\langle\psi|\psi_f\rangle}\langle\psi_f|H_k|\psi\rangle] = 0 \iff \text{Im}[\langle\psi|\psi_f\rangle\langle\psi_f|H_k|\psi\rangle] = 0 \end{aligned}$$

According to Lemma 4.1, for $\langle\psi|\psi_f\rangle \neq 0$,

$$\begin{aligned} \dot{V} = 0 &\iff \lambda\langle\psi_f|\psi\rangle = \langle\psi_f|H_k|\psi\rangle, \quad \lambda \in R \\ \text{i.e. } \dot{V} = 0 &\iff \langle\psi_f|\lambda_k I - H_k|\psi\rangle = 0, \quad k = 1, \dots, r, \lambda_k \in R \end{aligned} \quad (4.14)$$

(I) \iff (III) is proved.

The proof of (I) \Rightarrow (II) is as follows:

Substitution of Equation 4.14 into Equation 4.9 gives

$$u_k = K_k f_k (\text{Im}[e^{i\angle\langle\psi|\psi_f\rangle}\lambda\langle\psi_f|\psi\rangle]) = K_k f_k (\lambda|\langle\psi_f|\psi\rangle|\text{Im}[e^{i\angle\langle\psi|\psi_f\rangle}e^{i\angle\langle\psi_f|\psi\rangle}]) = 0$$

Then by substituting u_k into Equation 4.5, one obtains $i\hbar|\dot{\psi}(t)\rangle = H_0|\psi(t)\rangle$.

(II) \Rightarrow (I):

Comparing Equation 4.9 with Equation 4.5, one has

$$\begin{aligned} \sum_{k=1}^r H_k u_k |\psi\rangle = 0 &\Rightarrow \langle\psi_f| \sum_{k=1}^r H_k u_k |\psi\rangle = \sum_{k=1}^r u_k \langle\psi_f|H_k|\psi\rangle \\ &= 0 \Rightarrow \sum_{k=1}^r u_k e^{i\angle\langle\psi|\psi_f\rangle} \langle\psi_f|H_k|\psi\rangle = 0. \end{aligned}$$

Since u_k is a real scalar function, $\sum_{k=1}^r u_k |\langle\psi|\psi_f\rangle| \text{Im}[e^{i\angle\langle\psi|\psi_f\rangle}\langle\psi_f|H_k|\psi\rangle] = 0$ holds, that is,

$\dot{V} = 0$. So, (I) \iff (II).

To sum up, (I), (II), and (III) are equivalent to each other. ■

Lemma 4.4 The coupled Equation 4.13 has a non-zero solution $|\psi\rangle = |\psi_f\rangle$.

Proof One can see from Equation 4.13, when $|\psi\rangle = |\psi_f\rangle$ is satisfied, $u_k = 0$ ($k = 1, 2, \dots, r$) holds, therefore the above condition (II) holds, and thus condition (III) holds.

From the above three conditions, it is not hard to show that they are all *stationary* conditions at some specific evolution time. However, any one of these three equivalence conditions cannot explain the asymptotic stability of the system. In other words, it should be considered whether or not $\dot{V} = 0$ holds at the next moment that $\dot{V} = 0$ is satisfied: if $\dot{V} = 0$ holds, the system will not evolve toward the final state after the moment. Otherwise, the state at this moment is only a transition state in the evolution process. This is the so-called *dynamic* condition. From this

point of view, further study is as follows. Calculating the first-order time derivative of the two sides of Equation 4.13 gives

$$\langle \psi_f | \lambda_k I - H_k | \psi \rangle = 0, (k = 1, \dots, r, \lambda_k \in R)$$

Substitution of Equation 4.12 into this formula gives $\langle \psi_f | \lambda_k I - H_k | H_0 | \psi \rangle = 0$, and simplifying gives $\langle \psi_f | \lambda_k H_0 | \psi \rangle = \langle \psi_f | H_k H_0 | \psi \rangle$, where the left-hand side of the formula equals $\lambda_0 \lambda_k \langle \psi_f | \psi \rangle = \lambda_0 \langle \psi_f | \lambda_k I | \psi \rangle$. Substituting Equation 4.13 into this formula gives $\langle \psi_f | \lambda_k H_0 | \psi \rangle = \lambda_0 \langle \psi_f | H_k | \psi \rangle = \langle \psi_f | H_0 H_k | \psi \rangle$. Consequently, $\langle \psi_f | H_0 H_k | \psi \rangle = \langle \psi_f | H_k H_0 | \psi \rangle$ holds, that is

$$\langle \psi_f | [H_0, H_k] | \psi \rangle = 0, (k = 1, \dots, r) \quad (4.15)$$

Equation 4.15 shows that if $|\psi\rangle \in \Omega$ holds at some moment, $|\psi\rangle \in \Omega$ will still hold at the next moment. Otherwise, it means that if $|\psi\rangle \in \Omega$ holds at some moment, $|\psi\rangle \notin \Omega$ will hold at the next moment. So, one can generalize the following (asymptotic) stability theorem. ■

Theorem 4.2 Assume that $|\psi_f\rangle$ is an eigenstate of H_0 and is not an eigenstate of every H_k , ($k = 1, 2, \dots, r$). With the control function form in Equation 4.9, if coupled equations $\begin{cases} \langle \psi_f | \lambda_k I - H_k | \psi \rangle = 0, & (k = 1, 2, \dots, r) \\ \langle \psi_f | [H_0, H_k] | \psi \rangle = 0, & (k = 1, 2, \dots, r) \end{cases}$ have the only solution $|\psi\rangle = |\psi_f\rangle$, the control system will be asymptotically stable.

Lemma 4.5 The coupled Equation 4.15 has a non-zero solution $|\psi\rangle = |\psi_f\rangle$.

This conclusion is easily checked.

Deduction 4.1 If the coupled equation $\langle \psi_f | [H_0, H_k] | \psi \rangle = 0, (k = 1, \dots, r)$ only has the solution $|\psi\rangle = |\psi_f\rangle$, the control system will be asymptotically stable.

Based on Lemma 4.4, Lemma 4.5, and Theorem 4.2, this deduction can be proved.

4.2.4 Application to a Spin-1/2 Particle System

We give some system simulation experiments in this section to illustrate the effectiveness of the method proposed. Suppose that the spin-1/2 particle system is controlled only by one control field, and the control function $u(t)$ varies the electromagnetic field in the y -direction. The spin is discussed in the σ_z representation. The Schrödinger equation of the system is

$$i\hbar |\dot{\psi}(t)\rangle = (H_0 + u_1 H_1) |\psi(t)\rangle$$

where $H_0 = \sigma_z = \begin{bmatrix} 1 & 0 \\ 0 & -1 \end{bmatrix}$ and $H_1 = \sigma_y = \begin{bmatrix} 0 & -i \\ i & 0 \end{bmatrix}$, setting $\hbar = 1$.

To perform the simplest logic NOT-gate operation, the state $|\psi\rangle$ must be driven to switch between two eigenstates $|0\rangle = [1, 0]^T$ and $|1\rangle = [0, 1]^T$. Now select an initial state $|\psi(0)\rangle = |0\rangle$ and a final state $|\psi_f\rangle = |1\rangle$. When $K_1 > 0$, the condition in Lemma 4.3 is satisfied, therefore the control field in Equation 4.9 is fit for this system.

For this example, according to Deduction 4.1, one has $\langle \psi_f | [H_0, H_1] | \psi \rangle = 0$, that is, $\langle 1 | -2i\sigma_x | \psi \rangle = 0$. This equation admits the only solution $|\psi\rangle = |1\rangle$ (without regard to the phase). Consequently, the system is asymptotically stable.

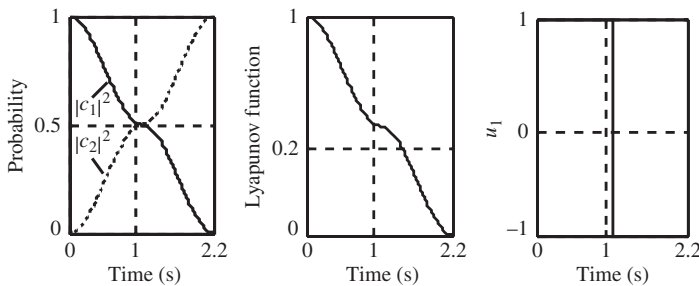


Figure 4.1 Simulation results of the spin-1/2 particle system: (a) probability of the state evolution, (b) Lyapunov function during the state evolution, and (c) control value

Setting $|\psi\rangle = [c_1, c_2]^T$ and choosing the simple sign function as the control function for the sake of easy realization, one has

$$u_1 = K_1 \text{sign}\{\text{Im}[e^{i\angle\langle\psi|\psi_f\rangle} \langle\psi_f| H_1 |\psi\rangle]\}$$

where $K_1 > 0$ and $\text{sign}(x) = \begin{cases} 1 & , x > 0 \\ 0 & , x = 0 \\ -1 & , x < 0 \end{cases}$. Apparently, when $x\text{sign}(x) \geq 0$, the requirement of the control field is satisfied. At the same time, the control function has the form of simple bang-bang control. With $K_1 = 1$, time step $\Delta t = 0.01$, and control time $t = 2.2$ a.u., the simulation results are shown in Figure 4.1, where Figure 4.1a is the probability of the state evolution, Figure 4.1b is the Lyapunov function during the state evolution, and Figure 4.1c is the control value.

According to Figure 4.1a, at an arbitrary moment $|c_1|^2 + |c_2|^2 = 1$ holds, that is, the probability preserves. Based on Figure 4.1b, one can draw a conclusion: at $t_f = 2.2$ seconds, basically $V = 0$ is satisfied and state transfer is finished.

After repeated experiments, the following rules are obtained: When the parameter K_1 is fixed, t_f (i.e., the time when the equivalence class of the final state is reached) does not vary with the time step Δt . The parameter t_f decreases as the parameter K_1 increases. In the applications, according to the control requirement of the system, one may properly select K_1 to get a smaller t_f .

4.3 Optimal Quantum Control Based on the Lyapunov Stability Theorem

In quantum systems such as NMR and chemical reactions, there are many practical problems that have to be solved by optimal control theories. Admittedly, the optimal control method is an important approach for realizing quantum control, but the current proposed optimal control methods are generally obtained by means of complex numeral iterative algorithms (Shi and Rabitz, 1990; Zhu and Rabitz, 1998; D'Alessandro and Dahleh, 2001), which are quite inconvenient to operate and realize. How to obtain an optimal method without iterative solutions is of great significance.

Benallou and Mellichamp proposed a design method for the optimal controller for bilinear systems (Benallou, Mellichamp, and Seborg, 1988). The method can stabilize the controlled system. Here, we give a brief introduction to the main idea of this method.

Consider the general bilinear system

$$\dot{\mathbf{x}} = \mathbf{A}\mathbf{x} + \sum_{i=1}^m (B_i\mathbf{x} + b_i)u_i \quad (4.16)$$

where $\mathbf{x} \in R^n$, $A, B_i \in R^{n \times n}$, A , and B_i are constant matrices.

The performance index is

$$J = \int_0^\infty L(\mathbf{x}, \mathbf{u})dt \quad (4.17)$$

and the Lyapunov function $V(\mathbf{x})$ is selected. The Hamiltonian function of the controlled system is

$$H(\mathbf{x}, \mathbf{u}) = L(\mathbf{x}, \mathbf{u}) + V_x(\mathbf{x}) \left[\mathbf{A}\mathbf{x} + \sum_{i=1}^m u_i \mathbf{d}_i(\mathbf{x}) \right]$$

where $V_x = (\frac{\partial V}{\partial \mathbf{x}})'$.

Finally, the optimal control law \mathbf{u}^* is obtained, which can not only stabilize the bilinear system but also minimize the performance index J . The major advantage of this method is that the control law is obtained through the solution of the Lyapunov equation without iteration.

4.3.1 Description of the System Model

The mathematical model of pure state quantum systems is formally a bilinear system. It can be described by the following Schrödinger equation:

$$i\hbar|\psi\rangle = H|\psi\rangle \quad (4.18)$$

where $\hbar = 1.0545 \times 10^{-34} \text{ J} \cdot \text{s}$ is the reduced Planck constant. In theoretical analysis \hbar often lies in H , so we can set $\hbar = 1$. $|\psi\rangle$ is the actual state of the quantum system, $|\psi\rangle \in C^n$, and $\| |\psi\rangle \| = 1$. H is the Hamiltonian operator, which corresponds to a special system and decides the state evolution in the system.

Assume that H consists of two parts:

$$H = H_0 + H_c(t) \quad (4.19)$$

where H_0 is the inner Hamiltonian, $H_c(t)$ is the interaction Hamiltonian generated by the interaction of the external controls and the system, and $H_c(t) = \sum_{i=1}^m H_i u_i(t)$. Both H_0 and H_i are linear Hermitian operators independent of time, that is, $H_0^\dagger = H_0$ and $H_i^\dagger = H_i$, where the superscript plus sign represents conjugate transpose. $u_i(t)$ is a realizable, scalar, real-valued control function.

Equation 4.18 can therefore be written in the following form:

$$i|\psi\rangle = \left(H_0 + \sum_{i=1}^m H_i u_i(t) \right) |\psi\rangle \quad (4.20)$$

The eigen-equation of operator H_0 is given by

$$H_0|\psi_n\rangle = \lambda_n|\psi_n\rangle \quad (4.21)$$

where λ_n is the eigenvalue of H_0 corresponding to the eigenstate $|\psi_n\rangle$. All the eigenstates $|\psi_n\rangle$ expand Hilbert space, hence the following equation holds:

$$|\psi\rangle = \sum_n C_n |\psi_n\rangle \quad (4.22)$$

where $C_n \in C$ and $\sum_n |C_n| = 1$. $|C_n|$ represents the quantum probability in the eigenstate $|\psi_n\rangle$.

The probability of the state vector $|\psi\rangle$ is equal to the probability of the state vector $e^{i\theta(t)}|\psi\rangle$. Physically, $|\psi\rangle$ and $e^{i\theta(t)}|\psi\rangle$ describe the same physical state for any globe phase factor $\theta(t)$, which is a time-dependent real function. $|\psi_1\rangle$ and $|\psi_2\rangle$ are identified when there exists $\theta \in \mathbb{R}$ such that $|\psi_1\rangle = e^{i\theta}|\psi_2\rangle$. Considering this characteristic, Mirrahimi and Rouchon proposed the introduction of a real control field ω according to $\dot{\theta}(t)$ in the system (Mirrahimi, Turinici, and Rouchon, 2005). The system state equation (Equation 4.20) can then be written in the following form:

$$i|\dot{\psi}\rangle = \left(H_0 + \sum_{i=1}^m H_i u_i(t) + \omega I \right) |\psi\rangle \quad (4.23)$$

It can be proved that the solution of Equation 4.23 is equal to the product of the solution of Equation 4.20 and the global phase factor $e^{-i\omega t}$. Accordingly, the introduced ω may be used to adjust the global phase without changing the physical quantities attached to $|\psi\rangle$. In quantum control, the target state is usually an eigenstate of the inner Hamiltonian, such as in quantum chemistry. We therefore assume that the target state $|\psi_f\rangle$ satisfies $H_0|\psi_f\rangle = \lambda_f|\psi_f\rangle$. Here, we fix $\omega = -\lambda_f$, then we can get $(H_0 + \omega I)|\psi_f\rangle = 0$.

The state steering of quantum systems is a major problem in quantum control. The purpose of quantum state steering is to seek some realizable control fields to drive the given initial states to the predetermined target ones. The system model described by Equation 4.23 is formally a bilinear system.

Although we can use the complex state-space to study quantum systems, for the convenience of analysis and calculation we use the real state-space to describe the controlled system here. In order to get the real state equation of Equation 4.23, we separate the real parts and the imaginary parts of the coefficient matrices and state variables in Equation 4.23. Let $|\psi\rangle = [x_1 + ix_{n+1} \ x_2 + ix_{n+2} \ \dots \ x_n + ix_{2n}]^T$. Because the real part and the imaginary part in each side of Equation 4.23 are respectively equal, the following equation about the real vector \mathbf{x} can be obtained:

$$\dot{\mathbf{x}} = \left(A + \sum_{i=1}^m B_i u_i(t) \right) \mathbf{x} \quad (4.24)$$

where $A = \begin{bmatrix} \Re(H_0 + \omega I) & \Im(H_0 + \omega I) \\ -\Im(H_0 + \omega I) & \Re(H_0 + \omega I) \end{bmatrix}$, $B_i = \begin{bmatrix} \Re(H_i) & \Im(H_i) \\ -\Im(H_i) & \Re(H_i) \end{bmatrix}$, and A and B_i are skew symmetric matrices that satisfy $A + A' = 0$ and $B_i + B_i' = 0$. Because $(H_0 + \omega I)|\psi_f\rangle = 0$, $Ax_f = 0$ can be obtained.

4.3.2 Optimal Control Law Design and Property Analysis

The optimal control law of Equation 4.24 is given by the following theorem.

Theorem 4.3 For the system defined by Equation 4.24, the performance index is given by

$$J = \frac{1}{2} \int_0^\infty \left\{ \sum_{i=1}^m \frac{1}{r_i} [(\mathbf{x} - \mathbf{x}_f)' P B_i \mathbf{x}]^2 + \mathbf{u}' R \mathbf{u} \right\} dt \quad (4.25)$$

where $\mathbf{u} = [u_1 \ u_2 \ \dots \ u_m]', R$ is a diagonal matrix with positive elements, $r_i > 0 (i = 1, 2, \dots, m)$, and P is a positive definite symmetric matrix that satisfies the equation

$$PA + A'P = 0 \quad (4.26)$$

There then exists an optimal control law:

$$u_i^* = -\frac{1}{r_i} (\mathbf{x} - \mathbf{x}_f)' P B_i \mathbf{x}, (i = 1, 2, \dots, m) \quad (4.27)$$

such that the system Equation 4.24 is stable and the performance index Equation 4.25 is minimum.

Proof

1. Proof of stability

Select the following the Lyapunov function:

$$V(\mathbf{x}) = \frac{1}{2} (\mathbf{x} - \mathbf{x}_f)' P (\mathbf{x} - \mathbf{x}_f) \quad (4.28)$$

where P is a positive definite symmetric solution of Equation 4.26. The first-order time derivative of $V(\mathbf{x})$ is:

$$\dot{V}(\mathbf{x}) = (\mathbf{x} - \mathbf{x}_f)' P \dot{\mathbf{x}} \quad (4.29)$$

Substituting Equation 4.24 into Equation 4.28 yields:

$$\dot{V}(\mathbf{x}) = (\mathbf{x} - \mathbf{x}_f)' P A \mathbf{x} + \sum_{i=1}^m (\mathbf{x} - \mathbf{x}_f)' P B_i u_i(t) \mathbf{x} \quad (4.30)$$

Because $PA + A'P = 0$ and $Ax_f = 0$, $(\mathbf{x} - \mathbf{x}_f)' P A \mathbf{x} = \frac{1}{2} \mathbf{x}' (PA + A'P) \mathbf{x} + (Ax_f)' P \mathbf{x} = 0$ holds. Hence, Equation 4.30 can be written as

$$\dot{V}(\mathbf{x}) = \sum_{i=1}^m (\mathbf{x} - \mathbf{x}_f)' P B_i u_i(t) \mathbf{x} \quad (4.31)$$

Substituting Equation 4.27 into Equation 4.31 yields

$$\dot{V}(\mathbf{x}) = - \sum_{i=1}^m \frac{1}{r_i} [(\mathbf{x} - \mathbf{x}_f)' P B_i \mathbf{x}]^2 \leq 0 \quad (4.32)$$

where $\mathbf{x} = \mathbf{x}_f$ and $\dot{V}(\mathbf{x}) = 0$.

According to the Lyapunov stability theorem, the control law given by Equation 4.27 stabilizes the system given by Equation 4.24. Next, we will proof the optimality of the control law.

2. Proof of optimality

The Hamiltonian function of the system is

$$H(\mathbf{x}, \mathbf{u}) = L(\mathbf{x}, \mathbf{u}) + V_x(\mathbf{x}) \left[A\mathbf{x} + \sum_{i=1}^m u_i B_i \mathbf{x} \right] \quad (4.33)$$

where $L(\mathbf{x}, \mathbf{u}) = \frac{1}{2} \sum_{i=1}^m \frac{1}{r_i} [(\mathbf{x} - \mathbf{x}_f)' P B_i \mathbf{x}]^2 + \frac{1}{2} \mathbf{u}' R \mathbf{u}$ and $V_x = (\frac{\partial V}{\partial \mathbf{x}})' = (\mathbf{x} - \mathbf{x}_f)' P$.

The sufficient condition for optimality proposed by Athans and Falb (1966) is

$$\min_{u_i^* \in R^m} [H(\mathbf{x}, \mathbf{u})] = 0 \quad (4.34)$$

From Equation 4.33, one can obtain:

$$\frac{\partial H}{\partial u_i} = r_i u_i + (\mathbf{x} - \mathbf{x}_f)' P B_i \mathbf{x} \quad (4.35)$$

Substituting Equation 4.27 into Equation 4.35 yields $\frac{\partial H}{\partial u_i} = 0$, and then substituting Equation 4.27 into Equation 4.33 gives

$$\begin{aligned} H(\mathbf{x}, \mathbf{u}^*) &= \frac{1}{2} \sum_{i=1}^m \frac{1}{r_i} [(\mathbf{x} - \mathbf{x}_f)' P B_i \mathbf{x}]^2 + \frac{1}{2} \sum_{i=1}^m \frac{1}{r_i} [(\mathbf{x} - \mathbf{x}_f)' P B_i \mathbf{x}]^2 \\ &\quad + \frac{1}{2} \mathbf{x}' (P A + A' P) \mathbf{x} + (A \mathbf{x}_f)' P \mathbf{x} - \sum_{i=1}^m \frac{1}{r_i} [(\mathbf{x} - \mathbf{x}_f)' P B_i \mathbf{x}]^2 \\ &= \frac{1}{2} \mathbf{x}' (P A + A' P) \mathbf{x} + (A \mathbf{x}_f)' P \mathbf{x} \end{aligned} \quad (4.36)$$

Because $A \mathbf{x}_f = 0$ and P satisfies $P A + A' P = 0$, one can obtain $H(\mathbf{x}, \mathbf{u}^*) = 0$. Thus, the control law (Equation 4.27) is optimal and minimizes the performance index (Equation 4.25).

The proof of the theorem is completed. ■

Remarks on Theorem 4.3

1. J in Equation 4.25 is a generalized quadratic performance index in which the integral term $\frac{1}{2} \int_0^\infty \sum_{i=1}^m \frac{1}{r_i} [(\mathbf{x} - \mathbf{x}_f)' P B_i \mathbf{x}]^2 dt$ reflects the accumulation of state error in control systems, while the integral term $\frac{1}{2} \int_0^\infty \mathbf{u}' R \mathbf{u} dt$ reflects the consumption of control energy in the whole control process.

2. From the theorem-proving process, we can see that $PA + A'P = 0$ is very important to minimize the performance index (Equation 4.25). This equation is quite different to that obtained from the control systems in the macroscopic field, where the coefficient matrix A is a Hurwitz matrix, P satisfies the Lyapunov function $PA + A'P = -Q$, and Q is a positive definite symmetric matrix. However, the research objective here is a quantum system in the microscopic field, in which the Hamiltonian operator is a Hermitian operator. After transforming the system equation to real state-space, the coefficient matrix A of the system is a skew symmetric matrix that satisfies $A + A' = 0$. Hence, the positive definite symmetric matrix P must satisfy $PA + A'P = 0$.
3. The selection of the Lyapunov function is not unique, thus the optimal control law obtained by the method in this subsection is not unique either. As long as a proper Lyapunov function $V(\mathbf{x})$ is selected, under the precondition of $\dot{V}(\mathbf{x}) \leq 0$, the control law can be obtained to ensure the controlled system is stable.
4. In the optimal control law and performance index obtained by Theorem 15, the weighting matrix R can be selected independently, while the positive definite matrix P is defined by Equation 4.26.

In the following we will give the optimal control law design steps based on Theorem 4.3.

1. Select the weighting on the control vector:

$$R = \text{diag}(r_i), r_i > 0, i = 1, 2, \dots, m$$

2. Solve Equation 4.26 for a positive definite matrix P .
3. Obtain the optimal stabilizing control law from Equation 4.27.

4.3.3 Simulation Experiments and the Results Comparisons

In order to illustrate the effectiveness of the method proposed in this subsection, numerical simulation experiments will be given. Here, we select the spin-1/2 particle system as the controlled system. Suppose that the spin-1/2 particle system is controlled by only one control field u_1 , which is the electromagnetic field in the y -direction. The particle is self-spin in σ_z . The system satisfies the following Schrödinger equation:

$$i|\psi\rangle = (H_0 + H_1 u_1)|\psi\rangle \quad (4.37)$$

where $H_0 = \sigma_z = \begin{bmatrix} 1 & 0 \\ 0 & -1 \end{bmatrix}$ and $H_1 = \sigma_y = \begin{bmatrix} 0 & -i \\ i & 0 \end{bmatrix}$. After introducing ω , Equation 4.37 can be written as

$$i|\psi\rangle = (H_0 + H_1 u_1 + \omega I)|\psi\rangle \quad (4.38)$$

where $\omega = -\lambda_f$, which is a constant.

Now assume that the initial state of the system is $|\psi_0\rangle = |0\rangle = [1 \ 0]^T$ and the desired final state is $|\psi_f\rangle = |1\rangle = [0 \ 1]^T$.

For Equation 4.38, let $|\psi\rangle = [x_1 + ix_3 \ x_2 + ix_4]^T$, then $|C_1|^2 = x_1^2 + x_3^2$ and $|C_2|^2 = x_2^2 + x_4^2$. The following state equation about the real vector \mathbf{x} can be obtained:

$$\dot{\mathbf{x}} = (A + B_1 u_1(t))\mathbf{x}$$

where $A = \begin{bmatrix} 0 & 0 & 2 & 0 \\ 0 & 0 & 0 & 0 \\ -2 & 0 & 0 & 0 \\ 0 & 0 & 0 & 0 \end{bmatrix}$, $B_1 = \begin{bmatrix} 0 & -1 & 0 & 0 \\ 1 & 0 & 0 & 0 \\ 0 & 0 & 0 & -1 \\ 0 & 0 & 1 & 0 \end{bmatrix}$, $\mathbf{x}_0 = [1 \ 0 \ 0 \ 0]'$, and $\mathbf{x}_f = [0 \ 1 \ 0 \ 0]'$. The performance index is $J = \frac{1}{2} \int_0^\infty \left\{ \frac{1}{r_1} [(\mathbf{x} - \mathbf{x}_f)' P B_1 \mathbf{x}]^2 + r_1 u_1^2 \right\} dt$, according to Equation 4.27, and the optimal control law can be obtained:

$$u_1^* = -\frac{1}{r_1} (\mathbf{x} - \mathbf{x}_f)' P B_1 \mathbf{x} \quad (4.39)$$

where P is a positive definite symmetric matrix that satisfies the equation $PA + A'P = 0$ and the solution of the equation is not unique.

Before the simulation experiment, we first study the influence of parameters P and r_1 in Equation 4.39. The control law with parameters P_0 and r_{01} is $u_{01} = -\frac{1}{r_{01}} (\mathbf{x} - \mathbf{x}_f)' P_0 B_1 \mathbf{x}$, where P_0 satisfies $P_0 A + A' P_0 = 0$. Let $r_{11} = \alpha r_{01}$ and $P_1 = \alpha P_0$, where $\alpha > 0$, hence P_1 satisfies $P_1 A + A' P_1 = 0$. Consequently, the control law with parameters P_1 and r_{11} is

$$u_{11} = -\frac{1}{r_{11}} (\mathbf{x} - \mathbf{x}_f)' P_1 B_1 \mathbf{x} = -\frac{1}{\alpha r_{01}} (\mathbf{x} - \mathbf{x}_f)' \alpha P_0 B_1 \mathbf{x} \quad (4.40)$$

from which one can see that multiplying P and r_1 by the same factor yields the same control law, so we only consider the influence of P here. In the simulation experiments, with sampling time $T = 0.01$ seconds and $r_1 = 1$, parameter P is adjusted by different values. When $|C_2|^2 = 0.995$, the simulation results are shown in Table 4.1. From Table 4.1 one can see that: (i) increasing all the elements in P simultaneously, the transfer time can be shorted, but the control variable and the performance index increase, that is, the consumptive control energy is increased, and (ii) if only some elements are increased in P , such as the third and fourth experiments in Table 4.1, both $|C_1|$ and $|C_2|$ will be affected because of the non-linear characteristic of the control law in Equation 4.40.

Accordingly, we can select P under the condition of $PA + A'P = 0$, and then realize the state transformation faster with a smaller control variable. In our simulation experiments, combining the transfer time and the performance index, we get the best result when $P = \text{diag}(2, 1, 2, 1)$. The shortest transfer time is 3.69 seconds, and the corresponding performance

Table 4.1 Simulation results with a different value of P

No.	Parameter P	Range of u_1	Transfer time	Performance index J
1	$\text{diag}(1, 1, 1, 1)$	(-0.78, 1.00)	6.57	1.00
2	$\text{diag}(2, 2, 2, 2)$	(-0.98, 2.00)	3.47	2.00
3	$\text{diag}(2, 1, 2, 1)$	(-1.09, 1.10)	3.69	1.49
4	$\text{diag}(1, 2, 1, 2)$	(-0.79, 2.00)	6.06	1.51

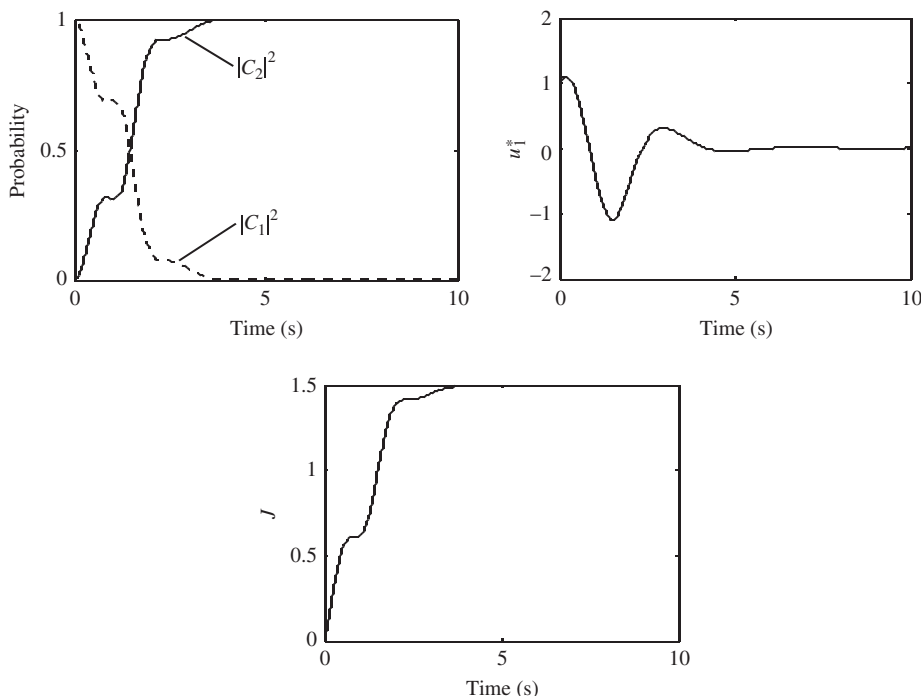


Figure 4.2 Simulation experimental results: (a) probability of the state's evolution, (b) control value of the system, and (c) performance index

index is 1.49. The simulation curves of the control system with $P = \text{diag}(2, 1, 2, 1)$ are shown in Figure 4.2a–c, in which Figure 4.2a shows the probability of the state evolution, Figure 4.2b shows the control variable u_1^* , and Figure 4.2c shows the performance index J . As can be seen from Figure 4.2, at any time $|C_1|^2 + |C_2|^2 = 1$ holds, that is, the probability is conservative. When the controlled state reaches the target state, the value of u_1^* tends to zero and stays at zero. The system state is also steady in the desired state. The value of J gradually increases with time, and it is almost unchanged with time when $t = 3.69$ seconds and $J = 1.49$, that is, the state transfer is finished.

4.4 Realization of the Quantum Hadamard Gate Based on the Lyapunov Method

The Hadamard gate is widely used in quantum computation (Shi, 2003). It is therefore one of the most important gates in quantum computation and is also a basic gate for performing quantum algorithms (Nielsen and Chuang, 2000). Any unitary operation can be approximated to arbitrary accuracy by means of a set of special gates, and the Hadamard gate is always in such a set. Many quantum algorithms use the Hadamard transform as a first step to initialize the state with random information. The function of the Hadamard gate as a one-bit gate is to put the un-superpositioned qubit into a superposition of basis states.

The aim of this section is to study the realization of the quantum Hadamard gate based on the spin of a single electron confined to a semiconductor quantum dot. Because the Hadamard gate cannot be realized by applying plane fields directly, we give the canonical form of the unitary rotation gate, which is possible by applying plane control fields first. The effect of the unitary rotation gate on the state can be realized by applying external tailored control fields. The Hadamard gate can then be decomposed into two canonical matrices which are feasible canonical forms. The two matrices correspond to rotate-operation and reflect-operation of the vector coordinates on the Bloch sphere, respectively. Thus the Hadamard gate can be realized in two steps by choosing appropriate control fields, so the realization of the Hadamard gate is to design external tailored control fields. Finally, the control fields which perform rotate-operation and reflect-operation are designed based on the Lyapunov stability theorem. Numerical simulation experiments and comparison results analysis are given for a specific example.

4.4.1 Mathematical Model

A qubit can be in a superposition of basis states and is defined in a two-dimensional space called Hilbert space, \mathcal{H} , which is spanned by a pair particular orthonormal basis $\{|0\rangle, |1\rangle\}$, that is:

$$\mathcal{H} = \text{span}\{|0\rangle, |1\rangle\} \quad (4.41)$$

Loss and Di Vincenzo first proposed this idea of using the spin states of individual electrons confined to semiconductor quantum dots as qubits, calling them spin qubits (Loss and DiVincenzo, 1997). Single qubit operations can be achieved by applying pulsed local electromagnetic fields to electrons in single quantum dots (Burkard, Loss, and DiVincenzo, 1999). The wave function of the electron confined to a quantum dot is

$$|\Psi(t)\rangle = \psi_1(t)|0\rangle + \psi_2(t)|1\rangle \quad (4.42)$$

in which $\psi_1(t)$ and $\psi_2(t)$ satisfy the normalization condition

$$|\psi_1(t)|^2 + |\psi_2(t)|^2 = 1 \quad (4.43)$$

The state $\Psi(t)$ satisfies the Schrodinger equation

$$\begin{cases} i\hbar |\Psi(t)\rangle = \mathbf{H}(t)|\Psi(t)\rangle, t > 0 \\ |\Psi(0)\rangle = |\Psi_0\rangle \in \mathcal{H} \end{cases} \quad (4.44)$$

where, \mathcal{H} is the Hilbert space in Equation 4.41 and $\mathbf{H}(t)$ is the Hamiltonian of the control system and can be written as:

$$\mathbf{H}(\mathbf{t}) = \hbar \cdot \boldsymbol{\Omega}(\mathbf{t}) \cdot \boldsymbol{\sigma} \quad (4.45)$$

where, $\boldsymbol{\Omega}(\mathbf{t})$ and $\boldsymbol{\sigma}$ are the external control field and the spin operator of the electron, respectively. $\boldsymbol{\Omega}(\mathbf{t})$ and $\boldsymbol{\sigma}$ are defined by Burkard, Engel, and Loss (2000):

$$\boldsymbol{\Omega}(\mathbf{t}) = \mu_B g(t) \mathbf{B}(t) \quad (4.46)$$

$$\boldsymbol{\sigma} = \sigma_x \mathbf{e}_x + \sigma_y \mathbf{e}_y + \sigma_z \mathbf{e}_z \quad (4.47)$$

where μ_B and $g(t)$ are the Bohr magneton and the effective g-factor, respectively, \mathbf{e}_x , \mathbf{e}_y , and \mathbf{e}_z are the unit vectors in directions of x , y , and z , and σ_x , σ_y , and σ_z are Pauli matrices.

4.4.2 Realization of the Quantum Hadamard Gate

1) Canonical form of the unitary rotation gate

The unitary rotation gate is a common form of a one-bit gate in atomic, molecular, and optical (AMO) devices and can be realized directly by applying plane control fields. The Hadamard gate cannot be realized by applying plane fields directly. In order to realize the Hadamard gate, one first needs to decompose it to several canonical forms of the unitary rotation gate and then realize these gates, which are put through decomposition by applying plane control fields. This can be done by selecting the following control field $\Omega(\mathbf{t})$ (Chen *et al.*, 2003):

$$\Omega(\mathbf{t}) = \Omega(t)\mathbf{e}(\varphi), t \in [0, T] \quad (4.48)$$

where the scalar control field $\Omega(t)$ and vector $\mathbf{e}(\varphi)$ satisfy:

$$\int_0^T \Omega(t)dt = \theta, \theta \in [0, 2\pi] \quad (4.49)$$

$$\mathbf{e}(\varphi) = \cos \varphi \cdot \mathbf{e}_x + \sin \varphi \cdot \mathbf{e}_y \quad (4.50)$$

Taking into account suppression of the unwanted effect of the Lorentz force, which produces an accumulated phase change, one can set the following constrained condition on the direction of the magnetic field:

$$\Omega(\mathbf{t}) \cdot \mathbf{e}_z = 0 \quad (4.51)$$

Substituting Equation 4.48 into Equation 4.45, the Hamiltonian of the system can be written as

$$\mathbf{H}(t) = \hbar \cdot \Omega(t)\mathbf{e}(\varphi) \cdot \boldsymbol{\sigma} \quad (4.52)$$

where

$$\mathbf{e}(\varphi) \cdot \boldsymbol{\sigma} = \begin{bmatrix} 0 & \cos \varphi - i \sin \varphi \\ \cos \varphi + i \sin \varphi & 0 \end{bmatrix} \stackrel{\Delta}{=} \tilde{\mathbf{H}}(\varphi) \quad (4.53)$$

Because of the commutation of the Hamiltonian in Equation 4.52 at different times, that is:

$$\begin{aligned} [\mathbf{H}(t_1), \mathbf{H}(t_2)] &= [\hbar \cdot \Omega(t_1)\mathbf{e}(\varphi) \cdot \boldsymbol{\sigma}, \hbar \cdot \Omega(t_2)\mathbf{e}(\varphi) \cdot \boldsymbol{\sigma}] \\ &= \hbar \cdot \Omega(t_1)\Omega(t_2)[\mathbf{e}(\varphi) \cdot \boldsymbol{\sigma}, \mathbf{e}(\varphi) \cdot \boldsymbol{\sigma}] \\ &= 0 \end{aligned} \quad (4.54)$$

on the basis of Equation 4.52, the time evolution operator of the quantum system $\mathbf{U}(T)$ will be (Nejad and Mehmandoost, 2010)

$$\begin{aligned} \mathbf{U}(T) &= e^{-i \int_0^T \mathbf{H}(t)dt / \hbar} \\ &= e^{-i\theta \mathbf{e}(\varphi) \cdot \boldsymbol{\sigma}} \end{aligned} \quad (4.55)$$

In the case that the eigenvalues of Equation 4.53 are ± 1 , the time evolution operator of the system becomes

$$\begin{aligned}\mathbf{U}(T) &= \frac{1}{2}e^{-i\theta}[1 + \tilde{\mathbf{H}}(\varphi)] + \frac{1}{2}e^{i\theta}[1 - \tilde{\mathbf{H}}(\varphi)] \\ &= \begin{bmatrix} \cos \theta & -ie^{-i\varphi} \sin \theta \\ -ie^{i\varphi} \sin \theta & \cos \theta \end{bmatrix} \\ &= \mathbf{U}(\theta, \varphi)\end{aligned}\quad (4.56)$$

which is the canonical form of the unitary rotation gate and is possible by applying plane control fields. According to parameters θ and φ , Equation 4.56 can be decomposed into:

$$\mathbf{U}(T) = \begin{bmatrix} 1 & 0 \\ 0 & e^{i\varphi} \end{bmatrix} \begin{bmatrix} \cos \theta & i \sin(-\theta) \\ i \sin(-\theta) & \cos(\theta) \end{bmatrix} \begin{bmatrix} 1 & 0 \\ 0 & e^{-i\varphi} \end{bmatrix} \quad (4.57)$$

From the right-hand side of Equation 4.57, one can see that the time evolution operator $\mathbf{U}(T)$ is composed of three matrices from left to right. The behaviors that are shown by these three matrices in the Bloch sphere are as follows: the first and third matrices make the qubit state on the Bloch sphere rotate by φ and $-\varphi$ around the z -axis, respectively, and the second matrix makes the qubit state on the Bloch sphere rotate by -2θ around the x -axis.

2) Realization process of the Hadamard gate

The quantum Hadamard gate, which is a one-input, one-output gate, causes a rotation followed by a reflection of the Bloch sphere representation of the qubit state, known as rotate-operation and reflect-operation, respectively (Nejad and Mehmundoost, 2010). Here, a simple example of the Hadamard operation is the input state of the Hadamard gate, $\frac{1}{\sqrt{2}}(|0\rangle + |1\rangle)$. In the first step under the effect of the evolution operator Equation 4.57, the input state is rotated by $\frac{\pi}{2}$ around the z -axis, then rotated by $-\frac{\pi}{2}$ around the x -axis and finally gets to state $|1\rangle$ by rotating $-\frac{\pi}{2}$ around the z -axis. The effects of all operations are equivalent to from the state $\frac{1}{\sqrt{2}}(|0\rangle + |1\rangle)$ around the y -axis rotation angle of $\frac{\pi}{2}$ to the state $|1\rangle$ on the Bloch sphere, so the operations in this step are collectively referred to as rotate-operation. In the second step operation, state $|1\rangle$ is rotated by 0 around the z -axis, then rotated by $-\pi$ around the x -axis and finally gets to state $|0\rangle$ by rotating 0 around the z -axis. The effects of all operations are equivalent to from the state $|1\rangle$ through the $x-y$ plane reflection to $|0\rangle$ on the Bloch sphere, so the operations in this step are collectively referred to as reflect-operation. This example illustrates the conclusion that the Hadamard operation is just a rotation of the sphere about the y -axis by $\frac{\pi}{2}$, followed by a rotation about the x -axis by π (Nielsen and Chuang, 2000). The Hadamard gate is mainly used for transforming a basis state into the superposition of basis states.

The matrix operator of the Hadamard gate is given by:

$$\mathbf{U}_H = \begin{bmatrix} \frac{1}{\sqrt{2}} & \frac{1}{\sqrt{2}} \\ \frac{1}{\sqrt{2}} & -\frac{1}{\sqrt{2}} \end{bmatrix} \quad (4.58)$$

Comparing Equation 4.58 with Equation 4.56, one can see that the Hadamard gate cannot be realized by using Equation 4.56 directly, but Equation 4.58 can be decomposed into two canonical matrices in the form of Equation 4.56, and the Hadamard gate can then be realized in two-step operations by choosing appropriate control fields. In the first step, the control field Ω_1 is chosen in direction of y and satisfies

$$\int_0^{T_m} \Omega_1(t) dt = \frac{\pi}{4} \quad (4.59)$$

which means that rotate-operation is realized in time interval $[0, T_m]$ using Ω_1 . According to Equations 4.59 and 4.56, the unitary rotation gate realized by applying Ω_1 will be

$$\mathbf{U}_1 = \begin{bmatrix} \frac{1}{\sqrt{2}} & -\frac{1}{\sqrt{2}} \\ \frac{1}{\sqrt{2}} & \frac{1}{\sqrt{2}} \end{bmatrix} = \mathbf{U}\left(\frac{\pi}{4}, \frac{\pi}{2}\right) \quad (4.60)$$

In the second step, the control field Ω_2 is chosen in the direction of x and satisfies

$$\int_{T_m}^T \Omega_2(t) dt = \frac{\pi}{2} \quad (4.61)$$

which means that reflect-operation is realized in time interval $[T_m, T]$ using Ω_2 . According to Equations 4.61 and 4.56, the unitary rotation gate realized by applying Ω_2 will be

$$\mathbf{U}_2 = \begin{bmatrix} 0 & -i \\ -i & 0 \end{bmatrix} = \mathbf{U}\left(\frac{\pi}{2}, 0\right) \quad (4.62)$$

The synthetic matrix of \mathbf{U}_1 and \mathbf{U}_2 is the Hadamard gate with an unwanted phase factor, that is:

$$\mathbf{U}_2 \cdot \mathbf{U}_1 = \mathbf{U}\left(\frac{\pi}{2}, 0\right) \cdot \mathbf{U}\left(\frac{\pi}{4}, \frac{\pi}{2}\right) = e^{-i\frac{\pi}{2}} \cdot \begin{bmatrix} \frac{1}{\sqrt{2}} & \frac{1}{\sqrt{2}} \\ \frac{1}{\sqrt{2}} & -\frac{1}{\sqrt{2}} \end{bmatrix} = e^{-i\frac{\pi}{2}} \cdot \mathbf{U}_H \quad (4.63)$$

Because \mathbf{U}_1 and \mathbf{U}_2 can be realized by applying Ω_1 and Ω_2 , respectively, the quantum Hadamard gate is realized.

4.4.3 Design of Control Fields

Consider a control system described by the Schrodinger equation

$$\begin{cases} i\hbar |\Psi(t)\rangle = H(\Omega(t))|\Psi(t)\rangle \\ |\Psi(0)\rangle = |\Psi_0\rangle \end{cases} \quad (4.64)$$

where $\mathbf{H}(\Omega(t)) = \hbar \cdot \tilde{\mathbf{H}}(\varphi)\Omega(t)$.

The realization of the Hadamard gate is to design control fields that drive the system from an initial state $|\Psi_0\rangle$ to a desired final state $|\Psi_T\rangle$, in which $|\Psi_0\rangle$ and $|\Psi_T\rangle$ satisfy

$$|\Psi_T\rangle = \mathbf{U}_H |\Psi_0\rangle \quad (4.65)$$

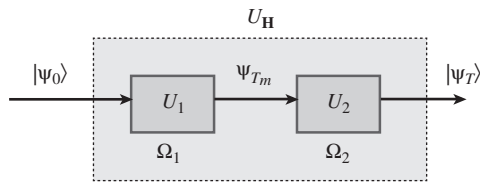


Figure 4.3 Schematic diagram of the realization process

According to the realization process of the Hadamard gate proposed in Section 4.4.2, the matrix operator of the Hadamard gate is first decomposed into the matrix operators in Equations 4.60 and 4.62, which can be realized using plane control fields directly, then the matrix operator \mathbf{U}_1 in Equation 4.60 can be realized by the control field Ω_1 in the direction of y , and the matrix operator \mathbf{U}_2 in Equation 4.62 can be realized by the control field Ω_2 in the direction of x , that is, for a given initial state $|\psi_0\rangle$. \mathbf{U}_1 transfers the state from $|\psi_0\rangle$ to the intermediate state $|\psi_{T_m}\rangle$ in time interval $[0, T_m]$, then \mathbf{U}_2 transfers the state from $|\psi_{T_m}\rangle$ to the final state $|\psi_T\rangle$ in time interval $[T_m, T]$. The schematic diagram of the realization process is shown in Figure 4.3.

According to Equation 4.55, \mathbf{U}_1 and \mathbf{U}_2 are

$$\begin{aligned} \mathbf{U}_1 &= e^{-i\sigma_y \int_0^{T_m} \Omega_1 dt} = e^{-i\sigma_y \cdot \frac{\pi}{4}} \\ \mathbf{U}_2 &= e^{-i\sigma_x \int_0^{T-T_m} \Omega_2 dt} = e^{-i\sigma_x \cdot \frac{\pi}{2}} \end{aligned} \quad (4.66)$$

Thus \mathbf{U}_1 and \mathbf{U}_2 can be realized as long as control fields Ω_1 and Ω_2 satisfy Equations 4.59 and 4.61, respectively. The realization of the Hadamard gate is then to design control fields Ω_1 and Ω_2 in which Ω_1 is used to drive the initial state $|\psi_0\rangle$ to the intermediate state $|\psi_{T_m}\rangle$ first, and then Ω_2 is used to drive $|\psi_{T_m}\rangle$ to the final state $|\psi_T\rangle$. $|\psi_0\rangle$, $|\psi_{T_m}\rangle$, and $|\psi_T\rangle$ satisfy Equation 4.65 and have the following relationships:

$$|\psi_{T_m}\rangle = \mathbf{U}_1 |\psi_0\rangle \quad (4.67)$$

$$|\psi_T\rangle = \mathbf{U}_2 |\psi_{T_m}\rangle \quad (4.68)$$

There are many control fields methods in which the Lyapunov method is adapted to time-varying and non-linear systems, and the control fields can ensure the stability of the controlled system. The Lyapunov method is therefore used to design the control fields Ω_1 and Ω_2 here. The idea of the Lyapunov method is to choose a suitable Lyapunov function V and then design a control by making V monotonically decrease along any dynamical evolution of the control system. For the convenience of the analysis and calculation, we use the real state-space to describe the quantum system. In order to get the real state equation of Equation 4.64, we separate the real part and the imaginary part of the state variables of Equation 4.64. Let $|\psi\rangle = [x_1 + ix_3 \quad x_2 + ix_4]^T$, because the real part and the imaginary part on each side of Equation 4.64 are respectively equal, and the equation of the real vector

$\mathbf{x} = [x_1 \ x_2 \ x_3 \ x_4]^T$ can be obtained as

$$\dot{\mathbf{x}}(t) = \mathbf{B}\Omega(t)\mathbf{x}(t) \quad (4.69)$$

where $\mathbf{B} = \begin{bmatrix} \Im(\tilde{\mathbf{H}}(\varphi)) & \Re(\tilde{\mathbf{H}}(\varphi)) \\ -\Re(\tilde{\mathbf{H}}(\varphi)) & \Im(\tilde{\mathbf{H}}(\varphi)) \end{bmatrix}$ and \Im and \Re represent the real and imaginary parts, respectively. Select the following Lyapunov function:

$$V(\mathbf{x}) = \frac{1}{2} \cdot (\mathbf{x} - \mathbf{x}_f)^T \mathbf{P} (\mathbf{x} - \mathbf{x}_f) \quad (4.70)$$

where \mathbf{P} is a positive definite symmetric matrix, so $V(\mathbf{x})$ is non-negative. The first-order derivative of $V(\mathbf{x})$ is:

$$\dot{V}(\mathbf{x}) = (\mathbf{x} - \mathbf{x}_f)^T \mathbf{P} \dot{\mathbf{x}} = (\mathbf{x} - \mathbf{x}_f)^T \mathbf{P} \mathbf{B} \Omega(t) \mathbf{x} \quad (4.71)$$

In order for the first-order derivative of $V(\mathbf{x})$ to be non-positive, choose the following control field:

$$\Omega(t) = -k(\mathbf{x} - \mathbf{x}_f)^T \mathbf{P} \mathbf{B} \mathbf{x}, k > 0 \quad (4.72)$$

Substituting Equation 4.72 into Equation 4.71, one has:

$$\dot{V}(\mathbf{x}) = -k[(\mathbf{x} - \mathbf{x}_f)^T \mathbf{P} \mathbf{B} \mathbf{x}]^2 \leq 0 \quad (4.73)$$

in which $\dot{V}(\mathbf{x}) = 0$ when $\mathbf{x} = \mathbf{x}_f$.

Let \mathbf{x} and \mathbf{x}_f be the real vectors that are obtained by separating the real and imaginary parts of $|\psi\rangle$ and $|\psi_{T_m}\rangle$, respectively. Ω_1 can be obtained by Equation 4.72, in which \mathbf{B} is composed of $\tilde{\mathbf{H}}(\varphi)$, which makes $\mathbf{U} = \mathbf{U}_1$. Then, let \mathbf{x} and \mathbf{x}_f be the real vectors that are obtained by separating the real and imaginary parts of $|\psi\rangle$ and $|\psi_T\rangle$, respectively. \mathbf{B} is composed by $\tilde{\mathbf{H}}(\varphi)$, which makes $\mathbf{U} = \mathbf{U}_2$, and Ω_2 can be obtained by Equation 4.72. Ω_1 and Ω_2 are therefore both obtained by Equation 4.72 and can be used to realize \mathbf{U}_1 and \mathbf{U}_2 , respectively, and then realize the Hadamard gate.

4.4.4 Numerical Simulations and Comparison Results Analyses

A specific numerical simulation will be used here to illustrate the effectiveness of the control fields proposed in this subsection. The input of the Hadamard gate is $\frac{1}{\sqrt{2}}(|0\rangle + |1\rangle)$. The first step operation is the rotate-operation, in which the input state is rotated by $\frac{\pi}{2}$ around the y-axis on the Bloch sphere to state $|1\rangle$, and the second step operation is the reflect-operation, in which $|1\rangle$ is reflected by the x - y plane to state $|0\rangle$ on the Bloch sphere. The rotate-operation in which the initial state and final state are $\frac{1}{\sqrt{2}}(|0\rangle + |1\rangle)$ and $|1\rangle$ realizes the matrix operator $\mathbf{U}_1 =$

$$\begin{bmatrix} \frac{1}{\sqrt{2}} & -\frac{1}{\sqrt{2}} \\ \frac{1}{\sqrt{2}} & \frac{1}{\sqrt{2}} \end{bmatrix} = \mathbf{U} \left(\frac{\pi}{4}, \frac{\pi}{2} \right), \text{ which is in accord with Equation 4.56, that is, } |1\rangle = \mathbf{U}_1 \cdot \frac{1}{\sqrt{2}}(|0\rangle +$$

$|1\rangle$), and one can get $\tilde{\mathbf{H}}(\varphi) = \tilde{\mathbf{H}}\left(\frac{\pi}{2}\right) = \begin{bmatrix} 0 & -i \\ i & 0 \end{bmatrix}$ on the basis of Equation 4.53. In this step, the control field (Equation 4.72) has the parameters $k = 0.21$, $\mathbf{P} = \text{diag}(2.5, 0.01, 2.5, 1)$, and

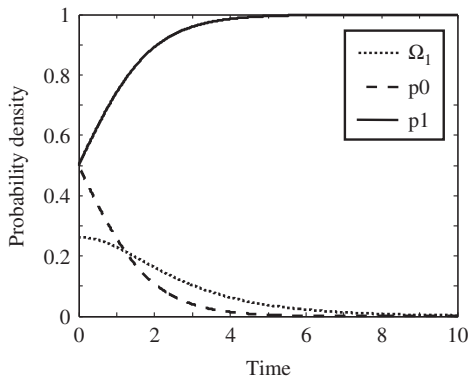


Figure 4.4 Rotate-operation

$\mathbf{x}_f = [0 \ 1 \ 0 \ 0]^T$. The simulation results are shown in Figure 4.4, in which p_0 is the probability density of the basis state $|0\rangle$ and p_1 is the probability density of the basis state $|1\rangle$.

It can be seen from Figure 4.4 that the probability density of state $|1\rangle$ tends to 1 from 0.5 and the probability density of state $|0\rangle$ tends to 0 from 0.5 under the control field. It means that the spin state turns into the intermediate state $|1\rangle$ from the initial state $\frac{1}{\sqrt{2}}(|0\rangle + |1\rangle)$. The reflect-operation for which the initial state and final state are $|1\rangle$ and $|0\rangle$ realize the matrix operator $\mathbf{U}_2 = \begin{bmatrix} 0 & -i \\ -i & 0 \end{bmatrix} = \mathbf{U}\left(\frac{\pi}{2}, 0\right)$, which is in accord with Equation 4.56, that is, $|0\rangle = \mathbf{U}_2 \cdot |1\rangle$, and one can get $\tilde{\mathbf{H}}(\varphi) = \tilde{\mathbf{H}}(0) = \begin{bmatrix} 0 & 1 \\ 1 & 0 \end{bmatrix}$ on the basis of Equation 4.53.

The control field of this step is in the form of Equation 4.72, with the parameters $k = 0.12$, $\mathbf{P} = \text{diag}(10, 9, 0.5, 1)$, and $\mathbf{x}_f = [1 \ 0 \ 0 \ 0]^T$. The simulation results are shown in Figure 4.5, in which one can see that the probability density of state $|1\rangle$ tends to 0 from 1 and the probability density of the state $|0\rangle$ tends to 1 from 0 under the control field.

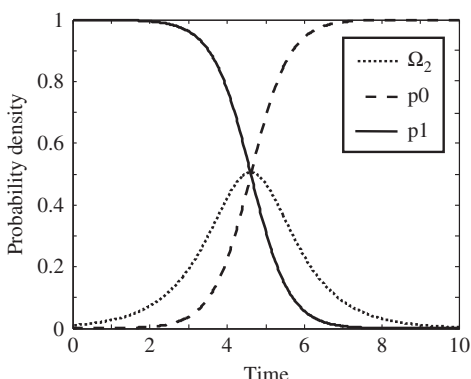


Figure 4.5 Reflect-operation

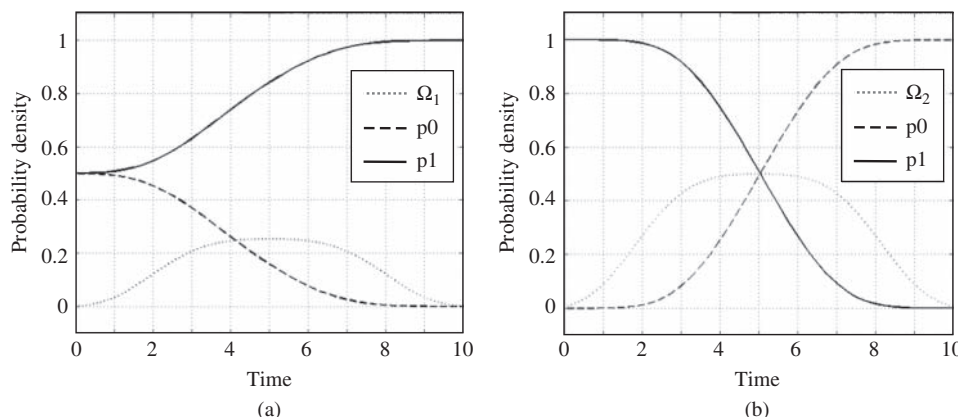


Figure 4.6 Simulation results from Nejad and Mehmandoost (2010). (a) Rotate-operation, (b) Reflect-operation

This means that the spin state turns into the final state $|0\rangle$ from the intermediate state $|1\rangle$. On the whole, the spin state is driven to $|0\rangle$ from $\frac{1}{\sqrt{2}}(|0\rangle + |1\rangle)$ under the control fields Ω_1 and Ω_2 , which is equivalent to the effect of the quantum Hadamard gate. Nejad and Mehmandoost also proposed the quantum Hadamard gate in 2010 and their simulation results are shown in Figure 4.6. The control fields proposed in this subsection have explicit mathematical expression compared with Nejad and Mehmandoost's simulation results.

References

- Altafini, C. (2007) Feedback stabilization of isospectral control systems on complex flag manifolds: application to quantum ensembles. *IEEE Transactions on Automatic Control*, **52**(11), 2019–2028.
- Athans, M. and Falb, P.L. (1966) *Optimal Control*, McGraw-Hill, New York.
- Benallou, A., Mellichamp, D.A. and Seborg, D.E. (1988) Optimal stabilizing controllers for bilinear systems. *International Journal of Control*, **48**(4), 1487–1501.
- Burkard, G., Engel, H. and Loss, D. (2000) Spintronics and quantum dots for quantum computing and quantum communication, in *Complexity from Microscopic to Macroscopic Scales: Coherence and Large Deviations*, vol. **63**, Kluwer Academic Publishers, pp. 83–104.
- Burkard, G., Loss, D. and DiVincenzo, D.P. (1999) Coupled quantum dots as quantum gates. *Physical Review B*, **59**(3), 2070–2078.
- Chen, G., Church, D.A., Englert, B.G. et al. (2003) Mathematical models of contemporary elementary quantum computing devices. *RM Proceedings and Lecture Notes*, **33**, 79–118.
- Cong, S. and Kuang, S. (2007) Quantum control strategy based on state distance. *Acta Automatica Sinica*, **33**(1), 28–31.
- Cong, S. and Zhang, Y.Y. (2008) Superposition state preparation based on Lyapunov stability theorem in quantum systems. *Journal of University of Science and Technology of China*, **38**(7), 821–827.
- Cong, S. and Zhang, Y.Y. (2009) Lyapunov-based optimal quantum pure state control strategy. International Conference on Automation, Robotics and Control Systems, Florida, pp. 89–96.
- D'Alessandro, D. and Dahleh, M. (2001) Optimal control of two-level quantum systems. *IEEE Transaction on Automatic Control*, **46**(6), 866–876.

- Ferrante, A., Pavon, M., and Raccanelli, G. (2002a) Driving the propagator of a spin system: a feedback approach. Proceedings of the 41st IEEE Conference on Decision and Control, Las Vegas, Nevada, Vol. 1, pp. 46–50.
- Ferrante, A., Pavon, M., and Raccanelli, G. (2002b) Control of quantum systems using model-based feedback strategies. 15th International Symposium on Mathematical Theory of Networks and Systems, Indiana, pp. 1–9.
- Grivopoulos, S. and Bamieh, B. (2003) Lyapunov-based control of quantum systems. Proceedings of the 42nd IEEE Conference on Decision and Control, Maui, pp. 434–438.
- Jing, X.G. (2004) *Quantum Mechanics*, Harbin Institute of Technology Press, Harbin.
- Kuang, S. and Cong, S. (2008) Lyapunov control methods of closed quantum systems. *Automatica*, **44**(1), 98–108.
- Loss, D. and DiVincenzo, D.P. (1997) Quantum computation with quantum dots. *Physical Review A*, **57**(1), 120–126.
- Mirrahimi, M. and Rouchon, P. (2004) Trajectory tracking for quantum systems: a Lyapounov approach. Proceedings of the International Symposium MTNS, Leuven, Belgium.
- Mirrahimi, M., Rouchon, P. and Turinici, G. (2005) Lyapunov control of bilinear Schrödinger equations. *Automatica*, **41**(11), 1987–1994.
- Mirrahimi, M., Turinici, G. and Rouchon, P. (2005) Reference trajectory tracking for locally designed coherent quantum controls. *Journal of Physical Chemistry A*, **109**(11), 2631–2637.
- Nejad, S.M. and Mehmandoost, M. (2010) Realization of quantum Hadamard gate by applying optimal control fields to a spin qubit. 2nd International Conference on Mechanical and Electronics Engineering, Vol. 2, pp. 292–296.
- Nielsen, M.A. and Chuang, I.L. (2000) *Quantum Computation and Quantum Information*, Cambridge University Press, Cambridge.
- Paolo, V. (2002). On the convergence of a feedback control strategy for multilevel quantum systems. In Fifteenth International Symposium MTNS'2002, 1–10.
- Shi, Y. (2003) Both Toffoli and Controlled-NOT need little help to do universal quantum computation. *Quantum Information and Computation*, **3**, 84–92.
- Shi, S. and Rabitz, H. (1990) Quantum mechanical optimal control of physical observables in microsystems. *Journal of Chemical Physics*, **92**(1), 364–376.
- Sugawara, M. (2002) Local control theory for coherent manipulation of population dynamics. *Chemical Physics Letters*, **358**(3–4), 290–297.
- Sugawara, M. (2003) General formulation of locally designed coherent control theory for quantum system. *Journal of Chemical Physics*, **118**(15), 6784–6801.
- Wang, X. and Schirmer, S. (2010a) Analysis of Lyapunov method for control of quantum states. *IEEE Transactions on Automatic Control*, **55**(10), 2259–2270.
- Wang, X. and Schirmer, S. (2010b) Analysis of effectiveness of Lyapunov control for non-generic quantum states. *IEEE Transactions on Automation Control*, **55**(6), 1406–1411.
- Zhang, Y.Y. and Cong, S. (2008) Quantum control of nuclear wave packets by locally designed optimal pulses. *Journal of University of Science and Technology of China*, **38**(3), 331–336.
- Zhu, W. and Rabitz, H. (1998) A rapid monotonically convergent iteration algorithm for quantum optimal control over the expectation value of a positive definite operator. *Journal of Chemical Physics*, **109**(2), 385–392.

5

Population Control Based on the Lyapunov Method

5.1 Population Control of Equilibrium State

5.1.1 Preliminary Notions

Population control can be regarded as a particular state control, and it is of fundamental importance in quantum chemistry and quantum computation. So far, for the population control of quantum states several different strategies have emerged, for example optimal control (Shi and Rabitz, 1990; Werschnik and Gross, 2007), adiabatic control (Shapiro *et al.*, 2007), factorization techniques of the unitary group (Schirmer *et al.*, 2002), the Lyapunov method (Grivopoulos and Bamieh, 2003; Sugawara, 2003; Mirrahimi, Rouchon, and Turinici, 2005; Mirrahimi, Turinici, and Rouchon, 2005; Beaucharda *et al.*, 2007; Cong and Kuang, 2007; Kuang and Cong, 2008; Wang and Schirmer, 2009; Altafini, 2007), methods based on adaptive tracking (Sugawara *et al.*, 2007) and system decomposition (D'Alessandro, 2007), and so on.

Consider an N -level quantum system and assume that it is operator controllable:

$$\dot{\rho}(t) = -i \left[H_0 + \sum_{k=1}^m H_k u_k(t), \rho(t) \right], \quad \rho_0 = \rho(0) \quad (5.1)$$

where $\rho(t)$ is the density operator, H_0 is the inner Hamiltonian of the system, $u_k(t)$ is an applied real-valued control field, and H_k is the control Hamiltonian caused by the interaction between $u_k(t)$ and the system. Both H_0 and H_k are independent of time. We work in an orthonormal basis of energy eigenvectors, so ρ , H_0 , and H_k will take on the corresponding $N \times N$ matrix forms and H_0 is diagonal.

The system described by Equation 5.1 is closed and its evolution is unitary, so whatever values $u_k(t)$ takes, $\rho(t)$ and ρ_0 have the same spectrum. This is a necessary condition satisfied by any reachable state of ρ_0 .

In physics, the eigenvalues λ_j ($j = 1, 2, \dots, N$) of $H_0 = \text{diag}(\lambda_1, \lambda_2, \dots, \lambda_N)$ represent all the possible energy levels of the system, while $\omega_{jl} = \lambda_j - \lambda_l$ represents the Bohr frequency (transition frequency) between the energy levels λ_j and λ_l . Furthermore, we assume the following concepts. If all the energy levels of a quantum system are mutually different, then

the system is called non-degenerate. If all the Bohr frequencies of a quantum system are mutually different, then the system is called transitionally non-degenerate. If there exists $k' \in (1, 2, \dots, m)$ such that $(H_{k'})_{jl} \neq 0$ holds, then the energy-level pair (j, l) admits a direct transition and is called directly coupled. If for two arbitrary energy levels there exists a path connecting them via a series of direct transitions, then the system is called connected. If two arbitrary energy levels admit a direct transition, then the system is called fully connected. Furthermore, we call ρ satisfying $[H_0, \rho] = 0$ an equilibrium state of Equation 5.1, denoted by ρ_e .

This section assumes that the system under consideration is transitionally non-degenerate and connected.

5.1.2 Control Laws Design

The control goal is to design the control laws $u_k(t)$ via the Lyapunov method such that the system Equation 5.1 starts transits with a high probability from an initial state ρ_0 to the population of some equilibrium state ρ_f isospectral to ρ_0 .

Consider the Lyapunov function:

$$V(\rho) = \text{tr}(P\rho) \quad (5.2)$$

where P is a positive definite Hermitian operator to be constructed and can be regarded as an imaginary mechanical quantity. Mathematically, $V(\rho)$ is a tracing operation and represents the average value of P .

Now, we will design control laws by guaranteeing the monotonic decreasing of the Lyapunov function (Equation 5.2). Calculating the first-order time derivative of Equation 5.2, one has:

$$\dot{V}(\rho) = -i\text{tr}([P, H_0]\rho) - i \sum_{k=1}^m \text{tr}([P, H_k]\rho)u_k \quad (5.3)$$

Taking into account the independence of the first item on the right-hand side of Equation 5.3, let:

$$[P, H_0] = 0 \quad (5.4)$$

To ensure $\dot{V}(\rho) \leq 0$, one can design:

$$u_k = i\varepsilon_k \text{tr}([P, H_k]\rho), k = 1, \dots, m \quad (5.5)$$

where $\varepsilon_k > 0$ and is used to adjust the amplitude of u_k .

Considering that the density operator ρ evolves in a unitary fashion, one can prove the following proposition about the Lyapunov function (Equation 5.2) and its extreme points via the tool of Lie algebra $su(N)$ (D'Alessandro, 2007):

Proposition 5.1 On the premise that ρ changes in a unitary fashion, if ρ is any extreme point of $V(\rho)$, then $[\rho, P] = 0$ holds; contrarily, if ρ satisfies $[\rho, P] = 0$, then ρ must be an extreme point of $V(\rho)$.

Furthermore, one can also easily prove the following proposition about P :

Proposition 5.2 If H_0 is non-degenerate and satisfies $[H_0, P] = 0$, then P is diagonal.

Remark 5.1 The system considered here is non-degenerate, so by replacing P in Proposition 5.2 with ρ , it can be shown that its equilibrium states are also diagonal.

5.1.3 Analysis of the Largest Invariant Set

Since the system Equation 5.1 with the control field (Equation 5.5) is autonomous, that is, the system Hamiltonian is independent of time, the LaSalle invariance principle can be used to analyze at time t_0 . Then, the following three conditions are equivalent:

$$\dot{V}(\rho(t_0)) = 0 \quad (5.6)$$

$$\text{tr}(\rho(t_0)[P, H_k] = 0), k = 1, \dots, m \quad (5.7)$$

$$u_k(t_0) = 0, k = 1, \dots, m \quad (5.8)$$

Remark 5.2 Since Equations 5.3–5.5 do not involve concrete initial states, Equations 5.6–5.8 represent all the extreme states during the evolving processes starting from all the initial states. From $\text{tr}(A[B, C]) = \text{tr}(C[A, B])$, Proposition 5.1 and Equation 5.6, it is easily known that the extreme points of the Lyapunov function (Equation 5.2) with respect to ρ must be in S .

For the largest invariant set E contained in S we have:

Theorem 5.1 Consider the control system Equation 5.1 with the control field (Equation 5.5) and the following three conditions: (a) $[P, H_0] = 0$, (b) the system is non-degenerate, that is, H_0 is a non-degenerate diagonal matrix, and (c) the system is transitionally non-degenerate. Then, the following three conclusions are true:

1. If (a) holds, then the largest invariant set E contained in S of the control system is $E = \{\rho(0) : \dot{V}(\rho(t)) = 0, t \in R\}$, where $\rho(t)$ ($t \in R$) is the trajectory of the control system associated with the initial state $\rho(0)$.
2. If both (a) and (b) simultaneously hold, then the largest invariant set in conclusion 1 reduces to $E = \{\rho(0) : \text{tr}(e^{iH_0 t} H_k e^{-iH_0 t} [\rho(0), P]) = 0, k = 1, \dots, m; t \in R\}$
3. If both (a) and (c) simultaneously hold, then the (l, j) -th element of the state $\rho(0)$ belonging to the largest invariant set in conclusion (2) satisfies $(H_k)_{jl}(p_l - p_j)\rho_{jl}(0) = 0$, ($j, l = 1, \dots, N; k = 1, \dots, m; j < l$)
where p_l and p_j are the l -th and j -th diagonal elements of P , respectively.

Proof See Section 5.1.6. ■

Remark 5.3 The three conclusions in Theorem 5.1 cover three classes of cases about the system itself: conclusion 1 imposes no restriction on the system, conclusion 2 requires the system to be non-degenerate, and conclusion 3 requires the system to be transitionally non-degenerate. It can be seen from the three conclusions that the expression of the states in the largest invariant set is more and more able to be analytically decided along with the gradual strengthening of the conditions on the system itself.

Remark 5.4 Conditions (b) and (c) are in fact the conditions possessed by the system itself. The system considered satisfies condition (c), and thereby condition (b), that is, the largest invariant sets in the three conclusions of Theorem 5.1 are fully consistent for the system. Thus, from Proposition 5.1 and conclusion 2 of Theorem 5.1, it follows that the extreme points of the Lyapunov function (Equation 5.2) with respect to ρ must also be in the largest invariant set E .

1) Bloch vector and convergent state set

Conclusion 3 of Theorem 5.1 shows that the characteristics of each element of any state are contained in the largest invariant set E . However, it is difficult to decide of which states E is composed. In fact, given an initial state ρ_0 , all the states to which the control system may converge are those contained in E and isospectral to ρ_0 . We call the set of such states the convergent state set of the control system, denoted by $E(\rho_0)$. To find $E(\rho_0)$ and achieve the convergence to the population of some equilibrium state by constructing P , it is necessary to further search for the explicit expression of the states in E . To do this, the Bloch vector representation of density matrices will be introduced.

2) Bloch vector framework of density matrices

Assume that H_N is the Hilbert space associated with an N -level quantum system and isomorphic to C^N . Then, the set of all the bounded linear operators that act on H_N and endowed with the following inner product forms a Hilbert space, called the Liouville space, denoted by $L(H_N)$:

$$\langle\langle A|B\rangle\rangle = \text{tr}(A^\dagger B) \quad (5.9)$$

The inner product defined by Equation 5.9 is also called the Hilbert–Schmidt inner product. One can select the identity matrix I_N and the following generators of group $SU(N)$ as an orthonormal basis of $L(H_N)$ (Schirmer, Zhang, and Leahy, 2004; Kimura, 2003):

$$\sigma_{jl}^x = |j\rangle\langle l| + |l\rangle\langle j|, 1 \leq j < l \leq N \quad (5.10)$$

$$\sigma_{jl}^y = -i(|j\rangle\langle l| - |l\rangle\langle j|), 1 \leq j < l \leq N \quad (5.11)$$

$$\sigma_j^z = \frac{\sqrt{2}}{\sqrt{j(j+1)}} \left(\sum_{n=1}^j |n\rangle\langle n| - j|j+1\rangle\langle j+1| \right), 1 \leq j \leq N-1 \quad (5.12)$$

where x , y , and z are used to distinguish different generators, and are analogous to the Pauli matrices along the directions x , y , and z in the case of two-level systems. For convenience, this basis is written as:

$$\begin{aligned} \{\sigma_s\}_{s=0}^{N^2-1} &= \{I_N\} \cup \{\sigma_s\}_{s=1}^{N^2-1} \\ &= \{I_N\} \cup \{\sigma_{jl}^x, \sigma_{jl}^y, \sigma_{jl}^z\} = \{I_N, \sigma_{jl}^x, \sigma_{jl}^y, \sigma_{jl}^z\} \end{aligned} \quad (5.13)$$

where $1 \leq j < l \leq N$ and $1 \leq j \leq N-1$.

The set of all the density matrices in $L(H_N)$ will form the so-called density matrix space, denoted by $L_1(H_N)$. Thus, any density matrix ρ in $L_1(H_N)$ can be expressed by the basis

Equation 5.13. In view of the intrinsic properties of density matrices, such an expression has a fixed form:

$$\begin{aligned}\rho &= \frac{I_N}{N} + \frac{1}{2} \sum_{s=1}^{N^2-1} \gamma_s \sigma_s \\ &= \frac{I_N}{N} + \frac{1}{2} \sum_{j < l} \gamma_{jl}^x \sigma_{jl}^x + \frac{1}{2} \sum_{j < l} \gamma_{jl}^y \sigma_{jl}^y + \frac{1}{2} \sum_{j=1}^{N-1} \gamma_j^z \sigma_j^z\end{aligned}\quad (5.14)$$

where $\gamma_s = \text{tr}(\rho \sigma_s)$ ($1 \leq s \leq N^2 - 1$), which can be verified using Equation 5.9 and the orthogonality of the basis Equation 5.13.

The vector $\gamma_s = [\gamma_1, \gamma_2, \dots, \gamma_{N^2-1}]^T$ is the Bloch vector of ρ . Obviously, it is a real-valued vector in R^{N^2-1} . The set of all the Bloch vectors forms the Bloch space of the system in R^{N^2-1} , denoted by $B(R^{N^2-1})$. In general, given some members of the basis Equation 5.13, one cannot generate ρ by taking an arbitrary γ in Equation 5.14. Alternatively, it should be obtained by taking γ in the Bloch space $B(R^{N^2-1})$. For any N -level quantum system, Kimura proved the following proposition on its Bloch space in 2003:

Proposition 5.3 Let $\alpha_v(\gamma)$ be the coefficients of the characteristic polynomial $\det(\eta I_N - \rho)$ with respect to ρ in Equation 5.14, and define

$$B(R^{N^2-1}) = \{\gamma \in R^{N^2-1} : \alpha_v(\gamma) \geq 0 (v = 1, \dots, N)\}$$

Then, the map:

$\gamma \in R^{N^2-1} \rightarrow \rho = \frac{1}{N} I_N + \frac{1}{2} \sum_{s=1}^{N^2-1} \gamma_s \sigma_s \in L_1(H_N)$ is a bijection from the Bloch space $B(R^{N^2-1})$ to the density matrix space $L_1(H_N)$.

Proposition 5.3 is important in theory, as it directly indicates a one-to-one correspondence between the density matrix space and the Bloch space of any N -level system. In particular, it can be calculated by Proposition 5.3 that the Bloch space of any two-level system is a well-known unit ball $B(R^3) = \{\gamma \in R^3 : |\gamma| \leq 1\}$ in R^3 .

3) Convergent state set of the control system

Conclusion 3 of Theorem 5.1 does not cover the case of $j = l$. In fact, for $j = l$, the expression in conclusion 3 naturally holds, so all the basis members of diagonal type, σ_j^z ($j = 1, \dots, N - 1$), will become the generators of the largest invariant set E . For $j \neq l$, it is known from the expression in conclusion 3 that if at least one of the following two conditions is satisfied:

$$\exists j', l' \in \{1, \dots, N\}, \text{s.t. } p_{l'} = p_{j'}, j' < l' \quad (5.15)$$

and

$$\exists j', l' \in \{1, \dots, N\}, \text{s.t. } (H_k)_{j' l'} = 0, k = 1, \dots, m, j' < l' \quad (5.16)$$

then

$$\rho_{l' j'}(0) \in C, j' < l' \quad (5.17)$$

Equation 5.17 means that the basis members $\sigma_{j'l'}^x$ and $\sigma_{j'l'}^y$ are also the generators of E . Generally, when the control Hamiltonians $H_k(k = 1, \dots, m)$ are given and P is determined beforehand, it is not difficult to find all the pairs of the basis members acting as the generators of E . Thus, E can be ultimately calculated via Equation 5.14. Accordingly, the following theorem is obtained.

Theorem 5.2 Consider the transitionally non-degenerate system Equation 5.1 with the control field (Equation 5.5). If $[P, H_0] = 0$, then any trajectory of the control system converges to the largest invariant set contained in S :

$$E = \left\{ \rho : \rho = \frac{1}{N}I_N + \frac{1}{2} \sum_{j=1}^{N-1} \gamma_j^z \gamma_j^z + \frac{1}{2} \sum_{j < l} \gamma_{jl}^x \sigma_{jl}^x + \frac{1}{2} \sum_{j < l} \gamma_{jl}^y \sigma_{jl}^y, ((H_k)_{jl} = 0, k = 1, \dots, m, \right.$$

or $p_j = p_l; \gamma \in B(R^{N^2-1})\}$, where γ is the Bloch vector of dimension $N^2 - 1$ with $\gamma_{jl}^x, \gamma_{jl}^y$ and $\gamma_j^z(j = 1, \dots, N; j < l)$ as components and satisfies $\gamma_{jl}^x = \gamma_{jl}^y(j = 1, \dots, N; j < l) = 0$ for $(H_k)_{jl} \neq 0(k = 1, \dots, m)$.

Since the equilibrium states of the considered systems here are diagonal matrices, the set of all the equilibrium states to which the control system may converge is the set of all the diagonal matrices in the largest invariant set E , denoted by E_e . Furthermore, given an initial state ρ_0 , the set of all the equilibrium states to which the control system may converge is the set of all the diagonal matrices in the convergent state set $E(\rho_0)$, denoted by $E_e(\rho_0)$. Evidently, the number of elements in $E_e(\rho_0)$ is finite, denoted by $\rho_{e1}, \rho_{e2}, \dots, \rho_{en}(n \leq N!)$.

Note that when P is non-degenerate and the controlled system is fully connected, the following conclusion is easily obtained via Theorem 5.2, and Propositions 5.1 and 5.2.

Corollary 5.1 For the transitionally non-degenerate system Equation 5.1 with the control field (Equation 5.5), if P is non-degenerate and the system Equation 5.1 is fully connected, then the largest invariant set in Theorem 5.2 reduces to the equilibrium state set E_e , that is, any trajectory of the control system converges to one of the equilibrium states of the system Equation 5.1.

5.1.4 Considerations on the Determination of P

In this subsection, the determination problem of P will be studied so that the system Equation 5.1 can converge to or transit with a high probability to the population of some equilibrium state. This task is not too formidable since the system only needs to be steered to a state that has the same population as the target equilibrium state.

According to Theorem 5.2, the largest invariant set E depends not only on the pairs of energy levels that are not directly coupled in the control Hamiltonians but also on the diagonal elements of P . For the considered system, Theorem 5.2 and the diagonal type of the equilibrium states ensure that all the equilibrium states are in the largest invariant set. However, this does not mean that any control system trajectory can reach the population of the target equilibrium state. We solve this problem by constructing P .

In view of the diagonal type of P , Equation 5.2 can be written as

$$V(\rho) = \sum_{k=1}^N p_k \rho_{kk} \quad (5.18)$$

where ρ_{kk} is the (k,k) -th element of ρ and represents the population component on the k -th eigenstate. Equation 5.18 and the population conservation during the evolving process ensure that the population components on the eigenstates associated with the maximal and minimal diagonal elements of P change quickly with decreasing V . Based on this, the diagonal element of P associated with the maximal diagonal element of the target equilibrium state should be kept minimal, the diagonal element of P associated with the minimal diagonal element of the target equilibrium state should be kept maximal, and other diagonal elements should take suitable values.

Such an approach of roughly determining diagonal elements cannot guarantee the best approach to the population of the target equilibrium state, so it is necessary to further adjust those diagonal elements. One idea is to observe and alter the diagonal values of P via simulation experiments to resultantly alter the changing rate of the Lyapunov function (Equation 5.2) with respect to the population components on the eigenstates. Furthermore, altering the changing rate of the Lyapunov function (Equation 5.2) with respect to time can also alter the control system trajectory. Considering Equations 5.3–5.5, one can obtain:

$$\dot{V}(\rho) = -4 \sum_{k=1}^m \varepsilon_k \left(\sum_{j < l} (p_j - p_l) \Im(\rho_{jl}(H_k)_{jl})^2 \right) \quad (5.19)$$

It can be seen from Equation 5.19 that the pairs of energy levels that are directly coupled in the control Hamiltonians decide the diagonal elements of P that impact on the changing rate of the Lyapunov function (Equation 5.2), so adjusting the differences between the diagonal elements of P associated with the energy levels that are directly coupled can alter the decreasing rate of the Lyapunov function (Equation 5.2).

5.1.5 Illustrative Example

We will demonstrate the concrete determination method of P via a numerical example in this subsection. Consider a three-level system acted on only one control field. In the orthonormal basis $\{|0\rangle = [1, 0, 0]^T, |1\rangle = [0, 1, 0]^T, |2\rangle = [0, 0, 1]^T\}$, the inner and control Hamiltonians are given, respectively, as $H_0 = \begin{bmatrix} 0.3 & 0 & 0 \\ 0 & 0.5 & 0 \\ 0 & 0 & 0.9 \end{bmatrix}$ and $H_1 = \begin{bmatrix} 0 & 1 & 0 \\ 1 & 0 & 1 \\ 0 & 1 & 0 \end{bmatrix}$

Assume that this system is initially in the state $|\psi_1(0)\rangle = |0\rangle$ with probability 0.9 and the state $|\psi_2(0)\rangle = \frac{1}{\sqrt{2}}|0\rangle + \frac{i}{2}|1\rangle + \frac{i}{2}|2\rangle$ with probability 0.1, that is, the initial density operator is

$$\rho(0) = \begin{bmatrix} 0.95 & \frac{(-i\sqrt{2})}{40} & \frac{(-i\sqrt{2})}{40} \\ \frac{(i\sqrt{2})}{40} & 0.025 & 0.025 \\ \frac{(i\sqrt{2})}{40} & 0.025 & 0.025 \end{bmatrix}$$

According to Theorem 5.2, it is easy to find the largest invariant set E and the convergent state set $E(\rho_0)$, where the Bloch space $B(R^8)$ can be calculated by using Proposition 5.3. In addition, numerical computation shows that the three eigenvalues of $\rho(0)$ are equal to 0, 0.0472, and 0.9528. That is to say, the set $E_e(\rho(0))$ of the equilibrium states to which the control system may converge contains 3! elements:

$$\begin{aligned}\rho_{e1} &= \text{diag}\{0, 0.0472, 0.9528\}, \rho_{e2} = \text{diag}\{0, 0.9528, 0.0472\} \\ \rho_{e3} &= \text{diag}\{0.0472, 0, 0.9528\}, \rho_{e4} = \text{diag}\{0.0472, 0.9528, 0\} \\ \rho_{e5} &= \text{diag}\{0.9528, 0, 0.0472\}, \rho_{e6} = \text{diag}\{0.9528, 0.0472, 0\}.\end{aligned}$$

The control goal is to drive this system to the population of ρ_{e1} with a high probability. The following parameters are selected in the simulation experiments: $p_1 = 1, p_2 = 0.7, p_3 = 0.5$, and $\varepsilon_1 = 0.05$ in the control field (Equation 5.5). Simulation results show that when the control time period t_f is large enough (e.g., $t_f > 10\,000$ a.u.), the population on the three eigenstates finally reaches up to about 0.0003, 0.0472, and 0.9525, which is very close to the population on the three eigenstates of ρ_{e1} . To clearly see the key evolving process of the control system, the corresponding simulation curves in the time interval [0, 1500] are plotted in Figures 5.1 and 5.2.

It can be seen from Figures 5.1 and 5.2 that the population evolution of the system goes through the path $|1\rangle \rightarrow |2\rangle \rightarrow |3\rangle$. Evidently, the population exchange between the eigenstates $|1\rangle$ and $|2\rangle$ mainly happens in the time interval [0, 380], while the population exchange between $|2\rangle$ and $|3\rangle$ mainly happens in [380, 880]. Numerical calculation shows that the oscillatory frequencies of the control field in [0, 380] and [380, 880] are about 0.1984 and 0.4021, which are very close to the transition frequencies 0.2 (between $|1\rangle$ and $|2\rangle$) and 0.4 (between $|2\rangle$ and $|3\rangle$), respectively.

In fact, better control results can be obtained by suitably adjusting the diagonal elements of P . For instance, for $p_1 = 1.2, p_2 = 0.7$, and $p_3 = 0.3$, the population on the three eigenstates finally reaches about 0, 0.0472, and 0.9528.

The simulation experiments on the three-level system have verified the effectiveness of the research results. However, when the number of the energy levels in the system is relatively large or the structure of the largest invariant set is very complex, the trial determination method in this section appears weak. In this case, it is necessary to develop some new theoretical tools

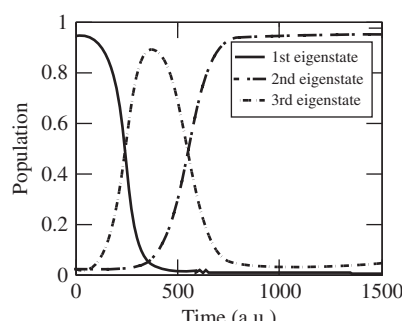


Figure 5.1 Population evolution curves in the time interval [0, 1500]

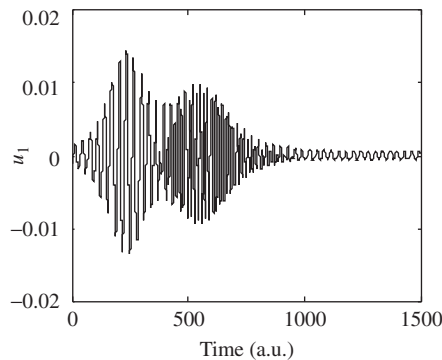


Figure 5.2 Control field in the time interval $[0, 1500]$

and search for some more rigorous determination principles, which will be investigated in the later chapters of this book.

5.1.6 Appendix: Proof of Theorem 5.1

1) Conclusion 1

It is known from Proposition 5.3 that the states satisfying $\dot{V}(\rho(t)) = 0$ ($t \in R$) are the ones that satisfy:

$$u_k(t) = i\epsilon_k \text{tr}([P, H_k]\rho(t)) = 0, k = 1, \dots, m, t \in R \quad (5.20)$$

which implies that $\rho(t)$ contained in the control field is the free evolving state of the system. Substituting the solution of $\dot{\rho}(t) = -i[H_0, \rho(t)]$ into Equation 5.20 equivalently gives

$$\text{tr}(e^{-iH_0 t} \rho(0) e^{iH_0 t} [P, H_k]) = 0, k = 1, \dots, m, t \in R \quad (5.21)$$

That is to say, the largest invariant set contained in S is

$$E = \{\rho(0) : \text{tr}(e^{-iH_0 t} \rho(0) e^{iH_0 t} [P, H_k]) = 0, k = 1, \dots, m, t \in R\} \quad (5.22)$$

Now, we use Equation 5.21 to prove the invariance and the largest property of E . Firstly, for showing the invariance, we suppose $\rho_1(0) \in E$, i.e.

$$\text{tr}(e^{-iH_0 t} \rho_1(0) e^{iH_0 t} [P, H_k]) = 0, k = 1, \dots, m, t \in R \quad (5.23)$$

Then, the system state at any time t_0 is equal to $\rho_1(t_0) = e^{-iH_0 t_0} \rho_1(0) e^{iH_0 t_0}$. Let $\rho_1(t_0)$ be a new initial state, denoted by $\rho_1(t_0)(0)$. Calculating the left-hand side of Equation 5.21 gives

$$\text{tr}(e^{-iH_0 t} \rho_1(t_0) e^{iH_0 t} [P, H_k]) = \text{tr}(e^{-iH_0(t+t_0)} \rho_1(t_0) e^{iH_0(t+t_0)} [P, H_k]) \quad (5.24)$$

Obviously, for $t \in R$, Equation 5.24 is equivalent to the left-hand side of Equation 5.23, that is, $\rho_1(t_0) \in E$. This ends the proof of the invariance.

Next, for proving the largest invariant property of E , suppose E' is any invariant set contained in S and $\rho'(0)$ is any point in E' . The invariance of E' ensures that the trajectory starting

from $\rho'(0)$ still belongs to E' and can be written as $\rho'(t) = e^{-iH_0 t} \rho'(0) e^{iH_0 t}$ ($t \in R$), that is, $\rho'(0) = e^{-iH_0 t} \rho'(t) e^{iH_0 t}$. Replacing $\rho(0)$ in Equation 5.21 with $\rho'(0)$ gives $\text{tr}(\rho'(t)[P, H_k]) = 0$ ($k = 1, \dots, m$; $t \in R$). This is exactly the characteristic of E expressed in Equation 5.20. The arbitrariness of $\rho'(0)$ in E' ensures $E' \subset E$. Furthermore, the arbitrariness of E' in S ensures that E is the largest invariant set contained in S .

2) Conclusion 2

Since H_0 is non-degenerate and diagonal, it can be known from Proposition 5.2 that P is also diagonal. So, one has $P = e^{-iH_0 t} P e^{iH_0 t}$. Combined with $\text{tr}(A[B, C]) = \text{tr}(C[A, B])$, the left-hand side of Equation 5.21 can be reduced to

$$\begin{aligned} \text{tr}(e^{-iH_0 t} \rho(0) e^{iH_0 t} [P, H_k]) &= \text{tr}(H_k [e^{-iH_0 t} \rho(0) e^{iH_0 t}]) \\ &= \text{tr}(H_k [e^{-iH_0 t} \rho(0) e^{iH_0 t}, e^{-iH_0 t} P e^{iH_0 t}]) = \text{tr}(H_k e^{-iH_0 t} [\rho(0), P] e^{iH_0 t}) \\ &= \text{tr}(e^{iH_0 t} H_k e^{-iH_0 t} [\rho(0), P]) \end{aligned}$$

Thus, Equation 5.21 is equivalent to

$$\text{tr}(e^{iH_0 t} H_k e^{-iH_0 t} [\rho(0), P]) = 0, k = 1, \dots, m, t \in R \quad (5.25)$$

and accordingly Equation 5.22 can be equivalently written as

$$E = \{\rho(0) : \text{tr}(e^{iH_0 t} H_k e^{-iH_0 t} [\rho(0), P]) = 0, k = 1, \dots, m, t \in R\} \quad (5.26)$$

3) Conclusion 3

Applying $e^A B e^{-A} = \sum_{n=0}^{\infty} \frac{[A^{(n)}, B]}{n!}$ to Equation 5.25, one obtains

$$\begin{aligned} \text{tr}(e^{iH_0 t} H_k e^{-iH_0 t} [\rho(0), P]) = 0 &\iff \text{tr}\left(\sum_{n=0}^{\infty} \frac{1}{n!} \left[\left(iH_0 t\right)^{(n)}, H_k\right] [\rho(0), P]\right) = 0 \\ &\iff \sum_n \frac{(i^n t^n)}{n!} \text{tr}([H_0^{(n)}, H_k] [\rho(0), P]) = 0 \end{aligned} \quad (5.27)$$

$$M = \begin{bmatrix} 1 & \cdots & 1 & 1 & \cdots & 1 & \cdots & 1 \\ \omega_{12}^2 & \cdots & \omega_{1N}^2 & \omega_{23}^2 & \cdots & \omega_{2N}^2 & \cdots & \omega_{N-1,N}^2 \\ \omega_{12}^4 & \cdots & \omega_{1N}^4 & \omega_{23}^4 & \cdots & \omega_{2N}^4 & \cdots & \omega_{N-1,N}^4 \\ \vdots & \ddots & \vdots & \ddots & \ddots & \vdots & \ddots & \vdots \\ \omega_{12}^{N(N-1)-2} & \cdots & \omega_{1N}^{N(N-1)-2} & \omega_{23}^{N(N-1)-2} & \cdots & \omega_{2N}^{N(N-1)-2} & \cdots & \omega_{N-1,N}^{N(N-1)-2} \end{bmatrix}$$

where $[H_0^{(n)}, H_k] = [H_0, [H_0, \dots, [H_0, H_K]]]$ and $[H_0^{(0)}, H_k] = H_k$.

By considering the linear independence of the time sequence $1, t, t^2, \dots$, Equation 5.27 can be written as

$$\text{tr}([H_0^{(n)}, H_k] [P, \rho(0)]) = 0, n = 0, 1, 2, \dots, k = 1, \dots, m \quad (5.28)$$

Denoting P as $P = \text{diag}\{p_1, p_2, \dots, p_N\}$ and considering the diagonal type of H_0 , one can calculate $[H_0^{(n)}, H_k]$ and $[P, \rho(0)]$ as

$$[H_0^{(n)}, H_k] = ((\lambda_j - \lambda_l)^n (H_k)_{jl}) = (\omega_{jl}^n (H_k)_{jl}), j, l = 1, \dots, N \quad (5.29)$$

and

$$[P, \rho(0)] = ((p_j - p_l) \rho_{jl}(0)), j, l = 1, \dots, N \quad (5.30)$$

respectively.

Substituting Equations 5.29 and 5.30 into Equation 5.28 gives

$$\sum_{j,l=1}^N \omega_{jl}^n (H_k)_{jl} (p_j - p_l) \rho_{jl}(0) = 0, n = 0, 1, 2, \dots, k = 1, \dots, m \quad (5.31)$$

By using the Hermitian property of H_k and $\rho(0)$, Equation 5.31 can be further written as

$$\sum_{j < l} (\omega_{jl}^n (H_k)_{jl} (p_j - p_l) \rho_{jl}(0) + \omega_{jl}^n (H_k)_{jl}^* (p_j - p_l)^* \rho_{jl}^*(0)) = 0 \quad (5.32)$$

For even n Equation 5.32 can be reduced to

$$\sum_{j < l} \omega_{jl}^n \Im(H_k)_{jl} (p_j - p_l) \rho_{jl}(0) = 0, n = 0, 2, \dots, k = 1, \dots, m \quad (5.33)$$

For odd n Equation 5.32 can be reduced to

$$\sum_{j < l} \omega_{jl}^n \Re(H_k)_{jl} (p_j - p_l) \rho_{jl}(0) = 0, n = 1, 3, \dots, k = 1, \dots, m \quad (5.34)$$

Denote

$$\xi_k = \begin{bmatrix} (H_k)_{12} (p_2 - p_1) \rho_{21}(0) \\ \vdots \\ (H_k)_{1N} (p_N - p_1) \rho_{N1}(0) \\ (H_k)_{23} (p_3 - p_2) \rho_{32}(0) \\ \vdots \\ (H_k)_{2N} (p_N - p_2) \rho_{N2}(0) \\ \vdots \\ (H_k)_{N-1,N} (p_N - p_{N-1}) \rho_{N,N-1}(0) \end{bmatrix}$$

$$\Lambda = \text{diag}\{\omega_{12}, \dots, \omega_{1N}, \omega_{23}, \dots, \omega_{2N}, \dots, \omega_{N-1,N}\}$$

Then Equations 5.33 and 5.34 are equivalent to

$$M \Im(\xi_k) = 0, k = 0, \dots, m \quad (5.35)$$

and

$$M \Re(\xi_k) = 0, k = 1, \dots, m \quad (5.36)$$

respectively.

Since the system is transitionally non-degenerate, both M and Λ are non-singular square matrices of order $[N(N - 1)]/2$. Thus, Equations 5.35 and 5.36 imply

$$\xi_k = 0, k = 1, \dots, m \quad (5.37)$$

that is,

$$(H_k)_{jl}(p_l - p_j)\rho_{lj}, j, l = 1, \dots, N, j < l \quad (5.38)$$

which is the condition satisfied by the element $\rho_{lj}(0)$ of any state $\rho(0)$ in the largest invariant set E .

Thus, we complete the proof of Theorem 5.1.

5.2 Generalized Control of Quantum Systems in the Frame of Vector Treatment

For the state steering problems in closed quantum systems, we solved the problem that an initial state is orthogonal to a target eigenstate by separating the modulus of the inner product of the controlled state with the target state from its phase factor in Chapter 4. We summarized and compared three Lyapunov-based methods for closed quantum systems in Section 5.1. On the basis of these research results, in this section we will utilize the vector treatment to design a kind of control to analyze the convergence of the control system in the formulation of vectors via the invariance principle. We will consider the problems involved in the following way: dividing the whole time coordinate axis into plentiful small intervals, and in every interval keeping constant controls and successively using Lyapunov technology and the invariance principle.

5.2.1 Design of Control Law

We only treat finite dimensional systems, and assume that the system of interest is controllable and its dimension is N .

The state evolution equation of a quantum system is:

$$i\hbar|\psi(t)\rangle = H|\psi(t)\rangle, H = H_0 + H_c, H_c = \sum_{k=1}^r H_k u_k(t) \quad (5.39)$$

where H_0 is the internal Hamiltonian and H_c is the interaction Hamiltonian. Both H_0 and H_c are independent of time. $u_k(t)$ is a realizable, scalar, real-valued control function, and \hbar is set to be 1.

We take the following distance as a Lyapunov function:

$$V = \frac{1}{2}(1 - |\langle\psi_f|\psi\rangle|^2) \quad (5.40)$$

where $|\langle\psi_f|\psi\rangle|^2$ represents the transition probability from $|\psi\rangle$ into $|\psi_f\rangle$.

In quantum control, the target state is usually an eigenstate of the inner Hamiltonian, for example in quantum chemistry. We therefore assume here that the target state $|\psi_f\rangle$ satisfies

$$H_0|\psi_f\rangle = \lambda_f|\psi_f\rangle \quad (5.41)$$

In order to obtain the designed control law in an explicit form, one can calculate the first-order time derivative of V as follows:

$$\begin{aligned}\dot{V} &= \frac{1}{2}(-\langle \psi_f | \psi \rangle \langle \psi | \psi_f \rangle - \langle \psi_f | \psi \rangle \langle \psi | \psi_f \rangle) \\ &= -\text{Im} \left(\langle \psi | \psi_f \rangle \langle \psi_f | \sum_{k=1}^r u_k H_k | \psi \rangle \right) \\ &= -\sum_{k=1}^r u_k \cdot \text{Im} (\langle \psi | \psi_f \rangle \langle \psi_f | H_k | \psi \rangle)\end{aligned}\quad (5.42)$$

It can be seen from Equation 5.42 that it is possible to achieve the desired control when the control law is designed as the function of $\text{Im} (\langle \psi | \psi_f \rangle \langle \psi_f | H_k | \psi \rangle)$ and the condition that if $\text{Im}(\cdot) = 0$ then $u_k = 0$ is set according to the Lyapunov stability theorem. In such a case, if an initial state is orthogonal to the final state $|\psi_f\rangle$, then the obtained control value is equal to zero. In other words, the designed control law is invalid for the system at the initial time.

We wrote the inner product $\langle \psi | \psi_f \rangle$ in Equation 5.42 as the product of its modulus and phase factor as follows:

$$\dot{V} = -\sum_{k=1}^r u_k \cdot |\langle \psi | \psi_f \rangle| \cdot \text{Im} (e^{i\angle(\psi|\psi_f)} \langle \psi_f | H_k | \psi \rangle) \quad (5.43)$$

It can be seen from Equation 5.43 that when an initial state is orthogonal to the final state $|\psi_f\rangle$ at the initial time, $\text{Im} (e^{i\angle(\psi|\psi_f)} \langle \psi_f | H_k | \psi \rangle) \neq 0$ holds. Furthermore, $u_k \neq 0$ holds. To guarantee $\dot{V} \leq 0$, one can let each item of the summation sign in Equation 5.43 be non-negative. However, we will relax such a requirement by utilizing the vector treatment. Therefore, we set:

$$u = \begin{bmatrix} u_1 \\ u_2 \\ \dots \\ u_r \end{bmatrix} \text{ and } I = \begin{bmatrix} I_1 \\ I_2 \\ \dots \\ I_r \end{bmatrix} = \begin{bmatrix} \text{Im} (e^{i\angle(\psi|\psi_f)} \langle \psi_f | H_1 | \psi \rangle) \\ \text{Im} (e^{i\angle(\psi|\psi_f)} \langle \psi_f | H_2 | \psi \rangle) \\ \dots \\ \text{Im} (e^{i\angle(\psi|\psi_f)} \langle \psi_f | H_r | \psi \rangle) \end{bmatrix},$$

then Equation 5.43 becomes:

$$\dot{V} = -|\langle \psi | \psi_f \rangle| \cdot (u, I) \quad (5.44)$$

where \cdot denotes the standard inner product in Euclidean space R^r .

Evidently, as long as $(u, I) \geq 0$ holds, one can obtain $\dot{V} \leq 0$. Thus, there is the need to introduce a parameter $\theta(t)$, $(0 \leq \theta(t) < \pi/2)$, which is the angle between the control vector u and the vector I . According to the definition of the inner product $(u, I) = |u| \cdot |I| \cdot \cos \theta(t)$ where $(u, I) = u_1 I_1 + u_2 I_2 + \dots + u_r I_r$, $|u| = \sqrt{u_1^2 + u_2^2 + \dots + u_r^2}$, and $|I| = \sqrt{I_1^2 + I_2^2 + \dots + I_r^2}$, one can obtain the following identity:

$$u_1 I_1 + u_2 I_2 + \dots + u_r I_r = \sqrt{u_1^2 + u_2^2 + \dots + u_r^2} \cdot \sqrt{I_1^2 + I_2^2 + \dots + I_r^2} \cdot \cos \theta(t) \quad (5.45)$$

By solving Equation 5.45 in real time, one can obtain the corresponding control values at each instant. However, it is difficult to directly solve Equation 5.45. For convenience in calculation, we make the following reduction:

Firstly, when $I(t) \neq 0$, one may let:

$$|u(t)| = K(t) \cdot |I(t)| \quad (5.46)$$

where $K(t) > 0$ represents the alterable coefficient of the modulus of the vector $u(t)$ and is decided by any designer. Consequently,

$$u_1 I_1 + u_2 I_2 + \cdots + u_r I_r = K(t) \cdot |I|^2 \cdot \cos \theta(t), \left(0 \leq \theta(t) < \frac{\pi}{2}\right) \quad (5.47)$$

Secondly, when $I(t) = 0$, the values of the controls in Equation 5.45 are of arbitrariness. To reduce the degree of freedom of the control values in this case, we stipulate the following: in the presence of $I(t) = 0$, the modulus of $u(t)$ obeys Equation 5.46.

In conclusion, as long as the vector $I(t)$ at every instant is given, one can obtain the corresponding control values satisfying Equations 5.46 and 5.47 instantaneously, so the controls satisfying both Equations 5.46 and 5.47 are the designed controls.

Remark 5.5

1. Here, by introducing the vector inner product $(u, I) = \sum_{i=1}^r u_i I_i$ and the angle $\theta(t)$ between u and I , we obtain a control law whose values may be obtained by a linear Equation 5.47 with the constraint Equation 5.46.
2. The quantity $\angle\langle\psi|\psi_f\rangle$ is included in the vector I of Equation 5.47. Its value is uncertain when $\langle\psi|\psi_f\rangle$ is equal to zero. To reduce the degree of freedom of the values of the phase in the case, we should endow it with a determinate angle. To do so, we define

$$\text{If } \langle\psi|\psi_f\rangle = 0, \text{ then } \angle\langle\psi|\psi_f\rangle = 0^\circ \quad (5.48)$$

3. If $r = 1$ (only one control), then $\theta(t) \equiv 0$ holds. Accordingly, Equation 5.46 becomes $I_1 \cdot u_1 = K(t) \cdot I_1^2$, that is, $u_1 = K(t) \cdot I_1$. Since $K(t) > 0$, the values of the obtained control law in this case are equivalent to the one in Chapter 4, and we can take every u_k in Equation 5.42 to be in the following form:

$$u_k = K_k \cdot f_k(I_k), I_k = \text{Im} (e^{i\angle\langle\psi|\psi_f\rangle} \langle\psi_f|H_k|\psi\rangle), (K_k > 0, k = 1, 2, \dots, r) \quad (5.49)$$

where the image of the function $y_k = f_k(x_k)$ passes the origin of the plane $x_k - y_k$ monotonically and lies in quadrant I or III. It can be proved that Equation 5.49 is a special case of Equations 5.46 and 5.47. In fact, writing u_k and I_k values ($k = 1, \dots, r$) in Equation 5.49 in terms of their vector forms and denoting as u' and I' , and considering the relation between u_k and I_k in Equation 5.49, one can conclude that if $I_{k'} \neq 0$ holds for some $k' \in \{1, 2, \dots, r\}$, then the angle $\theta'(t)$ between u' and I' satisfies $0 \leq \theta'(t) < \pi/2$. Equation 5.49 is therefore a special case of Equation 5.45. Of course, the special cases of Equation 5.45 are not unique, for example

$$u = A(t)_{r \times r} \cdot I \quad (5.50)$$

where $A(t)_{r \times r}$ is an arbitrary time-dependent, r -dimensional, positive definite matrix. It also can be proved that Equation 5.50 is another special case of Equation 5.45 via the vector theory, so the obtained control law here is more general.

5.2.2 Convergence Analysis

Theorem 5.3 Consider the system Equation 5.39 with the controls Equations 5.46 and 5.47. If the spectrum of H_0 is non-degenerate, then the largest invariant set of the control system is $S^{2N-1} \cap E$, $E = \{|\psi\rangle \mid \langle\psi_f|H_k|\psi\rangle = 0, k = 1, \dots, r\}$. If all the solutions of $\langle\psi_f|H_k|\psi\rangle = 0, (k = 1, \dots, r)$ are within the equivalence class of the goal state, then the control system will be asymptotically stable. If there exist two non-equivalent states in $S^{2N-1} \cap E$, then $S^{2N-1} \cap E$ can be reached.

Theorem 5.3 contains the main results on the convergence of the control system. In what follows we will prove and analyze this theorem via the invariance principle. Since the controlled state leaving the initial state and converging to the target state are of the coequal importance, we will give the conditions of the controlled state leaving an initial state in the following lemmas in advance.

Lemma 5.1 Under the action of the control functions (Equations 5.46 and 5.47), if $\langle\psi(0)|\psi_f\rangle \neq 0$, then $\langle\psi(t)|\psi_f\rangle \neq 0, (t > 0)$ holds.

Lemma 5.2 Under the action of the control functions (Equations 5.46 and 5.47), if the initial state of the system is an eigenstate of H_0 and satisfies $\langle\psi(0)|\psi_f\rangle = 0$, then the following conclusions hold:

1. If $\text{Im}\langle\psi_f|H_k|\psi(0)\rangle \neq 0$ holds for some $k \in \{1, 2, \dots, r\}$, then $\langle\psi(t)|\psi_f\rangle \neq 0, (t > 0)$.
2. If $\text{Im}\langle\psi_f|H_k|\psi(0)\rangle = 0$ holds for every $k \in \{1, 2, \dots, r\}$, $\text{Re}\langle\psi_f|H_k|\psi(0)\rangle \neq 0$ holds for some $k \in \{1, 2, \dots, r\}$, and the eigenvalue λ_0 corresponding to the eigenstate $|\psi(0)\rangle$ of H_0 is not equal to zero, then $\langle\psi(t)|\psi_f\rangle \neq 0, (t \geq t')$ holds for some small time t' ; otherwise, the designed control laws cannot achieve the target state.

Proof

1. When the system runs for a very small time period Δt , that is, $t = \Delta t$, it follows that $|\psi(\Delta t)\rangle = e^{-iH\Delta t}|\psi(0)\rangle = \sum_{m=0}^{\infty} \frac{(-iH\Delta t)^m}{m!}|\psi(0)\rangle$. Taking the first-order approximation, one has

$$\langle\psi_f|\psi(\Delta t)\rangle = \sum_{k=1}^r u_k(0)\langle\psi_f|H_k|\psi(0)\rangle.$$

Here, $u_k(0)$ satisfies

$$(u(0), I(0)) = K(0) \cdot |I(0)|^2 \cdot \cos \theta(0)$$

$$|u(0)| = K(0) \cdot |I(0)|$$

where

$$I(0) = \begin{bmatrix} \text{Im}\langle\psi_f|H_1|\psi(0)\rangle \\ \text{Im}\langle\psi_f|H_2|\psi(0)\rangle \\ \vdots \\ \text{Im}\langle\psi_f|H_r|\psi(0)\rangle \end{bmatrix}.$$

Therefore, only when $\sum_k u_k(0) \langle \psi_f | H_k | \psi(0) \rangle \neq 0$ is satisfied does $u(0) \neq 0$ hold. Equivalently, $\langle \psi_f | \psi(\Delta t) \rangle = \sum_{k=1}^r u_k(0) \langle \psi_f | H_k | \psi(0) \rangle \neq 0$ holds. Furthermore, this conclusion can be proved via Lemma 5.1.

2. Since $u_k(0) = 0, (k = 1, 2, \dots, r)$, the system evolves freely, so for a small time period $t' > 0$, one can obtain $|\psi(t')\rangle = e^{-iH_0 t'} |\psi(0)\rangle = e^{-i\lambda_0 t'} |\psi(0)\rangle$.

Considering $\langle \psi_f | H_k | \psi(0) \rangle \in R, (k = 1, 2, \dots, r)$, one has

$$\begin{aligned} I(t') &= \begin{bmatrix} \text{Im} \left(e^{-i\lambda_0 t'} \langle \psi_f | H_1 | \psi(0) \rangle \right) \\ \text{Im} \left(e^{-i\lambda_0 t'} \langle \psi_f | H_2 | \psi(0) \rangle \right) \\ \vdots \\ \text{Im} \left(e^{-i\lambda_0 t'} \langle \psi_f | H_r | \psi(0) \rangle \right) \end{bmatrix} = \text{Im} (e^{-i\lambda_0 t'}) \begin{bmatrix} \langle \psi_f | H_1 | \psi(0) \rangle \\ \langle \psi_f | H_2 | \psi(0) \rangle \\ \vdots \\ \langle \psi_f | H_r | \psi(0) \rangle \end{bmatrix} \\ &= -\sin(\lambda_0 t') \begin{bmatrix} \langle \psi_f | H_1 | \psi(0) \rangle \\ \langle \psi_f | H_2 | \psi(0) \rangle \\ \vdots \\ \langle \psi_f | H_r | \psi(0) \rangle \end{bmatrix} \end{aligned}$$

Evidently, when $\text{Re} \langle \psi_f | H_k | \psi(0) \rangle \neq 0$ holds for some $k \in \{1, 2, \dots, r\}$ and the eigenvalue λ_0 corresponding to the eigenstate $|\psi(0)\rangle$ of H_0 is not equal to zero, the control vector satisfies $u(t') \neq 0$ at $t = t'$. Thus,

$$\begin{aligned} \langle \psi_f | \psi(t' + \Delta t) \rangle &= \langle \psi_f | e^{-i \left(H_0 + \sum_{k=1}^r H_k u_k(t') \right) \Delta t} | \psi(t') \rangle \\ &\approx e^{-i\lambda_0 t'} \Delta t \langle \psi_f | (I - i \left(H_0 + \sum_{k=1}^r H_k u_k(t') \right)) | \psi(0) \rangle \\ &= -ie^{-i\lambda_0 t'} \Delta t \langle \psi_f | \sum_{k=1}^r H_k u_k(t') | \psi(0) \rangle \\ &= -ie^{-i\lambda_0 t'} \Delta t \cdot (u(t'), I'') \neq 0 \end{aligned}$$

Conclusion 2 is proved. ■

5.2.3 Numerical Simulation on a Spin-1/2 System

A spin-1/2 particle system is the simplest finite dimensional bilinear system. It may be used to constitute a qubit as an information unit in quantum communication and quantum computers,

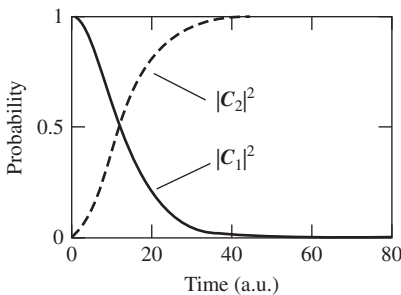


Figure 5.3 Probability of the state evolution

and its quantum state may be manipulated to achieve the corresponding information processing. For this example, we did some simulation experiments by using one control in Chapter 4 and Section 5.1. However, to illustrate the effectiveness of the proposed method, we suppose that the spin-1/2 particle system is controlled by two controls, $u_1(t)$ and $u_2(t)$, and the electromagnetic fields are varied in the x - and y -directions, respectively. The spin is discussed in the σ_z representation. The Schrödinger equation of the system is

$$i|\psi(t)\rangle = (H_0 + u_1 H_1 + u_2 H_2)|\psi(t)\rangle$$

where $H_0 = \sigma_z = \begin{bmatrix} 1 & 0 \\ 0 & -1 \end{bmatrix}$, $H_1 = \sigma_x = \begin{bmatrix} 0 & 1 \\ 1 & 0 \end{bmatrix}$, and $H_2 = \sigma_y = \begin{bmatrix} 0 & -i \\ i & 0 \end{bmatrix}$.

According to the linear superposition principle, to perform the simplest logic NOT-gate operation the state $|\psi\rangle$ must be driven to switch between the two eigenstates $|0\rangle = [1, 0]^T$ and $|1\rangle = [0, 1]^T$. Supposing that the actual state is $|\psi\rangle = [c_1, c_2]^T$, the initial state is $|\psi(0)\rangle = |0\rangle$ and the target state is $|\psi_f\rangle = |1\rangle$.

Since this system has two control inputs, to reduce the freedom of control values we obtain the values of the controls in both Equations 5.47 and 5.46 by rotating the vector $I(t) = \begin{bmatrix} \text{Im}[e^{i\angle(\psi|\psi_f)}\langle\psi_f|H_1|\psi\rangle] \\ \text{Im}[e^{i\angle(\psi|\psi_f)}\langle\psi_f|H_2|\psi\rangle] \end{bmatrix}$ anticlockwise by $\theta(t)$ ($0 \leq \theta(t) < \frac{\pi}{2}$) and multiplying by $K(t)$ ($K(t) > 0$) at every instant. Setting $K(t) = 0.2$ and $\theta(t) = 45^\circ$, the sample time is $\Delta t = 0.01$ a.u. and the control time duration is $t = 80$ a.u..

The simulation results are shown in Figures 5.3–5.6, and Figure 5.3 shows the evolution of the state probability $|\psi\rangle^2$. Figure 5.4 is the evolution of the Lyapunov function. Figure 5.5 shows the control value u_1 . Figure 5.6 shows the control value u_2 . From Figure 5.3 one can see that at any moment $|c_1|^2 + |c_2|^2 = 1$ holds, that is, the probability is conserved. Based on Figure 5.4, one can draw a conclusion: at $t_f = 45$ a.u., $V = 0$ is satisfied and the state transfer is completed.

After several repeated experiments, the following rule are obtained: If the coefficient $K(t)$ is fixed, the final time t_f does not vary with the sample time Δt and decreases with increasing $K(t)$.

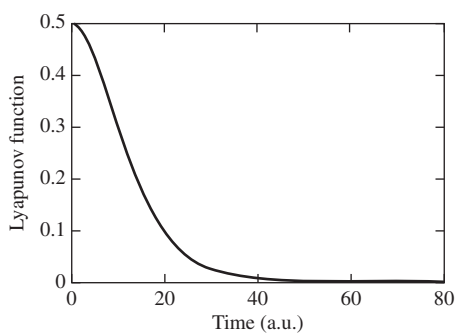


Figure 5.4 Lyapunov function during state evolution

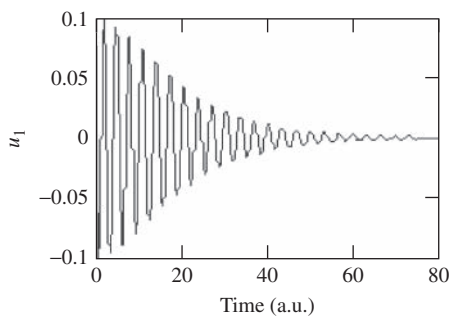


Figure 5.5 The first control value

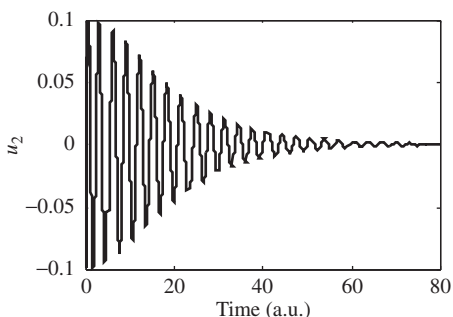


Figure 5.6 The second control value

5.3 Population Control of Eigenstates

Quantum Lyapunov methods have been extensively studied. Based on the average values of some observables, Sugawara discussed in 2003 some design methods of control laws for different tasks. Based on Hilbert–Schmidt norm, several researchers largely analyzed the convergence of the control system (Wang and Schirmer, 2010a; Altafini, 2007). In fact, it is expected that any control system trajectory could converge to a given target state. Unfortunately, the LaSalle invariance in the Lyapunov methods principle ensures that any control trajectory can only converge to the invariant set. In order to solve this problem, in 2005 Mirrahimi *et al.* achieved asymptotical approaching toward any eigenstate by the analysis of tracking conditions for a certain reference trajectory. We also preliminarily discussed the quantum Lyapunov method with degrees of freedom in Section 5.1, based on which we will give some strict theoretical results by classifying eigenstates and explain our methods by doing simulation experiments in the following subsection.

5.3.1 System Model and Control Laws

Consider N -level quantum systems described by the mathematical model

$$i|\dot{\psi}(t)\rangle = (H_0 + H_1 u_1(t))|\psi(t)\rangle \quad (5.51)$$

in which H_0 is diagonal and can be denoted by $H_0 = \text{diag}[\lambda_1, \lambda_2, \dots, \lambda_N]$.

The system Equation 5.51 has the following properties: Equation 5.51 is non-degenerate, it has no degenerate transition, and it is fully connected. In addition, the system Equation 5.51 is also assumed to be pure-state controllable.

The adopted Lyapunov function is

$$V = \langle\psi|P|\psi\rangle \quad (5.52)$$

where P is a real diagonal matrix and its diagonal elements need to be determined beforehand. For convenience, we denote P by $P = \text{diag}[P_1, P_2, \dots, P_N]$. The critical property of the Lyapunov function (Equation 5.52) can be characterized by the following proposition (Grivopoulos and Bamieh, 2003).

Proposition 5.4 The set of critical points of the Lyapunov function (Equation 5.52) defined on the complex surface $\langle\psi|\psi\rangle = 1$ is given by the normalized eigenvectors of P . The eigenvectors associated with the largest eigenvalue of P are the maximum points of V , the eigenvectors associated with the smallest eigenvalue are the minimum points of V , and all other eigenvectors are saddle points.

It is easily calculated that the first-order derivative of V is

$$\dot{V} = i\langle\psi|[H_0, P]|\psi\rangle + i\sum_{k=1}^r \langle\psi|[H_k, P]|\psi\rangle u_k \quad (5.53)$$

To ensure $\dot{V} \leq 0$ we let

$$[H_0, P] = 0 \quad (5.54)$$

and select the form of control field to be

$$u_1 = -iK_1 \langle \psi | [H_1, P] | \psi \rangle \quad (5.55)$$

with $K_1 > 0$.

5.3.2 Largest Invariant Set of Control Systems

The whole control system is autonomous. In this case, one can analyze its convergence directly by the LaSalle invariance principle. This principle guarantees that any control trajectory converges to the largest invariant set E contained in $M \stackrel{\Delta}{=} \left\{ \langle \psi | : \frac{d}{dt} \dot{V}(|\psi(t)\rangle) = 0 \right\}$.

For the largest invariant set, we can obtain the following results.

Proposition 5.5 In M , the largest invariant set of control systems is $E = \{|\psi(0)\rangle : \dot{V}(|\psi(t)\rangle) = 0, t \in R; |\psi(0)\rangle \in S^{2N-1}\}$.

Theorem 5.4 Consider the model (Equation 5.32) with the constraints (Equations 5.54 and 5.55). If $P_j \neq P_l (j \neq l)$, then any trajectory of control systems converges to the largest invariant set $E = \{|\psi(0)\rangle : \langle \lambda_l | \psi(0) \rangle \langle \psi(0) | \lambda_j \rangle (H_1)_{jl} = 0, j, l = 1, \dots, N; j \neq l, |\psi(0)\rangle \in S^{2N-1}\}$ contained in M .

5.3.3 Analysis of the Eigenstate Control

Let the number of the least invariant subsets which cover E be q , and denote such invariant subsets by E_1, E_2, \dots, E_q . The Rayleigh principle ensures

$$P_{\min}(E_a) \leq V(E_a) \leq P_{\max}(E_a), (a = 1, \dots, q), \quad (5.56)$$

where $P_{\min}(E_a)$ and $P_{\max}(E_a)$ represent the minimum and maximum eigenvalues of P restricted on E_a , respectively.

Now, assume that $|\lambda_g\rangle$ is the target eigenstate contained in the invariant subset E_b , ($b \in \{1, \dots, q\}$). For the sake of clarity, eigenstates will be divided into two classes: isolated and not isolated.

1) Isolated target eigenstate

This case means that the target eigenstate $|\lambda_g\rangle$ is directly coupled with all other eigenstates. Evidently, if the eigenvalue P_g of P associated with $|\lambda_g\rangle$ is the smallest one, then $|\lambda_g\rangle$ is the minimum point of V by Proposition 5.4. Thus, the LaSalle principle ensures that $|\lambda_g\rangle$ is locally asymptotically stable. In order to investigate the stability on a large scale, we consider two kinds of initial states.

Case 1: The initial states with non-zero projections on $|\lambda_g\rangle$. For such initial states, the following inequality with respect to P_j , ($j = 1, \dots, N$) has solutions:

$$\begin{cases} P_g < |c_{g0}|^2 P_g + \sum_{j \neq g} |c_{g0}|^2 P_j < P_1, \dots, P_{g-1}, P_{g+1}, \dots, P_N \\ |c_{g0}|^2 + \sum_{j \neq g} |c_{g0}|^2 = 1 \end{cases} \quad (5.57)$$

where $|c_{g0}|^2$ is the initial population component on $|\lambda_j\rangle$ and $|c_{g0}|^2 \neq 0$, that is to say, there exists P such that all system trajectories starting from such initial states necessarily converge to $|\lambda_g\rangle$.

Case 2: The initial states without projections on $|\lambda_g\rangle$. In this case, Equation 5.57 cannot hold. Dependent on different initial states and transition graphs, the problem will become complicated. However, one can easily find some alternative methods to achieve convergence to $|\lambda_g\rangle$. For instance, one may add an external field to excite $|\lambda_g\rangle$ and so transform this case into case 1.

2) Non-isolated target eigenstate

This situation means that the invariant subset E_b contains at least another eigenstate apart from $|\lambda_g\rangle$. Since the control Equation 5.55 cannot discriminate between states in any invariant set, it is difficult to establish exact convergence to $|\lambda_g\rangle$. Motivated by the transition path control proposed by Sugawara in 2003, we can artificially program at least one longest path to the end point $|\lambda_g\rangle$ in the transition graph as the system is connected, and set the corresponding diagonal elements in a decreasing order along these paths from far to near. Generally speaking, such diagonal elements can lead to a good control effect and also make the system trajectory converge to one invariant subset containing $|\lambda_g\rangle$. However, this does not mean the high-probability transition to $|\lambda_g\rangle$, so further adjustment for diagonal elements is also necessary. Here, we give some possible adjustment considerations.

1. Since P is diagonal, V can be written as:

$$V = \sum_{j=1}^N P_j |c_j|^2 \quad (5.58)$$

where $\sum_{j=1}^N P_j |c_j|^2 = 1$, and $|c_j|^2$ is the population component on $|\lambda_j\rangle$. Equation 5.58 implies that the population components on eigenstates associated with maximum or minimum eigenvalues of P will quickly vary.

2. In simulations, a possible reason why a certain system trajectory reaches E_b , but the population exponent on $|\lambda_g\rangle$ is relatively low, is that the trajectory has entered E_b before $|\lambda_g\rangle$ gains a sufficient population distribution. We can therefore try to decrease the changing rate of V to alter the trajectory. It can be calculated that

$$\dot{V} = K_1 \left(\sum_{l,j=1}^N (P_l - P_j) \langle \psi | \lambda_j \rangle \langle \lambda_l | \psi \rangle (H_1)_{jl} \right)^2 \quad (5.59)$$

Equation 5.59 shows that the decreasing rate of V is closely related to all differences between different eigenvalues of P associated with admissible direct transitions. It can be seen that the smaller the differences, the longer the time period to which E_b can reach.

5.3.4 Simulation Experiments

In this section, we verify the effectiveness of the methods proposed via some simulation experiments on a three-level system. The system and control Hamiltonians of this system are given as

$$H_0 = \text{diag}[0, 0.3, 0.9]$$

and

$$H_1 = \begin{bmatrix} 0 & 1 & 0 \\ 1 & 0 & 1 \\ 0 & 1 & 0 \end{bmatrix}$$

respectively. According to its energy-level transition graph, we can write the largest invariant set as $E = \text{spans}\{|\lambda_2\rangle\} \cup \text{spans}\{|\lambda_1\rangle, |\lambda_3\rangle\}$. In simulations, we uniformly set $K_1 = 0.15$.

1) Isolated target eigenstate

Assume that the isolated state $|\lambda_2\rangle$ is a target eigenstate. We consider two cases of initial states:

Case 1: The initial states with a non-zero projection on $|\lambda_2\rangle$, for example $|\psi(0)\rangle = \sqrt{3}/2|\lambda_1\rangle + 1/2|\lambda_2\rangle$. In this case, Equation 5.57 becomes $P_2 < 0.25P_2 + 0.75P_1 < P_1, P_3$. It can be verified that $P_1 = 2$, $P_2 = 1$, and $P_3 = 2.1$ satisfy this inequality, that is, $P = \text{diag}[2, 1, 2.1]$. The simulation result is shown in Figure 5.7.

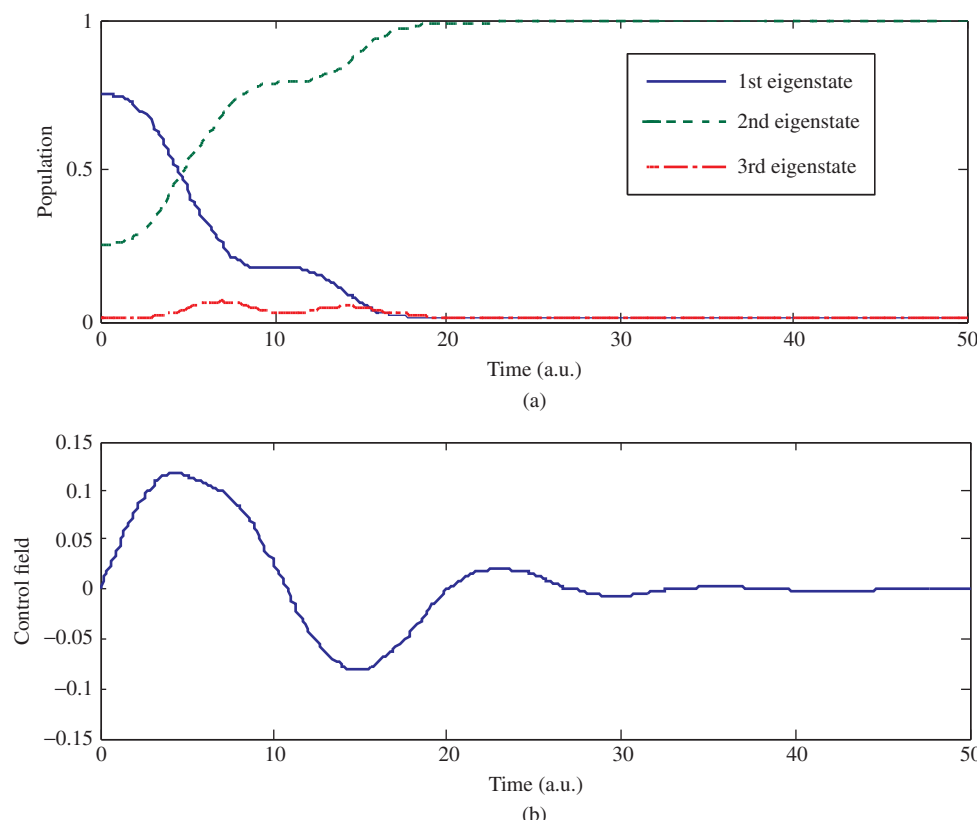


Figure 5.7 The simulation result with the isolated target eigenstate $|\lambda_2\rangle$ and the initial state $|\psi(0)\rangle = \sqrt{3}/2|\lambda_1\rangle + 1/2|\lambda_2\rangle$: (a) population evolving process and (b) control field

Case 2: The initial states without projections on $|\lambda_2\rangle$, for example $|\psi(0)\rangle = \sqrt{3}/2|\lambda_1\rangle + 1/2|\lambda_3\rangle$. In this case, we should add an external field to excite $|\lambda_2\rangle$, for example $u_0(t) = 0.15 \sin 0.3t$, $t \in [0, 10]$. It can be computed that the state at $t = 10$ is equal to $|\psi(10)\rangle = (0.6376 + 0.1575i)|\lambda_1\rangle - (0.5680 + 0.2835i)|\lambda_2\rangle - (0.3817 + 0.1414i)|\lambda_3\rangle$. Let $|\psi(10)\rangle$ be a new initial state. The control field (Equation 5.55) can then be used. Further calculation shows that $P = \text{diag}[2, 1, 2.1]$ is still one solution of Equation 5.57. The corresponding simulation result is shown in Figure 5.8, in which the applied field $u_0(t) = 0.15 \sin 0.3t$ works in the time interval $[0, 10]$, while the control field (Equation 5.55) works in the time interval $[0, 50]$. The simulation experiments shows that the control system trajectories finally converge to (the population of) the target eigenstate $|\lambda_2\rangle$.

2) Non-isolated target eigenstate

Assume that the non-isolated state $|\lambda_3\rangle$ is a target eigenstate. We select the path $1 \rightarrow 2 \rightarrow 3$ and accordingly set $P = \text{diag}[1, 2, 1, 0.4]$. The simulation result is shown in Figure 5.9, in which the initial state $|\psi(0)\rangle = \sqrt{3}/2|\lambda_1\rangle + 1/2|\lambda_2\rangle$.

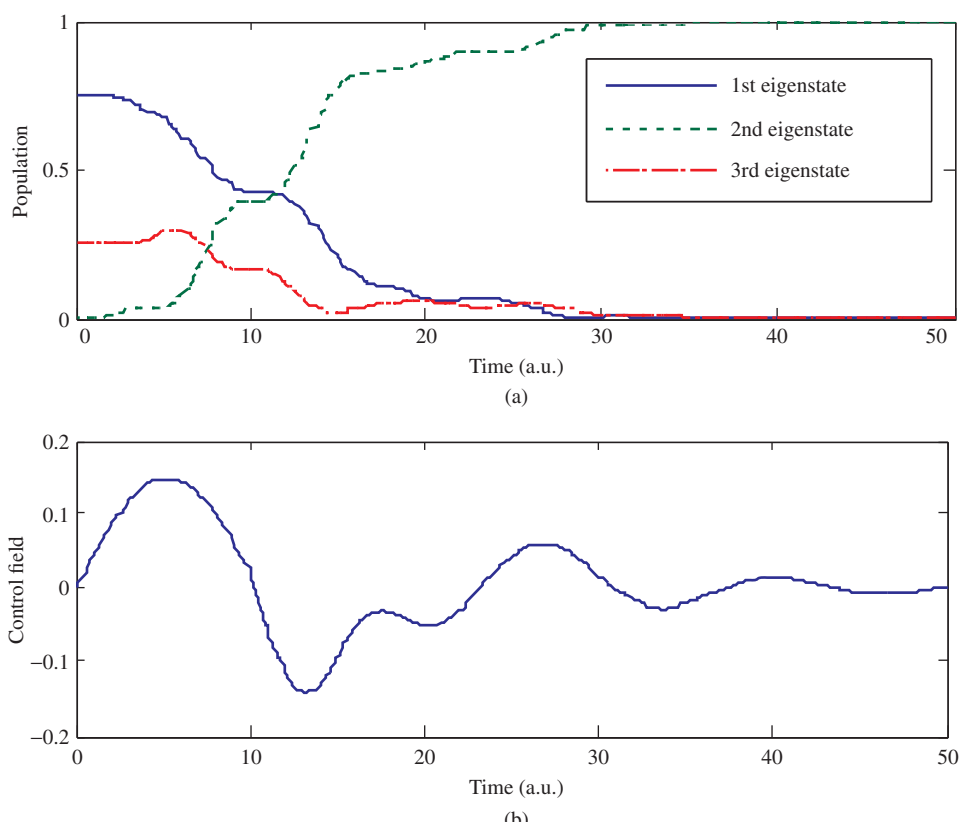


Figure 5.8 The simulation result with the isolated target eigenstate $|\lambda_2\rangle$ and the initial state $|\psi(0)\rangle = \sqrt{3}/2|\lambda_1\rangle + 1/2|\lambda_3\rangle$: (a) population evolving process and (b) control field

Obviously, the system trajectory finally reaches to $\text{span}\{|\lambda_1\rangle, |\lambda_3\rangle\}$. However, the population component on $|\lambda_3\rangle$ is not high enough. Based on Equation 5.59, we can increase P_3 to reduce the decreasing speed of V , for example for $P = \text{diag}[1.2, 1, 0.8]$, the simulation result is as shown in Figure 5.10. It can be seen from Figures 5.9 and 5.10 that the adjustment consideration is effective.

In this section, we have studied the high-probability transition to any eigenstate of quantum systems using the invariance principle and quantum energy-level transition graphs. For isolated target eigenstates, we have theoretically shown the existence of degrees of freedom that guarantees the convergence. For non-isolated target eigenstates, exact convergence cannot be guaranteed. Instead, we have given some methods for roughly determining degrees of freedom and also achieved the target with a high probability.

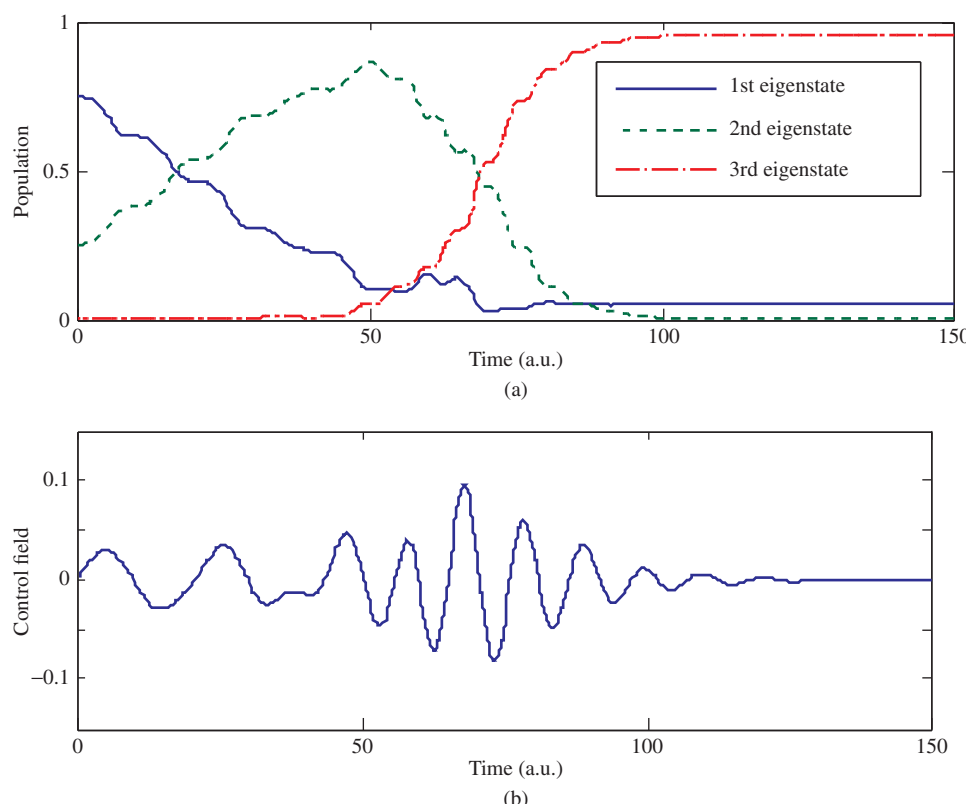


Figure 5.9 The simulation result with $|\psi(0)\rangle = \sqrt{3}/2|\lambda_1\rangle + 1/2|\lambda_2\rangle$ and $P = \text{diag}[1, 2, 1, 0.4]$: (a) population evolving process and (b) control field

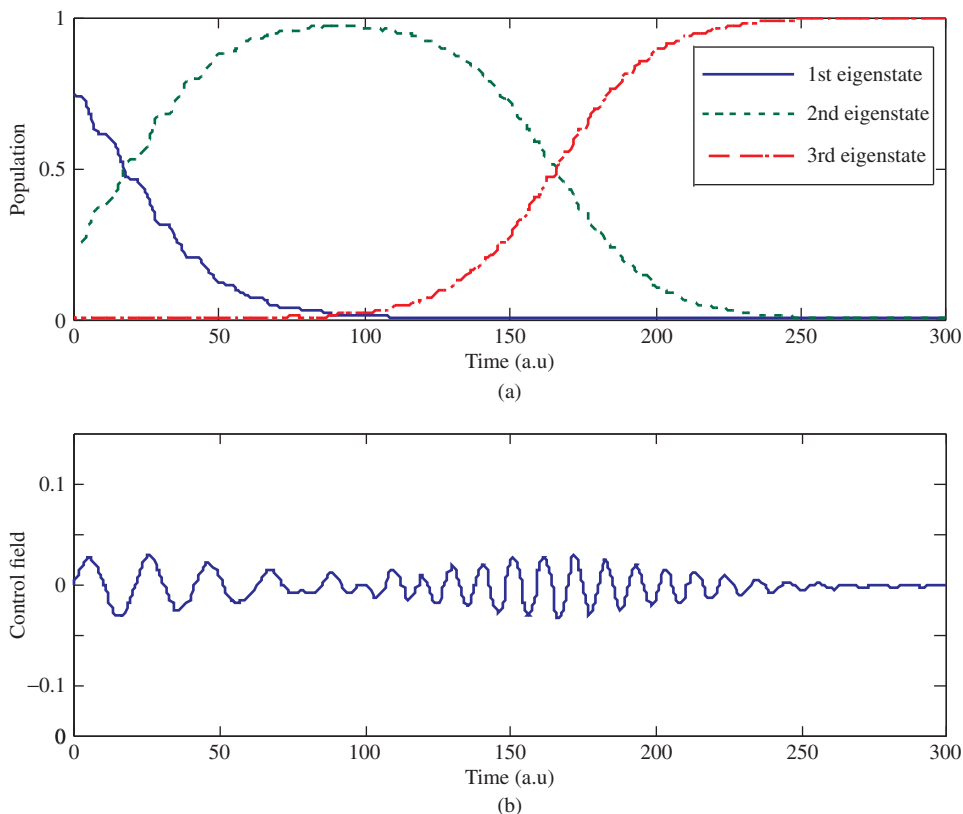


Figure 5.10 The simulation result with the non-isolated target eigenstate $|\lambda_3\rangle$, the initial state $|\psi(0)\rangle = \sqrt{3}/2|\lambda_1\rangle + 1/2|\lambda_2\rangle$, and $P = [1.2, 1, 0.8]$: (a) population evolving process and (b) control field

References

- Altafini, C. (2007) Feedback stabilization of isospectral control systems on complex flag manifolds: application to quantum ensembles. *IEEE Transactions on Automatic Control*, **52**(11), 2019–2028.
- Beaucharda, K., Coronb, J.M., Mirrahimic, M. et al. (2007) Implicit Lyapunov control of finite dimensional Schrödinger equations. *Systems & Control Letters*, **56**(5), 388–395.
- Cong, S. and Kuang, S. (2007) Quantum control strategy based on state distance. *Acta Automatica Sinica*, **33**(1), 28–31.
- D'Alessandro, D. (2007) *Introduction to Quantum Control and Dynamics*, Taylor & Francis Group, LLC, Boca Raton, FL.
- Grivopoulos, S. and Bamieh, B. (2003) Lyapunov-based control of quantum systems. Proceedings of the 42nd IEEE Conference on Decision and Control, Maui, pp. 434–438.

- Kimura, G. (2003) The Bloch vector for N-level systems. *Physics Letters A*, **314**(5–6), 339–349.
- Kuang, S. and Cong, S. (2008) Lyapunov control methods of closed quantum systems. *Automatica*, **44**(1), 98–108.
- Mirrahimi, M., Rouchon, P. and Turinici, G. (2005) Lyapunov control of bilinear Schrödinger equations. *Automatica*, **41**(11), 1987–1994.
- Mirrahimi, M., Turinici, G. and Rouchon, P. (2005) Reference trajectory tracking for locally designed coherent quantum controls. *Journal of Physical Chemistry A*, **109**(11), 2631–2637.
- Schirmer, S.G., Greentree, A.D., Ramakrishna, V. et al. (2002) Constructive control of quantum systems using factorization of unitary operators. *Journal of Physics A: Mathematical and General*, **35**(39), 8315–8339.
- Schirmer, S.G., Zhang, T. and Leahy, J.V. (2004) Orbits of quantum states and geometry of Bloch vectors for N-level systems. *Journal of Physics A: Mathematical and General*, **37**(4), 1389–1402.
- Shapiro, E.A., Milner, V., Menzel-Jones, C. et al. (2007) Piece-wise adiabatic passage with a series of femtosecond pulses. *Physical Review Letters*, **99**(3), 2–5.
- Shi, S. and Rabitz, H. (1990) Quantum mechanical optimal control of physical observables in microsystems. *Journal of Chemical Physics*, **92**(1), 364–376.
- Sugawara, M. (2003) General formulation of locally designed coherent control theory for quantum system. *Journal of Chemical Physics*, **118**(15), 6784–6801.
- Sugawara, M., Tamaki, M. and Yabushita, S. (2007) A new control scheme of multilevel quantum system based on effective decomposition by intense CW lasers. *Journal of Physical Chemistry A*, **111**(38), 9446–9453.
- Wang, X. and Schirmer, S. (2009) Entanglement generation between distant atoms by Lyapunov control. *Physical Review A*, **80**, 042305.
- Wang, X. and Schirmer, S. (2010a) Analysis of Lyapunov method for control of quantum states. *IEEE Transactions on Automatic Control*, **55**(10), 2259–2270.
- Werschnik, J. and Gross, E. (2007) Quantum optimal control theory. *Journal of Physics B: Atomic, Molecular and Optical Physics*, **40**(18), 175–211.

6

Quantum General State Control Based on Lyapunov Method

6.1 Pure State Manipulation

As an important method in control theory, the main idea of the method based on the Lyapunov stability theorem is to construct an appropriate Lyapunov function first and then obtain the control law when the first-order time derivative of the selected Lyapunov function is kept non-positive. The condition obtained from this method is a sufficient condition. The Lyapunov functions have different geometric or physical meanings. Among them the most commonly used are three types: the state distance-based Lyapunov function, the average valued-based Lyapunov function, and the state error-based Lyapunov function. The control laws in Section 4.2 are obtained under the assumption that the target state is an eigenstate, thus they can be used only when the desired final state is an eigenstate, especially in the population transfer in chemistry. On the other hand, often the arbitrary superposition target state has to be prepared in physical application fields. In this chapter we will solve the control goal of some general states controls such as the pure state, which is composed of eigenstate, the superposition state, and the mixed state.

6.1.1 Design of Control Law and Discussion

The mathematical model of a pure-state quantum system is described by the following Schrödinger equation:

$$i\hbar |\psi\rangle = H |\psi\rangle \quad (6.1)$$

where $\hbar = 1.0545 \times 10^{-34} J \cdot s$ is the Planck constant. In theoretical analysis \hbar often lies in H , so we can set $\hbar = 1$. $|\psi\rangle$ is the actual state of the quantum system: $|\psi\rangle \in C^n$ and $\| |\psi\rangle \| = 1$. H is the Hamiltonian operator and H consists of two parts:

$$H = H_0 + H_c(t) \quad (6.2)$$

where H_0 is the inner Hamiltonian, $H_c(t)$ is the interaction Hamiltonian generated by the interaction of the external controls and the system, and $H_c(t) = \sum_{k=1}^m H_k u_k(t)$. Both H_0 and H_k are

linear Hermitian operators independent of time, that is, $H_k^\dagger = H_k$, ($k = 0, 1, \dots, m$), where the superscript plus sign represents conjugate transpose. $u_k(t)$ is a realizable, scalar, real-valued control function, thus Equation 6.1 can be written in the following form:

$$i|\psi\rangle = \left(H_0 + \sum_{k=1}^m H_k u_k(t) \right) |\psi\rangle \quad (6.3)$$

The eigenequation of operator H_0 is:

$$H_0 |\psi_n\rangle = \lambda_n |\psi_n\rangle \quad (6.4)$$

where λ_n is the eigenvalue of H_0 corresponding to the eigenstate $|\psi_n\rangle$. All the eigenstates $|\psi_n\rangle$ expand Hilbert space, thus the following equation holds:

$$|\psi\rangle = \sum_n c_n |\psi_n\rangle \quad (6.5)$$

where $c_n \in \mathbb{C}$ and $\sum_n |c_n| = 1$. $|c_n|$ represents the quantum probability in the eigenstate $|\psi_n\rangle$.

Generally speaking, different Lyapunov functions will lead to different types of control laws and different control effectiveness. Designing the Lyapunov function from some special geometric or physical meaning is a good approach. The control strategy based on the error is widely applied to classical control systems in the Lyapunov method. It achieves the control object by continually reducing the error between the controlled state and the target state. This idea may be used in quantum systems.

In Section 4.2, the Lyapunov function based on the error between the initial state and the target one was selected as

$$V = \langle \psi - \psi_f | \psi - \psi_f \rangle \quad (6.6)$$

where $|\psi\rangle$ is the actual state of the controlled quantum system and $|\psi_f\rangle$ is the target state.

In Section 4.2 the $|\psi_f\rangle$ was assumed to be an eigenstate of the inner Hamiltonian H_0 , thus $|\psi_f\rangle$ satisfying $H_0 |\psi_f\rangle = \lambda_f |\psi_f\rangle$. The model discussed here is slightly different from Equation 6.3 and is given by

$$i|\psi\rangle = \left(H_0 + \sum_{k=1}^m H_k u_k(t) + \omega I \right) |\psi\rangle \quad (6.7)$$

where ω is a new real scalar control field. It can be proved that the solution of Equation 6.7 is equal to the product of the solution of Equation 6.3 plus the global phase factor $e^{-i\omega t}$. Thus, the introduction of ω may be used to adjust the global phase without changing the physical quantities attached to $|\psi\rangle$ (Mirrahimi and Rouchon, 2004; Mirrahimi, Rouchon, and Turinici, 2005).

The first-order time derivative of V is

$$\begin{aligned} \dot{V} &= -2 \sum_{k=1}^m \Im(\langle \psi_f | H_k | \psi \rangle) u_k - 2\Im(\langle \psi_f | (H_0 + \omega I) | \psi \rangle) \\ &= -2 \sum_{k=1}^m \Im(\langle \psi_f | H_k | \psi \rangle) u_k - 2(\lambda_f + \omega)\Im(\langle \psi_f | \psi \rangle) \end{aligned} \quad (6.8)$$

where \Im represents the imaginary part operation.

The simple and effective form of control laws can be selected as:

$$\lambda_f + \omega = K_0 f_0 (\Im(\langle \psi_f | \psi \rangle)) \quad (6.9)$$

$$u_k = K_k f_k \left(\Im \left(\langle \psi_f | H_k | \psi \rangle \right) \right), \quad (k = 1, \dots, m) \quad (6.10)$$

where $K_k > 0, (k = 0, 1, \dots, m)$ and the image of the function $y_k = f_k(x_k), (k = 0, 1, \dots, m)$ passes the origin of plane $x_k - y_k$ monotonically and lies in quadrants I and III. Thus the selected control laws can ensure $\dot{V} \leq 0$.

In Section 4.2 we realized the state transfer by introducing the control variable ω to adjust the global phase, but the method has a limitation: it can only transfer the system state to an eigenstate of the inner Hamiltonian.

What we want to do here is to make the system state transfer to the superposition state by eliminating the local phase.

Unitary transformation plays an important role in quantum systems: just as we perform linear transformation to simplify the calculation in the macroscopic systems, we can use the unitary transformation in the quantum system to simplify the process of operation. Assuming that $|\psi(t)\rangle$ satisfies the Schrödinger equation (Equation 6.3), we perform the following unitary transformation:

$$|\psi(t)\rangle = U(t)|\tilde{\psi}(t)\rangle \quad (6.11)$$

where the unitary matrix $U(t) = \text{diag}(e^{-i\lambda_1 t}, e^{-i\lambda_2 t}, \dots, e^{-i\lambda_n t})$. Substituting Equation 6.11 into Equation 6.3 gives

$$i|\tilde{\psi}\rangle = \left(\tilde{H}_0 + \sum_{k=1}^m \tilde{H}_k u_k(t) - \Lambda \right) |\tilde{\psi}\rangle \quad (6.12)$$

where $\Lambda = \text{diag}(\lambda_1, \lambda_2, \dots, \lambda_n)$, $\tilde{H}_0 = U^\dagger H_0 U$, and $\tilde{H}_k = U^\dagger H_k U$. From Equations 6.5 and 6.11 we obtain

$$|\tilde{\psi}\rangle = \sum_n \tilde{c}_n |\tilde{\psi}_n\rangle \quad (6.13)$$

where $\tilde{c}_n = e^{i\lambda_n t} c_n$. Because $|\tilde{c}_n| = |c_n|$, Equations 6.12 and 6.3 describe the same system (Boscain and Chambrion, 2002a). In the subsequent control law design and analysis we do not distinguish $|\tilde{\psi}\rangle$ and $|\psi\rangle$, and we use $|\psi\rangle$ instead of $|\tilde{\psi}\rangle$ for convenience.

Next, we design the controller according to the new system model described in Equation 6.12. Here, the Lyapunov function selected is the same as in Equation 6.6. It can be calculated that the first-order time derivative of V is given by

$$\dot{V} = \langle \dot{\psi} | \psi - \psi_f \rangle + \langle \psi - \psi_f | \dot{\psi} \rangle \quad (6.14)$$

Dividing both sides of Equation 6.12 by i gives the following form:

$$|\dot{\psi}\rangle = -i \left(\tilde{H}_0 + \sum_{k=1}^m \tilde{H}_k u_k(t) - \Lambda \right) |\psi\rangle \quad (6.15)$$

Substituting Equation 6.15 into Equation 6.14 gives:

$$\begin{aligned}
 \dot{V} &= \langle \psi | \left(-i\tilde{H}_0 - i \sum_{k=1}^m \tilde{H}_k u_k(t) + i\Lambda \right)^+ |\psi - \psi_f\rangle + \langle \psi - \psi_f | (-i\tilde{H}_0 - i \sum_{k=1}^m \tilde{H}_k u_k(t) + i\Lambda) |\psi\rangle \\
 &= 2\Im \left(\langle \psi | \sum_{k=1}^m \tilde{H}_k u_k(t) |\psi\rangle \right) - 2\Im \left(\langle \psi_f | \left(\tilde{H}_0 + \sum_{k=1}^m \tilde{H}_k u_k(t) - \Lambda \right) |\psi\rangle \right) \\
 &= -2\Im \left(\langle \psi_f - \psi | \sum_{k=1}^m \tilde{H}_k u_k(t) |\psi\rangle \right) - 2\Im (\langle \psi_f | (\tilde{H}_0 - \Lambda) |\psi\rangle)
 \end{aligned} \tag{6.16}$$

Because $|\psi_f\rangle = \sum_n c_n |\psi_n\rangle$ and $\tilde{H}_0 |\psi_n\rangle = \lambda_n |\psi_n\rangle$, we get $\Im (\langle \psi_f | (\tilde{H}_0 - \Lambda) |\psi\rangle) = 0$.

Finally the expression of \dot{V} is obtained:

$$\dot{V} = -2 \sum_{k=1}^m u_k(t) \Im (\langle \psi_f - \psi | \tilde{H}_k |\psi\rangle) \tag{6.17}$$

Observing Equation 6.17, the most reliable method of ensuring $\dot{V} \leq 0$ is to let each item of the summation sign be non-negative, that is, the sign of u_k is the same as $\Im (\langle \psi_f - \psi | H_k |\psi\rangle)$. We can choose the control law u_k to be

$$u_k = K_k \Im (\langle \psi_f - \psi | \tilde{H}_k |\psi\rangle) \tag{6.18}$$

where $K_k > 0$.

V decreases gradually under the action of u_k and reaches zero when $|\psi\rangle = |\psi_f\rangle$. At the moment when $u_k = 0$ and $\dot{V} = 0$, the system state is stabilized at the final state $|\psi_f\rangle$.

Comparing the design method proposed in this section with the one in Section 4.3, there are some similarities as well as differences between them.

First, both of them select the state errors as the Lyapunov functions and the control laws are derived from Lyapunov stability theorem, guaranteeing that the first-order time derivatives of the Lyapunov functions are non-positive. When the target state is an eigenstate of the inner Hamiltonian, the control system designed by either method is stable under the meaning of the Lyapunov method.

Second, transformations are performed in the system. In Section 4.3 we introduced a new imaginary real scalar control field ω . ω can be used to adjust the global phase of the controlled state, but does not change the probability distribution value of the system. Here we use unitary transformation to change the local phase, which does not affect the probability distribution.

Third, the transformation in Section 4.3 did not change the Hamiltonian of the system, but in here it does. Comparing Equation 6.10 with Equation 6.18, the two control laws have similar expressions, but the Hamiltonian in Equation 6.10 is time-independent and is still the original Hamiltonian of the system, while the Hamiltonian \tilde{H}_k in Equation 6.18 might be time-dependent and is not the original one. The simulation experiment may be more complex using the control law expressed in Equation 6.18 than using the one in Equation 6.10.

Fourth, considering Equation 6.8, when the target state is not an eigenstate of the inner Hamiltonian, the sign of $\Im (\langle \psi_f | (H_0 + \omega I) |\psi\rangle)$ used in Section 4.3 was not determined. It might be negative or positive, thus the stable control law under the meaning of Lyapunov cannot be

obtained. $\Im(\langle \psi_f | (\tilde{H}_0 - \Lambda) |\psi \rangle)$ in Equation 6.16 is always equal to zero, no matter what state $|\psi_f\rangle$ is. We can therefore obtain the arbitrary desired target state by designing the control variable u_k . This result is caused by different eigenequations in this section and in Section 4.3. The eigenequation satisfied in Section 4.3 is $H_0 |\psi_f\rangle = \lambda_f |\psi_f\rangle$, while it is $\tilde{H}_0 |\psi_n\rangle = \lambda_n |\psi_n\rangle$ in this section.

6.1.2 Control System Simulations and Results Analyses

In this subsection we will study the control properties of the proposed controller by control system simulation experiments.

Here we still select a spin-1/2 particle system as the controlled system. Suppose that the spin-1/2 particle system is controlled only by one control field u_1 and this control field is the electromagnetic field in the y -direction. The particle is self-spin in σ_z . Then the system satisfies the following Schrödinger equation:

$$i |\psi\rangle = (H_0 + H_1 u_1) |\psi\rangle \quad (6.19)$$

where $H_0 = \sigma_z = \begin{bmatrix} 1 & 0 \\ 0 & -1 \end{bmatrix}$ and $H_1 = \sigma_y = \begin{bmatrix} 0 & -i \\ i & 0 \end{bmatrix}$. The eigenstates of H_0 are $\lambda_1 = 1$ and $\lambda_2 = -1$. When we select the unitary operator $U = \text{diag}(e^{-it}, e^{it})$ and put it into Equation 6.19, the following form can be obtained:

$$i |\psi\rangle = (\tilde{H}_0 + \tilde{H}_1 u_1 - \Lambda) |\psi\rangle \quad (6.20)$$

where $\tilde{H}_0 = U^+ H_0 U = \begin{bmatrix} 1 & 0 \\ 0 & -1 \end{bmatrix}$, $\tilde{H}_1 = U^+ H_1 U = \begin{bmatrix} 0 & -ie^{2it} \\ ie^{-2it} & 0 \end{bmatrix}$, and $\Lambda = \text{diag}(\lambda_1, \lambda_2)$.

1) In the situation of the target eigenstate

Suppose that the initial state of the system is an eigenstate $|\psi_0\rangle = |0\rangle = \begin{bmatrix} 1 \\ 0 \end{bmatrix}$ and the desired final state is also an eigenstate $|\psi_f\rangle = |1\rangle = \begin{bmatrix} 0 \\ 1 \end{bmatrix}$. From Equation 6.18 we can get the following control law:

$$u_1 = K_1 \Im(\langle \psi_f | \tilde{H}_1 |\psi \rangle) \quad (6.21)$$

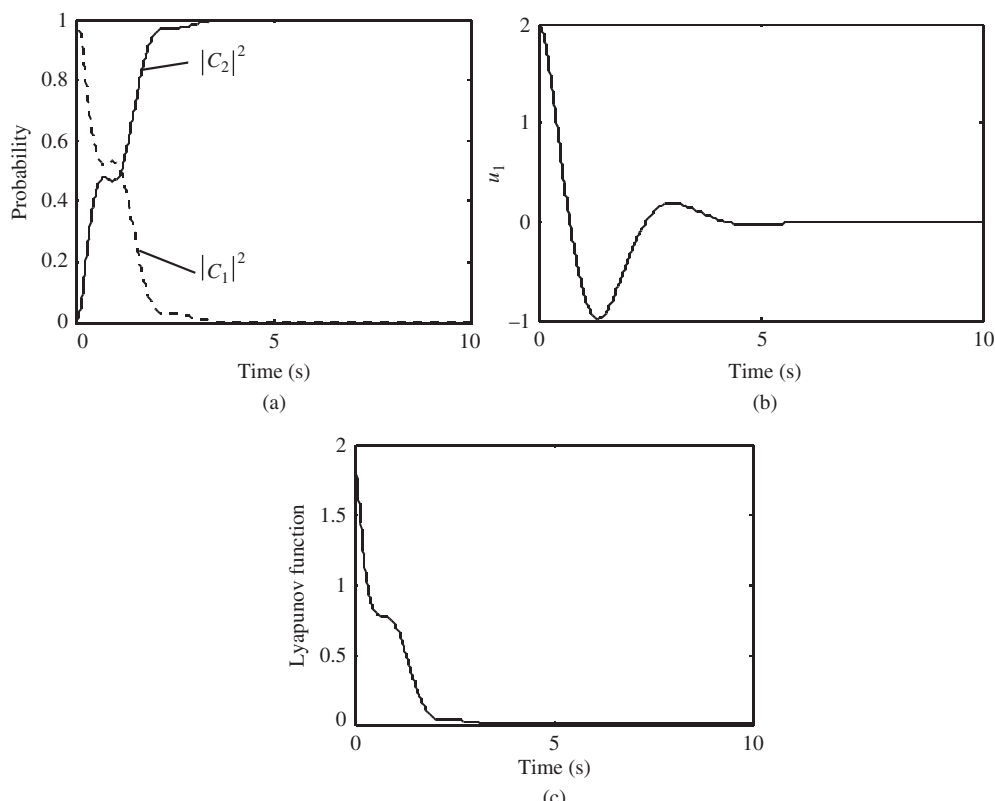
Next we analyze the influence of the parameter K_1 on the transfer time in the control by carrying out simulation experiments of the system described by Equation 6.20.

In the simulation experiments, the sampling time T is 0.01 seconds and the parameter K_1 is adjusted to different values. By analyzing the simulation results, we find that the transfer time decreases as the value of K_1 increases. On the other hand, the maximum of the control value increases as K_1 increases. When $|C_2|^2 = 0.995$, the simulation results under different values of K_1 are shown in Table 6.1, from which it can be seen that when $K_1 = 2$, it has the shortest transfer time of 3.47 seconds. Larger K_1 would induce a larger control value. In the actual application, the trade-off between the transfer time and the control variable must be taken into account.

Table 6.1 The simulation results with different values of K_1

Experiment number	Parameter K_1	Range of u_1	Transfer time (s)
1	0.5	(−0.47, 0.5)	13.09
2	1	(−0.78, 1.0)	6.57
3	2	(−0.98, 2.0)	3.47

The simulation results of the control system with $K_1 = 2$ are shown in Figure 6.1a–c, in which Figure 6.1a shows the probability of the state evolution, from which one can see that at any moment $|C_1|^2 + |C_2|^2 = 1$ holds, that is, the probability is conservative. Figure 6.1b shows the control value. It can be seen that when the controlled state reaches the target state, the control value u_1 tends to zero and stays at zero. The system state is also steady in the desired state. Figure 6.1c shows the Lyapunov function. It can be seen that $V = 0$ is satisfied and state transfer is finished when $t = 3.47$ seconds.

**Figure 6.1** The simulation results of the control system with $K_1 = 2$: (a) probability of the state evolution, (b) control value of the system, and (c) variation of the Lyapunov function

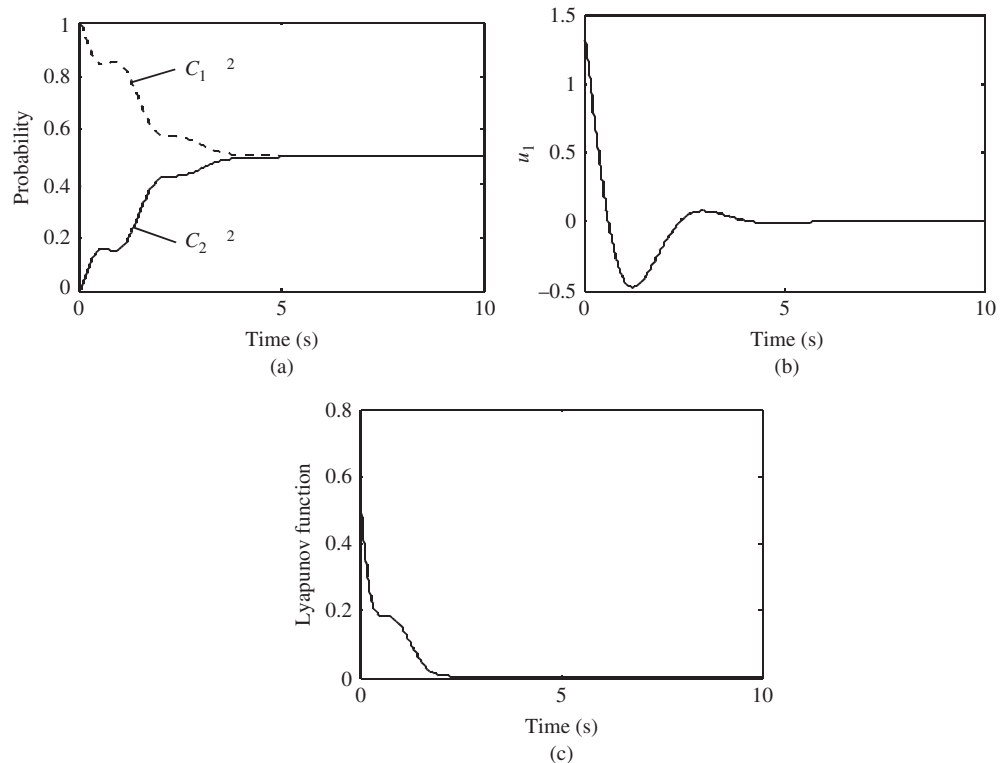


Figure 6.2 The simulation results of the control system with $K_1 = 2$: (a) probability of the state evolution, (b) control value of the system, and (c) variation of the Lyapunov function

2) In the situation of the target superposition state

Suppose that the initial state of the system is an eigenstate $|\psi_0\rangle = |0\rangle = \begin{bmatrix} 1 \\ 0 \end{bmatrix}$ and the desired target state is a superposition state $|\psi_f\rangle = \frac{1}{\sqrt{2}}(|0\rangle + |1\rangle)$. In this case, the expression of the control value is still Equation 6.21.

In the simulation experiments, the same situation that appeared in the process of eigenstate transfer can be found: the transfer time decreases and the maximum of control increases as K_1 increases. The simulation results under the conditions of $T = 0.01$ seconds and $K_1 = 2$ are shown in Figure 6.2a–c. Figure 6.2a shows that the system state is transferred to $|0\rangle$ and $|1\rangle$ with the same probability 1/2. In Figure 6.2b, the control value u_1 tends to zero and stays there once the controlled state reaches the target. In Figure 6.2c, the Lyapunov function decreases continuously and tends to zero.

6.2 Optimal Control Strategy of the Superposition State

In quantum chemistry and quantum physics, the eigenstates or superposition states of quantum systems need to be prepared according to practical applications. The design process of

the control law for a quantum system is a special case in that both the initial and the target states are eigenstates. When the target state is an arbitrary superposition state, it is difficult to steer the initial state to the target one and keep the state steady. Benallou *et al.* proposed a design method for an optimal stabilizing controller for bilinear systems without iteration (Benallou, Mellichamp, and Seborg, 1988). Because the mathematical model of the pure state quantum system is formally a bilinear system, in this section we will apply the design idea in the macroscopic field proposed by Benallou *et al.* to the pure state quantum systems. For the situation in which the target state is an arbitrary superposition state, this section will design the control law.

6.2.1 Preliminary Knowledge

In Section 4.2 we presented the Lyapunov stability theorem, which is used throughout this section. For a given system $\dot{\mathbf{x}} = \mathbf{f}(\mathbf{x})$, one can determine its stability without solving it, which can be done by using the Lyapunov stability theorem. This theorem requires one to seek a function called the Lyapunov function $V(\mathbf{x})$, which satisfies some specified properties. One can determine whether the controlled system of interest is stable according to the sign of the derivative of $V(\mathbf{x})$.

Here we will also use the principle of optimality and the sufficient condition for optimality. We suppose that the controlled system is in the form of $\dot{\mathbf{x}}(t) = \mathbf{f}[\mathbf{x}(t), \mathbf{u}(t), t]$, where $t \in [T_1, T_2]$, $\mathbf{x}(t) \subset \mathbb{R}^n \times [T_1, T_2]$, and $\mathbf{u}(t) \subset \mathbb{R}^m \times [T_1, T_2]$. Let X be a given region in $\mathbb{R}^n \times [T_1, T_2]$ and contain the target set S . For each (\mathbf{x}_0, t_0) in X , we need to determine the control \mathbf{u} which transfers (\mathbf{x}_0, t_0) to S and minimizes the performance index $J(\mathbf{x}, \mathbf{u}, t) = \int_{t_0}^{t_1} L[\mathbf{x}(t), \mathbf{u}(t), t] dt$. We define $J^*(\mathbf{x}, t)$ as the minimum of $J(\mathbf{x}, \mathbf{u}, t)$. The Hamiltonian $H(\mathbf{x}, \mathbf{p}, \mathbf{u}, t)$ is given by $H(\mathbf{x}, \mathbf{p}, \mathbf{u}, t) = L(\mathbf{x}, \mathbf{u}, t) + \langle \mathbf{p}, \mathbf{f}(\mathbf{x}, \mathbf{u}, t) \rangle$.

Principle of Optimality: If $\mathbf{u}^*(t)$ is an optimal control and if $\mathbf{x}^*(t)$, for $t \in [t_0, t_1]$, is the optimal trajectory corresponding to $\mathbf{u}^*(t)$, then the restriction of $\mathbf{u}^*(t)$ to a subinterval $[t, t_1]$ of $[t_0, t_1]$ is an optimal control for the initial pair $(\mathbf{x}^*(t), t)$.

Theorem 6.1 (Athans and Falb, 1966) Suppose that $X = \mathbb{R}^n \times (T_1, T_2)$, H is normal relative to $\mathbb{R}^n \times (T_1, T_2)$, and $\mathbf{u}(\mathbf{x}, \mathbf{p}, t)$ is the H -minimal control relative to $\mathbb{R}^n \times (T_1, T_2)$. Let $\mathbf{u}^*(t)$ be an admissible control such that:

1. $\mathbf{u}^*(t)$ transfers (\mathbf{x}_0, t_0) to set S and
2. there is a solution $J^*(\mathbf{x}, t)$ of the Hamilton–Jacobi equation

$$\frac{\partial J}{\partial t}(\mathbf{x}, t) + H \left[\mathbf{x}, \frac{\partial J}{\partial \mathbf{x}}(\mathbf{x}, t), \mathbf{u} \left(\mathbf{x}, \frac{\partial J}{\partial \mathbf{x}}(\mathbf{x}, t), t \right), t \right] = 0$$

satisfying the boundary condition $J(\mathbf{x}, t) = 0$ for $(\mathbf{x}, t) \in S$, such that $\mathbf{u}^*(t) = \left(\mathbf{x}^*(t), \frac{\partial J^*}{\partial \mathbf{x}}(\mathbf{x}^*(t), t), t \right)$ for t in (t_0, t_1) . Then $\mathbf{u}^*(t)$ is an optimal control.

Theorem 6.1 is a global sufficiency condition for the optimality, and the Hamilton–Jacobi equation is most often used as a check on the optimality of a control derived from the minimum principle.

6.2.2 Control Law Design

The controlled system of interest is the pure state of a quantum system, which can be described as the following Schrödinger equation:

$$i\hbar |\psi\rangle = H |\psi\rangle, H = H_0 + H_c(t), H_c(t) = \sum_{i=1}^m H_i u_i(t) \quad (6.22)$$

where H_0 is the inner Hamiltonian and $H_c(t)$ is the interaction Hamiltonian generated by the interaction of the external controls and the system. Both H_0 and H_i are linear Hermitian operators independent of time. $u_i(t)$ is a realizable, scalar, real-valued control function. Here \hbar is set to 1.

Considering the Schrödinger equation (Equation 6.22), in order to make the system state reach the arbitrary state, one needs first to eliminate the drift term $H_0 = \text{diag}(\lambda_1, \lambda_2, \dots, \lambda_n)$ in Equation 6.22, which can be done by performing a unitary transformation. Assuming that $|\psi(t)\rangle$ satisfies Equation 6.22, the form of the unitary transformation is as follows:

$$|\psi(t)\rangle = U(t) |\tilde{\psi}(t)\rangle \quad (6.23)$$

where the unitary matrix $U(t) = \text{diag}(e^{-i\lambda_1 t}, e^{-i\lambda_2 t}, \dots, e^{-i\lambda_n t})$. Substituting Equation 6.23 into Equation 6.22, one can obtain:

$$i |\tilde{\psi}\rangle = \left(\tilde{H}_0 + \sum_{i=1}^m \tilde{H}_i u_i(t) - i U^\dagger \dot{U} \right) |\tilde{\psi}\rangle \quad (6.24)$$

where $\tilde{H}_0 = U^\dagger H_0 U = H_0$, $\tilde{H}_i = U^\dagger H_i U$, and $i U^\dagger \dot{U} = H_0$.

In such a way, the drift term H_0 is eliminated and Equation 6.24 can be written into the following form:

$$i |\tilde{\psi}\rangle = \sum_{i=1}^m \tilde{H}_i u_i(t) |\tilde{\psi}\rangle \quad (6.25)$$

One can write $|\psi\rangle = \sum_n C_n |\psi_n\rangle$ and $|\tilde{\psi}\rangle = \sum_n \tilde{C}_n |\tilde{\psi}_n\rangle$, where $\tilde{C}_n = e^{i\lambda_n t} C_n$. Then $|\tilde{C}_n| = |C_n|$, that is, Equations 6.25 and 6.22 describe the same system (Boscain and Chambrion, 2002b). In the following discussion we will not distinguish $|\tilde{\psi}\rangle$ and $|\psi\rangle$.

Let $|\psi\rangle = [x_1 + ix_{n+1} \ x_2 + ix_{n+2} \ \dots \ x_n + ix_{2n}]^T$. Equation 6.25 in real state-space is given by:

$$\dot{\mathbf{x}} = \sum_{i=1}^m \tilde{B}_i u_i(t) \mathbf{x} \quad (6.26)$$

where $\tilde{B}_i = \begin{bmatrix} \Re(\tilde{H}_i) & \Im(\tilde{H}_i) \\ -\Im(\tilde{H}_i) & \Re(\tilde{H}_i) \end{bmatrix}$ and \tilde{B}_i is a skew symmetric matrix that satisfies $\tilde{B}_i + \tilde{B}_i^T = 0$. The optimal control law of Equation 6.26 is given by Theorem 6.2.

Theorem 6.2 For the system defined by Equation 6.26, give the performance index:

$$J = \frac{1}{2} \int_0^\infty \left\{ \sum_{i=1}^m \frac{1}{r_i} \left[(\mathbf{x} - \mathbf{x}_f)^T P \tilde{B}_i \mathbf{x} \right]^2 + \mathbf{u}^T R \mathbf{u} \right\} dt \quad (6.27)$$

where $\mathbf{u} = [u_1 \ u_2 \ \dots \ u_m]^T$, R is a diagonal matrix with positive elements $r_i > 0 (i = 1, 2, \dots, m)$, and P is a positive definite symmetric matrix. Then there exists an optimal control law:

$$u_i^* = -\frac{1}{r_i}(\mathbf{x} - \mathbf{x}_f)^T P \tilde{B}_i \mathbf{x}, (i = 1, 2, \dots, m) \quad (6.28)$$

such that the system Equation 6.26 is stable and the performance index (Equation 6.27) is minimum.

The proof method of Theorem 6.2 is the same as that of Theorem 4.3, thus it will not be repeated. Comparing the control law given by Theorem 4.3 with the one given by Theorem 6.2, the following conclusions can be obtained.

Remarks on Theorem 6.2

1. Theorems 6.1 and 6.2 are suitable for different models. Theorem 4.3 in Section 4.3.2 is suitable for the model (Equation 4.24), which is obtained by introducing a new imaginary real scalar control field ω in Equation 6.22. ω can be used to adjust the global phase of the controlled state, but does not change the probability distribution value of the system. Theorem 6.2 is suitable for the model (Equation 6.25), which is obtained by performing a unitary transformation to Equation 6.26. The unitary transformation changes the local phase, but does not affect the probability distribution either.
2. Theorem 4.3 is only suitable for the target eigenstate, and the positive definite matrix P is defined by Equation 4.26. While the drift term is eliminated in Equation 6.25 by the unitary transformation, Theorem 6.2 is effective for the arbitrary target pure state, and the weighting matrix P can be selected independently.
3. The transformation in Equation 6.2 does not change the Hamiltonian of the system, but the transformation in Equation 6.25 does. Comparing the optimal control law (Equation 4.27) in the eigenstate case with Equation 6.21, the two control laws have similar expressions, but B_i in Equation 6.6 is time-independent, while \tilde{B}_i in Equation 6.21 might be time-dependent. In the numerical simulations, it may be more complex to use the control law expressed in Equation 6.21 than in Equation 6.6.

In the next subsection, we will give the design method for the optimal control law for a concrete quantum system, and analyze the influence of the parameters on the control law.

6.2.3 Numerical Simulations

Suppose that the spin-1/2 particle system is controlled by only one control field u_1 , which is the electromagnetic field in the y -direction. The particle is self-spin in σ_z . The system satisfies the following Schrödinger equation:

$$i|\psi\rangle = (H_0 + H_1 u_1)|\psi\rangle \quad (6.29)$$

where $H_0 = \sigma_z = \begin{bmatrix} 1 & 0 \\ 0 & -1 \end{bmatrix}$ and $H_1 = \sigma_y = \begin{bmatrix} 0 & -i \\ i & 0 \end{bmatrix}$.

Suppose that the initial state of the system is an eigenstate $|\psi_0\rangle = |0\rangle = \begin{bmatrix} 1 \\ 0 \end{bmatrix}$ and the target state is a superposition state $|\psi_f\rangle = \frac{1}{\sqrt{2}}(|0\rangle + |1\rangle)$. The unitary operator $U = \text{diag}(e^{-it}, e^{it})$ is selected. After unitary transformation Equation 6.29 can be written as:

$$i|\dot{\psi}\rangle = \tilde{H}_1 u_1 |\psi\rangle \quad (6.30)$$

$$\text{where } \tilde{H}_1 = U^\dagger H_1 U = \begin{bmatrix} 0 & -ie^{2it} \\ ie^{-2it} & 0 \end{bmatrix}.$$

Transform Equation 6.30 into the following real state equation:

$$\dot{x} = \tilde{B}_1 u_1(t) x \quad (6.31)$$

$$\text{where } \tilde{B}_1 = \begin{bmatrix} 0 & -\cos(2t) & 0 & \sin(2t) \\ \cos(2t) & 0 & \sin(2t) & 0 \\ 0 & -\sin(2t) & 0 & -\cos(2t) \\ -\sin(2t) & 0 & \cos(2t) & 0 \end{bmatrix} \text{ and } x_0 = [1 \ 0 \ 0 \ 0]^T, x_f = \begin{bmatrix} \frac{1}{\sqrt{2}} & \frac{1}{\sqrt{2}} & 0 & 0 \end{bmatrix}^T.$$

According to Theorem 6.2, $J = \frac{1}{2} \int_0^\infty \left\{ \frac{1}{r_1} \left[(\mathbf{x} - \mathbf{x}_f)^T P \tilde{B}_1 \mathbf{x} \right]^2 + r_1 u_1^2 \right\} dt$ is selected as the performance index, and the obtained optimal control law is

$$u_1^* = -\frac{1}{r_1} (\mathbf{x} - \mathbf{x}_f)^T P \tilde{B}_1 \mathbf{x} \quad (6.32)$$

in which the effect of the parameters P and r_1 is the same as in Equation 4.39. In the numerical simulation, the sampling time $T = 0.01$ seconds. When the parameters $P = \text{diag}(2, 1, 2, 1)$ and $r_1 = 1$, the simulation curves of the control system are as shown in Figure 6.3a–c, from which one can see that in Figure 6.3a, the system state transforms to $|0\rangle$ and $|1\rangle$ with the same probability 1/2. In Figure 6.3b, the control value u_1^* tends to zero and stays there once the controlled state reaches the target state. In Figure 6.3c, J gradually increases with time and tends to a constant.

In fact, the method in Theorem 6.2 can also steer the system states to the eigenstates. Considering the practical needs and operating convenience, if the control strategy used in Theorem 4.3 can meet demands, one need not use the control strategy in Theorem 6.2. However, when the preparation of superposition state is needed, the control strategy in Theorem 4.3 is invalid, so we have to use the control strategy in Theorem 6.2.

6.3 Optimal Control of Mixed-State Quantum Systems

In the applications of optimal control theory, one can select different performance indices and get different control laws. Here we will select the error between the states as a performance index of the control law. We have applied this method to a superposition state in Section 6.2. As a further step, in this section we will consider the mixed-state control problem based on the formulas of statistical mechanics for the Liouville equation.

In a quantum system, two reasons lead to a mixed state. The first is quantum dissipation due to quantum system entanglement with environment. In such a situation, the system will be open.

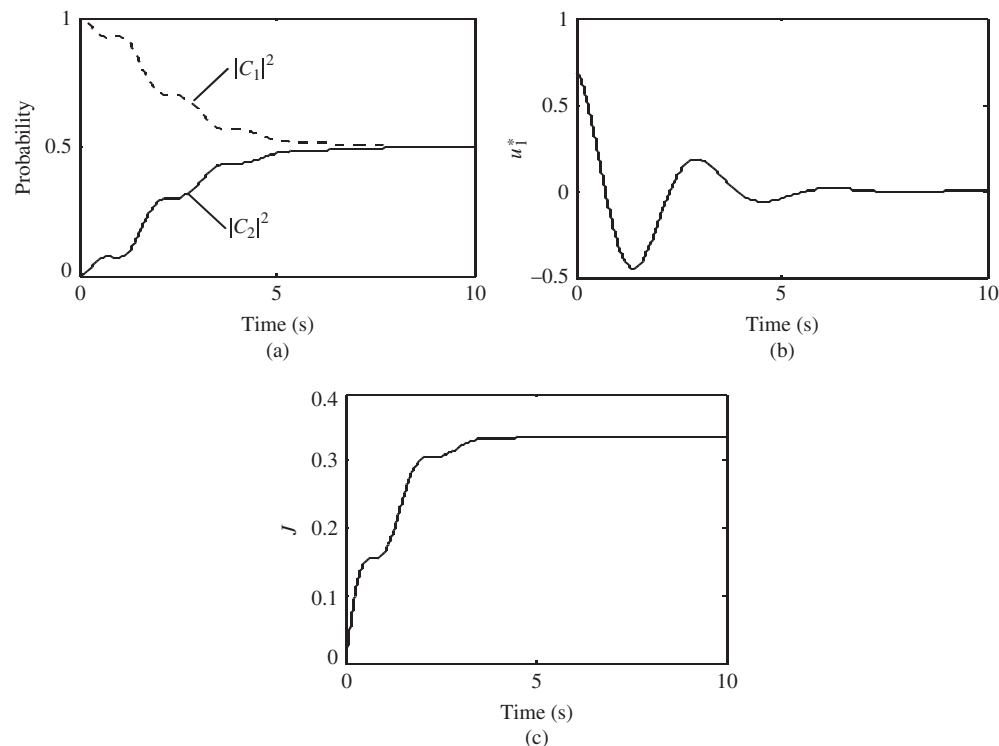


Figure 6.3 System simulation results with superposition target state: (a) probability of the state evolution, (b) control value of the system, and (c) variation of the performance index

A quantum state will become a mixed-state even though it is a pure state at the beginning, and the evolution of the density matrix in this open system will not be unitary. The second reason is that the large amount of the same particles in different pure states are incoherent mixed, which would be a quantum ensemble. Particles in different pure states are in this ensemble with some probability, viz. average statistics. In this section, we only consider a closed quantum system without interaction with the environment, so mixed-state here refers to mixed-state in ensemble.

6.3.1 Model of the System to be Controlled

The state of a quantum mechanical system can be described in various ways. When a system is in a pure state not entangled with its environment, the state of the system can be described by a wave function that evolves according to a control-dependent Schrödinger equation. One can also describe the state of the system by a density operator $\hat{\rho}(t)$, which can represent not only a pure state but also a mixed state. The density operator $\hat{\rho}(t)$ acting on the system's Hilbert space \mathcal{H} evolves with time according to the quantum Liouville equation:

$$i\hbar \frac{\partial}{\partial t} \hat{\rho}(t) = [\hat{H}(t), \hat{\rho}(t)], \quad \hat{H}(t) = \hat{H}_0 + \sum_{m=1}^M f_m(t) \hat{H}_m \quad (6.33)$$

where \hat{H}_0 is the system's internal (or free) Hamiltonian and \hat{H}_m is the interaction (or control) Hamiltonian. Both of these will be assumed to be time-independent. $f_m(t)$ is the admissible real-valued external control field. We set the Planck constant $\hbar = 1$ for convenience.

Because $\hat{\rho}(t)$ is a $N \times N$ density matrix in Hilbert space, it is difficult to solve the differential Equation 6.33. One may introduce the Liouville operator in Liouville space according to the concept of the Dirac operator to simplify this problem. There is a natural connection between the density matrix and Liouville space (Barnett and Dalton, 1987; Ohtsuki and Fujimura, 1989). In Liouville space, Equation 6.33 can be represented in the same form as the Schrödinger equation:

$$i \frac{\partial}{\partial t} |\rho(t)\rangle\rangle = \mathcal{L}(t) |\rho(t)\rangle\rangle, \quad \mathcal{L}(t) = \mathcal{L}_0 + \sum_{m=1}^M f_m(t) \mathcal{L}_m \quad (6.34)$$

where $|\rho(t)\rangle\rangle$ is defined as a Liouville ket and \mathcal{L} is the Liouville operator defined by the dual correspondence:

$$\mathcal{L}(t) |\rho(t)\rangle\rangle \leftrightarrow [\hat{H}, \hat{\rho}(t)] \quad (6.35)$$

The basis vectors belonging to Liouville space and Hilbert space are defined by the objective correspondence $|mn\rangle\rangle \leftrightarrow |m\rangle\langle n|$ (Schirmer, 2000). Then one has:

$$\begin{aligned} \mathcal{L}_{jk,mn} &= \langle\langle jk | \mathcal{L} | mn \rangle\rangle = \langle j | [\hat{H}, |m\rangle\langle n|] | k \rangle \\ &= tr(|k\rangle\langle j| [\hat{H}, |m\rangle\langle n|]) \\ &= \sum_i (\langle i | |k\rangle\langle j| [\hat{H}] | m \rangle\langle n | |i\rangle - \langle i | |k\rangle\langle j| | m \rangle\langle n | [\hat{H}] | i \rangle) \\ &= \langle j | [\hat{H}] | m \rangle\delta_{nk} - \langle n | [\hat{H}] | k \rangle\delta_{jm} = H_{jm}\delta_{nk} - H_{kn}^*\delta_{jm} \end{aligned} \quad (6.36)$$

For a $N \times N$ density matrix $\hat{\rho}(t)$ in Hilbert space, its replacement form $|\rho(t)\rangle\rangle$ is an N^2 column vector in Liouville space and \mathcal{L} is an $N^2 \times N^2$ matrix. In such a way it is much easier to solve Equation 6.34 than Equation 6.33 expressed in terms of some commutators. Hence, Equation 6.34 will be adopted as the investigated model in the following subsections.

6.3.2 Control Law Design

Quantum control problems can be formulated in the state steering (or transfer) problem, that is to say steer the system from a given initial state to a desired target state. In this section we will develop an optimal control method based on the Lyapunov theorem for the Liouville equation.

First we will introduce the principle of the optimality and the sufficient condition for optimality. Suppose the controlled system is in the form of $\dot{\mathbf{x}}(t) = \mathbf{f}[\mathbf{x}(t), \mathbf{u}(t), t]$, where $t \in [T_1, T_2]$, $\mathbf{x}(t) \subset \mathbb{R}^n \times [T_1, T_2]$, and $\mathbf{u}(t) \subset \mathbb{R}^m \times [T_1, T_2]$. Let X be a given region in $\mathbb{R}^n \times [T_1, T_2]$ and contain the target set S . For each (\mathbf{x}_0, t_0) in X , one needs to determine the control \mathbf{u} which transfers (\mathbf{x}_0, t_0) to S and minimizes the performance index $J(\mathbf{x}, \mathbf{u}, t) = \int_{t_0}^{t_1} L[\mathbf{x}(t), \mathbf{u}(t), t] dt$. Defining $J^*(\mathbf{x}, t)$ as the minimum of $J(\mathbf{x}, \mathbf{u}, t)$, the Hamiltonian $H(\mathbf{x}, \mathbf{p}, \mathbf{u}, t)$ is given by $H(\mathbf{x}, \mathbf{p}, \mathbf{u}, t) = L(\mathbf{x}, \mathbf{u}, t) + \langle \mathbf{p}, \mathbf{f}(\mathbf{x}, \mathbf{u}, t) \rangle$.

Principle of Optimality: If $\mathbf{u}^*(t)$ is an optimal control and if $\mathbf{x}^*(t)$, for $t \in [t_0, t_1]$, is the optimal trajectory corresponding to $\mathbf{u}^*(t)$, then the restriction of $\mathbf{u}^*(t)$ to a subinterval $[t, t_1]$ of $[t_0, t_1]$ is an optimal control for the initial pair $(\mathbf{x}^*(t), t)$.

Sufficient Condition for Optimality (Athans and Falb, 1966): Suppose that $X = \mathbb{R}^n \times (T_1, T_2)$, H is normal relative to $\mathbb{R}^n \times (T_1, T_2)$, and $\mathbf{u}(\mathbf{x}, \mathbf{p}, t)$ is the H -minimal control relative to $\mathbb{R}^n \times (T_1, T_2)$. Let $\mathbf{u}^*(t)$ be an admissible control such that:

1. $\mathbf{u}^*(t)$ transfers (\mathbf{x}_0, t_0) to S .
2. There is a solution $J^*(\mathbf{x}, t)$ of the Hamilton–Jacobi equation

$$\frac{\partial J}{\partial t}(\mathbf{x}, t) + H\left[\mathbf{x}, \frac{\partial J}{\partial \mathbf{x}}(\mathbf{x}, t), \mathbf{u}\left(\mathbf{x}, \frac{\partial J}{\partial \mathbf{x}}(\mathbf{x}, t), t\right)\right] = 0$$

satisfying the boundary condition $J(\mathbf{x}, t) = 0$ for $(\mathbf{x}, t) \in S$, such that

$$\mathbf{u}^*(t) = \left(\mathbf{x}^*(t), \frac{\partial J^*}{\partial \mathbf{x}}(\mathbf{x}^*(t), t), t\right)$$

for t in (t_0, t_1) . Then $\mathbf{u}^*(t)$ is an optimal control.

1) Stationary target state

Assume the target state is the statistical incoherent mixtures of energy eigenstates: $\hat{\rho}_f = \sum_{n=1}^N w_n |n\rangle \langle n|$ and $\hat{\rho}_f$ is a stationary target state, for example $\hat{\rho}_f = |0\rangle \frac{1}{4} \langle 0| + |1\rangle \frac{3}{4} \langle 1| = \frac{1}{4} \begin{pmatrix} 1 & 0 \\ 0 & 3 \end{pmatrix}$. In this case, all of the off-diagonal elements in the target state are zeros. If so, the optimal control law is given by Theorem 6.3.

Theorem 6.3 For the system defined in Liouville space by Equation 6.34, given the performance index:

$$J = \frac{1}{2} \int_0^\infty \left\{ \sum_{m=1}^M \frac{1}{r_m} \left[\text{Im} \left(\langle \langle \rho - \rho_f | P \mathcal{L}_m | \rho \rangle \rangle \right) \right]^2 + \mathbf{f}(t)^T R \mathbf{f}(t) \right\} dt \quad (6.37)$$

where $\mathbf{f}(t) = [f_1(t) f_2(t) \dots f_M(t)]^T$, R is a diagonal matrix with positive elements, $r_m > 0$, ($m = 1, 2, \dots, M$), and P is a positive definite symmetric matrix that satisfies the equation:

$$P \mathcal{L}_0 - \mathcal{L}_0^\dagger P = 0 \quad (6.38)$$

then there exists an optimal control law:

$$f_m^* = -\frac{1}{r_m} \text{Im}(\langle \langle \rho - \rho_f | P \mathcal{L}_m | \rho \rangle \rangle), (m = 1, 2, \dots, M) \quad (6.39)$$

such that the system Equation 6.34 is stable and the performance index (Equation 6.37) is minimum.

In fact, according to the Lyapunov indirect stability theorem, P is a positive definite symmetric matrix that should satisfy the Lyapunov equation $P(i\mathcal{L}_0) + (i\mathcal{L}_0)^\dagger P = -Q$. Because \mathcal{L}_0

is a linear Hermitian operator whose eigenvalues are real, $i\mathcal{L}_0$ is a skew Hermitian operator whose eigenvalues are pure imaginary. Accordingly, $Q = 0$, which results in Equation 6.38.

Proof

1. Proof of stability

Select the following Lyapunov function:

$$V(|\rho\rangle\rangle) = \frac{1}{2} \langle\langle \rho - \rho_f | P | \rho - \rho_f \rangle\rangle \quad (6.40)$$

where P is a positive definite symmetric matrix satisfying Equation 6.38. The first-order time derivative of $V(|\rho\rangle\rangle)$ is:

$$\dot{V}(|\rho\rangle\rangle) = \text{Re}(\langle\langle \rho - \rho_f | P | \dot{\rho} \rangle\rangle) \quad (6.41)$$

Substituting Equation 6.34 into Equation 6.41 yields:

$$\dot{V}(|\rho\rangle\rangle) = \text{Im}(\langle\langle \rho - \rho_f | P \mathcal{L}_0 | \rho \rangle\rangle) + \sum_{m=1}^M f_m(t) \text{Im}(\langle\langle \rho - \rho_f | P \mathcal{L}_m | \rho \rangle\rangle) \quad (6.42)$$

Since $P \mathcal{L}_0 - \mathcal{L}_0^\dagger P = 0$ and $\mathcal{L}_0 | \rho_f \rangle\rangle = 0$, $\text{Im}(\langle\langle \rho - \rho_f | P \mathcal{L}_0 | \rho \rangle\rangle) = 0$ holds. Hence, Equation 6.42 can be re-written as:

$$\dot{V}(|\rho\rangle\rangle) = \sum_{m=1}^M f_m(t) \text{Im}(\langle\langle \rho - \rho_f | P \mathcal{L}_m | \rho \rangle\rangle) \quad (6.43)$$

Substituting the control law (Equation 6.39) into Equation 6.43 yields:

$$\dot{V}(|\rho\rangle\rangle) = - \sum_{m=1}^M \frac{1}{r_m} [\text{Im}(\langle\langle \rho - \rho_f | P \mathcal{L}_m | \rho \rangle\rangle)]^2 \leq 0 \quad (6.44)$$

Thus, the system Equation 6.34 is stable under the control law (Equation 6.39). Next we will prove that this control law is optimal.

2. Proof of optimality

(a) The sufficient condition for the optimality says that if a system can be transferred from some initial state to a target set by applying an admissible control, then an optimal control exists and may be found by determining the admissible control f_m^* that causes the system to reach the target set S . The description of the target set S is assumed to be known, so for the system Equation 6.34 it now only remains that one needs to construct a proper target set S . Here we use the same way we proved in Section 4.2 to construct the target set S . In fact, in the Lyapunov-based control design, the Lyapunov function V , can be seen as a target set S . One can therefore define the target set S as the Lyapunov function V by constructing an appropriate matrix P . P is selected using a positive definite symmetric matrix that satisfies Equation 6.38. At the same time, the eigenvectors with the largest eigenvalue are the maxima of V , the eigenvectors with the smallest eigenvalue are the minima, and all others are saddle points. The smallest eigenvalue of P is P_f , with the

corresponding target state ρ_f . The value of P that corresponds to the eigenvalues of the initial state is placed the closest to the target state. In such a way, a target set S with a monotonic function and the target state as the minima value are constructed, and the initial state can be transferred to the target state by the control law f_m^* .

(b) From Equations 6.39 and 6.44 we can get $J^*(|\rho\rangle\rangle, t)$ as follows:

$$\begin{aligned} J^*(|\rho\rangle\rangle, t) &= \frac{1}{2} \int_t^\infty \left\{ \sum_{m=1}^M \frac{1}{r_m} [\text{Im}(\langle\langle \rho - \rho_f | P\mathcal{L}_m | \rho \rangle\rangle)]^2 + \mathbf{f}^*(t)^T R \mathbf{f}^*(t) \right\} dt \\ &= \int_t^\infty \left\{ \sum_{m=1}^M \frac{1}{r_m} [\text{Im}(\langle\langle \rho - \rho_f | P\mathcal{L}_m | \rho \rangle\rangle)]^2 \right\} dt \\ &= - \int_t^\infty \dot{V}(|\rho\rangle\rangle) dt = V(|\rho\rangle\rangle) \end{aligned} \quad (6.45)$$

Thus, the Hamiltonian function of the system can be:

$$H(|\rho\rangle\rangle, \mathbf{f}) = L(|\rho\rangle\rangle, \mathbf{f}) + \text{Im} \left[\left(\frac{\partial V(|\rho\rangle\rangle)}{\partial |\rho\rangle\rangle} \right)^\dagger \left(\mathcal{L}_0 + \sum_{m=1}^M f_m(t) \mathcal{L}_m \right) |\rho\rangle\rangle \right] \quad (6.46)$$

where

$$L = \frac{1}{2} \sum_{m=1}^M \frac{1}{r_m} [\text{Im}(\langle\langle \rho - \rho_f | P\mathcal{L}_m | \rho \rangle\rangle)]^2 + \mathbf{f}(t)^T R \mathbf{f}(t)$$

Because $\frac{\partial J^*}{\partial t}(|\rho\rangle\rangle, t) = 0$, a part of the sufficient condition for the optimality is:

$$\min_{\mathbf{f} \in R^M} [H(|\rho\rangle\rangle, \mathbf{f})] = 0 \quad (6.47)$$

From Equation 6.46 one can obtain:

$$\begin{aligned} H(|\rho(t)\rangle\rangle, \mathbf{f}) &= \frac{1}{2} \sum_{m=1}^M \frac{1}{r_m} [\text{Im}(\langle\langle \rho - \rho_f | P\mathcal{L}_m | \rho \rangle\rangle)]^2 + \mathbf{f}(t)^T R \mathbf{f}(t) \\ &\quad + \text{Im}(\langle\langle \rho - \rho_f | P(\mathcal{L}_0 + \sum_{m=1}^M f_m(t) \mathcal{L}_m) | \rho \rangle\rangle) \\ &= \frac{1}{2} \sum_{m=1}^M \frac{1}{r_m} [\text{Im}(\langle\langle \rho - \rho_f | P\mathcal{L}_m | \rho \rangle\rangle)]^2 + \sum_{m=1}^M r_m f_m^2(t) \\ &\quad + \sum_{m=1}^M f_m(t) \text{Im}(\langle\langle \rho - \rho_f | P\mathcal{L}_m | \rho \rangle\rangle) \\ &= \frac{1}{2} \sum_{m=1}^M \frac{1}{r_m} [\text{Im}(\langle\langle \rho - \rho_f | P\mathcal{L}_m | \rho \rangle\rangle) + r_m f_m(t)]^2 \geq 0 \end{aligned} \quad (6.48)$$

Substituting Equation 6.39 into Equation 6.48 yields $H(|\rho(t)\rangle\rangle, \mathbf{f}^*) = 0$. Thus, the control law (Equation 6.39) is optimal and minimizes the performance index (Equation 6.37). The proof of Theorem 6.3 is completed. ■

The design steps of the optimal control law proposed based on Theorem 6.3 are as follows:

1. Select the weighting R of the control vector $R = \text{diag}(r_i)$, $r_i > 0$, $i = 1, 2, \dots, m$.
2. Solve Equation 6.38 to obtain the positive define matrix P .
3. Calculate the optimal stabilizing control law from Equation 6.39.

2) Non-stationary target state

If not all of the off-diagonal elements in the target state are zeros, which is also the case for a mixed-state, for example

$$\hat{\rho}_f = |1\rangle \frac{1}{2} \langle 1| + \left(\frac{\sqrt{2}}{2} |0\rangle + \frac{\sqrt{2}}{2} |1\rangle \right) \frac{1}{2} \left(\frac{\sqrt{2}}{2} \langle 0| + \frac{\sqrt{2}}{2} \langle 1| \right) = \frac{1}{4} \begin{pmatrix} 1 & 1 \\ 1 & 3 \end{pmatrix}$$

the target state $\hat{\rho}_f(t)$ is in fact not stationary but evolves under \hat{H}_0 according to the Liouville–von Neumann equation:

$$i \frac{\partial}{\partial t} \hat{\rho}_f(t) = [\hat{H}_0, \hat{\rho}_f(t)] \quad (6.49)$$

Now the target state is a time-dependent function, and the control problem becomes a trajectory tracking problem. From the system control point of view, a trajectory tracking problem can be solved by translating it into a state steering problem. To do this we first carry out the following unitary transformations:

$$\tilde{\rho}(t) = U(t) \tilde{\rho} U^\dagger(t) \quad (6.50)$$

and

$$\hat{\rho}_f(t) = U(t) \hat{\rho}_f U^\dagger(t) \quad (6.51)$$

in which $\tilde{\rho}_f$ is a stationary target state that equals $U(t) = \text{diag}(e^{-iE_1 t}, e^{-iE_2 t}, \dots, e^{-iE_N t})$ and $E_i, i = 1, \dots, N$, satisfying $\hat{H}_0 = \text{diag}(E_1, E_2, \dots, E_N)$ in Equation 6.33.

Substituting Equation 6.50 into Equation 6.33 one can obtain:

$$i \frac{\partial}{\partial t} \tilde{\rho}(t) = \left[\sum_{m=1}^M f_m(t) \tilde{H}_m(t), \tilde{\rho}(t) \right] \quad (6.52)$$

where $\tilde{H}_m(t) = U^\dagger(t) \hat{H}_m U(t)$.

Owing to the unitary transformation, $\hat{\rho}(t)$ and $\tilde{\rho}(t)$ have the same populations, which means that Equations 6.33 and 6.52 describe the same physical system. In such a way, the problem of system Equation 6.33 tracking a time-dependent target state $\hat{\rho}_f(t)$ in Equation 6.49 is equivalent to a problem of steering the state in system Equation 6.52 to the stationary target state $\tilde{\rho}_f$.

In the Liouville space, Equation 6.52 can be represented as:

$$i \frac{\partial}{\partial t} |\tilde{\rho}(t)\rangle\rangle = \sum_{m=1}^M f_m(t) \tilde{L}_m(t) |\tilde{\rho}(t)\rangle\rangle \quad (6.53)$$

The optimal control law of Equation 6.53 is given by Theorem 6.4.

Theorem 6.4 For the system defined by Equation 6.53 give the performance index:

$$J = \frac{1}{2} \int_0^\infty \left\{ \sum_{m=1}^M \frac{1}{r_m} \left[\text{Im} \left(\langle \langle \tilde{\rho} - \tilde{\rho}_f | P \tilde{\mathcal{L}}_m(t) | \tilde{\rho} \rangle \rangle \right) \right]^2 + \mathbf{f}(t)^T R \mathbf{f}(t) \right\} dt \quad (6.54)$$

where $\mathbf{f}(t) = [f_1(t) f_2(t) \dots f_M(t)]^T$, R is a diagonal matrix with positive elements, $r_m > 0$, ($m = 1, 2, \dots, M$), and P is a positive definite symmetric matrix. Then there exists an optimal control law:

$$f_m^* = -\frac{1}{r_m} \text{Im}(\langle \langle \tilde{\rho} - \tilde{\rho}_f | P \tilde{\mathcal{L}}_m(t) | \tilde{\rho} \rangle \rangle), (m = 1, 2, \dots, M) \quad (6.55)$$

such that system Equation 6.53 is stable and the performance index (Equation 6.54) is minimum.

The proof method of Theorem 6.4 is the same as that of Theorem 6.2, thus it will not be repeated here. In computer simulation, we need to choose an appropriate discrete propagation method to solve the differential Equation 6.34 or 6.53. A simple approach would be to adopt the first-order Euler method. However, in order to obtain a more efficient result, we employ the four-order Runge-Kutta method, which has higher precision and faster convergence rate.

6.3.3 Numerical Simulations and Results Analyses

As an explicit example we consider a typical diatomic molecule model with N discrete vibrational energy levels E_n corresponding to independent states $|n\rangle$ of the system. The internal Hamiltonian is given by:

$$\hat{H}_0 = \sum_{n=1}^N E_n |n\rangle \langle n| \quad (6.56)$$

Assume that the diatomic molecular system is controlled by a single control field $f(t)$. Then the total Hamiltonian of the system can be represented as $\hat{H}(t) = \hat{H}_0 + f(t)\hat{H}_1$, and the corresponding Liouville operator is $\hat{\mathcal{L}}(t) = \hat{\mathcal{L}}_0 + f(t)\hat{\mathcal{L}}_1$. The interaction Hamiltonian can be chosen as the dipole form:

$$\hat{H}_1 = \sum_{n=1}^{N-1} d_n (|n\rangle \langle n+1| + |n+1\rangle \langle n|) \quad (6.57)$$

Next we will separately study the diatomic molecules described by the Morse oscillator model and the Harmonic oscillator model.

1) Control system simulation of a Morse oscillator model

To simplify the calculation, we consider a hydrogen fluoride (HF) molecule described by a four-level Morse oscillator model. The vibrational energy levels are as follows (Schirmer and Solomon, 2001):

$$E_n = \hbar\omega_0 \left(n - \frac{1}{2} \right) \left[1 - \frac{1}{2} \left(n - \frac{1}{2} \right) B \right] \quad (6.58)$$

where $\omega_0 = 7.8 \times 10^{-14} \text{ s}^{-1}$ and $B = 0.0419$. Thus the corresponding energy levels are $E_1 = 0.4948$, $E_2 = 1.4529$, $E_3 = 2.3691$, and $E_4 = 3.2434$ in units of $\hbar\omega_0$. In the following calculations, all the parameters are expressed in atomic units (a.u.). Here the dipole moments in Equation 6.57 are $d_n = \sqrt{n}$, $n = 1, 2, 3$. This system is completely controllable, as verified in Schirmer and Solomon (2001).

Assume that the system is initially in the thermal equilibrium, that is, $\hat{\rho}_0 = \sum_{n=1}^4 w_n |n\rangle\langle n|$ with weights $w_n = C \exp[-E_n/(E_4 - E_1)]$. This is a Boltzmann distribution and the normalization constant $C = (e^{-E_1/kT} + e^{-E_2/kT} + e^{-E_3/kT} + e^{-E_4/kT})^{-1}$ with $kT = E_4 - E_1$. Concretely, $w_1 = 0.3877$, $w_2 = 0.2736$, $w_3 = 0.1961$, and $w_4 = 0.1426$. The control task is to determine the control field $f(t)$ so as to steer the system from the initial state $\hat{\rho}_0$ to the target state $\hat{\rho}_f = \sum_{n=1}^4 w_{5-n} |n\rangle\langle n|$. The state control problem and the observable control problem are inter-convertible. The control goal is to maximize the expectation value of the observable $\hat{A} = \hat{H}_0$.

According to Theorem 6.3, the optimal control law can be obtained as:

$$f(t) = -\frac{1}{r_1} \text{Im}(\langle\langle \rho - \rho_f | P\mathcal{L}_1 | \rho \rangle\rangle) \quad (6.59)$$

The initial state of the system lies within the set of states resulting in $\text{Im}(\langle\langle \rho_0 - \rho_f | P\mathcal{L}_1 | \rho_0 \rangle\rangle) = 0$, at the moment the control field $f_0 = 0$. This problem can be solved by applying an initial small magnitude disturbance to excite the system out of its initial equilibrium state (Beaucharda *et al.*, 2007). In our numerical system simulations, the initial control field $f_0 = 0.05$ a.u., the target time $t_f = 200$ a.u., and the sampling time $dt = 0.1$ a.u. The choice of suitable parameters r_1 and P is crucial to get good results. In order to obtain a higher probability for the target state, P can be chosen to make the Lyapunov function described by Equation 6.40 larger at the initial time, and the diagonal elements of the initial state are ordered in a non-increasing sequence. The corresponding elements of P are also arrayed in non-increasing sequence. After several trials of tuning, we select $r_1 = 1$ and

$$P = \text{diag}(18, 1, 1, 1, 1, 1.5, 1, 1, 1, 1, 1, 1, 1, 1, 0.01).$$

The numerical simulation results are shown in Figure 6.4a–d, where Figure 6.4a shows the control field. The corresponding evolution populations of energy levels 1–4 are shown in Figure 6.4b, from which one can see that the populations are inverted, that is, the most energetic state $|4\rangle$ has the highest population and the second one has the second highest population. The final populations of energy levels are 0.1547, 0.1927, 0.2680, and 0.3845, respectively. Figure 6.4c shows the performance index and Figure 6.4d shows the distance from the target state. At the final time 200 a.u. the distance is $\|\hat{\rho} - \hat{\rho}_f\|^2 = 0.0034$, so that the mixed-state control is completed.

2) Control system simulation of a harmonic oscillator model

In comparison to the above completely controllable Morse oscillator model, in this subsection we consider the diatomic molecule described by a four-level harmonic oscillator model. The

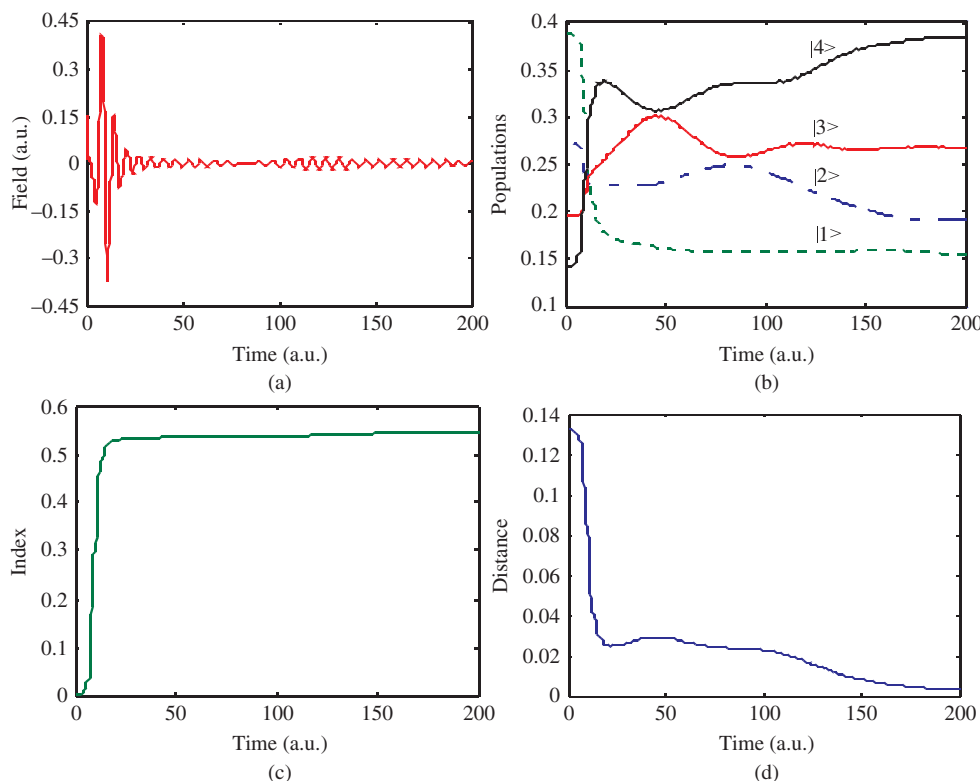


Figure 6.4 The numerical simulation results: (a) optimal control field for a four-level Morse oscillator model, (b) evolution of populations for a four-level Morse oscillator model, (c) performance index for a four-level Morse oscillator model, and (d) distance from the target state for a four-level Morse oscillator model

vibrational energy levels are determined by:

$$E_n = n - \frac{1}{2} \quad (6.60)$$

Thus the energy levels are $E_1 = 0.5$, $E_2 = 1.5$, $E_3 = 2.5$, and $E_4 = 3.5$. The dipole moments in this model are $d_n = 1$, $n = 1, 2, 3$. The system is not completely controllable because the dimension of the Lie algebra generated by \hat{H}_0 and \hat{H}_1 is less than 16 (Barnett and Dalton, 1987). We still suppose that the initial density is $\hat{\rho}_0 = \sum_{n=1}^4 w_n |n\rangle \langle n|$, in which $w_1 = 0.3850$, $w_2 = 0.2758$, $w_3 = 0.1976$, and $w_4 = 0.1416$. The target state and the control law are the same as for the Morse oscillator model. Starting with $f_0 = 0.15$ a.u., $dt = 0.1$ a.u., $r_1 = 1$, and $P = \text{diag}(4, 1, 1, 1, 1, 3, 1, 1, 1, 1, 2, 1, 1, 1, 1, 1)$, the simulation curves are shown in Figure 6.5a–c. At the final time, the populations of energy levels are 0.1482, 0.2003, 0.2732, and 0.3783, respectively, and the distance from the target state is $\|\hat{\rho} - \hat{\rho}_f\|^2 = 0.0036$. Although the system is not completely controllable, the method proposed in this section is still efficient.

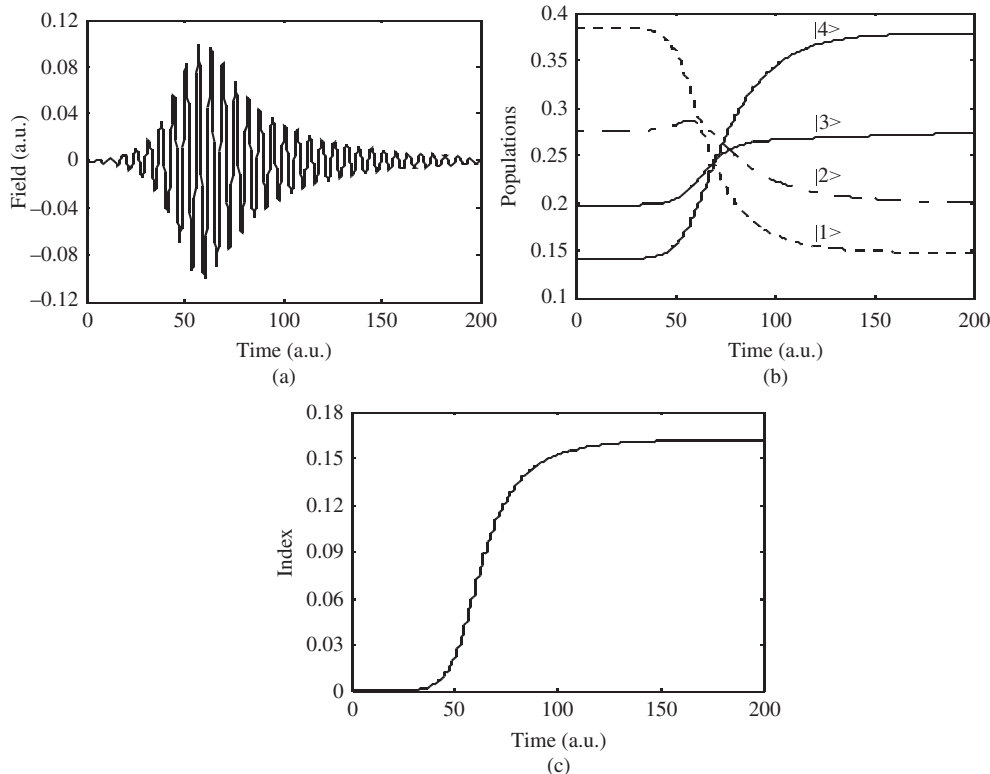


Figure 6.5 The simulation results for a four-level harmonic oscillator model: (a) optimal control field, (b) evolution of populations, and (c) distance from target state

6.4 Arbitrary Pure State to a Mixed-State Manipulation

Mixed state plays an important role in quantum computation, so it is worth studying its preparation. For the initial state as a mixed state, the method for getting the target mixed state was presented in Section 6.3. However, the pure state can be prepared more easily. When the initial state is the pure state, the method of transferring an initial pure state to a mixed state is discussed in this section. We want to seek an effective control strategy to drive the arbitrary pure state to the target mixed state.

Banks, Peskin, and Susskind suggested a Liouville equation for the density matrix ρ . Its generic form is:

$$i\hbar \frac{\partial}{\partial t} \rho = [H, \rho] + i \sum_{n,m} h_{nm} (Q_m Q_n \rho + \rho Q_m Q_n - 2 Q_n \rho Q_m) \quad (6.61)$$

where Q_n is any Hermitian operator and h_{nm} is the c-number Hermitian matrix. A sufficient condition that can ensure the positivity of ρ is that the matrix h_{nm} is positive. ρ is a Hermitian matrix for quantum systems, so its eigenvalues are non-negative and $\text{tr}(\rho) = 1$. Nevertheless, Equation 6.61 cannot preserve the value of $\text{tr}(\rho^2)$. When ρ represents a pure state, the value of $\text{tr}(\rho^2)$ is 1, and the value is less than 1 when ρ represents a mixed state, from which one can see that the pure state can indeed evolve to a mixed state (Reznik, 1996).

In this section, we propose a control strategy that drives an arbitrary pure state to a target mixed state for two-level systems via three-step controls. The first step is the preparation of the eigenstate: an arbitrary pure state is driven to an eigenstate through the control of pure state quantum systems. The second step is to drive the eigenstate to a mixed state in which not all of the off-diagonal elements in the density matrices are zeros. In this step we use an auxiliary system that interacts with the controlled system and achieve the transfer through the interaction of two systems. If the target state is the mixed state in which all of the off-diagonal elements in the density matrices are zeros, then one needs to drive the mixed state obtained in the second step to the target state through the control of mixed-state quantum systems.

6.4.1 Transfer from an Arbitrary Pure State to an Eigenstate

Considering a closed-loop quantum system S , its mathematical model is described as the following Schrödinger equation:

$$i\hbar |\psi_S\rangle = H |\psi_S\rangle, H = H_0 + H_c(t) \quad (6.62)$$

where H_0 is the inner Hamiltonian, $H_c(t)$ is the interaction Hamiltonian, and $H_c(t) = \sum_{k=1}^m H_k u_k(t)$. Both H_0 and H_k are linear Hermitian operators. $u_k(t)$ is a real-valued control function and the Planck constant is set at $\hbar = 1$.

First, the following unitary transformation is performed:

$$|\psi_S(t)\rangle = U(t) |\tilde{\psi}_S(t)\rangle \quad (6.63)$$

where $U(t) = \text{diag}(e^{-i\lambda_1 t}, e^{-i\lambda_2 t}, \dots, e^{-i\lambda_n t})$ is a unitary matrix and λ_i is the eigenvalue of H_0 . Substituting Equation 6.63 into Equation 6.62 gives:

$$i |\tilde{\psi}_S\rangle = \left(\tilde{H}_0 + \sum_{k=1}^m \tilde{H}_k u_k(t) - \Lambda \right) |\tilde{\psi}_S\rangle \quad (6.64)$$

where $\Lambda = \text{diag}(\lambda_1, \lambda_2, \dots, \lambda_n)$, $\tilde{H}_0 = U^\dagger H_0 U$, and $\tilde{H}_k = U^\dagger H_k U$. Equations 6.62 and 6.64 describe the same system (Boscain, Chambrion, and Gauthier, 2002a), so we design a control law based on the system model described by Equation 6.64. The design of control methods is plentiful, the Lyapunov method is adapted to the time-varying and non-linear systems, and the control can ensure the stability of the controlled system. The Lyapunov method is therefore used to design all controls in this section. The idea of Lyapunov control is to choose a suitable Lyapunov function V and then try to find a control that ensures that V is monotonically decreasing along any dynamical evolution of the control system. Here, V , as selected by the Lyapunov function, is taken to be:

$$V = \langle \psi_S - \psi_{Sf} | \psi_S - \psi_{Sf} \rangle \quad (6.65)$$

where $|\psi_S\rangle$ is the actual state of the system S , $|\psi_{Sf}\rangle$ is the target state, and $\psi_{Sf} = \sum_n c_n |\psi_n\rangle$.

$|c_n|$ is the probability of $|\psi_{Sf}\rangle = |\psi_n\rangle$.

It can be calculated that the first-order time derivative of V is given by:

$$\begin{aligned}\dot{V} &= \langle \dot{\psi}_S | \psi_S - \psi_{Sf} \rangle + \langle \psi_S - \psi_{Sf} | \dot{\psi}_S \rangle \\ &= -2\Im \left(\langle \psi_{Sf} - \psi_S | \sum_{k=1}^m \tilde{H}_k u_k(t) | \psi_S \rangle \right) - 2\Im \left(\langle \psi_{Sf} | (\tilde{H}_0 - \Lambda) | \psi_S \rangle \right)\end{aligned}\quad (6.66)$$

Because $\psi_{Sf} = \sum_n c_n |\psi_n\rangle$ and $\tilde{H}_0 |\psi_n\rangle = \lambda_n |\psi_n\rangle$, we can get $\Im(\langle \psi_{Sf} | (\tilde{H}_0 - \Lambda) | \psi_S \rangle) = 0$. So the expression \dot{V} in Equation 6.66 can be written as:

$$\dot{V} = -2 \sum_{k=1}^m u_k(t) \Im(\langle \psi_{Sf} - \psi_S | \tilde{H}_k | \psi_S \rangle) \quad (6.67)$$

Observing Equation 6.67, for the sake of ensuring $\dot{V} \leq 0$, we choose the control law u_k as:

$$u_k = K_k \Im(\langle \psi_{Sf} - \psi_S | \tilde{H}_k | \psi_S \rangle) \quad (6.68)$$

where $K_k > 0$. V decreases gradually under the action of u_k and reaches zero when $|\psi_S\rangle = |\psi_{Sf}\rangle$.

At the moment $\dot{V} = 0$ and $u_k = 0$, the system state would be stabilized at $|\psi_{Sf}\rangle$. Just choosing $|\psi_{Sf}\rangle$ to be an eigenstate of the system S , one can drive an arbitrary initial pure state to $|\psi_{Sf}\rangle$ by using the control law (Equation 6.68), and the state remains in the eigenstate.

6.4.2 Transfer from an Eigenstate to a Mixed State by Interaction Control

1) Establishment of mathematical model

In quantum control, the effect of control on the dynamics of the controlled system is the same for performing a suitable unitary transformation. However, the unitary transformation cannot change the purity of state; it is impossible to drive a pure state to a mixed state for a single particle using a unitary transformation. Thus we need an initially uncorrelated auxiliary system P that interacts with the controlled system S , and the transfer of states is achieved through the interaction of the two systems (Romano and D'Alessandro, 2006).

We have driven an arbitrary pure state to the eigenstate of system S through the control used in Section 6.4.1. An eigenstate can be expressed by the density matrix as $\rho_S = |\psi_{Sf}\rangle \langle \psi_{Sf}|$. The initial state of the auxiliary system P is a mixed state $\rho_P = \rho_P(u)$, and the ability to modify the state of the controlled system S depends on the correlation between S and P , which is generated by the interaction. The dynamics of S are given by

$$\rho_S(t, u) = Tr_P \rho_T(t) \quad (6.69)$$

with

$$\rho_T = \gamma_t [\rho_S(0) \otimes \rho_P(u)] \quad (6.70)$$

where T denotes the composite system $S + P$, and γ_t is an operator. If T is a closed system, then γ_t is given by

$$\gamma_t[\cdot] = e^{-iH_T t} \cdot e^{iH_T t} \quad (6.71)$$

According to Equation 6.69 and in consideration of Equations 6.70 and 6.71, when system S and P comprise a closed composite system, the dynamics of S are given by

$$\rho_S(t, u) = \text{Tr}_P(U(t)\rho_S \otimes \rho_P(u)U^\dagger(t)) \quad (6.72)$$

where $U(t) = e^{-iH_T t}$ is a unitary propagator and H_T is the total Hamiltonian, given by

$$H_T = H_S + H_P + H_I \quad (6.73)$$

where H_S and H_P are the free Hamiltonians of S and P , respectively. H_I is the interaction Hamiltonian of S and P .

When systems S and P are both two-level, H_S is given by considering a particular dynamical model (Romano, 2007):

$$H_S = \omega_S \sigma_z^S, H_P = \omega_P \sigma_z^P, H_I = g \sigma_x^S \otimes \sigma_x^P \quad (6.74)$$

where ω_S and ω_P are the eigen-frequencies of S and P , and g is the coupling constant. σ_z^S and σ_x^S are the Pauli matrices in system S , and σ_z^P and σ_x^P are the Pauli matrices in P .

We define the purity of a state ρ_S as the von Neumann distance of the state ρ_S from the maximally mixed state $I/2$:

$$\pi = \sqrt{2\text{Tr}\left(\rho_S - \frac{I}{2}\right)^2} = \sqrt{2\text{Tr}(\rho_S^2) - 1} \quad (6.75)$$

If the state ρ_S is represented by a Bloch vector:

$$\rho_S(t) = \frac{1}{2}(I + s(t) \cdot \boldsymbol{\sigma}^S) \quad (6.76)$$

then the time-dependent purity $\pi(t)$ is given by

$$\pi(t) = \|s(t)\| \quad (6.77)$$

The task of transferring a state from an initial pure state to a mixed state becomes a decreasing process of $\pi(t)$.

2) Design of control law

Considering the mathematical model of system T in Equation 6.72, the total Hamiltonian of T contains two parts: one is the local Hamiltonian $H_L = H_S + H_P$ composed of the free Hamiltonians S and P , and the other is the interaction Hamiltonian H_I . We still use the Lyapunov method to design the control law $u(t)$ in this section.

When T is a closed system, T follows the Liouville equation (with $\hbar = 1$):

$$\dot{\rho}_T(t) = -i[H_L + u(t)H_I, \rho_T(t)] \quad (6.78)$$

where $H_L = H_S + H_P$ and the dynamics of T are:

$$\rho_T(t) = U(t)\rho_S \otimes \rho_P(u)U^\dagger(t) \quad (6.79)$$

where $U(t) = e^{-iH_T t}$ is a unitary propagator.

The initial states of S and P are the eigenstate and mixed state, respectively, and S and P are initially uncorrelated. ρ_S^f and ρ_P^f represent the final states of S and P , respectively, so the final state of T is:

$$\rho_T^f = \rho_S^f \otimes \rho_P^f \quad (6.80)$$

where ρ_S^f is a mixed state.

The Hilbert–Schmidt distance $\|\rho_T(t) - \rho_T^f\|_2$ is chosen as the Lyapunov function:

$$V(\rho_T(t), \rho_T^f) = \frac{1}{2} \|\rho_T(t) - \rho_T^f\|_2^2 = \frac{1}{2} \text{Tr}[(\rho_T(t) - \rho_T^f)^2] \quad (6.81)$$

The first-order time derivative of V is:

$$\dot{V} = \text{Tr}((\rho_T(t) - \rho_T^f) \cdot \dot{\rho}_T(t)) \quad (6.82)$$

Substituting Equation 6.78 into Equation 6.82, one has:

$$\begin{aligned} \dot{V} &= \text{Tr}((\rho_T(t) - \rho_T^f) \cdot (-i[H_L + u(t)H_I, \rho_T(t)])) \\ &= \text{Tr}((\rho_T(t) - \rho_T^f) \cdot (-i[H_L, \rho_T(t)] - i[u(t)H_I, \rho_T(t)])) \\ &= \text{Tr}(i\rho_T^f \cdot [H_L, \rho_T(t)] + i\rho_T^f \cdot [u(t)H_I, \rho_T(t)]) \\ &= -\text{Tr}(i[H_L, \rho_T^f] \cdot \rho_T(t)) - u(t)\text{Tr}(\rho_T^f \cdot [-iH_I, \rho_T(t)]) \end{aligned} \quad (6.83)$$

When $[H_L, \rho_T^f] = 0$ is satisfied, the first term on the right-hand side of Equation 6.83 is zero. In order for \dot{V} to be non-negative, the second term on the right-hand side of Equation 6.83 should be non-negative. So assuming $k > 0$, we choose the following control:

$$u(t) = k\text{Tr}(\rho_T^f \cdot [-iH_I, \rho_T(t)]) \quad (6.84)$$

and Equation 6.83 becomes

$$\dot{V} = -\frac{1}{k}u(t)^2 \leq 0, k > 0 \quad (6.85)$$

The Lyapunov function V is monotonically decreasing along any dynamical evolution because $\dot{V} \leq 0$. On the basis of the Lyapunov stability theorem, the closed quantum system T is stable under the action of the control law (Equation 6.84), which drives the system state $\rho_T(t)$ to the final state ρ_T^f at the same time as the final state in S evolves to ρ_S^f :

$$\text{Tr}_P(\rho_T^f) = \text{Tr}_P(\rho_S^f \otimes \rho_P^f) = \rho_S^f \quad (6.86)$$

As long as the final state of T satisfies $[H_L, \rho_T^f] = 0$, the control (Equation 6.84) can drive an eigenstate to the mixed state in which not all of the off-diagonal elements in the density matrices are zeros for system S through the interaction between the controlled system S and the auxiliary system P .

6.4.3 Control Design for a Mixed-State Transfer

The state of controlled system S has been driven from an arbitrary pure state to the mixed state in which not all the off-diagonal elements in the density matrices are zeros via the controls in Sections 6.4.1 and 6.4.2. When the target state is the mixed state in which all the off-diagonal

elements in density matrices are zeros, it is necessary to perform the further control to the mixed state which is obtained in Section 6.4.2, so that the state of system S can be driven to the target mixed state. This subsection will give the specific design procedure for the controller.

The density matrix $\rho_S(t)$ of the controlled system S follows the Liouville equation:

$$i\hbar \frac{\partial}{\partial t} \rho_S(t) = [H(t), \rho_S(t)], H(t) = H_0 + \sum_{m=1}^M f_m(t) H_m \quad (6.87)$$

where H_0 is the inner Hamiltonian, H_m is the interaction Hamiltonian generated by the interaction of external controls and the system, and $f_m(t)$ is the external control.

The collection of bounded linear operators in Hilbert space forms its own Hilbert space, called the Liouville space. Every bounded linear operator A in Hilbert space corresponds to a vector $|A\rangle\rangle$ in Liouville space. Using $|\rho_S(t)\rangle\rangle$ to express the density matrix $\rho_S(t)$ in the Liouville space, Equation 6.87 can be written as (Ohtsuki and Fujimura, 1989):

$$i \frac{\partial}{\partial t} |\rho_S(t)\rangle\rangle = L(t) |\rho_S(t)\rangle\rangle, \quad L(t) = L_0 + \sum_{m=1}^M f_m L_m \quad (6.88)$$

The control law is designed based on the Lyapunov stability theorem in this subsection and the Lyapunov function selected is the following equation:

$$V(|\rho_S\rangle\rangle) = \frac{1}{2} \langle\langle \rho_S - \rho_{Sf} | P | \rho_S - \rho_{Sf} \rangle\rangle \quad (6.89)$$

where ρ_S is the actual state of S and ρ_{Sf} is the target mixed state. P is a positive definite symmetric matrix and satisfies

$$PL_0 - L_0^\dagger P = 0 \quad (6.90)$$

According to Equations 6.88 and 6.90, the first-order time derivative of $V(|\rho_S\rangle\rangle)$ is given by

$$\begin{aligned} \dot{V}(|\rho_S\rangle\rangle) &= \text{Re}(\langle\langle \rho_S - \rho_{Sf} | P | \rho_S \rangle\rangle) \\ &= \text{Im}(\langle\langle \rho_S - \rho_{Sf} | PL_0 | \rho_S \rangle\rangle) + \sum_{m=1}^M f(t) \text{Im}(\langle\langle \rho_S - \rho_{Sf} | PL_m | \rho_S \rangle\rangle) \\ &= \sum_{m=1}^M f(t) \text{Im}(\langle\langle \rho_S - \rho_{Sf} | PL_m | \rho_S \rangle\rangle) \end{aligned} \quad (6.91)$$

In order to ensure $\dot{V} \leq 0$, we choose the control law to be:

$$f_m = -\frac{1}{r_m} \text{Im}(\langle\langle \rho_S - \rho_{Sf} | PL_m | \rho_S \rangle\rangle), (m = 1, 2, \dots, M) \quad (6.92)$$

and Equation 6.91 becomes:

$$\dot{V}(|\rho_S\rangle\rangle) = \sum_{m=1}^M \frac{1}{r_m} [\text{Im}(\langle\langle \rho_S - \rho_{Sf} | PL_m | \rho_S \rangle\rangle)]^2 \leq 0 \quad (6.93)$$

In this way the drive of the state of S to the mixed state in which all of the off-diagonal elements in density matrices are zeros is realized under the action of the control law

(Equation 6.92). Note that the purity of the initial state is equal to the purity of the final state when the control law (Equation 6.92) is adopted. This means that the final state in Section 6.4.2 is not arbitrary when it is needed to perform the third step. The purity of the final state selected in Section 6.4.2 should be equal to the purity of the target state.

6.4.4 Numerical Simulation Experiments

In this section we illustrate the effectiveness of the proposed control strategy through a specific numerical simulation. The simulation experiment is to drive the state of the controlled system S from the initial superposition state $S(0) = (0.866, 0, -0.5)$ to the target mixed state $S_{final} = (0, 0, 0.7)$. The states of the systems are all expressed in Bloch vectors in the simulation.

The first step: Drive a controlled system S from a superposition state $S(0) = (0.866, 0, -0.5)$ to the eigenstate $S'(0) = (1, 0, 0)$. We can obtain the required control law according to Equation 6.68: $u_k = K_k \Im(\langle \psi_{S'} | \psi_S | \tilde{H}_k | \psi_S \rangle)$. K_k is set to 1 in the experiment. The control system simulation results are shown in Figure 6.6, in which Figure 6.6a shows the evolution trajectory of system S and Figure 6.6b shows the value of the control.

From Figure 6.6a one can see that the state of S is driven from the superposition state $S(0) = (0.866, 0, -0.5)$ to the eigenstate $S'(0) = (1, 0, 0)$ under the action of the designed control. One can see from Figure 6.6b that the value of the control stays at zero once the eigenstate is reached and the state can remain in the eigenstate stably and continuously. The state of S therefore reaches the eigenstate at the end of the control.

The second step: Drive the eigenstate $S'(0) = (1, 0, 0)$ to the mixed state $S_f = (0.7, 0, 0)$ in which not all of the off-diagonal elements in the density matrices are zeros. The initial state of the auxiliary system P is set to be $P(0) = (0.7, 0, 0)$ and its final state is $P_f = (0, 0, 1)$. The eigen-frequencies ω_S and ω_P are both 1. $H_S = \text{diag}(1, -1)$ and $H_P = \text{diag}(1, -1)$ are the Hamiltonians of S and P , respectively, and the Hamiltonians of T are $H_L = \delta_z^S \otimes I + I \otimes \delta_z^P$ and $H_I = \delta_x^S \otimes \delta_x^P$. The control law in this step is designed by Equation 6.84, $u(t) = kTr(\rho_T^f[-iH_I, \rho_T(t)])$, in which k is chosen to be 1 in the experiment. The second step control simulation results are shown in Figure 6.7, in which Figure 6.7a shows the evolution trajectory

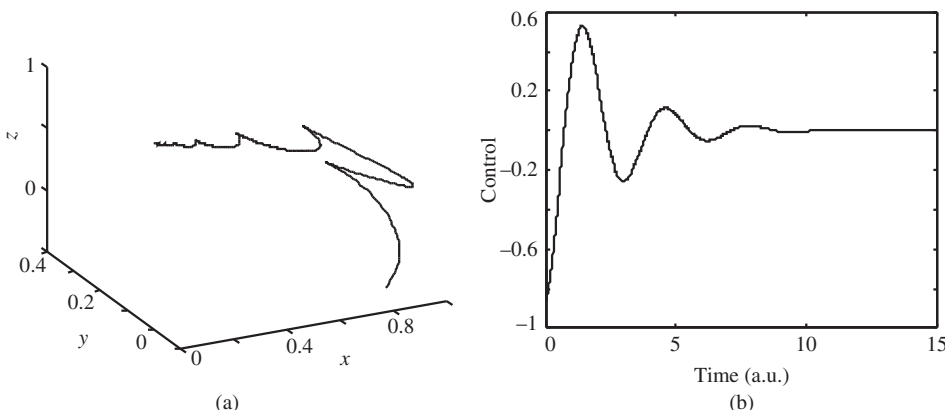


Figure 6.6 Simulation results of the first-step control for system S : (a) trajectory of system S and (b) value of control u

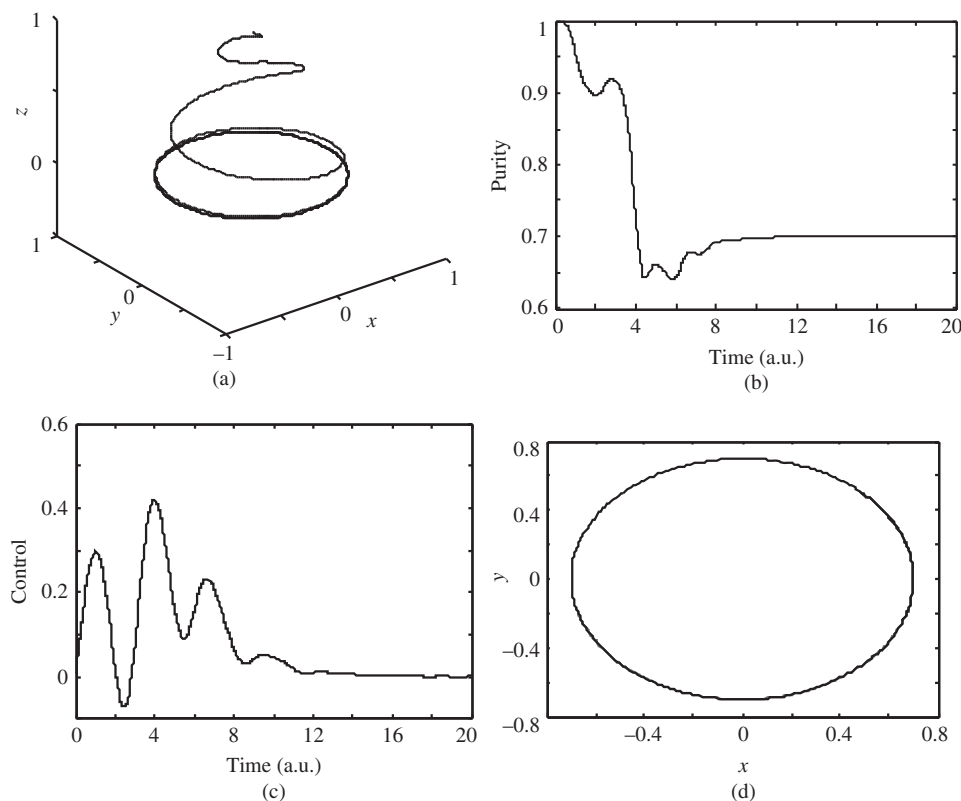


Figure 6.7 Simulation of the second-step control for system S : (a) trajectory of system S , (b) purity of system S , (c) value of control u , and (d) projection of trajectory for $15 \leq t \leq 20$ in the x - y plane

of S , Figure 6.7b shows the purity curve of S , Figure 6.7c shows the value of the control, and Figure 6.7d shows the projection of the evolution trajectory in the time period $15-20$ in the x - y plane. It can be seen from Figure 6.7a that the evolution trajectory enters the inside from the north pole of the Bloch ball under the control and makes a circular motion around the z -axis after the interaction. According to the definition of purity, the purity is 1 when in the pure state and less than 1 in the mixed state. Figure 6.7b shows that the purity of S decreases from 1 to 0.7, so the controlled system S is driven to the mixed state from the eigenstate. From Figure 6.7c one can see that the value of the control tends to zero when time is about 15, which means the end of the interaction of S and P .

From Figure 6.7a and Figure 6.7d it can be concluded that S is driven to the mixed state in which not all of the off-diagonal elements in the density matrices are zeros from the eigenstate under the control.

In order to drive the controlled system S to the target mixed state in which all of the off-diagonal elements are zeros, it is necessary to control the mixed-state quantum system. This can be achieved using the control law (Equation 6.92). The initial state of the third step is $S_f = (0.7, 0, 0)$, which is the final state of the second step, and the final state is the target mixed state $S_{final} = (0, 0, 0.7)$. The purities of S_f and S_{final} are all 0.7 and satisfy the limiting

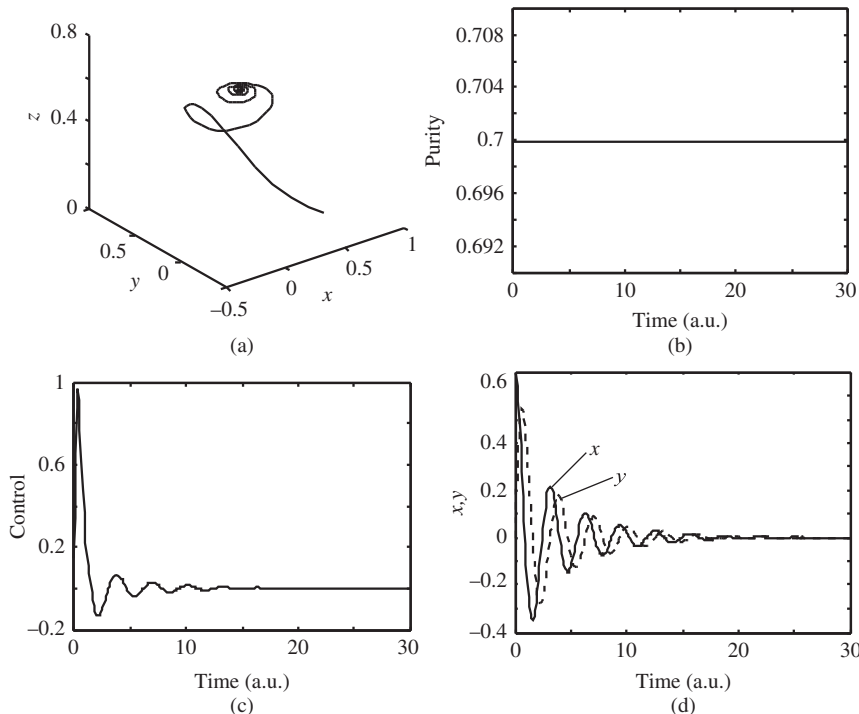


Figure 6.8 Simulation of the third-step control for system S : (a) trajectory of system S , (b) purity of system S , (c) value of control u , and (d) value of coordinates x and y in the Bloch vector

condition of the control law (Equation 6.92). The Hamiltonian of the controlled system S is $H_0 = \text{diag}(1, -1)$, $H_I = \begin{bmatrix} 0 & 1 \\ 1 & 0 \end{bmatrix}$ and the parameter P in the control law is $P = \text{diag}(16.5, 1, 1, 1)$.

The third-step control simulation results are shown in Figure 6.8, in which Figure 6.8a shows the evolution trajectory, Figure 6.8b shows the purity curve, Figure 6.8c shows the value of the control, and Figure 6.8d shows the curves of coordinates x and y in the Bloch vector, which represent the state of system S .

One can see from Figure 6.8a that system S is driven to the target mixed state under the control law and the purity of the state has been kept at 0.7 in the control process. The control law (Equation 6.92) does not change the purity. The control law (Equation 6.92) is related to the choice of parameter P , and the different parameters will have different results and effects on the controls so it is important to select a suitable parameter for the control. P is selected as $P = \text{diag}(16.5, 1, 1, 1)$ in our experiment.

One can see from Figure 6.8c that the control value tends to zero finally, which indicates that P is suitable. When coordinates x and y in the Bloch vector are zero, all the off-diagonal elements in the density matrices are zeros.

It can be seen from Figure 6.8d that the values of coordinates x and y tend to zero, so the final state is the mixed state in which all of the off-diagonal elements in the density matrices are zeros. Thus the state of S is driven to the target mixed state from the initial superposition state via three-step controls. When the initial state of the controlled system is an eigenstate, the

first-step control is not necessary and the second-step control can be performed directly. When the target state is the mixed state in which not all of the off-diagonal elements in the density matrices are zeros, the third-step control is not necessary and the transfer can be achieved through the first two steps. In addition, S can be driven to the target mixed state in which not all of the off-diagonal elements are zeros only when the initial state of P is the same as the final state of S in the second step.

References

- Athans, M. and Falb, P.L. (1966) *Optimal Control*, McGraw-Hill, New York.
- Barnett, S.M. and Dalton, B.J. (1987) Liouville space description of thermofields and their generalizations. *Journal of Physics A: Mathematical and General*, **20**, 411–418.
- Beaucharda, K., Coronb, J.M., Mirrahimic, M. et al. (2007) Implicit Lyapunov control of finite dimensional Schrödinger equations. *Systems and Control Letters*, **56**(5), 388–395.
- Benallou, A., Mellicharmp, D.A. and Seborg, D.E. (1988) Optimal stabilizing controllers for bilinear systems. *International Journal of Control*, **48**(4), 1487–1501.
- Boscain, U., Chambrion, T. and Gauthier, J.P. (2002a) On the K+P problem for a three-level quantum systems: optimality implies resonance. *Journal of Dynamical Control Systems*, **8**(4), 547–572.
- Boscain, U., Chambrion, T. and Gauthier, J.P. (2002b) On the K+P problem for a three-level quantum systems: optimality implies resonance. *Journal of Dynamical Control Systems*, **8**(4), 547–572.
- Mirrahimi, M. and Rouchon, P. (2004) Trajectory tracking for quantum systems: a Lyapounov approach. *Proceedings of the International Symposium MTNS*, Leuven, Belgium.
- Mirrahimi, M., Rouchon, P. and Turinici, G. (2005) Lyapunov control of bilinear Schrödinger equations. *Automatica*, **41**(11), 1987–1994.
- Ohtsuki, Y. and Fujimura, Y. (1989) Bath-induced vibronic coherence transfer effects on femtosecond time-resolved resonant light scattering spectra from molecules. *Journal of Chemical Physics*, **91**(7), 3903–3915.
- Reznik, B. (1996) Unitary evolution between pure and mixed states. *Physical Review Letters*, **76**(8), 1192–1195.
- Romano, R. (2007) Resonant purification of mixed states for closed and open quantum systems. *Physical Review A*, **75**(2), 024301.
- Romano, R. and D'Alessandro, D. (2006) Incoherent control and entanglement for two-dimensional coupled systems. *Physical Review A*, **73**(2), 022323.
- Schirmer, S.G. (2000) Theory of Control of Quantum Systems. PhD Thesis. Oregon University.
- Schirmer, S.G., Fu, H. and Solomon, A.I. (2001) Complete controllability of quantum systems. *Physical Review A*, **63**(6), 063410.

7

Convergence Analysis Based on the Lyapunov Stability Theorem

7.1 Population Control of Quantum States Based on Invariant Subsets with the Diagonal Lyapunov Function

The quantum Lyapunov control method, initially called the local (optimization) control method, has been applied to many concrete quantum problems. From the viewpoint of control design, one always expects that any trajectory of a control system can asymptotically converge to a prescribed target state. In Lyapunov control methods, however, LaSalle's invariance principle ensures that any system trajectory can only converge to an invariant subset of the system, therefore to reliably achieve the task of state control, one should combine control design with convergence analysis. In 2005 Mirrahimi *et al.* proposed the asymptotical approach toward an eigenstate of the inner Hamiltonian by using the quantum adiabatic theorem on the basis of analyzing the conditions of the asymptotical tracking of the closed loop system to any reference trajectory. However, the method proposed cannot achieve a high-probability convergence to the superposition state in the invariant set, which is a general phenomenon in Lyapunov control methods. In this section we will utilize the idea of partially constructing the Lyapunov function to solve this issue, that is, to converge on a target pure state in the related invariant set with a high probability.

The core of quantum Lyapunov methods lies in the selection of Lyapunov functions. For pure states, our research in Section 5.3 shows that the Lyapunov function based on the average values of a mechanical quantity has more generality and flexibility. In this section we will therefore adopt the Lyapunov function used in Section 5.3.

7.1.1 System Model and Control Design

Consider the quantum systems:

$$i\hbar|\psi(t)\rangle = \left(H_0 + \sum_{k=1}^r H_k u_k(t) \right) |\psi(t)\rangle \quad (7.1)$$

in which H_0 is diagonal and can be denoted by $H_0 = \text{diag}[\lambda_1, \lambda_2, \dots, \lambda_N]$.

For convenience, atomic units are used and $\hbar = 1$. Assuming the dimension of the system is N , then the state of the system (Equation 7.1), $|\psi(t)\rangle$, varies on the unit complex ball surface of dimension $2N - 1$, S^{2N-1} .

The Lyapunov function used in control design is given as

$$V = \langle \psi | P | \psi \rangle \quad (7.2)$$

where P is a Hermitian operator to be constructed and can be considered as an observable of the system. In mathematics V is a quadratic function of $|\psi\rangle$, while in physics it represents the average value of P .

It is easily calculated that the first-order time derivative of V is

$$\dot{V} = i \langle \psi | [H_0, P] | \psi \rangle + i \sum_{k=1}^r \langle \psi | [H_k, P] | \psi \rangle u_k \quad (7.3)$$

Considering the first item on the right-hand side of Equation 7.3, which is dependent on the control component, to ensure $\dot{V} \leq 0$, we let

$$[H_0, P] = 0 \quad (7.4)$$

and select the form of the control field as

$$u_k = -i K_k \langle \psi | [H_k, P] | \psi \rangle \quad (7.5)$$

where $K_k > 0$.

Equation 7.4 means the Hermitian operators P and H_0 are commutative. Because H_0 is diagonal, so is P when H_0 is non-degenerate. Thus, the Hermitian property of P ensures that P is a real diagonal matrix, that is, P can be written as

$$P = \text{diag} [P_1, P_2, \dots, P_N] \quad (7.6)$$

where $P_1, P_2, \dots, P_N \in R$. This is to say, we only need to construct all the real diagonal elements of P , P_1, P_2, \dots, P_N in order to achieve the control goal.

7.1.2 Correspondence between any Target Eigenstate and the Value of the Lyapunov Function

In Lyapunov design methods one expects that the controlled state will be precisely transferred to the target state as the Lyapunov function decreases to some value by designing control laws. It is therefore crucial to decide the correspondence between the value and the target state. Evidently, when the minimum value of the Lyapunov function corresponds to the target state, the controlled state will be transferred to the target state as the Lyapunov function decreases to its minimum value because the minimum point is unique.

Equation 7.4 also implies that the normalized eigenvectors of H_0 are those of P when H_0 is non-degenerate. So, P can also be written as

$$P = \sum_{m=1}^N P_m |\lambda_m\rangle \langle \lambda_m| \quad (7.7)$$

where P_m ($m = 1, 2, \dots, N$) is an eigenvalue of P and $|\lambda_m\rangle$ is the eigenvector associated with the eigenvalue of H_0 .

In 2003 Grivopoulos and Bamieh proved the following lemma:

Lemma 7.1 The set of critical points of the Lyapunov function (Equation 7.2) defined on the unit complex ball surface $\langle\psi|\psi\rangle = 1$ is given by the normalized eigenvectors of P . The eigenvector associated with the largest eigenvalue of P is the maximum point of V , the eigenvector associated with the smallest eigenvalue is the minimum point of V , and all other eigenvectors are saddle points.

According to this Lemma 7.1 and Equation 7.7, if the eigenvalue associated with the target eigenstate $|\psi_f\rangle \in \{|\lambda_1\rangle, |\lambda_2\rangle, \dots, |\lambda_N\rangle\}$, $P_f \in \{P_1, P_2, \dots, P_N\}$, is the smallest eigenvalue of P , then the controlled state will be driven to $|\psi_f\rangle$ when one makes V decrease to P_f . Thus, we can obtain the first construction principle on diagonal elements: the eigenvalue of P associated with the target eigenstate should be kept to a minimum.

7.1.3 Invariant Set of Control Systems

It is easily seen from Equation 7.5 that the control system is an autonomous system defined by S^{2N-1} . One can therefore analyze the convergence of the control system by using the dynamical system theory and LaSalle's invariance principle, and study the related invariant set.

1) Mathematical expression of the invariant set

The state-space of the control system is S^{2N-1} since the target eigenstate can be assumed stationary, regardless of the global phase caused by the inner Hamiltonian, which is not observable in physics. The fact that S^{2N-1} is a compact manifold ensures that any solution of the system (Equation 7.1) with the control field (Equation 7.5) is bounded. Thus, by applying LaSalle's principle we can obtain:

Theorem 7.1 With the control field in Equation 7.5, all the trajectories of the control system converge to its invariant set $E = \{|\psi(t_0)\rangle \mid \dot{V}(|\psi(t)\rangle) = 0, t \geq t_0 \geq 0; |\psi(t_0)\rangle \in S^{2N-1}\}$.

Proof The invariance of E is evident. The convergence is proved as follows.

Let $|\psi(t)\rangle$ be any solution of the control system and Γ^+ be the positive limit set of $|\psi(t)\rangle$. From the definition of the positive limit set, if $|\psi(t)\rangle$ is bounded for $t \geq 0$, then $|\psi(t)\rangle$ will tend to any set including Γ^+ as $t \rightarrow \infty$. So, we only need to prove $\Gamma^+ \subset E$. The continuity and monotony of V ensures that, along the trajectory $|\psi(t)\rangle$, V will continuously decrease to its extreme value associated with the trajectory and take this extreme value at each point in Γ^+ .

Next, we show that the positive limit set induced by any solution $|\psi(t)\rangle$, Γ^+ , is a subset of E . For any point $|x_\infty(t_0)\rangle \in \Gamma^+$, Γ^+ may also be the positive limit set of other system trajectories. We therefore mark $|x_\infty(t)\rangle$ to be any trajectory through point $|x_\infty(t_0)\rangle$ at time t_0 . Considering that Γ^+ is invariant and V takes constant in Γ^+ , one can easily conclude $\dot{V}(|x_\infty(t)\rangle) = 0$ ($t \geq t_0$), that is, $|x_\infty(t_0)\rangle \in E$ or $\Gamma^+ \subset E$. ■

Now, we consider the following conditions:

Assumption 7.1 $P_l \neq P_j$, $l \neq j$.

Assumption 7.2 $\omega_{lj} \neq \omega_{uv}$, $(l,j) \neq (u,v)$, where $\omega_{lj} = \lambda_l - \lambda_j$.

Remark 7.1 Assumption 7.1 means that a new constraint condition is imposed on the diagonal elements to be constructed. In principle, this is feasible. We will relax this condition in the next subsection. Assumption 7.2 says that the transition energies between arbitrary different levels are clearly identified. In principle, it is possible to use tailored radio-frequency pulses to selectively transfer populations between two levels (D'Alessandro, 2007).

By calculating the concrete expression of the invariant set E , we can obtain the following theorem.

Theorem 7.2 Consider the non-degenerate system (Equation 7.1) with the control field in Equation 7.5. Under Assumption 7.1, Assumption 7.2, and condition $[H_0, P] = 0$, any trajectory of the control system converges to the invariant set $E = \{|\psi(t_0)\rangle \mid |\langle\lambda_l|\psi(t_0)\rangle\langle\psi(t_0)|\lambda_j\rangle(H_k)_{jl} = 0, (j,l = 1, \dots, N; j \neq l; k = 1, \dots, r); |\psi(t_0)\rangle \in S^{2N-1}\}$.

Proof It is known from Equations 7.3 and 7.5 that $\dot{V}(|\psi(t)\rangle) = 0$ ($t \geq t_0 \geq 0$) is equivalent to $u_k(t) = 0$ ($t \geq t_0 \geq 0, k = 1, \dots, r$), that is,

$$u_k(t) = -iK_k\langle\psi(t)|[H_k, P]|\psi(t)\rangle = 0, \quad t \geq t_0 \quad (7.8)$$

Substituting the free-evolution state of the system $|\psi(t)\rangle = e^{-iH_0(t-t_0)}|\psi(t_0)\rangle$ into Equation 7.8 gives

$$\langle\psi(t_0)|e^{iH_0(t-t_0)}[H_k, P]e^{-iH_0(t-t_0)}|\psi(t_0)\rangle = 0, \quad t \geq t_0 \quad (7.9)$$

The system state at time t_0 can be expanded in a set of complete, orthogonal, normalized bases of H_0 as

$$|\psi(t_0)\rangle = \sum_{j=1}^N \langle\lambda_j|\psi(t_0)\rangle |\lambda_j\rangle \quad (7.10)$$

Set $|\lambda_1\rangle = [1, \dots, 0]^T, \dots$, and $|\lambda_N\rangle = [0, \dots, 1]^T$. Substituting Equation 7.10 into Equation 7.9, one can obtain

$$\sum_{j,l=1}^N (P_l - P_j) \langle\lambda_l|\psi(t_0)\rangle \langle\psi(t_0)|\lambda_j\rangle (H_k)_{jl} e^{-i\omega_j(t-t_0)} = 0 \quad (7.11)$$

In view of the linear independence of the exponential functions, Equation 7.11 can be written as

$$\langle\lambda_l|\psi(t_0)\rangle \langle\psi(t_0)|\lambda_j\rangle (H_k)_{jl} = 0, \quad (j,l = 1, \dots, N; j \neq l; k = 1, \dots, r) \quad (7.12)$$

The set of all the states satisfying Equation 7.12, $\{|\psi(t_0)\rangle\}$, forms the invariant set E . ■

2) Analysis of the invariant set based on the connectivity graph of energy levels

The form of the invariant set in Theorem 7.2 seems to be complex and it is necessary to further analyze it. It can be seen from Equation 7.12 that the invariant set E is closely related to the control Hamiltonian which indicates whether the direct transition between arbitrary energy levels is allowed or not. We can therefore use the connectivity graph of energy level transition to intuitively study the set. Based on Equation 7.12, two rules can easily be obtained.

Firstly, when $(H_k)_{jl} = 0, k = 1, \dots, r$, the subspace generated by $|\lambda_j\rangle$ and $|\lambda_l\rangle$, $\text{span}\{|\lambda_j\rangle, |\lambda_l\rangle\}$, is sure to be an invariant subset of E .

Secondly, when $(H_k)_{jl} \neq 0, k \in \{1, \dots, r\}$, the subspace generated by at most one of $|\lambda_j\rangle$ and $|\lambda_l\rangle$ is consequentially an invariant subset of E . Reflecting the two rules on the connectivity graph of energy level transition, we can directly write out the invariant set E along the following steps:

Step 1: Take eigenstate $|\lambda_1\rangle$ as the first basis element of the invariant subset $E_1 \subset E$ to be generated. All the eigenstates that are directly connected with it do not participate in generating E_1 .

Step 2: Out of the set of all the eigenstates that are not directly connected with $|\lambda_1\rangle$, $\bar{E}_1 = \{|\lambda_{11}\rangle, |\lambda_{12}\rangle, \dots, |\lambda_{1q}\rangle\}$, choose the first eigenstate $|\lambda_{11}\rangle$ as the second basis element of E_1 . Then all the eigenstates in \bar{E}_1 that are directly connected with $|\lambda_{11}\rangle$ do not participate in generating E_1 . Furthermore, mark the set of all the eigenstates in \bar{E}_1 that are not directly connected with $|\lambda_{11}\rangle$ as \bar{E}_{11}, \dots . Repeating this process we can obtain the first form of the invariant subset E_1 . Taking $|\lambda_{1s}\rangle, s = 2, \dots, q$ as the second basis element of E_1 in turn and following the above method to choose other basis elements of E_1 in the above-mentioned three cases, then all the possible forms of E_1 will be obtained finally.

Step 3: For each $|\lambda_m\rangle, m = 2, \dots, N$, write out all the possible forms of the invariant subset E_m . Then, the union of all the obtained invariant subsets is E .

Remark 7.2 One can see from Equation 7.12 that every single eigenstate of the inner Hamiltonian is in the invariant set E . In fact, one can further know that every eigenstate is in an invariant subset of E by analyzing the connectivity graph.

3) Construction principle of diagonal elements

The invariance analysis based on the connectivity graph implies that any trajectory of the control system converges to one of the invariant subsets of E . It is therefore natural to consider any state in an invariant subset as the target state. Here, we mainly expatiate on the case where one eigenstate belongs to only one invariant subset. The case where one eigenstate simultaneously belongs to several invariant subsets will be given in the simulation experiments of Section 7.1.4.

Mark all the invariant subsets of E as E_1, E_2, \dots, E_q , and assume that $|\lambda_f\rangle$ is one eigenstate which participates in constituting the target state in $E_a, a \in \{1, 2, \dots, q\}$. Given any initial state $|\psi(0)\rangle$, one expects that a trajectory starting from $|\psi(0)\rangle$ will converge into E_a . In view of the continuity of V and Lemma 7.1, the second construction principle of diagonal elements of P is obtained:

$$\begin{aligned} P_f < P_{\bar{f}}(E_a) &< V(|\psi(0)\rangle) < P(E_b), \\ (b = 1, \dots, q; b \neq a; P(E_b) \neq P(E_a)) \end{aligned} \quad (7.13)$$

where P_f represents the eigenvalue of P associated with the eigenstate $|\lambda_f\rangle$ in E_a , $P_{\bar{f}}(E_a)$ is the eigenvalue of P associated with any eigenstate in E_a except $|\lambda_f\rangle$, $P(E_b)$ is the eigenvalue of P associated with any eigenstate in E_b , and $P(E_a)$ is the eigenvalue of P associated with any eigenstate in E_a .

Equation 7.13 ensures that any trajectory starting from $|\psi(0)\rangle$ converges to nothing but E_a rather than E_b , ($b \neq a$). Generally, under normalization condition, the more eigenstates which participate in constituting an initial state, the more easily is Equation 7.13 satisfied.

4) Adjustment principle of diagonal elements

It should be pointed out that Equation 7.13 is a quite conservative expression of construction relation. In other words, Equation 7.13 cannot ensure that the system trajectory will converge to a prescribed target state in E_a with a high probability, for example an eigenstate in E_a . This means that the system trajectory has entered an invariant subset before the target state gains a sufficient population distribution. To solve this problem we provide two measures to improve the construction of P .

Firstly, we calculate the rate of change of V along the system trajectory. From Equations 7.3 and 7.5 one has:

$$\dot{V} = \sum_{k=1}^r K_k \left(\sum_{j,l=1}^N (P_l - P_j) \langle \psi | \lambda_j \rangle \langle \lambda_l | \psi \rangle (H_k)_{jl} \right)^2 \quad (7.14)$$

Equation 7.14 shows that the decreasing rate of V is closely related to all the differences between different eigenvalues of P associated with the eigenstates between which direct transitions exist. Evidently, the smaller the differences are, the longer the time it takes for the system to reach an invariant subset. This provides a possibility for sufficient population distribution on the target state.

Secondly, with decreasing V , the population conservation of the system usually makes the population of eigenstate associated with the largest eigenvalue of P attenuate quickly. Thus, if permitted, we may gradually increase (or decrease) $P_{\bar{f}}(E_a)$ in Equation 7.13 to achieve the decrease (or increase) in the population on the eigenstate associated with $P_{\bar{f}}(E_a)$.

5) A particular consideration on initial states

Here, we discuss an usual case where the initial state is a stationary eigenstate of H_0 . Since all the eigenstates of H_0 are in the invariant set E , the control law (Equation 7.5) cannot be directly used. In this case, an initial disturbance should be applied to force the system to leave this initial state. Furthermore, one can take the post-disturbance state as a new initial state and use the control law in Equation 7.5 to achieve the control goal.

6) Extension of the invariant set

This subsection discusses how to achieve a high-probability convergence to the target pure state in some invariant subset. If the invariant set of the system is small, the scope of target states for convergence will be small. To improve the status, it is necessary to study the problem of extending the invariant set.

We try to relax the condition of Assumption 7.1, that is, to enable

$$P_l = P_j \quad (l, j \in \{1, 2, \dots, N\}; l \neq j) \quad (7.15)$$

in Equation 7.11. Reconsidering the linear independence of the exponential functions, one has

$$(P_l - P_j) \langle \lambda_l | \psi(t_0) \rangle \langle \psi(t_0) | \lambda_j \rangle (H_k)_{jl} = 0, \quad j, l \in \{1, \dots, N\}; j \neq l; k = 1, \dots, r \quad (7.16)$$

Equation 7.16 means that, when Equation 7.15 is satisfied, the direct connectivity path between the l th and j th eigenstates is cut off, so the invariant set of the control system is sure to become big. Generally, the higher the number of pairs of the set equal eigenvalues, the bigger the scope of the target states for convergence. At the same time, it may be more difficult to construct appropriate diagonal elements.

7.1.4 Numerical Simulations

We use a five-level system (Kuang and Cong, 2008; D'Alessandro, 2007; Turinici and Rabitz, 2001) to numerically verify the control method proposed. It will be seen that the above construction and adjustment principles are only indicatory and some special considerations are necessary for concrete cases. The inner and control Hamiltonians are given as

$$H_0 = \begin{bmatrix} 1 & 0 & 0 & 0 & 0 \\ 0 & 1.2 & 0 & 0 & 0 \\ 0 & 0 & 1.3 & 0 & 0 \\ 0 & 0 & 0 & 2 & 0 \\ 0 & 0 & 0 & 0 & 2.15 \end{bmatrix}, H_1 = \begin{bmatrix} 0 & 0 & 0 & 1 & 1 \\ 0 & 0 & 0 & 1 & 1 \\ 0 & 0 & 0 & 1 & 1 \\ 1 & 1 & 1 & 0 & 0 \\ 1 & 1 & 1 & 0 & 0 \end{bmatrix},$$

Only one control field will be used in the simulation and its proportional coefficient will be uniformly taken as $K_1 = 0.15$.

1) Eigenvalues of P are different

Our task is to achieve the convergence to the equal-probability superposition state of $|\lambda_4\rangle$ and $|\lambda_5\rangle$ with a high probability. Considering that the invariant set of the control system is $E = E_1 \cup E_2 = \text{span}\{|\lambda_1\rangle, |\lambda_2\rangle, |\lambda_3\rangle\} \cup \text{span}\{|\lambda_4\rangle, |\lambda_5\rangle\}$, one can construct the values of diagonal elements according to the following steps:

Step 1: Let $P_4 = P_5 < P_1, P_2, P_3$ and observe the status of population distribution on $|\lambda_4\rangle$ and $|\lambda_5\rangle$ when the system trajectory enters the invariant subset E_2 .

Step 2: Based on the result of step 1, gradually adjust the relative values of P_4 until the equal-probability superposition state of $|\lambda_4\rangle$ and $|\lambda_5\rangle$ is obtained.

Remark 7.3 Since both $|\lambda_4\rangle$ and $|\lambda_5\rangle$ are in E_2 , the construction relation in step 1 will not change the invariant set of the system and the convergence of the system trajectory to E_2 . To pick up the rate of convergence, we can choose the eigenvalues associated with E_1, P_1, P_2 , and P_3 , which are much bigger than P_4 and P_5 .

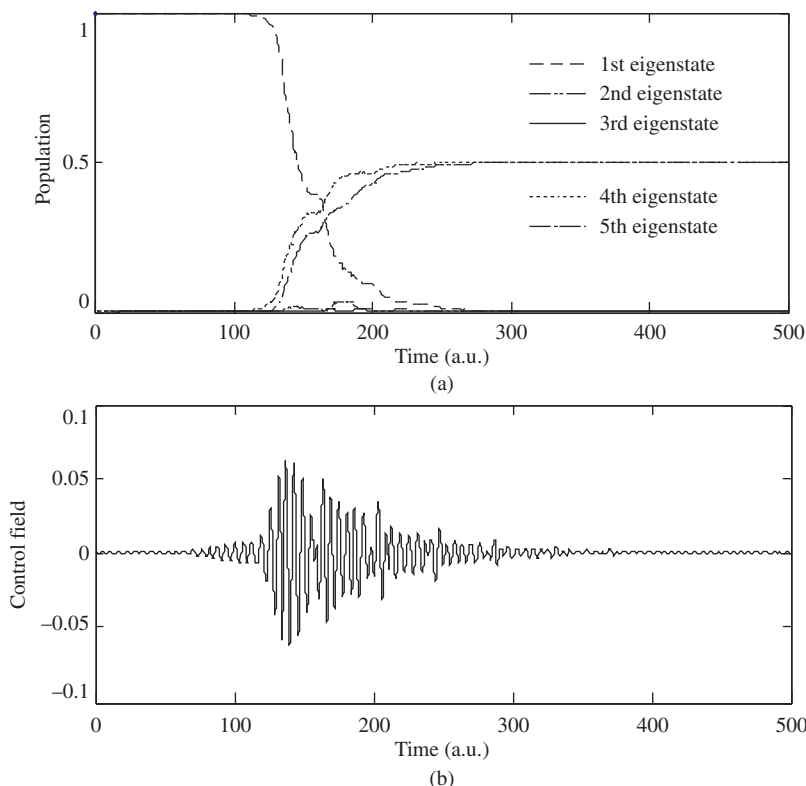


Figure 7.1 The simulation result in the case where the eigenvalues of P are different and the target state is the equal-probability superposition state of $|\lambda_4\rangle$ and $|\lambda_5\rangle$: (a) the population of the system and (b) the associated control field

Assume the initial state of the system is $|\psi(0)\rangle = |\lambda_1\rangle$ and add to the system an initial constant disturbance with amplitude 0.015 in the duration time 0.001, that is, take the post-disturbance state as a new initial state. According to the above two steps, if one takes $P_1 = 1, P_2 = 1.2, P_3 = 1.3$, and $P_4 = P_5 = 0.5$, then it can be observed that the population on $|\lambda_4\rangle$ is much higher than that of $|\lambda_5\rangle$. By gradually increasing P_4 , one can obtain a diagonal matrix that achieves the equal-probability population distribution on $|\lambda_4\rangle$ and $|\lambda_5\rangle$, $P = \text{diag}[1, 1.2, 1.3, 0.55352, 0.5]$. The simulation results are shown in Figure 7.1.

2) P has the same eigenvalues

If $P_3 = P_4$, the invariant set of the system will change. The new invariant set can be written as $E' = E'_1 \cup E'_2 \cup E'_3 = \text{span}\{|\lambda_1\rangle, |\lambda_2\rangle, |\lambda_3\rangle\} \cup \text{span}\{|\lambda_3\rangle, |\lambda_4\rangle\} \cup \text{span}\{|\lambda_4\rangle, |\lambda_5\rangle\}$. Thus, it is possible to achieve the equi-probability distribution of the system on $|\lambda_3\rangle$ and $|\lambda_4\rangle$. Unlike the case in Section 7.1.4, condition $P_3 = P_4$ restrains us from singly adjusting P_3 or P_4 . However, as the two eigenstates $|\lambda_3\rangle$ and $|\lambda_4\rangle$ in E'_2 belong to E'_1 and E'_3 , respectively, we can try to adjust the eigenvalues associated with the other eigenstates in E'_1 and E'_3 to accomplish the control task.

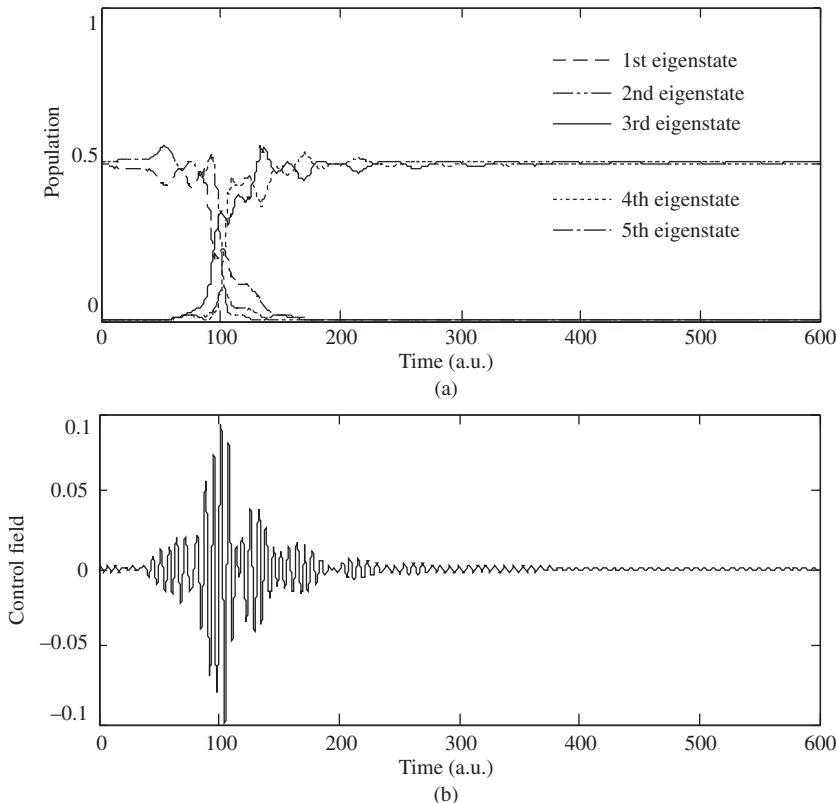


Figure 7.2 The simulation result in the case where P is of the same eigenvalues and the target state is the equi-probability superposition state of $|\lambda_3\rangle$ and $|\lambda_4\rangle$: (a) the population of the system and (b) the control field

Assume that the initial state is given as $|\psi(0)\rangle = \frac{1}{\sqrt{2}}|\lambda_1\rangle + \frac{1}{\sqrt{2}}|\lambda_5\rangle$.

Choosing $P_1 = 1, P_2 = 1.2, P_3 = P_4 = 0.3$, and $P_5 = 0.8$, one can observe that the trajectory of the control system finally converges to E'_2 , but the population on $|\lambda_3\rangle$ is much higher than the one on $|\lambda_4\rangle$. We may therefore try to gradually decrease P_1 or P_2 , or increase P_5 to reduce the population on $|\lambda_3\rangle$ and increase the one on $|\lambda_4\rangle$. Here, we adopt the means of gradually increasing P_5 . Via several trials, one can obtain the diagonal matrix $P = \text{diag}[1, 1.2, 0.3, 0.3, 0.9886]$. The corresponding simulation results are shown in Figure 7.2.

3) Target state is an eigenstate

In this case, we only change the control Hamiltonian as

$$H_1 = \begin{bmatrix} 0 & 1 & 0 & 1 & 1 \\ 1 & 0 & 0 & 1 & 1 \\ 0 & 0 & 0 & 0 & 1 \\ 1 & 1 & 0 & 0 & 0 \\ 1 & 1 & 1 & 0 & 0 \end{bmatrix}.$$

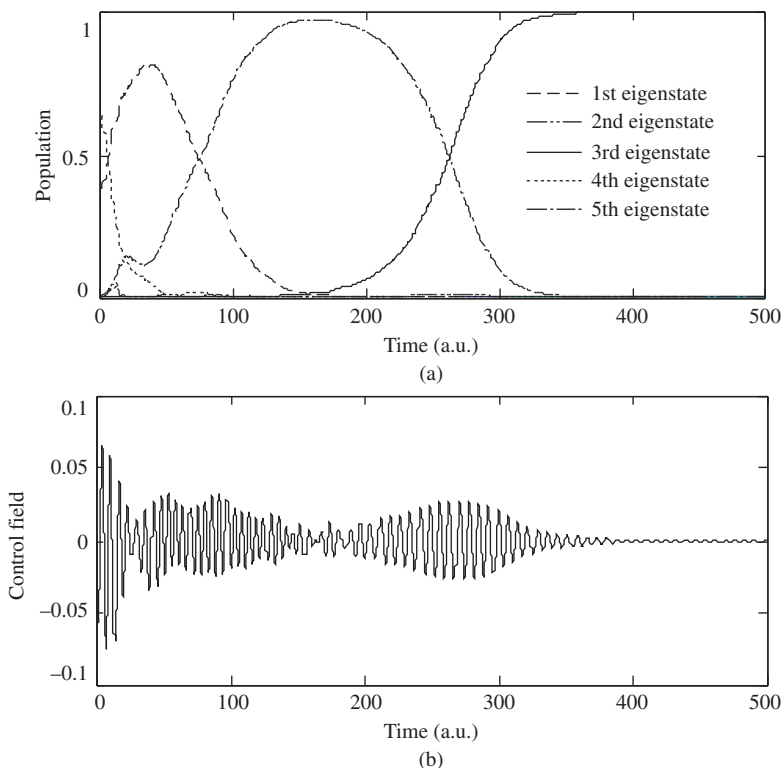


Figure 7.3 The simulation results in the case where the target state is an eigenstate: (a) the population of the system and (b) the control field

Assume that the initial state is $|\psi(0)\rangle = \frac{1}{\sqrt{3}}|\lambda_1\rangle + \frac{\sqrt{2}}{\sqrt{3}}|\lambda_4\rangle$ and the target state is the eigenstate $|\psi_f\rangle = |\lambda_3\rangle$, which simultaneously belongs to the three invariant subsets. It can be seen from the connectivity graph of the system that the population transition to $|\lambda_3\rangle$ has to pass through the medium energy state $|\lambda_5\rangle$. P_3 should therefore be kept to a minimum and P_5 should be second smallest. Furthermore, according to the form of its invariant set and the indicatory construction principles, we can find many groups of diagonal elements that achieve the control goal with a high probability, for example $P = \text{diag}[0.8, 1.1, 0.4, 1.2, 0.6]$. The simulation results are shown in Figure 7.3.

7.1.5 Summary and Discussion

In essence, the designed control laws cannot distinguish between arbitrary eigenstates in an invariant subset. It is therefore reasonable to regard each invariant subset as a whole and to determine its region of attraction. However, it is known that the structure of the invariant set E may be very complex. Even though P is given, determining the region of attraction of each invariant subset is extremely difficult. In this section, we find the construction and

adjustment principles of P . However, when the structure of the related invariant subsets is very complicated, the construction and adjustment principles in this section appear weak and insufficient. In this case, it is necessary to seek further theoretical tools to develop some extra new construction principles, which are studied in Chapter 8.

7.2 A Convergent Control Strategy of Quantum Systems

In this section an absolute of average value with an observable quantity P is chosen as the Lyapunov-like function, called the energy function. We will derive an explicit general expression of P that could be used to obtain the control law directly, and this P makes the target state the minimum point of the energy function. In addition, we will prove a sufficient and necessary condition of guaranteeing the convergence of the control system on control Hamiltonians by analyzing the dynamical stability of the critical points of the derivative of energy function. In addition, when the controlled system cannot be transferred to the target state, we will propose a route extension strategy to solve this problem by adding new evolving routes, which can also track an arbitrary time-varying target state.

7.2.1 Problem Description

Consider a closed quantum system with dimension of n :

$$i\hbar\dot{\rho} = [H(t), \rho] \quad (7.17a)$$

$$H(t) = H_0 + \sum_{j=1}^n H_j u_j(t) \quad (7.17b)$$

where H_0 is a free Hamiltonian, which is a Hermite diagonal matrix, H_j is a control Hamiltonian, u_j is a control quantity, and ρ is the state density matrix of the system. By transforming the system (Equation 7.17a) into the interaction picture, viz. setting $\rho' = e^{iH_0 t/\hbar} \rho e^{-iH_0 t/\hbar}$, the Liouville equation of the closed quantum system after the transformation can be written as

$$\dot{\rho}' = \left[\sum_j A_j(t) u_j(t), \rho' \right] \quad (7.18a)$$

$$A_j(t) = e^{iH_0 t/\hbar} H_j e^{-iH_0 t/\hbar} / i\hbar \quad (7.18b)$$

where $A_j(t)$ is the control Hamiltonian in the interaction picture. It can be verified that such a transformation does not change the population distribution of the system state. In the next part of this section we will omit the label “ $'$ ” in Equation 7.18 for convenience.

Define a bounded Lyapunov-like function $E(\rho)$ as

$$|E(\rho)| = |tr(P\rho)| \leq M \quad (7.19a)$$

in which P is the observable operator and M is a finite positive number.

We call this Lyapunov-like function $E(\rho)$ as energy function. The main difference between the energy function and the Lyapunov function is that the former can be either positive or negative and it needs to be only boundary, while the latter must be positive (semi) definite.

The Lyapunov function is defined strictly. The energy function definition is reasonable in the study of closed quantum systems, in which P is not limited to be positive definite. For the sake of convenience, we may define an energy function $E(\rho)$ by

$$E(\rho) = \text{tr}(P\rho) \quad (7.19\text{b})$$

where P is an observable operator without positive definite limitations.

The control task is to steer an arbitrary initial state in Equation 7.18 to the desired target state, which can be an eigenstate, a superposition state, or a mixed state, by designing a convergent control law. Clearly, one could achieve such a task by associating the minimum point of energy function (Equation 7.19b) with the target state ρ_f and guaranteeing the monotonic decrease of energy function (Equation 7.19b). Let the first-order time derivative be negative semi-definite:

$$\dot{E}(\rho(t)) = \sum_j u_j \text{tr}([\rho(t), P]A_j) \leq 0 \quad (7.20)$$

The following control laws can be derived:

$$u_j(t) = -\kappa_j(t) \text{tr}([\rho(t), P]A_j(t)), \kappa_j(t) > 0 \quad (7.21)$$

where $\kappa_j(t)$ is control gain, used to adjust the convergence speed of the system.

Generally, the control law (Equation 7.21) is only a stable control. The system can only converge to a local extreme point of some system trajectories instead of the global minimum point. In order to solve such a problem, an observable operator P will be designed. The conditions on control Hamiltonians will be proposed in this section under certain assumptions. Finally, a route extension strategy is proposed to fully solve the convergence problem.

7.2.2 Construction Method of the Observable Operator

This section presents the construction method of the observable operator P , which makes ρ_f the minimum point of Equation 7.19b, and gives the conditions on control Hamiltonians such that control laws are convergent.

Consider the transition from a fixed initial state to a desired target state ρ_f . The task is to make ρ_f the minimum point of Equation 7.19b with a fixed P , which means that the state ρ_f makes the following equations hold:

$$\text{tr}(P\rho_f) = \min_{\rho} \text{tr}(P\rho) \quad (7.22\text{a})$$

$$\text{tr}([\rho_f, P]A_j(t)) = 0 \quad (7.22\text{b})$$

where ρ is any possible system state.

Now, we discuss Equation 7.22 using Lie algebra $u(n)$. A state density matrix ρ with n dimensions can be written as

$$\rho = I/n + \sum x_l X_l \quad (7.23)$$

where X_l are the basis of $u(n)$ that satisfies $\text{tr}(X_l X_j) = \delta_{lj}$ and x_l is a real number. The vector V_ρ is formed by x_1, x_2, \dots and x_{n^2-1} is called the coherent vector of density matrix ρ , that is,

$$V_\rho = (x_1, x_2, \dots, x_{n^2-1})^T \quad (7.24)$$

The module of a coherent vector V_ρ indicates the purity of a state. Because of the unitary nature of closed quantum system's evolution, the purity will be unchanged during the whole evolution process of the system, and the module of V_ρ is equal to $\sum_l |x_l|^2 = C$, where C is a constant.

Likewise, ρ_f and P can be written as:

$$\rho_f = I/n + \sum_j f_j X_j \quad (7.25a)$$

$$P = c_0 I + \sum_k c_k X_k \quad (7.25b)$$

According to $\text{tr}(X_i X_j) = \delta_{ij}$ and Equation 7.25, one has:

$$\text{tr}(P \rho_f) = c_0 + V_P^T V_{\rho_f} \quad (7.26)$$

Because the module of V_ρ is constant, Equation 7.22a ensures that coherent vectors V_ρ and V_{ρ_f} have opposite directions:

$$V_P = \lambda V_{\rho_f}, \lambda < 0 \quad (7.27)$$

It can be verified that such a P is commutative with ρ_f , and Equation 7.22b is satisfied. Thus we have:

Theorem 7.3 Suppose the system Equation 7.18a is expected to evolve from a given initial state to the target state ρ_f . In order for the target state ρ_f to be the minimum point of energy function (Equation 7.19b), the coherent vectors of P and ρ_f must have opposite directions, that is, $V_P = \lambda V_{\rho_f}, \lambda < 0$.

Theorem 7.3 implies that P is not unique. For instance, the simplest way to get an observable operator P is to let $P = -\rho_f$, which is the coincidence of the solution in the case of the target eigenstate, but here we develop a general formation for constructing P . For a two-level system with target state $\rho_f = |0\rangle\langle 0|$, V_P and V_{ρ_f} have opposite directions when one takes $P = a|0\rangle\langle 0| + b|1\rangle\langle 1|$ with $a < b$. Generally, for pure states, the following conclusion holds:

Corollary 7.1 Suppose the system state and the target state are both pure states, that is, $\rho = |\psi\rangle\langle\psi|$ and $\rho_f = |\psi_f\rangle\langle\psi_f|$. In order for ρ_f to be the minimum point of Equation 7.19b, an observable operator P can be constructed by an orthogonal basis containing the target state ρ_f :

$$P = p_h \sum_{\langle\psi_j|\psi_f\rangle=0} |\psi_j\rangle\langle\psi_j| + p_l |\psi_f\rangle\langle\psi_f|, \text{ for } \langle\psi_j|\psi_f\rangle = \delta_{jk} \text{ and } p_l < p_h \quad (7.28)$$

Remark 7.4 It can be proven from Equation 7.28 that energy function (Equation 7.19b) reaches its minimum if and only if $|\psi\rangle = |\psi_f\rangle$ for a two-level system with pure states. According to Theorem 7.3, the coherent vector of P in Equation 7.28 has an opposite direction to that of ρ_f , that is, $E(\rho) = -\text{tr}(\rho\rho_f) \leq 0$. This energy function is not a standard Lyapunov function with $E(\rho) \geq 0$ because P is no longer positive definite. That is the reason why we define a bounded energy function.

Theorem 7.3 and Corollary 7.1 are the construction methods and the expression of observable operator P for general states and pure states, respectively. Such an observable operator guarantees that the target state ρ_f is the minimum point of energy function (Equation 7.19b) and control laws (Equation 7.21) are stable controls. In order to make such controls convergent, some restrictions on control Hamiltonians should be placed. To this end, three assumptions are given in advance.

Assumption 7.3 System (Equation 7.17) is strongly regular, that is, all the transition frequencies are different, viz. $\Delta_{jk} \neq \Delta_{pq}$ and $(j, k) \neq (p, q)$, where $\Delta_{jk} = \lambda_j - \lambda_k$ and λ_j is an eigenvalues of H_0 .

Assumption 7.4 The control Hamiltonian H_l has a particular structure: $H_l \in \{\hbar h_{jk} | h_{jk} = |j\rangle\langle k| + |k\rangle\langle j|, j > k\}$, where $|j\rangle$ is the eigenstate associated with λ_j .

Assumption 7.5 The initial and target states are unitarily equivalent, that is, there exists a unitary transform U such that $\rho_f = U\rho U^\dagger$.

Remark 7.5 Assumption 7.3 indicates that transition frequencies between all the energy levels are distinct, so that each transition can be distinguished and selected. This enables Assumption 7.4 to hold by considering rotating wave approximation. The operator h_{jk} denotes that the transition between energy levels j and k is admitted. If two transitions are the same, for example, $\Delta_{12} = \Delta_{34}$, then h_{12} and h_{34} should be incorporated as $h = h_{12} + h_{34}$.

Next, we will give a sufficient and necessary condition that guarantees convergence of the control system:

Theorem 7.4 Based on Assumptions 7.3, 7.4, and 7.5, for any given initial and target states the observable operator P is constructed by Equation 7.27. A sufficient and necessary condition that system Equation 7.17a with control laws (Equation 7.21) converges to the target state is: for $\forall j, k, \exists l$, s.t. $H_l = \hbar h_{jk}$.

7.2.3 Proof of Convergence

If the controlled system is asymptotically stable, the system will converge to the target state. For autonomous systems, asymptotic stability can be analyzed by the LaSalle principle. In the present situation, however, the controlled system becomes non-autonomous in the interaction picture. However, one can get an analogous conclusion by the Barbalat lemma:

Lemma 7.2 The scalar function $E(x, t)$ satisfies: (i) $E(x, t)$ is lower bounded, (ii) $\dot{E}(x, t)$ is negative semi-definite, and (iii) $\dot{E}(x, t)$ is uniformly continuous in time. Then, $\dot{E}(x, t) \rightarrow 0$ as $t \rightarrow \infty$.

Energy function $E(\rho) = -\text{tr}(\rho\rho_f) \geq -\text{tr}(\rho_f^2)$ is lower bounded. Its first derivative is negative semi-definite under control laws (Equation 7.21). The second derivative is:

$$\ddot{E}(\rho, t) = \sum_j \{u_j \text{tr}([\dot{\rho}(t), P]A_j(t)) + u_j \text{tr}([\rho(t), P]\dot{A}_j(t))\} \quad (7.29)$$

Equation 7.29 is bounded when the inputs are bounded. Thus, $\dot{E}(\rho, t)$ is uniformly continuous in time. According to Lemma 7.2, the first-order time derivative of the energy function converges to zero, viz., $\lim_{t \rightarrow \infty} \dot{E}(\rho(t), t) = 0$.

Let R be the set of critical points on any dynamic trajectory, viz.

$$R \equiv \{\rho : tr([\rho, P]A_j(t)) = 0, \forall j, t\} \quad (7.30)$$

Then, the controlled system converges to R .

Moreover, system Equation 7.18a is homogeneous, and the states in R make their controls zero according to Equation 7.21. The largest invariant set in R is therefore itself.

Theorem 7.5 System Equation 7.18a with control laws (Equation 7.21) converges to the set R defined by Equation 7.30.

In 2008 Wang and Schirmer indicated that kinematically critical points ρ_s can be defined by $[\rho_s, \rho_f] = 0$, and if the system is controllable, then all the critical points except the maximum and minimum points are kinematically critical stable. However, kinematical analysis implicates that the direction fields of state evolution are unrestricted. In fact, the direction fields determined by the Hamiltonians are usually non-arbitrary. This means that some trajectories in kinematics are forbidden in dynamics. That is to say, the results in kinematics and in dynamics may be different. The dynamic stability of critical points in R will be further analyzed as follows.

First, we show that if the conditions in Theorem 7.4 are satisfied, then critical points in kinematics and in dynamics are the same.

Lemma 7.3 If the conditions in Theorem 7.4 are satisfied, then critical points ρ_s and ρ_f are unitarily equivalent. ρ_s can then be defined by $[\rho_s, \rho_f] = 0$, viz., the invariant set R in Theorem 7.5 can be redefined by

$$R \equiv \{\rho : [\rho, P] = D\} \quad (7.31)$$

where D is a diagonal matrix.

Lemma 7.4 Given a generic P , if $\text{rank}\tilde{A}(\vec{P}) = n^2 - n$ holds, then the invariant set R is regular, viz. $R \equiv \{\rho_s : [\rho_s, P] = 0\}$, where $[\rho, P] = Ad_p(\vec{P})$ and Ad_p is a linear map from Hermitian or anti-Hermitian matrices into $su(n)$ (Wang and Schirmer, 2010b). Let $A(\vec{P})$ be the real $(n^2 - 1) * (n^2 - 1)$ matrix corresponding to the Bloch representation of Ad_p . Denote $su(n) = T \oplus C$ and $R^{n^2-1} = S_T \oplus S_C$, where S_C and S_T are real subspaces corresponding to the Cartan and non-Cartan subspaces C and T , respectively. Then $\tilde{A}(\vec{P})$ is the first $n^2 - n$ rows of $A(\vec{P})$.

For target state ρ_f with diagonal type, the invariant set with $P = -\rho_f$ in Equation 7.31 can be simplified as

$$R \equiv \{\rho : [\rho, P] = 0\} \quad (7.32)$$

For the non-diagonal target state ρ_f including some mixed states and superposition states, Lemma 7.4 is employed. If ρ_f satisfies Lemma 7.4 automatically, one obtains Equation 7.32 with $P = -\rho_f$. Otherwise, taking superposition states, for example, P is

chosen for Equation 7.28. We can always choose eigenvalues p_i to meet the condition of Lemma 7.4 and then Equation 7.32 is obtained. To sum up, for most diagonal target states, the superposition states, and some mixed states satisfy Lemma 7.4, there are two ways to construct P : one is $P = -\rho_f$ and the other is Equation 7.28, by which the invariant set can be reduced to Equation 7.32. All the convergence analysis will be carried out based on Equation 7.32.

Next, we will give a sufficient and necessary condition on control Hamiltonians such that all the states in R except the maximum and minimum points are dynamically critically stable under Assumptions 7.3 and 7.4.

For a dynamically minimum point, $\ddot{E}(\rho_s, t) \geq 0$ holds for any time and any control $u = (u_1, u_2, \dots, u_N)$. Otherwise, the state will be critically stable. That is to say, it is enough to consider the second derivative of the energy function.

For $\text{tr}([\rho_s, P]\dot{A}_j(t)) = \frac{i}{\hbar}\text{tr}([\rho_s, P][H_0, A_j]) = 0$, the following equation holds:

$$\begin{aligned}\ddot{E}(\rho_s, t) &= \text{tr}\left(\sum_j u_j \dot{A}_j(t)[\rho_s, P]\right) + \text{tr}\left(\left[\sum_j u_j A_j(t), \rho_s\right] \left[P, \sum_j u_j A_j(t)\right]\right) \\ &= \text{tr}\left(\left[\sum_j u_j A_j(t), \rho_s\right] \left[P, \sum_j u_j A_j(t)\right]\right)\end{aligned}$$

If $P = -\rho_f$, one has

$$\ddot{E}(\rho_s, t) = \text{tr}\left(\left[\sum_j u_j A_j(t), \rho_s\right] \left[\sum_j u_j A_j(t), \rho_f\right]\right) \quad (7.33a)$$

If P is chosen according to Equation 7.28, where we denote $\rho_h = |\psi_h\rangle\langle\psi_h|$, one obtains:

$$\begin{aligned}\ddot{E}(\rho_s, t) &= p_l \text{tr}\left(\left[\sum_j u_j A_j(t), \rho_s\right] \left[\sum_j u_j A_j(t), \rho_f\right]\right) \\ &\quad + \sum_h p_h \text{tr}\left(\left[\sum_j u_j A_j(t), \rho_s\right] \left[\sum_j u_j A_j(t), \rho_h\right]\right) \\ &= p_l \text{tr}\left(\left[\sum_j u_j A_j(t), \rho_s\right] \left[\sum_j u_j A_j(t), \rho_f\right]\right) \quad (7.33b)\end{aligned}$$

Obviously, ρ_f is a stable point since $\ddot{E}(\rho_f, t) \geq 0$ holds for $\forall t$. Further analysis implicates Lemma 7.5.

Lemma 7.5 For any diagonal target state ρ_f , a sufficient and necessary condition such that all the states in R except the minimum point are dynamically critically stable is, for $\forall l_0, r_0$, $\exists A_q(t)$, such that $(A_q(t))_{l_0 r_0} \neq 0$.

Proof Necessity. It is equivalent to prove that if $\exists l_0, r_0$, such that $(A_q(t))_{l_0 r_0} = 0$ for $A_q(t), (A_q(t))_{lr} \neq 0$, then $\exists \rho_f, \rho_s \neq \rho_f$ such that $\ddot{E}(\rho_s, t) \geq 0$ holds for $\forall t$ and any controls.

We can denote diagonal matrices ρ_f and ρ_s as follows. Let the two smallest elements of ρ_f be $(\rho_f)_{r_0 r_0}$ and $(\rho_f)_{l_0 l_0}$. Then, ρ_s can be selected by exchanging the l_0 th and r_0 th elements of ρ_f , that is, $(\rho_s)_{l_0 l_0} = (\rho_f)_{r_0 r_0}$ and $(\rho_s)_{r_0 r_0} = (\rho_f)_{l_0 l_0}$. Obviously, ρ_f and ρ_s are commutable, viz., $\rho_s \in R$.

According to Assumptions 7.3 and 7.4, one has:

$$i\hbar A_q(t) \in \{|j\rangle\langle k|e^{i\omega_{jk}t/\hbar} + |k\rangle\langle j|e^{-i\omega_{jk}t/\hbar}, j < k\} \quad (7.34)$$

Denote H_q by H_{lr} and u_q by u_{lr} . If $(A_q(t))_{lr} \neq 0$, it can be obtained from Equation 7.33a that

$$\ddot{E}(\rho_s) = \sum_{l \neq l_0, r \neq r_0} u_{lr}^2 ((\rho_s)_{rr} - (\rho_s)_{ll}) ((\rho_f)_{rr} - (\rho_f)_{ll}) \quad (7.35)$$

For $\forall j \neq l_0, j \neq r_0$, $(\rho_s)_{jj} = (\rho_f)_{jj}$, $((\rho_s)_{rr} - (\rho_s)_{ll})((\rho_f)_{rr} - (\rho_f)_{ll}) \geq 0$ holds, therefore $\ddot{E}(\rho_s, t) \geq 0$ holds for $\forall t$ and any controls. The necessity is proven.

Sufficiency: It is enough to prove that $\exists u$, $\ddot{E}(\rho_s) < 0$.

For $[\rho_s, \rho_f] = 0$, ρ_s is also a diagonal matrix. Since ρ_f and ρ_s are unitarily equivalent, ρ_s has the same spectrum with ρ_f , that is, the diagonal element of ρ_s is a permutation of that of ρ_f . Suppose the largest element of the permutation is $(\rho_f)_{l_0 l_0}$ or $(\rho_s)_{r_0 r_0}$, then we have $(\rho_s)_{r_0 r_0} - (\rho_s)_{l_0 l_0} > 0$ and $(\rho_f)_{r_0 r_0} - (\rho_f)_{l_0 l_0} < 0$. According to Equation 7.35, if $u_{l_0 r_0} \neq 0$ and other controls are equal to zero, then $\ddot{E}(\rho_s) < 0$. The sufficiency is proven.

Lemma 7.5 is proven. ■

For a general ρ_f , the of the necessity is the same as Lemma 7.5 and one needs only to prove the sufficiency.

Now, suppose $\rho_f = \sum_j c_j |\varphi_j\rangle\langle\varphi_j|$, where $|\varphi_j\rangle = \sum_k \alpha_{jk}|k\rangle$. Let $U = \sum_j |j\rangle\langle\psi_j|$. There must be $U = \sum_j |j\rangle\langle\psi_j|$ to diagonalize ρ_f and ρ_s simultaneously, then:

$$\begin{aligned} \ddot{E}(\rho_s) &= \text{tr} \left(\left[\sum_j u_j U A_j(t) U^\dagger, U \rho_s U^\dagger \right] \left[\sum_j u_j U A_j(t) U^\dagger, U \rho_f U^\dagger \right] \right) \\ &\equiv \text{tr} \left(\left[\sum_j u_j U A_j(t) U^\dagger, D_s \right] \left[\sum_j u_j U A_j(t) U^\dagger, D_f \right] \right) \end{aligned} \quad (7.36)$$

where D_s and D_f are two diagonal matrices. In particular, if ρ_f is a superposition state, P is chosen according to Equation 7.28. Equation 7.36 is also obtained from Equation 7.33b. Calculating $\sum_j u_j U A_j(t) U^\dagger$ one gets:

$$\begin{aligned} \sum_j u_j U A_j(t) U^\dagger &= -i \sum_j 2\text{Re} \left\{ \left(\sum_{l < r} u_{lr} \alpha_{jl}^* \alpha_{jr} e^{i\omega_{lr}t} \right) |j\rangle\langle j| \right\} \\ &\quad - i \sum_{j < k} \left\{ \left[\sum_{l < r} u_{lr} \left(\alpha_{jl}^* \alpha_{kr} e^{i\omega_{lr}t} + \alpha_{jr}^* \alpha_{kl} e^{-i\omega_{lr}t} \right) \right] |j\rangle\langle k| \right. \\ &\quad \left. + \left[\sum_{l < r} u_{lr} \left(\alpha_{kl}^* \alpha_{jr} e^{i\omega_{lr}t} + \alpha_{kr}^* \alpha_{jl} e^{-i\omega_{lr}t} \right) \right] |k\rangle\langle j| \right\} \end{aligned} \quad (7.37)$$

in which the first sum on the right hand side is a diagonal matrix, which commutes with D_s and D_f so it can be ignored. Let

$$\begin{aligned} f_{jk} &\equiv \sum_{l < r} u_{lr} (\alpha_{jl}^* \alpha_{kr} e^{i\omega_{lr} t} + \alpha_{jr}^* \alpha_{kl} e^{-i\omega_{lr} t}) = \langle \psi_j | e^{iH_0 t} \left(\sum_{l < r} u_{lr} H_{lr} \right) e^{-iH_0 t} | \psi_k \rangle \\ &= \langle \psi'_j | \left(\sum_{l < r} u_{lr} H_{lr} \right) | \psi'_k \rangle \end{aligned} \quad (7.38)$$

Then

$$\ddot{E}(\rho_s) = \sum_{j,k} |f_{jk}|^2 ((D_s)_{kk} - (D_s)_{jj}) ((D_f)_{kk} - (D_f)_{jj}) \quad (7.39)$$

Equation 7.38 can be rewritten as

$$\begin{pmatrix} \langle \psi'_1 | H_{12} | \psi'_2 \rangle & \langle \psi'_1 | H_{13} | \psi'_2 \rangle & \dots & \langle \psi'_1 | H_{(n-1)n} | \psi'_2 \rangle \\ \langle \psi'_1 | H_{12} | \psi'_3 \rangle & \langle \psi'_1 | H_{13} | \psi'_3 \rangle & \dots & \langle \psi'_1 | H_{(n-1)n} | \psi'_3 \rangle \\ \vdots & \vdots & \ddots & \vdots \\ \langle \psi'_{n-1} | H_{12} | \psi'_{n-1} \rangle & \langle \psi'_{n-1} | H_{13} | \psi'_{n-1} \rangle & \dots & \langle \psi'_{n-1} | H_{(n-1)n} | \psi'_{n-1} \rangle \end{pmatrix} \begin{pmatrix} u_{12} \\ u_{13} \\ \vdots \\ u_{(n-1)n} \end{pmatrix} = \begin{pmatrix} f_{12} \\ f_{13} \\ \vdots \\ f_{(n-1)n} \end{pmatrix} \quad (7.40)$$

If the square matrix in Equation 7.40 is noted as M , it is easy to verify that if the condition in Theorem 7.4 is satisfied, M has full rank. If there exists a linear combination of some columns in the square matrix which is zero, then for $\forall j, k$ there is:

$$\langle \psi'_j | \left(\sum_{l < r} \beta_{lr} H_{lr} \right) | \psi'_k \rangle = 0 \quad (7.41)$$

Consider two states $|\psi'_j\rangle$ and $|\psi'_k\rangle$ to be arbitrary. Equation 7.36 holds for only $\beta_{lr} = 0$, viz. the matrix M is full rank.

In the following we will seek the control u that makes $\ddot{E}(\rho_s, u) < 0$. Equation 7.41 can be rewritten as

$$\ddot{E}(\rho_s, u) = f^\dagger K f = u^\dagger M^\dagger K M u \quad (7.42)$$

in which K is a diagonal matrix and defined by:

$$K = \begin{pmatrix} ((D_s)_{22} - (D_s)_{11}) ((D_f)_{22} - (D_f)_{11}) & \dots & 0 \\ \vdots & \ddots & \vdots \\ 0 & \dots & ((D_s)_{nn} - (D_s)_{(n-1)(n-1)}) ((D_f)_{nn} - (D_f)_{(n-1)(n-1)}) \end{pmatrix} \quad (7.43)$$

Matrix K has at least one negative element because the two matrices D_s and D_f satisfy $D_f \neq D_s$, and their diagonal elements are an arrangement of the same numbers. In other words, matrix is non-positive definite. The matrix $M^\dagger K M$ is therefore also non-positive definite, and its eigenvalues include at least one real negative element, viz.:

$$M^\dagger K M = T^\dagger Q T \quad (7.44)$$

where Q is a real negative diagonal matrix in its k_0 th element and T is a unitary matrix whose k_0 th row is supposed to be z^\dagger . The matrix T and the vector z can be separated into real and imaginary parts, respectively, as:

$$T = A + iB \quad (7.45)$$

and

$$z = x + iy \quad (7.46)$$

Because $\ddot{E}(\rho_s, u)$ is a real number, the imaginary part of the matrix $M^\dagger KM$ has no contribution to $\ddot{E}(\rho_s, u)$, which can be written as

$$\ddot{E}(\rho_s, u) = u^\dagger (A' QA + B' QB) u \quad (7.47)$$

If the control u is replaced by z :

$$\begin{aligned} \ddot{E}(\rho_s, z) &= (Q)_{k_0 k_0} \\ &= z^\dagger (A' QA + B' QB) z \\ &= x'(A' QA + B' QB)x + y'(A' QA + B' QB)y \\ &< 0 \end{aligned} \quad (7.48)$$

then one can see that at least one of the two items $x'(A' QA + B' QB)x$ and $y'(A' QA + B' QB)y$ is negative. It does no harm to suppose that $x'(A' QA + B' QB)x < 0$, then if only the control is the real part of the vector z , one has $\ddot{E}(\rho_s, \text{Re}(z)) < 0$. So if the condition in Theorem 7.4 is satisfied, all the states in the set R except the target state are dynamically critically stable, that is, Theorem 7.4 can be obtained.

Theorem 7.4 means that any restriction on the evolution direction will produce new dynamically stable points, which may have a strong impact on control design. The conditions in Theorem 7.4 are obtained based on Assumption 7.4, which in fact defines a basic orthogonal basis for permissible state-evolving directions. This basis spans a full space of evolving direction fields when the conditions in Theorem 7.4 are satisfied. In fact, Assumption 7.4 is not necessary: if another basis spans the same space of evolving direction fields, then all the states in invariant set R except the target state are dynamically critically stable and the control laws (Equation 7.21) are still convergent.

7.2.4 Route Extension Strategy

There may be many critical points between the initial state and the target state that may result in the system converging in a final state that is not the desired target state. In addition, for some initial states the target state is not achievable. In these cases, we propose a route extension strategy that can weaken or remove the restriction on the state evolution direction fields by adding new control Hamiltonians to provide new evolving routes and make the system converge to the target state. The detailed procedure of realizing the route extension strategy will be introduced in Section 7.3.

Remark 7.6 Of course, a route extension might not always be realizable because it changes transition structure between energy levels and is forbidden in some cases. For many situations, it is permitted. For instance, in quantum computation, the controlled systems are just carriers of information and they could be displaced by other particles via which a route extension is realizable.

Another solution for the convergence problem, which can be called trajectory programming, can be adopted if one knows some exact information about evolution from an initial state to a target state. Trajectory programming selects one or more realizable intermediate states on

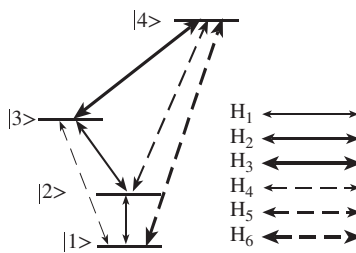


Figure 7.4 The transitions among energy levels and the related control Hamiltonians

the evolution path as transitional target states through which the system evolves step by step and finally converges to the desired target state. Naturally, there may be many transitional target states. A particular case is that the target state varies throughout the time period, thus the control problem is transferred to track a dynamic target state. In this case, control laws (Equation 7.21) are required to be convergent controls. The conditions in Theorem 7.4 must be satisfied and P can be designed as

$$P(t) = -\rho_f(t) \quad (7.49)$$

7.2.5 Numerical Simulations

Numerical examples are simulated on a four-level quantum system in this subsection to verify the effectiveness of the control strategy proposed.

The free Hamiltonian of the controlled system is

$$H_0 = \sum_{j=1}^n E_j |j\rangle\langle j| \quad (7.50)$$

where $E_1 = 0.4948$, $E_2 = 1.4529$, $E_3 = 2.3691$, and $E_4 = 3.2434$. Their energy-level differences are $\Delta_{21} = 0.9581$, $\Delta_{31} = 1.8743$, $\Delta_{41} = 2.7486$, $\Delta_{32} = 0.9162$, $\Delta_{42} = 1.7905$, and $\Delta_{43} = 0.8743$, separately. They are mutually distinct so that Assumption 7.3 is satisfied.

The control goal is to reverse the population of initial state $\rho_0 = \text{diag}(0.3850, 0.2758, 0.1976, 0.1416)$, that is, to drive the system to target state $\rho_f = \text{diag}(0.1416, 0.1976, 0.2758, 0.3850)$.

First, consider a ladder-type system in which the transitions between energy levels 1 and 2, 2 and 3, and 3 and 4 are permissible, as shown by the solid line in Figure 7.4. There are three control Hamiltonians for the system:

$$H_1 = \begin{pmatrix} 0 & 1 & 0 & 0 \\ 1 & 0 & 0 & 0 \\ 0 & 0 & 0 & 0 \\ 0 & 0 & 0 & 0 \end{pmatrix}, H_2 = \begin{pmatrix} 0 & 0 & 0 & 0 \\ 0 & 0 & 1 & 0 \\ 0 & 1 & 0 & 0 \\ 0 & 0 & 0 & 0 \end{pmatrix}, H_3 = \begin{pmatrix} 0 & 0 & 0 & 0 \\ 0 & 0 & 0 & 0 \\ 0 & 0 & 0 & 1 \\ 0 & 0 & 1 & 0 \end{pmatrix} \quad (7.51)$$

The control law is designed based on Equations 7.21 and 7.51, in which the observable operator is constructed according to Theorem 7.3 and is taken as $P = -\rho_f$ in simulation experiments, $\kappa_1 = \kappa_2 = \kappa_3 = 20$. Figure 7.5 shows the evolution curves of the system population and the control fields, from which one can see that the controlled system does not reach the target state after 150 time units.

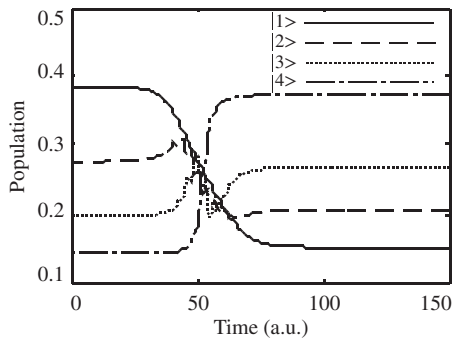


Figure 7.5 Simulation results with three control fields

The system state in numerical simulation after 150 a.u. of time is:

$$\rho_s = \begin{pmatrix} 0.1514 & 0 & -0.0254 + 0.019i & 0.0178 + 0.0079i \\ 0 & 0.2063 & 0 & -0.0238 + 0.0321i \\ -0.0254 - 0.019i & 0 & 0.2679 & 0 \\ 0.0178 - 0.0079i & -0.0238 - 0.0321i & 0 & 0.3744 \end{pmatrix} \quad (7.52)$$

In fact, it can be verified that the condition in Theorem 7.4 is not satisfied in the case that control Hamiltonians are in the form shown in Equation 7.51. In the following, the route extension and dynamic state-tracking strategies proposed in this paper are used to complete the control task.

1) Route extension

According to Theorem 7.4, if the transitions between energy levels 1 and 3, 2 and 4, and 1 and 4 are permitted, as shown by the dashed line in Figure 7.4, then three more control Hamiltonians are available:

$$H_4 = \begin{pmatrix} 0 & 0 & 1 & 0 \\ 0 & 0 & 0 & 0 \\ 1 & 0 & 0 & 0 \\ 0 & 0 & 0 & 0 \end{pmatrix}, H_5 = \begin{pmatrix} 0 & 0 & 0 & 0 \\ 0 & 0 & 0 & 1 \\ 0 & 0 & 0 & 0 \\ 0 & 1 & 0 & 0 \end{pmatrix}, H_6 = \begin{pmatrix} 0 & 0 & 0 & 1 \\ 0 & 0 & 0 & 0 \\ 0 & 0 & 0 & 0 \\ 1 & 0 & 0 & 0 \end{pmatrix} \quad (7.53)$$

Now, redesign the control laws and do simulation experiments again with $\kappa_4 = \kappa_5 = \kappa_6 = 20$. The evolution curves of the system population and the control fields are shown in Figure 7.6, from which one can see that the controlled system reaches the target state ρ_f after 100 a.u.

2) Dynamic state tracking

Control laws (Equation 7.21) with the control Hamiltonians (Equations 7.51 and 7.53) can also be used to track a dynamic state. Suppose that initial state is $\rho_0 = |1\rangle\langle 1|$ and that target state is $\rho_f(t) = |\psi_f(t)\rangle\langle\psi_f(t)|$, in which $|\psi_f(t)\rangle$ is defined as

$$|\psi_f(t)\rangle = \cos(\omega_1 t)|1\rangle + i \sin(\omega_1 t) \cos(\omega_2 t)|2\rangle - \sin(\omega_1 t) \sin(\omega_2 t) \cos(\omega_3 t)|3\rangle - i \sin(\omega_1 t) \sin(\omega_2 t) \sin(\omega_3 t)|4\rangle \quad (7.54)$$

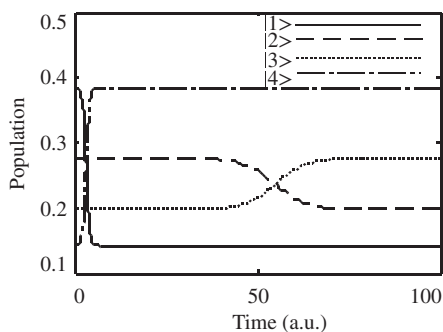


Figure 7.6 Simulation results for route extension

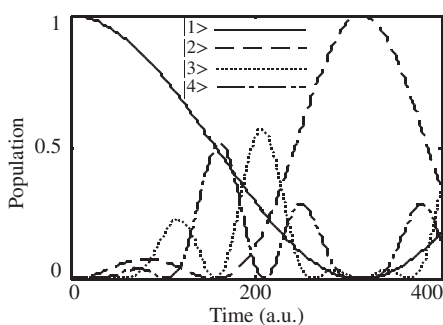


Figure 7.7 Simulation results for dynamic state tracking

with $\omega_1 = 0.005$, $\omega_2 = 0.01$, and $\omega_3 = 0.03$. Figure 7.7 shows the experimental tracking results of the route extension strategy. It can be concluded from the simulation experiments that the system tracks well when the target state varies less quickly or when the target state varies quickly and the feedback gains are large enough.

7.3 Path Programming Control Strategy of Quantum State Transfer

In this section we study the control field design by the Lyapunov-based method. A transition path programming control strategy is proposed to solve the convergence problem. The average value of an observable is selected as the Lyapunov function. We propose an observable operator construction method that guarantees that the target state is a stable point in the Lyapunov sense. Then the transition path of system states are implemented by two steps: in the first step several intermediate states are selected to program a suitable transition path, and in the second one observable operators are designed according to each intermediate state. In such a way control fields can be designed using the Lyapunov-based method, and the controlled system state would evolve along this transition path and converge to the target state at last.

7.3.1 Control Law Design Based on the Lyapunov Method in the Interaction Picture

The Lyapunov-based control is generally a program control with feedback, so we will restrict our attention in this section to closed finite-level quantum systems with a discrete energy spectrum, such a closed quantum system with n dimensions that can be described by the Liouville equation:

$$i\hbar\dot{\rho} = [H(t), \rho] \quad (7.55a)$$

$$\mathbf{H}(t) = \mathbf{H}_0 + \sum_{j=1} u_j(t) \quad (7.55b)$$

where \mathbf{H}_0 is the free Hamiltonian, which is a Hermite diagonal matrix, \mathbf{H}_j is a control Hamiltonian, u_j is a control field, and ρ is the state density matrix of the system, which is also Hermite. By transforming system Equation 7.55a into the interaction picture, viz. setting $\rho' = e^{i\mathbf{H}_0 t/\hbar} \rho e^{-i\mathbf{H}_0 t/\hbar}$, the Liouville equation of the closed quantum system after transformation can be written as:

$$\dot{\rho}' = \left[\sum_j A_j(t) u_j(t), \rho' \right] \quad (7.56)$$

where $A_j(t) = e^{i\mathbf{H}_0 t/\hbar} \mathbf{H}_j e^{-i\mathbf{H}_0 t/\hbar} / i\hbar$ is the control Hamiltonian in the interaction picture. The interaction transformation maps the system states into rotational coordinates, that is, the local phases of states are rotary. It can be verified that such a transformation does not change the population distribution of the system state. In the next part of this section we will omit the label “’” in Equation 7.56 for convenience.

Define the Lyapunov function as the average value of an observable quantity:

$$V(\rho) = C_{\rho_f} + \text{tr}(\mathbf{P}\rho) \quad (7.57)$$

where \mathbf{P} is the observable operator. It is not necessary for \mathbf{P} to be positive definite here. C_{ρ_f} is a constant used to adjust the value of the Lyapunov function.

It is expected that the target state is stable in the Lyapunov sense, viz. the following three conditions are satisfied:

- (a) The Lyapunov function (Equation 7.57) is positive semi-definite, that is, $V(\rho) = C_{\rho_f} + \text{tr}(\mathbf{P}\rho) \geq 0$.
- (b) The Lyapunov function (Equation 7.57) equals zero only when the system is on the target state, and the system is able to remain on the target state from then on.
- (c) The first-order derivative of the Lyapunov function (Equation 7.57) is negative semi-definite, that is, $\dot{V}(\rho) \leq 0$. According to this condition one has:

$$\dot{V}(\rho) = \sum_j u_j \text{tr}([\rho, \mathbf{P}] A_j) \leq 0 \quad (7.58)$$

The following control law is suggested:

$$u_j(t) = -\kappa_j(t) \text{tr}([\rho(t), \mathbf{P}]A_j(t)), \quad \kappa_j(t) > 0 \quad (7.59)$$

where $\kappa_j(t)$ is the control gain, used to adjust the convergence speed of the system.

One can see from the procedure of control law design that the constant C_{ρ_f} in Equation 7.57 does not play any role. However, it can guarantee that the minimum of the Lyapunov function is zero so that condition (a) is satisfied. In fact, condition (a) can broaden to show that the Lyapunov function is a bounded function, which can be called as energy function: $E(\rho) = \text{tr}(\mathbf{P}\rho)$.

Generally speaking, the Lyapunov-based control method in a quantum system can be regarded as an optimal control obtained by the elimination method, that is, the term $\dot{\rho}$ in $\dot{V}(\rho)$ is eliminated by means of the Liouville equation (Equation 7.56). For a general Lyapunov function, the control law may not be obtained by letting the first derivative of the Lyapunov function equal zero. One can only make the first derivative of the Lyapunov function be negative semidefinite, which is a local optimal solution. In fact, if the performance index in an optimal control is selected as

$$J(\rho, u) = \text{tr}(\mathbf{P}\rho) + \int_0^t \sum_j u_j^2(\tau)/\kappa_j(\tau) d\tau \quad (7.60)$$

then the control law (Equation 7.59) makes $J(\rho, u) = 0$, so it can be seen as an optimal control law with a performance index (Equation 7.60).

The transformation of the interaction picture is used to facilitate the mathematical treatment of the problem. The system after the transformation becomes strictly bilinear, and the drift item (without being multiplied by $u_j(t)$) disappears in the first derivative of the Lyapunov function, consequently greatly reducing the difficulty and complexity of the control design.

7.3.2 Transition Path Programming Control Strategy

To transfer the state of the controlled system from a given initial state to the desired target state, the control law (Equation 7.59) is obtained using the Lyapunov-based method in Section 7.3.1; the observable operator \mathbf{P} can be constructed according to Theorem 7.3 in Section 7.2.2. However, the Lyapunov-based method is a local optimization method and it is just a stable control. The condition for constructing the observable operator \mathbf{P} in Theorem 7.3 can only guarantee that the target state ρ_f is the minimum point of the Lyapunov function, but cannot guarantee that the system will converge, especially for a multi-level quantum system. In this case, there must be something wrong with the Lyapunov-based control. In practice, there are usually two problems. One is that the system state is on a critical stable point of the evolution trajectory. The other is that the controlled state falls into other local extreme points instead of the desired target state.

If the state is on a critical stable point, the control fields will be zero. In such a case, the issue can be resolved by adding a disturbance to the system, which makes the state move away from the critical stable point.

For the second situation, that is, the system state falls into other local extreme points, a transition path programming strategy is proposed here to ensure that the control law designed is convergent. The idea of the strategy is that several intermediate states are selected as transitional

target states which form a transition path together with the initial state and the desired target state. The transition path can naturally be divided into different parts. The evolutions between these states can be determined by the designed control law (Equation 7.59), in which the observable operators should be reconstructed after the system state moves into a new part of the transition path. The selection of these intermediate states must ensure that when the system evolves through one part of the transition path, it will not fall into any other local extreme point except the transitional target one of the parts. In such a way, the system evolves step by step and finally converges to the desired target state.

For example, if there is only one transitional target state ρ_s , then the transition path of system is

$$\rho(0) \rightarrow \rho_s \rightarrow \rho_f \quad (7.61)$$

First, the observable operator $\mathbf{P}^{(1)}$ can be constructed as

$$\mathbf{P}^{(1)} = -\rho_s \quad (7.62)$$

According to Equation 7.59, control field $u^{(1)}$ is designed to transfer the system state $\rho(0)$ to ρ_s .

Then the observable operator $\mathbf{P}^{(2)}$ can be constructed as

$$\mathbf{P}^{(2)} = -\rho_f \quad (7.63)$$

and the design control law is $u^{(2)}$ again. In such a way, the system state can be transferred to the desired target state ρ_f eventually by the two successive control fields.

In the transition path programming strategy, selection of the intermediate states is the key point. To ensure the system does not fall into other local extreme points apart from the transitional target state, the selection of intermediate states is of course not optional. Here we introduce Lie group decomposition technology to complete the task of selecting those states. In Lie group decomposition technology, the control pulses, which are resonant with different energy-level transitions, are acted on the quantum system in sequence so the state transition matrix can be decomposed into a sequence of transitions caused by a single control pulse. The state transition matrix $\mathbf{T}(t)$ is defined by the initial state and the desired state:

$$\rho(t) = \mathbf{T}(t)\rho_0\mathbf{T}^\dagger(t) \quad (7.64)$$

The state transition matrix satisfies the Schrodinger equation:

$$\dot{\mathbf{T}}(t) = \left(\sum_j u_j(t) \mathbf{A}_j(t) \right) \mathbf{T}(t) \quad (7.65)$$

Defining the unitary operator Ω_l as the transition factor of the l th control pulse with corresponding control Hamiltonian $\hbar\mathbf{h}_{js}$, then according to Assumption 7.4 Ω_l has the following form:

$$\Omega_l = a|j\rangle\langle j| + b|j\rangle\langle s| + c|s\rangle\langle j| + d|s\rangle\langle s| + \sum_{k\neq j,s} |k\rangle\langle k| \quad (7.66)$$

where a , b , c , and d are complex numbers. Now suppose the state transition matrix T of the desired target state has the following decomposition:

$$\mathbf{T} = \Omega_k \Omega_{k-1} \dots \Omega_1 \quad (7.67)$$

Then the intermediate states can be chosen as

$$\rho_k = \Omega_k \rho_{k-1} \Omega_k^+ \quad (7.68)$$

We will now explain how to obtain Ω_k and ρ_k . Because of the unitarity of quantum system evolution, the state transition matrix is unitary. Equation 7.67 can be rewritten as

$$\mathbf{I} = \Omega_k \Omega_{k-1} \dots \Omega_1 \mathbf{T}^+ \quad (7.69)$$

Equation 7.67 is a procedure of $\mathbf{I} \rightarrow \mathbf{T}$ and can be translated to Equation 7.69, viz. the procedure of $\mathbf{T}^+ \rightarrow \mathbf{I}$, from which each transition factor Ω_j can be derived. A four-level system will be taken into account next as an example to illustrate the procedure for obtaining the intermediate states in detail.

Suppose the system is a ladder level system, viz. only transitions between level 1 and 2, 2 and 3, and 3 and 4 are allowed. The energy level differences are distinct so the control pulses can take effect in sequence. Thus the three types of transition factor can be described as

$$\Omega_{12} = \begin{pmatrix} a_1 & b_1 & 0 & 0 \\ c_1 & d_1 & 0 & 0 \\ 0 & 0 & 1 & 0 \\ 0 & 0 & 0 & 1 \end{pmatrix}, \Omega_{23} = \begin{pmatrix} 1 & 0 & 0 & 0 \\ 0 & a_2 & b_2 & 0 \\ 0 & c_2 & d_2 & 0 \\ 0 & 0 & 0 & 1 \end{pmatrix}, \Omega_{34} = \begin{pmatrix} 1 & 0 & 0 & 0 \\ 0 & 1 & 0 & 0 \\ 0 & 0 & a_3 & b_3 \\ 0 & 0 & c_3 & d_3 \end{pmatrix} \quad (7.70)$$

The state transition matrix of the desired state is:

$$T^+ = \begin{pmatrix} a_{11} & a_{12} & a_{13} & a_{14} \\ a_{21} & a_{22} & a_{23} & a_{24} \\ a_{31} & a_{32} & a_{33} & a_{34} \\ a_{41} & a_{42} & a_{43} & a_{44} \end{pmatrix} \quad (7.71)$$

First, one can select the factor Ω_{12} and make the element a_{14} in Equation 7.71 zero, viz. the fourth column of T^+ becomes $(0 \ a'_{24} \ a_{34} \ a_{44})^T$. Second, select the factor Ω_{23} and make a'_{24} zero, which makes the fourth column of the state transition matrix become $(0 \ 0 \ a'_{34} \ a_{44})^T$. Third, the fourth column of the state transition matrix becomes $(0 \ 0 \ 0 \ 1)^T$ by operating the factor Ω_{34} . Then the state transition matrix T^+ becomes T'^+ . Because $T T'^+ T' = \mathbf{I}$, one can verify that the fourth row of T'^+ is $(0 \ 0 \ 0 \ 1)$, that is, the state transition matrix becomes

$$\Omega_{34} \Omega_{23} \Omega_{12} T^+ = T'^+ = \begin{pmatrix} b_{11} & b_{12} & b_{13} & 0 \\ b_{21} & b_{22} & b_{23} & 0 \\ b_{31} & b_{32} & b_{33} & 0 \\ 0 & 0 & 0 & 1 \end{pmatrix} \quad (7.72a)$$

The elements of factor Ω_{js} used in Equation 7.72a can be calculated according to operations of the above three steps, for example one calculates Ω_{12} in the first step. Suppose $a_{14} \neq 0$, according to $\begin{pmatrix} a_1 & b_1 \\ c_1 & d_1 \end{pmatrix} \begin{pmatrix} a_{14} \\ a_{24} \end{pmatrix} = \begin{pmatrix} 0 \\ a'_{24} \end{pmatrix}$ and $\begin{pmatrix} a_1 & b_1 \\ c_1 & d_1 \end{pmatrix} \begin{pmatrix} a_1^* & c_1^* \\ b_1^* & d_1^* \end{pmatrix} = \mathbf{I}$. It can be calculated that $|b_1|^2 = |c_1|^2 = 1/(1 + |a_{24}/a_{14}|^2)$, $a_1 = -b_1 a_{24}/a_{14}$, and $d_1 = c_1 a_{24}^*/a_{14}^*$. The phase of b_1 and c_1 can be selected freely because it only affects the phases of the non-diagonal elements of the intermediate states, which have no means when using the control law (Equation 7.59). In such a way, one can calculate each element of Ω_{12} , Ω_{23} , and Ω_{34} , respectively.

For the state transition matrix T'^+ in Equation 7.72a, one can define new factors Ω'_{12} and Ω'_{23} , and operate them on T'^+ , which makes the state transition matrix become

$$\Omega'_{23}\Omega'_{12}\Omega_{34}\Omega_{23}\Omega_{12}T^+ = \begin{pmatrix} c_{11} & c_{12} & 0 & 0 \\ c_{21} & c_{22} & 0 & 0 \\ 0 & 0 & 1 & 0 \\ 0 & 0 & 0 & 1 \end{pmatrix} \quad (7.72b)$$

In a similar way, one can calculate each element of Ω'_{12} and Ω'_{23} , respectively.

Fianlly, after the factor Ω''_{12} has acted, one has:

$$\Omega'_{12}\Omega'_{23}\Omega'_{12}\Omega_{34}\Omega_{23}\Omega_{12}T^+ = \mathbf{I} \quad (7.72c)$$

Then the intermediate target state can be obtained according to Equation 7.68.

According to the above derivation and discussion, it can be seen if all energy levels can be connected by transitions, such as the example of a ladder level system, any state transition matrix can be decomposed into the form of Equation 7.67.

Theorem 7.6 Under Assumptions 7.3 and 7.4, if all energy levels of the controlled system are connected by transitions, then any state transition matrix T of the system can be decomposed into a sequence of transition factors, viz. it can be written as Equation 7.67, $T = \Omega_k\Omega_{k-1} \dots \Omega_1$, where Ω_l is the transition factor.

When the state transition matrix T is decomposed into a sequence of transition factors, and intermediate states ρ_k are determined, the evolution between ρ_{k-1} and ρ_k can be achieved by acting on the k th pulse, which means a control $u_l(t)$ corresponding to the k th pulse will minimize the Lyapunov function $V_{\rho_k}(\mathbf{a})$. Here $V_{\rho_k}(\mathbf{a})$ is the Lyapunov function with observable operator \mathbf{P} constructed by ρ_k . If $u_l(t)$ corresponds to the control Hamiltonian $\hbar\mathbf{h}_{js}$, then any state ρ on the path ρ_{k-1} through ρ_k satisfies

$$\rho = \mathbf{U}_{js}\rho_k\mathbf{U}_{js}^\dagger \quad (7.73a)$$

where \mathbf{U}_{js} has the same form with Ω_{js} , viz.:

$$\mathbf{U}_{js} = \gamma_1|j\rangle\langle j| + \gamma_2|j\rangle\langle s| + \gamma_3|s\rangle\langle j| + \gamma_4|s\rangle\langle s| + \sum_{k\neq j,s} |k\rangle\langle k| \quad (7.73b)$$

So when we use the control laws (Equation 7.59) to design the control field to steer the system from ρ_{k-1} to ρ_k , it is necessary to ensure that only $u_l(t)$ is not zero, that is, to ensure the following equation is satisfied:

$$\begin{aligned} \text{tr}([\rho, \mathbf{p}_k]A_{q\neq l}(t)) &= \text{tr}([\mathbf{U}_{js}\rho_k\mathbf{U}_{js}^\dagger, \mathbf{p}_k]A_{q\neq l}(t)) \\ &= 0 \end{aligned} \quad (7.74)$$

In this condition, all controls $u_{j\neq l}(t)$ do not exist, and they will not change the value of the Lyapunov function $V_{\rho_k}(\rho)$, so the system will converge to ρ_k . However, Equation 7.74 cannot be always satisfied unless the following condition is satisfied:

$$(\mathbf{p}_k)_{pq} = 0, \{pq|p \neq j, s q = j, s \text{ or } p = j, s q \neq j, s\} \quad (7.75)$$

In order to satisfy Equation 7.75 (if it is not satisfied), one can let those elements of ρ_k be zero and denote the new matrix $\tilde{\rho}_k$. Correspondingly, we can modify ρ_{k-1} to get $\tilde{\rho}_{k-1}$. Then we can use $\tilde{\rho}_{k-1}$ and $\tilde{\rho}_k$ as the transitional initial and target states to design $u_l(t)$. Such control $u_l(t)$ of course also steers ρ_{k-1} to ρ_k .

To illustrate the process, now suppose we have the decomposition (Equation 7.72c) and intermediate states (Equation 7.68). The transition from the initial state ρ_0 to transitional target state ρ_1 is achieved by Ω_{12} , as described in Equation 7.70. Then $\tilde{\rho}_0$ and $\tilde{\rho}_1^{(1)}$ are as follows:

$$\tilde{\rho}_0 = \begin{pmatrix} (\rho_0)_{1,1} & (\rho_0)_{1,2} & 0 & 0 \\ (\rho_0)_{2,1} & (\rho_0)_{2,2} & 0 & 0 \\ 0 & 0 & (\rho_0)_{3,3} & (\rho_0)_{3,4} \\ 0 & 0 & (\rho_0)_{4,3} & (\rho_0)_{4,4} \end{pmatrix}, \tilde{\rho}_1^{(1)} = \begin{pmatrix} (\rho_1)_{1,1} & (\rho_1)_{1,2} & 0 & 0 \\ (\rho_1)_{2,1} & (\rho_1)_{2,2} & 0 & 0 \\ 0 & 0 & (\rho_1)_{3,3} & (\rho_1)_{3,4} \\ 0 & 0 & (\rho_1)_{4,3} & (\rho_1)_{4,4} \end{pmatrix} \quad (7.76a)$$

The observable operator $\mathbf{P}^{(1)} = -\tilde{\rho}_1^{(1)}$ and the first control field is designed according to Equation 7.59. Next, ρ_1 is transferred by Ω_{23} to ρ_2 , and the corresponding $\tilde{\rho}_1^{(2)}$ and $\tilde{\rho}_2^{(1)}$ can be written as

$$\tilde{\rho}_1^{(2)} = \begin{pmatrix} (\rho_1)_{1,1} & 0 & 0 & (\rho_1)_{1,4} \\ 0 & (\rho_1)_{2,2} & (\rho_1)_{2,3} & 0 \\ 0 & (\rho_1)_{3,2} & (\rho_1)_{3,3} & 0 \\ (\rho_1)_{4,1} & 0 & 0 & (\rho_1)_{4,4} \end{pmatrix}, \tilde{\rho}_2^{(1)} = \begin{pmatrix} (\rho_2)_{1,1} & 0 & 0 & (\rho_2)_{1,4} \\ 0 & (\rho_2)_{2,2} & (\rho_2)_{2,3} & 0 \\ 0 & (\rho_2)_{3,2} & (\rho_2)_{3,3} & 0 \\ (\rho_2)_{4,1} & 0 & 0 & (\rho_2)_{4,4} \end{pmatrix} \quad (7.76b)$$

The observable operator $\mathbf{P}^{(2)} = -\tilde{\rho}_2^{(1)}$ and the second control field can be designed. Similar processes can be done until the last control field is designed.

Theorem 7.7 Suppose the state transition matrix T of the desired target state can be decomposed into a sequence of state transition factors as Equation 7.67, and the corresponding intermediate state ρ_k satisfies Equation 7.68, which divides the transition path into different parts. Then the evolution through these parts can be achieved by the control law (Equation 7.59), in which the observable operator \mathbf{P} is constructed using a corresponding transitional target state $\tilde{\rho}_k^{(1)}$ described by Equation 7.76.

Theorems 7.6 and 7.7 together guarantee the convergence of the transition path programming strategy.

7.3.3 Numerical Simulations and Results Analyses

In this subsection, a four-level system will be used to illustrate the effectiveness of the control strategy proposed. The free Hamiltonian of the controlled system is

$$H_0 = \sum_{j=1}^n E_j |j\rangle\langle j| \quad (7.77)$$

where $E_1 = 0.4948$, $E_2 = 1.4529$, $E_3 = 2.3691$, and $E_4 = 3.2434$. Thus the free Hamiltonian of the system becomes $\mathbf{H}_0 = \text{diag}(0.4948, 1.4529, 2.3691, 3.2434)$, where $\text{diag}(\cdot)$ denotes a diagonal matrix. The energy level differences are $\Delta_{12} = E_2 - E_1 = 0.9581$, $\Delta_{23} = 0.9162$, and $\Delta_{34} = 0.8743$. Our goal is to reverse the probability of the initial system

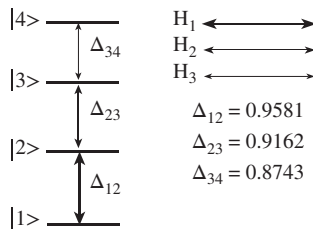


Figure 7.8 Energy structure of a ladder level system and its relationship with the control Hamiltonians

state $\rho_0 = \text{diag}(0.3850, 0.2758, 0.1976, 0.1416)$, namely to transfer the system from the initial state ρ_0 to the target state $\rho_f = \text{diag}(0.1416, 0.1976, 0.2758, 0.3850)$.

For convenience a ladder level system as discussed above is considered, which permits transitions between level 1 and level 2, level 2 and level 3, and level 3 and level 4. The energy structure of a ladder level system and its relationship with the control Hamiltonians are shown in Figure 7.8.

There are three control Hamiltonians under the controllable situation described:

$$\mathbf{H}_1 = \begin{pmatrix} 0 & 1 & 0 & 0 \\ 1 & 0 & 0 & 0 \\ 0 & 0 & 0 & 0 \\ 0 & 0 & 0 & 0 \end{pmatrix}, \mathbf{H}_2 = \begin{pmatrix} 0 & 0 & 0 & 0 \\ 0 & 0 & 1 & 0 \\ 0 & 1 & 0 & 0 \\ 0 & 0 & 0 & 0 \end{pmatrix}, \mathbf{H}_3 = \begin{pmatrix} 0 & 0 & 0 & 0 \\ 0 & 0 & 0 & 0 \\ 0 & 0 & 0 & 1 \\ 0 & 0 & 1 & 0 \end{pmatrix} \quad (7.78)$$

First of all, according to Equation 7.78, we design a control law under the condition in Theorem 7.3 and the control system simulation experiments are implemented. In the simulation experiments, the evolution is discrete, namely, the time scale is divided into numerous intervals, each interval so short that the Hamiltonian in it is regarded as unchanged. Then the evolution of the system can be obtained by iteration. In order to avoid the accumulative errors, we choose the following formula rather than iteration for Equation 7.56:

$$\rho(t + \Delta t) = e^{i \sum_j A_j(t) u_j(t) \Delta t} \rho(t) e^{-i \sum_j A_j(t) u_j(t) \Delta t} \quad (7.79)$$

which has $\text{tr}(\rho^2(t + \Delta t)) = \text{tr}(\rho^2(t))$ and guarantees unitarity during the evolution. The control field is Equation 7.59: $u_j(t) = -\kappa_j(t) \text{tr}([\rho(t), \mathbf{P}] A_j(t))$, in which $\kappa_1 = \kappa_2 = \kappa_3 = 20$. Figure 7.9 shows the experimental results with three control fields, in which Figure 7.9a is the probability of the system state and Figure 7.9b is the control fields applied.

From Figure 7.9 one can see that the system state applied by the control law designed after 150 a.u. of time is

$$\rho_s = \begin{pmatrix} 0.1514 & 0 & -0.0254 + 0.019i & 0.0178 + 0.0079i \\ 0 & 0.2063 & 0 & -0.0238 + 0.0321i \\ -0.0254 - 0.019i & 0 & 0.2679 & 0 \\ 0.0178 - 0.0079i & -0.0238 - 0.0321i & 0 & 0.3744 \end{pmatrix} \quad (7.80)$$

From Equation 7.80 one can see that the system controlled cannot reach the desired target state ρ_f .

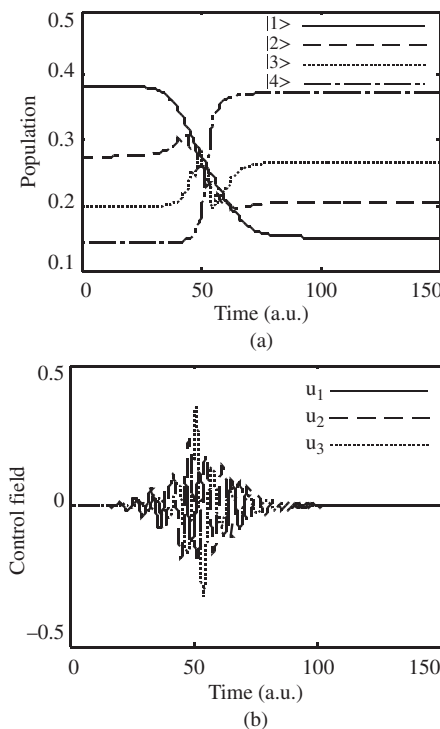


Figure 7.9 Experimental results with three control fields: (a) the probability of the system state and (b) the control fields applied

The transition path programming method proposed is applied to the controlled system. The state transition matrix is:

$$\mathbf{T} = \begin{pmatrix} 0 & 0 & 0 & 1 \\ 0 & 0 & 1 & 0 \\ 0 & 1 & 0 & 0 \\ 1 & 0 & 0 & 0 \end{pmatrix} \quad (7.81)$$

According to Equation 7.72, the transition factors can be calculated as:

$$\Omega_{12} = \Omega'_{12} = \Omega'_{12} = \begin{pmatrix} 0 & 1 & 0 & 0 \\ 1 & 0 & 0 & 0 \\ 0 & 0 & 1 & 0 \\ 0 & 0 & 0 & 1 \end{pmatrix} \quad (7.82a)$$

$$\Omega_{23} = \Omega'_{23} = \begin{pmatrix} 1 & 0 & 0 & 0 \\ 0 & 0 & 1 & 0 \\ 0 & 1 & 0 & 0 \\ 0 & 0 & 0 & 1 \end{pmatrix} \quad (7.82b)$$

$$\Omega_{34} = \begin{pmatrix} 1 & 0 & 0 & 0 \\ 0 & 1 & 0 & 0 \\ 0 & 0 & 0 & 1 \\ 0 & 0 & 1 & 0 \end{pmatrix} \quad (7.82c)$$

According to Equation 7.68, the transitional states are chosen, respectively, as:

$$\rho_1 = \text{diag}(0.2758, 0.3850, 0.1976, 0.1416) \quad (7.83a)$$

$$\rho_2 = \text{diag}(0.2758, 0.1976, 0.3850, 0.1416) \quad (7.83b)$$

$$\rho_3 = \text{diag}(0.2758, 0.1976, 0.1416, 0.3850) \quad (7.83c)$$

$$\rho_4 = \text{diag}(0.1976, 0.2758, 0.1416, 0.3850) \quad (7.83d)$$

$$\rho_5 = \text{diag}(0.1976, 0.1416, 0.2758, 0.3850) \quad (7.83e)$$

which means that the evolution path of the system state is

$$\rho_0 \rightarrow \rho_1 \rightarrow \rho_2 \rightarrow \rho_3 \rightarrow \rho_4 \rightarrow \rho_5 \rightarrow \rho_f \quad (7.84)$$

Because the states in Equation 7.83a–e satisfy Equation 7.74, $\tilde{\rho}_k = \rho_k$. Observable operators and control fields can be directly designed. The experimental results with path programming are shown in Figure 7.10, in which Figure 7.10a is the probability of system state with path programming and Figure 7.10b is the corresponding control fields. From Figure 7.10 one can see that the system state achieves the desired target state ρ_f after 700 a.u. of time, while Figure 7.9

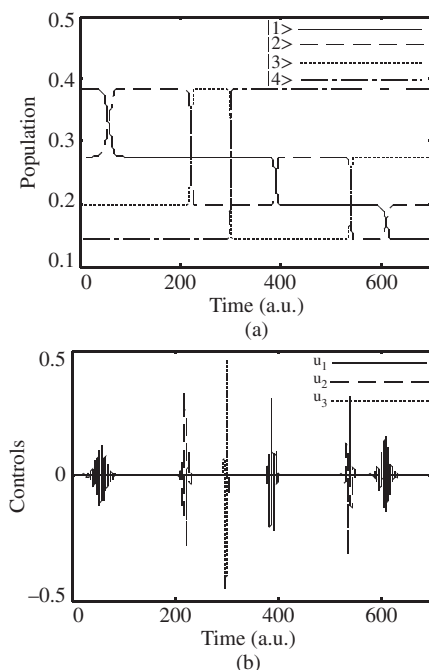


Figure 7.10 Experimental results with path programming: (a) the probability of the system state with path programming and (b) the corresponding control fields

shows that the direct transfer from the initial state to the desired target state cannot be realized by using three control fields. The path programming proposed demonstrates the significant effectiveness. The suitable selection of transitional states and the design of corresponding transition factors are two key points in this control strategy.

Figure 7.10 also shows that there is a sequence of six control fields, which act as π pulse sequences, reversing the probability of state and making the system evolve to the desired target state eventually. In addition, it is shown in Figures 7.9 and 7.10 that each control field corresponds to a distinct oscillating frequency, and each oscillating frequency of the control field is equal to the energy level difference between the energy levels corresponding to the control Hamiltonian, for example the oscillating frequency of the control field u_1 is just the energy level difference between level 1 and level 2, which is $\Delta_{12} = 0.9581$. This means that the single-frequency electromagnetic field can be used to choose the probability transferring between specific levels, just as the π pulse control does.

References

- D'Alessandro, D. (2007) *Introduction to Quantum Control and Dynamics*, Taylor & Francis Group, LLC, Boca Raton, FL.
- Kuang, S. and Cong, S. (2008) Lyapunov control methods of closed quantum systems. *Automatica*, **44**(1), 98–108.
- Turinici, G. and Rabitz, H. (2001) Quantum wavefunction controllability. *Chemical Physics*, **267**(1-3), 1–9.
- Wang, X. and Schirmer, S. (2010a) Analysis of Lyapunov method for control of quantum states. *IEEE Transactions on Automatic Control*, **55**(10), 2259–2270.
- Wang, X. and Schirmer, S. (2010b) Analysis of effectiveness of lyapunov control for non-generic quantum states. *IEEE Transactions on Automation Control*, **55**(6), 1406–1411.

8

Control Theory and Methods in Degenerate Cases

8.1 Implicit Lyapunov Control of Multi-Control Hamiltonian Systems Based on State Error

In the last 30 years, the control theory of quantum systems has developed rapidly and it has been widely used in quantum chemistry, nanotechnology, quantum information, and quantum physics. Many quantum methods exist, such as quantum optimal control, adiabatic control, Lyapunov-based control, and optimal Lyapunov-based quantum control. The design idea of the Lyapunov-based control is based on the Lyapunov stability theorem, that is, the control laws are designed by means of ensuring that the first-order time derivative of a selected Lyapunov function is not positive. The control system based on the Lyapunov stability theorem is at least stable. However, the probability control in the quantum system requires a convergent control strategy because a stable quantum control method may mean that the control system cannot reach the desired target state. To make the control system converge to the target state, it is therefore necessary to study the convergence of the control system, which is one of the research focuses of the Lyapunov-based control method.

Existing research results have indicated that for the Schrödinger equation, when the target state is an eigenstate, by using the Lyapunov control method based on the state distance or the state error (Kuang and Cong, 2008; Mirrahimi *et al.*, 2005a) the control system can be asymptotically stabilized if two conditions are satisfied: (i) the control system is strongly regular and (ii) all other eigenstates, which are different from the target state, are directly coupled to the target state. Condition (i) means that all the differences of the two energy levels are not mutually equal, that is, the spectrum of the internal Hamiltonian is non-degenerate. Using the Lyapunov method based on the average value of an imaginary mechanical quantity, two conditions which make the control system asymptotically stable are: (i) the internal Hamiltonian is strongly regular and (ii) all the eigenstates different from the target state are directly coupled to the target state (Cong and Kuang, 2007; Grivopoulos and Bamieh, 2003). If the control system satisfies these two convergence conditions, it is called a non-degenerate case. In fact many real systems do not satisfy these conditions. These cases are called degenerate cases. In order to solve the convergence problems of degenerate cases, several researchers have introduced an implicit

function to make the single control Hamiltonian quantum system converge to an eigenstate from any pure state (Beaucharda *et al.*, 2007; Zhao *et al.*, 2009, 2012). In the multi-control Hamiltonians system, when the target state is an eigenstate, one can control the design laws by introducing a series of perturbations which are implicit functions and choosing an implicit Lyapunov function based on the state distance.

So far, for the Schrodinger equation in the degenerate cases, the existing Lyapunov control methods can only make the control system converge to an eigenstate from any pure state. Where the target state is a superposition state, the convergence problem of the control system has not been resolved.

This section has two main purposes. First, for the Schrödinger equation, in degenerate cases and the case where the target state is an arbitrary pure state, by using an implicit Lyapunov quantum control method based on the state error we will solve the convergence problem of the multi-control Hamiltonians system. Thus, in degenerate cases, the control system can completely transfer between two arbitrary pure states. Our basic idea is as follows: in order to solve the convergence problem of degenerate cases for the multi-control Hamiltonians system, we introduce a series of implicit function perturbations and select a state error-based Lyapunov function that is also an implicit function. This method is not a simple extension from the single-control Hamiltonian case (Zhao *et al.*, 2012) to the multi-control Hamiltonians case. For the multi-control Hamiltonians case, the derivation process of the control laws and the convergence proof will become more complex, especially in the calculation of the first-order time derivative of the Lyapunov function. On the other hand, to make the control system also converge to a superposition state; we introduce a series of constant disturbances. The second purpose of this section is to analyze the relationship between the implicit Lyapunov functions based on the state distance and the state error, and compare the control effects of these two implicit Lyapunov control methods.

8.1.1 Control Design

A N -level closed quantum system with multi-control Hamiltonians can be modeled as the following bilinear Schrödinger equation:

$$i|\dot{\psi}(t)\rangle = \left(H_0 + \sum_{k=1}^r H_k u_k(t) + \omega I \right) |\psi(t)\rangle \quad (8.1)$$

where $|\psi(t)\rangle$ is the state vector, H_0 is the internal Hamiltonian, H_k ($k = 1, \dots, r$) are the control Hamiltonians, $u_k(t)$ are scalar and real control laws, and ω is the global phase control law.

For the Schrodinger equation, in degenerate cases, the existing Lyapunov control methods can only make the control system converge to an eigenstate from any pure state. To allow the control system to also converge to the target superposition state $|\psi_f\rangle$, we introduce a series of constant disturbances η_k . The dynamic (Equation 8.1) will become

$$i|\dot{\psi}(t)\rangle = \left(H_0 + \sum_{k=1}^r H_k (v_k(t) + \eta_k) + \omega I \right) |\psi(t)\rangle \quad (8.2)$$

where $v_k(t)$ and η_k are the control laws which need to be designed. Our basic idea is that we add η_k to make the target state $|\psi_f\rangle$ an eigenstate of $H_0 + \sum_{k=1}^r H_k \eta_k$, that is,

$$\left(H_0 + \sum_{k=1}^r H_k \eta_k \right) |\psi_f\rangle = \lambda'_f |\psi_f\rangle \quad (8.3)$$

where λ'_f is the eigenvalue of $H'_0 = H_0 + \sum_{k=1}^r H_k \eta_k$ corresponding to the target state $|\psi_f\rangle$. We can view H'_0 as the new internal Hamiltonian of the control system.

In degenerate cases, to solve the convergence problem of the control system we introduce perturbations $\gamma_k(t)$, which are implicit functions in the control laws $u_k(t)$ ($k = 1, \dots, r$) of Equation 8.1. The dynamic Equation 8.2 will become

$$i|\dot{\psi}(t)\rangle = \left(H_0 + \sum_{k=1}^r H_k (\gamma_k(t) + v_k(t) + \eta_k) + \omega I \right) |\psi(t)\rangle \quad (8.4)$$

where $\gamma_k(t) + v_k(t) + \eta_k = u_k$ and ω are the total control laws.

The basic idea is as follows: denote the system with the internal Hamiltonian H_0 , the control Hamiltonians H_k ($k = 1, \dots, r$) and the control laws $\gamma_k(t) + v_k(t) + \eta_k = u_k$ as system 1, the system with the internal Hamiltonian $H'_0 = H_0 + \sum_{k=1}^r H_k \eta_k$, the control Hamiltonians H_k ($k = 1, \dots, r$) and the control laws $\gamma_k(t) + v_k(t)$ as system 2, and the system with the internal Hamiltonian $H_{03} = H_0 + \sum_{k=1}^r H_k (\gamma_k(t) + \eta_k)$, the control Hamiltonians H_k ($k = 1, \dots, r$) and the control laws $v_k(t)$ as system 3. These three systems can be depicted by Equation 8.4. Denote the eigenvalues and eigenstates of H'_0 as $\lambda'_1, \lambda'_2, \dots, \lambda'_N$ and $|\phi'_1\rangle, |\phi'_2\rangle, \dots, |\phi'_N\rangle$, respectively. Denote the eigenvalues and eigenstates of H_{03} as $\lambda'_{1,\gamma_1, \dots, \gamma_r}, \dots, \lambda'_{N,\gamma_1, \dots, \gamma_r}$, and $|\phi'_{1,\gamma_1, \dots, \gamma_r}\rangle, \dots, |\phi'_{N,\gamma_1, \dots, \gamma_r}\rangle$, respectively, which are functions of the perturbations $\gamma_k(t)$. Without loss of generality, assume $|\psi_g\rangle = |\phi_g\rangle$, $1 \leq g \leq N$. Denote $|\psi'_{f,\gamma_1, \dots, \gamma_r}\rangle = |\phi'_{g,\gamma_1, \dots, \gamma_r}\rangle$. If one can design the perturbations $\gamma_k(t)$ such that (i) $\omega'_{l,m,\gamma_1, \dots, \gamma_r} \neq \omega'_{i,j,\gamma_1, \dots, \gamma_r}$, $(l, m) \neq (i, j)$, $i, j, l, m \in \{1, 2, \dots, N\}$, where $\omega'_{l,m,\gamma_1, \dots, \gamma_r} = \lambda'_{l,\gamma_1, \dots, \gamma_r} - \lambda'_{m,\gamma_1, \dots, \gamma_r}$ holds and (ii) for any $|\phi'_{i,\gamma_1, \dots, \gamma_r}\rangle \neq |\psi'_{f,\gamma_1, \dots, \gamma_r}\rangle$ ($i = 1, 2, \dots, N$), there exists at least a $k \in \{1, \dots, r\}$ satisfying $\langle \phi'_{i,\gamma_1, \dots, \gamma_r} | H_k | \psi'_{f,\gamma_1, \dots, \gamma_r} \rangle \neq 0$ ($k = 1, \dots, r$), and select the specific Lyapunov function based on the state error as

$$V(|\psi\rangle) = \frac{1}{2} \langle \psi - \psi'_{f,\gamma_1, \dots, \gamma_r} | \psi - \psi'_{f,\gamma_1, \dots, \gamma_r} \rangle \quad (8.5)$$

then system 3 will converge to $|\psi'_{f,\gamma_1, \dots, \gamma_r}\rangle$. When system 3 converges to $|\psi'_{f,\gamma_1, \dots, \gamma_r}\rangle$, if the perturbations $\gamma_k(t)$ at $|\psi'_{f,\gamma_1, \dots, \gamma_r}\rangle$ are designed to equal zero, then system 3 will become system 2, and $|\psi'_{f,\gamma_1, \dots, \gamma_r}\rangle$ will become $|\psi_f\rangle$. Because the convergence of system 2 to $|\psi_f\rangle$ is equivalent to that of system 1 to $|\psi_f\rangle$, the convergence of system 1 to $|\psi_f\rangle$ will be ensured. In fact, the evolution of system 1 can be viewed as a composite of two evolution processes. One is system 3 converging to $|\psi'_{f,\gamma_1, \dots, \gamma_r}\rangle$ from the initial state $|\psi_0\rangle$, another is $\gamma_k(t)$ converging to 0. To make

the introduced perturbations take effect to make system 1 in the non-degenerate case converge to $|\psi_f\rangle$, the speed of $\gamma_k(t)$ ($k = 1, \dots, r$) converging to 0 must be slower than the speed at which system 3 converges toward $|\psi'_{f,\gamma_1, \dots, \gamma_r}\rangle$. For convenience, the control system in the following sections means system 1.

From the above analyses, we can design $\gamma_k(t)$ to be a monotonically increasing function on $V(t)$ as

$$\gamma_k(|\psi\rangle) = \theta_k(V(|\psi\rangle)) = \theta_k\left(\frac{1}{2}\left\langle\psi - \psi'_{f,\gamma_1, \dots, \gamma_r}|\psi - \psi'_{f,\gamma_1, \dots, \gamma_r}\right\rangle\right) \quad (k = 1, \dots, r) \quad (8.6)$$

where functions $\theta_k(\cdot)$ satisfy $\theta_k(0) = 0$, $\theta_k(s) > 0$, $\theta'_k(s) > 0$ for every $s > 0$, and s is the independent variable of the function $\theta_k(\cdot)$. From Equations 8.5 and 8.6, one can see that when we introduce implicit function perturbations in the control laws to solve the convergence problems of the degenerate cases, the selected Lyapunov function should be a implicit function of the time t . The existence of these implicit function perturbations $\gamma_k(|\psi\rangle)$ in Equation 8.6 can be depicted by Lemma 8.1.

Lemma 8.1 Let $\theta_k \in C^\infty(R^+; [0, \gamma_k^*]), k = 1, \dots, r, \gamma_k^* > 0$ satisfy $\theta_k(0) = 0$, $\theta_k(s) > 0$, and $\theta'_k(s) > 0$ for every $s > 0$, $\|\theta'_k\|_\infty < 1/rC^*$, and $C^* = 1 + C: C = \max\{\|(\partial|\psi'_{f,\gamma_1, \dots, \gamma_r}\rangle/\partial\gamma_k)|_{(\gamma_{10}, \dots, \gamma_{r0})}\|_\infty; \gamma_{k0} \in [0, \gamma_k^*]\}$, $\gamma_{k0} = \gamma_k(0)$. Then for every state $|\psi\rangle \in S^{2N-1} = \{x \in C^N; \|x\| = 1\}$, there exists a unique $\gamma_1, \gamma_2, \dots$, and γ_r with $\gamma_k \in C^\infty(\gamma_k \in [0, \gamma_k^*]) (k = 1, \dots, r)$ satisfying $\gamma_k(|\psi\rangle) = \theta_k\left(\frac{1}{2}\left\langle\psi - \psi'_{f,\gamma_1, \dots, \gamma_r}|\psi - \psi'_{f,\gamma_1, \dots, \gamma_r}\right\rangle\right)$.

According to the implicit theorem (Krantz and Parks, 2002), Lemma 8.1 can be proved.

Next, on the basis of the Lyapunov stability theorem let us design the control laws $v_k(t)$ and ω . The basic idea is that we design control laws to make the time derivative of the selected Lyapunov function be less than or equal to 0, that is, $\dot{V}(t) \leq 0$. Denote the eigenvalue of $H_{03} = H_0 + \sum_{k=1}^r H_k(\gamma_k(t) + \eta_k)$ corresponding to $|\psi'_{f,\gamma_1, \dots, \gamma_r}\rangle$ as $\lambda'_{f,\gamma_1, \dots, \gamma_r}$. By Equations 8.4 and 8.5, the time derivative of the selected Lyapunov function defined by Equation 8.5 is

$$\begin{aligned} \dot{V} = & -\sum_{k=1}^r \Re(\langle(\partial|\psi'_{f,\gamma_1, \dots, \gamma_r}\rangle/\partial\gamma_k)|\psi\rangle)\dot{\gamma}_k(t) - (\lambda'_{f,\gamma_1, \dots, \gamma_r} + \omega) \\ & \times \Im(\langle|\psi'_{f,\gamma_1, \dots, \gamma_r}\rangle|\psi\rangle) - \sum_{k=1}^r \Im(\langle|\psi'_{f,\gamma_1, \dots, \gamma_r}\rangle|H_k|\psi\rangle)v_k(t) \end{aligned} \quad (8.7)$$

Equation 8.7 contains the time derivative of the implicit function perturbation $\dot{\gamma}$, which needs to be eliminated. From Equation 8.6 one can deduce

$$\begin{aligned} \dot{\gamma}_j(t) = & -\theta'_j\left(\sum_{k=1}^r \Re\left(\left\langle\left(\partial|\psi'_{f,\gamma_1, \dots, \gamma_r}\rangle/\partial\gamma_k\right)|\psi\right\rangle\right)\dot{\gamma}_k(t) + (\lambda'_{f,\gamma_1, \dots, \gamma_r} + \omega)\Im(\langle|\psi'_{f,\gamma_1, \dots, \gamma_r}\rangle|\psi\rangle)\right. \\ & \left. + \sum_{k=1}^r \Im\left(\left\langle\psi'_{f,\gamma_1, \dots, \gamma_r}\right|H_k|\psi\rangle\right)v_k(t)\right) \end{aligned} \quad (8.8)$$

Summing each item on both sides of Equation 8.8 gives

$$\begin{aligned} \sum_{j=1}^r \dot{\gamma}_j(t) = & - \sum_{j=1}^r \theta'_j \left(\sum_{k=1}^r \Re \left(\left\langle \left(\partial |\psi'_{f,\gamma_1, \dots, \gamma_r}\rangle / \partial \gamma_k \right) |\psi\rangle \right) \dot{\gamma}_k(t) \right. \\ & \left. + (\lambda'_{f,\gamma_1, \dots, \gamma_r} + \omega) \Im(\langle \psi'_{f,\gamma_1, \dots, \gamma_r} | \psi \rangle) + \sum_{k=1}^r \Im \left(\langle \psi'_{f,\gamma_1, \dots, \gamma_r} | H_k | \psi \rangle \right) v_k(t) \right) \end{aligned} \quad (8.9)$$

Assuming $\partial |\psi'_{f,\gamma_1, \dots, \gamma_r}\rangle / \partial \gamma_1 = \dots = \partial |\psi'_{f,\gamma_1, \dots, \gamma_r}\rangle / \partial \gamma_r$ and from Equation 8.8, Equation 8.9 becomes

$$\begin{aligned} \dot{V} = & - \left(1 / \left(1 + \Re \left(\left\langle \left(\partial |\psi'_{f,\gamma_1, \dots, \gamma_r}\rangle / \partial \gamma_k \right) |\psi\rangle \right) \sum_{j=1}^r \theta'_j \right) \right) \right. \\ & \cdot \left. \left((\lambda'_{f,\gamma_1, \dots, \gamma_r} + \omega) \Im(\langle \psi'_{f,\gamma_1, \dots, \gamma_r} | \psi \rangle) + \sum_{k=1}^r \Im(\langle \psi'_{f,\gamma_1, \dots, \gamma_r} | H_k | \psi \rangle) v_k(t) \right) \right) \end{aligned} \quad (8.10)$$

From the condition $\|\theta'_j\| < 1/(rC^*)$ in Lemma 8.1, $(1 + \Re(\langle \partial |\psi'_{f,\gamma_1, \dots, \gamma_r}\rangle / \partial \gamma_k) |\psi\rangle) \sum_{j=1}^r \theta'_j > 0$ holds. In order to ensure $\dot{V} \leq 0$, let us design ω and $v_k(t)$ as

$$\omega = -\lambda'_{f,\gamma_1, \dots, \gamma_r} + cf_0(\Im(\langle \psi'_{f,\gamma_1, \dots, \gamma_r} | \psi \rangle)) \quad (8.11)$$

$$v_k(t) = K_k f_k(\Im(\langle \psi'_{f,\gamma_1, \dots, \gamma_r} | H_k | \psi \rangle)) \quad (k = 1, \dots, r) \quad (8.12)$$

where $K_k > 0$, $c > 0$, and $y_k = f_k(x_k)$ ($k = 0, 1, \dots, r$) are monotonic increasing functions through the coordinate origin of the plane $x_k - y_k$.

Equations 8.11 and 8.12 are the designed control laws using the Lyapunov stability theorem for the control system (Equation 8.4) with the Lyapunov function Equation 8.5.

In fact, the above designed control laws can only ensure that the control system (Equation 8.4) is stable. In order to make the control system converge to the target state, we must analyze the convergence of the control system. The results of this analysis are described by Theorem 8.1.

Theorem 8.1 Consider the control system (Equation 8.7) with control fields $\gamma_k(t)$ designed in Lemma 8.1, η_k defined by Equation 8.3, $v_k(t)$ designed in Equation 8.13, and ω designed in Equation 8.12. If the control system satisfies (i) $\omega'_{l,m,\gamma_1, \dots, \gamma_r} \neq \omega'_{i,j,\gamma_1, \dots, \gamma_r}$, $(l, m) \neq (i, j)$, $i, j, l, m \in \{1, 2, \dots, N\}$, where $\omega'_{l,m,\gamma_1, \dots, \gamma_r} = \lambda'_{l,\gamma_1, \dots, \gamma_r} - \lambda'_{m,\gamma_1, \dots, \gamma_r}$ holds and (ii) for any $|\phi'_{i,\gamma_1, \dots, \gamma_r}\rangle \neq |\psi'_{f,\gamma_1, \dots, \gamma_r}\rangle$ ($i = 1, 2, \dots, N$) there exists at least a $k \in \{1, \dots, r\}$ satisfying $\langle \phi'_{i,\gamma_1, \dots, \gamma_r} | H_k | \psi'_{f,\gamma_1, \dots, \gamma_r} \rangle \neq 0$ ($k = 1, \dots, r$), then any state trajectory of the control system will converge toward $S^{2N-1} \cap E$, $E = \{|\psi\rangle = e^{i\theta}|\psi_f\rangle, \theta \in R\}$.

This convergence theorem will be proved in Section 8.1.2.

8.1.2 Convergence Proof

According to the LaSalle invariance principle, as $t \rightarrow \infty$ any state trajectory will converge to the largest invariant set contained in the set E in which the states satisfy $\dot{V} = 0$. The basic idea of the proof of Theorem 8.1 is as follows. First, the state set satisfying $\dot{V} = 0$ at some specific evolving moment is characterized. Then, whether $\dot{V} = 0$ holds after that moment is considered. Finally, by using the LaSalle invariance principle, the convergence theorem is proved.

By means of ω designed in Equation 8.11 and $v_k(t)$ designed in Equation 8.12, one can obtain

$$\dot{V} = 0 \iff \Im(\langle \psi | \psi'_{f,\gamma_1, \dots, \gamma_r} \rangle) = 0, \Im(\langle \psi'_{f,\gamma_1, \dots, \gamma_r} | H_k | \psi \rangle) = 0 \quad (8.13)$$

Without loss of generality, assume $\dot{V}(t) = 0$ ($t \geq t_0$). After the time t_0 , $\dot{V}(t) = 0$ holds and V is constant, thus γ_k ($k = 1, 2, \dots, r$) are constants, denoted by $\gamma_k = \bar{\gamma}_k$. By means of Equation 8.13 and ignoring higher-order terms of dt in the Taylor expansion formula of the state at time t_0 , $t_1 = t_0 + dt$, $t_2 = t_1 + dt$, \dots , we can obtain in turn:

$$t_0 : \Im(\langle \psi'_{f,\bar{\gamma}_1, \dots, \bar{\gamma}_r} | \psi(t_0) \rangle) = 0, \Im(\langle \psi'_{f,\bar{\gamma}_1, \dots, \bar{\gamma}_r} | H_k | \psi(t_0) \rangle) = 0 \quad (8.14)$$

$$t_1 : \Im(\langle \psi'_{f,\bar{\gamma}_1, \dots, \bar{\gamma}_r} | \psi(t_0 + dt) \rangle) = \Im(\langle \psi'_{f,\bar{\gamma}_1, \dots, \bar{\gamma}_r} | \psi(t_0) \rangle) = 0$$

$$\Im(i\langle \psi'_{f,\bar{\gamma}_1, \dots, \bar{\gamma}_r} | [H_{03}, H_k] | \psi(t_0) \rangle) = 0, \quad (8.15)$$

...

$$\Im(\langle \psi'_{f,\bar{\gamma}_1, \dots, \bar{\gamma}_r} | \psi(t_0) \rangle) = 0$$

$$\Im(i^n \langle \psi'_{f,\bar{\gamma}_1, \dots, \bar{\gamma}_r} | [H_{03}]^{(n)}, H_k | \psi(t_0) \rangle) = 0, (n = 0, 1, \dots) \quad (8.16)$$

where $H_{03} = H_0 + \sum_{k=1}^r H_k (\bar{\gamma}_k + \eta_k)$ and $[H_{03}]^{(n)}, H_k = \underbrace{[H_{03}, [H_{03}, \dots, [H_{03}, H_k]]]}_{n \text{ times}}$. Set

$U = (|\phi'_{1,\gamma_1, \dots, \gamma_r}\rangle, \dots, |\phi'_{N,\gamma_1, \dots, \gamma_r}\rangle)$, then the system in the eigenbasis of H_{03} is

$$i\dot{|\bar{\psi}(t)\rangle} = \left(\bar{H}_0 + \sum_{k=1}^r \bar{H}_k (\gamma_k(t) + v_k(t) + \eta_k) + \omega I \right) |\bar{\psi}(t)\rangle \quad (8.17)$$

where

$$|\psi(t)\rangle = U |\bar{\psi}(t)\rangle, H_0 = U \bar{H}_0 U^\dagger, H_k = U \bar{H}_k U^\dagger \quad (8.18)$$

Denote $|\bar{\psi}'_{f,\gamma_1, \dots, \gamma_r}\rangle = U_1^\dagger |\psi'_{f,\gamma_1, \dots, \gamma_r}\rangle$. Substituting Equation 8.18 into Equation 8.16 gives

$$\begin{aligned} \Im(\langle \bar{\psi}'_{f,\bar{\gamma}_1, \dots, \bar{\gamma}_r} | \bar{\psi}(t_0) \rangle) &= 0 \\ \Im(i^n \langle \bar{\psi}'_{f,\bar{\gamma}_1, \dots, \bar{\gamma}_r} | [\bar{H}_{03}]^{(n)}, \bar{H}_k | \bar{\psi}(t_0) \rangle) &= 0, (n = 0, 1, 2, \dots) \end{aligned} \quad (8.19)$$

where $\bar{H}_{03} = (\bar{H}_0 + \sum_{k=1}^r \bar{H}_k (\bar{\gamma}_k + \eta_k)) = \text{diag}[\lambda'_{1,\bar{\gamma}_1, \dots, \bar{\gamma}_r}, \dots, \lambda'_{N,\bar{\gamma}_1, \dots, \bar{\gamma}_r}]$. Set $|\bar{\psi}(t_0)\rangle = [\psi_1, \dots, \psi_N]^T$. By condition (i), the spectrum of H_{03} is not degenerate so N eigenstates of H_{03} can be written as $[1, 0, \dots, 0]^T$, \dots , and $[0, 0, \dots, 1]^T$. For convenience, assume $|\bar{\psi}'_{f,\bar{\gamma}_1, \dots, \bar{\gamma}_r}\rangle = [0, 0, \dots, 1]^T$. Then Equation 8.19 can be written as

$$\begin{aligned} \Im(\langle \bar{\psi}'_{f,\bar{\gamma}_1, \dots, \bar{\gamma}_r} | \bar{\psi}(t_0) \rangle) &= 0 \\ \Im \left(i^n \sum_{j=1}^N \left(\lambda'_{N,\bar{\gamma}_1, \dots, \bar{\gamma}_r} - \lambda'_{j,\bar{\gamma}_1, \dots, \bar{\gamma}_r} \right)^n (\bar{H}_k)_{Nj} \psi_j \right) &= 0 \end{aligned} \quad (8.20)$$

Set

$$\xi = [(\bar{H}_k)_{N1} \psi_1, (\bar{H}_k)_{N2} \psi_2, \dots, (\bar{H}_k)_{NN-1} \psi_{N-1}]^T \quad (8.21a)$$

$$\Lambda = \text{diag}[\omega'_{N,1,\bar{\gamma}_1, \dots, \bar{\gamma}_r}, \dots, \omega'_{N,(N-1),\bar{\gamma}_1, \dots, \bar{\gamma}_r}] \quad (8.21b)$$

$$M = \begin{bmatrix} 1 & \cdots & 1 \\ \omega'_{N,1,\bar{\gamma}_1, \dots, \bar{\gamma}_r}^2 & \cdots & \omega'_{N,(N-1),\bar{\gamma}_1, \dots, \bar{\gamma}_r}^2 \\ \vdots & \vdots & \vdots \\ \omega'_{N,1,\bar{\gamma}_1, \dots, \bar{\gamma}_r}^{2(N-2)} & \cdots & \omega'_{N,(N-1),\bar{\gamma}_1, \dots, \bar{\gamma}_r}^{2(N-2)} \end{bmatrix} \quad (8.21c)$$

By conditions (i) and (ii), one can obtain $\psi_j = 0$ ($j = 1, \dots, N-1$), therefore Equation 8.20 is equivalent to $|\bar{\psi}(t_0)\rangle = \psi_N |\bar{\psi}'_{f,\bar{\gamma}_1, \dots, \bar{\gamma}_r}\rangle = e^{i\theta} |\bar{\psi}'_{f,\bar{\gamma}_1, \dots, \bar{\gamma}_r}\rangle$. Thus one can obtain $|\psi(t_0)\rangle = e^{i\theta} |\psi'_{f,\bar{\gamma}_1, \dots, \bar{\gamma}_r}\rangle$. If $\gamma_k(e^{i\theta} |\psi'_{f,\bar{\gamma}_1, \dots, \bar{\gamma}_r}\rangle) = 0$, then $|\psi(t_0)\rangle = e^{i\theta} |\psi_f\rangle$ holds. According to the LaSalle invariance principle (LaSalle and Lefschetz, 1961), as $t \rightarrow \infty$, any state trajectory of the control system will converge toward $E = \{|\psi\rangle = e^{i\theta} |\psi_f\rangle, \theta \in R\}$. Theorem 8.1 is proved.

8.1.3 Relation between Two Lyapunov Functions

In Liouville space, the Hilbert–Schmidt distance between two density operators ρ_1 and ρ_2 is

$$d_{HS}(\rho_1, \rho_2) = \sqrt{\text{tr}(\rho_1 - \rho_2)^2} \quad (8.22)$$

The inner product of two operators A and B is defined as $\langle A | B \rangle = \text{tr}(A^\dagger B)$, where the operation A^\dagger refers to the conjugate transpose of A . By $\rho = |\psi\rangle\langle\psi|$, the square of the Hilbert–Schmidt distance between the density operator ρ and the target density operator $\rho_{f,\bar{\gamma}_1, \dots, \bar{\gamma}_r}$ is

$$d_{HS}^2(\rho, \rho_{f,\bar{\gamma}_1, \dots, \bar{\gamma}_r}) = 2(1 - |\langle\psi|\psi'_{f,\bar{\gamma}_1, \dots, \bar{\gamma}_r}\rangle|^2) \quad (8.23)$$

By Equation 8.23 and the implicit Lyapunov functions based on the state distance $V(\psi) = \frac{1}{2}(1 - |\langle\psi|\psi'_{f,\bar{\gamma}_1, \dots, \bar{\gamma}_r}\rangle|^2)$ and the state error $V(|\psi\rangle) = \frac{1}{2}\langle\psi - \psi'_{f,\bar{\gamma}_1, \dots, \bar{\gamma}_r} | \psi - \psi'_{f,\bar{\gamma}_1, \dots, \bar{\gamma}_r} \rangle$ used in this section, we can conclude that two implicit Lyapunov functions are equivalent in the sense of replacing the pure states with their equivalent density operators.

8.1.4 Numerical Simulation and Result Analysis

In this subsection, a four-level multi-control Hamiltonian quantum system in a degenerate case is considered. The experiment is done to verify the effectiveness of the implicit Lyapunov

control method proposed and compare the control effectiveness of implicit Lyapunov control based on the state error with that of the state distance.

In the numerical simulation experiment, the Hamiltonians of the selected four-level quantum system are

$$H_0 = \text{diag}(1.1, 1.83, 2.56, 3.05)$$

$$H_1 = \begin{bmatrix} 0 & 0 & 1 & 1 \\ 0 & 0 & 1 & 0 \\ 1 & 1 & 0 & 0 \\ 1 & 0 & 0 & 0 \end{bmatrix}, \quad H_2 = \begin{bmatrix} 0 & 1 & 0 & 0 \\ 1 & 0 & 0 & 1 \\ 0 & 0 & 0 & 1 \\ 0 & 1 & 1 & 0 \end{bmatrix} \quad (8.24)$$

Assume the initial state is a superposition state, $|\psi_0\rangle = 0.5(1 \ 1 \ 1 \ 1)^T$, and the target state is an eigenstate, $|\psi_f\rangle = (0 \ 0 \ 0 \ 1)^T$.

According to the design idea proposed, the control laws based on the state error are $u_k(t) = \gamma_k(t) + v_k(t) + \eta_k$ ($k = 1, 2$) and ω . The implicit functions $\gamma_k(t)$ ($k = 1, 2$) are designed according to Lemma 8.1 as $\gamma_k(|\psi\rangle) = \theta_k \left(\frac{1}{2} \langle \psi - \psi'_{f,\gamma_1,\gamma_2} | \psi - \psi'_{f,\gamma_1,\gamma_2} \rangle \right)$ ($k = 1, 2$), where $\theta_1(s) = C_1 s$ and $\theta_2(s) = C_2 s$. According to Equation 8.3, η_k are designed as $\eta_1 = \eta_2 = 0$. The control fields $v(t)$ are designed according to Equation 8.12 as $v_1(t) = K_1 \Im(\langle \psi'_{f,\gamma_1,\gamma_2} | H_1 | \psi \rangle)$ and $v_2(t) = K_2 \Im(\langle \psi'_{f,\gamma_1,\gamma_2} | H_2 | \psi \rangle)$. ω is designed according to Equation 8.11 as $\omega = -\lambda'_{\gamma_1,\gamma_2} + c \Im(\langle \psi'_{f,\gamma_1,\gamma_2} | \psi \rangle)$. After tuning these control parameters repeatedly and carefully, we choose the control parameters as $C_1 = 0.04$, $C_2 = 0.02$, $K_1 = 0.3$, $K_2 = 0.7$, and $c = 0.16$.

In the numerical simulation experiment, the sample step is set to be 0.01 a.u. and the control duration is 50 a.u. The results of the numerical simulation experiment are shown in Figures 8.1–8.3, where Figure 8.1 shows the population evolution curves of the control system and $|c_i|^2$ ($i = 1, 2, 3, 4$) is the population of level $|i\rangle$. Figure 8.2 shows the designed control fields $u_1(t)$ and $u_2(t)$. Figure 8.3 shows the designed ω .

One can see from Figure 8.1 that at time 31 a.u., the populations of the four energy levels are $|c_1|^2 = 2.4334 \times 10^{-5}$, $|c_2|^2 = 1.1384 \times 10^{-6}$, $|c_3|^2 = 2.6292 \times 10^{-7}$, and $|c_4|^2 = 0.99997$. The transition probability is over 99.997% after time 35 a.u.

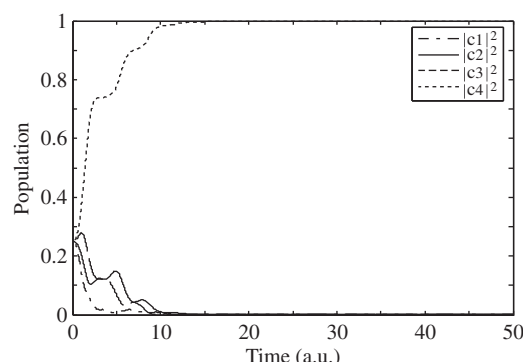


Figure 8.1 Populations of four energy levels

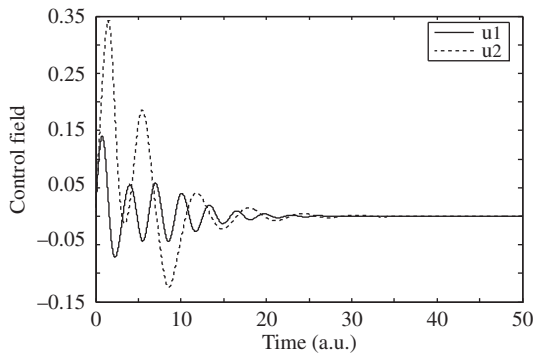


Figure 8.2 Control fields $u_1(t)$ and $u_2(t)$

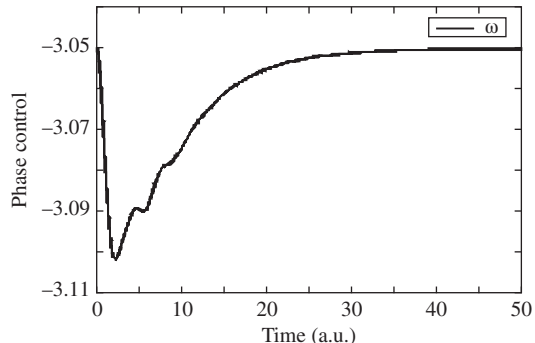


Figure 8.3 Imaginary control field ω

8.2 Quantum Lyapunov Control Based on the Average Value of an Imaginary Mechanical Quantity

8.2.1 Control Law Design and Convergence Proof

Consider the N -level closed quantum system governed by the following bilinear Schrödinger equation:

$$i|\psi(t)\rangle = \left(H_0 + \sum_{k=1}^r H_k v_k(t) \right) |\psi(t)\rangle \quad (8.25)$$

where $|\psi(t)\rangle$ is the quantum state vector, H_0 is the internal Hamiltonian, H_k ($k = 1, \dots, r$) are control Hamiltonians, and $v_k(t)$ ($k = 1, \dots, r$) are control laws.

In order to solve the problem of convergence of the control system in the degenerate cases, a series of perturbations $\gamma_k(t)$, which are implicit functions of state $|\psi(t)\rangle$ and time t , are introduced into the control laws. Equation 8.25 then becomes

$$i|\psi(t)\rangle = \left(H_0 + \sum_{k=1}^r H_k (\gamma_k(t) + v_k(t)) \right) |\psi(t)\rangle \quad (8.26)$$

Where $\gamma_k(t) + v_k(t) = u_k(t)$ ($k = 1, \dots, r$) are the total control laws.

Our control task is to make the control system governed by Equation 8.26 transfer from an arbitrary initial pure state $|\psi_0\rangle$ to an arbitrary target pure state $|\psi_f\rangle$ by designing appropriate control laws $u_k(t) = \gamma_k(t) + v_k(t)$ ($k = 1, \dots, r$). In order to complete this control task, first the perturbations $\gamma_k(t)$ and $v_k(t)$ are designed. Second, the convergence of the control system is proved. Third, the way in which the convergence conditions can be satisfied is analyzed.

First, let us design $\gamma_k(t)$ ($k = 1, \dots, r$). After introducing perturbations $\gamma_k(t)$, $H_0 + \sum_{k=1}^r H_k \gamma_k(t)$ can be regarded as the new internal Hamiltonian of the control system. In order to understand the basic idea of this method, we describe the system in the eigenbasis of $H_0 + \sum_{k=1}^r H_k \gamma_k(t)$:

$$i|\dot{\hat{\psi}}(t)\rangle = \left(\left(\hat{H}_0 + \sum_{k=1}^r \hat{H}_k \gamma_k(t) \right) + \sum_{k=1}^r \hat{H}_k v_k(t) \right) |\hat{\psi}(t)\rangle \quad (8.27)$$

where $|\hat{\psi}\rangle = U_1^\dagger |\psi\rangle$, $\hat{H}_0 = U_1^\dagger H_0 U_1$, $\hat{H}_k = U_1^\dagger H_k U_1$, $U_1 = (|\phi_{1,\gamma_1, \dots, \gamma_r}\rangle, \dots, |\phi_{N,\gamma_1, \dots, \gamma_r}\rangle)$, and $|\phi_{n,\gamma_1, \dots, \gamma_r}\rangle$, $1 \leq n \leq N$ are eigenstates of $H_0 + \sum_{k=1}^r H_k \gamma_k(t)$ corresponding to the eigenvalues $\lambda_{n,\gamma_1, \dots, \gamma_r}$. Accordingly, $|\psi_f\rangle$ will become $|\hat{\psi}_f\rangle = U_1^\dagger |\psi_f\rangle$, which is also a functional of $\gamma_k(t)$.

The design idea of $\gamma_k(t)$ is as follows: (i) $\gamma_k(t)$ are designed to satisfy the convergence conditions for Hamiltonians so that the control system can converge toward $|\hat{\psi}_f\rangle$ by designing appropriate control laws $u_k(t) = \gamma_k(t) + v_k(t)$ ($k = 1, \dots, r$), (ii) at the same time, $\gamma_k(t)$ ($k = 1, \dots, r$) themselves need converge to zero, and their convergent speed must be slower than that of the control system to $|\hat{\psi}_f\rangle$ to make $\gamma_k(t)$ take effect, and (iii) $\gamma_k(|\psi_f\rangle) = 0$ must hold to make the control system asymptotically stable at the target state.

In Section 7.1.3 we proposed the restriction $V(|\psi_f\rangle) < V(|\psi_0\rangle) < V(|\psi_{other}\rangle)$ to make the system in non-degenerate cases converge to the target state $|\psi_f\rangle$ from the initial state $|\psi_0\rangle$, where $|\psi_{other}\rangle$ represents any other state in the invariant set $E = \{|\psi\rangle | \dot{V}(|\psi\rangle) = 0\}$ except the target state. However, it is difficult to design the imaginary mechanical quantity required to make this restriction on the Lyapunov function be satisfied for any initial state and any target state.

For degenerate cases, to make the system converge to the target state we choose a simpler restriction: $V(|\psi_f\rangle) < V(|\psi_{other}\rangle)$, which can be satisfied for any initial state and any target state by designing the imaginary mechanical quantity. In order to ensure the system converges to the target state by adding this restriction, we design all the perturbations $\gamma_k(t) = 0$ to hold for $k = 1, \dots, r$ only at $|\psi_f\rangle$, that is, (i) $\gamma_k(|\psi_f\rangle) = 0$ ($k = 1, \dots, r$) and (ii) for $|\psi\rangle \neq |\psi_f\rangle$ there exists at least one k such that $\gamma_k(|\psi\rangle) \neq 0$.

According to the analysis mentioned above, let us design the specific $\gamma_k(t)$ ($k = 1, \dots, r$). Since the evolution of the system's state relies on the continuous decrease of the Lyapunov function $V(t)$ in the Lyapunov control, we design $\gamma_k(t)$ be a monotonically increasing functional of $V(t)$ as

$$\gamma_k(|\psi\rangle) = C_k \cdot \theta_k(V(|\psi\rangle) - V(|\psi_f\rangle)) \quad (8.28)$$

where $C_k \geq 0$ and for $k = 1, \dots, r$ there exists at least a $C_k > 0$. $\theta_k(\cdot)$ also satisfies $\theta_k(0) = 0$, $\theta_k(s) > 0$, and $\theta'_k(s) > 0$ for every $s > 0$. The specific Lyapunov function based on the average value of an imaginary mechanical quantity is selected as

$$V(|\psi\rangle) = \langle \psi | P_{\gamma_1, \dots, \gamma_r} | \psi \rangle \quad (8.29)$$

where $P_{\gamma_1, \dots, \gamma_r} = f(\gamma_1(t), \dots, \gamma_r(t))$ is a functional of $\gamma_k(t)$ and a positive definite.

The existence of $\gamma_k(t)$ can be depicted by Lemma 8.2.

Lemma 8.2 If $C_k = 0$, $\gamma_k(|\psi\rangle) = 0$. Else if $C_k > 0$, $\theta_k \in C^\infty(R^+; [0, \gamma_k^*]), k = 1, \dots, r$ (γ_k^* is a positive constant) satisfies $\theta_k(0) = 0$, $\theta_k(s) > 0$, and $\theta'_k(s) > 0$ for every $s > 0$, and $|\theta'_k| < 1/(2C_k C^*)$, $C^* = 1 + C$, and $C = \max\{\|\partial P_{\gamma_1, \dots, \gamma_r}/\partial \gamma_k\|_\infty, \gamma_k \in [0, \gamma_k^*]\}$, then for every $|\psi\rangle \in S^{2N-1}$, there is a unique $\gamma_k \in C^\infty(\gamma_k \in [0, \gamma_k^*])$ satisfying $\gamma_k(|\psi\rangle) = C_k \cdot \theta_k(\langle\psi|P_{\gamma_1, \dots, \gamma_r}|\psi\rangle - \langle\psi_f|P_{\gamma_1, \dots, \gamma_r}|\psi_f\rangle)$.

Proof Assume $P_{\gamma_1, \dots, \gamma_r}$ are analytic functions of the parameters $\gamma_k(\psi) \in [0, \gamma_k^*]$ ($k = 1, \dots, r$). $\partial P_{\gamma_1, \dots, \gamma_r}/\partial \gamma_k$ are bounded on $[0, \gamma_k^*]$, thus $C < \infty$. Define

$$F_k(\gamma_1, \dots, \gamma_r, |\psi\rangle) = \gamma_k - C_k \cdot \theta_k(\langle\psi|P_{\gamma_1, \dots, \gamma_r}|\psi\rangle - \langle\psi_f|P_{\gamma_1, \dots, \gamma_r}|\psi_f\rangle) \quad (8.30)$$

where $F_k(\gamma_1, \dots, \gamma_r, |\psi\rangle)$ are regular. For a fixed $|\psi\rangle$, $F_k(\gamma_1(|\psi\rangle), \dots, \gamma_r(|\psi\rangle), |\psi\rangle) = 0$ holds. Some deductions show that $\partial F_k(\gamma_1, \dots, \gamma_r, |\psi\rangle)/\partial \gamma_k \neq 0$ holds. Thus according to the implicit theorem (Krantz and Parks, 2002), Lemma 8.2 is proved. ■

Remark 8.1 For the sake of simplicity, set $\gamma_k(t) = 0$ for some k , and other $\gamma_k(t)$ are equal to $\gamma(t)$, that is, set

$$\begin{aligned} \gamma_k(t) &= \gamma(t) = \theta(\langle\psi|P_\gamma|\psi\rangle - \langle\psi_f|P_\gamma|\psi_f\rangle), k = k_1, \dots, k_m; \\ \gamma_k(t) &= 0, k \neq k_1, \dots, k_m (1 \leq k_1, \dots, k_m \leq r) \end{aligned} \quad (8.31)$$

where $\theta(\cdot) = \theta_{k_1}(\cdot) = \dots = \theta_{k_m}(\cdot)$ and P_γ are functionals of $\gamma(t)$.

Then let us design $v_k(t)$ to make $\dot{V}(t) \leq 0$ hold. Setting $\left[P_\gamma, H_0 + \sum_{n=k_1}^{k_m} H_n \gamma(t)\right] = 0$, one can obtain the time derivative of the selected Lyapunov function as

$$\begin{aligned} \dot{V} &= \sum_{k=1}^r i v_k(t) \langle\psi|[H_k, P_\gamma]|\psi\rangle \cdot (1 + \theta'(\langle\psi_f|(\partial P_\gamma/\partial \gamma)|\psi_f\rangle)) \\ &\quad / (1 - \theta'(\langle\psi|(\partial P_\gamma/\partial \gamma)|\psi\rangle - \langle\psi_f|(\partial P_\gamma/\partial \gamma)|\psi_f\rangle)) \end{aligned} \quad (8.32)$$

According to Lemma 8.2, one can obtain

$$(1 + \theta'(\langle\psi_f|(\partial P_\gamma/\partial \gamma)|\psi_f\rangle)) / (1 - \theta'(\langle\psi|(\partial P_\gamma/\partial \gamma)|\psi\rangle - \langle\psi_f|(\partial P_\gamma/\partial \gamma)|\psi_f\rangle)) > 0$$

In order to ensure $\dot{V}(t) \leq 0$, $v_k(t)$ ($k = 1, \dots, r$) are designed as

$$v_k(t) = -K_k f_k(i \langle\psi|[H_k, P_\gamma]|\psi\rangle) \quad (k = 1, \dots, r) \quad (8.33)$$

where K_k is a constant and $K_k > 0$ and $y_k = f_k(x_k)$ ($k = 1, 2, \dots, r$) are monotonic increasing functions through the coordinate origin of the plane $x_k - y_k$.

Based on LaSalle's invariance principle (LaSalle and Lefschetz, 1961), the convergence of the control system governed by Equation 8.26 can be obtained as follows:

Theorem 8.2 Consider the control system governed by Equation 8.26 with control fields $u_k(t) = \gamma_k(t) + v_k(t)$ ($k = 1, \dots, r$), where $\gamma_k(t)$ is defined by Lemma 8.2 and Equation 8.31,

and $v_k(t)$ is defined by Equation 8.33. If the control system satisfies: (i) $\omega_{l,m,\gamma} \neq \omega_{i,j,\gamma}$, $(l, m) \neq (i, j)$, $i, j, l, m \in \{1, 2, \dots, N\}$, and $\omega_{l,m,\gamma} = \lambda_{l,\gamma} - \lambda_{m,\gamma}$, where $\lambda_{l,\gamma}$ is the l th eigenvalue of $H_0 + \sum_{n=k_1}^{k_m} H_n \gamma(t)$ corresponding to the eigenstate $|\phi_{l,\gamma}\rangle$, (ii) for any $i \neq j$, $i, j \in \{1, 2, \dots, N\}$, there exists at least one k such that $(\hat{H}_k)_{lm} \neq 0$, where $(\hat{H}_k)_{lm}$ is the (l, m) th element of $\hat{H}_k = U_1^\dagger H_k U_1$, $U_1 = (|\phi_{1,\gamma}\rangle, \dots, |\phi_{N,\gamma}\rangle)$, (iii) $\left[P_\gamma, H_0 + \sum_{n=k_1}^{k_m} H_n \gamma(t) \right] = 0$, and (iv) $(\hat{P}_\gamma)_{ll} \neq (\hat{P}_\gamma)_{mm}$, $l \neq m$, where $(\hat{P}_\gamma)_{ll}$ is the (l, l) th element of $U_1^\dagger P_\gamma U_1$, then any trajectory will converge toward $E_1 = \{|\psi_{t_0}\rangle |e^{i\theta_l}| \phi_{l,\gamma}(\psi_{t_0})\}; \theta_l \in R, l \in \{1, \dots, N\}\}$.

Proof Without loss of generality, assume that for $t \geq t_0$ ($t_0 \in R$), $\dot{V} = 0$ is satisfied. By Equations 8.32 and 8.33, one obtains

$$\dot{V} = 0 \iff \langle \psi | [H_k, P_\gamma] | \psi \rangle = 0 \iff v_k(t) = 0 \quad (8.34)$$

As $\dot{V} = 0$, γ is a constant, denoted by $\bar{\gamma}$. The state $|\psi(t_0)\rangle$ can be written as $|\psi(t_0)\rangle = \sum_{l=1}^N c_l(t_0) |\phi_{l,\gamma}\rangle$. Then $|\hat{\psi}(t_0)\rangle$ can be written as $|\hat{\psi}(t_0)\rangle = \sum_{l=1}^N c_l(t_0) U_1^H |\phi_{l,\gamma}\rangle$. Substituting the solution of Equation 8.27 with $\gamma = \bar{\gamma}$ and $v_k(t) = 0$ into $\langle \hat{\psi} | [\hat{H}_k, \hat{P}_\gamma] | \hat{\psi} \rangle = \langle \psi | [H_k, P_\gamma] | \psi \rangle = 0$, gives

$$\sum_{l,m=1}^N e^{i\omega_{l,m,\bar{\gamma}}(t-t_0)} ((\hat{P}_{\bar{\gamma}})_{mm} - (\hat{P}_{\bar{\gamma}})_{ll}) c_l^*(t_0) c_m(t_0) (\hat{H}_k)_{lm} = 0 \quad (8.35)$$

By conditions (i), (ii), and (iv), one can have

$$c_l^*(t_0) c_m(t_0) = 0 \quad (l, m \in \{1, \dots, N\}) \quad (8.36)$$

which implies that there is at most one $c_l(t_0)$ ($l \in \{1, \dots, N\}$) that is non-zero. Theorem 8.2 is proved. ■

Theorem 8.2 guarantees that the control system converges to the set E_1 , but it cannot guarantee that the control system converges to the target state. From Theorem 8.2, one can see that if the target state $|\psi_f\rangle$ is an eigenstate, $|\psi_f\rangle$ is contained in E_1 because $\gamma(|\psi_f\rangle) = 0$. In order to make the system converge to the target state, on the one hand, as $\dot{V} \leq 0$, we design P_γ to make

$$V(|\psi_f\rangle) < V(|\psi_{other}\rangle) \quad (8.37)$$

hold, where $|\psi_{other}\rangle$ represents any other state in the set E_1 except the target state. On the other hand, because $\partial\gamma/\partial V > 0$, $\dot{V} \leq 0$, $\gamma \geq 0$ holds, we set $\gamma = \bar{\gamma} - \alpha$ ($0 < \alpha \ll \bar{\gamma}$) when $v_k(t) = 0$, $\gamma(t) = \bar{\gamma} \neq 0$ holds for some time to make the state trajectory evolve but not stay in E_1 until $|\psi_f\rangle e^{i\theta_l}$, which is the equivalent state of the target state $|\psi_f\rangle$, is reached.

From the above analysis, we can see that if the control system satisfies the conditions (i)–(iv) in Theorem 8.2 and Equation 8.37, and at the same time set $\gamma = \bar{\gamma} - \alpha$ ($0 < \alpha \ll \bar{\gamma}$) when $v_k(t) = 0$, $\gamma(t) = \bar{\gamma} \neq 0$ holds for some time, the control system can converge to the target eigenstate from an arbitrary initial pure state.

Next we will analyze how to satisfy these conditions in detail. Conditions (i) and (ii) in Theorem 8.2 are associated with H_0 , H_k ($k = 1, \dots, r$) and $\gamma_k(t)$. By designing appropriate $\gamma_k(t)$, these two conditions can be satisfied in most cases. Condition (iii) means that P_γ and

$H_0 + \sum_{n=k_1}^{k_m} H_n \gamma(t)$ have the same eigenstates. If we design the eigenvalues of P_γ to be constant, denoted by P_1, P_2, \dots, P_N , and design P_γ as

$$P_\gamma = \sum_{j=1}^N P_j |\phi_{j,\gamma}\rangle\langle\phi_{j,\gamma}| \quad (8.38)$$

condition (iii) can then be satisfied. If we design $P_l \neq P_j (\forall l \neq j; 1 \leq l, j \leq N)$ to make condition (iv) hold then let us analyze how to make Equation 8.37 hold. The research result is given by Theorem 8.3.

Theorem 8.3 If one designs $P_i > P_f$ ($i = 1, \dots, N, P_i \neq P_f$), then $V(|\psi_f\rangle) < V(|\psi_{other}\rangle)$ holds, where P_f is the eigenvalue of $P_{\gamma(|\psi_f\rangle)}$ corresponding to $|\psi_f\rangle$.

Proof Set $|\psi_s\rangle = (e^{i\theta_l} |\phi_{l,\gamma}\rangle)|_{\gamma=0}$. According to Proposition 1 in Krantz and Parks in 2002, if one designs $P_i > P_f$, ($i = 1, \dots, N, P_i \neq P_f$), then $V(|\psi_f\rangle) < V(|\psi_s\rangle)$ holds because $\partial\gamma/\partial V > 0, \dot{V} \leq 0, \gamma > 0, V(|\psi_s\rangle) < V(|\psi_{other}\rangle)$ holds. Thus $V(|\psi_f\rangle) < V(|\psi_{other}\rangle)$ holds. Theorem 8.3 is proved. ■

Remark 8.2 According to the above analysis and Theorem 8.3, the design principle of the imaginary mechanical quantity is $P_i > P_f$ ($i = 1, \dots, N, P_i \neq P_f$) and $P_l \neq P_j (\forall l \neq j)$.

In order to solve the problem of convergence to the target state being a superposition state, a series of disturbances η_k whose values are constant are introduced into the control laws. Thus the mechanical equation (Equation 8.26) will become

$$i|\dot{\psi}(t)\rangle = \left(H_0 + \sum_{k=1}^r H_k (\eta_k + \gamma_k(t) + v_k(t)) \right) |\psi(t)\rangle \quad (8.39)$$

Our basic idea is to design η_k to make the target state $|\psi_f\rangle$ be an eigenstate of $H'_0 = H_0 + \sum_{k=1}^r H_k \eta_k$. H'_0 can be viewed as the new internal Hamiltonian of the control system. If the number of the control Hamiltonians r is large enough, by designing appropriate η_k , $(H_0 + \sum_{k=1}^r H_k \eta_k) |\psi_f\rangle = \lambda'_f |\psi_f\rangle$ can be satisfied in most cases, where λ'_f is the eigenvalue of H'_0 corresponding to $|\psi_f\rangle$. Then the design of the control laws and the convergence proof can follow the target eigenstate cases. One can prove that the designed control laws are also valid. Theorems 8.2 and 8.3 also hold with changing H_0 into H'_0 .

8.2.2 Numerical Simulation and Result Analysis

In order to verify the effectiveness of the proposed method, consider a three-level system with H_0 and H_1 as

$$H_0 = \begin{bmatrix} 0.3 & 0 & 0 \\ 0 & 0.5 & 0 \\ 0 & 0 & 0.9 \end{bmatrix}, \quad H_1 = \begin{bmatrix} 0 & 1 & 0 \\ 1 & 0 & 0 \\ 0 & 0 & 0 \end{bmatrix}, \quad H_2 = \begin{bmatrix} 0 & 0 & 1 \\ 0 & 0 & 0 \\ 1 & 0 & 0 \end{bmatrix} \quad (8.40)$$

According to H_0 and H_1 , the system is in the degenerate case. Assume that the initial state is an eigenstate as $|\psi_0\rangle = (0 \ 0 \ 1)^T$ and the target state is a superposition state as $|\psi_f\rangle = (\sqrt{2/3} \ -\sqrt{1/3} \ 0)^T$.

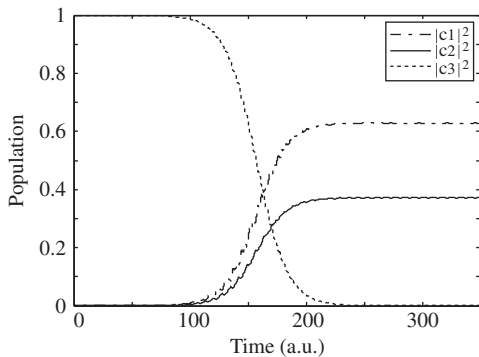


Figure 8.4 Population

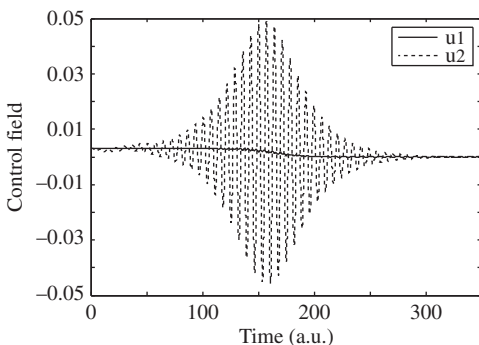


Figure 8.5 Control fields

According to the design ideas in Section 8.2.1, the control law is designed as $u_k(t) = \gamma_k(t) + v_k(t) + \eta_k$ ($k = 1, 2$). Design $\eta_1 = -0.3771, \eta_2 = 0$ to make the target state $|\psi_f\rangle$ be an eigenstate of $H'_0 = H_0 + \sum_{k=1}^2 H_k \eta_k$, and design $\gamma_1 = \gamma_2 = \gamma = 0.01 \cdot (\langle\psi|P_\gamma|\psi\rangle - \langle\psi_f|P_\gamma|\psi_f\rangle)$, $v_1(t) = -0.2 \cdot (i\langle\psi|[H_1, P_\gamma]|\psi\rangle)$, and $v_2(t) = -0.2 \cdot (i\langle\psi|[H_2, P_\gamma]|\psi\rangle)$, where $P_\gamma = \sum_{j=1}^3 P_j |\phi_{j,\gamma}\rangle$. According to Theorem 8.3 in Section 8.2.1, set $P_f = 0.1$ and other two eigenvalues of P_γ are 0.4 and 0.6.

In the simulations, the time step size is set as 0.01 a.u. and the control duration is 300 a.u. The results of numerical simulations are shown in Figures 8.4 and 8.5. Figure 8.4 shows the population evolution curves of the system, where $|c_i|^2$ ($i = 1, 2, 3$) is the population of level $|i\rangle$. Figure 8.5 shows the designed control fields. According to numerical results, we can see that the proposed method is effective.

8.3 Implicit Lyapunov Control for the Quantum Liouville Equation

As we know, the convergence of the quantum system can be analyzed based on LaSalle's invariance principle. According this principle, as $t \rightarrow \infty$ any state trajectory will converge to the largest invariant set in the set E in which the states satisfy that the first-order time derivative of the Lyapunov function equals zero. In fact, the set E contains not only the target state but

also the other states, and in such a case the system may converge to other states rather than the target state. Thus, in order to enable the control system to converge to the target state, the main idea is to add restrictions to make the set E as small as possible. In recent years, according to the quantum system governed by the Schrödinger equation or quantum Liouville equation, the research results on system convergence can be divided into two categories:

1. Consider the Schrödinger equation $i\hbar|\psi(t)\rangle = \left(H_0 + \sum_{k=1}^r H_k u_k(t) \right) |\psi(t)\rangle$, where $|\psi(t)\rangle$ is the quantum state vector, H_0 is the internal Hamiltonian, H_k ($k = 1, \dots, r$) are control Hamiltonians, and $u_k(t)$ ($k = 1, \dots, r$) are control laws. For the target state $|\psi_f\rangle$ being an eigenstate, the conditions which make the control system converge to the target state are:
 - a. The internal Hamiltonian is strongly regular, that is, $\omega_{lm} \neq \omega_{ij}$, $(i,j) \neq (l,m)$, $i,j,l,m \in \{1, 2, \dots, N\}$, where $\omega_{lm} = \lambda_l - \lambda_m$ represents the Bohr frequency (transition frequency) between the energy levels λ_l and λ_m , and λ_l is the l th eigenvalue of H_0 corresponding to the eigenstate $|\phi_l\rangle$.
 - b. i. For the Lyapunov function based on the state distance $V = 1/2(1 - |\langle\psi_f|\psi\rangle|^2)$ or state error $V = 1/2\langle\psi - \psi_f|\psi - \psi_f\rangle$, the condition is: all the eigenstates different from the target state are directly coupled to the target state, that is, for any eigenstate $|\phi_i\rangle \neq |\psi_f\rangle$, there exists at least a k such that $\langle\phi_i|H_k|\psi_f\rangle \neq 0$.
 - ii. For the Lyapunov function based on the average value of an imaginary mechanical quantity $V = \langle\psi|P|\psi\rangle$, where P is an imaginary mechanical quantity, the condition is: any two levels are coupled directly, that is, for any $|\phi_i\rangle \neq |\phi_j\rangle$, there exists at least a k such that $\langle\phi_i|H_k|\phi_j\rangle \neq 0$.
2. Consider the quantum Liouville equation $i\hbar\dot{\rho}(t) = \left[H_0 + \sum_{k=1}^r H_k u_k(t), \rho(t) \right]$, where $\rho(t)$ is the density operator. For the target state to be a diagonal matrix, the convergence conditions are (Wang and Schirmer, 2010b; Kuang and Cong, 2010a,b):
 - a. the internal Hamiltonian is strongly regular and
 - b. the control Hamiltonians are full connected, that is, $\forall j \neq l$, for $k = 1, \dots, r$, there exists at least a $(H_k)_{jl} \neq 0$, where $(H_k)_{jl}$ is the (j,l) th element of H_k .

The control systems that satisfy the conditions mentioned above are called ideal systems or non-degenerate cases. The systems that do not satisfy these conditions are called degenerate cases. For degenerate systems, a modified control design based on an “implicit” Lyapunov function has been used to make the control system converge to an arbitrary eigenstate from any pure state for the Schrödinger equation. However, little research has focused on the problems of convergences to the superposition and mixed states.

We will propose a solution to these problems in this section. Another important area in this section is to analyze how to satify these convergence conditions. The explicit design principle of the imaginary mechanical quantity is proposed.

8.3.1 Description of Problem

Consider the N -level closed quantum system governed by the following quantum Liouville equation:

$$i\dot{\rho}(t) = \left[H_0 + \sum_{k=1}^r H_k u_k(t), \rho(t) \right], \rho_0 = \rho(0), (\hbar = 1) \quad (8.41)$$

where $\rho(t)$ is the density operator, H_0 is the internal Hamiltonian, H_k ($k = 1, \dots, r$) are control Hamiltonians, and $u_k(t)$ ($k = 1, \dots, r$) are control laws.

Here we introduce perturbations $\gamma_k(t)$ into the control laws. Thus Equation 8.41 becomes

$$i\dot{\rho}(t) = \left[H_0 + \sum_{k=1}^r H_k (\gamma_k(t) + v_k(t)), \rho(t) \right], \rho_0 = \rho(0) \quad (8.42)$$

where $\gamma_k(t)$ are the control laws specially used to solve the convergence problem for the degenerate cases, $v_k(t)$ are the designed control laws based on the Lyapunov stability theorem, and $\gamma_k(t) + v_k(t) = u_k(t)$ ($k = 1, \dots, r$) are the total control laws.

We call the system that is composed of the internal Hamiltonian H_0 , the control Hamiltonians H_k ($k = 1, \dots, r$), and the control laws $u_k(t) = \gamma_k(t) + v_k(t)$ system 1, and the system that is composed of the internal Hamiltonian $H_{02} = H_0 + \sum_{k=1}^r H_k \gamma_k(t)$, the control Hamiltonians H_k ($k = 1, \dots, r$), and the control laws $v_k(t)$ system 2. Both these systems can be depicted by Equation 8.42. In order to understand how to solve the convergence problem of the control system in degenerate cases, we describe system 2 by means of the eigenbasis of H_{02} . Assume the eigenvalues and eigenstates of H_{02} are $\lambda_{n,\gamma_1, \dots, \gamma_r}$ and $|\phi_{n,\gamma_1, \dots, \gamma_r}\rangle$, $1 \leq n \leq N$, respectively. Set $U_1 = (|\phi_{1,\gamma_1, \dots, \gamma_r}\rangle, \dots, |\phi_{N,\gamma_1, \dots, \gamma_r}\rangle)$, then system 2 in the eigenbasis of H_{02} is

$$i\dot{\hat{\rho}}(t) = \left[\left(\hat{H}_0 + \sum_{k=1}^r \hat{H}_k \gamma_k(t) \right) + \sum_{k=1}^r \hat{H}_k v_k(t), \hat{\rho}(t) \right] \quad (8.43)$$

where $\hat{\rho} = U_1^\dagger \rho U_1$, $\hat{H}_0 = U_1^\dagger H_0 U_1$, $\hat{H}_k = U_1^\dagger H_k U_1$.

Accordingly, the target state ρ_f will become $\hat{\rho}_f = U_1^\dagger \rho_f U_1$, which is a functional of $\gamma_k(t)$. Because U_1 is unitary, the eigenvalues of H_{02} and $\hat{H}_{02} = \hat{H}_0 + \sum_{k=1}^r \hat{H}_k \gamma_k(t)$ are equivalent. The basic idea of solving the convergence problem for the degenerate cases is: if we design $\gamma_k(t)$ to make condition (i) $\omega_{l,m,\gamma_1, \dots, \gamma_r} \neq \omega_{i,j,\gamma_1, \dots, \gamma_r}$, $(l, m) \neq (i, j)$, $i, j, l, m \in \{1, 2, \dots, N\}$ hold, $\omega_{l,m,\gamma_1, \dots, \gamma_r} = \lambda_{l,\gamma_1, \dots, \gamma_r} - \lambda_{m,\gamma_1, \dots, \gamma_r}$, where $\lambda_{l,\gamma_1, \dots, \gamma_r}$ is the l th eigenvalue of H_{02} and (ii) $\forall j \neq l$, for $k = 1, \dots, r$, there exists at least a $(\hat{H}_k)_{jl} \neq 0$, where $(\hat{H}_k)_{jl}$ is the (j,l) th element of \hat{H}_k . According to existing research results (Wang and Schirmer, 2010b; Kuang and Cong, 2010a,b), system 2 can converge from $\hat{\rho}_0 = U_1^\dagger \rho_0 U_1$ to $\hat{\rho}_f = U_1^\dagger \rho_f U_1$ by designing appropriate control laws $u_k(t) = \gamma_k(t) + v_k(t)$. If we design $\gamma_k(t) = 0$ when system 2 governed by Equation 8.43 converges to $\hat{\rho}_f$, that is, system 2 governed by Equation 8.42 converges to ρ_f , system 2 will become system 1, then the convergence of system 1 to ρ_f will be ensured. In fact, the evolution of system 1 can be viewed as a composite of two evolution processes: one is system 2 converging to ρ_f from ρ_0 and the other is $\gamma_k(t)$ converging to 0.

The control goal can be stated as follows: to design control laws $u_k(t) = \gamma_k(t) + v_k(t)$ such that the control system 1 depicted by Equation 8.42 can completely transfer from any initial state ρ_0 to the target state $\rho_f = U^\dagger \rho_0 U$, $U \in SU(N)$. For convenience, the control system in the following sections means system 1.

8.3.2 Derivation of Control Laws

The Lyapunov quantum control method based on the average value of an imaginary mechanical quantity is used here. The so-called imaginary mechanical quantity means that it is a linear Hermitian operator to be designed, and maybe not a physical observable.

We select the specific Lyapunov function as:

$$V(\rho) = \text{tr}(P_{\gamma_1, \dots, \gamma_r} \rho) \quad (8.44)$$

where $P_{\gamma_1, \dots, \gamma_r} = f(\gamma_1(t), \dots, \gamma_r(t))$ is a functional of $\gamma_k(t)$ and is positive definite.

For non-degenerate cases, the restriction $V(\rho_f) < V(\rho_0) < V(\rho_{\text{other}})$ should be held to make the system converge to the target state ρ_f from the initial state ρ_0 , where ρ_{other} represents any other state in the set $E = \{\rho | \dot{V}(\rho) = 0\}$ except the target state. Without this restriction, the system state trajectory may evolve to ρ_{other} , at which point all the control laws vanish because of $\dot{V}(\rho) = 0 \iff u_k(t) = 0 \ (k = 1, \dots, r)$ and the control system stay in ρ_{other} .

Here what we do is to design all the perturbations where $\gamma_k(t) = 0 \ (k = 1, \dots, r)$ holds only in the target state, that is, (i) $\gamma_k(\rho_f) = 0 \ (k = 1, \dots, r)$ and (ii) for $\rho \neq \rho_f$, there exists at least one k such that $\gamma_k(\rho) \neq 0$. Thus the restriction only needs to be $V(\rho_f) < V(\rho_{\text{other}})$ for degenerate cases.

In conclusion, the introduced perturbations $\gamma_k(t)$ have two tasks. One task is to solve the convergent problem of the control system in degenerate cases and the other is to choose a simpler restriction $V(\rho_f) < V(\rho_{\text{other}})$. According to the analysis mentioned above, let us design $\gamma_k(t) \ (k = 1, \dots, r)$. We design $\gamma_k(t)$ to be a monotonically increasing functional of $V(t)$ as:

$$\gamma_k(\rho) = C_k \cdot \theta_k(V(\rho) - V(\rho_f)) \quad (8.45)$$

where $C_k \geq 0$ and for $k = 1, \dots, r$, there exists at least a $C_k > 0$; $\theta_k(\cdot)$ is a function and satisfies $\theta_k(0) = 0$, $\theta_k(s) > 0$, $\theta'_k(s) > 0$ for every $s > 0$, where s is the independent variable of the function $\theta_k(\cdot)$.

From Equations 8.44 and 8.45, one can see that $V(t)$ and $\gamma_k(t)$ are the implicit functions of time t . The existence of $\gamma_k(t)$ can be depicted by Lemma 8.3.

Lemma 8.3 If $C_k = 0$, $\gamma_k(\rho) = 0$. Else if $C_k > 0$, $\theta_k \in C^\infty(R^+; [0, \gamma_k^*])$, $k = 1, \dots, r$ (γ_k^* is a positive constant) satisfies $\theta_k(0) = 0$, $\theta_k(s) > 0$, and $\theta'_k(s) > 0$ for every $s > 0$, and $|\theta'_k| < 1/(2C^*C_k)$, $C^* = 1 + C$, and $C = \max\{\|\partial P_{\gamma_1, \dots, \gamma_r}/\partial \gamma_k\|_{m_1}, (k = 1, \dots, r)\}$, then for every ρ there is a unique $\gamma_k \in C^\infty(\gamma_k \in [0, \gamma_k^*])$ satisfying $\gamma_k(\rho) = C_k \cdot \theta_k(\text{tr}(P_{\gamma_1, \dots, \gamma_r} \rho) - \text{tr}(P_{\gamma_1, \dots, \gamma_r} \rho_f)) \ (k = 1, \dots, r)$, where $\|\cdot\|_{m_1}$ represents m_1 norm.

Proof Assume $P_{\gamma_1, \dots, \gamma_r}$ are analytic functions of the perturbations $\gamma_k(\rho)$. $\partial P_{\gamma_1, \dots, \gamma_r}/\partial \gamma_k \ (k = 1, \dots, r)$ are bounded on $[0, \gamma_k^*]$, thus $C < \infty$. By Equations 8.44 and 8.45, the derivative of θ_k on γ_k is

$$\partial \theta_k / \partial \gamma_k = \theta'_k \text{tr}(\partial P_{\gamma_1, \dots, \gamma_r} / \partial \gamma_k (\rho - \rho_f)) \quad (8.46)$$

Define

$$F_k(\gamma_1, \dots, \gamma_r, \rho) = \gamma_k - C_k \cdot \theta_k(\text{tr}(P_{\gamma_1, \dots, \gamma_r} \rho) - \text{tr}(P_{\gamma_1, \dots, \gamma_r} \rho_f)) \quad (8.47)$$

where $F_k(\gamma_1, \dots, \gamma_r, \rho) \ (k = 1, \dots, r)$ are regular.

For a fixed ρ

$$F_k(\gamma_1(\rho), \dots, \gamma_r(\rho), \rho) = 0 \ (k = 1, \dots, r) \quad (8.48)$$

holds. By Equation 8.46, one can obtain

$$\partial F_k / \partial \gamma_k = 1 - C_k \theta'_k \text{tr}(\partial P_{\gamma_1, \dots, \gamma_r} / \partial \gamma_k \cdot (\rho - \rho_f)) \quad (8.49)$$

Some deduction shows that

$$|tr(\partial P_{\gamma_1, \dots, \gamma_r} / \partial \gamma_k \cdot (\rho - \rho_f))| \leq 2 \|\partial P_{\gamma_1, \dots, \gamma_r} / \partial \gamma_k\|_{m_1} \quad (8.50)$$

According to the given conditions, one can have

$$|C_k \theta'_k tr(\partial P_{\gamma_1, \dots, \gamma_r} / \partial \gamma_k \cdot (\rho - \rho_f))| < 1 \quad (8.51)$$

Then

$$\partial F_k(\gamma_1(\rho), \dots, \gamma_r(\rho), \rho) / \partial \gamma_k \neq 0 \quad (8.52)$$

holds. Thus, according to the implicit theorem (Krantz and Parks, 2002), Lemma 8.3 is proved. ■

The basic idea of designing $v_k(t)$ is to design the control laws $v_k(t)$ such that the first-order time derivative of the selected Lyapunov function $\dot{V}(t) \leq 0$ holds. For the sake of simplicity, set $\gamma_k(t) = 0$ for some k and other $\gamma_k(t)$ are equal, denoted by $\gamma(t)$, that is, set

$$\begin{aligned} \gamma_k(t) &= \gamma(t), C_k = 1, k = k_1, \dots, k_m; \\ C_k &= 0, k \neq k_1, \dots, k_m (1 \leq k_1, \dots, k_m \leq r) \end{aligned} \quad (8.53)$$

Correspondingly, Equation 8.44 can be rewritten as $V(\rho) = tr(P_\gamma \rho)$, where P_γ is a functional of $\gamma(t)$. By Equation 8.42, one can obtain the first-order time derivative of the selected Lyapunov function as:

$$\dot{V} = -itr \left(\left[P_\gamma, H_0 + \sum_{n=k_1}^{k_m} H_n \gamma(t) \right] \rho \right) - i \sum_{k=1}^r v_k(t) tr([P_\gamma, H_k] \rho) + \dot{\gamma} tr((\partial P_\gamma / \partial \gamma) \rho) \quad (8.54)$$

The sign of the first term in the right-hand side of Equation 8.54 is difficult to determine and this term can be eliminated by setting $\left[P_\gamma, H_0 + \sum_{n=k_1}^{k_m} H_n \gamma(t) \right] = 0$. How to satisfy the condition $\left[P_\gamma, H_0 + \sum_{n=k_1}^{k_m} H_n \gamma(t) \right] = 0$ will be specifically analyzed in Section 8.3.3. Then Equation 8.54 becomes

$$\dot{V} = -i \sum_{k=1}^r v_k(t) tr([P_\gamma, H_k] \rho) + \dot{\gamma} tr((\partial P_\gamma / \partial \gamma) \rho) \quad (8.55)$$

Equation 8.55 contains the time derivative of the implicit function perturbation $\dot{\gamma}(t)$, which needs to be eliminated. By Equations 8.45 and 8.53 one can obtain the time derivative of the implicit function perturbation $\dot{\gamma}(t)$ as:

$$\dot{\gamma}(t) = \left(i \theta' \sum_{k=1}^r v_k tr ([P_\gamma, H_k] \rho) \right) / (\theta' tr((\partial P_\gamma / \partial \gamma)(\rho - \rho_f)) - 1) \quad (8.56)$$

Substituting Equation 8.56 into Equation 8.55, one has

$$\dot{V} = - \frac{1 + \theta' tr((\partial P_\gamma / \partial \gamma) \rho_f)}{1 - \theta' tr((\partial P_\gamma / \partial \gamma)(\rho - \rho_f))} \sum_{k=1}^r itr([P_\gamma, H_k] \rho) v_k(t) \quad (8.57)$$

According to Equations 8.51 and 8.53, one can obtain $|\theta' \text{tr}((\partial P_\gamma / \partial \gamma) \rho_f)| < 1/2$, then $(1 + \theta' \text{tr}((\partial P_\gamma / \partial \gamma) \rho_f)) / (1 - \theta' \text{tr}((\partial P_\gamma / \partial \gamma)(\rho - \rho_f))) > 0$ holds. In order to ensure $\dot{V}(t) \leq 0$, $v_k(t)$ ($k = 1, \dots, r$) can be designed as

$$v_k(t) = K_k f_k(\text{itr}([P_\gamma, H_k] \rho)) \quad (k = 1, \dots, r) \quad (8.58)$$

where K_k is a constant, $K_k > 0$, and $y_k = f_k(x_k)$ ($k = 1, 2, \dots, r$) are monotonic functions through the coordinate origin and in the first quadrant and the third quadrant of the plane $x_k - y_k$.

8.3.3 Convergence Analysis

In this subsection, the convergence of the control system governed by Equation 8.42 will be analyzed based on LaSalle's invariance principle. According to this principle, if the Lyapunov function $V(t)$ satisfies $V(t) > 0$, $\dot{V}(t) \leq 0$, as $t \rightarrow \infty$, any trajectory will converge to the largest invariant set in $E = \{\rho | \dot{V}(\rho) = 0\}$. After this analysis, the convergence of the control system governed by Equation 8.42 can be depicted by Theorem 8.4.

Theorem 8.4 Consider the control system described by Equation 8.42 with control laws $\gamma_k(t)$ defined by Lemma 8.3, Equations 8.45 and 8.53, and $v_k(t)$ defined by Equation 8.58 if the control system satisfies the following four conditions:

1. $\omega_{l,m,\gamma} \neq \omega_{i,j,\gamma}$, $(l, m) \neq (i, j)$, $i, j, l, m \in \{1, 2, \dots, N\}$, $\omega_{l,m,\gamma} = \lambda_{l,\gamma} - \lambda_{m,\gamma}$, where $\lambda_{l,\gamma}$ is the l th eigenvalue of $H_0 + \sum_{n=k_1}^{k_m} H_n \gamma(t)$ corresponding to the eigenstate $|\phi_{l,\gamma}\rangle$.
2. $\forall j \neq l$, for $k = 1, \dots, r$, there exists at least a $(\hat{H}_k)_{jl} \neq 0$, where $(\hat{H}_k)_{jl}$ is the (j, l) th element of $\hat{H}_k = U_1^\dagger H_k U_1$ with $U_1 = (|\phi_{1,\gamma}\rangle, \dots, |\phi_{N,\gamma}\rangle)$.
3. $\left[P_\gamma, H_0 + \sum_{n=k_1}^{k_m} H_n \gamma(t) \right] = 0$, $1 \leq k_1, \dots, k_m \leq r$.
4. For any $l \neq j$ ($1 \leq l, j \leq N$), $(\hat{P}_\gamma)_{ll} \neq (\hat{P}_\gamma)_{jj}$ holds, where $(\hat{P}_\gamma)_{ll}$ is the (l, l) th element of $\hat{P}_\gamma = U_1^\dagger P_\gamma U_1$, then the control system will converge toward $E = \{\rho_{t_0} | (U_1^\dagger \rho_{t_0} U_1)_{ij} = 0, i \neq j, \gamma = \gamma(\rho_{t_0}), t_0 \in R\}$, where $\rho_{t_0} = \rho(t_0)$.

Proof Without loss of generality, assume that for $t \geq t_0$ ($t_0 \in R$), $\dot{V} = 0$ is satisfied. By Equations 8.57 and 8.58, one can obtain

$$\dot{V} = 0 \iff \text{tr}([P_\gamma, H_k] \rho) = 0 \iff v_k(t) = 0 \quad (8.59)$$

As $\dot{V} = 0$, γ are constants, which are denoted by $\bar{\gamma}$. According to the property of the trace, Equation 8.59 can be written as

$$\dot{V} = 0 \iff \text{tr}([\hat{P}_{\bar{\gamma}}, \hat{H}_k] \hat{\rho}) = 0 \iff v_k(t) = 0 \quad (8.60)$$

where $\hat{P}_{\bar{\gamma}} = U_1^\dagger P_{\bar{\gamma}} U_1$. Setting $\hat{\rho}_{t_0} = \hat{\rho}(t_0)$, the solution of Equation 8.44, with $\gamma_k(t)$ defined by Equations 8.45 and 8.53, $\gamma = \bar{\gamma}$ and $v_k(t) = 0$ is

$$\hat{\rho}(t) = e^{-i\left(\hat{H}_0 + \sum_{n=k_1}^{k_m} \hat{H}_n \bar{\gamma}\right)(t-t_0)} \hat{\rho}_{t_0} e^{i\left(\hat{H}_0 + \sum_{n=k_1}^{k_m} \hat{H}_n \bar{\gamma}\right)(t-t_0)} \quad (8.61)$$

Thus $\text{tr}([\hat{P}_{\bar{\gamma}}, \hat{H}_k] \hat{\rho}) = 0$ can be written as

$$\text{tr} \left(e^{-i\left(\hat{H}_0 + \sum_{n=k_1}^{k_m} \hat{H}_n \bar{\gamma}\right)(t-t_0)} \hat{\rho}_{t_0} e^{i\left(\hat{H}_0 + \sum_{n=k_1}^{k_m} \hat{H}_n \bar{\gamma}\right)(t-t_0)} [\hat{P}_{\bar{\gamma}}, \hat{H}_k] \right) = 0 \quad (8.62)$$

By condition (iii), $\hat{P}_{\bar{\gamma}}$ is a diagonal matrix, therefore $\hat{P}_{\bar{\gamma}} = e^{-i\left(\hat{H}_0 + \sum_{n=k_1}^{k_m} \hat{H}_n \bar{\gamma}\right)(t-t_0)}$ holds. Substituting this into Equation 8.62 one can obtain

$$\text{tr} \left(e^{i\left(\hat{H}_0 + \sum_{n=k_1}^{k_m} \hat{H}_n \bar{\gamma}\right)(t-t_0)} \hat{H}_k e^{-i\left(\hat{H}_0 + \sum_{n=k_1}^{k_m} \hat{H}_n \bar{\gamma}\right)(t-t_0)} [\hat{\rho}_{t_0}, \hat{P}_{\bar{\gamma}}] \right) = 0 \quad (8.63)$$

By $e^A B e^{-A} = \sum_{n=0}^{\infty} (1/n!) [A^{(n)}, B]$, one gets

$$\sum_{n=0}^{\infty} (1/n!) (i^n (t - t_0)^n) \text{tr} \left[\left(\left(\hat{H}_0 + \sum_{n=k_1}^{k_m} \hat{H}_n \bar{\gamma} \right)^{(n)}, \hat{H}_k \right) [\hat{\rho}_{t_0}, \hat{P}_{\bar{\gamma}}] \right] = 0 \quad (8.64)$$

where

$$\left[\left(\hat{H}_0 + \sum_{n=k_1}^{k_m} \hat{H}_n \bar{\gamma} \right)^{(n)}, \hat{H}_k \right] = \underbrace{\left[\left(\hat{H}_0 + \sum_{n=k_1}^{k_m} \hat{H}_n \bar{\gamma} \right), \left[\left(\hat{H}_0 + \sum_{n=k_1}^{k_m} \hat{H}_n \bar{\gamma} \right), \dots, \hat{H}_k \right] \right]}_{n \text{ times}}$$

Then one has

$$\sum_{j,l=1}^N \omega_{j,l,\bar{\gamma}}^n (\hat{H}_k)_{jl} ((\hat{P}_{\bar{\gamma}})_{ll} - (\hat{P}_{\bar{\gamma}})_{jj}) (\hat{\rho}_{t_0})_{lj} = 0, (k = 1, \dots, r) \quad (8.65)$$

where $(\hat{P}_{\bar{\gamma}})_{ll}$ is the (l, l) th element of $\hat{P}_{\bar{\gamma}}$. Set

$$\xi_k = \begin{bmatrix} (\hat{H}_k)_{12} ((\hat{P}_{\bar{\gamma}})_{22} - (\hat{P}_{\bar{\gamma}})_{11}) (\hat{\rho}_{t_0})_{21} \\ \vdots \\ (\hat{H}_k)_{(N-1)N} ((\hat{P}_{\bar{\gamma}})_{NN} - (\hat{P}_{\bar{\gamma}})_{(N-1)(N-1)}) (\hat{\rho}_{t_0})_{N(N-1)} \end{bmatrix} \quad (8.66a)$$

$$\Lambda = \text{diag}(\omega_{1,2,\bar{\gamma}}, \dots, \omega_{N-1,N,\bar{\gamma}}) \quad (8.66b)$$

$$M = \begin{bmatrix} 1 & 1 & \cdots & 1 \\ \omega_{1,2,\bar{\gamma}}^2 & \omega_{1,3,\bar{\gamma}}^2 & \cdots & \omega_{N,N-1,\bar{\gamma}}^2 \\ \vdots & \vdots & \vdots & \vdots \\ \omega_{1,2,\bar{\gamma}}^{N(N-1)-2} & \omega_{1,3,\bar{\gamma}}^{N(N-1)-2} & \cdots & \omega_{N,N-1,\bar{\gamma}}^{N(N-1)-2} \end{bmatrix} \quad (8.66c)$$

For $n = 0, 2, 4, \dots$, Equation 8.65 reads $M\mathfrak{F}(\xi_k) = 0$. For $n = 1, 3, 5, \dots$, Equation 8.65 reads $M\Lambda\mathfrak{R}(\xi_k) = 0$. By condition (i), M and Λ are non-singular real matrices. One can obtain $\xi_k = 0$, that is,

$$(\hat{H}_k)_{jl}((\hat{P}_{\bar{\gamma}})_{ll} - (\hat{P}_{\bar{\gamma}})_{jj})(\hat{\rho}_{t_0})_{lj} = 0 \quad (k = 1, \dots, r) \quad (8.67)$$

By condition (ii), one can have

$$((\hat{P}_{\bar{\gamma}})_{ll} - (\hat{P}_{\bar{\gamma}})_{jj})(\hat{\rho}_{t_0})_{lj} = 0 \quad (8.68)$$

that is, $[\hat{P}_{\bar{\gamma}}, \hat{\rho}_{t_0}] = 0$. Denote $\rho_{t_0} = \rho(t_0)$, then $[P_{\bar{\gamma}}, \rho_{t_0}] = 0$. According to condition (iv) in Theorem 8.4

$$(\hat{\rho}_{t_0})_{lj} = 0 \quad (8.69)$$

holds. Then Theorem 8.4 is proved based on LaSalle's invariance principle. ■

$\hat{\rho}_{t_0}$ is a diagonal matrix according to Equation 8.69. Since the evolution of $\hat{\rho}(t)$ is unitary in closed quantum systems, $\hat{\rho}(t)$ for $t \geq 0$ are isospectral. Denote the eigenvalues of the initial state $\hat{\rho}_0$ by $\hat{\lambda}_{01}, \hat{\lambda}_{02}, \dots, \hat{\lambda}_{0N}$. Then the diagonal elements of the states in $E_1 = \{\hat{\rho}|(\hat{\rho})_{ij} = 0\}$ are the various permutations of $\hat{\lambda}_{01}, \hat{\lambda}_{02}, \dots, \hat{\lambda}_{0N}$. According to Lemma 8.3, for every $\hat{\rho}_{t_0}$ there is a unique $\bar{\gamma}$, therefore E has at most $N!$ elements. For the target state ρ_f being a diagonal matrix, ρ_f is contained in E because $\gamma(\rho_f) = 0$. In the evolution process of the system's states, as $\dot{V}(t) \leq 0$, the Lyapunov function decreases. In order to make the system converge to the target state ρ_f , on the one hand, we need to design $P_{\bar{\gamma}}$ to make $V(\rho_f)$ small, that is,

$$V(\rho_f) < V(\rho_{\text{other}}) \quad (8.70)$$

where ρ_{other} represents any other state in the set E except the target state. On the other hand, we design $\gamma = \bar{\gamma} - \alpha$, ($0 < \alpha \ll \bar{\gamma}$) when $v_k(t) = 0$ and $\gamma(t) = \bar{\gamma} \neq 0$ hold for some time to make the state trajectory evolve but not stay in E until ρ_f is reached. For the target state which commutes with H_0 , that is, $[\rho_f, H_0] = 0$, if the control system satisfies the conditions in Theorem 8.4 and Equation 8.70, the state trajectory can converge to the target state from an arbitrary initial state unitarily equivalent to the target state.

Next we will analyze how to satisfy these conditions in detail.

Conditions (i) and (ii) in Theorem 8.4 are associated with H_0, H_k ($k = 1, \dots, r$), and $\gamma_k(t)$. By appropriately designing $\gamma_k(t)$, these two conditions can be satisfied in most cases. Condition (iii) means that $P_{\bar{\gamma}}$ and $H_0 + \sum_{n=k_1}^{k_m} H_n \gamma(t)$ have the same eigenstates $|\phi_{j,\gamma}\rangle$ ($j = 1, \dots, N$). If the eigenvalues of $P_{\bar{\gamma}}$ are designed to be constant, denoted by P_1, P_2, \dots, P_N , then $P_{\bar{\gamma}}$ can be written as

$$P_{\bar{\gamma}} = \sum_{j=1}^N P_j |\phi_{j,\gamma}\rangle \langle \phi_{j,\gamma}| \quad (8.71)$$

By condition (iii), \hat{P}_γ and $\hat{H}_0 + \sum_{n=k_1}^{k_m} \hat{H}_n \gamma(t)$ have the same eigenstates and $\hat{P}_\gamma = \text{diag}(P_1, P_2, \dots, P_N)$. If we design $P_l \neq P_j (\forall l \neq j; 1 \leq l, j \leq N)$, condition (iv) can be satisfied. As P_γ should be positive definite, we design $P_i > 0 (i = 1 \dots N)$. Then let us analyze how to make Equation 8.70 hold. The result is as follows:

Theorem 8.5 For the diagonal target state ρ_f , if $(\rho_f)_{ii} < (\rho_f)_{jj}, 1 \leq i, j \leq N$ holds, then design $P_i > P_j$; if $(\rho_f)_{ii} = (\rho_f)_{jj}, 1 \leq i, j \leq N$ holds, design $P_i \neq P_j$; else if $(\rho_f)_{ii} > (\rho_f)_{jj}, 1 \leq i, j \leq N$ holds, design $P_i < P_j$, then $V(\rho_f) < V(\rho_{\text{other}})$ holds.

Proof First, some useful propositions are proposed as follows. ■

Proposition 8.1 If the diagonal elements of the diagonal target state $\{(\rho_f)_{11}, (\rho_f)_{22}, \dots, (\rho_f)_{NN}\}$ are arranged in decreasing order, and $\{P_1, P_2, \dots, P_N\}$ are arranged in increasing order, then $V(\rho_f) < V(\rho_{\text{other}})$ holds.

Proof Denote $\rho_s = \text{diag}((\rho_f)_{11(\tau)}, (\rho_f)_{22(\tau)}, \dots, (\rho_f)_{NN(\tau)})$, where $\{11(\tau), 22(\tau), \dots, NN(\tau)\}$ is a permutation of $\{11, 22, \dots, NN\}$. First, we prove $V(\rho_f) < V(\rho_s)$ holds.

As H_0 is diagonal, $P_\gamma|_{\gamma=0} = \text{diag}(P_1, P_2, \dots, P_N)$, thus the Lyapunov function $V(\rho) = \text{tr}(P_\gamma \rho)$ for $\gamma = 0$ can be written as

$$V(\rho)|_{\gamma=0} = \sum_{j=1}^N P_j \rho_{jj} \quad (8.72)$$

Assume $(\rho_f)_{11} > (\rho_f)_{22} > \dots > (\rho_f)_{NN} \geq 0$ and $0 < P_1 < P_2 < \dots < P_N$.

For the level of the system $n=2$, one has

$$V(\rho_f)_2 - V(\rho_s)_2 = (P_1 - P_2)((\rho_f)_{11} - (\rho_f)_{22}) < 0 \quad (8.73)$$

where the subscript “2” in $V(\rho_f)_2$ and $V(\rho_s)_2$ means $n=2$. $V(\rho_f) < V(\rho_s)$ holds.

Assume that $V(\rho_f) < V(\rho_s)$ holds for $n=N-1$. Then

$$\begin{aligned} V(\rho_f)_{N-1} - V(\rho_s)_{N-1} &= \sum_{j=1}^{N-1} P_j ((\rho_f)_{jj} - (\rho_f)_{jj(\tau)}) \\ &= \sum_{j=1}^{N-1} (P_{j(\tau)} - P_j)(\rho_f)_{jj(\tau)} < 0 \end{aligned} \quad (8.74)$$

where $P_{j(\tau)} = (P_\gamma|_{\gamma=0})_{jj(\tau)}$. For $n=N$

$$V(\rho_f)_N - V(\rho_s)_N = \sum_{j=1}^{N-1} (P_{j(\tau)} - P_j)(\rho_f)_{jj(\tau)} + (P_{N(\tau)} - P_N)(\rho_f)_{NN(\tau)} \quad (8.75)$$

By Equation 8.75 and $0 < P_1 < P_2 < \dots < P_N$, one can get

$$V(\rho_f)_N - V(\rho_s)_N < 0 \quad (8.76)$$

Because $\partial \gamma / \partial V > 0$, $\dot{V} \leq 0$, and $V(\rho_s) < V(\rho_{\text{other}})$ holds, Proposition 8.1 is proved. ■

Proposition 8.2 If the diagonal elements of the diagonal target state $\{(\rho_f)_{11}, (\rho_f)_{22}, \dots, (\rho_f)_{NN}\}$ are arranged in a non-decreasing order with $(\rho_f)_{k_{11}k_{11}} = \dots = (\rho_f)_{k_{1L_1}k_{1L_1}} < (\rho_f)_{k_{21}k_{21}} = \dots = (\rho_f)_{k_{2L_2}k_{2L_2}} < \dots < (\rho_f)_{k_{Q1}k_{Q1}} = \dots = (\rho_f)_{k_{QL_Q}k_{QL_Q}}, \quad 1 \leq k_{ij} \leq N, k_{11} = 1, k_{QL_Q} = N$, where $i = 1, 2, \dots, Q$, and $j = 1, 2, \dots, L_1$ when $i = 1$, $j = 1, 2, \dots, L_2$ when $i = 2, \dots$, and $j = 1, 2, \dots, L_Q$ for $i = Q$. Design $\{P_1, P_2, \dots, P_N\}$ as follows: $P_{k_{11}} > \dots > P_{k_{1L_1}} > \dots > P_{k_{Q1}} > \dots > P_{k_{QL_Q}} > 0$, then $V(\rho_f) < V(\rho_{other})$ holds.

Proof Obviously, $V(\rho_f) < V(\rho_s)$ holds for $n = 2$. Assume that for $n = N - 1$, $V(\rho_f) < V(\rho_s)$ is true. Then Equation 8.74 holds. For $n = N$, if $(\rho_f)_{(N-1)(N-1)} < (\rho_f)_{NN}$, design $P_{k_{11}}, \dots, P_{k_{1L_1}} > \dots > P_N$, then Equation 8.76 holds. If $(\rho_f)_{k_{Q1}k_{Q1}} = (\rho_f)_{k_{Q2}k_{Q2}} = \dots = (\rho_f)_{NN}$, then $NN(\tau) \neq k_{Q1}k_{Q1} \neq \dots \neq k_{QL_Q-1}k_{QL_Q-1}$ in Equation 8.75. Design $P_{k_{11}}, \dots, P_{k_{1L_1}} > \dots > P_{k_{Q1}}, \dots, P_{k_{QL_Q}}$, then Equation 8.76 holds. Proposition 8.2 is proved. ■

Obviously, according to Propositions 8.1 and 8.2 we can obtain Theorem 8.5.

From the convergence analysis mentioned above, one can see that the proposed method can only ensure that the control system converges to the target state ρ_f which commutes with H_0 , that is, $[\rho_f, H_0] = 0$. For the target state which does not commute with H_0 , that is, $[\rho_f, H_0] \neq 0$, further research needs to be done. We introduce a series of disturbances η_k ($k = 1, \dots, r$) whose values are constant. Thus the dynamical Equation 8.42 will become

$$i\dot{\rho}(t) = \left[H_0 + \sum_{k=1}^r H_k (\gamma_k(t) + v_k(t) + \eta_k), \rho(t) \right] \quad (8.77)$$

where $\gamma_k(t) + v_k(t) + \eta_k = u_k(t)$ are the total control laws. Our basic idea is to design η_k to make the target state ρ_f satisfy $[\rho_f, (H_0 + \sum_{k=1}^r H_k \eta_k)] = 0$, where r is an integer number. Define $H'_0 = H_0 + \sum_{k=1}^r H_k \eta_k$, which can be regarded as the new internal Hamiltonian of the control system. If r is large enough, $[\rho_f, H'_0] = 0$ can be satisfied in most cases by designing η_k appropriately. Then one can design control laws according to Section 8.3.2.

8.3.4 Numerical Simulations

In order to verify the effectiveness of the proposed method, a three-level system is considered in this subsection and numerical simulations are done for a non-diagonal target state case.

Consider a three-level system with H_0 and H_1 as:

$$H_0 = \begin{bmatrix} 0.3 & 0 & 0 \\ 0 & 0.6 & 0 \\ 0 & 0 & 0.9 \end{bmatrix}, \quad H_1 = \begin{bmatrix} 0 & 1 & 1 \\ 1 & 0 & 0 \\ 1 & 0 & 0 \end{bmatrix} \quad (8.78)$$

According to H_0 and H_1 , the system is a degenerate case. Assume that the initial state is a mixed state:

$$\rho_0 = \begin{bmatrix} 0.1 & 0.1 & 0.04 \\ 0.1 & 0.5 & 0.08 \\ 0.04 & 0.08 & 0.4 \end{bmatrix}$$

and that the target state is also a mixed state:

$$\rho_f = \begin{bmatrix} 0.1085 & 0.0755 & 0.0745 \\ 0.0755 & 0.3354 & 0 \\ 0.0745 & 0 & 0.5560 \end{bmatrix}$$

According to the design ideas introduced in Section 8.3.3, the control law is $u_1(t) = \gamma_1(t) + v_1(t) + \eta_1$, where perturbation $\gamma_1(t)$ is designed as

$$\gamma_1(\rho) = M_1 \cdot (tr(P_{\gamma_1} \rho) - tr(P_{\gamma_1} \rho_f)) \quad (8.79)$$

and $v(t)$ is designed as

$$v_1(t) = K_1 (itr([P_{\gamma_1}, H_1] \rho)) \quad (8.80)$$

where M_1 is the proportional coefficient of γ_1 , $M_1 > 0$, and $P_{\gamma_1} = \sum_{j=1}^3 P_j |\phi'_{j,\gamma_1}\rangle \langle \phi'_{j,\gamma_1}|$, where $|\phi'_{j,\gamma_1}\rangle$ is the j th eigenvector of $[H_0 + H_1(\gamma_1(t) + \eta_1)]$.

In order to make $[\rho_f, (H_0 + H_1\eta_1)] = 0$ hold, we set $\eta_1 = 0.1$. Then the control system in the eigenbasis of $H'_0 = H_0 + H_1\eta_1$ is

$$i\dot{\hat{\rho}}(t) = [\hat{\tilde{H}}_0 + \hat{\tilde{H}}_1(\gamma_1(t) + v_1(t) + \eta_1), \hat{\tilde{\rho}}(t)] \quad (8.81)$$

where $\hat{\tilde{H}}_0 = diag(0.9171, 0.6275, 0.2555)$, and

$$\hat{\tilde{H}}_1 = \begin{bmatrix} 0.3488 & -0.4185 & 0.9142 \\ -0.4185 & 0.4550 & -0.7083 \\ 0.9142 & -0.7083 & -0.8037 \end{bmatrix}.$$

Accordingly, the target state ρ_f will be transformed to $\hat{\tilde{\rho}}_f = diag(0.5687, 0.3562, 0.075)$.

In the numerical simulations, according to the specific design principle of the imaginary mechanical quantity proposed in Section 8.3.3, design P_1, P_2, P_3 such that $P_1 < P_2 < P_3$. Denoting the terminal time of the numerical simulations as t_f , the principle of regulating P_1, P_2, P_3 is as follows: in general, if $(\hat{\tilde{\rho}}(t_f))_{ii} < (\hat{\tilde{\rho}}_f(t_f))_{ii}$, decrease P_i ; else if $(\hat{\tilde{\rho}}(t_f))_{ii} > (\hat{\tilde{\rho}}_f(t_f))_{ii}$, increase P_i , where $(\hat{\tilde{\rho}}(t_f))_{ii}$ and $(\hat{\tilde{\rho}}_f(t_f))_{ii}$ are the (i,i) th elements of $\hat{\tilde{\rho}}(t_f)$ and $\hat{\tilde{\rho}}_f(t_f)$, respectively. Sometimes this method dose not work because P_i influences not only $\hat{\tilde{\rho}}_{ii}$ but also other elements of $\hat{\tilde{\rho}}$. The principle of regulating K_1 is: the larger K_1 is, the faster the system converges to the target state. However, after K_1 exceeds a certain value, the transition probability will decrease, the control effect will deteriorate, and the system even may oscillate. The principle of regulating M_1 is: regulate M_1 to be as small as possible on the premise that the perturbations take effect to make the control system exhibit a behavior of trending to the target state. After tuning the control parameters repeatedly and carefully, the control parameters are selected as $M_1 = 0.1$, $K_1 = 0.34$, $P_1 = 0.01$, $P_2 = 2$, and $P_3 = 2.9$.

In the simulations, the sample time is set as 0.01 a.u. and the control duration is 500 a.u. The results of numerical simulations are shown in Figures 8.6 and 8.7, in which Figure 8.6 displays the evolution curves of ρ_{ij} ($i, j = 1, 2, 3$), where ρ_{ij} is the $(i,-j)$ th diagonal element of ρ . Figure 8.7 shows the designed control laws $v_1(t)$, $\gamma_1(t)$, and $u_1(t)$.

According to numerical results, the state at 500 a.u. is $\rho_{11} = 0.10827$, $\rho_{12} = 0.075312$, $\rho_{13} = 0.074573$, $\rho_{22} = 0.33582$, and $\rho_{33} = 0.5559$. The transition probability is able to reach more than 99.92%.

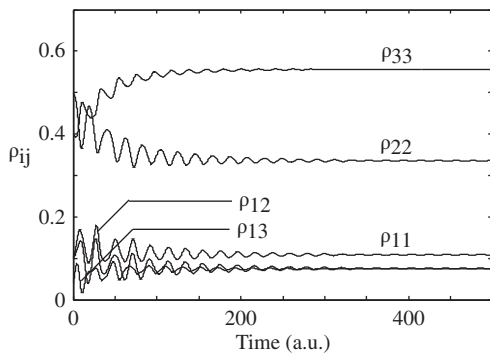


Figure 8.6 Evolution curves of ρ_{ij}

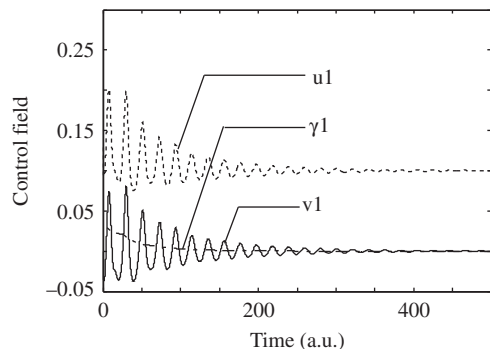


Figure 8.7 Control fields

In this chapter, for non-degenerate and degenerate cases, the existing quantum Lyapunov control based on the state distance, state error, and average value of an imaginary mechanical quantity for the control systems have been summarized and analyzed. For the target state being the eigenstate, the mixed state which commutes with the internal Hamiltonian, the superposition state, and the mixed state which does not commute with the internal Hamiltonian state the design methods of the control laws have been summarized, and the convergence to the target state has been summarized and analyzed. Research results show that the Lyapunov-based quantum control method can make the control system converge from any initial state to the target state in both non-degenerate and degenerate cases. After 10 years of development, the quantum control theory based on the Lyapunov stability theorem has been established.

References

- Beaucharda, K., Coronb, J.M., Mirrahimic, M. et al. (2007) Implicit Lyapunov control of finite dimensional Schrödinger equations. *Systems & Control Letters*, **56**(5), 388–395.
 Cong, S. and Kuang, S. (2007) Quantum control strategy based on state distance. *Acta Automatica Sinica*, **33**(1), 28–31.

- Grivopoulos, S. and Bamieh, B. (2003) Lyapunov-based control of quantum systems. Proceedings of the 42nd IEEE Conference on Decision and Control, Maui, pp. 434–438.
- Krantz, S.G. and Parks, H.R. (2002) *The Implicit Function Theorem: History, Theory, and Applications*, Birkhauser, Boston, MA.
- Kuang, S. and Cong, S. (2008) Lyapunov control methods of closed quantum systems. *Automatica*, **44**(1), 98–108.
- Kuang, S. and Cong, S. (2010a) Population control on equilibrium states of quantum systems via Lyapunov method. *Acta Automatica Sinica*, **36**(9), 1257–1263.
- Kuang, S. and Cong, S. (2010b) Lyapunov stabilization strategy of mixed-state quantum systems with ideal conditions. *Control and Decision*, **25**(2), 273–277.
- LaSalle, J. and Lefschetz, S. (1961) *Stability By Liapunov's Direct Method With Applications*, Academic Press, New York.
- Mirrahimi, M., Rouchon, P. and Turinici, G. (2005a) Lyapunov control of bilinear Schrödinger equations. *Automatica*, **41**(11), 1987–1994.
- Mirrahimi, M., Turinici, G. and Rouchon, P. (2005b) Reference trajectory tracking for locally designed coherent quantum controls. *Journal of Physical Chemistry A*, **109**(11), 2631–2637.
- Wang, X. and Schirmer, S. (2010a) Analysis of Lyapunov method for control of quantum states. *IEEE Transactions on Automatic Control*, **55**(10), 2259–2270.
- Wang, X. and Schirmer, S. (2010b) Analysis of effectiveness of Lyapunov control for non-generic quantum states. *IEEE Transactions on Automation Control*, **55**(6), 1406–1411.
- Zhao, S.W., Lin, H., Sun, J.T. et al. (2009) Implicit Lyapunov control of closed quantum systems. Joint 48th IEEE Conference on Decision and Control and 28th Chinese Control Conference, Shanghai, P.R. China, pp. 3811–3815.
- Zhao, S.W., Lin, H., Sun, J.T. et al. (2012) An implicit Lyapunov control for finite-dimensional closed quantum systems. *International Journal of Robust and Nonlinear Control*, **22**(11), 1212–1228.

9

Manipulation Methods of the General State

9.1 Quantum System Schmidt Decomposition and its Geometric Analysis

The essential difference between a quantum system and a classical system in engineering is quantum entanglement. Since this concept was proposed in the last century it has played a critical role in quantum theory and is believed to be the key point in quantum information science. Entanglement means non-local property in physical theory and the entanglement of a multi-particle system cannot be described by the combination of several single-particle system states. However, the Schmidt decomposition can be used to analysis the entanglement of a two-particle quantum system. Considering the pure state of a two-qubit system $|\psi\rangle_{AB}$, if the quantum state can be separated into a product, then $|\psi\rangle_{AB} = |\psi\rangle_A \otimes |\psi\rangle_B$ is said to be separable, where $|\psi\rangle_A \in H_A$, $|\psi\rangle_B \in H_B$, and H_A and H_B are the Hilbert spaces of the individual particles. Otherwise, the state is called an entangled state. There are a great number of good definitions of the entanglement for the degree of a two-particle quantum system pure state (Ayman *et al.*, 2001; Ekert, 1991). The definition of the entanglement of formation was proposed by Hill and Wootters in a two spin-1/2 particles quantum system (Hill and William, 1997; William, 1998). Vedral proposed a definition of entanglement based on the distance (Vedral and Plenio, 1998). The Schmidt decomposition is an effective mathematical tool for understanding quantum entanglement. The pure state of a two-qubit system $|\psi\rangle_{AB}$ could be decomposed as follows, if it is an entangled state:

$$|\psi\rangle = \sqrt{p_1}|u_1\rangle \otimes |v_1\rangle + \sqrt{p_2}|u_2\rangle \otimes |v_2\rangle = \sum_i \sqrt{p_i}|u_i\rangle \otimes |v_i\rangle \quad (9.1)$$

in which $\sum_i p_i = 1$, $p_1, p_2 \neq 0$; $\{|u\rangle\}$ is the unit orthogonal vectors of the Hilbert space H_A , and $\{|v\rangle\}$ is the unit orthogonal vectors of the Hilbert space H_B . This decomposition is called the Schmidt decomposition (Ekert and Peter, 1995). Moreover, this decomposition always exists for a two-particle pure state of a quantum system, but it does not always exist for a three-particle system pure state or more.

A quantum system can be described by the intuitionistic mathematical language of geometric algebra (Shyamal, Anthony, and Chris, 1999), which provides an effective mathematical instrument for a multi-particle quantum system. Geometric algebra can be used to express the Schmidt decomposition of a two-qubit pure state. This geometric algebra expression contains the geometric products of single spinor part and a two-particle spinor part, which will help us to understand the quantum system more deeply. The Bloch vector is used to describe the geometric prospect of each subsystem, so the information of the quantum system can be learned from the interactional information of the subsystem.

In this section, the Schmidt decomposition of a two-particle quantum system is first introduced, and then the entanglement degree is discussed based on this decomposition. Moreover, the geometric prospect of the quantum system is proposed using the Bloch vector, which will demonstrate the character of the quantum system incisively and vividly.

9.1.1 Schmidt Decomposition of Quantum States

Considering a two-particle quantum system in the Hilbert space, the interactional Hilbert space of a two-particle quantum system can be denoted by $H_A \otimes H_B$, where H_A and H_B are the Hilbert spaces of the individual particles. The pure state of the quantum system $|\psi\rangle \in H_A \otimes H_B$ can be described by $|\psi\rangle = \sum_{i,j} a_i b_j |i\rangle \otimes |j\rangle = \sum_{i,j} a_i b_j |i\rangle |j\rangle = \sum_{i,j} a_i b_j |i, j\rangle$. If more than one of the coefficients a_i, b_j is non-zero, it is an entangled state.

We introduce the theorem of the Schmidt decomposition here: The composite system of two subsystems H_A and H_B forms the Hilbert space $H_A \otimes H_B$. To any pure state of this space $|\psi\rangle_{AB} = \sum_{i,j} a_{ij} |i\rangle_A \otimes |j\rangle_B$, the state can be decomposed into state $|\psi\rangle_{AB} = \sum_i \sqrt{p_i} |i\rangle_A |i'\rangle_B$, where $\sum_i p_i = 1$, and $\sum_{i,j} a_{ij}^2 = 1$, $\{|i\rangle_A\}$ and $\{|i'\rangle_A\}$ are the unit orthogonal vectors of the Hilbert space H_A , and $\{|j\rangle_B\}$ and $\{|i'\rangle_B\}$ are the unit orthogonal vectors of the Hilbert space H_B .

The properties of the Schmidt decomposition are as follows:

1. The Schmidt decomposition can only be used in pure state of a two-particle quantum system. Different states $|\psi\rangle_1$ and $|\psi\rangle_2$ have different decompositions.
2. The two subsystems do not need to have the same dimension in the Schmidt decomposition, and the summation over the single index in the Schmidt decomposition goes to the smaller of the dimensionalities of the Hilbert spaces.
3. The reduced density matrices of systems ρ_A and ρ_B have the same eigenvalues, so ρ_A and ρ_B have the same von Neumann entropy.
4. The Schmidt decomposition cannot, in general, be extended to more than two subsystems.

Next, we prove that the Schmidt decomposition cannot be extended to more than two subsystems by using the example of a three-particle quantum system. If the Schmidt decomposition exists in a three-particle quantum system, the state could be expressed as follows:

$$|\varphi\rangle_{ABC} = \sum_i \sqrt{p_i} |i\rangle_A \otimes |i\rangle_B \otimes |i\rangle_C$$

in which $|\varphi\rangle$ is a normalized state and $\{|i\rangle_A\}$, $\{|i\rangle_B\}$, and $\{|i\rangle_C\}$ are the unit orthogonal vectors of the Hilbert spaces H_A , H_B , and H_C separately.

Then the diagonal reduced density matrices of subsystems A, B, and C can be calculated under the Schmidt orthogonal vectors, and the three matrices have the same eigenvalues $\sqrt{p_i}$. The eigenvalues of the subsystem are not changed under the local unitary transformation, and all the reduced-density matrices have the same eigenvalues. In conclusion, the necessary condition of the existence of the Schmidt decomposition is that all the reduced-density matrices have the same eigenvalues. However, not any pure state $|\varphi\rangle_{ABC}$ satisfies this necessary condition. Consider the following quantum state:

$$|\psi\rangle_{ABC} = |0\rangle_A \left(\frac{1}{\sqrt{2}} (|00\rangle_{BC} + |11\rangle_{BC}) \right)$$

$$\rho_{ABC} = |\psi\rangle_{ABC} \langle \psi| = \frac{1}{2} (|000\rangle \langle 000| + |000\rangle \langle 011| + |011\rangle \langle 000| + |011\rangle \langle 011|)$$

The reduced density matrices of subsystem ρ_A , ρ_B , and ρ_C are

$$\rho_A = \text{tr}_B \text{tr}_C \rho_{ABC} = |0\rangle_{AA} \langle 0| = \begin{bmatrix} 1 & 0 \\ 0 & 0 \end{bmatrix}, \quad \rho_B = \rho_C = \begin{bmatrix} 1/2 & 0 \\ 0 & 1/2 \end{bmatrix} \quad (9.2)$$

Based on property (3) of the Schmidt decomposition mentioned above, if $|\psi\rangle_{ABC}$ can be decomposed, ρ_A , ρ_B , and ρ_C must have the same eigenvalues. However, Equation 9.2 denotes that ρ_A , ρ_B , and ρ_C do not have the same eigenvalues, so $|\psi\rangle_{ABC}$ does not exist the Schmidt decomposition. Based on the above analysis we can obtain the conclusion that no pure state of a three-particle quantum system can be decomposed in this way. In general, this conclusion can be extended to more than two subsystems.

9.1.2 Definition of Entanglement Degree Based on the Schmidt Decomposition

A definition of the entanglement degree of a two-qubit system based on the Schmidt decomposition will be proposed in this subsection. Considering the Schmidt decomposition in Equation 9.1, the reduced-density matrices ρ_A and ρ_B of two subsystems A and B have the same eigenvalues $\sqrt{p_i}$. The two subsystems also have the same von Neumann entropy, $S(\rho_A) = S(\rho_B)$. Now we can define the entanglement degree of the system $E(\psi)$:

$$E(\psi) = S(\rho_A) = S(\rho_B) = -\text{tr}(\rho_A \log_2 \rho_A) = -\sum_i p_i \log_2 p_i$$

Because the two-qubit system has the property of $p_1 + p_2 = 1$, let $p_1 = p$ and $p_2 = 1 - p$. Then another expression of entanglement degree can be obtained as:

$$E(\psi) = -p \log_2 p - (1 - p) \log_2 (1 - p)$$

The entanglement degree E changes with p as shown in Figure 9.1. The range of entanglement degree is from 0 to 1. When $p_1 = p_2 = 1/2$, the entanglement degree is maximal, which is equal to 1. At this time, the state is called the maximal entangled state. When $p_1 = 0$ or $p_2 = 0$, the quantum state is separable, and the entanglement degree is 0. The Bell states $|\psi^\pm\rangle$ and $|\varphi^\pm\rangle$ are maximal entangled states.

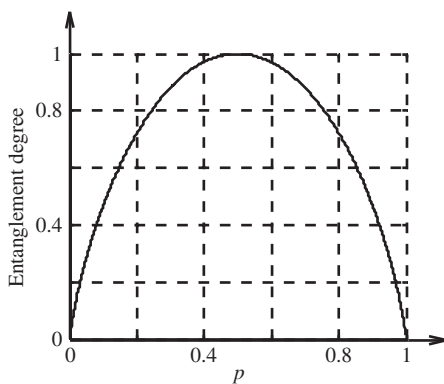


Figure 9.1 The entanglement degree of a quantum system changed with p

9.1.3 Application of the Schmidt Decomposition

The simplest form of the Hamiltonian for a system of n coupled nuclear spins is:

$$H_{\text{sys}} = - \sum_i \hbar \omega_0^i I_z^i + \hbar \sum_{i < j} 2\pi J_{ij} I_z^i I_z^j$$

in which $\omega_0^i/2\pi$ is the Larmor frequency of the i th qubit:

$$I_z = \frac{1}{2} \sigma_z = \frac{1}{2} \begin{bmatrix} 1 & 0 \\ 0 & -1 \end{bmatrix}$$

A quantum system can be described by this Hamilton clearly in nuclear magnetic resonance (NMR) quantum computation (Lieven and Chuang, 2005). A two-qubit logical gate can be produced by the interactional Hamilton, and this Hamilton can be expressed as

$$H_J = \hbar 2\pi J I_z^1 I_z^2$$

The time-dependent operator can be obtained as

$$U_J(t) = \exp(-i2\pi J I_z^1 I_z^2 t)$$

If the original state is $|\psi(0)\rangle$, the state $|\psi(t)\rangle = U_J(t)|\psi(0)\rangle$ can be obtained by applying a unitary transformation $U_J(t)$. The unitary operator $U_J(t)$ can be expressed as

$$U_J(t) = \begin{bmatrix} e^{-i\pi J t/2} & 0 & 0 & 0 \\ 0 & e^{i\pi J t/2} & 0 & 0 \\ 0 & 0 & e^{i\pi J t/2} & 0 \\ 0 & 0 & 0 & e^{-i\pi J t/2} \end{bmatrix}$$

The CNOT gate U_{CNOT} and controlled phase gate U_{CPHASE} can be constructed by $U_J(t)$.

The theorem of quantum computation (Lieven and Chuang, 2005) indicates that any unitary transformations of n -qubit can be constructed by using CNOT gates U_{CNOT} and single qubit gates $R_{\hat{n}}(\theta)$, so the quantum control can be simplified to the realization of U_{CNOT} and $R_{\hat{n}}(\theta)$.

The CNOT gate flips the second qubit (the target) if and only if the control is $|1\rangle$, and this gate is the analog of the classical exclusive-or gate, since $U_{\text{CNOT}}|i\rangle|j\rangle = |i\rangle|i \oplus j\rangle$, where $i, j \in \{0, 1\}$. Choose the original state

$$|\psi(0)\rangle_{AB} = c_0|00\rangle + c_1|01\rangle + c_2|10\rangle + c_3|11\rangle$$

where $|c_0|^2 + |c_1|^2 + |c_2|^2 + |c_3|^2 = 1$. The state of the quantum system at time t is

$$\begin{aligned} |\psi(t)\rangle_{AB} &= U_J(t)|\psi(0)\rangle_{AB} = c_0e^{-i\pi Jt/2}|00\rangle + c_1e^{i\pi Jt/2}|01\rangle \\ &\quad + c_2e^{i\pi Jt/2}|10\rangle + c_3e^{-i\pi Jt/2}|11\rangle \end{aligned}$$

To decompose the state $|\psi(t)\rangle$, let $\{u_i(t)\}$ and $\{v_i(t)\}$ be the unit orthogonal vectors of the Hilbert space H_A and H_B separately; the orthogonal vectors are time-dependent. So the expression of the Schmidt decomposition is

$$|\psi(t)\rangle_{AB} = k_1(t)|u_1(t)\rangle \otimes |v_1(t)\rangle + k_2(t)|u_2(t)\rangle \otimes |v_2(t)\rangle$$

in which $|k_1(t)|^2 + |k_2(t)|^2 = 1$.

The reduced density matrices of the subsystems are expressed as:

$$\begin{aligned} \rho_A &= |k_1(t)|^2|u_1(t)\rangle\langle u_1(t)| + |k_2(t)|^2|u_2(t)\rangle\langle u_2(t)| \\ \rho_B &= |k_1(t)|^2|v_1(t)\rangle\langle v_1(t)| + |k_2(t)|^2|v_2(t)\rangle\langle v_2(t)| \end{aligned}$$

and ρ_A and ρ_B have the same eigenvalues, $|k_1(t)|^2$ and $|k_2(t)|^2$, and they also have the same von Neumann entropy.

The density matrix of the composite system ρ_{AB} is now:

$$\begin{aligned} \rho_{AB}(t) &= |\psi(t)\rangle_{AB}\langle\psi(t)| \\ &= |c_0|^2|0\rangle_A\langle 0| \otimes |0\rangle_B\langle 0| + |c_1|^2|0\rangle_A\langle 0| \otimes |1\rangle_B\langle 1| + |c_2|^2|1\rangle_A\langle 1| \otimes |0\rangle_B\langle 0| \\ &\quad + |c_3|^2|1\rangle_A\langle 1| \otimes |1\rangle_B\langle 1| \\ &\quad + c_0\bar{c}_1e^{-i\pi Jt}|0\rangle_A\langle 0| \otimes |0\rangle_B\langle 1| + c_0\bar{c}_2e^{-i\pi Jt}|0\rangle_A\langle 1| \otimes |0\rangle_B\langle 0| + c_0\bar{c}_3|0\rangle_A\langle 1| \otimes |0\rangle_B\langle 1| \\ &\quad + c_1\bar{c}_0e^{i\pi Jt}|0\rangle_A\langle 0| \otimes |1\rangle_B\langle 0| + c_1\bar{c}_2|0\rangle_A\langle 1| \otimes |1\rangle_B\langle 0| + c_1\bar{c}_3e^{i\pi Jt}|0\rangle_A\langle 1| \otimes |1\rangle_B\langle 1| \\ &\quad + c_2\bar{c}_0e^{i\pi Jt}|1\rangle_A\langle 0| \otimes |0\rangle_B\langle 0| + c_2\bar{c}_1|1\rangle_A\langle 0| \otimes |0\rangle_B\langle 1| + c_2\bar{c}_3e^{i\pi Jt}|1\rangle_A\langle 1| \otimes |0\rangle_B\langle 1| \\ &\quad + c_3\bar{c}_0|1\rangle_A\langle 0| \otimes |1\rangle_B\langle 0| + c_3\bar{c}_1e^{-i\pi Jt}|1\rangle_A\langle 0| \otimes |1\rangle_B\langle 1| + c_3\bar{c}_2e^{-i\pi Jt}|1\rangle_A\langle 1| \otimes |1\rangle_B\langle 0| \end{aligned}$$

The density matrices of subsystems A and B under the orthogonal vectors $\{|0\rangle, |1\rangle\}$ are:

$$\rho_A(t) = \begin{bmatrix} |c_0|^2 + |c_1|^2 & c_0\bar{c}_2e^{-i\pi Jt} + c_1\bar{c}_3e^{i\pi Jt} \\ c_2\bar{c}_0e^{i\pi Jt} + c_3\bar{c}_1e^{-i\pi Jt} & |c_2|^2 + |c_3|^2 \end{bmatrix} \quad (9.3a)$$

$$\rho_B(t) = \begin{bmatrix} |c_0|^2 + |c_2|^2 & c_0\bar{c}_1e^{-i\pi Jt} + c_2\bar{c}_3e^{i\pi Jt} \\ c_1\bar{c}_0e^{i\pi Jt} + c_3\bar{c}_2e^{-i\pi Jt} & |c_1|^2 + |c_3|^2 \end{bmatrix} \quad (9.3b)$$

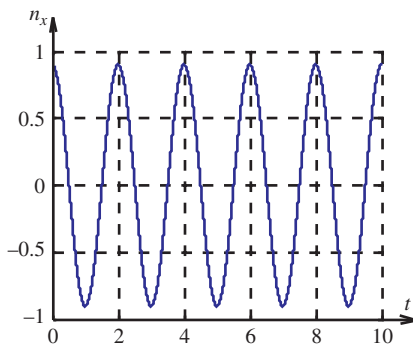


Figure 9.2 The sub-vector of the Bloch vector n in σ_x

Now we use the Bloch vector to analysis the subsystem:

$$\rho_A = \frac{1}{2}(I + \vec{\sigma} \cdot \vec{n}_A) = \frac{1}{2} \begin{bmatrix} 1 + n_{A3}(t) & n_{A1}(t) + in_{A2}(t) \\ n_{A1}(t) - in_{A2}(t) & 1 - n_{A3}(t) \end{bmatrix} \quad (9.4)$$

Comparing Equations 9.3a and 9.4 we can obtain:

$$\begin{aligned} n_{A1}(t) &= c_0\bar{c}_2e^{-i\pi Jt} + c_1\bar{c}_3e^{i\pi Jt} + c_2\bar{c}_0e^{i\pi Jt} + c_3\bar{c}_1e^{-i\pi Jt} \\ n_{A2}(t) &= -i(c_0\bar{c}_2e^{-i\pi Jt} + c_1\bar{c}_3e^{i\pi Jt} - c_2\bar{c}_0e^{i\pi Jt} - c_3\bar{c}_1e^{-i\pi Jt}) \\ n_{A3}(t) &= |c_0|^2 + |c_1|^2 - |c_2|^2 - |c_3|^2 \end{aligned}$$

in which $n_{A1}(t)$ and $n_{A2}(t)$ are time-dependent, so the Bloch vector of subsystem A is also time-dependent. The orthogonal vectors of the Hilbert space, which is obtained by the Schmidt decomposition, also change with time. If the norm of the Bloch vector of subsystem A is time-dependent, the eigenvalues and entanglement degree are also time-variable. When the norm of Bloch vector is 0, the state of subsystem A is called the maximal mixed state and the composite system reaches the maximal entangled stated. When the norm of the Bloch vector is 1, the state of subsystem A is a pure state and the composite system is separable.

Now supposing the original state is

$$|\psi(0)\rangle_{AB} = \sqrt{\frac{1}{8}}|00\rangle + \sqrt{\frac{1}{4}}|01\rangle + \sqrt{\frac{7}{16}}|10\rangle + \sqrt{\frac{3}{16}}|11\rangle$$

The subvectors of the Bloch vector of subsystem A in the directions σ_x , σ_y , and σ_z are shown in Figures 9.2–9.4, respectively.

The Bloch vector of subsystem A is shown in Figure 9.5. The Bloch vector n is always in the unit sphere, which indicates that the quantum state is entangled. The two-qubit state is always an entangled state.

The Bloch vector of the subsystem has the same direction as one of the decomposed vectors of Schmidt decomposition and has the opposite direction to the other decomposed vectors of the Schmidt decomposition. For example, the decomposed vectors of the Schmidt decompositions $|u_1(t)\rangle$ and $|u_2(t)\rangle$ correspond to the Bloch vectors \mathbf{m}_1 and \mathbf{m}_2 . $|u_1(t)\rangle$ and $|u_2(t)\rangle$ are

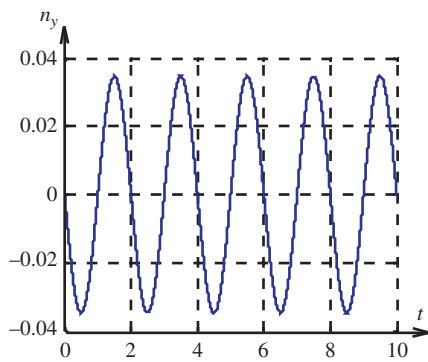


Figure 9.3 The sub-vector of the Bloch vector n in σ_y

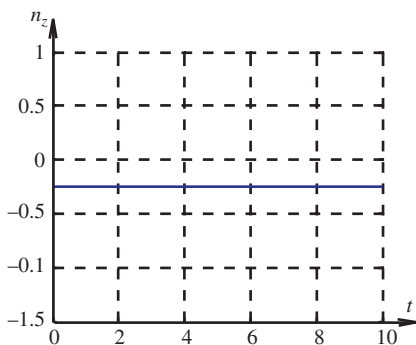


Figure 9.4 The sub-vector of the Bloch vector n in σ_z

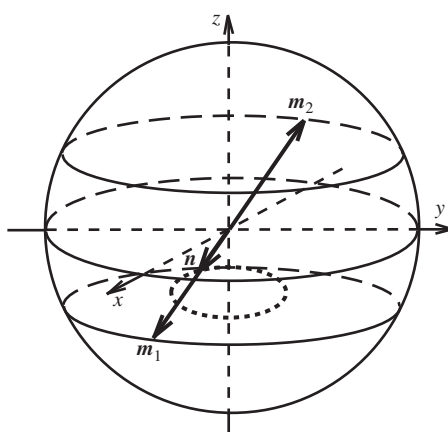


Figure 9.5 The variation of the Bloch vector n

orthogonal vectors, and the corresponding Bloch vectors \mathbf{m}_1 and \mathbf{m}_2 have opposite directions whose norms are both equal to 1. The Bloch vector \mathbf{m}_1 has the same direction as the Bloch vector \mathbf{n} , and the Bloch vector \mathbf{m}_2 has the opposite direction to the Bloch vector \mathbf{n} , which is shown in Figure 9.5.

9.2 Preparation of Entanglement States in a Two-Spin System

Quantum entanglement, as the most important resource of the quantum information technique (QIT), has many applications (Nielsen and Chuang, 2010), such as quantum communication (Bennett *et al.*, 1993), quantum dense coding (Mattle *et al.*, 1996), and quantum computation (Bennett and DiVincenzo, 2000). How to prepare the entangled state and keep it are therefore key issues for QIT. Along with the rapid growth of the quantum control theory (QCT), the numerous strategies based on QCT offer us potent tools for solving this issue. The earliest strategy is coherent control technology (Basharov, Bashkeev, and Manykin, 2005; Xie, Jia, and Yang, 2009; Osnaghi *et al.*, 2001), where one assumes that the controls enter the Hamiltonian of the control model as appropriate functions. For instance, in 2005 Basharov *et al.* utilized a resonant classical electromagnetic field to generate entanglement between two two-level atoms coupled by dipole–dipole interactions. In 2009 Xie *et al.* proposed that the frequency of the field varies with time in the forms of sine and rectangle. Stimulated Raman adiabatic passage (STIPAP) strategy is another important method of preparing entangled states (Bergmann, Theuer, and Shore, 1998). Although these works about the two strategies can generate an entangled state, the entangled state can only be kept for a short time, which is not enough to allow designed tasks to be fulfilled. Because of the form of control function being predetermined, the preparation of the entangled state relies largely on one's intuition.

Although Wang and Schirmer applied Lyapunov control design to the problem of entanglement creation in 2009, their method can only transfer some initial states to maximally entangled states. Thus we want to derive a convergent control law that is effective for the arbitrary initial states.

To accomplish this task, a two-spin system was chosen, in which we focused on maximally entangled states, that is, the Bell states. Because the generic Heisenberg interaction model is an inhomogeneous equation that is hard to use, we applied unitary transformations to the Hamiltonian of the controlled system to get a homogeneous equation. Based on this, we designed the control law in which a general form of the observable operator P is constructed under the condition of guaranteeing the controlled system to be stable. Then we analyzed the convergence of the system controlled and demonstrated that the Bell states are asymptotically stable under the control law designed. In other words, we proposed the general form of the Lyapunov-based control method to make the controlled system converge to the maximally entangled state from an arbitrary initial state.

9.2.1 Construction of the Two-Spin Systems Model in the Interaction Picture

The quantum state of an n -dimensional system can be represented by a complex vector $\psi \in C^n$, and $\|\psi\| := \sqrt{\psi^\dagger \psi} = 1$ holds. Here the label “ \dagger ” denotes the complex conjugate. For example, for a single-spin system, its spin-up and spin-down states along an axis are

represented as $\psi_u = [1 \ 0]^T$ and $\psi_d = [0 \ 1]^T$, respectively. According to the superposition principle in quantum theory, any state of the single-spin system can be described in the form $\psi = a\psi_u + b\psi_d$ in which the complex coefficients $a, b \in C$ satisfy $|a|^2 + |b|^2 = 1$.

In this section, we focus on a system composed of two spins, which is described in the product space of the single-spin, that is, $C^4 = C^2 \otimes C^2$. The four bases can be taken as up-up, up-down, down-up, and down-down states. In such a way, one can obtain four bases as follows (Yamamoto, Tsumura, and Hara, 2007):

$$\begin{aligned} \{\psi_u \otimes \psi_u, \psi_u \otimes \psi_d, \psi_d \otimes \psi_u, \psi_d \otimes \psi_d\} &= \{|1\rangle, |2\rangle, |3\rangle, |4\rangle\} \\ &= \left\{ [1 \ 0 \ 0 \ 0]^T, [0 \ 1 \ 0 \ 0]^T, [0 \ 0 \ 1 \ 0]^T, [0 \ 0 \ 0 \ 1]^T \right\} \end{aligned} \quad (9.5)$$

Any quantum state of the two-spin system can be described by a superposition of four bases (Equation 9.5), that is, $\psi = [a_1 \ a_2 \ a_3 \ a_4]^T$. If there is no correlation between the spins then this two-spin state takes a special form

$$\psi = \psi_1 \otimes \psi_2 = \begin{bmatrix} a \\ b \end{bmatrix} \otimes \begin{bmatrix} c \\ d \end{bmatrix} = [ac \ ad \ bc \ bd]^T \quad (9.6)$$

On the other hand, a quantum state that cannot be expressed by a product state shown as Equation 9.6 has a specific quantum correlation called entanglement. For example, an entangled state

$$\psi = a\psi_u \otimes \psi_d + b\psi_d \otimes \psi_u = [0 \ a \ b \ 0]^T, a \neq 0, b \neq 0 \quad (9.7)$$

cannot be written by a product form.

The following four Bell states, which are maximally entangled states, are considered for the preparation:

$$|\Psi^+\rangle = \frac{1}{\sqrt{2}}(\psi_u \otimes \psi_d + \psi_d \otimes \psi_u) = \frac{1}{\sqrt{2}}[0 \ 1 \ 1 \ 0]^T \quad (9.8a)$$

$$|\Phi^-\rangle = \frac{1}{\sqrt{2}}(\psi_u \otimes \psi_u + \psi_d \otimes \psi_d) = \frac{1}{\sqrt{2}}[1 \ 0 \ 0 \ 1]^T \quad (9.8b)$$

$$|\Phi^-\rangle = \frac{1}{\sqrt{2}}(\psi_u \otimes \psi_u - \psi_d \otimes \psi_d) = \frac{1}{\sqrt{2}}[1 \ 0 \ 0 \ -1]^T \quad (9.8c)$$

$$|\Psi^-\rangle = \frac{1}{\sqrt{2}}(\psi_u \otimes \psi_d - \psi_d \otimes \psi_u) = \frac{1}{\sqrt{2}}[0 \ 1 \ -1 \ 0]^T \quad (9.8d)$$

The Hamiltonian of such a two-spin system is composed of internal Hamiltonian H_0 and external Hamiltonian $H_1(t)$, that is:

$$H(t) = H_0 + H_1(t) \quad (9.9)$$

According to the generic Heisenberg interaction model, the internal Hamiltonian H_0 is given by

$$H_0 = -J \sum_{k=x,y,z} I_{1k} I_{2k} \quad (9.10)$$

in which the constant $J > 0$ is the coupling constant between two particles. For $k = x, y, z$, one has $I_{1k} = \frac{1}{2}\sigma_k \otimes I$, $I_{2k} = I \otimes \frac{1}{2}\sigma_k$, and $I_{1k}I_{2k} = \sigma_k \otimes \sigma_k$, where σ_k are the components of the spin operator in the x , y , and z directions, $\sigma_x = \begin{pmatrix} 0 & 1 \\ 1 & 0 \end{pmatrix}$, $\sigma_y = \begin{pmatrix} 0 & -i \\ i & 0 \end{pmatrix}$, and $\sigma_z = \begin{pmatrix} 1 & 0 \\ 0 & -1 \end{pmatrix}$, and I is the identity operator.

If the external control field is applied along the x , y , and z directions to the system, the external Hamiltonian $H_1(t)$ can be defined as

$$H_1(t) = - \sum_{k=x,y,z} (\gamma_1 I_{1k} + \gamma_2 I_{2k}) u_k(t) \quad (9.11)$$

in which the constants γ_1 and γ_2 are the gyromagnetic ratios of particle 1 and particle 2, respectively. From Equations 9.9–9.11, one has

$$H(t) = - \sum_{k=x,y,z} (\gamma_1 I_{1k} + \gamma_2 I_{2k}) u_k(t) - J \sum_{k=x,y,z} I_{1k} I_{2k} \quad (9.12)$$

Generally, the state of the quantum mechanical system $|\psi(t)\rangle$ is determined by the Schrödinger equation:

$$i\hbar |\dot{\psi}\rangle = H(t) |\psi\rangle \quad (9.13)$$

Putting Equation 9.12 into Equation 9.13 one has:

$$|\psi\rangle = (\bar{A} + \bar{B}_x \bar{u}_x + \bar{B}_y \bar{u}_y + \bar{B}_z \bar{u}_z) |\psi\rangle \quad (9.14)$$

where $\bar{B}_z = i\gamma_1(I_{1z} + rI_{2z})$, $r = \gamma_2/\gamma_1$, and $\bar{A} = iJ \sum_{k=x,y,z} I_{1k} I_{2k}$, $\bar{B}_x = i\gamma_1(I_{1x} + rI_{2x})$, and $\bar{B}_y = i\gamma_1(I_{1y} + rI_{2y})$. Here the Planck constant has been assigned to be 1. The matrices $\bar{A}, \bar{B}_x, \bar{B}_y$ and \bar{B}_z change on the Lie group $SU(4)$.

In order to diagonalize the matrix \bar{A} , we perform a unitary transformation, that is, $|\psi'\rangle = T|\psi\rangle$, $T^\dagger = T^{-1}$ holds, and:

$$T := \frac{1}{\sqrt{2}} \begin{pmatrix} 0 & i & -i & 0 \\ 0 & 1 & 1 & 0 \\ -i & 0 & 0 & -i \\ -1 & 0 & 0 & 1 \end{pmatrix} \quad (9.15)$$

By adjusting the amplitude of the control field, Equation 9.14 becomes

$$|\dot{\psi}'\rangle = (A + B_x u_x + B_y u_y + B_z u_z) |\psi'\rangle \quad (9.16)$$

and the four Bell states in Equations 9.8a–c are transformed into:

$$|\Psi^+\rangle' = T|\Psi^+\rangle = [0 \ 1 \ 0 \ 0]^T \quad (9.17a)$$

$$|\Phi^+\rangle' = T|\Phi^+\rangle = [0 \ 0 \ -i \ 0]^T \quad (9.17b)$$

$$|\Phi^-\rangle' = T|\Phi^-\rangle = [0 \ 0 \ 0 \ -1]^T \quad (9.17c)$$

$$|\Psi^-\rangle' = T|\Psi^-\rangle = [i \ 0 \ 0 \ 0]^T \quad (9.17d)$$

For convenience, we label the four Bell states from Equations 9.17a–9.17d as $\psi_1, \psi_2, \psi_3, \psi_4$, respectively. Then for the system in Equation 9.16 the task is to prepare the four Bell states in Equation 9.17a and Equation 9.17d. We will omit the label “ \rangle ” in the following text for convenience. That is:

$$|\psi\rangle = (A + B_x u_x + B_y u_y + B_z u_z) |\psi\rangle \quad (9.18)$$

where $A = T\bar{A}T^{-1} = \text{diag}(-3i, i, i, i)$,

$$\begin{aligned} B_x &= T\bar{B}_x T^{-1} = \begin{pmatrix} 0 & 0 & 0 & 1-r \\ 0 & 0 & r+1 & 0 \\ 0 & -r-1 & 0 & 0 \\ r-1 & 0 & 0 & 0 \end{pmatrix}, \\ B_y &= T\bar{B}_y T^{-1} = \begin{pmatrix} 0 & 0 & 1-r & 0 \\ 0 & 0 & 0 & -r-1 \\ r-1 & 0 & 0 & 0 \\ 0 & r+1 & 0 & 0 \end{pmatrix}, \text{ and} \\ B_z &= T\bar{B}_z T^{-1} = \begin{pmatrix} 0 & 1-r & 0 & 0 \\ r-1 & 0 & 0 & 0 \\ 0 & 0 & 0 & r+1 \\ 0 & 0 & -r-1 & 0 \end{pmatrix}. \end{aligned}$$

It is evident that the four Bell states in Equation 9.17a–d are the eigenvectors of A . In fact, in the original system model Equation 9.14, one can verify that the eigenvectors of \bar{A} are the Bell states in Equation 9.8a–d, which indicates that the two models (Equations 9.14 and 9.18) are equivalent.

Transforming the system into the interaction picture, viz. setting $|\psi''\rangle = \exp(-At)|\psi\rangle$, the Schrödinger equation of the closed quantum system after transformation can be written as:

$$|\psi''\rangle = \sum_{k=x,y,z} A_k(t) u_k |\psi''\rangle \quad (9.19)$$

where $A_k(t) = \exp(-At)B_k \exp(At)$, $k = x, y, z$, satisfies $A_k^\dagger = -A_k$. The unitary transformation in the interaction picture changes the relative phase of states, while the probability distributions of eigenstates are unchanged. $|\psi\rangle$ is therefore equivalent to $|\psi''\rangle$, and we will omit the label “ \rangle ” in the following text for convenience. Equation 9.19 is therefore just the mathematical model of a two-spin system in the interaction picture.

9.2.2 Design of the Control Field Based on the Lyapunov Method

The design idea of the control field in this subsection is based on the Lyapunov-based method, which is a type of control law widely used in macroscopic system control. The control law is obtained under the condition that the first-order time derivative of a selected Lyapunov function is kept non-positive. This condition can guarantee that the controlled system is stable, so the key to control law designing is to select a suitable Lyapunov function. The average value of

an observable quantity is selected here, that is,

$$V = \langle \psi | P | \psi \rangle \quad (9.20)$$

where P is the Hermitian observable operator.

According to Equation 9.19, the time derivative of V is:

$$\begin{aligned} \dot{V} &= \langle \psi | P | \psi \rangle + \langle \psi | P | \dot{\psi} \rangle \\ &= \sum_{k=x,y,z} u_k \langle \psi | A_k(t) | P | \psi \rangle + \sum_{k=x,y,z} u_k \langle \psi | P A_k(t) | \psi \rangle \\ &= \sum_{k=x,y,z} u_k \langle \psi | A_k^\dagger(t) P | \psi \rangle + \sum_{k=x,y,z} u_k \langle \psi | P A_k(t) | \psi \rangle \\ &= \sum_{k=x,y,z} u_k \langle \psi | [P, A_k(t)] | \psi \rangle \end{aligned} \quad (9.21)$$

If we choose the control law as:

$$u_k = -K_k \langle \psi | [P, A_k] | \psi \rangle, k = x, y, z \quad (9.22)$$

where $K_k > 0$ is used to adjust the control amplitude, one can verify that $\dot{V} \leq 0$, which means the controlled system is stable. To make the target state stable in the Lyapunov sense, the following two conditions need to be satisfied:

- The Lyapunov function Equation 9.20 reaches a minimum only when the system is in the target state.
- The system is able to remain in the target state from then on.

In fact, condition (b) can be obtained from condition (a). If we assume condition (a) is satisfied, the control field is certainly equal to 0 when the system reaches the target state, otherwise the Lyapunov function will keep decreasing under the action of the control law, which means the Lyapunov function does not reach a minimum. This is in contradiction to our assumption, therefore condition (b) is satisfied as long as condition (a) is met. The only thing left is to construct an observable operator P to satisfy condition (a), that is, to make target state ψ_f be the minimum point of the Lyapunov function. The design process of P is as follows.

For the sake of convenience, the Hermitian matrix is expressed as coherent vectors. The bases of a unitary Lie algebra $su(n)$ are recorded as

$$\{iX_1, \dots, iX_m\}, m = n^2 - 1 \quad (9.23)$$

which has the relations

$$\text{tr}(X_l) = 0 \quad (9.24a)$$

$$\text{tr}(X_l X_j) = \delta_{lj} \quad (9.24b)$$

According to the idea proposed in Section 7.2.2, a state density matrix $\rho = |\psi\rangle\langle\psi|$ with n dimensions can be rewritten as

$$\rho = I/n + \sum x_l X_l \quad (9.25)$$

where x_l is real number. In such a way, the coherent vector V_ρ of a state density matrix ρ can be written as

$$V_\rho = (x_1, x_2, \dots, x_{n^2-1})^T \quad (9.26)$$

The modulus of a coherent vector V_ρ indicates the purity of a state, which is a maximum $\sqrt{(n-1)/n}$ when the state is pure and is zero for a maximum mixed-state I/n . Because of the unitary nature of the closed quantum system's evolution, the purity will be unchanged during the whole evolution process of the system, namely, all the time one has

$$\sum_l |x_l|^2 = C, \text{ where } C \text{ is a constant} \quad (9.27)$$

Now assume

$$\rho_f = I/n + \sum_j f_j X_j \quad (9.28a)$$

$$P = c_0 I + \sum_k c_k X_k \quad (9.28b)$$

Then

$$V = \langle \psi | P | \psi \rangle = \text{tr}(P \rho_f) = c_0 + \sum_k c_k f_k \quad (9.29)$$

In order to make Equation 9.29 achieve the minimum under the condition of Equation 9.27, one has

$$c_k = \lambda f_k, \lambda < 0 \quad (9.30)$$

which means that the coherent vector V_P of the observable operator P has an opposite direction to that of the target state ρ_f :

$$V_P = \lambda V_{\rho_f}, \lambda < 0 \quad (9.31)$$

Suppose a system described by Equation 9.19 needs to evolve from an initial state to a target state ρ_f , whose coherent vector obtained through Equation 9.29a is $V_{\rho_f} = (f_1, f_2, \dots, f_{n^2-1})^T$. In order to make the target state ψ_f be the minimum point of the Lyapunov function the coherent vector V_P of the observable operator P constructed must satisfy the condition of Equation 9.31. The matrix P can be constructed by a set of orthogonal bases with target state

$$P = p_h \sum_{\langle \psi_j | \psi_f \rangle = 0} |\psi_j\rangle \langle \psi_j| + p_l |\psi_f\rangle \langle \psi_f|, \quad p_h > p_l \quad (9.32)$$

According to Equation 9.32, the simplest way to get the observable operator P is to let

$$P = -\rho_f \quad (9.33)$$

Obviously, the observable operator P constructed by Equation 9.33 is commutative with the density matrix of the target state. At the same time, the observable operator P ensures that the Lyapunov function reaches a minimum when the system evolves to the target state ψ_f , therefore the target state is stable in the Lyapunov sense under the action of the control law (Equation 9.22).

9.2.3 Proof of Convergence for the Bell States

In Section 9.2.2 we derived the Lyapunov control laws that make the system only stable but not asymptotically stable, that is, the condition for constructing the observable operator P can only guarantee that the target state ψ_f is the minimum point of the Lyapunov function, but cannot guarantee the system's convergence. In this subsection we will prove that the system driven by the control law (Equation 9.22) converges to the desired the Bell state, that is, for any initial state one can prepare any of the Bell states by the control law (Equation 9.22) designed by Lyapunov-based method.

If the controlled system is asymptotically stable, the system will converge to the target state. For autonomous systems, asymptotic stability can be analyzed by the LaSalle principle, but in the present situation the controlled system becomes non-autonomous in the interaction picture. However, one can get an analogous conclusion by the Lemma 7.2:

For the pure state, the Lyapunov function $V(\psi) = \langle\psi|P|\psi\rangle = -|\langle\psi|\psi_f\rangle|^2 \geq -1$ is lower bounded. Its first derivative is negative semi-definite under the control law (Equation 9.22). The second derivative is

$$\ddot{V}(\psi, t) = \sum_j \{u_j \text{tr}([\dot{\rho}(t), P]A_j(t)) + u_j \text{tr}([\rho(t), P]\dot{A}_j(t))\} \quad (9.34)$$

Equation 9.34 is bounded when the inputs are bounded. Thus, $\dot{V}(\psi, t)$ is uniformly continuous in time. According to Lemma 7.2, the first derivative of the Lyapunov function converges to zero, viz., $\dot{V}(\psi(\infty), \infty) = 0$. Then, the controlled system converges to the set \mathcal{R} , where

$$\mathcal{R} \equiv \{\psi : \langle\psi|[P, A_k]|\psi\rangle, k = x, y, z \text{ and } \forall t\} \quad (9.35)$$

Moreover, the system in Equation 9.19 is homogeneous, and the states in \mathcal{R} make their controls are zero according to Equation 9.22, so the largest invariant set in \mathcal{R} is itself. Then we can obtain the theorem 9.1:

Theorem 9.1 The system in Equation 9.19 with the control law in Equation 9.22 converges to the set \mathcal{R} defined by Equation 9.35.

This set \mathcal{R} is in general of finite dimension, indicating that it is easy to manipulate the system to a state in the set but difficult to control it from an arbitrary initial state to a given target state. Fortunately we just focus on convergence of the Bell states, that is, we need to prove the following theorem:

Theorem 9.2 For any a given target state $\psi_f, f \in \{1, 2, 3, 4\}$ which is a Bell state, the system in Equation 9.19 with the control law in Equation 9.22 in which the observable operator P is given by $P = -|\psi_f\rangle\langle\psi_f|$ converges to ψ_f .

Proof Because P , A_k , and the density matrix $\rho = |\psi\rangle\langle\psi|$ are Hermitian, combined with $\text{tr}(A[B, C]) = \text{tr}(B[C, A])$, one can compute

$$\langle\psi|[P, A_k]|\psi\rangle = \text{tr}(\rho[P, A_k]) = \text{tr}(P[\rho, A_k]) = -\langle\psi_f|[\rho, A_k]|\psi_f\rangle \quad (9.36)$$

Thus, Equation 9.35 is equivalent to

$$\langle \psi_f | [\rho, A_k] | \psi_f \rangle = 0, k = x, y, z, \text{ for } \forall t \quad (9.37)$$

Namely,

$$([\rho, A_k])_{ff} = 0, k = x, y, z, \text{ for } \forall t \quad (9.38)$$

where $(A)_{jj}$ represents the j th row and j th column of the matrix A . Substituting the expression of A_k into Equation 9.38, we have

$$\rho_{jf} = (|\psi\rangle\langle\psi|)_{jf} = 0, j \neq f \text{ and } j \in \{1, 2, 3, 4\} \quad (9.39)$$

Because the system is closed, the state is the pure state at any time, so it can be expressed as $|\psi\rangle = \sum_{i=1}^4 c_i |\psi_i\rangle$, $\sum_{i=1}^4 |c_i|^2 = 1$. Then Equation 9.39 is equivalent to

$$c_j^* c_f = 0, j \neq f \text{ and } j \in \{1, 2, 3, 4\} \quad (9.40)$$

which means the state in the set \mathcal{R} can be expressed as

$$\left\{ |\psi\rangle : |\psi\rangle = \sum_{i=1}^4 c_i |\psi_i\rangle, c_f = 0 \right\} \text{ or } \left\{ |\psi\rangle : |\psi\rangle = \sum_{i=1}^4 c_i |\psi_i\rangle, |c_f| = 1 \text{ and } c_j = 0 \text{ for } \forall j \neq f \right\} \quad (9.41)$$

Therefore the set \mathcal{R} is

$$\mathcal{R} = \mathcal{R}_1 \cup \mathcal{R}_2 \quad (9.42)$$

where

$$\mathcal{R}_1 = \text{span}\{|\psi_f\rangle\}, \mathcal{R}_2 = \text{span}\{|\psi_j\rangle, j \neq f\} \quad (9.43)$$

According to Theorem 9.1, the system converges to the set \mathcal{R} . Note that \mathcal{R}_2 is the orthogonal space of the set \mathcal{R}_1 , thus the intersection of \mathcal{R}_1 and \mathcal{R}_2 is empty. As a result, the system converges to either \mathcal{R}_1 or \mathcal{R}_2 . In fact, the system can only converge to \mathcal{R}_1 . The states in \mathcal{R}_2 make the Lyapunov function a maximum, therefore for any initial state $|\psi_0\rangle \notin \mathcal{R}_2$, that is, the initial value of the Lyapunov function is not the maximum, the system converges to \mathcal{R}_1 because $\dot{V} \leq 0$. For $|\psi_0\rangle \in \mathcal{R}_2$, the state is on a critical stable point, which makes the initial control zero. For this case a disturbance introduced to the system can enable the value of the Lyapunov function to decrease, which means that the system state leaves and no longer reaches the set \mathcal{R}_2 . Then, the controlled state converges to \mathcal{R}_1 , therefore for any initial state, the system will converge to ψ_f under control law (Equation 9.22) with the observable operator P given by $P = -|\psi_f\rangle\langle\psi_f|$.

The proof is finished. ■

9.2.4 Numerical Simulations

In this subsection, we will present numerical experiments to illustrate how to design our strategy in detail. In the system simulation experiment, we will demonstrate the effectiveness of the method proposed, that is, we will illustrate that the four Bell states are asymptotically stable, and the target states are $\psi_1, \psi_2, \psi_3, \psi_4$, respectively. Assume the system is initially in the

states $|\psi_0\rangle = \psi_u \otimes \psi_d$, which means the two particles of a composite system are in the spin-up and spin-down states, respectively. The system model is transformed into Equation 9.19, with $r = \gamma_2/\gamma_1 = 2$. Then the transformed initial state for the system model (Equation 9.19) is $|\psi_0\rangle = T\psi_u \otimes \psi_d = 1/\sqrt{2}[i \ 1 \ 0 \ 0]^T$.

The control goal is to drive this system from the initial state $|\psi_0\rangle$ to the four Bell states ψ_1, ψ_2, ψ_3 , and ψ_4 in Equations 9.17a–d, respectively. Then the corresponding control laws $u^{(1)}, u^{(2)}, u^{(3)}$, and $u^{(4)}$ are designed based on Equation 9.22 as

$$u_k^{(j)} = -K_k \langle \psi | [P^{(j)}, A_k] | \psi \rangle, k = x, y, z \text{ and } j = 1, 2, 3, 4 \quad (9.44)$$

where $K_x = K_y = K_z = 0.1$, $A_k(t) = \exp(-At)B_k \exp(At)$, $A = \bar{T}AT^{-1} = \text{diag}(-3i, i, i, i)$, and T is selected as in Equation 9.15. According to Equation 9.33, the observable operators are given by

$$P^{(1)} = \begin{pmatrix} 0 & 0 & 0 & 0 \\ 0 & -1 & 0 & 0 \\ 0 & 0 & 0 & 0 \\ 0 & 0 & 0 & 0 \end{pmatrix}, P^{(2)} = \begin{pmatrix} 0 & 0 & 0 & 0 \\ 0 & 0 & 0 & 0 \\ 0 & 0 & -1 & 0 \\ 0 & 0 & 0 & 0 \end{pmatrix}, P^{(3)} = \begin{pmatrix} 0 & 0 & 0 & 0 \\ 0 & 0 & 0 & 0 \\ 0 & 0 & 0 & 0 \\ 0 & 0 & 0 & -1 \end{pmatrix}, P^{(4)} = \begin{pmatrix} -1 & 0 & 0 & 0 \\ 0 & 0 & 0 & 0 \\ 0 & 0 & 0 & 0 \\ 0 & 0 & 0 & 0 \end{pmatrix}$$

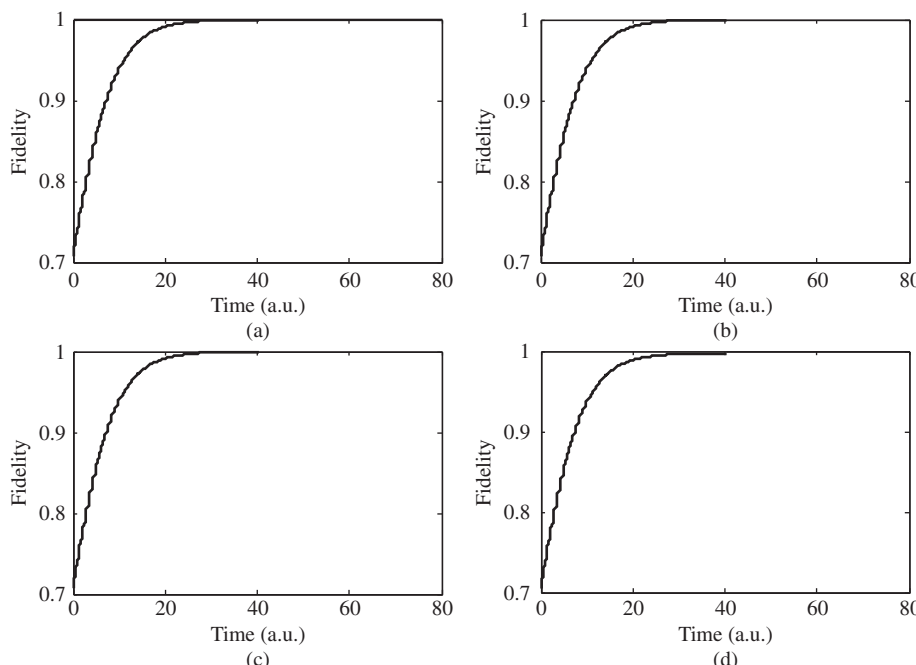


Figure 9.6 The Fidelity evolving curves in the interval $[0, 80]$ for four target states: (a) the fidelity for the target state ψ_1 , (b) the fidelity for the target state ψ_2 , (c) the fidelity for the target state ψ_3 , and (d) the fidelity for the target state ψ_4

The fidelity between $|\psi(t)\rangle$ and the target state $|\psi_f\rangle$ is defined as $F(t) = |\langle\psi(t)|\psi_f\rangle|$. This represents the transition probability from $|\psi(t)\rangle$ to $|\psi_f\rangle$. The greater F is, the higher the transition probability is. $F = 1$ means the system reaches the target state. Time step $\Delta t = 0.01$ and control time $t = 40$, the time evolution of the fidelity for different target states, are displayed in Figure 9.6, in which Figures 9.6a–d correspond to the target state being ψ_1 , ψ_2 , ψ_3 and ψ_4 , respectively. It can be seen from Figure 9.6 that the fidelity for each target state reaches one, that is, the four Bell states are prepared by the control laws in Equation 9.44.

The results indicate that our strategy is effective. The changing curves of the control laws are showed in Figure 9.7. It can be seen from Figure 9.7 that all the control laws $u^{(1)}$, $u^{(2)}$, $u^{(3)}$, and $u^{(4)}$ ultimately vanish, that is, the system would stay in the Bell states, which is consistent with Theorem 9.2 in Section 9.2.3. Furthermore, the controls along different directions are needed for different target states. For instance, to prepare the target states ψ_1 and ψ_4 , the control along the z direction $u_z^{(j)}$, $j=1,4$, plays the dominant role, whereas the controls along the x and y directions do not work. By contrast, for the target states ψ_2 and ψ_3 , the z direction's control almost does not affect the system. Comparing Figure 9.7b with Figure 9.7c, the control laws

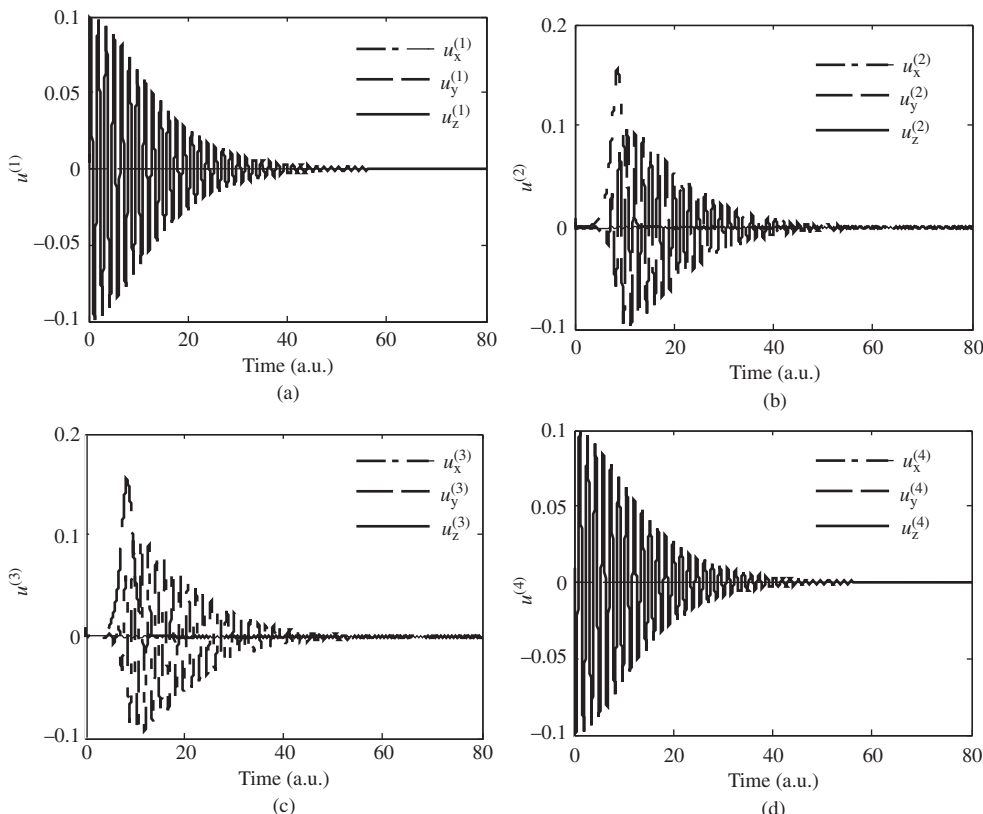


Figure 9.7 The curves of the control laws in $[0 \ 100]$ for four target states: (a) the control for the target state ψ_1 , (b) the control for the target state ψ_2 , (c) the control for the target state ψ_3 , and (d) the control for the target state ψ_4

for the target states ψ_2 and ψ_3 have similar shapes. The only difference is that the system is mainly influenced by the x direction's control in the time interval $[0, 13]$, then by the y direction's control in Figure 9.7b. Conversely in Figure 9.7c, $u_y^{(3)}$ influences the system first, then $u_x^{(3)}$.

9.3 Purification of the Mixed State for Two-Dimensional Systems

The states of quantum systems as the information carrier must be prepared in pure states for the implementation of quantum information processing. However, quantum systems often exist naturally in mixed states due to environmental noise, and decoherence becomes one main obstacle to practical quantum information processing. To overcome the decoherence of the environment it is important to decouple the system as much as possible from it (Dowling and Milburn, 2003; Ticozzi and Ferrante, 2006) or to study methods for preserving (or restoring) the entanglement and the purity of the states.

The purification study of a quantum system (Benenti and Strini, 2009; Kleinmann *et al.*, 2006; Bouda and Bužek, 2002; Pan *et al.*, 2003; Ralph *et al.*, 2006; Griffith, Hill, and Ralph, 2007; Wiseman and Ralph, 2006) in which continuous measurements and the feedback control were utilized, and state purifications were realized. Recently, a different control scheme has been developed that does not assume coherent control and quantum measurements (Romano and D'Alessandro, 2006). This non-coherent control protocol relies on the use of an initially uncorrelated auxiliary system, the probe P , which interacts with the relevant system S and is discarded at the end of the procedure. In 2006 Romano and D'Alessandro investigated the accessibility and controllability of such a composite system in the two-dimensional Hilbert spaces. Furthermore, some results of the purification of mixed states for closed and open quantum systems were achieved by Romano in 2007, from which the main result is that the purification process exhibits a resonant behavior depending on the energy difference between S and P . However, this strategy suffered because the mixed state cannot be purified completely for cases of non-zero energy difference.

In order to resolve this issue, based on the method proposed by Romano in 2007, in this section we will propose a purification strategy that purifies an arbitrary mixed state into a pure state by controlling the interaction between S and P . Generally, the pure state can be either an eigenstate or a superposition state. For the sake of simplicity, the eigenstate is selected as the target state. The coupling between S and P is a time- and controls-dependent function. The control is designed by Lyapunov-based control, in which the Lyapunov indirect stability theorem is used. It will be seen that the mixed state can be completely purified and steered to the eigenstate even if the energy difference between S and P is not zero.

9.3.1 Purification by Means of a Probe

Generally, for a closed quantum system, a control law directly affects the dynamics of the controlled system and corresponds to a suitable unitary transformation. However, the purity of a mixed state ρ remains constant under the action of unitary transformations. It is therefore impossible to drive a mixed state of a single quantum system to a pure state.

In order to obtain a non-unitary transformation, one idea is to introduce a second system to the original system so that the dynamics of the original system is a non-unitary transformation.

This second system is called the probe. Following this, a purification protocol by means of a probe can be developed. In this protocol, the system S is allowed to interact with the probe P , and initially they are in an uncorrelated state $\rho_s \otimes \rho_P$. It is assumed that the controls enter the dynamics of S through $\rho_P = \rho_P(u)$. Under the assumption that the composite system $T = S + P$ is closed, the dynamics of system S is given by:

$$\rho_S(t, u) = \text{Tr}_P(X(t)\rho_s \otimes \rho_P(u)X^\dagger(t)) \quad (9.45)$$

in which Tr_P is the partial trace over the degrees of freedom of P , $X(t) = e^{-iH_T t}$ is the unitary propagator, and $H_T = H_S + H_P + H_I$ is the Hamiltonian of T where H_S and H_P are the free Hamiltonian of S and P , respectively. The coupling between S and P is given by the interaction Hamiltonian H_I .

Now we simply review the purification strategy proposed by Romano, which pays attention to the two-dimensional S and P . The particular dynamical model is given by $H_S = \omega_S \sigma_z^S$, $H_P = \omega_P \sigma_z^P$, and $H_I = g \sigma_x^S \otimes \sigma_x^P$, where ω_S and ω_P are the characteristic energies in S and P , g is the coupling constant, and σ_i^S and σ_i^P ($i = x, y, z$) are the Pauli matrices in S and P , respectively. The purity of a state ρ_S is defined as the von Neumann distance of this state from the maximally mixed state $I/2$, that is

$$\pi = \sqrt{2\text{Tr}\left(\rho_S - \frac{I}{2}\right)^2} = \sqrt{2\text{Tr}(\rho_S^2) - 1} \quad (9.46)$$

For the sake of convenience, the Bloch vector representation for the states is adopted as

$$\rho_S(t) = \frac{1}{2} \left[I + \vec{s}(t) \cdot \vec{\sigma}^S \right], \rho_P(t) = \frac{1}{2} \left[I + \vec{p}(t) \cdot \vec{\sigma}^P \right] \quad (9.47)$$

in which I is a 2×2 identical matrix and $\vec{s}(t) = (s_x \ s_y \ s_z) = (\text{tr}\{\rho_s \sigma_x^S\} \text{tr}\{\rho_s \sigma_y^S\} \text{tr}\{\rho_s \sigma_z^S\})$, $\vec{p}(t) = (p_x \ p_y \ p_z) = (\text{tr}\{\rho_P \sigma_x^P\} \text{tr}\{\rho_P \sigma_y^P\} \text{tr}\{\rho_P \sigma_z^P\})$ are Bloch vectors with $\|\vec{s}(t)\| \leq 1$, $\|\vec{p}(t)\| \leq 1$, and $\vec{\sigma}^S$ and $\vec{\sigma}^P$ are the vectors of Pauli matrices in S and P , respectively, where $\sigma_x = \begin{pmatrix} 0 & 1 \\ 1 & 0 \end{pmatrix}$, $\sigma_y = \begin{pmatrix} 0 & -i \\ i & 0 \end{pmatrix}$ and $\sigma_z = \begin{pmatrix} 1 & 0 \\ 0 & -1 \end{pmatrix}$.

In this representation, the time-dependent purity is presented by $\pi(t) = \|\vec{s}(t)\|$, in which if $\pi(t) = 1$, the state is a pure state, otherwise it is a mixed state.

Generally, it is impossible to derive the analytic solutions of purity $\pi(t)$, but if the initial state of the system S is chosen as the maximally mixed state $\rho_S(0) = I/2$ and the interaction between S and P is depressed, that is, $g < \omega_S, \omega_P$, the maximal amplitude of the function $\pi_M = \max_{t \geq 0} \pi(t)$ can be derived, that is,

$$\pi_M \approx \frac{|p_z|g^2}{\delta\omega^2 + g^2} \quad (9.48)$$

where $\delta\omega = \omega_S - \omega_P$ is just the energy difference between S and P . One can see from Equation 9.48 that the complete purification of the maximally mixed state is realized only for $|p_z| = 1$ and $\delta\omega = 0$. These results do not completely satisfy the goal of transferring an arbitrary mixed state to a pure state in the cases $\omega_S \neq \omega_P$. In order to realize this goal, we will propose a new strategy in Section 9.3.2.

9.3.2 Purification by Interaction Control

In the method proposed by Romano, the purification protocol was realized by the action of the probe, which was affected by the control variables and then interacted with the quantum system to obtain control. In such a case, the dynamics of the system S is determined and not controllable once the initial state of the probe is determined. This is the main reason why Romano could not completely purify the spin system when $\omega_S \neq \omega_P$. Here, we will propose a new purification strategy: adjusting the control variables to effect the desired interaction between S and P for the purification of the mixed state. In such a case, the dynamics of the system S is determined by the control u .

In this time scale the Hamiltonian evolution is still a good approximation, and many physical systems satisfy the quantum Liouville equation (with $\hbar = 1$). Considering the same system T used by Romano, the dynamics of the composite system T under interaction control can be described as

$$\dot{\rho}_T(t) = -i [H_{\text{local}} + u(t) H_I, \rho_T(t)] \quad (9.49)$$

where $[A, B] = AB - BA$ is a commutator, $H_I = \delta_x^S \otimes \delta_x^P$ is the interaction Hamiltonian, and $H_{\text{local}} = H_S + H_P$ is the local Hamiltonian. The dynamics of the system S is given by $\rho_S(t) = \text{tr}_P(\rho_T(t))$. Here, it must be stressed that the coupling strength between S and P is not a constant but influenced by u , which is time dependent and must be designed to effect the desired interaction. The following thing is to find one method to design u to purify the mixed state to an eigenstate.

Here we select the same Lyapunov function as

$$V(\rho_T, \rho_{Tf}) = \frac{1}{2} \left\| \rho_T(t) - \rho_{Tf} \right\|_2 = \frac{1}{2} \text{Tr} \left[(\rho_T(t) - \rho_{Tf})^2 \right] \quad (9.50)$$

in which ρ_{Tf} is the target state of the composite system T , which is an uncorrelated state and can be chosen as $\rho_{Tf} = \rho_{Se} \otimes \rho_{Pf}$ such that $\rho_{Sf} = \text{Tr}_P(\rho_{Tf}) = \rho_{Se}$, where ρ_{Se} represents an eigenstate of S , that is, we desire to drive a mixed state in S to an eigenstate, and ρ_{Pf} represents the final state of system P and can be an arbitrary diagonal density matrix so that $[H_{\text{local}}, \rho_{Tf}] = 0$.

Because $[H_{\text{local}}, \rho_{Tf}] = 0$, according to Equation 9.49, one can derive that the first-order derivative of the Lyapunov function Equation 9.50 is

$$\begin{aligned} \dot{V}(t) &= \dot{V}(\rho_T(t), \rho_{Tf}) = \text{Tr} \left((\rho_T(t) - \rho_{Tf}) \dot{\rho}_T(t) \right) \\ &= \text{Tr} \left(-i (\rho_T(t) - \rho_{Tf}) [H_{\text{local}} + u(t) H_I, \rho_T(t)] \right) \\ &= \text{Tr} \left(i \rho_{Tf} [H_{\text{local}} + u(t) H_I, \rho_T(t)] \right) = -u(t) \text{Tr} \left(\rho_{Tf} [-i H_I, \rho_T(t)] \right) \end{aligned} \quad (9.51)$$

In order to ensure $\dot{V} \leq 0$, one can obtain the interaction control law:

$$u(t) = k \text{Tr} \left(\rho_{Tf} [-i H_I, \rho_T(t)] \right) \quad (9.52)$$

where $k > 0$ is used to adjust the control amplitude. Equation 9.52 is just the interaction control law, and one can verify that $\dot{V}(t) \leq 0$ holds under the control law (Equation 9.52), which means that the Lyapunov function V is monotonically decreasing during the evolution of the system state. The composite system T will converge to its stable point, which makes $V(\rho_T, \rho_{Tf}) = 0$, that is, $\rho_T(t) = \rho_{Tf}$.

Our control goal is to design a control law to drive the system state $\rho_T(t)$ to the target state ρ_{Tf} , namely, the final state of system S evolves to $\rho_{Sf} = \text{Tr}_P(\rho_{Tf}) = \rho_{Se}$, that is, the state ρ_S is driven from a mixed state $\rho_S(t) = \text{Tr}_P(\rho_T(t))$ to an eigenstate ρ_{Se} by means of interaction control (Equation 9.52). In such a way, we completely purify the system S .

9.3.3 Numerical Experiments and Results Comparisons

In order to compare the results with Romano's, the same parameters for different $\delta\omega$ are used and simplified models are analyzed in the following numerical simulation experiments. The fidelity between ρ_S and the target eigenstate ρ_{Se} is defined as

$$F(\rho_S, \rho_{Se}) = \text{tr}(\sqrt{\sqrt{\rho_S}\rho_{Se}\sqrt{\rho_S}}) \quad (9.53)$$

In numerical experiments, the Bloch vector representation for the states is adopted and the initial states in S and P are $\vec{s}(0) = (0.7, 0, 0)$ and $\vec{p}(0) = (0, 0, 1)$, respectively. Let $\omega_S = 1$ and the final state of the composite system T be $\rho_{Tf} = \rho_{Se} \otimes \rho_{Pf}$, with $\vec{p}_f = (0, 0, 0)$ and $\vec{s}_f = (0, 0, 1)$. With time step length $\Delta t = 0.01$ and control time $t = 100$, the evolution trajectories of the system states are as shown in Figure 9.8, in which there are four cases with $\delta\omega = 0$, $\delta\omega = 0.2$, $\delta\omega = 0.5$, and $\delta\omega = 0.9$.

From the data of the experiments, we find the values of fidelity $F(\rho_{Sf}, \rho_{Se})$ for different $\delta\omega$ are all almost 1, that is, the state in S $\rho_S(t)$ converges to ρ_{Se} . It can therefore be concluded

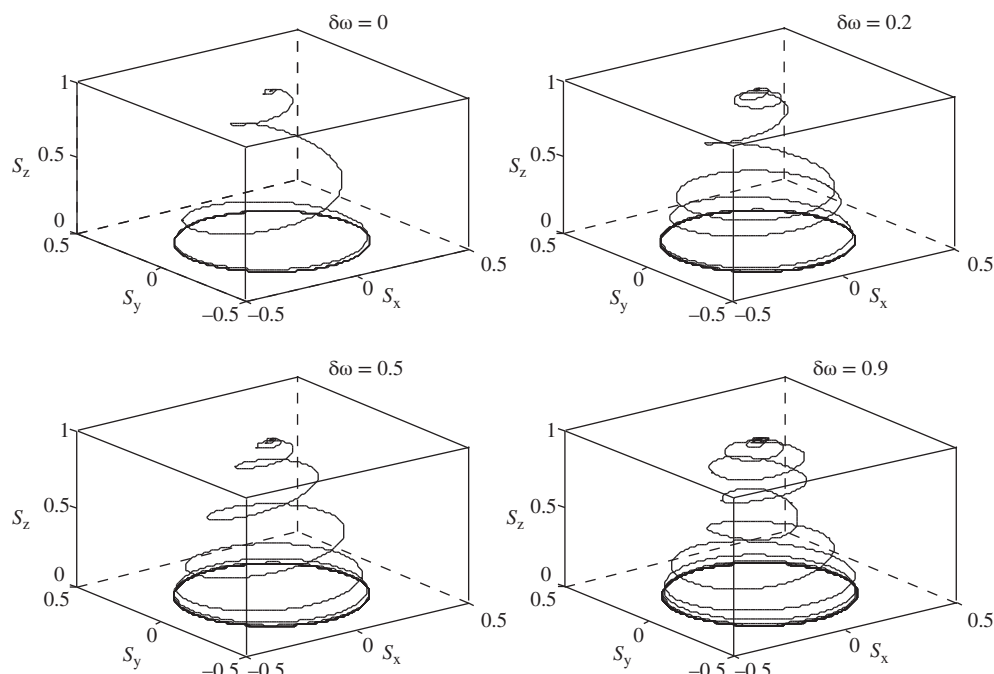


Figure 9.8 Evolution trajectories of $\vec{s}(t)$ for $0 \leq t \leq 100$

that the mixed state $\vec{s}(0) = (0.7, 0, 0)$ is transferred to $\vec{s}_f = (0, 0, 1)$ for any positive value of $\delta\omega$, while this result can be realized only in the case of $\delta\omega = 0$ by Romano. This difference can be clearly seen in Figure 9.8. The control strategy proposed in this paper therefore greatly increases the quality of purification of the mixed state.

The control law is designed based on Equation 9.52 with $k = 1$, and the control functions are shown in Figure 9.9, in which there are four cases with the same situations as in Figure 9.8. One can see from Figure 9.9 that the control function oscillates more and more intensively as $\delta\omega$ increases. The control function for $\delta\omega = 0$ approximates to the Gauss pulse, which is used frequently in practical experiments. All the control values in different cases turn to zero finally. In other words, the control design is robust.

9.3.4 Discussion

We have proposed a strategy that completely purifies the mixed state for arbitrary $\delta\omega$ in this section. In our method the interaction is modified by the Lyapunov-based control to stable the system. A two-level quantum system S based on its interaction with an auxiliary two-level system P is considered and by assuming particular forms of free Hamiltonians of S and P we derived the control model. The control u is designed to effect the desired interaction by the

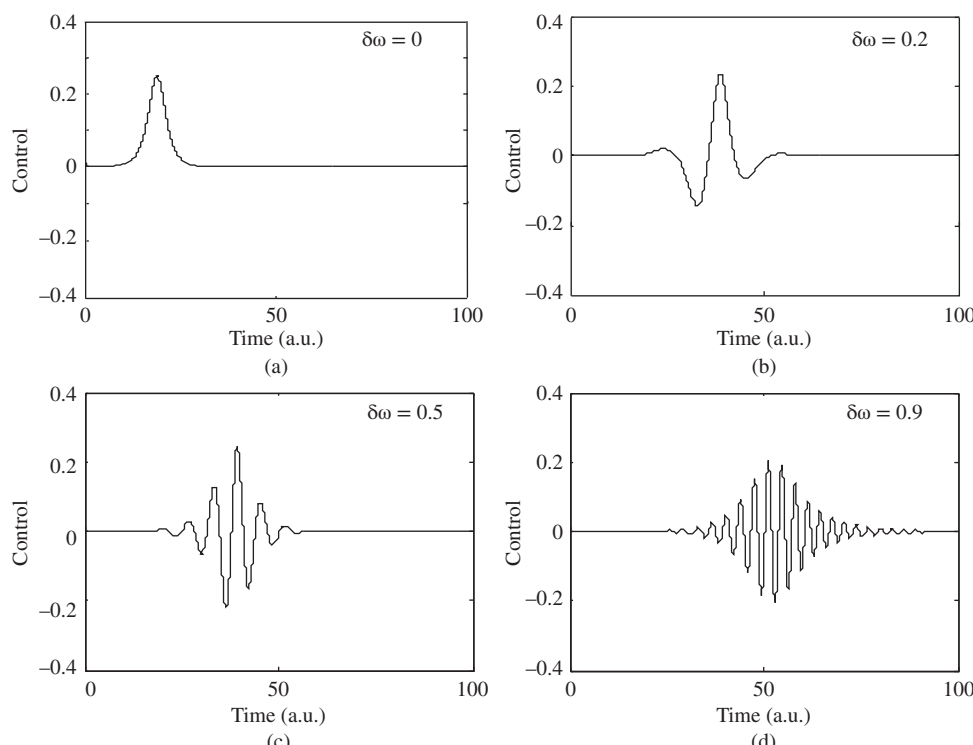


Figure 9.9 Control function for different values of $\delta\omega$

Lyapunov-based control method. As a result, an eigenstate in S is achieved by control that is not dependent on the energy difference. This result is demonstrated by the numerical experiments. Furthermore, we analyzed the feasibility of our protocol, which indicates that it is possible to realize purification by our strategy in practice.

Although particular models have been considered, the results are not exceptional. In fact our protocol is feasible for the more general Hamiltonian terms of a two-dimensional system and some higher-dimensional systems.

References

- Ayman, F.A., Bahaa, E.A.S., Alexander, V.S. *et al.* (2001) Degree of entanglement for two qubits. *Physical Review A*, **64**(5), 050101.
- Basharov, A.M., Bashkeev, A.A. and Manykin, É.A. (2005) Coherent control of quantum correlations in atomic systems. *Journal of Experimental and Theoretical Physics*, **100**(3), 475–486.
- Benenti, G. and Strini, G. (2009) Optimal purification of a generic n-qudit state. *Physical Review A*, **79**(5), 052301.
- Bennett, C.H., Brassard, G., Crepeau, C. *et al.* (1993) Teleporting an unknown quantum state via dual classical and Einstein–Podolsky–Rosen channels. *Physical Review Letters*, **70**(13), 2895–1899.
- Bennett, C.H. and DiVincenzo, D.P. (2000) Quantum information and computation. *Nature*, **404**, 247–255.
- Bergmann, K., Theuer, H. and Shore, B.W. (1998) Coherent population transfer among quantum states of atoms and molecules. *Reviews of Modern Physics*, **70**(3), 1003–1025.
- Bouda, J. and Bužek, V. (2002) Purification and correlated measurements of bipartite mixed state. *Physical Review A*, **65**(3), 034304.
- Dowling, J.P. and Milburn, G.J. (2003) Quantum technology: the second quantum revolution. *Philosophical Transactions of the Royal Society A*, **361**(1809), 1655–1674.
- Ekert, A.K. (1991) Correlations in Quantum Optics. PhD Thesis. Clarendon Laboratory, Oxford.
- Ekert, A. and Peter, L.K. (1995) Entangled quantum system and the Schmidt decomposition. *American Journal of Physics*, **63**(5), 415–423.
- Griffith, E.J., Hill, C.D. and Ralph, J.F. (2007) Rapid-state purification protocols for Cooper pair box. *Physical Review B*, **75**(1), 014511.
- Hill, S. and William, K.W. (1997) Entanglement of a pair of quantum bits. *Physical Review Letters*, **78**(26), 5022–5025.
- Kleinmann, M., Kampermann, H., Meyer, T. *et al.* (2006) Physical purification of quantum states. *Physical Review A*, **73**(6), 062309.
- Lieven, M.V. and Chuang, I.L. (2005) NMR techniques for quantum control and computation. *Reviews of Modern Physics*, **76**(4), 1037–1069.
- Mattle, K., Weinfurter, H., Kwiat, P.G. *et al.* (1996) Dense coding in experimental quantum communication. *Physical Review Letters*, **76**(25), 4656–4659.
- Nielsen, M.A. and Chuang, I.L. (2010) *Quantum Computation and Quantum Information*, Cambridge University Press, Cambridge.
- Osnaghi, S., Bertet, P., Ufferves, A. *et al.* (2001) Coherent control of an atomic collision in a cavity. *Physical Review Letters*, **87**(3), 037902.
- Pan, J., Gasparoni, S., Ursin, R. *et al.* (2003) Experimental entanglement purification of arbitrary unknown states. *Nature*, **423**, 417–422.
- Romano, R. and D'Alessandro, D. (2006) Incoherent control and entanglement for two-dimensional coupled systems. *Physical Review A*, **73**(2), 022323.
- Shyamal, S., Anthony, L. and Chris, D. (1999) Geometric algebra and the causal approach to multiparticle quantum mechanics. *Journal of Mathematical Physics*, **40**(7), 3327–3341.

- Ticozzi, F. and Ferrante, A. (2006) Dynamical decoupling in quantum control: a system theoretic approach. *Systems & Control Letters*, **55**(7), 578–584.
- Vedral, V. and Plenio, M.B. (1998) Entanglement measures and purification procedures. *Physical Review A*, **57**(3), 1619–1633.
- William, K.W. (1998) Entanglement of formation of an arbitrary state of two qubits. *Physical Review Letters*, **80**(10), 2245–2248.
- Wiseman, H.M. and Ralph, J.F. (2006) Reconsidering rapid qubit purification by feedback. *New Journal of Physics*, **8**(6), 90.
- Xie, S., Jia, F. and Yang, Y. (2009) Dynamic control of the entanglement in the presence of the time-varying field. *Optics Communications*, **282**(13), 2642–2649.
- Yamamoto, N., Tsumura, K. and Hara, S. (2007) Feedback control of quantum entanglement in a two-spin system. *Automatica*, **43**(6), 981–992.

10

State Control of Open Quantum Systems

10.1 State Transfer of Open Quantum Systems with a Single Control Field

In this section we will study the state transfer control of open quantum systems in the environment, in which states evolve along with phase decoherence and population relaxation. The Liouville–von Neumann equation of open quantum systems in a matrix form was transformed into a vector form using the Liouville super-operator to get a more easily solvable equation. Given the dynamical model of a dissipative quantum system in the presence of a time-dependent external control field, we chose the states transfer of system as the performance index, and derived a control law for the external field to drive the system state to transfer to the desired target state by a kind of no-iteration optimal control method. In the numerical simulation experiments, we will study the dynamics of a spin-1/2 particle system in a bath under the influence of an external control field. Different states transfer paths between eigenstates, pure states, and mixed states will be demonstrated on Bloch spheres to locate the specific evolution tracks by means of making each state of the spin-1/2 particle system correspond to a single point on or in the sphere uniquely. Finally, a detailed comparative analysis will be given.

10.1.1 *Dynamical Model of Open Quantum Systems*

The system of interest is coupled with the bath, whose evolution follows the dynamics of an open quantum system ($\hbar = 1$ is chosen):

$$\dot{\rho}_s = -\frac{i}{\hbar}[H_0, \rho_s] + L_D(\rho_s) \quad (10.1)$$

where ρ_s denotes the density matrix of the system state without the external control fields, H_0 is the Hamiltonian of the system, and L_D describes the bath-induced decoherence dynamics,

conveniently cast into the Lindblad semigroup form:

$$L_D(\rho_s) = \frac{1}{2} \sum_{j=1}^{N^2-1} r_j \left(\left[L_j \rho_s, L_j^\dagger \right] + \left[L_j, \rho_s L_j^\dagger \right] \right) \quad (10.2)$$

where L are operators in the Hilbert space of the system and r denotes the decoherence rate of the system under the bath. The nature of the bath interaction determines the form of the Lindblad operators L . The choice of L determines the dissipative model considered.

Our objective here is to design a time-dependent external control field $\vec{f}(t) = (f_1(t), f_2(t), \dots, f_M(t))$ to steer an open quantum system coupled with a bath, which makes sure that the system state will achieve the expected target state ρ_{tar} and maintain it for some time. The external control field is coupled to the subjected system by transition of molecular dipoles. At this point, the control Hamiltonian becomes $H_c = \sum_{m=1}^M H_m f_m(t)$ and the dynamical equation of the subjected system can be written as:

$$\dot{\rho}_c = -i[H_0, \rho_c] - i[H_c, \rho_c] + L_D(\rho_c) \quad (10.3)$$

where $\rho_c(t)$ is the system's state under the external control fields. The task now is how to design a control field $f(t)$ so that the evolution of the system state ρ_c will approach the target state ρ_{tar} as closely as possible.

10.1.2 Derivation of Optimal Control Law

In order to evaluate the extent of the transfer of system state ρ_c to the target state ρ_{tar} , the performance index here is chosen to be the Mayer type in optimal control, which only emphasizes the performance of the system on the terminal point of time.

$$J(t) = \text{Tr}(\rho_c(t) - \rho_{tar})^2 \quad (10.4)$$

One characteristic of the density matrix of a quantum system state is the complex conjugate, therefore at any time the density matrix of the system state $\rho_c(t)$ and the target state ρ_{tar} can be written as

$$\rho_c(t) = \begin{pmatrix} a_{11}(t) & a_{12}(t) & \cdots & a_{1n}(t) \\ a_{12}^*(t) & a_{22}(t) & \cdots & a_{2n}(t) \\ \vdots & \vdots & \ddots & \vdots \\ a_{1n}^*(t) & a_{2n}^*(t) & \cdots & a_{nn}(t) \end{pmatrix}, \rho_{tar} = \begin{pmatrix} b_{11} & b_{12} & \cdots & b_{1n} \\ b_{12}^* & b_{22} & \cdots & b_{2n} \\ \vdots & \vdots & \ddots & \vdots \\ b_{1n}^* & b_{2n}^* & \cdots & b_{nn} \end{pmatrix} \quad (10.5)$$

Substituting Equation 10.5 into Equation 10.4, one can get

$$J(t) = \sum_{i=1}^n (a_{ii}(t) - b_{ii})^2 + 2 \sum_{i,j=1, i \neq j}^n |a_{ij}(t) - b_{ij}|^2 \quad (10.6)$$

from which one can see that the performance index $J(t)$ will achieve the minimum value of zero if and only if $a_{ij}(t) = b_{ij}$ ($i, j = 1, 2, \dots, n$), which means the system state $\rho_c(t)$ equals the target state ρ_{tar} including non-diagonal elements and diagonal elements.

It is necessary for control fields to change the system states and reduce the value of the performance index $J(t)$ until the minimum, which means a suitable $f_m(t)$ needs be designed

so that the subjected system states ensure that the time derivative of the performance index

$$\frac{d}{dt}J(t) = \frac{d}{dt}\text{Tr}(\rho_c(t) - \rho_{tar})^2 \quad (10.7)$$

is non-positive at all time in $t \in [t_0, t_f]$.

By simple computation of Equation 10.7, one can obtain (for the sake of simplicity, we shorten $\rho_c(t)$ to ρ_c in the rest of this section)

$$\frac{d}{dt}\text{Tr}(\rho_c - \rho_{tar})^2 = \frac{d}{dt}\text{Tr}(\rho_c^2 - 2\rho_c\rho_{tar} + \rho_{tar}^2) = \text{Tr}(2\dot{\rho}_c\rho_c - 2\dot{\rho}_c\rho_{tar}) = 2\text{Tr}(\dot{\rho}_c(\rho_c - \rho_{tar})) \quad (10.8)$$

According to the control Hamiltonian $H_c = \sum_{m=1}^M H_m f_m(t)$ and substituting the dynamical equation of the open quantum systems as Equation 10.3 into Equation 10.8, one can get

$$\begin{aligned} \frac{d}{dt}\text{Tr}(\rho_c - \rho_{tar})^2 &= 2\text{Tr}(\dot{\rho}_c(\rho_c - \rho_{tar})) \\ &= 2\text{Tr}((-i[H_0, \rho_c] - i[H_c, \rho_c] + L_D)(\rho_c - \rho_{tar})) \\ &= 2\text{Tr}\left(\left((-i[H_0, \rho_c] - i\left[\sum_{m=1}^M H_m f_m, \rho_c\right] + L_D)\right)(\rho_c - \rho_{tar})\right) \\ &= -2i\sum_{m=1}^M f_m \text{Tr}([H_m, \rho_c](\rho_c - \rho_{tar})) + 2\text{Tr}((L_D - i[H_0, \rho_c])(\rho_c - \rho_{tar})) \end{aligned} \quad (10.9)$$

To ensure that $\frac{d}{dt}\text{Tr}(\rho_c - \rho_{tar})^2 \leq 0$, namely, that the right-hand side of Equation 10.9 is negative, one must have

$$\sum_{m=1}^M f_m i\text{Tr}([H_m, \rho_c](\rho_c - \rho_{tar})) \geq \text{Tr}((L_D - i[H_0, \rho_c])(\rho_c - \rho_{tar})) \quad (10.10)$$

To make Equation 10.10 hold, we let

$$f_m i\text{Tr}([H_m, \rho_c](\rho_c - \rho_{tar})) \geq \text{Tr}((L_D - i[H_0, \rho_c])(\rho_c - \rho_{tar}))/M \quad m = 1, \dots, M \quad (10.11)$$

from which one can obtain the range of control fields f_m by making the performance index Equation 10.4 be the smallest

$$\begin{cases} f_m \geq C/(MD) & \text{if } D > 0 \\ f_m \leq C/(MD) & \text{if } D < 0 \end{cases} \quad m = 1, \dots, M \quad (10.12)$$

where $C = \text{Tr}((L_D - i[H_0, \rho_c])(\rho_c - \rho_{tar}))$ and $D = i\text{Tr}([H_m, \rho_c](\rho_c - \rho_{tar}))$.

When the system state achieves the desired target state, $C = 0$ and $D = 0$. Transforming the inequality Equation 10.12 into an equation, one can get a group of control fields as

$$f_m = \begin{cases} K_1 C/(MD) & \text{if } D > 0 \text{ and } C \geq 0 \\ -K_2 C/(MD) & \text{if } D > 0 \text{ and } C < 0 \\ K_3 C/(MD) & \text{if } D < 0 \text{ and } C \geq 0 \\ -K_4 C/(MD) & \text{if } D < 0 \text{ and } C < 0 \end{cases} \quad m = 1, \dots, M \quad (10.13)$$

where the proportional coefficients $K_{1,2,3,4} > 1$.

A group of feasible control fields can then be obtained by simultaneously solving Equation 10.13:

$$f_m = \begin{cases} K_1 C / (MD) & \text{if } C \geq 0 \\ -K_2 C / (MD) & \text{if } C < 0 \end{cases} \quad m = 1, \dots, M \quad (10.14)$$

where $K_{1,2} > 1$.

Re-inspecting the scope of control fields Equation 10.12 that enables the performance index to be smallest, we let

$$K_{1,3} = k_{1,3}/D = k_{1,3}/(iTr([H_m, \rho_c](\rho_c - \rho_{tar}))) \quad (10.15)$$

where $k_{1,3} > 1$.

In Equation 10.15, D can be removed from the denominator of f_m and integrated into adjustable proportional coefficients $K_{1,3}$, while the ranges of $K_{2,4}$ do not change because of the bounded value of D . Then one can obtain a group of control fields that still meets the inequality Equation 10.12:

$$f_m = \begin{cases} K_1 C/M & \text{if } D > 0 \text{ and } C \geq 0 \\ -K_2 C/M & \text{if } D > 0 \text{ and } C < 0 \\ -K_3 C/M & \text{if } D < 0 \text{ and } C \geq 0 \\ K_4 C/M & \text{if } D < 0 \text{ and } C < 0 \end{cases} \quad m = 1, \dots, M \quad (10.16)$$

where $K_{1,3} = k_{1,3}/D$, $k_{1,3} > 1$, $K_{2,4} > 0$, $C = Tr((L_D - i[H_0, \rho_c])(\rho_c - \rho_{tar}))$, and $D = iTr([H_m, \rho_c](\rho_c - \rho_{tar}))$.

Remark 10.1 Equation 10.16 is the control law designed for optimal state transfer control when the control time t_f is not fixed. The advantage of the control design method used in this section is that the iterative process which exists in the standard quantum optimal control method can be avoided in the deriving process of the control law Equation 10.16 owing to the unfixed t_f . Because the control law is an analytical solution rather than a numerical one, one can adjust the proportional coefficients $K_j (j = 1, 2, 3, 4)$ in Equation 10.16 to make the system state ρ_c completely transfer into the target state ρ_{tar} at a given time $t = t_f$. The control problem with a given final time t_f can therefore be solved by the optimal control method designed here.

Remark 10.2 The control law Equation 10.16 is obviously segmented, which may affect the control effect. We therefore discuss here the continuous problem of boundary points in Equation 10.16 as follows. $C = 0$ or $D = 0$ both lead to $\rho_c = \rho_{tar}$, therefore $K_1 C/M, -K_2 C/M, -K_3 C/M$, and $K_4 C/M$ are all equal to zero when $C = 0$ or $D = 0$, which means that the control law Equation 10.16 is a continuous function without any break point.

Remark 10.3 From Equation 10.16 one can see that $C = Tr((L_D - i[H_0, \rho_c])(\rho_c - \rho_{tar}))$ in the numerator and $D = iTr([H_m, \rho_c](\rho_c - \rho_{tar}))$ in the denominator will both approach zero when

the system state ρ_c approaches the desired target state ρ_{tar} . According to Hospital's rule, one can derive that:

$$\lim_{\rho_c \rightarrow \rho_{tar}} f_m = \begin{cases} k_1 \text{Tr} \left(\sum_{j=1}^{N^2-1} \gamma_j (L_j L_j^\dagger - L_j^\dagger L_j) - i[H_0, \rho_{tar}] \right) / (iM \text{Tr}([H_m, \rho_{tar}])) & \text{if } D > 0 \text{ and } C \geq 0 \\ -K_2/M & \text{if } D > 0 \text{ and } C < 0 \\ -k_3 \text{Tr} \left(\sum_{j=1}^{N^2-1} \gamma_j (L_j L_j^\dagger - L_j^\dagger L_j) - i[H_0, \rho_{tar}] \right) / (iM \text{Tr}([H_m, \rho_{tar}])) & \text{if } D < 0 \text{ and } C \geq 0 \\ K_4/M & \text{if } D < 0 \text{ and } C < 0 \end{cases} \quad m = 1, \dots, M \quad (10.17)$$

from which one can see that when the system state achieves the target state $\rho_c \rightarrow \rho_{tar}$, the control values in Equation 10.16 are not infinite, namely, the value of the control law is bounded and cannot drive the system divergence.

Remark 10.4 The control law Equation 10.16 contains the system state ρ_c , which is a feedback quantity in each sampling period of optimal control. In model-based feedback control, the value of ρ_c comes from the system model (Equation 10.3) rather than measurements.

10.1.3 Control System Design

In this subsection we will specifically design a control law for the spin-1/2 particle system. The Lindblad equation of the controlled system can be written as:

$$\dot{\rho}_c = -i[H, \rho_c] + \frac{1}{2} \sum_{j=1}^3 \left([L_j \rho, L_j^\dagger] + [L_j, \rho L_j^\dagger] \right) \quad (10.18)$$

where the Lindblad operators L_j ($j = 1, 2, 3$) are related to the population relaxation rate γ and the pure phase relaxation rate $\tilde{\Gamma}$:

$$L_1 = \begin{bmatrix} 0 & 0 \\ \sqrt{\gamma_{21}} & 0 \end{bmatrix}, L_2 = \begin{bmatrix} 0 & \sqrt{\gamma_{12}} \\ 0 & 0 \end{bmatrix}, L_3 = \begin{bmatrix} \sqrt{2\tilde{\Gamma}_{12}} & 0 \\ 0 & 0 \end{bmatrix} \quad (10.19)$$

The phase relaxation rate between state $|1\rangle$ and state $|2\rangle$ is:

$$\Gamma_{12} = (\gamma_{12} + \gamma_{21})/2 + \tilde{\Gamma}_{12} \quad (10.20)$$

The Hamiltonian for the spin-1/2 particle model can be written as:

$$H := w \begin{bmatrix} 1 & 0 \\ 0 & -1 \end{bmatrix} + f_x \begin{bmatrix} 0 & 1 \\ 1 & 0 \end{bmatrix} + f_y \begin{bmatrix} 0 & -i \\ i & 0 \end{bmatrix} \quad (10.21)$$

where f_x and f_y are the external control fields imposed on directions x and y , respectively.

Substituting Equations 10.19 and 10.21 into Equation 10.18 gives the dynamical equation of the two-level open quantum system under external control fields. This is a matrix differential equation. In order to simplify the solving process, the $N \times N$ dimension density matrix $\rho(t)$ is

rewritten into a $1 \times N^2$ dimension column vector by column stacking, recorded as $|\rho(t)\rangle\rangle$. If $|\rho(t)\rangle\rangle$ is the independent variable, one can get the dynamical equation of the two-level open quantum system in the form of the Liouville super-operator:

$$\frac{d}{dt}|\rho(t)\rangle\rangle = \begin{bmatrix} -\gamma_{21} & if_x - f_y & -if_x - f_y & \gamma_{12} \\ if_x + f_y & -2iw - \Gamma_{12} & 0 & -if_x - f_y \\ -if_x + f_y & 0 & 2iw - \Gamma_{12} & if_x - f_y \\ \gamma_{21} & -if_x + f_y & if_x + f_y & -\gamma_{12} \end{bmatrix} |\rho(t)\rangle\rangle \quad (10.22)$$

where the values of parameters are set as

$$w = 20, \gamma_{12} = 19.8 \text{ cm}^{-1}, \gamma_{21} = 20 \text{ cm}^{-1}, \Gamma_{12} = 29.9 \text{ cm}^{-1} \quad (10.23)$$

The external control fields can change the evolution path of the state in an open quantum system and drive the state to the target state. In this subsection we study the transfers of the states with both diagonal and non-diagonal elements in a density operator. In order to demonstrate the trajectory of the state and consider that the system state corresponds with the point on or in the Bloch sphere, the Bloch sphere is chosen to display the evolution path from the initial state to the expected target state.

From the form of the system Hamiltonian (Equation 10.21) one can see that the external control fields have two possible directions, x and y . An external field in the x direction only enables transfer between the states in the $y - z$ plane in the Bloch sphere. Another external field in the y direction only enables transfer between the states in the $x - z$ plane in the Bloch sphere. External fields in both x and y directions enable transfer between the states with arbitrary phases in the Bloch sphere. For convenience, the control field only in one direction is imposed on the subjected system here. Assuming the electromagnetic field is imposed in direction y only, the dynamical equation of the subjected system is simplified to

$$\dot{\rho}_c = -i[H_0, \rho_c] - i[H_1 f_y, \rho_c] + \frac{1}{2} \sum_{j=1}^3 \left([L_j \rho, L_j^\dagger] + [L_j, \rho L_j^\dagger] \right) \quad (10.24)$$

Substituting the parameters in Equation 10.23 and $f_x = 0$ into Equation 10.22, the evolution equation in the super-operator form can be written as

$$\frac{d}{dt}|\rho(t)\rangle\rangle = \begin{bmatrix} -20 & -f_y & -f_y & 19.8 \\ f_y & -40i - 29.9 & 0 & -f_y \\ f_y & 0 & 40i - 29.9 & -f_y \\ 20 & f_y & f_y & -19.8 \end{bmatrix} |\rho(t)\rangle\rangle \quad (10.25)$$

The simulation experiments in the next subsection will all adopt the dynamical equation in super-operator formation (Equation 10.25).

10.1.4 Numerical Simulations and Results Analyses

An eigenstate ρ_{0a} , a pure state ρ_{0b} , and a mixed state ρ_{0c} are chosen to be the initial system states, respectively, in our experiments:

$$\rho_{0a} = \begin{bmatrix} 0 & 0 \\ 0 & 1 \end{bmatrix}, \rho_{0b} = \begin{bmatrix} 3/4 & \sqrt{3}/4 \\ \sqrt{3}/4 & 1/4 \end{bmatrix}, \rho_{0c} = \begin{bmatrix} 3/8 & \sqrt{3}/8 \\ \sqrt{3}/8 & 5/8 \end{bmatrix} \quad (10.26)$$

The control field as Equation 10.16 is adopted to be f_m , where the proportional coefficients are $K_{1,3} = k_{1,3}/(iTr([H_m, \rho_c](\rho_c - \rho_{tar}))$ and $K_{2,4} = k_{2,4}$. The greater the control quantity, the more obviously the environment is suppressed, but the control field should take a smaller value in view of the perturbative feature of the quantum control system. The proportional coefficients of control fields in the following experiments are therefore all values of the smallest integers, which enables the system states to achieve the target states. In addition, from Equation 10.16 one can see that the scope of the proportional coefficients of the control field is

$$k_{1,3} > 1, k_{2,4} > 0 \quad (10.27)$$

Experiments will be simulated according to different target states. The sampling period in the experiments is $\Delta t = 10^{-4}$.

1) Free evolution of systems without an external control field

The control field $f_m = 0$ when the external field is absent. The eigenstate, pure state, and mixed state specified in Equation 10.26 are chosen as the initial states in the experiments. The corresponding free evolutions of system states on the Bloch sphere are shown in Figure 10.1, in which “o” denotes the initial state of the system and “+” denotes the final state of the system. From the Bloch spheres in Figure 10.1 one can see that all the system states eventually terminate on the equilibrium state $\rho_f = \text{diag}\{99/199, 100/199\}$ without external control fields whenever the initial states are any of those three. These free evolutions display the relaxation processes of both phase and population of the two-level open quantum system.

2) Situation when the equilibrium state is the target state

Set the equilibrium state to be the target state:

$$\rho_{tar} = \text{diag}\{99/199, 100/199\} \quad (10.28)$$

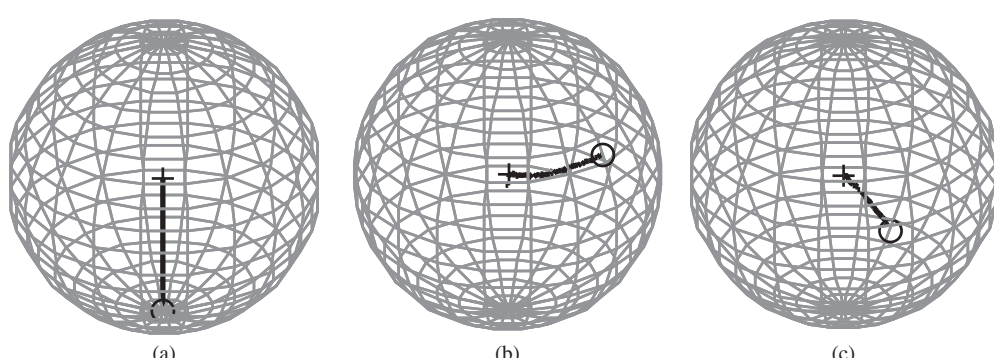


Figure 10.1 Free evolution trajectories without control fields in three initial states: (a) initial eigenstate, (b) initial pure state, and (c) initial mixed state

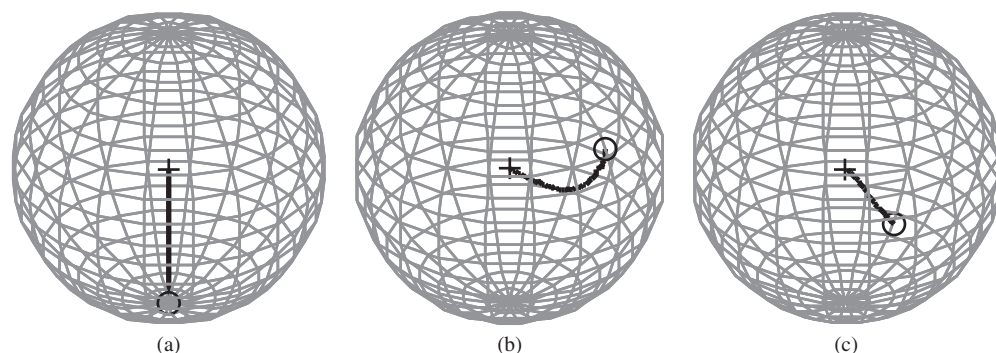


Figure 10.2 The paths of evolutions when the target state is the equilibrium state for $k_{1,3} = 2$ and $k_{2,4} = 1$: (a) initial eigenstate, (b) initial pure state, and (c) initial mixed state

As before, the eigenstate, pure state, and mixed state specified in Equation 10.26 are chosen to be the initial states. The external control fields in Equation 10.16 are adopted in the experiments. The corresponding evolutions of system states on the Bloch sphere obtained from the experiments are shown in Figure 10.2, in which “o” denotes the initial system state and “+” denotes the target system state. The proportional coefficients of control fields in Figure 10.2 are $k_{1,3} = 2$ and $k_{2,4} = 1$.

From the Bloch spheres in Figure 10.2 one can see that the system states all smoothly evolve to the target state (the equilibrium state) with 100% under the external control fields designed, no matter what point on or in Bloch sphere the initial states are. In fact, Figures 10.1b and 10.2b have the same system initial state and final state, between which the only difference is that an external control field exists in Figure 10.2b but not in Figure 10.1b. In order to analyze the experiments in this section (with an external control field) and the previous section (without an external control field), which have the same system initial state and final state, the population transferring graphs Figures 10.1b and 10.2b are presented in Figure 10.3, where the horizontal axes are the timeline and the longitudinal axes show the populations on the two qubits. From Figure 10.3 one can see that the time for the system in Figure 10.1b to achieve the target state is 0.08, while the time for the system in Figure 10.2b to achieve the target state is 0.03, which indicates that the external control field greatly speeds up the evolution from the initial state to the target state. This effect cannot be demonstrated in figures of evolution on the Bloch sphere.

3) Situation when the mixed state is the target state

When mixed states are the target states, we do the simulation experiments for two cases: the mixed state on the z -axis and a general case.

In the first case, a mixed state on the z -axis is set to be the target state:

$$\rho_{tar2} = \text{diag}\{1/3, 2/3\} \quad (10.29)$$

As before, the eigenstate, the pure state, and the mixed state specified in Equation 10.26 are chosen to be the initial states. An external control field in Equation 10.16 is again adopted.

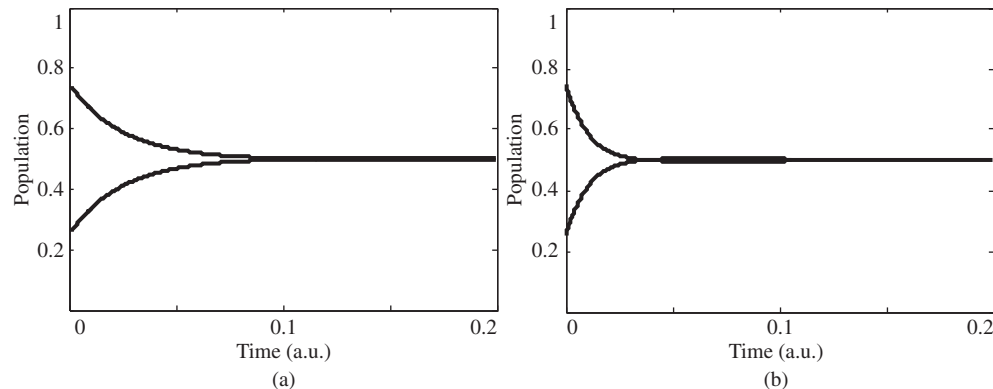


Figure 10.3 The population transfer with and without external control fields from the initial pure state to the target equilibrium state: (a) population transfer in the free evolution and (b) population transfer under the control

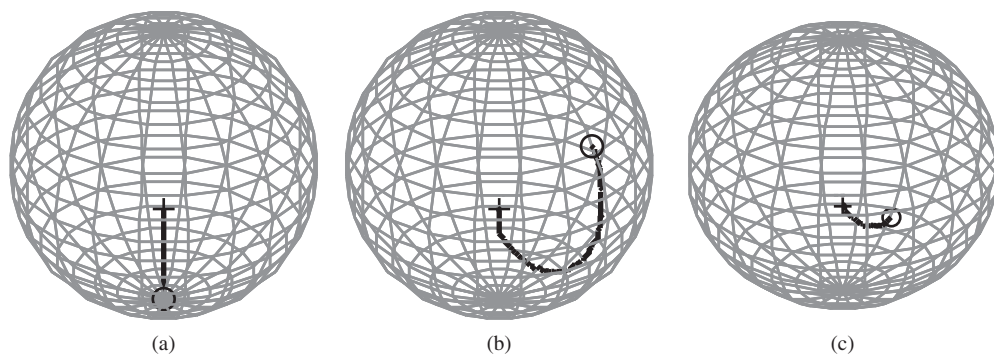


Figure 10.4 The paths of evolutions when the target state is a mixed state on the z -axis: (a) initial eigenstate and $k_{1,3} = 2$, $k_{2,4} = 1$, (b) initial pure state and $k_{1,3} = 2$, $k_{2,4} = 8$, and (c) initial mixed state and $k_{1,3} = 2$, $k_{2,4} = 58$

The corresponding evolution of system states on the Bloch sphere are shown in Figure 10.4, in which “o” denotes the initial system state and “+” denotes the target system state. In Figure 10.4 the proportional coefficients are $k_{1,3} = 2$ and $k_{2,4} = 1$ when the initial state is an eigenstate, $k_{1,3} = 2$ and $k_{2,4} = 8$ when the initial state is a pure state, and $k_{1,3} = 2$ and $k_{2,4} = 58$ when the initial state is a mixed state. From Figure 10.4 one can see that when the target state is a mixed state on the z -axis, the system states evolve to the z -axis first and then evolve to the target states along the z -axis. In Figures 10.4b and 10.4c control fields that are strong enough to suppress the relaxation effect caused by the environment and drive the system states to evolve to the target state are needed.

In the second case a general mixed state is set to be the target state:

$$\rho_{tar3} = \begin{bmatrix} 3/8 & 1/8 \\ 1/8 & 5/8 \end{bmatrix} \quad (10.30)$$

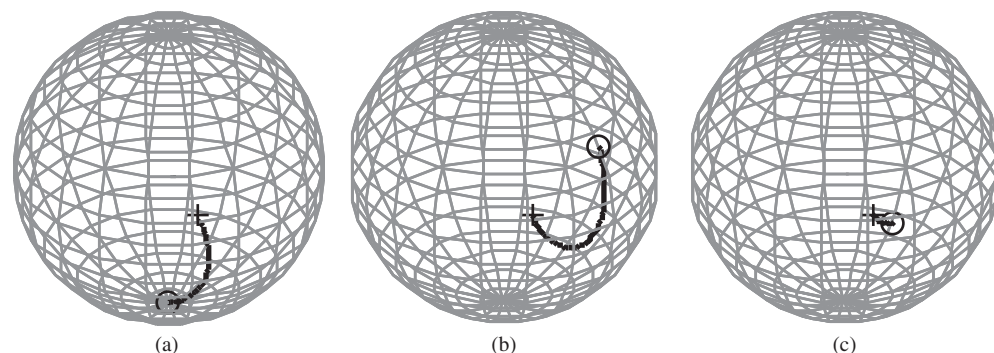


Figure 10.5 The paths of evolutions when the target state is a general mixed state: (a) initial eigenstate and $k_{1,3} = 2$, $k_{2,4} = 3$, (b) initial pure state and $k_{1,3} = 2$, $k_{2,4} = 6$, and (c) initial mixed and $k_{1,3} = 2$, $k_{2,4} = 27$

As before, the eigenstate, pure state, and mixed state specified in Equation 10.26 are chosen to be the initial states. An external control field in Equation 10.16 is again adopted for the simulation experiments. The corresponding evolution of system states on the Bloch sphere is shown in Figure 10.5, where “o” denotes the initial system state and “+” denotes the target system state. In Figure 10.5 the proportional coefficients are $k_{1,3} = 2$ and $k_{2,4} = 3$ when the initial state is an eigenstate, $k_{1,3} = 2$ and $k_{2,4} = 6$ when the initial state is a pure state, and $k_{1,3} = 2$ and $k_{2,4} = 27$ when the initial state is a mixed state.

From Figure 10.5 one can see that the system state can evolve to a general mixed state from an eigenstate, pure state, or mixed state by control fields to suppress the relaxation effect caused by the environment.

From the four groups of experiments above, one can see that an open quantum system has its own evolution path when there is no external control field. In this way both phase and population relax, and the system state ultimately evolves to the equilibrium state. If the desired target state is not on this evolution path, one can impose an external control field to change the evolution path to pass the target state and accomplish the transfer from the initial state to the target state. If the desired target state happens to fall on the original evolution path of the open quantum system, one can transfer the system state from the initial state to the target state whether or not there is a control field. In that case, the effect of the control field is to speed up the evolution to the target state.

The environment can produce a slow decline in the purity of the system state, which leads to a limitation with which the initial state and the target state should comply. This limitation is that the purity of the initial state must be bigger than that of the target state, otherwise transfer control cannot be achieved. With this limitation, the initial state and the target state can be selected as any state.

10.2 Purity and Coherence Compensation through the Interaction between Particles

As a main goal of quantum control, the preservation of state purity and coherence retains the information of quantum systems, thus it is of primary importance in the quantum

information process (Nielsen and Chuang, 2010) and quantum coherent control (Brumer and Shapiro, 2003). Various methods have been developed for this goal, for example quantum error-correcting coding (Steane, 1999; Shor, 1995; MacWilliams and Sloane, 1977), a decoherence-free subspace or noiseless subsystem (Lidar, Chuang, and Whaley, 1998; Duan and Guo, 1997, 1998; Zanardi, 1998), strategies based on feedback or stochastic control (Mancini and Bonifacio, 2001; Wiseman, Mancini, and Wang, 2002), and dynamical decoupling (Viola, Knill, and Lloyd, 1999; Viola, 2002; Vitali and Tombesi, 2001; Byrd and Lidar, 2003; Facchi *et al.*, 2005). Both the logical coding in quantum error-correcting coding and the states recoding in decoherence-free subspace need an assistant quantum system that provides information redundancy. Strategies based on feedback manipulate the evolutions of quantum system states and need no assistant system. Decoherence may be suppressed for a while but cannot be prevented completely because of the unitary of the control operation. In such a case, state purity is uncontrollable (Facchi *et al.*, 2005).

In order to compensate for purity and coherence leaking to the environment, non-unitary operations that increase the purity and coherence of the controlled system should be induced, but it is difficult for the continuous wave control method to do this. We therefore propose a new method in this section, which is similar to error-correcting coding and decoherence-free subspace methods in some ways. The method proposed needs an assistant quantum system. The main idea is that purity and coherence are transferred from an assistant particle to the target one by carefully selecting the types of interactions between these two particles to compensate for the purity and leaking of coherence to the environment of the target particle.

10.2.1 Method of Compensation for Purity and Coherence

In order to purify a target particle with a mixed state or counteract the process of decoherence, one can transfer an assistant particle into the purity or coherence. The transference may compensate the purity of the target particle or the leaking of coherence due to decoherence process. Such a method is based on the assumption that the types of interaction between the two particles can be chosen freely, and the interaction intensities can be controlled.

1) Interaction model of spin-1/2 particles

In present work we choose spin-1/2 particles as the target and assistant particles. The target particle 1 and the assistant particle 2 compose a closed quantum system, and between them there are nine basic types of interaction Hamiltonian:

$$\sigma_m \otimes \sigma_n, \quad m, n = x, y, z \quad (10.31)$$

where $\sigma_{x,y,z}$ are Pauli matrices, which denote rotations around the x -, y -, and z -axes.

The von Neumann equation describing the evolution of the density matrix for the closed quantum system under the action of the interaction Hamiltonians is:

$$i\hbar\dot{\rho} = [H_i, \rho] \quad (10.32a)$$

$$H_i = -\frac{\hbar}{2} \left(\sum_{m,n=x,y,z} J_{mn}(t) \sigma_m \otimes \sigma_n \right) \quad (10.32b)$$

where H_i are time-dependent interaction Hamiltonians. $J_{mn}(t) \geq 0$ denotes the intensity of interaction $\sigma_m \otimes \sigma_n$, $m, n = x, y, z$.

The system density matrix ρ can be decomposed into the following form:

$$\rho = \sum_{k=0}^{15} \text{Tr}(4\rho X_k) X_k = \sum_{k=0}^{15} p_k X_k \quad (10.33a)$$

where $p_k \in [-1, 1]$, and X_k is defined as

$$\{X_k\} = \frac{1}{4} \left\{ I \otimes I, \sigma_x \otimes I, \sigma_y \otimes I, \sigma_z \otimes I, I \otimes \sigma_x, I \otimes \sigma_y, I \otimes \sigma_z, \right. \\ \left. \sigma_x \otimes \sigma_x, \sigma_x \otimes \sigma_y, \sigma_x \otimes \sigma_z, \sigma_y \otimes \sigma_x, \sigma_y \otimes \sigma_y, \sigma_y \otimes \sigma_z, \sigma_z \otimes \sigma_x, \sigma_z \otimes \sigma_y, \sigma_z \otimes \sigma_z \right\}, \quad (10.33b)$$

Equation 10.33a establishes one-to-one correspondence between density matrix ρ and vector $P = (p_1, p_2, \dots, p_{15})^T$. The vector $P = (p_1, p_2, \dots, p_{15})^T$ is called the coherent vector. $B_1 = (p_1, p_2, p_3)^T$ and $B_2 = (p_4, p_5, p_6)^T$ correspond to vector $B = (x, y, z)^T$ on the Bloch sphere of particles 1 and 2. p_7 through p_{15} are quantities describing the relation between the two particles. For example, all zeros denote the closed system in a separable state that can be expressed as a tensor product of the states of particles 1 and 2.

An inner product of two Bloch vectors is defined as

$$D(B_1, B_2) = (p_1 p_4 + p_2 p_5 + p_3 p_6)^{1/2} \quad (10.34)$$

The purity of a particle is defined as the module of its Bloch vector, viz. the inner product to itself. While the coherence is defined as the projection length of the Bloch vector on the $x-y$ plane, thus purity and coherence of particle 1 can be expressed as

$$pu_1 = (p_1^2 + p_2^2 + p_3^2)^{1/2} = D(B_1) \quad (10.35a)$$

$$co_1 = (p_1^2 + p_2^2)^{1/2} = D(P_{xy} B_1) \quad (10.35b)$$

$$P_{xy} = \begin{pmatrix} 1 & 0 & 0 \\ 0 & 1 & 0 \\ 0 & 0 & 0 \end{pmatrix} \quad (10.35c)$$

where P_{xy} is the projection factor to the $x-y$ plane.

This definition of purity is equivalent to the usual definition $p \equiv \text{tr}(\rho^2)$. We are interested in a two-level quantum particle denoted particle 1, whose purity under the usual definition can be calculated by

$$p = \text{tr}(\rho_1^2) = \text{tr}(\text{tr}_2(\rho_{12})^2) = 1/2 \sum_{i=1,2,3} p_i^2 + 1/2 = 1/2 pu_1^2 + 1/2$$

which gives a one-to-one correspondence between p and pu_1 , where the latter is more intuitionistic to comprehend and convenient to discuss.

Rewrite Equation 10.32 into coherent vector form and replace $J_{xx}, J_{xy}, J_{xz}, J_{yx}, J_{yy}, J_{yz}, J_{zx}, J_{zy}, J_{zz}$ with J_1 through J_9 , respectively as:

$$\dot{\rho}(t) = \tilde{H}(t)\rho(t) \quad (10.36a)$$

$$\tilde{H}(t) = \begin{pmatrix} 0 & 0 & 0 & 0 & 0 & 0 & 0 & 0 & J_7 & J_8 & J_9 & -J_4 & -J_5 & -J_6 \\ 0 & 0 & 0 & 0 & 0 & 0 & -J_7 & -J_8 & -J_9 & 0 & 0 & J_1 & J_2 & J_3 \\ 0 & 0 & 0 & 0 & 0 & 0 & J_4 & J_5 & J_6 & -J_1 & -J_2 & -J_3 & 0 & 0 \\ 0 & 0 & 0 & 0 & 0 & 0 & 0 & J_3 & -J_2 & 0 & J_6 & -J_5 & 0 & J_9 & -J_8 \\ 0 & 0 & 0 & 0 & 0 & 0 & -J_3 & 0 & J_1 & -J_6 & 0 & J_4 & -J_9 & 0 & J_7 \\ 0 & 0 & 0 & 0 & 0 & 0 & J_2 & -J_1 & 0 & J_5 & -J_4 & 0 & J_8 & -J_7 & 0 \\ 0 & J_7 & -J_4 & 0 & J_3 & -J_2 & 0 & 0 & 0 & 0 & 0 & 0 & 0 & 0 & 0 \\ 0 & J_8 & -J_5 & -J_3 & 0 & J_1 & 0 & 0 & 0 & 0 & 0 & 0 & 0 & 0 & 0 \\ 0 & J_9 & -J_6 & J_2 & -J_1 & 0 & 0 & 0 & 0 & 0 & 0 & 0 & 0 & 0 & 0 \\ -J_7 & 0 & J_1 & 0 & J_6 & -J_5 & 0 & 0 & 0 & 0 & 0 & 0 & 0 & 0 & 0 \\ -J_8 & 0 & J_2 & -J_6 & 0 & J_4 & 0 & 0 & 0 & 0 & 0 & 0 & 0 & 0 & 0 \\ -J_9 & 0 & J_3 & J_5 & -J_4 & 0 & 0 & 0 & 0 & 0 & 0 & 0 & 0 & 0 & 0 \\ J_4 & -J_1 & 0 & 0 & J_9 & -J_8 & 0 & 0 & 0 & 0 & 0 & 0 & 0 & 0 & 0 \\ J_5 & -J_2 & 0 & -J_9 & 0 & J_7 & 0 & 0 & 0 & 0 & 0 & 0 & 0 & 0 & 0 \\ J_6 & -J_3 & 0 & J_8 & -J_7 & 0 & 0 & 0 & 0 & 0 & 0 & 0 & 0 & 0 & 0 \end{pmatrix}, \quad (10.36b)$$

where $J_k(t)$ is simplified to J_k for convenience.

If we consider further the decoherence process of particle 1 due to interactions with the environment, then the equation for the state evolution of the complex system composed of target particle 1 and assistant particle 2 is:

$$\dot{P}(t) = (\tilde{H}(t) + \tilde{L}(t))P(t) + \lambda(t) \quad (10.37)$$

where $\tilde{L}(t)$ and $\lambda(t)$ denote the effect induced by interactions between target particle 1 and the environment.

In fact it is not necessary to use nine types of interaction to transfer the purity or coherence from the assistant particle to the target one. Choosing too many basic types of interaction will complicate the problem while too few will be incapable of completing the compensation effectively. The proper selection of basic interaction types can be done through analyses of the structure of $\tilde{H}(t)$.

2) Selection of the interaction type

According to the structure of $\tilde{H}(t)$, one can obtain the relations between quantities of the Bloch vector as shown in Figure 10.6, from which one can consider $p_A \xrightarrow{J_k} p_B$. This has two significant points: it shows, on one side, that p_A promotes the increase in p_B , viz. $\dot{p}_B = J_k p_A$; on the other side p_B induces the decrease of p_A , that is, $\dot{p}_A = -J_k p_B$. It should be noted that $p_A + p_B$ is not a conservational quantity, but $p_A^2 + p_B^2$, that is, the decrease rate of p_A^2 equals the increase rate of p_B^2 . Because there are extractions in the definition of the purity and coherence, they are not conservational quantities.

The compensation for the purity or coherence of the target particle increases $pu_1^2 = p_1^2 + p_2^2 + p_3^2$ or $co_1^2 = p_1^2 + p_2^2$, and the increment is obtained from the assistant particle, therefore the interactions selected should establish a passage from p_4, p_5, p_6 to p_1, p_2, p_3 . At least three basic interaction types are needed for such a passage, made up of three different kinds of one-to-one connectedness:

$$\sigma_x \otimes \sigma_x, \sigma_y \otimes \sigma_y, \sigma_z \otimes \sigma_z \iff J_1(t)J_5(t)J_9(t) \neq 0 \iff \begin{cases} p_4 \leftrightarrow p_1 \\ p_5 \leftrightarrow p_2 \\ p_6 \leftrightarrow p_3 \end{cases} \quad (10.38a)$$

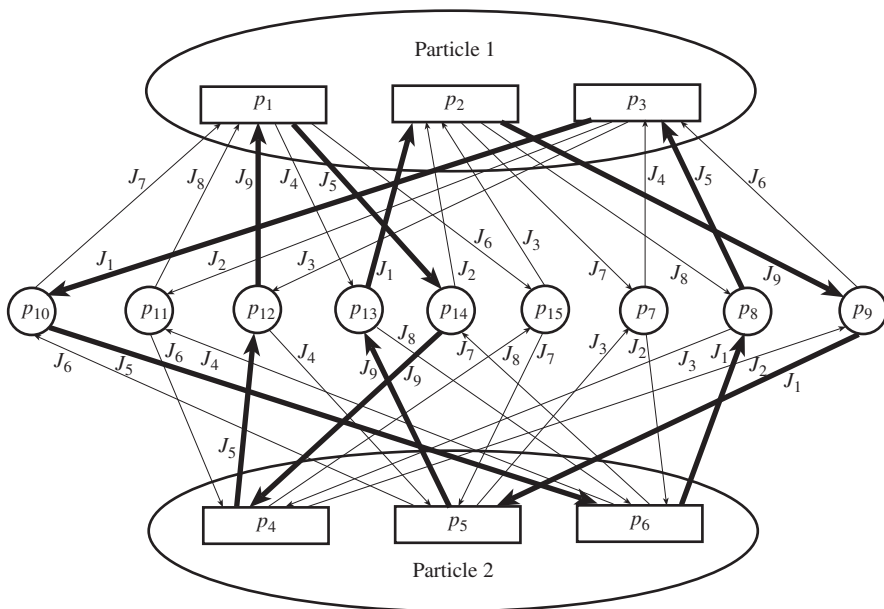


Figure 10.6 The relations between quantities of the Bloch vector are obtained according to the structure of $\tilde{H}(t)$

$$\sigma_x \otimes \sigma_y, \sigma_y \otimes \sigma_z, \sigma_z \otimes \sigma_x \iff J_2(t)J_6(t)J_7(t) \neq 0 \iff \begin{cases} p_4 \leftrightarrow p_3 \\ p_5 \leftrightarrow p_1 \\ p_6 \leftrightarrow p_2 \end{cases} \quad (10.38b)$$

$$\sigma_x \otimes \sigma_z, \sigma_y \otimes \sigma_x, \sigma_z \otimes \sigma_y \iff J_3(t)J_4(t)J_8(t) \neq 0 \iff \begin{cases} p_4 \leftrightarrow p_2 \\ p_5 \leftrightarrow p_3 \\ p_6 \leftrightarrow p_1 \end{cases} \quad (10.38c)$$

Equations 10.38a–c show the three simplest cases. For the other three cases, at least six basic interaction types are needed, which makes the problem more complex and more cumbersome to deal with.

Equation 10.38a will be analyzed in the following. The connection between the quantities of the two Bloch vectors is marked with thick lines in Figure 10.6, from which one can see that quantities $p_8, p_9, p_{10}, p_{12}, p_{13}, p_{14}$ are located on the passages, while p_7, p_{11}, p_{15} are isolated, and therefore they are invariable during the evolution of the system.

10.2.2 Analysis of System Evolution

For convenience we suppose that

$$J_1(t) = J_5(t) = J_9(t) = J(t) \quad (10.39)$$

If we take no account of the decoherence, Equation 10.36a has an analytical solution:

$$P(t) = \exp \left(\int_0^t \tilde{H}(s) ds \right) P(0) \quad (10.40)$$

where $P(0)$ is the initial coherent vector of the complex system. It is reasonable to assume that the complex system is in a separable state before the interaction of the two particles, that is, $p_7(0)$ through $p_{15}(0)$ are all zero. Let

$$Q(t) = \int_0^t J(s) ds \quad (10.41)$$

then the quantities of the Bloch vectors of particles 1 and 2 have analytical forms:

$$\begin{aligned} p_1(t) &= \frac{p_1(0) - p_4(0)}{2} \cos(2Q(t)) + \frac{p_1(0) + p_4(0)}{2} \\ p_2(t) &= \frac{p_2(0) - p_5(0)}{2} \cos(2Q(t)) + \frac{p_2(0) + p_5(0)}{2} \\ p_3(t) &= \frac{p_3(0) - p_6(0)}{2} \cos(2Q(t)) + \frac{p_3(0) + p_6(0)}{2} \end{aligned} \quad (10.42a)$$

$$\begin{aligned} p_4(t) &= \frac{p_4(0) - p_1(0)}{2} \cos(2Q(t)) + \frac{p_1(0) + p_4(0)}{2} \\ p_5(t) &= \frac{p_5(0) - p_2(0)}{2} \cos(2Q(t)) + \frac{p_2(0) + p_5(0)}{2} \\ p_6(t) &= \frac{p_6(0) - p_3(0)}{2} \cos(2Q(t)) + \frac{p_3(0) + p_6(0)}{2} \end{aligned} \quad (10.42b)$$

Thus the purity and coherence of particle 1 can be derived according to Equations 10.35a and 10.35b:

$$pu_1(t) = \frac{1}{2} D(B_1(0)(1 + \cos(2Q(t))) + B_2(0)(1 - \cos(2Q(t)))) \quad (10.43a)$$

$$co_1(t) = \frac{1}{2} D(P_{xy}(B_1(0)(1 + \cos(2Q(t))) + B_2(0)(1 - \cos(2Q(t))))) \quad (10.43b)$$

Some properties of the system evolution can be obtained from Equations 10.42a and 10.42b, for example if $Q(t) = \pi/2$, we can exchange the states of those two particles. Equations 10.43a and 10.43b show that the sufficient and essential condition to preserve the purity (coherence) is that the projections to the $x-y$ plane of two initial Bloch vectors are the same. In such a situation the states of two particles are invariant. Another important property of system evolution is that the track of two particle states on the Bloch sphere can be found according to two initial Bloch vectors:

Theorem 10.1 The track for the states evolution of two particles on the Bloch sphere is the length of a straight line ascertained by two initial states.

Proof If the initial Bloch vectors of two particles are $B_1(0) = (p_1(0), p_2(0), p_3(0))^T$ and $B_2(0) = (p_4(0), p_5(0), p_6(0))^T$, then the coordinates of dots on the straight line ascertained by two initial states satisfy the following equations

$$\begin{cases} (y - p_2(0))(p_4(0) - p_1(0)) = (p_5(0) - p_2(0))(x - p_1(0)) \\ (z - p_3(0))(p_4(0) - p_1(0)) = (p_6(0) - p_3(0))(x - p_1(0)) \end{cases} \quad (10.44)$$

which come into existence when x , y , and z are substituted in Equations 10.42a and 10.42b. This gives the states at any time location on the line described by Equation 10.44.

Considering $\cos(2Q(t)) \in [-1, 1]$ we have

$$p_1(t) \in [\min\{p_1(0), p_4(0)\}, \max\{p_1(0), p_4(0)\}] \quad (10.45)$$

In the same way we know that $p_2(t) \sim p_6(t)$ satisfies conditions similar to Equation 10.45, therefore the track for states evolution of those two particles on the Bloch sphere is the length of a straight line ascertained by two initial states.

End. ■

According to Theorem 10.1, one can obtain the following deduction.

Deduction 10.0 The sufficient and necessary condition to compensate for the purity (coherence) of the target particle with an assistant particle is that the purity (coherence) of the assistant particle must be larger than that of the target particle. The largest compensation must be equal to the difference between the purities (coherences) of the two particles.

For a target particle in a mixed state, Deduction 10.1 tells us that to compensate for the purity or coherence with an assistant particle, whose purity or coherence must be larger than that of the target one, and the magnitude of compensation can be controlled by $Q(t)$.

Now consider the effect of decoherence. Suppose the purity-leaking rate (coherence-leaking rate) of the target particle due to interactions with the environment is $V_{de}(t)$, and the purity (coherence) can be also preserved through compensation with an assistant particle. In this case the conditions that the assistant particle satisfies are more rigorous than in Deduction 10.1.

Theorem 10.2 The sufficient and necessary condition to preserve the purity (or coherence) of the target particle for a period of time after the beginning of purity leaking (or decoherence) is that the Bloch vectors (or their projection onto $x-y$ plane) of the two particles form an obtuse triangle, whose longest side is the Bloch vector of the assistant particle (or its projection), that is,

$$D^2(B_2(0)) - D^2(B_1(0)) - D^2(B_2(0) - B_1(0)) > 0 \quad (10.46a)$$

$$D^2(P_{xy}B_2(0)) - D^2(P_{xy}B_1(0)) - D^2(P_{xy}B_2(0) - P_{xy}B_1(0)) > 0 \quad (10.46b)$$

Proof Consider the purity differential coefficient of the target particle without the effect of decoherence according to Equation 10.43a:

$$p\dot{u}_1(t) = \frac{J(t) \sin(2Q(t))}{2} \frac{D^2(B_2(0)) - D^2(B_1(0)) - D^2(B_2(0) - B_1(0)) \cos(2Q(t))}{D(B_1(0)[1 + \cos(2Q(t))] + B_2(0)[1 - \cos(2Q(t))])} \quad (10.47)$$

At the beginning of time dt , in order to compensate for the purity leaking of the target particle due to the interactions with the environment, the purity differential coefficient induced by interactions with the assistant particle must be equal to the purity-leaking rate:

$$p\dot{u}_1(dt) = V_{de}(dt) \quad (10.48)$$

For a finite $J(t)$, dt could be small enough to make a sufficiently small $Q(dt)$, thus according to Equations 10.47 and 10.48:

$$\begin{aligned} J(dt) &= \frac{2V_{de}(dt)D(B_1(0)[1 + \cos(2Q(dt))] + B_2(0)[1 - \cos(2Q(dt))])}{\sin(2Q(dt))[D^2(B_2(0)) - D^2(B_1(0)) - D^2(B_2(0) - B_1(0))\cos(2Q(dt))]} \\ &\approx \frac{2V_{de}(dt)D(B_1(0))}{Q(dt)[D^2(B_2(0)) - D^2(B_1(0)) - D^2(B_2(0) - B_1(0))]} \end{aligned} \quad (10.49)$$

the sufficient and necessary condition for $J(dt)$ to be existent is therefore that Equation 10.46a comes into existence. In a similar way it can be found that the sufficient and essential condition for the coherence situation is Equation 10.46b.

The proof is complete. ■

To preserve particle purity (coherence), intensities of interactions between the two particles should be controlled. At any time t the purity-increase (coherence-increase) rate of the target particle due to interactions with the assistant particle should be equal to its purity-leaking (coherence-leaking) rate $V_{de}(t)$, thus it can be found from Equation 10.36a that:

$$p\dot{u}_1(t) = \frac{J(t)(p_1(t)p_{12}(t) - p_1(t)p_{14}(t) + p_2(t)p_{13}(t) - p_2(t)p_9(t) + p_3(t)p_8(t) - p_3(t)p_{10}(t))}{p u_1(t)} = V_{de}(t) \quad (10.50a)$$

$$co_1(t) = \frac{J(t)(p_1(t)p_{12}(t) - p_1(t)p_{14}(t) + p_2(t)p_{13}(t) - p_2(t)p_9(t))}{co_1(t)} = V_{de}(t) \quad (10.50b)$$

In the next section system numerical simulation experiments will be done to validate the validity of compensation with an assistant particle for the situations of purity compensation of the mixed state and coherence preservation in the decoherence process.

10.2.3 Numerical Simulations

1) Compensation of purity for mixed state

Suppose the target particle and the assistant particle are in a maximum mixed state and a ground state initially, and the complex closed system is in a separable state. The initial coherent vector of the system is supposed to be:

$$P(0) = (0, 0, 0, 0, 0, 1, 0, \dots, 0)_{15}^T \quad (10.51)$$

so the maximum compensation of purity for the target particle is 1 with $Q(t) = \pi/2$ according to Deduction 10.1. The interaction intensities are therefore designed to be:

$$J(t) = \begin{cases} (1 - \cos t)^2 / 6, & 0 \leq t \leq 2\pi \\ 0, & \text{else} \end{cases} \quad (10.52)$$

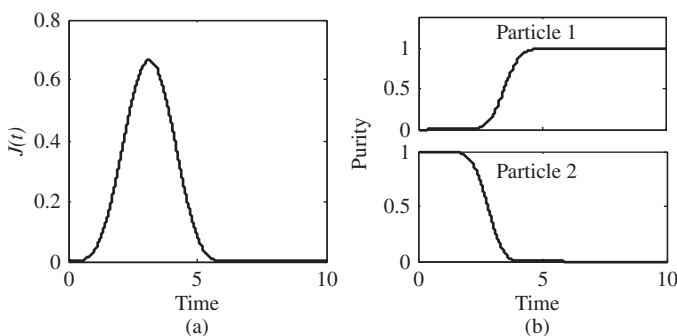


Figure 10.7 (a) Interaction intensity curves between the target particle and the assistant particle. (b) Purities of two particle

In the simulation experiment, simulation step τ is 0.01 and the simulation time is 7. Interaction intensities $J(t)$ are considered to be invariant in a simulation step τ . Evolution of the system coherent vector can be derived using Equation 10.53 iteratively, and purity curves for the two particles can be drawn as Figure 10.7:

$$P(t + \tau) = \exp(\tilde{H}(t)\tau)P(t) \quad (10.53)$$

Figure 10.7a shows the curves of the interaction intensities $J(t)$ between the two particles, and Figure 10.7b shows their purity curves. It can be seen from Figure 10.7b that the purity of particle 1 increases during the interaction and finally arrives at 1, while the purity of particle 2 decreases to 0; the purity compensation for the target particle is achieved successfully.

2) Counteraction for the decoherence process

The decoherence process of the target particle induced by interactions with the environment can be counteracted by an assistant particle. Considering the pure dephasing decoherence process, in this case

$$\lambda(t) = 0 \quad (10.54a)$$

and $\tilde{L}(t)$ has the form

$$\tilde{L}(t) = \begin{pmatrix} -\gamma & 0 & 0 & \cdots & 0 \\ 0 & -\gamma & 0 & \cdots & 0 \\ 0 & 0 & 0 & \cdots & 0 \\ \vdots & \vdots & \vdots & \ddots & 0 \\ 0 & 0 & 0 & 0 & 0 \end{pmatrix}_{15 \times 15} \quad (10.54b)$$

The coherence-leaking rate of the target particle can therefore be found according to Equations 10.37, 10.54a and 10.54b:

$$V_{de}(t) = \gamma co_1(t) \quad (10.55)$$

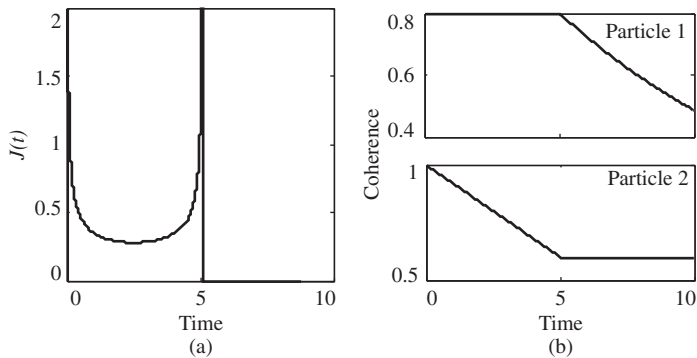


Figure 10.8 (a) Interaction intensities. (b) Particle coherence curves

According to Equation 10.50b, the condition to preserve the coherence of the target particle is that the interaction intensities of $J(t)$ should satisfy the following equation:

$$J(t) = \frac{\gamma co_1^2(t)}{p_1(t)p_{12}(t) - p_1(t)p_{14}(t) + p_2(t)p_{13}(t) - p_2(t)p_9(t)} \quad (10.56a)$$

Because the denominator of Equation 10.56a may be zero, an upper limit J_{\max} is needed for $J(t)$. When $J(t)$ calculated by a too small denominator is too large, it will be set to J_{\max} , and when the denominator becomes a negative, $J(t)$ is set to zero. Thus in the simulation experiment the interaction intensity $J(t)$ is designed as

$$J(t) = \begin{cases} 0, & J(t) \leq 0 \\ J_{\max}, & J(t) \geq J_{\max} \\ \frac{\gamma co_1^2(t)}{p_1(t)p_{12}(t) - p_1(t)p_{14}(t) + p_2(t)p_{13}(t) - p_2(t)p_9(t)}, & \text{else} \end{cases} \quad (10.56b)$$

Figure 10.8 show the interaction intensities and particle coherence curves for $\gamma = 0.1$, $P(0) = (0.8, 0, 0, 1, 0, 0, 0, \dots, 0)_{15}^T$, $J_{\max} = 2$, and $\tau = 0.01$. It is shown in Figure 10.8 that when the coherence of particle 1 leaks to the environment, the existence of the assistant particle and interaction with it preserves the coherence of particle 1 during time (0,5). After that the interactions come to a halt, the coherence of particle 1 decreases and particle 2 is preserved. One can see from Figure 10.8b that when the coherence of particle 1 is invariant, the coherence-decrease rate of particle 2 is constant and equal to the coherence-leaking rate of particle 1.

10.2.4 Discussion

Deduction 10.1 gives the condition for compensating for the purity of the target particle in a mixed state with an assistant particle. In order to get the maximum purity compensation $Q(t) = \pi/2$ should come into the existence, which actually exchanges the states of the two particles. A single particle in a mixed state is in fact entangled with some particles in the

environment; the exchange of states for the two particles predicates the invariance of states for those particles entangled with the target particle during purification. This may be useful in some situations, for instance the particles entangled to the target particle are considered to be part of the interested system whose states need to be retained during the purification of the target particle. If the target particle is purified through the measurement, collapse would be induced, which changes the states of the particles entangled to the target one.

To compensate for the decoherence process, Theorem 10.2 gives the condition for preserving the coherence of the target particle with an assistant particle, which is not very rigorous. In Equation 10.49, a very small $Q(dt)$ within a short time dt after the beginning of the interaction may lead to a large $J(dt)$, which means the compensation of coherence for particle 1 cannot sufficiently counteract the coherence that leaks to the environment. The coherence of the target particle therefore decreases a short time after the beginning of the interaction. The decrement is very small because such a time is very short. It can be seen from Figure 10.8a that the period when the interaction intensities are at the maximum of 2 is the period when the coherence of the target particle decreases. The decrement cannot be seen in Figure 10.8b because it is too small. It can also be seen from Figure 10.8a that intensities achieve the maximum at the end of the interaction because the denominator of Equation 10.56a is close to zero then. When the denominator of Equation 10.56a becomes negative, the existence of interactions cannot compensate for the leaking of the coherence of particle 1 to the environment but transfers the coherence to particle 2, thus accelerating the decrement of the coherence of particle 1. This is why interaction intensities are set to zero in this situation.

It is natural to ask how long the coherence of the target particle can be preserved when counteracting the decoherence process. Although for general situations we give no solution to this, there is an answer when conditions for the initial coherent vectors of the two particles are satisfied.

Theorem 10.3 When counteracting the pure dephasing process, if the angle formed by two projections on the x - y plane of the two initial Bloch vectors is zero, that is,

$$P_{xy}B_2(0) = \alpha P_{xy}B_1(0), \quad \alpha > 1 \quad (10.57)$$

then the time the coherence of particle 1 can be preserved through controlling interactions between the two particles can be calculated as

$$T = \frac{2(co_2(0) - co_1(0))}{\gamma co_1(0)} \quad (10.58)$$

Proof It can be proved with mathematical induction (see Appendix 10.A) that when Equation 10.57 is satisfied, Equation 10.59 comes into the existence during the simulation iterative process:

$$\frac{p_2(t)}{p_1(t)} = \frac{p_5(t)}{p_4(t)} = \frac{p_{13}(t)}{p_{12}(t)} = \frac{p_9(t)}{p_{14}(t)} = \kappa \quad (10.59)$$

where κ is the tangent of the phase of the coherent vectors' projections on the x - y plane.

For the proof of Equation 10.59 for the simulation iterative process see Appendix 10.A.

Using Equations 10.50b, 10.55, and 10.59, the following equation can be obtained:

$$\begin{aligned} c\dot{o}_2(t) &= \frac{-J(t)(p_{12}(t) - p_{14}(t) + \kappa(p_{13}(t) - p_9(t)))}{\sqrt{1 + \kappa^2}} \frac{p_4(t)}{|p_4(t)|} \\ &= \frac{-J(t)(p_{12}(t) - p_{14}(t) + \kappa(p_{13}(t) - p_9(t)))}{\sqrt{1 + \kappa^2}} \frac{p_1(t)}{|p_1(t)|} \\ &= -V_{de}(t) = -\gamma co_1(0) \end{aligned} \quad (10.60)$$

If the coherence of the target particle can be preserved within time T under the compensation, and considering the conservation of $\sum_k p_k^2(t)$, we find

$$\begin{aligned} co_1^2(0) + co_2^2(0) &= co_1^2(T) + co_2^2(T) + \sum_{k=9,12,13,14} p_k^2(T) \\ &\approx co_1^2(0) + (co_2(0) - \gamma co_1(0)T)^2 \end{aligned} \quad (10.61)$$

where the approximation appears at the end of the interaction when $p_k^2(T), k = 9, 12, 13, 14$ Are very small. According to Equation 10.61 the time T within which coherence of particle 1 can be preserved can be calculated by Equation 10.58.

The proof is complete. ■

Theorem 10.3 tells us that when condition Equation 10.57 is satisfied, the coherence of particle 1 can be preserved within time T by utilizing interactions with an assistant particle. Considering Equation 10.59 further, states of particle 1 can be regarded as invariant within time T . Thus the pure dephasing process of the target particle can be counteracted completely using interactions with an assistant particle whose initial coherent vector can be selected freely to satisfy the conditions in Equation 10.57.

Appendix 10.A Proof of Equation 10.59

According to Equations 10.37 and 10.54, the differential coefficients of $p_{1,2,4,5,9,12,13,14}(t)$ are

$$\left\{ \begin{array}{l} \dot{p}_1(t) = J(t)(p_{12}(t) - p_{14}(t)) - \gamma p_1(t) \\ \dot{p}_2(t) = J(t)(p_{13}(t) - p_9(t)) - \gamma p_2(t) \\ \dot{p}_4(t) = -J(t)(p_{12}(t) - p_{14}(t)) \\ \dot{p}_5(t) = -J(t)(p_{13}(t) - p_9(t)) \\ \dot{p}_{12}(t) = J(t)(p_4(t) - p_1(t)) = -\dot{p}_{14}(t) \\ \dot{p}_{13}(t) = J(t)(p_5(t) - p_2(t)) = -\dot{p}_9(t) \end{array} \right. \quad (A1)$$

If at initial time $T = 0$ there are equations $\frac{p_5(0)}{p_4(0)} = \frac{p_2(0)}{p_1(0)} = \kappa$ and $p_{9,12,13,14}(0) = 0$ because of the separability of the complex system, then equations $\frac{p_{13}(\tau)}{p_{12}(\tau)} = \frac{p_9(\tau)}{p_{14}(\tau)} = \kappa$ and $\frac{p_5(\tau)}{p_4(\tau)} = \frac{p_2(\tau)}{p_1(\tau)} = \kappa$ come into existence after one step of the iterative process.

Now suppose at some time t_k there are equations $\frac{p_{13}(k\tau)}{p_{12}(k\tau)} = \frac{p_9(k\tau)}{p_{14}(k\tau)} = \kappa$ and $\frac{p_5(k\tau)}{p_4(k\tau)} = \frac{p_2(k\tau)}{p_1(k\tau)} = \kappa$. According to Equation 10.62, Equation 10.63 can be obtained after one step of the iterative process:

$$\left\{ \begin{array}{l} p_1((k+1)\tau) = p_1(k\tau) + J(k\tau)(p_{12}(k\tau) - p_{14}(k\tau))\tau \\ p_2((k+1)\tau) = p_2(k\tau) + J(k\tau)(p_{13}(k\tau) - p_9(k\tau))\tau = \kappa p_1((k+1)\tau) \\ p_4((k+1)\tau) = p_3(k\tau) - J(k\tau)(p_{12}(k\tau) - p_{14}(k\tau))\tau \\ p_5((k+1)\tau) = p_4(k\tau) - J(k\tau)(p_{13}(k\tau) - p_9(k\tau))\tau = \kappa p_4((k+1)\tau) \\ p_{12}((k+1)\tau) = p_{12}(k\tau) + J(k\tau)(p_4(k\tau) - p_1(k\tau))\tau \\ p_{13}((k+1)\tau) = p_{13}(k\tau) + J(k\tau)(p_5(k\tau) - p_2(k\tau))\tau = \kappa p_{12}((k+1)\tau) \\ p_{14}((k+1)\tau) = p_{14}(k\tau) - J(k\tau)(p_4(k\tau) - p_1(k\tau))\tau \\ p_9((k+1)\tau) = p_9(k\tau) - J(k\tau)(p_5(k\tau) - p_2(k\tau))\tau = \kappa p_{14}((k+1)\tau) \end{array} \right. \quad (\text{A2})$$

Equation 10.59 therefore comes into existence during the iterative process when Equation 10.57 is satisfied.

The proof is complete.

References

- Brumer, P.W. and Shapiro, M.(2003) *Principles of the Quantum Control of Molecular Processes*, Wiley, Hoboken, NJ.
- Byrd, M.S. and Lidar, D.A.(2003) Empirical determination of dynamical decoupling operations. *Physical Review A*, **67**(1), 012324.
- Duan, L.M. and Guo, G.C.(1997) Preserving coherence in quantum computation by pairing quantum bits. *Physical Review Letters*, **79**(10), 1953–1956.
- Duan, L.M. and Guo, G.C.(1998) Reducing decoherence in quantum-computer memory with all quantum bits coupling to the same environment. *Physical Review A*, **57**(2), 737–741.
- Facchi, P., Tasaki, S., Pascazio, S. et al. (2005) Control of decoherence: analysis and comparison of three different strategies. *Physical Review A*, **2005**(71), 2.
- Lidar, D.A., Chuang, I.L. and Whaley, K.B.(1998) Decoherence-free subspaces for quantum computation. *Physical Review Letters*, **81**(12), 2594–2597.
- MacWilliams, F.J. and Sloane, N.J.A.(1977) *The Theory of Error-correcting Codes*, North-Holland, Amsterdam.
- Mancini, S. and Bonifacio, R.(2001) Quantum Zeno-like effect due to competing decoherence mechanisms. *Physical Review A*, **64**(4), 042111.
- Nielsen, M.A. and Chuang, I.L.(2010) *Quantum Computation and Quantum Information*, Cambridge University Press, Cambridge.
- Shor, P.W.(1995) Scheme for reducing decoherence in quantum computer memory. *Physical Review A*, **52**(4), R2493–R2496.
- Steane, A.M.(1999) in *Introduction to Quantum Computation and Information*(eds H.K. Lo, S. Popescu and T.P. Spiller), World Scientific, Singapore.
- Viola, L.(2002) Quantum control via encoded dynamical decoupling. *Physical Review A*, **66**(1), 012307.
- Viola, L., Knill, E. and Lloyd, S.(1999) Dynamical decoupling of open quantum systems. *Physical Review Letters*, **82**(12), 2417–2421.

- Vitali, D. and Tombesi, P.(2001) Heating and decoherence suppression using decoupling techniques. *Physical Review A*, **65**(1), 012305.
- Wiseman, H.M., Mancini, S. and Wang, J.(2002) Bayesian feedback versus Markovian feedback in a two-level atom. *Physical Review A*, **66**(1), 013807.
- Zanardi, P.(1998) Dissipation and decoherence in a quantum register. *Physical Review A*, **57**(5), 3276–3284.

11

State Estimation, Measurement, and Control of Quantum Systems

11.1 State Estimation Methods in Quantum Systems

State is a mathematical description of the physical system that provides past and future information for this system. Leohart once made a standard statement on state (Raymer and Beck, 2004): “Knowing the state means knowing the maximally available statistical information about all physical quantities of a physical object.” The technique of state estimation is a method, that can obtain a system’s true state as far as possible by measurement. In essence, quantum state estimation and the corresponding classical state estimation mainly differ in three points. First of all, the state of a classical system usually has a clear physical significance, which is a real physical quantity of the system. The direct measurement of this physical quantity can usually give the corresponding state value in the permitted condition, but the state of a quantum system-wave function or a density operator is not a real physical quantity. It cannot acquire a certain value of a quantum state by direct state measurement. However, one can deduce the state with the aid of measurement of some observable quantities of the quantum system. Second, a classical system is determinism in theory. If the system is input by a signal, the state of the system at any time will be perfectly determined by the initial state. When the system suffers the impact of the disturbance, the instantaneous state of the system will have all kinds of noise. With the aid of the corresponding estimation technique, one can deal with the system noise and obtain the real state as far as possible. In contrast, in essence a quantum system is ruled by probability theory. Even though the quantum system does not suffer the consequence of any interference, one can only acquire a random result from the measurement of the quantum system. What is more, if the quantum system is disturbed, in order to obtain the state, additional handling of the relevant noise is needed. Third, as regards the method of realization of the measurement, the measurement of the classical system does not result in substantial damage to the system so in principle this system can be measured many times. Nevertheless, a quantum system is very fragile and the measurement usually will cause substantial damage, which the same quantum system from being reused to make multiple measurements.

Classical state estimation methods are more developed than state estimation methods in quantum systems. In reality, most state estimation methods are aimed at the reconstruction of

the initial state of a quantum system. If we can perfectly reconstruct the initial state of the quantum system, this will have a significant effect on experiments in the fields of physics and chemistry, and in the research of quantum control. Considering the particularity of the quantum system state estimation and in order to enable readers to have a whole understanding of the state estimation of the quantum system, in this section we will review the current development of quantum state estimation methods, and focus on the advantages and disadvantages of some estimation methods.

11.1.1 *Background of State Estimation of Quantum Systems*

According to the Heisenberg uncertainty principle of quantum systems (Neumann, 1955) and the quantum no-cloning theorem (Yuen, 1986), one cannot do any series of measurements on a single system without introducing a back-action correction and cannot reconstruct the state of a single quantum system by repeating the measurements. These inherent characteristics of quantum systems mean state estimation can only be carried out in the following way (D'Ariano, Paris, and Sacchi, 2004): use the same macro procedure to prepare many systems with identical copies of the same state, and make different state measurements of observable quantities for each copy system. This scheme in the field of quantum experiments has been very common. However, with the gradual introduction of control theory to the quantum field, it appears that quantum state measurement methods and estimation techniques are completely different. For example, the initial state estimation of the finite dimensional quantum system (D'Alessandro, 2003); state estimation based on the information of an observable quantity (Silberfarb, Jessen, and Deutsch, 2005).

The initial quantum state reconstruction process is similar to X-ray tomography in the medical field, thus state estimation methods in quantum systems (or state reconstruction techniques) are often known as quantum tomography (Baier *et al.*, 2005). It is worthwhile noting that in the physics literature, quantum tomography includes state estimation and parameter estimation; the former is called state tomography and the latter is often called process tomography. In engineering literature, quantum tomography is also involved with state estimation and parameter estimation problems in quantum systems, but here these processes are known as state filter and parameter identification (Baier *et al.*, 2005).

11.1.2 *Quantum State Estimation Methods Based on the Measurement of Identical Copies*

Any quantum state reconstruction scheme is based on a set of measurement data and the density operator of quantum mechanics systems carried out by a posteriori estimation. This set of measurement data must rely on macro-measuring instruments. The quality of the reconstruction depends on the quality of the measured data and the reconstruction procedure efficiency. In essence, based on multiple reconstructions of identical copies of the quantum system's state of the system obtained by repeating the measurement of these replica systems, different observables constitute a measured ensemble and the statistical properties of the observables measured can be reconstructed.

With the continuous development of the estimation techniques, five representative state reconstructions have now been formed: the state tomography (ST) method, the maximum

entropy (MaxEnt) estimation method, the ML estimation method, the Bayesian estimation method, and the least square-variance (LS) estimation. These typical reconstruction schemes can be specified in three different situations (Buzek, 2004). First, all observable systems can be measured accurately. This could be an arbitrary initial unknown state that is completely reconstructed. This reconstruction is called the reconstruction of the complete observation level. A typical example is the standard tomographic reconstruction of the quantum state of light. Second, only some of the observables of the system can be measured accurately and a complete reconstruction of the density operator cannot be made. However, the reconstructed density operator will still uniquely determine the average value of the measured observables. This reconstruction is known as the reconstruction of the incomplete observation level. The maximum entropy principle can be used in this situation. Third, the measurement cannot provide sufficient information to accurately determine the average value of the measured observable (or probability distribution), only the frequency of the measured observed eigenstates. At this time, methods such as ML estimation or the quantum Bayesian inference method can be used for state reconstruction.

1) State tomography (ST) method

In 1957 Fano first systematically discussed the problem of determining the quantum state on the basis of repeated measurements on the same copy of the prepared system. He realized that at least two or more observables are required to determine the state. A group of mechanics quantities is sufficient to fully determine the system density operator, which is called the quorum. However, for a particle, in addition to position, momentum, and energy, it was difficulty to design other observables. There was no breakthrough in measuring the quantum state until progress in the field of quantum optics theory in the 1990s. In 1989, Vogel and Risken derived the relationship between the probability distribution of the rotating orthogonal phase of a single-mode electromagnetic field and the pseudo probability distribution of the Wigner function, and pointed out that the marginal probability distribution obtained by the same difference detection is the Radon transform of the Wigner function. Thus, as for classic imaging processing technology, one can obtain the Wigner function from the inverse Radon transformation by means of homodyne tomography, the same difference measured the marginal probability distribution, and then get the matrix elements of the density operator from the Wigner function, which is very common in quantum optics: homodyne tomography. In essence, this estimation method requires the simultaneous measurement of a few kinds of non-commutative observables. In 1993, the Raymer research group of Oregon University in the USA first made use of this method to acquire the measurement of the harmonic oscillator position of a single-mode electromagnetic field and the momentum of linear combination, and reconstructed the coherent states and squeezed states of a single-mode field. However, this method suffers the impact of approximate factors.

Because the marginal probability distribution in an analytical form cannot be obtained based on a limited number of measurements, the conditions of the smooth parameters required by Radon inverse transformation are not met. In 1994, D'Ariano proposed the first accurate technology of the density matrix of the experimental determination of the radiation field in the photon number representation, which is realized by a function of the simple average of the difference data, and avoided the inverse Radon transform. D'Ariano also expressed the density operator as a convolution between the marginal distribution of the homodyne output with

the same difference and a kernel function to further simplify the technology (D'Ariano, Leonhardt, and Paul, 1995). Although these improved methods are not used with inverse Radon transformation, they are derived from the method of optical homodyne tomography. They are still classified as homodyne tomography. The success of the optical homodyne tomography stimulated the development of atomic beam state reconstruction, and solved the problems of state determination in experiments with molecular vibration (Dunn, Walmsley, and Mukamel, 1995), helium atomic ensembles (Kurtsiefer, Pfau, and Mlynek, 1997), and single particles in a Paul trap.

By quantum tomography and in the limit of infinite measurements, the state can be perfectly reproduced. However, the actual situation is that the number of measurements is always limited, so there will always be a statistical error in the state reconstruction. For infinite-dimensional systems, the statistical error propagation in the elements of the density matrix would have a serious impact on the final estimation quality. To solve this problem, in 2000 D'Ariano proposed a general estimation method according to the measurements on a quorum observable in homodyne tomography to estimate the ensemble average of all observables. An ensemble average of any mechanical quantity is expressed by appropriate Lie group unitary representation. This method was strictly proved in mathematics through the unitary Lie group square integrable representation theory. Obviously, this approach assumes that the corresponding Lie group representation is unitary, although the promotion of the non-unitary Lie group is also worth further study. D'Ariano *et al.* realized the generalization of homodyne tomography from single mode to any mode. Many researchers extended the tomography method from the harmonic oscillator system to any quantum system by means of group theory (D'Ariano, 2000a,b; Cassinelli, D'Ariano, and De Vito, 2000). In general, instrument noise will make the estimation algorithm biased. For any known noise, D'Ariano designed a general method of data analysis to make the estimation procedure unbiased. In addition, in order to improve the statistical error on the set of experimental samples, an "adaptive tomography" algorithm was designed (D'Ariano and Paris., 1999).

2) Maximum entropy estimation method

In the actual experiment, only a finite number of independent moments of the system operator can usually be measured, so only a subset of the observables of a quorum are measured. In this case, one cannot get all the information for the system. In other words, the experimental data do not give us enough information to uniquely determine the density operator of the system (Buzek, Drobny, and Adam, 1997), which means that there may be many density operators to meet the constraints imposed by the experimental data measured. Based on the degree of deviation of its pure state for the density operators, they can be separated from each other: each of the density operators has a different uncertainty measure. With respect to the expectation obtained by the selected observation, people want in an unbiased way to meet the requirements of the particular density operator (Buzek, 2004). On the basis of Jayne's principle of maximum entropy, the density operator must have the greatest uncertainty measure. The density operator can then be uniquely reconstructed with this additional criteria.

The premise of using the maximum entropy reconstruction must be able to accurately measure the expected value of the given observable quantities or probability distribution. In theory, this means that an ensemble of identical preparation systems should have an unlimited number of measurements to get those expectations. In fact, it can be considered that the average value

is a sufficiently accurate measurement as long as the measurement frequency is enough. If the observation level consists of all the observable quantities of a quorum, then the maximum entropy reconstruction can replace the standard quantum tomography reconstruction.

The maximum entropy reconstruction scheme does not require any a priori assumptions on the purity of the reconstructed state, namely, it can be used to reconstruct not only the pure state but also the statistical mixed state. This method has been used in the quantum state reconstruction of the monochromatic light field, the quantum state reconstruction of the spin system, and the reconstruction of the Wigner function of incomplete tomography data.

3) Maximum likelihood estimation method

Like the classical case, the basic idea of ML is that constructing a likelihood function from the overall state most likely to produce the observed data takes into account a priori knowledge between the density matrix elements, so one can naturally keep the structure of quantum theory, such as closure and the uncertainty relation. This technique has been used in the estimation of the quantum phase, the estimation of the photon number distribution, the reconstruction of the optical entangled state, and so on (D'Ariano, Maccone, and Paris, 2001; Hradil *et al.*, 2004). In 2000, Banaszek *et al.* proposed a general ML technique to reconstruct the density matrix that maintains the positive definiteness and normality, and can be used for the construction of multimode radiation field and spin systems, essentially reducing the statistical error, but they did not give an explicit reconstruction algorithm. In 2004 Lvovsky proposed a kind of iteration expectation maximization algorithm of the optical ensemble density matrix on the basis of a balanced homodyne measurement, which avoided the intermediate step of the measurement of the marginal probability distribution and can be used to directly measure the data.

Compared with the standard reconstruction methods used in ST, ML has the following characteristics (Lvovsky, 2004). First of all, for limited experimental data and the statistical noise caused by discreteness, ML extracts complete information as far as possible by adding low-pass filtering to the Fourier image of the Wigner function. Standard homodyne tomography handles this problem by attaching some mathematical hypothesis, but this is not physically easy to implement. Second, the back-to-back projection algorithm in the standard homodyne tomography does not consider the constraints of the density operator, which can cause some non-physical characteristics, such as the negative diagonal element in the density matrix. The ML allows people to consider the constraints condition of the positive definiteness of the density operator and unitary trace in the reconstruction process, so that one can always produce a physically reasonable ensemble. Third, the ML can be used where the efficiency of the detector is not high. While statistical errors can rapidly grow with the lower efficiency of a detector that causes orthogonal noise behavior, the ST will have the additional corrective in the reconstruction procedure. The disadvantage of ML is that the estimation procedure involves complex calculations and even with the help of numerical calculation it is still a very complex numerical optimization problem.

4) Bayesian estimation method

The core of the Bayesian method is the Bayes rule, that is, how to update knowledge of the current state according to the latest measured data (Schack, Brun, and Caves, 2001). Initially,

quantum Bayesian inference was developed for the reconstruction of the pure state of quantum mechanics. Because the average of the pure state usually is not pure, the deviation of the reconstructed density operator from the pure state, that is, the von Newman entropy measure, is used as the measurement of the reconstruction quality (Buzek *et al.*, 1998). Helston, Holevo, and Jones pointed out that the Bayesian reconstruction of the unknown pure state is affected by some ambiguity that is related to the choice of the cost function. In general, based on the choice of the cost function, people can get different estimators. In 2001 Schack *et al.* deduced a quantum Bayesian rule, which is applicable to the pure state and the mixed state, and this method has been successfully used in the N -qubit reconstruction.

5) Least variance estimation method

In essence, the LS method is based on the following facts: for any physical quantum state, the density operator element ρ_{mn} would ultimately increase with a decrease in mn , so that the density matrix can be effectively truncated when mn becomes large. Obviously, the truncation always causes a system error, but one can choose a truncation parameter that can ensure that the system error is less than the statistical error to solve this problem. The LS method is based on the method of the linear transformation of the measured data and it has a low computation cost, so it can be used to reconstruct the density matrix element in real time, but at the same time “negative probability” caused by the inaccuracy of the experiment may be produced. Generally, increasing the number of measurements can limit the emergence of “negative probability.”

The LS method has a very good advantage in reducing the statistical error of the estimation (Opatrny, Welsch, and Vogel, 1997), and its flexibility allows the reconstruction of the density matrix element on the basis of the recorded data in a short time interval. If the measured data are more sensitive to some of the density matrix elements, then one can construct so-called rules to resolve this, that is, the element value of the reconstructed density matrix is set to 0, rather than dealing with a strong fluctuation in value. Such rules reduce the statistical error of the reconstructed density matrix elements, but at the same time cause a system error. It is therefore essential to optimize the rules so that the system error caused is smaller than the statistical error.

The principle of the LS method appeared in the Legendre and Gauss era and is now used in quantum state reconstruction problems, for example the quantum state reconstruction of the cavity field with quantum state endoscopies (Bardroff *et al.*, 1996), trapping ion vibrational quantum state reconstruction, and light field quantum state reconstruction with the help of balanced and unbalanced homodyne detection. In short, the LS method assumes experimental data with ideal Gaussian noise. As previously stated, it allows the statistical noise to be reduced, using appropriate rules, but in principle it cannot guarantee that the reconstructed density matrix is positive definite, which requires a large number of measurements.

Isotactic copies have been estimated based on the measurement of the quantum state by a large number of studies and experiments. The current literature focuses on the features of the above methods to study the corresponding improvement algorithms and the respective improvement algorithms for the corresponding simulations.

In 2005 Artiles *et al.* for the first time studied the statistical properties of the type function projection estimator and filtered the ML estimator in tomography reconstruction. They gave the consistency theorem of these two kinds of estimators under different norms, and they left a few open questions, such as the processing problem of the non-Gaussian noise in the case of low

detector efficiency, the problem of the convergence rate of the algorithm, the design problem of the optimal estimator in the case of low detection efficiency, the problem of properly determining the kernel estimator of the Wigner function in the case of noise, whether the estimation methods can be applied into the vibration of measuring equipment, and the estimate problem of state transformation under the influence of quantum mechanical equipment, and so on.

11.1.3 *Quantum State Reconstruction Methods Based on System Theory*

With the development of the theory of quantum control, there has been some progress from a control point of view in solving the quantum state estimation. The way used to solve the problem is completely different from the method of measuring many identical copies of a quantum system. For specific measuring modes and ways of solving problems it appears there are three kinds of state estimation schemes. The way of dealing with problems with above measurement of a quantum system of many identical copies of the system is completely different. For specific measuring modes and specific ways of solving questions it appears there are three kinds of state estimations.

In 2003 D'Alessandro, at Iowa State University, USA, considered the problem of determining the initial state of a single finite-dimensional quantum system, which is known to be a non-degenerate observable amount of the expected value of one or more of the readings (D'Alessandro, 2003). He pointed out that by generating all the unitary evolution on a Lie group, and with the appropriate controlled evolution and measurement, information on the initial state can be extracted from the perspective of system observability. The research results show that observability does not always mean that appropriate evolution and measurement will be able to infer all the parameters of the initial state; coupling the system with the auxiliary system of a known state (a probe system), it is possible to obtain complete information for the initial state. In 2004 D'Alessandro studied the case in which this problem was extended to the possible degenerate observables with the help of a series of appropriate controlled evolution and selective measurements (D'Alessandro, 2004), and he gave a general algorithm for determining the maximum number of unknown parameters of the initial state. At the same time he discussed the problem of how to determine all the parameters on the quantum state when the system and probe were jointly controllable. This method is theoretically feasible, but the occurrence of noise in the experiment is a serious challenge for the whole algorithm.

In 2005 Silberfarb *et al.* proposed a new kind of scheme of quantum state reconstruction, which is based on the continuous weak measurement of a single observable quantity on an ensemble of identical preparation systems (Silberfarb, Jessen, and Deutsch, 2005). He required that this ensemble is driven so that every member's experience is the same and has a well-designed dynamical evolution, which required that the new information is continuously mapped to the measured quantities. He extends the state estimation scheme of Gaussian random variables of classical dynamical evolution with the help of a classical Bayesian filtering method. This estimation is in real time and has minimum disturbance for every member. It may realize quantum closed-loop feedback control on the basis of the extracted information from the measured information.

In 2001 Gambetta and Wiseman studied the state estimation problem where there is a system of unknown parameters by means of the quantum trajectory theory, which describes open-system evolution detected continuously. The random master equation (ME) of state evolution can be obtained by considering the system interaction with the environment and

real-time environmental measurement. In addition, the best estimate can be made according to the continuously detected measuring records and the classic probability statistical methods to the state of the system. Gambetta and Wiseman applied their estimating methods to the state estimation of a two-level atom coupled with the classical electromagnetic field with unknown Rabi frequency. They pointed out that the quality of estimation greatly depends on the different ways of testing the environment. In fact, the estimation of each moment will have a large error in obtaining the true state of the system; there is still a large amount of research required to accurately obtain the true state of the system.

In summary, the quantum state estimation method is not much different from classical state estimation in its mathematical principles. The fundamental difference is the special nature of the quantum state itself. Different quantum state estimation methods will eventually lead to the different application results.

11.2 Entanglement Detection and Measurement of Quantum Systems

In 1932, Einstein, Podolsky, and Rosen (Einstein, Podolsky, and Rosen, 1935) and Schrödinger (Schrödinger, 1935) recognized a “spooky” feature of quantum machinery, which implies the existence of global states of a composite system that cannot be written as a product of the states of individual subsystems. This phenomenon, existing only in composite systems, is known as entanglement, which is considered to be the qualitative feature of quantum theory that most strikingly distinguishes it from the classical intuition in the early days. Later, the subsequent development of Bell’s inequalities in terms of the local hidden variable model (LHVM) and the discovery of some entangled quantum states that violated the Bell inequality showed that one could create controllable quantum entanglement (Bell, 1964). Together with the rapid development of quantum information technology, the entanglement as an important resource is used in the fields of quantum communication (Bennett *et al.*, 1993), quantum coding (Ekert, 1991), and quantum computation (Raussendorf and Briegel, 2001; Leibfried *et al.*, 2005). The rapid experimental progress on quantum control led to a rapidly growing interest in entanglement theory and many experiments nowadays aim at the generation of entanglement.

In recent years enormous progress on the generation of entanglement has been achieved, for instance six or eight ions have been entangled (Häffner *et al.*, 2005). Photons have been used to demonstrate the entanglement between 6 particles or 10 qubits (Lu *et al.*, 2007; Gao *et al.*, 2010) and in diamond nuclear and electronic spins have been entangled (Neumann *et al.*, 2008). These entanglements are generated between individual particles. In other types of systems only collective measurements are possible. Through spin squeezing, the entanglement of 10^7 atoms was created in cold atomic clouds (Hald *et al.*, 1999) and large-scale entangling operations were realized in optical lattices of 10^5 two-state atoms (Mandel *et al.*, 2003). As the underlying techniques of quantum control improve continuously, it can be expected that in the near future even larger systems could be entangled. In any of these experiments, typical questions arise: How can one detect the presence of entanglement? Can we quantify the entanglement in the experiment? To tackle these problems, entanglement detection has been proposed. In addition, the quantification of entanglement should be concerned, which is essential the theory of entanglement measures. Entanglement detection and measurement are fundamental problems of the theory of entanglement. Obviously, Bell’s inequalities are the first powerful tool for the detection of entanglement. Peres proved that if the partial transposition of a two-body composite system’s density matrix is a positive definite matrix, then the quantum

system state is a separate state (Peres, 1996). Surprisingly, Peres' condition appeared to be a strong test for entanglement. As the partial transpose is a positive map it was realized that positive maps can serve as strong detectors of entanglement. Jamiolkowski isomorphism provided positive maps with a "footbridge" to use physical measurable quantities – the Hermitian's operators (Jamiolkowski, 1972). This becomes a necessary and sufficient condition for separability on the both physical level of observables and the non-physical one engaging positive maps, providing a basis for a general theory of the detection of entanglement. Later abundant separability criteria to detect entanglement were constructed. Terhal was the first to construct a family of indecomposable positive linear maps based on entangled quantum states. She also pointed out that a violation of a Bell inequality can formally be expressed as a witness for entanglement. From then on, the theory of entanglement witnesses was intensively developed, including theory analysis and its applications in experiments.

As we know, the main virtue of entanglement witnesses is that they provide an economic way of detecting entanglement that does not need full information about the state. This poses a natural question: How can the amount of entanglement of compound systems of an unknown state be estimated optimally if only incomplete data in the form of averages values of some operators are accessible? This question involves a principle of the minimization of entanglement under a chosen measure of entanglement with constraints in the form of an incomplete data set from experiments (Horodecki, Oppenheim, and Horodecki, 2002). It leads to two other issues: the definition of entanglement measure and its estimation. To qualify entanglement, two fundamental measures, entanglement distillation and what is now called entanglement cost, appeared in the context of manipulating entanglement, which has an operational meaning, but they cannot be calculated since they are limiting measures. Vedral and Plenio therefore proposed in 1998 an axiomatic approach to quantifying entanglement, in which a "good" measure of entanglement is any function that satisfies some postulates. The main idea is the monotonicity condition, that is, entanglement should not increase under local operations and classical communication (LOCC) (Bennett *et al.*, 1996). Up to now few effective measures have been proposed, such as relative entropy of entanglement and entanglement of formation. Although the measure of entanglement for pure bipartite states is unique and ordered, it seems that measures of entanglement do not exhibit any ordered behavior for other cases (Eisert and Plenio, 1999). After choosing a measure of entanglement, the remaining problem is to estimate the quality of entanglement with an incomplete set of data from experiments, for which a general method is to use the Legendre transform. For some witnesses, the Legendre transform can be determined analytically or estimated numerically.

The following section concerns two issues. One is entanglement detection. We will introduce the notions of entanglement and separability, analyze the relationship between several separability and positive maps, and introduce entanglement witnesses as a theoretical concept and explain how to construct and apply them in experiments. Several separability criteria for multipartite entangled states are also discussed. The other issue is entanglement measure, including its theoretical concept and application in experiments. Finally, we review non-linear entanglement witnesses.

11.2.1 Entanglement States

In quantum systems, the total state space of a multipartite system consisting of n subsystems is a tensor product of the subsystem spaces, that is, $H = \bigotimes_{l=1}^n H_l$. Then the superposition principle

allows us to write the total state of the system in the form of

$$|\psi\rangle = \sum_{\mathbf{i}_n} c_{\mathbf{i}_n} |\mathbf{i}_n\rangle \quad (11.1)$$

where $\mathbf{i}_n = i_1, i_2, \dots, i_n$ is the multi-index and $|\mathbf{i}_n\rangle = |i_1\rangle \otimes |i_2\rangle \otimes \dots \otimes |i_n\rangle$, which cannot be, in general, described as a product of states of individual subsystems, that is, $|\psi\rangle \neq |\psi_1\rangle \otimes |\psi_2\rangle \otimes \dots \otimes |\psi_n\rangle$. In this case it is called the entangled state. This is the case of pure states. In practice, we often encounter the mixed state. A state is called a mixed state of n systems entangled if it cannot be written as a convex combination of product states:

$$\rho \neq \sum_i p_i \rho_1^i \otimes \dots \otimes \rho_n^i \quad (11.2)$$

Since the separability criterion has given a close relationship with the positive map, we start with the definition of the positive map and the completely positive map. A linear map Λ is called positive if it maps the Hermitian operators onto the Hermitian operators, fulfilling $\Lambda(X^\dagger) = \Lambda(X)^\dagger$, and preserves the positivity, that is, if $X \geq 0$ then $\Lambda(X) \geq 0$. A positive map Λ is called a completely positive (CP) map if for an arbitrary Hilbert space $H_A \otimes H_N$ the map $I_A \otimes \Lambda$ is positive. A state ρ is separable if and only if for all positive maps Λ , the relation

$$(I_A \otimes \Lambda)(\rho) \geq 0 \quad (11.3)$$

holds. In this sense, the separability problem is equivalent to the classification of all positive maps. Of course, in order to develop a separability criterion, in Equation 11.3 only the positive, but not completely positive, maps are of interest. If the map Λ is transpose map T , the well-known Peres criterion can be obtained: if the state is separable, then after the partial transpose of the density matrix on one of the subsystems of a compound bipartite system, it is still a legitimate state. Another example of a not CP map is the reduction map $\Lambda(X) = \text{Tr}(X).I - X$. Consequently a separable state has to fulfill $\rho_A \otimes I - \rho \geq 0$. This is the reduction criterion for separability, which is weaker than the Peres criterion. Furthermore, one can extend the reduction map in the following way: If U is a unitary matrix with $U^T = -U$, then the map $\Lambda(X) = \text{Tr}(X).I - X - UX^T U^\dagger$ is a positive, but not completely positive, map. The majorization criterion relates the eigenvalues of the total state with the reduced states. For a general state ρ one takes $\rho_A = \text{Tr}_B(\rho)$ as the reduced state with respect to Alice and denotes it by (p_1, p_2, \dots) , the decreasingly ordered eigenvalues of ρ , and by (q_1, q_2, \dots) , the decreasingly ordered eigenvalues of ρ_A . The majorization criterion states that if ρ is separable, then $\sum_{i=1}^k p_i \leq \sum_{i=1}^k q_i$ holds for all k .

A simple and strong criterion is the computable cross norm or realignment (CCNR) criterion. In order to formulate it, one utilizes the Schmidt decomposition in operator space. For a density matrix, such a decomposition is

$$\rho = \sum_k \lambda_k G_A^k \otimes G_B^k \quad (11.4)$$

where $\lambda_k \geq 0$ and G_A^k and G_B^k are orthonormal bases of the observable spaces of H_A and H_B , which have to fulfill $\text{Tr}(G_A^k G_A^l) = \text{Tr}(G_B^k G_B^l) = \delta_{kl}$. One can then formulate the CCNR criterion:

if the state ρ is separable then $\sum_k \lambda_k \leq 1$. Hence, if $\sum_k \lambda_k > 1$ the state must be entangled. The remarkable fact is that the CCNR criterion allows one to prove the entanglement for many states where the Peres criterion fails.

In addition, there are many other approaches to derive separability criteria, such as one based on covariance matrices and W–Z criteria (Zhang, 2005), and several criteria based on non-CP maps (Augusiak and Stasińska, 2008).

Compared to bipartite entanglement, the multipartite case is much more complicated. Nonetheless, several criteria for the bipartite case can be extended to the general case. For instance, Peres criteria can be generalized to more parties, that is, the generalized partial transpose (GPT) criteria: if the density matrix is separable, after the partial transpose of the density matrix on any one of the subsystems of a compound multipartite system, the trace is less or equal to one. Permutation criterion can be viewed as the generalization from CCNR. It says the density matrix $\rho = \sum_{i_1, j_1, \dots, i_N, j_N} \rho_{i_1 j_1, \dots, i_N j_N} |i_1\rangle\langle j_1| \otimes \dots \otimes |i_N\rangle\langle j_N|$ is separable if

$$\left\| \rho_{\pi(i_1 j_1, \dots, i_N j_N)} \right\|_1 \leq 1 \quad (11.5)$$

where $\pi(\dots)$ is an arbitrary permutation of the indices.

It has already been demonstrated (Uffink, 2002) that quadratic Bell-type inequalities can be a useful tool for the investigation of multipartite entanglement. There is a series of other approaches that try to extend bipartite criteria to the multipartite case. These include positive maps (Horodecki *et al.*, 2001) and the conditions for the generalization of the Bloch vector (Yu and Song, 2005).

11.2.2 Entanglement Witnesses

The criteria mentioned above all have something in common: they all assume that the density matrix is already known and require to apply certain operations to a density matrix in order to decide whether the state is entangled or not. There is, however, a necessary and sufficient entanglement criterion in terms of directly measurable observables. These are the so-called entanglement witnesses, which are main methods of detecting entanglement experimentally. In this subsection, we start with the definition of witnesses, then introduce their applications to bipartite and multipartite entanglement, and the methods to construct them.

An observable W is called an entanglement witness (or witness for short), if $\text{Tr}(W\rho_s) \geq 0$ for all separable ρ_s and $\text{Tr}(W\rho_e) < 0$ for at least one entangled ρ_e . Thus, if one measures $\text{Tr}(W\rho) < 0$ one knows for sure that the state ρ is entangled. One detects W through $\text{Tr}(W\rho) < 0$. For each entangled state ρ_e there exists an entanglement witness to detect it (Horodecki *et al.*, 1996). Namely, any entangled state can be detected in principle with an entanglement witness; the task remains how to construct witnesses, which is not an easy problem. Let us discuss in three simple examples how the witnesses for bipartite entanglement can be constructed. Typically, if a state violates some criterion for the separability, an entanglement witness detecting the state can be written down.

As the first example, let us take a state ρ_e that is contrary to the Peres criterion. If there is a negative eigenvalue λ_- of $\rho_e^{\text{T}_A}$ and a corresponding eigenvector $|\eta\rangle$, then

$$W = |\eta\rangle\langle\eta|^{\text{T}_A} \quad (11.6)$$

is a witness of detecting ρ_e because $\text{Tr}(W\rho_e) = \text{Tr}(|\eta\rangle\langle\eta|^{\text{T}_A}\rho_e) = \text{Tr}(|\eta\rangle\langle\eta|\rho_e^{\text{T}_A}) = \lambda_- < 0$ and $\text{Tr}(W\rho_s) = \text{Tr}(|\eta\rangle\langle\eta|\rho_s^{\text{T}_A}) \geq 0$ for all separable ρ_s .

As a second example, let us consider the case when ρ_e violates the CCNR criterion. Then, by definition, we have the Schmidt decomposition in Equation 11.4, $\sum_k \lambda_k > 1$. A witness is now given by

$$W = I - \sum_k G_A^k \otimes G_B^k \quad (11.7)$$

Clearly, for an entangled state ρ_e one has $\text{Tr}(W\rho_e) = 1 - \sum_k \lambda_k < 0$. A general separable state $\rho_s = \sum_{kl} \mu_{kl} G_k^A \otimes G_l^B$ can be expressed on the basis of $G_k^{A/B}$. Then $\text{Tr}(W\rho_s) = 1 - \sum_k \mu_{kk} \geq 0$, where the last estimate comes from the CCNR criterion and the fact that a trace of a matrix is always smaller than the sum of its singular values.

As a third example, the witnesses can also be constructed from the consideration that states close to an entangled state must also be entangled. Therefore, one may try for a given entangled pure state $|\psi\rangle$ to write down a projector-based witness such as

$$W = \alpha I - |\psi\rangle\langle\psi| \quad (11.8)$$

which can be interpreted as follows. The quantity $\text{Tr}(\rho W) = \alpha - \text{Tr}(\rho|\psi\rangle\langle\psi|) = \alpha - \langle\psi|\rho|\psi\rangle$ is the fidelity of the state $|\psi\rangle$ in the mixed state ρ , and if this fidelity exceeds a critical value α , then the expectation value of the witness is negative and the state ρ must be entangled. In order to ensure that W is still positive on all separable states, take

$$\alpha = \max_{\rho \text{ is separable}} \text{Tr}(\rho|\psi\rangle\langle\psi|) = \max_{|\phi\rangle=|a\rangle\otimes|b\rangle} |\psi|\phi|^2 \quad (11.9)$$

It is worth mentioning that the witness W in Equation 11.8 can be generalized to the multipartite case, such as Greenberger-Horne-Zeilinger (GHZ), graph state, Dick state, and so on. The only difference is the value of α , for example $\alpha = 3/4$ for GHZ, 0.5 for the graph state, and 4/9 for the W_3 state.

Because of the linearity of the witness, all the states satisfying $\text{Tr}(W\rho) = 0$ form a hyperplane. All the separable states form a convex set, which is a subset of $\text{Tr}(W\rho) > 0$. Every entanglement witness can, by definition, detect some entangled states. However, some witnesses are better in this task than others. In this sense, one can optimize entanglement witnesses. A necessary condition for a witness to be optimal is that it “touches” the set of separable states, that is, there must be a separable ρ with $\text{Tr}(W\rho) = 0$. This is, however, not a sufficient condition, and witnesses which fulfill this condition are sometimes also called weakly optimal. Even optimal witnesses cannot completely divide separable states and entanglement states. Similarly, the witnesses can be used to distinguish the different classes of multiparticle entanglement, but not all of a class of entanglement can be detected (Gühne and Hyllus, 2003). For instance, witnesses give the possibility of proving that a state belongs to the GHZ class. However, it is not clear how one can show that a state is tripartite entangled and belongs to the W class. This cannot be done with witnesses, since they are designed to show that a state lies outside a convex set, and they fail to prove that a state is inside a convex set. Therefore, it is necessary to add a non-linear term such that $\text{Tr}(W\rho) = 0$ is a hyper-surface to increase the performance of witness. This is a so-called non-linear witness.

The witness W cannot easily be implemented in an experiment since it is usually a non-local observable that is not straightforward to measure in practice. The observables that can easily be measured in any experiment are local observables like $\langle \sigma_z \otimes \sigma_z \rangle$ or projectors. Therefore, for the experimental implementation it is necessary to decompose the witness into operators that can be measured locally. Thus, one needs a decomposition into projectors onto product vectors of the form

$$W = \sum_{i=1}^m M_i = \sum_{i=1}^m \sum_{k,l=1}^d c_{kl}^i |a_k^i\rangle\langle a_k^i| \otimes |b_l^i\rangle\langle b_l^i| \quad (11.10)$$

where $\langle a_s^i | a_t^i \rangle = \langle b_s^i | b_t^i \rangle = \delta_{st}$. M_i represents a local von Neumann measurement (LvNM), which measures the probabilities of these states $|a_k b_l\rangle$ and adds their results with the weights c_{kl} using one collective setting and some classical communication. It is therefore reasonable to find an optimal number of device settings, that is, a minimal m . In this sense m is the minimal number of measurements one has to perform. It should be noted that once the observable $\sigma_z \otimes \sigma_z$ is chosen all expectation values like $\langle \sigma_z \otimes \sigma_z \rangle$, $\langle \sigma_z \otimes I \rangle$, and $\langle I \otimes \sigma_z \rangle$ can be determined from the same data. The optimal number of decompositions for a two-qubit system is three (Guhne and Hyllus, 2003) and the optimal decomposition of witnesses for several entanglement states of a three-qubit system is obtained (Guhne *et al.*, 2003).

Furthermore, to determine the effectiveness of an entanglement detection scheme, one should consider its robustness to noise. As a simple approximation, one may consider a mixed state ρ of the form

$$\rho(p) = p|\psi\rangle\langle\psi| + (1-p)\frac{I}{\alpha} \quad (11.11)$$

where the pure state $|\psi\rangle\langle\psi|$ is the particular pure state to be produced and p is the noise probability. The robustness of the scheme is the maximal probability p_{\max} with which the entanglement can be detected, that is, $p_{\max} = \max_{\text{Tr}(W\rho(p))<0} \{p\}$. It is difficult to prove that a local decomposition is optimal.

11.2.3 Entanglement Measures

The initial idea to quantify entanglement was connected to its usefulness in terms of communication (Bennett *et al.*, 1996). As should be known, one can teleport one qubit by means of a two-qubit maximally entangled state. However, if the state is not maximally entangled, then this kind of teleportation is not credible. According to the Shannon communication theory, when there are many copies in such a state, one can obtain asymptotically faithful teleportation at some rate r and two basic measures of entanglement E_D (distillable entanglement) and E_C (entanglement cost) have been proposed to describe r .

Alice and Bob start from n copies of state ρ_{AB} and apply a LOCC operation. Finally $r \times n$ Einstein, Podolsky, and Rosen pairs $\phi(2^m)$ are obtained at most, with $\phi(2^m) = |\psi_{2^m}^+\rangle\langle\psi_{2^m}^+|$. The distillable entanglement can be defined concisely (Plenio and Virmani, 2006) as follows

$$E_D(\rho) = \sup \left\{ r : \lim_{n \rightarrow \infty} \left[\inf_{\Lambda} \text{tr} \left| \Lambda (\rho^{\otimes n}) - \phi(2^m) \right| \right] \right\} \quad (11.12)$$

Entanglement cost is a measure dual to E_D , and it reports how many qubits we have to communicate in order to create n states. The definition is

$$E_C(\rho) = \inf \left\{ r : \lim_{n \rightarrow \infty} \left[\inf_{\Lambda} \text{tr} |\rho^{\otimes n} - \Lambda(\phi(2^m))| \right] \right\} \quad (11.13)$$

where Λ represents an LOCC operation. The two measures of entanglement appeared in the context of manipulating entanglement and have an operational meaning. E_D (E_C) is the supremum (infimum) of all the measures of entanglement.

1) Entanglement measures: axiomatic approach

One can apply an axiomatic point of view by allowing any function of state to be a measure, provided it satisfies some postulates. The most important postulate for entanglement measures is monotonicity under LOCC: entanglement cannot increase under local operations and classical communication. Other postulates follow from this basic axiom: (i) the entanglement measure of separable states vanishes, (ii) convexity, that is, $E\left(\sum_i p_i \rho_i\right) \leq \sum_i p_i E(\rho_i)$, (iii) any *local* measurement will not increase entanglement *on average*, and (iv) invariance under local unitary transformations. The entanglement follows these axioms optionally. Here we will review bipartite entanglement measures built on an axiomatic basis.

One class of entanglement measures is based on the natural intuition that the closer the state is to the set of separable states, the less entangled it is. The measure is the minimum distance between the given state and the states in S : $E_{D,S}(\rho) = \inf_{\sigma \in S} D(\rho, \sigma)$, where the set S is chosen to be closed under LOCC operations. Once a good distance is chosen, one can consider different measures by changing the sets S . In this way one obtains E_R^{PPT} and E_R^{ND} (the distance from non-distillable states) (Rains, 2001). The greater the set is, the smaller the measure is.

According to the monotonicity condition, a distance measured must satisfy $D(\rho, \sigma) \geq D(\Lambda(\rho), \Lambda(\sigma))$. In 1998 Vedral and Plenio proposed two distances to satisfy this condition and convexity: square of Bures metric $B^2 = 2 - 2\sqrt{F(\rho, \sigma)}$ where $F(\rho, \sigma) = [\text{Tr}(\sqrt{\rho\sigma}\sqrt{\rho})]^{1/2}$ is fidelity and relative entropy $S(\rho|\sigma) = \text{Tr} \rho(\log \rho - \log \sigma)$. Originally, the set of separable states was used and the resulting measure

$$E_R = \inf_{\sigma \in \text{SEP}} \text{Tr} \rho(\log \rho - \log \sigma) \quad (11.14)$$

is called the relative entropy of entanglement. It is one of the fundamental entanglement measures, as relative entropy is one of the most important functions in quantum information theory. Its other versions – the relative entropy distance from PPT states and from non-distillable states – are denoted E_R^{PPT} and E_R^{ND} , respectively.

Furthermore, we consider the following method of obtaining entanglement measures: one starts by imposing a measure E on pure states and then extends it to mixed ones by constructing the convex function

$$E(\rho) = \inf \sum_i p_i E(\psi_i), \quad \sum_i p_i = 1, p_i \geq 0 \quad (11.15)$$

where $\{\rho_i, \psi_i\}$ can be any pure state ensemble. We call such an ensemble an optimal ensemble. Thus E is equal to the average under the optimal ensemble. The first entanglement measure

built in this way was called an entanglement of formation E_F (Bennett, *et al.*, 1996), where $E(\psi)$ is the von Neumann entropy of the reduced density matrix of ψ . If replace ρ as $\rho^{\otimes n}$, the entanglement of formation when $n \rightarrow \infty$, that is, E_F^∞ , is entanglement cost E_C .

A very popular measure for the quantification of bipartite quantum correlations is the concurrence (Hill and Wootters, 1997). This quantity can be defined for pure states and can be analytically calculated as $C(\rho) = \max\{0, \lambda_1 - \lambda_2 - \lambda_3 - \lambda_4\}$, where the λ_i are the decreasingly ordered eigenvalues of the matrix $\sqrt{\sqrt{\rho}\sigma_y \otimes \sigma_y\rho^*\sigma_y \otimes \sigma_y\rho\sqrt{\rho}}$. Moreover, for two qubits the entanglement of formation can be expressed in terms of the concurrence as

$$E_F(\rho) = H\left(\frac{1 + \sqrt{1 - C^2(\rho)}}{2}\right) \quad (11.16)$$

where $H(x) = -x \log x - (1 - x) \log(1 - x)$ is the binary entropy function. For higher dimensions, however, such a relation does not hold and the physical interpretation of the concurrence is not so clear.

The negativity (Vidal and Werner, 2002) is just given as the violation of the PPT criterion

$$N(\rho) = \frac{\|\rho^{T_B}\|_1 - 1}{2} \quad (11.17)$$

It is shown to be LOCC monotone. Two of the main advantages are that negativity is very easy to calculate and it is convex. In order to make this quantity additive, one can consider the logarithmic negativity $E_N(\rho) = \log_2 \|\rho^{T_B}\|_1$.

The robustness of entanglement is defined as the minimal t such that the state $\frac{1}{1+t}(\rho + t\sigma_{sep})$ is separable, where σ_{sep} is the separable state. There is also another entanglement which is called maximum cross norm (Rudolph, 2001). One decomposes ρ into the sum of product operators $\rho = \sum_i A_i \otimes B_i$, then the measure is given by

$$E(\rho) = \sup \sum_i \|A_i\|_1 \cdot \|B_i\|_1 \quad (11.18)$$

Squashed entanglement is defined as $E_{sq} = \inf_{\rho_{ABE}} \frac{1}{2}(S_{AE} + S_{BE} - S_E - S_{ABE})$, where S denotes von Neumann entropy and the infimum is taken over all density matrices ρ_{ABE} satisfying $\text{Tr}_E \rho_{ABE} = \rho_{AB}$. The measure has proved to be monotone and additive on tensor product and superadditive in general. It is not known whether it vanishes if and only if the state is separable.

Besides the above entanglement measure, there are a few measures that are not introduced here in detail, for example best separable approximation measure (Karnas and Lewenstein, 2001) and witnessed entanglement $E = -\inf_W \text{Tr}(\rho W)$ (Brandão and Vianna, 2004), where the infimum is taken over some set of entanglement witnesses, and Rains bound, which combines two different concepts (relative entropy of entanglement and negativity) (Rains, 2001), and conditioning entanglement (Yang *et al.*, 2005).

2) Multipartite entanglement measures

Many of the axiomatic measures can be immediately extended to the multipartite case. For example, relative entropy of entanglement is generalized by taking a suitable set in place

of bipartite separable states. For multipartite states, many more parameters to describe entanglement are needed, therefore many new entanglement measures have been designed, especially for pure states. They can be extended to all states by convex functions. Now we review multipartite entanglement measures for pure states.

There are measures that are simple functions of the sums of bipartite entanglement measures. An example is “global entanglement,” which is the sum of concurrences between a single qubit versus all other qubits. The first measure, which is neither an easy combination of bipartite measures nor an obvious generalization of such a measure, is the three-tangle, defined as $\tau(A : B : C) = \tau(A : BC) - \tau(AB) - \tau(AC)$, where the two tangles on the right-hand side are squares of concurrence, and $A : BC$ represents a segmentation of a three-qubit system. Shortly after introducing a tangle, a concept of another measure for tripartite states was introduced in the context of the asymptotic rate of transitions $E(\psi_{ABC}) = E_R(\rho_{AB}) + S(\rho_C)$, where ρ_{AB} and ρ_C are reductions of ψ_{ABC} .

One of the first measures designed specifically for multipartite states is the Schmidt measure. This is the minimum of $\log r$ where r is the number of terms in an expansion of the state in product basis. For GHZ this measure is 1 because there are just two terms, $|000\rangle$ and $|111\rangle$. Geometric measure is defined as $E_g(\psi) = 1 - \sum_{\phi \in S_k} 1 - |\psi\rangle\langle\phi|^2$, with S_k being the set of k -separable states. There are other attempts to generalize concurrence: concurrence-like measures works for even number of qubits and is given by $\langle\psi^*|\sigma_y^n|\psi\rangle$. The other measures include multipartite version of squashed entanglement, local entanglement, and so on (Horodecki, Horodecki, and Horodecki, 2009).

3) Estimation of entanglement measures

In the previous sections we introduced methods to qualify entanglement based on the quantum state being known. In principle, one can determine the full quantum state via ST, and apply some separability criteria afterwards. However, the tomography requires an effort that grows exponentially with the number of parties. This leads to the problem of how to estimate optimally the amount of entanglement of a compound system in an unknown state if only incomplete data in the form of average values of some operators detecting entanglement are accessible. This question involves a principle of minimization of entanglement under a chosen measure of entanglement with constraints in the form of an incomplete set of data from experiments.

Let us consider the following situation. In an experiment, n entanglement witnesses $W_k, k = 1, 2, \dots, n$ (or indeed any Hermitian operators) have been measured $w_k = \langle W_k \rangle = \text{Tr}(\rho W_k)$ along with some entanglement measure E . On the basis of these numbers we want to calculate a lower bound on $E(\rho)$ or, more precisely, the best lower bound $\inf_{\rho} \{E(\rho) | \text{Tr}(\rho W_k) = w_k\}$.

In order to derive such lower bounds, one can use the Legendre transform (Eisert, Brandão, and Audenaert, 2007) of E for the witness W , defined by the maximization

$$\hat{E}(W) = \sup_{\rho} \left\{ \sum_k r_k \text{Tr}(\rho W_k) - E(\rho) \right\} \quad (11.19)$$

As this is defined by the maximum over all ρ , for any fixed ρ we have $E(\rho) \geq \text{Tr}(\rho W) - \hat{E}(W)$, for which the first term on the right-hand side is the given measurement data, while the second

term can be calculated. A measurable bound on $E(\rho)$ can therefore be obtained. The remaining issue is to calculate $\hat{E}(W)$. If one can derive the optimal solution for any arbitrary chosen set of parameters (r_1, r_2, \dots, r_n) , the problem is simplified to optimizing over r , that is,

$$\epsilon(r) = \sup_r \left\{ \sum_k r_k w_k - \hat{E} \left(\sum_k r_k W_k \right) \right\} \quad (11.20)$$

Once again this is a Legendre transform formula. The main problem in this scheme lies in the calculation of the Legendre transform. The difficulty of this task clearly depends on the witness W and on the measure E chosen. For this problem, the following results have been obtained: for the entanglement of formation one can design a simple iterative algorithm that can perform the calculation numerically, and for the geometric measure of entanglement one can also construct an iterative algorithm for general witnesses (Guhne, Reimpell, and Werner, 2007). For some other witnesses one can analytically estimate the Legendre transform (Eisert, Brando, and Audenaert, 2007).

11.2.4 Non-linear Separability Criteria

The non-linear separability criteria are divided into two different classes. The first one is based on functions of results of some measurements performed in a non-collective manner. This comprises separability conditions in terms of uncertainty relations and non-linear witness. The second class of non-linear separability conditions is based on collective measurements on several copies.

Let us recall briefly the key of the approach of the local uncertainty relations (LURs). Consider the set of local observables $\{A_i\}_{i=0}^N, \{B_i\}_{i=0}^N$ on Hilbert spaces H_A and H_B . Suppose that one has bounds on the sum of local variances, that is, $\sum_i (\Delta A_i)^2 \geq c_a, \sum_i (\Delta B_i)^2 \geq c_b$ with some non-negative values c_a, c_b and the variance definition $\Delta(M)_\rho^2 = \langle M^2 \rangle_\rho - M_\rho^2$. Then for any separable state ρ_{AB} and the observable operator $M_i = A_i \otimes I + I \otimes B_i$ in $H_A \otimes H_B$, the following inequality holds

$$\sum_i (\Delta M_i)_{\rho_{AB}}^2 \geq c_a + c_b \quad (11.21)$$

Note that this inequality can be extended to the multipartite case by the induction.

The entanglement witness can be deemed as an inequality of the average value of the observable operator. Then one interest is to derive non-linear separability criteria like Equation 11.21 via operator variance. They are non-linear for the density matrix and therefore are called non-linear entanglement witnesses. Furthermore, they can approach the convex set of separable states better. The general form of the non-linear improvement of the witness W is

$$F_\rho = \langle W \rangle_\rho - \sum_k \alpha_k |\langle X_k \rangle_\rho|^2 \quad (11.22)$$

where the real numbers α_k and operators X_k are both chosen in such a way that for all possible separable states the condition $F_\rho \geq 0$ is satisfied. Then a state ρ satisfying $F_\rho < 0$ is entangled. One can see that the second term is a quadratic correction to the original (linear) mean value of entanglement witness. Higher-order corrections are also possible.

In a multi-qubit system, the qubits cannot be accessed individually so that collective measurement is needed. The quantities that can be measured collectively are the components of the collective angular momentum $J_l := \frac{1}{2} \sum_{k=1}^N \sigma_l^{(k)}$, where $l = x, y, z$ and $\sigma_l^{(k)}$ are the Pauli spin matrices. Several generalized spin squeezing inequalities based on the collective angular momentum have been developed. In 2007 Tóth *et al.* found a unifying framework for all these inequalities. It turned out that the first- and second-order moments of collective angular momenta for fully separable states fulfill eight inequalities that define a polytope in the three-dimensional ($\langle J_x^2 \rangle, \langle J_y^2 \rangle, \langle J_z^2 \rangle$) space. Separable states lie inside this polytope. If one of the inequalities is violated, then the state is on the outside and hence is entangled. The Hamiltonian of the system can also be chosen as collective measurement. To give a simple example, consider the one-dimensional Heisenberg Hamiltonian H_H on N spins: one can directly see that for a fully separable state $\langle H_H \rangle \geq -N$ has to hold.

11.3 Decoherence Control Based on Weak Measurement

The theory in quantum feedback control usually uses projective measurements to get the information about the quantum system controlled (Ezawa and Murayama, 1993; Wiseman, 1994; Ganesan and Tarn, 2007). A projective measurement is also called a strong measurement; it is carried out by orthogonal projective operators corresponding to the Hamiltonian's eigenspace of the observed quantities. After a projective measurement, the state of the controlled quantum system is projected to an eigenstate of the Hamiltonian with a certain probability. Such measurements typically disturb the controlled quantum system and destroy the quantum coherence. At the same time they give a stochastic characteristic to the quantum feedback control process. However, the projective measurement is not the only way to acquire information about quantum systems. The concept of a more general measurement is widely proposed afterwards, namely positive-operator valued measurement (POVM) or the generalized measurement. The POVM has a more common form and some properties that are not provided for by projective measurement, for instance the POVM can be non-orthogonal, informational incomplete, and unrepeatable. The POVM therefore has wider applications such as optimal differentiation for a set of quantum states in quantum computation and quantum information processes (Nielsen and Chuang, 2000).

As a special form of POVM, weak measurement has been widely studied in recent years (Bennett *et al.*, 1999; Lloyd and Slotine, 2000; Audretsch, Diósi, and Konrad, 2002; Johansen, 2004; Oreshkov and Brun, 2005; Ruskov, Korotkov, and Mize, 2006; Wang, Jin, and Li, 2007). The quantum feedback control usually requires continuous information of the controlled system with its state undestroyed. A weak measurement is a measurement that only slightly disturbs the quantum system controlled, and it is usually used in quantum feedback control systems, for example nuclear magnetic resonance (NMR) systems (Vandersypen and Chuang, 2004; Negrevergne *et al.*, 2005), which can be weakly coupled with the measurement equipment. The weak measurement therefore plays an important role in quantum feedback control processes and makes it possible to implement closed-loop quantum feedback controls. However, it is inconvenient to study weak measurement for general situations because there are various forms of it. A particular kind of POVM operators is therefore proposed in the following section, based on which the applicability of weak measurement is discussed and some

properties are studied. In addition the dephasing and depolarization process of a two-level single quantum system can be suppressed as a potential application.

11.3.1 Construction of a Weak Measurement Operator

In quantum theory, any state of a quantum system can be described by a density matrix ρ , which is defined as follows:

$$\rho = \sum_j c_j |\varphi_j\rangle\langle\varphi_j| \quad (11.23)$$

in which $|\varphi_j\rangle$ is a normalized pure state and c_j denotes corresponding probability satisfying $\sum_j c_j = 1$. Now assume A is a space of density matrix, that is, $\rho \in A$, then define the norm of the density matrix as

$$\|\rho\| = \sqrt{\text{tr}(\rho^2)} = \left(\sum_{ij} |\rho_{ij}|^2 \right)^{1/2} \quad (11.24)$$

It is easy to testify that $(A, \|\cdot\|)$ is a normed linear space (Ye, 1991), namely the following conditions are satisfied: (i) $\|\rho\| = 0 \iff \rho = 0$, (ii) $\|\lambda\rho\| = |\lambda| \cdot \|\rho\|$, and (iii) $\|\rho + \chi\| \leq \|\rho\| + \|\chi\|$, ($\rho, \chi \in A$). In addition, it can also be proved that $\|\rho\chi\| \leq \|\rho\| \cdot \|\chi\|$ and $\|U\rho U^+\| = \|\rho\|$, where $\rho, \chi \in A$, $UU^\dagger = U^\dagger U = I$. For the proof of normed linear space $(A, \|\cdot\|)$ see Appendix 11.A.

According to the quantum measurement assumption, the probability of getting a corresponding result is $p_j = \text{tr}(F_j^2 \rho)$ for a given measurement operator F_j , and after the measurement the density matrix of the observed quantum system becomes $\rho_j = (F_j \rho F_j)/p_j$. A weak measurement can therefore be defined to be such a measurement that satisfies the following formula (Lloyd and Slotine, 2000):

$$\sum_j p_j \|\rho - \rho_j\| < \epsilon, 0 < \epsilon \ll 1 \quad (11.25)$$

Definition 11.1 Assume $\{M_j\}$, $1 \leq j \leq n$, is the orthogonal projective measurement operators of a n -dimension quantum system. The measurement operator F_j is defined as:

$$F_j = \sum_k \alpha_{jk} M_k, \quad \alpha_{jk} \geq 0 \quad (11.26)$$

Operator F_j is obviously positive. According to the restriction of POVM measurement, $\sum_j F_j^2 = I$ and $\text{tr}(F_j^2) = 1$, one can get

$$\sum_j \alpha_{jk}^2 = 1 \quad (11.27a)$$

$$\sum_k \alpha_{jk}^2 = 1 \quad (11.27b)$$

In the rest of this section, we assume that operators $\{M_j\}$ are natural projections for convenience, namely projections to natural bases $\{|e_j\rangle\}$. In fact, if $\{M_j = |g_j\rangle\langle g_j|\}$ are not natural

projections, there is a transform U between bases $\{|e_j\rangle\}$ and $\{|g_j\rangle\}$, viz. $U(|e_1\rangle, \dots, |e_n\rangle) = (|g_1\rangle, \dots, |g_n\rangle)$, $E_j = |e_j\rangle\langle e_j| = U^\dagger M_j U$. If the expressions of density matrices corresponding to the bases $\{|g_j\rangle\}$ and $\{|e_j\rangle\}$ are ρ_g and ρ_e , respectively, then $\rho_g = U\rho_e U^\dagger$. Thus $p_j = \text{tr}(M_j \rho_g M_j) = \text{tr}(E_j \rho_e E_j)$ and $\rho_j = (M_j \rho_g M_j)/p_j = U(E_j \rho_e E_j)U^\dagger/p_j$, which means that the density matrix expression can be transformed to the bases corresponding to the projective measurement operators before the measurement, and after the measurement process it can be transformed back to the former bases. According to the characteristic of $\|U\rho U^\dagger\| = \|\rho\|$, the module is invariant under such transforms, therefore the assumption of natural projection is available.

A sufficient condition for the weak measurement operator F_j defined by Equation 11.26 can be derived according to the restriction in Equation 11.25.

Theorem 11.1 The sufficient condition of the weak measurement operator F_j defined by Equation 11.26 is

$$\sum_j (\max_k \alpha_{jk}^2 - \min_l \alpha_{jl}^2) < \epsilon, \quad 0 < \epsilon \ll 1 \quad (11.28)$$

Proof

$$\begin{aligned} & \sum_j p_j \|\rho - \rho_j\| \\ &= \sum_j \left(\sum_{kl} (p_j - \alpha_{jk}\alpha_{jl})^2 |\rho_{kl}|^2 \right)^{1/2} \leq \sum_j \left(\sum_{kl} (p_j - \alpha_{jk}\alpha_{jl})^2 |\rho_{kk}\rho_{ll}| \right)^{1/2} \\ &\leq \sum_j \left(\max_{kl} (p_j - \alpha_{jk}\alpha_{jl})^2 \sum_{kl} |\rho_{kk}\rho_{ll}| \right)^{1/2} \\ &\leq \left(\sum_j \max_{kl} |p_j - \alpha_{jk}\alpha_{jl}| \right) \left(\sum_k |\rho_{kk}|^2 \right)^{1/4} \left(\sum_l |\rho_{ll}|^2 \right)^{1/4} \\ &\leq \sum_j \max_{kl} |p_j - \alpha_{jk}\alpha_{jl}| = \sum_j \max_{kl} \left| \sum_m \alpha_{jm}^2 \text{tr}(M_m \rho) - \alpha_{jk}\alpha_{jl} \right| \leq \sum_j (\max_k \alpha_{jk}^2 - \min_l \alpha_{jl}^2) \\ &< \epsilon \end{aligned} \quad (11.29)$$

The proof has utilized the Hölder inequality (Ye, 1991), $|\rho_{kl}| \leq |\rho_{kk}\rho_{ll}|$, $\sum_k |\rho_{kk}|^2 \leq 1$, and the fact $\sum_m \text{tr}(M_m \rho) = 1$. The sufficient condition of weak measurement is therefore Equation 11.28. ■

11.3.2 Applicability of Weak Measurement

Weak measurement makes the system density matrix resistant to a degree of error $\pm\epsilon$, accordingly it obtains little information about the system, which indicates that the operator F_j is approximately in direct proportion to an identity matrix. The density matrix is unchanged

after the measurement with a probability close to 1, but it is changed with a very small probability. In order to get much more precise probabilities, the repetition measurements on the single quantum system are required, or there should be a mass of identical non-interacting quantum systems. Of course, perfectly non-interacting is impossible, but in many situations, such as liquid-state NMR and quantum optics, the non-interacting approximation is tolerable. Actually, some research indicates that when the number of identical quantum systems is large enough, and the interacting intensities are weak enough, one can acquire accurate system information with the system states perturbed by an arbitrarily small amount (Lloyd and Slotine, 2000).

For a single quantum system, although the mathematical descriptions of the states cannot be distinguished from that of a pure state ensemble, a quantum measurement is usually unrealized because collapses caused by the measurement are irreversible and the statistical information about the original state cannot be acquired, viz. the wave function of the original state cannot be ascertained. This is not always the case. The weak measurement changes the state of the observed system to some extent, and the repetition measurements are still valid to acquire the probability information. Practically, a system can restore its initial state after a series of weak measurements are acted on.

Lemma 11.1 There exists a weak measurement operator such that when it is acted on a single quantum system the state of the quantum system can be left unchanged.

Proof Consider

$$\prod_j F_j = \sum_k \left(\prod_j \alpha_{jk} \right) M_k \quad (11.30)$$

If it is made that

$$\prod_j \alpha_{jk} = \prod_j \alpha_{jl} = \beta \quad (11.31)$$

then Equation 11.30 becomes

$$\prod_j F_j = \beta \cdot I \quad (11.32)$$

Thus the state of the single system will be restored to the initial one after being sequentially acted on by a series of weak measurement operators F_j . This result is independent of the operators' order. There always exist the coefficients $\{\alpha_{jk}\}$ in Equation 11.31. If $\{\alpha_{11}, \alpha_{21}, \dots, \alpha_{s1}, s \geq n\}$ satisfies the inequation $\max_k \alpha_{j1}^2 - \min_k \alpha_{k1}^2 < \epsilon/n$ and Equation 11.27a holds, one can adopt $\alpha_{jk}, k > 1$ as $\alpha_{nk} = \alpha_{1,k-1}$ and $\alpha_{jk} = \alpha_{j+1,k-1}$, $j < n$, thus $\{\alpha_{jk}, k \neq 1, k \text{ is fixed}\}$ is a permutation of $\{\alpha_{11}, \alpha_{21}, \dots, \alpha_{n1}\}$, where different k values denote different permutations that guarantee that Equation 11.31 holds. Thus one can construct the operator F_j with coefficients $\{\alpha_{jk}, j \text{ is fixed}\}$, which has the same elements as $\{\alpha_{j1}\}$, so meets Equation 11.27b and the inequation $\max_k \alpha_{jk}^2 - \min_l \alpha_{jl}^2 < \epsilon/n$, which makes Equation 11.28 hold. Thus the operator F_j is obviously a weak measurement operator. When $n \geq 2$, the number of permutations is $s! \geq n$, hence such a weak measurement operator always exists, viz. the Lemma is true.

The Lemma implies that weak measurement defined by Equations 11.26 and 11.28 is applicable not only to a mass of identical non-interacting quantum systems, but also to a single

quantum system if any measurement operator can be selectively implemented. For a given weak measurement operator one can correspondingly construct a series of weak measurement operators, which are supposed to be sequentially acted on the system. The effect of those operators is to restore the system state from the one perturbed by the former operator to the initial one. In this way, it is equivalent to the situation where there is a mass of identical non-interacting quantum systems to be measured, therefore accurate statistical information could be acquired. It should be emphasized that for a single quantum system if any measurement operator can be selectively implemented, one could not only obtain the probability information of the system observed, but also keep the system state unchanged. ■

11.3.3 Effects on States

Now consider the change in an average of state density matrix when a weak measurement is acted on a set of identical non-interacting quantum systems. For the systems with identical initial density matrix ρ , the average state in the density matrix becomes $\rho^1 = \sum_j F_j \rho F_j$ after a weak measurement. Its matrix element is

$$\rho_{kl}^1 = \left(\sum_j \alpha_{jk} \alpha_{jl} \right) \rho_{kl} \quad (11.33a)$$

when $l = k$,

$$\rho_{kk}^1 = \left(\sum_j \alpha_{jk}^2 \right) \rho_{kk} = \rho_{kk} \quad (11.33b)$$

and when $l \neq k$,

$$\rho_{kl}^1 = \left(\sum_j \alpha_{jk} \alpha_{jl} \right) \rho_{kl} \leq \left(\sum_j \alpha_{jk}^2 \right)^{1/2} \left(\sum_j \alpha_{jl}^2 \right)^{1/2} \rho_{kl} = \rho_{kl} \quad (11.33c)$$

Therefore after N weak measurements being acted on, the average of state density matrix becomes

$$\rho_{kk}^N = \rho_{kk} \quad (11.34a)$$

$$\rho_{kl}^N = \left(\sum_j \alpha_{jk} \alpha_{jl} \right)^N \rho_{kl} \quad (11.34b)$$

where $N \rightarrow \infty$ and $\rho_{kl}^\infty \rightarrow 0$. This is equivalent to a projective measurement with operators $\{M_j\}$. In fact, it could be proved that this conclusion is still correct when $\{M_j\}$ are not natural projections. This means that any projective measurement can be done as a sequence of weak measurements. Moreover, it has been shown that any POVM can be achieved through weak measurements by using an additional ancilla system and a joint unitary transformation (Bennett *et al.*, 1999; Oreshkov and Brun, 2005). This property of weak measurement allows us to consider the collapse of a wave packet due to measurements resulting from continuous evolutions.

The characteristic mentioned above is deduced without the consideration of evolution induced by the system Hamiltonians, but N weak measurements are usually done in a relative

long time. Let us assume that one weak measurement is acted on every time period Δt , then the dynamical equation of the systems under continuous weak measurements, which is similar to the MEs of continuous quantum measurements (Walls and Milburn, 1994), can be derived.

Proposition 11.1 Under actions of continuous weak measurements, the evolution of the average of the state density matrix ρ follows this equation:

$$i\hbar\dot{\rho} = [H, \rho] - \frac{i\hbar}{2}\eta \sum_j [F_j, [F_j, \rho]] \quad (11.35)$$

where H is the system Hamiltonian, F_j is the weak measurement operator, and η is the measurement intensity.

Proof Consider Equation 11.33a:

$$\begin{aligned} \rho_{kl}^1 &= \left(\sum_j \alpha_{jk} \alpha_{jl} \right) \rho_{kl} \\ &= \sum_j \left(\alpha_{jk} \alpha_{jl} + \frac{\alpha_{jk}^2 + \alpha_{jl}^2}{2} - \frac{\alpha_{jk}^2 + \alpha_{jl}^2}{2} \right) \rho_{kl} = \left(\sum_j F_j \rho F_j \right)_{kl} + \rho_{kl} - \frac{1}{2} \sum_j (F_j^2 \rho + \rho F_j^2)_{kl} \\ &= \rho_{kl} - \frac{1}{2} \sum_j \left[F_j, [F_j, \rho] \right]_{kl} \end{aligned} \quad (11.36a)$$

The interval between two weak measurements is Δt and the change of average density matrix in interval Δt is $\Delta\rho = \rho^1 - \rho = -\frac{1}{2} \sum_j [F_j, [F_j, \rho]]$. If $\Delta t \rightarrow 0$:

$$\dot{\rho} = -\frac{1}{2}\eta \sum_j [F_j, [F_j, \rho]] \quad (11.36b)$$

where the measurement intensity $\eta = 1$ means an overall measurement on the set of non-interacting systems. Taking into consideration the evolution due to the system Hamiltonian gives Equation 11.35.

Proposition 11.1 implies that the non-diagonal elements of the average of the state density matrix decrease to zero gradually on continuous weak measurements, which is equivalent to a dephasing process. However, the situation is quite different when the weak measurements are acted on a single quantum system. When a single quantum system is in a mixed state, it has different physical meanings from that of a set of non-interacting systems, although their density matrices may be the same. If the density matrix of a set of non-interacting systems is in a mixed state, then it is a mix of many pure states, viz. an ensemble of pure states. If a single quantum system is in a mixed state, then it implies that the system is to some extent entangled with other systems, but because one knows nothing about (or may be not interested in) those other systems, the density matrix is only a partial trace of the overall systems' state. The mixed states of a single system and a pure state ensemble have the same results of probability when they are measured, so they have the same mathematical description. Therefore, after a measurement is acted on a single quantum system, the state is unique, that is, $\rho^1 = (F_j \rho F_j) / p_j$, where j depends

on the measurement result. It is different from the situation of a pure state ensemble, whose state after a measurement is a statistical result: $\rho^1 = \sum_j F_j \rho F_j$. Then according to Lemma 11.1, if an action of a weak measurement operator diminishes the coherence of the system, viz. the modules of the non-diagonal elements decrease, but the initial state can be restored, then there must be an operator that could enhance the coherence of the system. Thus if such a measurement operator is acted on the system continuously, decoherence processes could be suppressed. Taking a two-level system as an example, we will show how one can construct such a measurement operator. ■

Theorem 11.2 For a two-level quantum system, the operator which can suppress the dephasing processes can be constructed as $F_0 = \alpha_1 |0\rangle\langle 0| + \alpha_2 |1\rangle\langle 1|$, where α_1 and α_2 can be calculated by

$$\alpha_1 = \frac{1}{\sqrt{1 + 4\rho_{11}^2 e^{2\zeta\Delta t}}}, \quad \alpha_2 = \frac{2\rho_{11} e^{\zeta\Delta t}}{\sqrt{1 + 4\rho_{11}^2 e^{2\zeta\Delta t}}} \quad (11.37a)$$

The probability of successfully dephasing suppression for a single measurement is

$$p_0 = \alpha_1^2 \rho_{11} + \alpha_2^2 \rho_{22} \quad (11.37b)$$

and the measurement defined by $F_0 = \alpha_1 |0\rangle\langle 0| + \alpha_2 |1\rangle\langle 1|$ and $F_1 = \alpha_2 |0\rangle\langle 0| + \alpha_1 |1\rangle\langle 1|$ can also suppress the depolarization of the system.

Proof Assume that the state density matrix of system is ρ , its dephasing rate is ζ , $\zeta \ll 1$, viz. $\dot{\rho}_{12} = -\zeta\rho_{12}$, and the measurement operator acted on the system is $F_0 = \alpha_1 |0\rangle\langle 0| + \alpha_2 |1\rangle\langle 1|$, then the non-diagonal element of ρ after the measurement is $\rho'_{12} = \frac{\alpha_1 \alpha_2}{\alpha_1^2 \rho_{11} + \alpha_2^2 \rho_{22}} \rho_{12}$. The decrease of ρ_{12} after interval Δt due to the dephasing is $\Delta\rho_{12} = (e^{\zeta\Delta t} - 1)\rho_{12}(\Delta t)$. Therefore if the dephasing could be suppressed, the following inequation must be satisfied:

$$\left(\frac{\alpha_1 \alpha_2}{\alpha_1^2 \rho_{11}(\Delta t) + \alpha_2^2 \rho_{22}(\Delta t)} - 1 \right) |\rho_{12}(\Delta t)| \geq (e^{\zeta\Delta t} - 1) |\rho_{12}(\Delta t)| \quad (11.38)$$

According to the inequation (Equations 11.37a and 11.37b) one can get

$$\left(1 - \sqrt{1 - 4\rho_{11}\rho_{22}e^{2\zeta\Delta t}} \right) / 2\rho_{11}e^{\zeta\Delta t} \leq \frac{\alpha_1}{\alpha_2} \leq \left(1 + \sqrt{1 - 4\rho_{11}\rho_{22}e^{2\zeta\Delta t}} \right) / 2\rho_{11}e^{\zeta\Delta t} \quad (11.39a)$$

$$0 < \rho_{11} < \left(1 - \sqrt{1 - e^{-2\zeta\Delta t}} \right) / 2 \text{ or } \left(1 + \sqrt{1 - e^{-2\zeta\Delta t}} \right) / 2 < \rho_{11} < 1 \quad (11.39b)$$

Hence one can adopt $\alpha_1/\alpha_2 = 1/(2\rho_{11}e^{\zeta\Delta t})$. Considering Equation 11.27b, viz. $\alpha_1^2 + \alpha_2^2 = 1$, one can calculate α_1 and α_2 as Equation 11.37a.

The probability of getting the expected outcome is $p_0 = \alpha_1^2 \rho_{11} + \alpha_2^2 \rho_{22}$. On the other side, an unexpected outcome can be obtained corresponding to the measurement operator $F_1 = \alpha_2 |0\rangle\langle 0| + \alpha_1 |1\rangle\langle 1|$ with probability $1 - p_0$. If the outcome of corresponding to F_0 is obtained, then the dephasing process of the system is suppressed successfully with probability p_0 , and

one just waits for Δt to do another measurement. Otherwise, if the outcome of corresponding to F_1 is obtained, the dephasing process is accelerated instead. In order to suppress the dephasing from a global point of view, the probability of successful suppression should be larger than a half, viz. $p_0 > 1/2$. However, according to $\alpha_1/\alpha_2 = 1/(2\rho_{11}e^{\varsigma\Delta t})$, $\alpha_1^2 + \alpha_2^2 = 1$, and $p_0 > 1/2$, one can calculate that $1/(2e^{\varsigma\Delta t}) < \rho_{11} < 1/2$. It is easy to verify that $(1 - \sqrt{1 - e^{-2\varsigma\Delta t}})/2 < 1/(2e^{\varsigma\Delta t})$, thus the ρ_{11} described by Equation 11.39b makes the probability less than a half, viz. $p_0 < 1/2$ is always true.

Although from a global point of view the dephasing cannot be suppressed by simply using the weak measurement, it does not mean the weak measurement is useless for quantum decoherence control. When one only needs to keep the coherence of a single system for a short period of time, and if there are a lot of distinguishable quantum systems, which are in the same state, then after a measurement the systems on which F_0 has been acted can be picked out. The dephasing of these picked-out systems has been suppressed successfully, so if the number of the systems is large enough, it is possible to implement several instances of such a measurement and pick them out, and then one can get a single system whose dephasing is suppressed successfully in a short period of time.

It should be emphasized here that this method of decoherence control is applicable only if there are lots of distinguishable quantum systems. If these quantum systems are indistinguishable, those systems whose dephasing processes are successfully suppressed after a measurement cannot be picked out and then only the ensemble average of the state density matrix could be calculated, which is the situation in Proposition 11.1, viz. the effect of weak measurements for a mass of quantum systems is equivalent to a dephasing process.

Furthermore, let us consider the diagonal elements' change in the state density matrix due to the operator F_0 . The difference between ρ_{11} before the measurement and after the measurement is

$$\Delta\rho_{11} = \left(\frac{\alpha_1^2}{\alpha_1^2\rho_{11} + \alpha_2^2\rho_{22}} - 1 \right) \rho_{11} = \frac{1 - \rho_{11}}{\alpha_1^2\rho_{11}/\alpha_2^2 + \rho_{22}} \left(\frac{\alpha_1}{\alpha_2} + 1 \right) \left(\frac{\alpha_1}{\alpha_2} - 1 \right) \rho_{11} \quad (11.40)$$

It is easy to verify that $\Delta\rho_{11} > 0$ if $0 < \rho_{11} < (1 - \sqrt{1 - e^{-2\varsigma\Delta t}})/2$ and $\Delta\rho_{11} < 0$ if $(1 + \sqrt{1 - e^{-2\varsigma\Delta t}})/2 < \rho_{11} < 1$. Looking from the Bloch sphere, the operator F_0 moves the Bloch vector toward the x - y plane. Equation 11.39b is the condition for the existence of such a measurement operator, but its restriction is not strong because as long as $\rho_{11} < 1/2$, it could be satisfied through shortening the measurement interval Δt . Because of the movement toward the x - y plane induced by the operator F_0 , Equation 11.39b may be disobeyed after several measurements, and then the interval Δt should be readjusted in time. Measurements will be more and more frequent until $\rho_{11} = 1/2$ at some time, and from then on the dephasing process cannot be suppressed any longer.

Similarly, it can be verified that if the operator F_1 takes effect, $\Delta\rho_{11} < 0$ if $0 < \rho_{11} < (1 - \sqrt{1 - e^{-2\varsigma\Delta t}})/2$ and $\Delta\rho_{11} > 0$ if $(1 + \sqrt{1 - e^{-2\varsigma\Delta t}})/2 < \rho_{11} < 1$. This means the operator F_1 moves the Bloch vector toward the two poles of the Bloch sphere. Considering that the probability of successful suppression is always less than a half, viz. $p_0 < 1/2$, and $F_0F_1 = F_1F_0 = \beta I$, then from a global point of view only the operator F_1 takes effect. If $\varsigma\Delta t \rightarrow 0$, then $e^{\varsigma\Delta t} \rightarrow 1$. In such a situation, according to Equation 11.37a, when $\rho_{11} < 1/2$, $\alpha_1 > \alpha_2$, $(F_1)^m \xrightarrow{m \rightarrow \infty} \xi|1\rangle\langle 1|$, and when $\rho_{11} > 1/2$, $\alpha_1 < \alpha_2$, $(F_1)^m \xrightarrow{m \rightarrow \infty} \xi|0\rangle\langle 0|$. This indicates

that a lot of weak measurements are equivalent to a projective operator M_0 or M_1 . Whether it is M_0 or M_1 depends on the population of the initial state, therefore one can see that the measurement constructed above can suppress the depolarization of a single two-level quantum system. In fact, if projective operators $\{M_j\}$ can be designed arbitrarily, then any decoherence processes can be prevented by utilizing the quantum Zeno effect, viz. quantum measurements frequently enough can fix the system on the initial state. ■

Appendix 11.A Proof of Normed Linear Space ($A, \|\bullet\|$)

Conditions (i) and (ii) are obvious, now consider condition (iii). Utilizing the Minkowski inequation (Ye, 1991), one can get

$$\|\rho + \chi\| = \left(\sum_{ij} |\rho_{ij} + \chi_{ij}|^2 \right)^{1/2} \leq \left(\sum_{ij} |\rho_{ij}|^2 \right)^{1/2} + \left(\sum_{ij} |\chi_{ij}|^2 \right)^{1/2} = \|\rho\| + \|\chi\| \quad (\text{A.1})$$

The proof of $\|\rho\chi\| \leq \|\rho\| \cdot \|\chi\|$, ($\rho, \chi \in A$):

Utilizing the Hölder inequation, it can be found that

$$\begin{aligned} \|\rho\chi\| &= \left(\sum_{ij} \left| \sum_k \rho_{ik} \chi_{kj} \right|^2 \right)^{1/2} \\ &= \left(\sum_{ij} \sum_{pq} \left| \rho_{ip} \chi_{pj} \rho_{iq} \chi_{qj} \right| \right)^{1/2} \leq \left(\left(\sum_{pq} \sum_{ij} \left| \rho_{ip} \chi_{qj} \right|^2 \right)^{1/2} \left(\sum_{pq} \sum_{ij} \left| \rho_{iq} \chi_{pj} \right|^2 \right)^{1/2} \right)^{1/2} \\ &= \left(\sum_{ip} \sum_{qj} \left| \rho_{ip} \chi_{qj} \right|^2 \right)^{1/2} = \|\rho\| \cdot \|\chi\| \end{aligned} \quad (\text{A.2})$$

The proof of $\|U\rho U^+\| = \|\rho\|$, ($\rho \in A, UU^+ = U^+U = I$):

According to $UU^+ = U^+U = I$:

$$\sum_i u_{pi} u_{qi}^* = \sum_i u_{ip} u_{iq}^* = \begin{cases} 0, & p \neq q \\ 1, & p = q \end{cases} \quad (\text{A.3a})$$

$$\begin{aligned} \|U\rho U^+\| &= \left(\sum_{pq} \left| \sum_{ik} u_{pi} \rho_{ik} u_{qk}^* \right|^2 \right)^{1/2} = \left(\sum_{pq} \left(\sum_{ik} u_{pi} \rho_{ik} u_{qk}^* \right) \left(\sum_{jl} u_{pj}^* \rho_{jl}^* u_{ql} \right) \right)^{1/2} \\ &= \left(\sum_{pqijkl} u_{pi} \rho_{ik} u_{qk}^* u_{pj}^* \rho_{jl}^* u_{ql} \right)^{1/2} \\ &= \left[\sum_{ijkl} \left(\sum_p u_{pi} u_{pj}^* \right) \left(\sum_q u_{ql} u_{qk}^* \right) \rho_{ik} \rho_{jl}^* \right]^{1/2} \stackrel{i=j, k=l}{=} \left(\sum_{ik} \left| \rho_{ik} \right|^2 \right)^{1/2} \\ &= \|\rho\| \end{aligned} \quad (\text{A.3b})$$

References

- Audretsch, J., Diósi, L. and Konrad, T. (2002) Evolution of a qubit under the influence of a succession of weak measurements with unitary feedback. *Physical Review A*, **66**(2), 022310.
- Augusiak, R. and Stasińska, J. (2008) General scheme for construction of scalar separability criteria from positive maps. *Physical Review A*, **77**(1), 010303R.
- Baier, J., Jodlauk, S., Kriener, M. et al. (2005) Spin-state transition and metal-insulator transition in La_{1-x}EuxCoO₃. *Physical Review B*, **71**(1), 014443.
- Bardroff, P.J., Mayr, E., Schleich, W.P. et al. (1996) Simulation of quantum state endoscopy. *Physical Review A*, **53**(4), 2736–2741.
- Bell, J.S. (1964) On the Einstein Podolsky Rosen paradox. *Physics*, **1**, 195.
- Bennett, C.H., Brassard, G., Crepeau, C. et al. (1993) Teleporting an unknown quantum state via dual classical and Einstein–Podolsky–Rosen channels. *Physical Review Letters*, **70**(13), 2895–1899.
- Bennett, C.H., Brassard, G., Popescu, S. et al. (1996) Purification of noisy entanglement and faithful teleportation via noisy channels. *Physical Review Letters*, **76**(5), 722–725.
- Bennett, C.H., DiVincenzo, D.P., Fuchs, C.A. et al. (1999) Quantum nonlocality without entanglement. *Physical Review A*, **59**(2), 1070–1090.
- Brandão, F. and Vianna, R.O. (2004) Separable multipartite mixed states – operational asymptotically necessary and sufficient conditions. *Physical Review Letters*, **93**(22), 220503.
- Buzek, V. (2004) Quantum tomography from incomplete data via maxEnt principle, in *Quantum State Estimation*, Lecture Notes in Physics, vol. **649**, Springer-Verlag, Berlin, pp. 189–234.
- Buzek, V., Derka, R., Adam, G. et al. (1998) Reconstruction of quantum states of spin systems: from quantum Bayesian inference to quantum tomography. *Annals of Physics*, **266**(2), 454–496.
- Buzek, V., Drobny, G. and Adam, G. (1997) Reconstruction of quantum states of spin systems via the Jaynes principle of maximum entropy. *Journal of Modern Optics*, **44**(11–12), 2607–2627.
- Cassinelli, G., D'Ariano, G.M., De Vito, E. et al. (2000) Group theoretical quantum tomography. *Journal of Mathematical Physics*, **41**(12), 7940–7951.
- D'Alessandro, D. (2003) On quantum state observability and measurement. *Journal of Physics A: Mathematical and General*, **36**(37), 9721–9735.
- D'Alessandro, D. (2004) On the observability and state determination of quantum mechanical systems. Proceedings of the 43rd Conference on Decision and Control, Nassau, Vol. 1, pp. 352–357.
- D'Ariano, G.M. (2000a) Universal quantum estimation. *Physics Letters A*, **268**(3), 151–157.
- D'Ariano, G.M. (2000b) In *Quantum Communications, Computing, and Measurement*, Plenum Publishing, London.
- D'Ariano, G.M., Leonhardt, U. and Paul, H. (1995) Homodyne detection of the density matrix of the radiation field. *Physical Review A*, **52**(3), R1801–R1804.
- D'Ariano, G.M., Maccone, L. and Paris, M.G.A. (2001) Quorum of observables for universal quantum estimation. *Journal of Physics A: Mathematical and General*, **34**(1), 93–103.
- D'Ariano, G.M. and Paris, M.G.A. (1999) Adaptive quantum homodyne tomography. *Physical Review A*, **60**(1), 518–528.
- D'Ariano, G.M., Paris, M.G.A. and Sacchi, M.F. (2004) Quantum tomographic methods, in *Quantum State Estimation*, Lecture Notes in Physics, vol. **649**, Springer, Berlin, pp. 7–58.
- Dunn, T.J., Walmsley, I.A. and Mukamel, S. (1995) Experimental determination of the quantum-mechanical state of a molecular vibrational mode using fluorescence tomography. *Physical Review Letters*, **74**(6), 884–887.
- Einstein, A., Podolsky, B. and Rosen, N. (1935) Can quantum-mechanical description of physical reality be considered complete?, **47**(10), 777–780.
- Eisert, J., Brandão, F. and Audenaert, K. (2007) Quantitative entanglement witnesses. *New Journal of Physics*, **9**(46), 34392.
- Eisert, J. and Plenio, M.B. (1999) A comparison of entanglement measure. *Journal of Modern Optics*, **46**(1), 145–154.

- Ekert, A.K. (1991) Correlations in Quantum Optics, PhD Thesis. Clarendon Laboratory, Oxford.
- Ezawa, H. and Murayama, Y. (1993) *Quantum Control and Measurement*, North-Holland, Amsterdam.
- Ghne, O. and Hyllus, P. (2003) Investigating three qubit entanglement with local measurement. *International Journal of Theoretical Physics*, **42**(5), 1001–1013.
- Ghne, O., Hyllus, P., Bruss, D. et al. (2003) Experimental detection of entanglement via witness operators and local measurements. *Journal of Modern Optics*, **50**(6–7), 1079–1102.
- Ghne, O., Reimpell, M. and Werner, R.F. (2007) Estimating entanglement measures in experiments. *Physical Review Letters*, **98**(11), 110502.
- Ganesan, N. and Tarn, T.-J. (2007) Decoherence control in open quantum systems via classical feedback. *Physical Review A*, **75**(3), 032323.
- Gao, W.B., Lu, C.Y., Yao, X.C. et al. (2010) Experimental demonstration of a hyper-entangled ten-qubit Schrdinger cat state. *Nature Physics*, **6**, 331–335.
- Hffner, H., Hnsel, W., Roos, C.F. et al. (2005) Scalable multiparticle entanglement of trapped ions. *Nature*, **438**, 643–646.
- Hald, J., Srensen, J.L., Schori, C. et al. (1999) Spin squeezed atoms: A macroscopic entangled ensemble created by light. *Physical Review Letters*, **83**(77), 1319–1322.
- Hill, S. and Wootters, W.K. (1997) Entanglement of a pair of quantum bits. *Physical Review Letters*, **78**(26), 5022–5025.
- Horodecki, M., Horodecki, P. and Horodecki, R. (1996) Separability of mixed states: necessary and sufficient conditions. *Physical Letters A*, **223**(1–2), 1–8.
- Horodecki, M., Horodecki, P. and Horodecki, R. (2001) Separability of n-particle mixed states: necessary and sufficient conditions in terms of linear maps. *Physical Letters A*, **283**(1–2), 1–7.
- Horodecki, R., Horodecki, P. and Horodecki, M. (2009) Quantum entanglement. *Reviews of Modern Physics*, **81**(2), 865–942.
- Horodecki, M., Oppenheim, J., and Horodecki, R. (2002) Are the laws of entanglement theory thermodynamical? *Physical Review Letters*, **89**(24), 240403.
- Hradil, Z., Rehacek, J., Fiurasek, J. et al. (2004) Maximum-likelihood methods in quantum mechanics, in *Quantum State Estimation*, Lecture Notes in Physics, vol. **649**, Springer, Berlin, pp. 59–112.
- Jamiolkowski, A. (1972) Linear transformations which preserve trace and positive semidefiniteness of operators. *Reports on Mathematical Physics*, **3**, 275–278.
- Johansen, L.M. (2004) Weak measurements with arbitrary probe states. *Physical Review Letters*, **93**(12), 120402.
- Karnas, S. and Lewenstein, M. (2001) Separable approximations of density matrices of composite quantum systems. *Journal of Physics A: Mathematical and General*, **34**(35), 6919–6937.
- Kurtsiefer, C., Pfau, T. and Mlynek, J. (1997) Measurement of the Wigner function of an ensemble of helium atoms. *Nature*, **386**, 150–153.
- Leibfried, D., Knill, E., Seidelin, S. et al. (2005) Creation of a six-atom ‘Schrdinger cat’ state. *Nature*, **438**, 639–642.
- Lloyd, S. and Slotine, J.J.E. (2000) Quantum feedback with weak measurements. *Physical Review A*, **62**(1), 012307.
- Lu, C.Y., Zhou, X.Q., Ghne, O. et al. (2007) Experimental entanglement of six photons in graph states. *Nature Physics*, **3**, 91–95.
- Lvovsky, A.I. (2004) Iterative maximum-likelihood reconstruction in quantum homodyne tomography. *Journal of Optics B: Quantum Semiclass Optcas*, **6**(6), S556–S559.
- Mandel, O., Greiner, M., Widera, A. et al. (2003) Controlled collisions for multi-particle entanglement of optically trapped atoms. *Nature*, **425**, 937.
- Negrevergne, C., Somma, R., Ortiz, G. et al. (2005) Liquid-state NMR simulations of quantum many-body problems. *Physical Review A*, **71**(3), 032344.
- Neumann, J. V. (1955) *Mathematical Foundations of Quantum Mechanics*, Princeton University Press, Princeton, NJ.

- Neumann, P., Mizuuchi, N., Rempp, F. et al. (2008) Multipartite entanglement among single spins in diamond. *Science*, **320**(5881), 1326–1329.
- Nielsen, M.A. and Chuang, I.L. (2000) *Quantum Computation and Quantum Information*, Cambridge University Press, Cambridge.
- Opatrny, T., Welsch, D.G. and Vogel, W. (1997) Least-squares inversion for density-matrix reconstruction. *Physical Review A*, **56**(3), 1788–1799.
- Oreshkov, O. and Brun, T.A. (2005) Weak measurements are universal. *Physical Review Letters*, **95**(11), 110409.
- Peres, A. (1996) Collective tests for quantum nonlocality. *Physical Review A*, **54**(4), 2685–2689.
- Plenio, M.B. and Virmani, S. (2007) An introduction to entanglement measures. *Quantum Information & Computation*, **7**(1), 1–51.
- Rains, E.M. (2001) A semidefinite program for distillable entanglement. *IEEE Transactions on Information Theory*, **47**(1), 2921–2933.
- Raussendorf, R. and Briegel, H.J. (2001) A one-way quantum computer. *Physical Review Letters*, **86**(22), 5188–5191.
- Raymer, M.G. and Beck, M. (2004) Experimental quantum state tomography of optical fields and ultra fast statistical sampling, in *Quantum State Estimation*, Lecture Notes in Physics, vol. **649**, Springer, pp. 235–295.
- Rudolph, O. (2001) A new class of entanglement measures. *Journal of Mathematical Physics*, **42**(11), 5306–5314.
- Ruskov, R., Korotkov, A.N. and Mize, A. (2006) Signatures of quantum behavior in single-qubit weak measurements. *Physical Review Letters*, **96**(20), 200404.
- Schack, R., Brun, T.A. and Caves, C.M. (2001) Quantum Bayes rule. *Physical Review A*, **64**(1), 014305.
- Schrödinger, E. (1935) Die gegenwärtige situation in der Quantenmechanik. *Die Naturwissenschaften*, **23**(49), 823–828.
- Silberfarb, A., Jessen, P.S. and Deutsch, I.H. (2005) Quantum state reconstruction via continuous measurement. *Physical Review Letters*, **95**(3), 030402.
- Uffink, J. (2002) Quadratic Bell inequalities as tests for multipartite entanglement. *Physical Review Letters*, **88**(23), 230406.
- Vandersypen, L.M.K. and Chuang, I.L. (2004) NMR techniques for quantum control and computation. *Reviews of Modern Physics*, **76**(4), 1037–1069.
- Vidal, G. and Werner, R.F. (2002) Computable measure of entanglement. *Physical Review A*, **65**(3), 032314.
- Walls, D. and Milburn, G. (1994) *Quantum Optics*, Springer, Berlin.
- Wang, S.K., Jin, J.S. and Li, X.Q. (2007) Continuous weak measurement and feedback control of a solid-state charge qubit: a physical unraveling of non-Lindblad master equation. *Physical Review B*, **75**(15), 155304.
- Wiseman, H.M. (1994) Quantum theory of continuous feedback. *Physical Review A*, **49**(3), 2133–2150.
- Yang, T., Zhang, Q., Zhang, J. et al. (2005) All-versus-nothing violation of local realism by two-photon, four-dimensional entanglement. *Physical Review Letters*, **95**(24), 240406.
- Ye, H.A. (1991) *Consolidation and Fonctionnelle*, University of Science and Technology of China Press, Hefei.
- Yu, C.S. and Song, H.S. (2005) Separability criterion of tripartite qubit systems. *Physical Review A*, **72**(2), 022333.
- Yuen, H.P. (1986) Amplification of quantum states and noiseless photon amplifiers. *Physics Letters A*, **113**(8), 405–407.
- Zhang, Y.D. (2005) *Principles of Quantum Information Physics*, Science Press, Beijing.

12

State Preservation of Open Quantum Systems

12.1 Coherence Preservation in a Λ -Type Three-Level Atom

Decoherence is a serious obstacle to the preservation of quantum superposition and entanglement over long periods of time (Giulini *et al.*, 1996). Decoherence means non-unitary evolutions (Ai, Li, and Long, 2006; Niwa, Matsumoto, and Imai, 2002; Facchi *et al.*, 2005) and results in the loss of information and/or probability leakage toward the environment. This issue has attracted much attention and a number of interesting schemes have been proposed to preserve coherence. Among these schemes are quantum error-correction (QEC) codes (Shor, 1995; Cirac and Pellizzari, 1996; Knill and Laflamme, 1997; Laflamme *et al.*, 1996; Calderbank and Shor, 1996; Lidar, Bacon, and Whaley, 1999), error-avoiding codes (Ticozzi and Viola, 2008; Duan and Guo, 1998; Zanardi and Rasetti, 1997), decoherence-free subspaces (DFSs) (Lidar and Whaley, 2003; Lidar, Chuang, and Whaley, 1998; Bacon *et al.*, 2000; Lidar *et al.*, 2001; Kiffner, Evers, and Keitel, 2007; Cappellaro, Hodges, and Havel, 2006; Karasik *et al.*, 2008), bang-bang control (Viola, Knill, and Lloyd 1999; Hao, Huo, and Long, 2008; Du *et al.*, 2009; Tasaki *et al.*, 2004; Uhrig, 2008; Viola and Knill, 2005; Kern and Alber, 2005; Khodjasteh and Lidar, 2005; Khodjasteh and Lidar, 2007; Santos and Viola, 2006), and combinations thereof (Byrd, Wu, and Lidar, 2004). Error-avoiding codes encode information into the degenerate subspace of the error operators so that the information will not be affected by the error operators, while error-correcting codes restore the loss of information due to decoherence or quantum dissipation by monitoring the system and conditionally carrying on suitable feedback control. Their applications are limited by the requirement of using redundant qubit resources. Bang-bang control uses high-frequency pulses to average out the decoherence effect. However, it has the essential requirement that the bath retains some memory of its interaction with the system, so it is not useful for a system subject to Markovian decoherence. Lidar and Schneider (2005) therefore proposed a new method called tracking-control to solve the problem of stabilizing the coherence of a single qubit subject to Markovian decoherence. Recently, Zhang *et al.* (2010) proposed a feedback control strategy based on quantum weak measurements to protect the coherence of a qubit system in which the stochastic noise was considered. However, their work was restricted to a single-qubit system and they only

considered the unital-decoherence channel. In fact, three-level and higher dimension systems have attracted much interest for their applications in quantum control and quantum computation (Wang and Tan, 2003; Huang *et al.*, 2006) and so preserving the coherence of such a multilevel system has become a hot topic. However, non-unital decoherence channels are also frequently used, that is, spontaneous emission, and they exhibit completely distinct properties from the unital ones. Here we take the two points mentioned above into account and study the coherence preservation of higher dimension systems subject to the Markovian decoherence characterized by non-unital decoherence channels. As Lidar and Schneider pointed out in their open questions in 2005, the controllability could be improved if one expands the Hilbert space of the quantum system by including additional levels, which helps to maintain coherence. We consider a simple but typical problem: preserving the coherence between two levels of a Λ -type three-level atom subject to Markovian decoherence. This problem involves two issues: the feasibility of the coherence preservation of the multi-level system and the singularities issues encountered by Lidar and Schneider.

First we should demonstrate the feasibility of preserving the coherence of Markovian open quantum systems. To do this we choose the coherence between a ground state and the excited state as the control object, and apply a classical field to drive the states between these two. By imposing the constant coherence condition, the control parameters involving the initial phase and the field envelope are designed. It has been proved that such a control field does exist.

Second, the critical factor in our work is the singularity issue: the control field diverges after the breakdown time, namely, the coherence can be maintained only within the breakdown time. Although it is obtained analytically in the case of pure dephasing for a single qubit system in Lidar and Schneider, we find in our case that the analytical solution of breakdown time cannot be derived. Nonetheless, we qualitatively analyze the breakdown time and obtain the region in which the initial state maintains the coherence for a long time under the special conditions. At the same time it is proved by the numerical experiment that the coherence can be maintained longer when the initial state resides in this region than in other cases.

12.1.1 Models and Objectives

As is well known, the mathematical model of the Markovian open quantum system can be written as the following master equation:

$$\frac{\partial \rho}{\partial t} = -\frac{i}{\hbar} [H, \rho] + \mathcal{L}(\rho) \quad (12.1)$$

where the quantum state is represented by the density matrix ρ . The system Hamiltonian H is composed of H_0 and H_C , where H_0 and H_C refer to the free Hamiltonian and the control Hamiltonian, respectively. The Lie-bracket on the operator space is defined as $[A, B] = AB - BA$. The Lindbladian

$$\mathcal{L}(\rho) = \frac{1}{2} \sum_k \gamma_k \left\{ \left[L_k, \rho L_k^\dagger \right] + \left[L_k \rho, L_k^\dagger \right] \right\} \quad (12.2)$$

is induced by interactions between the system and the environment through different decoherence channels (represented by the system operator L_j with damping rate γ_j). Different decoherence channels exhibit distinct dynamics. For instance, the unital Lindblad generator, that is, $\mathcal{L}(I) = 0$, can make the purity function decrease regardless of the Hamiltonian

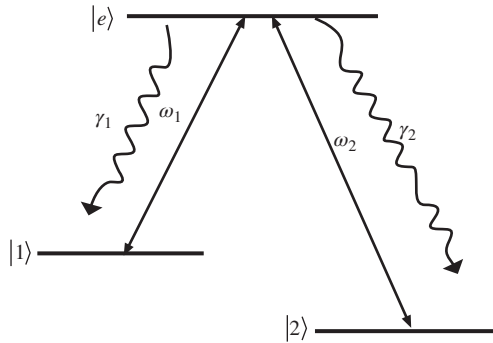


Figure 12.1 Atomic configurations: two ground states coupled to an excited state $|e\rangle$ with coupling constants ω_1 and ω_2

control existing. The situation is different for non-unital decoherence channels. These channels can increase the purity even without the action of the control. For example, under spontaneous emission an arbitrary qubit mixed state is gradually purified to the ground state. In this work, we consider only the non-unital Lindbladian over finite dimensional Hilbert space.

The system considered is the atom in the Λ -type shown in Figure 12.1, where two ground states, namely $|1\rangle$ and $|2\rangle$, are coupled to an excited state $|e\rangle$ with resonance frequencies ω_1 , and ω_2 , respectively. The corresponding eigenvalues are labeled E_1 , E_2 , and E_e , where $\omega_1 = (E_e - E_1) / \hbar$ and $\omega_2 = (E_e - E_2) / \hbar$. Similarly, we define $\omega_3 = (E_1 - E_2) / \hbar$ to be the resonant frequency between $|1\rangle$ and $|2\rangle$ for the atom and the laser field, although it does not correspond to an available transition here.

The following notations are defined as

$$\begin{aligned}\delta_z^{(j)} &= |e\rangle\langle e| - |j\rangle\langle j|, \delta_x^{(j)} = |e\rangle\langle j| + |j\rangle\langle e|, \delta_y^{(j)} = -i|e\rangle\langle j| + i|j\rangle\langle e| \\ \delta_-^{(j)} &= |j\rangle\langle e|, \delta_+^{(j)} = |e\rangle\langle j|, j = 1, 2\end{aligned}\quad (12.3)$$

The free Hamiltonian of such a system can then be written as

$$H_0 = \frac{\omega_1}{3} \delta_z^{(1)} + \frac{\omega_2}{3} \delta_z^{(2)} + \frac{\omega_3}{3} \delta_z^{(3)} \quad (12.4)$$

where $\delta_z^{(3)} = |1\rangle\langle 1| - |2\rangle\langle 2|$, and the constant energy term $(E_1 + E_2 + E_e) / 3$ has been ignored.

The excited state is not stable, it decays to the two ground states at rates γ_1 and γ_2 , respectively, as shown in Figure 12.1. Assuming the decay process is Markovian, then the decoherence channel can be characterized by the Lindblad operator $\delta_-^{(j)} = |j\rangle\langle e|$, $j = 1, 2$, and the Lindbladian can be expressed as

$$\mathcal{L}(\rho) = \frac{1}{2} \sum_{k=1,2} \gamma_k \left\{ \left[\delta_-^{(k)}, \rho \delta_+^{(k)} \right] + \left[\delta_-^{(k)} \rho, \delta_+^{(k)} \right] \right\} \quad (12.5)$$

One can verify $\mathcal{L}(I) \neq 0$, indicating the Lindbladian is non-unital.

Without loss of generality, we aim to preserve the coherence between the ground state $|1\rangle$ and the excited state $|e\rangle$, and the coherence function can be characterized by

$$C_1(\rho) = \sqrt{\left\langle \delta_x^{(1)} \right\rangle_{\rho}^2 + \left\langle \delta_y^{(1)} \right\rangle_{\rho}^2} \quad (12.6)$$

where $\langle A \rangle_{\rho} = \text{Tr}(A\rho)$. The loss of coherence between two levels $|1\rangle$ and $|e\rangle$ is due to the decay process from the higher level $|e\rangle$ to the lower level $|1\rangle$. One can apply a classical field to drive the states between $|1\rangle$ and $|e\rangle$, thus the decay process is likely to be inhibited.

We assume here that the transition dipole moments for the linearly polarized field are real. Then the control field, in the dipole approximation, can be expressed as (Scully and Zubairy, 1997)

$$E(t) = \varepsilon(t) \cos(\omega_d t + \phi_d)$$

The resulting expression for the control Hamiltonian is

$$H_C = \varepsilon(t) (e^{i\phi_d} |1\rangle\langle e| + \varepsilon(t) e^{-i\phi_d} |e\rangle\langle 1|) \cos \omega_d t \quad (12.7)$$

where the parameters ω_d and ϕ_d are the frequency and initial phase of the driving field and the parameter $\varepsilon(t)$ is the envelope of the field. They are the control parameters of the field to be designed. According to Equations 12.2, 12.4, 12.5, and 12.7, the decoherence equation under the action of control can be written as

$$\frac{\partial \rho}{\partial t} = -i [H_0 + H_C, \rho] + \frac{1}{2} \sum_{k=1,2} \gamma_k \left\{ [\delta_-^{(k)}, \rho \delta_+^{(k)}] + [\delta_-^{(k)} \rho, \delta_+^{(k)}] \right\} \quad (12.8)$$

Equation 12.8 is just the mathematic model of the control system. To make the coherence remain constant during the whole evolution, we impose the following constraint:

$$C_1(\rho(t)) = C_1(\rho_0) \quad (12.9)$$

The next thing is to design the control parameters to satisfy constraint in Equation 12.9.

12.1.2 Design of Control Field

In this subsection, we investigate the first issue mentioned above, that is, the design of a control field to preserve the coherence of a high-dimension system. One can see from Equation 12.8 that the drift Hamiltonian H_0 complicates the derivation of the control. For the sake of simplicity we are going to analyze the system dynamics in the interaction picture, where an operator X in Hilbert space is transformed into

$$X^I = e^{iH_0 t} X e^{-iH_0 t} \quad (12.10)$$

Then Equation 12.11 for $\rho^I(t)$ in the interaction picture can be obtained:

$$\frac{\partial \rho^I}{\partial t} = -i [H_C^I, \rho^I] + \frac{1}{2} \sum_k \gamma_k \left\{ [\delta_-^{(k)I}, \rho^I \delta_+^{(k)I}] + [\delta_-^{(k)I} \rho^I, \delta_+^{(k)I}] \right\} \quad (12.11)$$

and the coherence constraint Equation 12.9 turns to be

$$C_1(\rho^I(t)) = C_1(\rho_0) \quad (12.12)$$

The interaction transformation maps the system states into rotational coordinates, that is, the states are rotary. It can be verified that such a transformation does not change the population distribution of the system state and the expectation value of the operator.

In the interaction picture, the system Hamiltonian H turns out to be

$$H_C^I = e^{iH_0 t} H_C e^{-iH_0 t} = \varepsilon(t) e^{i\phi_d} |1\rangle\langle e| + \varepsilon(t) e^{-i\phi_d} |e\rangle\langle 1| = \varepsilon(t) (\cos \phi_d \delta_x^{(1)} + \sin \phi_d \delta_y^{(1)}) \quad (12.13)$$

where we assume the resonance condition, that is, $\omega_d = \omega_1$. Furthermore, one can derive that

$$\delta_-^{(1)I} = e^{-i\omega_1 t} \delta_-^{(1)}, \delta_-^{(2)I} = e^{-i\omega_2 t} \delta_-^{(2)} \quad (12.14)$$

Thus, substituting Equation 12.14 into Equation 12.11 gives

$$\frac{\partial \rho^I}{\partial t} = -i [H_C^I, \rho^I] + \frac{1}{2} \sum_{k=1,2} \gamma_k \left\{ \left[\delta_-^{(k)}, \rho^I \delta_+^{(k)} \right] + \left[\delta_-^{(k)} \rho^I, \delta_+^{(k)} \right] \right\} \quad (12.15)$$

which is just the models of the controlled system dynamics under the Markovian decoherence in the interaction picture. The transformation of the interaction picture is used to facilitate the mathematical treatment of the problem. The system after the transformation becomes more concise: the drift item H_0 disappears and consequently the difficulty and complexity of the control design are greatly reduced.

We now design the parameters ϕ_d and $\varepsilon(t)$ of the control field to satisfy the coherence constraint in Equation 12.12. We start by deriving the equations of motion of $\langle \delta_x^{(1)} \rangle_{\rho^I}$ and $\langle \delta_y^{(1)} \rangle_{\rho^I}$. According to Equation 12.15 one has

$$\begin{aligned} \frac{d\langle \delta_y^{(1)} \rangle_{\rho^I}}{dt} &= \text{Tr}(\delta_y^{(1)} \dot{\rho}^I) = \text{Tr}(\delta_y^{(1)} (-i[H_C^I, \rho^I] + \mathcal{L}(\rho))) = -i\text{Tr}([\delta_y^{(1)}, H_C^I] \rho^I) + \sum \text{Tr}(\delta_y^{(1)} \mathcal{L}(\rho)) \\ &= -i\varepsilon(t) \cos \phi_d \text{Tr}([\delta_y^{(1)}, \delta_x^{(1)}] \rho^I) + \frac{1}{2} \sum_{k=1,2} \gamma_k \left(\text{Tr}([\delta_y^{(1)}, \delta_-^{(k)}] \rho^I \delta_+^{(k)}) + \text{Tr}(\delta_-^{(k)} \rho^I [\delta_+^{(k)}, \delta_y^{(1)}]) \right) \\ &= -2\varepsilon(t) \cos \phi_d \langle \delta_z^{(1)} \rangle_{\rho^I} - \frac{\gamma_1 + \gamma_2}{2} \langle \delta_y^{(1)} \rangle_{\rho^I} \end{aligned} \quad (12.16)$$

Likewise, the motion of equation for $\langle \delta_x^{(1)} \rangle_{\rho^I}$ can be obtained:

$$\frac{d\langle \delta_x^{(1)} \rangle_{\rho^I}}{dt} = \text{Tr}(\delta_x^{(1)} \dot{\rho}^I) = 2\varepsilon(t) \sin \phi_d \langle \delta_z^{(1)} \rangle_{\rho^I} - \frac{\gamma_1 + \gamma_2}{2} \langle \delta_x^{(1)} \rangle_{\rho^I} \quad (12.17)$$

Obviously, by setting the phase ϕ_d and the amplitude $\varepsilon(t)$ as the following form:

$$\varepsilon(t) = \frac{(\gamma_1 + \gamma_2) C_1(\rho_0)}{4\langle \delta_z^{(1)} \rangle_{\rho^I}} \quad (12.18)$$

$$\phi_d = \begin{cases} \arctan \left(-\langle \delta_x^{(1)} \rangle_{\rho_0} / \langle \delta_y^{(1)} \rangle_{\rho_0} \right), & \langle \delta_y^{(1)} \rangle_{\rho_0} < 0 \\ \pi/2, & \langle \delta_y^{(1)} \rangle_{\rho_0} = 0 \\ \pi + \arctan \left(-\langle \delta_x^{(1)} \rangle_{\rho_0} / \langle \delta_y^{(1)} \rangle_{\rho_0} \right), & \langle \delta_y^{(1)} \rangle_{\rho_0} > 0 \end{cases} \quad (12.19)$$

we have $d\langle \delta_y^{(1)} \rangle_{\rho^I} / dt \equiv 0$ and $d\langle \delta_x^{(1)} \rangle_{\rho^I} / dt \equiv 0$, which means that $\langle \delta_x^{(1)} \rangle_{\rho^I} = \langle \delta_x^{(1)} \rangle_{\rho_0}$ and $\langle \delta_y^{(1)} \rangle_{\rho^I} = \langle \delta_y^{(1)} \rangle_{\rho_0}$, which naturally lead to $C_1(\rho^I(t)) = C_1(\rho_0)$, that is, the coherence between $|1\rangle$ and $|e\rangle$ is preserved under the control field given by Equation 12.7 with parameters ϕ_d and $\epsilon(t)$ specified by Equations 12.18 and 12.19.

The purity and coherence are both important qualities of quantum dynamics. The former reflects the entire unitary dynamics and the latter reflects the partial quantum dynamics. The purity in general comprises the coherence and other variables which relate to diagonal elements of density matrix. In the uncontrolled dynamics, the coherence keeps decreasing under the decoherence effect until it vanishes. In the controlled scenario, the control fields trade changing the variation trend of other variables in purity for fixing the coherence. In general, the purity for N -dimension quantum systems can be defined as $p = \frac{\text{Ntr}(\rho^2) - 1}{N-1}$. From this definition, the purity of the pure state and the maximum mixed state I_N/N are 1 and 0, respectively. In our case, the purity can be computed as

$$p = \frac{3}{2} \text{tr}(\rho^{I2}) - \frac{1}{2} = \frac{3}{2} \sum_{i,k=1,2,e} |\rho_{ik}^I|^2 - \frac{1}{2} = \frac{3}{4} \sum_{j=1,2,3} \left(\langle \delta_x^{(j)} \rangle_{\rho^I}^2 + \langle \delta_y^{(j)} \rangle_{\rho^I}^2 \right) + \frac{1}{2} \sum_{j=1,2,3} \langle \delta_z^{(j)} \rangle_{\rho^I}^2 \quad (12.20)$$

where $\delta_x^{(3)} = |1\rangle\langle 2| + |2\rangle\langle 1|$ and $\delta_y^{(3)} = -i|1\rangle\langle 2| + i|2\rangle\langle 1|$.

Equations 12.6 and 12.20 can be expressed as

$$p = \frac{3}{4} C_1^2 + \frac{3}{4} \sum_{j=2,3} \left(\langle \delta_x^{(j)} \rangle_{\rho^I}^2 + \langle \delta_y^{(j)} \rangle_{\rho^I}^2 \right) + \frac{1}{2} \sum_{j=1,2,3} \langle \delta_z^{(j)} \rangle_{\rho^I}^2 \quad (12.21)$$

Thus, the purity relates to not only the coherence function concerned, but also the coherence between $|2\rangle$ and $|e\rangle$ as well as the coherence between $|1\rangle$ and $|2\rangle$, and the population distribution. In the two-level system subject to the dephasing decoherence, the control fields trade decrease in purity in return for stabilization of coherence until the purity is equal to the coherence ($c = C_1^2$) (Lidar and Schneider, 2005). However, the trade-off for the three-level system becomes impossible as soon as $\langle \delta_z^{(1)} \rangle = 0$ at some time t_b . One can see from Equation 12.21 that the purity could be larger than the coherence at time t_b , namely, there is remaining “purity” not traded for the stabilization of coherence. Thus the time one can preserve the coherence in a high-dimension system is shorter than in a lower-dimension system under the same initial conditions if only the unital decoherence channels are considered. The situation is different for non-unital decoherence. Because the purity increases, the variation of $\langle \delta_z^{(1)} \rangle$ is not determined, so the time when the trade-off becomes impossible is not determined. We must therefore analyze the time of $\langle \delta_z^{(1)} \rangle = 0$, which is just the second issue mentioned above. We will work out the singularities of the control field in the next section.

12.1.3 Analysis of Singularities Issues

We will study the singularities of the control field, that is, the control field diverges as soon as $\langle \delta_z^{(1)} \rangle_{\rho^I}$ turns to zero. The breakdown time t_M , that is, the time of the control field diverges, represents how long one can maintain the coherence, and we analyze the breakdown time in this subsection.

First, derive the equation of motion for $\langle \delta_z^{(1)} \rangle_{\rho^I}$. According to Equation 12.15, one has

$$\frac{d\langle \delta_z^{(1)} \rangle_{\rho^I}}{dt} = \frac{-(\gamma_1 + \gamma_2) C_1^2(\rho_0)}{2\langle \delta_z^{(1)} \rangle_{\rho^I}} - (2\gamma_1 + \gamma_2) \rho_{ee}^I \quad (12.22)$$

where $\rho_{ee}^I = \langle e | \rho^I | e \rangle$. Due to the variation of $\langle \delta_z^{(1)} \rangle_{\rho^I}$ depending on ρ_{ee}^I , one needs to derive the equation of motion for ρ_{ee}^I . Similarly, one has

$$\frac{d\rho_{ee}^I}{dt} = \langle e | \dot{\rho}^I | e \rangle = \frac{-(\gamma_1 + \gamma_2) C_1^2(\rho_0)}{4\langle \delta_z^{(1)} \rangle_{\rho^I}} - (\gamma_1 + \gamma_2) \rho_{ee}^I \quad (12.23)$$

Obviously, Equations 12.22 and 12.23 are not analytically solvable, so the analytical solution of the breakdown time cannot be derived. Nonetheless, it is evident that the breakdown time is concerned with some parameters, for example $C_1(\rho_0)$, $\langle \delta_z^{(1)} \rangle_{\rho_0}$, and $\rho_{0,ee}$. It is important to ascertain how these parameters affect the breakdown time as this motivates us to make qualitative analysis for it.

In fact, there is no need to discuss the case of $\langle \delta_z^{(1)} \rangle_{\rho_0} \geq 0$ because in this case one can directly see from Equations 12.22 and 12.23 that the breakdown time is inversely proportional to $C_1^2(\rho_0)$ and $\rho_{0,ee}$, and proportional to $\langle \delta_z^{(1)} \rangle_{\rho_0}$.

Thus, in what follows we assume $\langle \delta_z^{(1)} \rangle_{\rho_0} < 0$. We analyze the motion of $\langle \delta_z^{(1)} \rangle_{\rho^I}$ based on the $\langle \delta_z^{(1)} \rangle_{\rho^I} - \rho_{ee}^I$ phase plane. From Equations 12.22 and 12.23 it is evident that $d\langle \delta_z^{(1)} \rangle_{\rho^I}/d\rho_{ee}^I \approx 2$ holds if the decay rates satisfy $\gamma_2/\gamma_1 \ll 1$. In such a case, there exist many pairs of real numbers (c_1, c_2) such that $\langle \delta_z^{(1)} \rangle_{\rho^I} = c_1$, $\rho_{ee}^I = c_2$, and $4c_1c_2 = -C_1^2(\rho_0)$, leading to $d\langle \delta_z^{(1)} \rangle_{\rho^I} = d\rho_{ee}^I = 0$, thus $\langle \delta_z^{(1)} \rangle_{\rho^I}$ is kept as c_1 . In fact, such pairs of real numbers form the curve $4\langle \delta_z^{(1)} \rangle_{\rho^I} \rho_{ee}^I = -C_1^2(\rho_0)$ in the $\langle \delta_z^{(1)} \rangle_{\rho^I} - \rho_{ee}^I$ phase plane. Therefore for some initial states, the control field makes $\langle \delta_z^{(1)} \rangle_{\rho^I}$ vary to and remain at the same points on the curve, and these initial states form the region S_0 . In other words, one can preserve the coherence almost forever if the initial states of the system reside in S_0 in the case of $\gamma_2/\gamma_1 \ll 1$. In the other cases, for any initial state, there exists a time t_M such that $\langle \delta_z^{(1)}(t_M) \rangle_{\rho^I} = 0$ and t_M is just the breakdown time. The problem is therefore divided into two parts: one is to seek S_0 and the other to analyze how different parameters influence the breakdown time t_M .

In the first case of $\gamma_2/\gamma_1 \ll 1$, by analyzing the $\left\langle \delta_z^{(1)} \right\rangle_{\rho^I} - \rho_{ee}^I$ phase plane one can see that the variable $\left\langle \delta_z^{(1)}(t) \right\rangle_{\rho^I}$ is constant for $\forall t > t_b$ if $\left\langle \delta_z^{(1)}(t_b) \right\rangle_{\rho^I} = -C_1^2(\rho_0) / [4(1-\tau)\rho_{ee}^I(t_b)]$, in which $\tau = \gamma_2 / (\gamma_1 + \gamma_2) \ll 1$. Considering the natural condition $\rho_{11}^I(t) + \rho_{ee}^I(t) \leq 1$, that is, $\left\langle \delta_z^{(1)}(t) \right\rangle_{\rho^I} \geq 2\rho_{ee}^I(t) - 1$, the region S_0 is given by

$$S_0 = \left\{ \rho_0 : C_1^2(\rho_0) \leq \frac{1-\tau}{2}, -1 \leq \left\langle \delta_z^{(1)} \right\rangle_{\rho_0} - 2\rho_{0,ee} \leq \frac{-2C_1(\rho_0)}{\sqrt{1-\tau}}, C_1^2(\rho_0) + 4(1-\tau)\left\langle \delta_z^{(1)} \right\rangle_{\rho_0}\rho_{0,ee} \leq 0, \rho_{0,ee} \geq 0 \right\} \quad (12.24)$$

We can conclude that if the initial states of the system reside in S_0 and the decay rates satisfy $\gamma_2/\gamma_1 \ll 1$, the coherence can be maintained for a long time. In this case, due to the weak coupling between $|2\rangle$ and $|e\rangle$, the quantum system is nearly equivalent to a two-level system. In such a system, the coherence can be preserved almost forever if the initial state resides in S_0 . By contrast, the coherence can be preserved within the breakdown time in Lidar and Schneider. This obvious difference comes from the fact that the mathematic model of our system has a non-unital Lindblad operator $\delta_- = |1\rangle\langle e|$ that describes the relaxation effect, while the decoherence-channel in Lidar and Schneider is a pure dephasing channel described by the unital Lindblad operator δ_z . This difference will be verified by the first numerical experiment in next subsection.

In fact, the reduced two-level system can be represented by Bloch sphere, and the trade-off between the coherence and purity can be interpreted geometrically. The uncontrolled relaxation channel makes any point in the Bloch sphere flow toward the stable point at the North Pole (Nielsen and Chuang, 2010). This process can be represented by the transformation of the Block vector, that is

$$(v_x, v_y, v_z) \rightarrow \left(v_x \sqrt{1-\Gamma}, v_y \sqrt{1-\Gamma}, v_z(1-\Gamma) + \Gamma \right) \quad (12.25)$$

where Γ is a time-dependent function that converges to 1. Equation 12.25 indicates that the $x-y$ plane is contracted, and at the same time the z component v_z moves toward the north pole. In the controlled scenario, the components of the $x-y$ plane (coherence) are invariant, and the z component moves to the south pole. The control field is thus able to trade the contraction in the $x-y$ plane for the motion of the z component to the south pole. For all the initial states in the northern hemisphere, therefore, v_z turns to zero, whereas for some initial state in the southern hemisphere, for example the states in S_0 , v_z does not reach zero almost forever. For the two-level system subject to dephasing decoherence, the trade-off between the coherence and purity has distinct geometric interpretation (Lidar and Schneider, 2005). The uncontrolled phase-flip channel maps the Bloch sphere to an ellipsoid with the z -axis as the major axis and the minor axis in the $x-y$ plane. The major axis is invariant under the uncontrolled dynamics, while the minor axis is contracted. The control field attempts to rotate the ellipsoid so that the minor axis becomes as aligned as possible with the z -axis, where it would experience no contraction. The fields diverge as long as the contraction is so strong that the control field is no longer capable of sustaining the required rotation. In this case, the two initial states symmetric about the $x-y$ plane have the same breakdown time.

For the other case, the atom is a real three-level system, and the analytical solution of t_M cannot be obtained as well. Similarly, we qualitatively analyze the motion of $\langle \delta_z^{(1)} \rangle_{\rho^I}$ in the $\langle \delta_z^{(1)} \rangle_{\rho^I} - \rho_{ee}^I$ phase plane. Now the special region in the $\langle \delta_z^{(1)} \rangle_{\rho^I} - \rho_{ee}^I$ phase plane is defined as

$$S = \left\{ \rho^I : C_1^2(\rho^I) \leq \frac{1-\tau}{2}, -1 \leq \langle \delta_z^{(1)} \rangle_{\rho^I} - 2\rho_{ee}^I \leq \frac{-2C_1(\rho^I)}{\sqrt{1-\tau}}, C_1^2(\rho^I) + 4(1-\tau)\langle \delta_z^{(1)} \rangle_{\rho^I} \rho_{ee}^I \leq 0, \rho_{ee}^I \geq 0 \right\} \quad (12.26)$$

Note that if the initial state resides in S_0 , the state of the system first evolves in the region S , then leaves it, and ultimately reaches the point that makes $\langle \delta_z^{(1)}(t) \rangle_{\rho^I}$ be zero.

It inspires us to make a conjecture that the breakdown time is longer for the case of the initial state residing in S_0 than that for other cases. In addition, the breakdown time is proportional to the distance between the initial state and S_0 .

This conjecture cannot be demonstrated theoretically and rigorously, but we can verify it by numerical experiments. Obviously, one can see from Equation 12.24 that the shape of S_0 relies on some parameters such as $C_1(\rho_0)$, τ , $\langle \delta_z^{(1)} \rangle_{\rho_0}$, and $\rho_{0,ee}$. Thus the breakdown time t_M is concerned with these parameters. We will take $C_1(\rho_0)$ and τ for examples to verify the conjecture by the second simulation example in the next section.

12.1.4 Numerical Simulations

To demonstrate the effectiveness of the strategy proposed in this subsection, we will implement some numerical examples with different parameters and give some analysis. The propagation of the dynamical equation in Equation 12.13 is carried out by fourth-order Runge–Kutta integration.

The first simulation example is to verify that the control field can preserve the coherence of the system for a long time, provided that the initial states reside in S_0 and $\tau \ll 1$. Therefore the decay rates can be chosen as $\gamma_1 = 0.1$, $\gamma_2 = 0.001$ such that $\tau \ll 1$ and the initial state is assumed to be

$$\rho_0 = \begin{pmatrix} 0.21 & 0.195 - 0.195i & 0 \\ 0.195 + 0.195i & 0.78 & 0 \\ 0 & 0 & 0.01 \end{pmatrix}$$

which resides in S_0 . The parameters of control field are designed according to Equations 12.18 and 12.19. The dynamical equations are solved over the total propagation time intervals of $T = 500$ with a time step of 0.01.

The evolution of coherence function $C_1(\rho^I)$ is displayed in Figure 12.2, from which one can see that the coherence between the ground state $|1\rangle$ and the excited state $|e\rangle$ is completely and quickly lost in the absence of control, while one can keep the coherence constant almost forever under the action of the control field with the designed control parameters (Equations 12.18 and 12.19).

In fact, the initial state indicates that the initial populations distribute mainly on levels $|e\rangle$ and $|1\rangle$, and the relaxation rate γ_2 is much smaller compared with γ_1 , so the three-level system

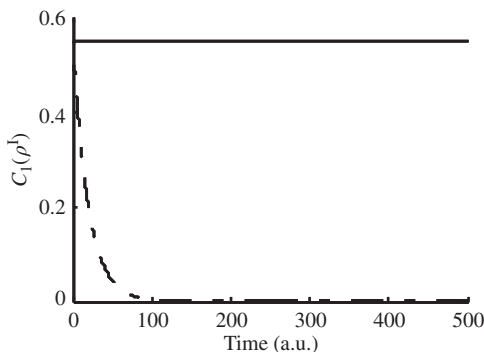


Figure 12.2 Evolution of coherence function $C_1(\rho^I)$. The solid line corresponds to the trajectories under the action of control and the dashed lines correspond to the uncontrolled trajectories with decoherence

can be regarded as a two-level one. Furthermore, the initial state also indicates that the purity is $p = 0.8047$ and the initial coherence is $C_1(\rho_0) = 0.55$ (according to the definition of the coherence c in Lidar and Schneider, $c = C_1^2$ holds for the two-level system, so the coherence is $c = 0.3$). Then we can deem that all the parameters in this simulation are the same as those in Lidar and Schneider, except the decoherence channels. The simulation results are different: the coherence in Lidar and Schneider can only be maintained within 8 a.u., which is very short compared to the case of the non-unital channel in our case.

The second simulation example is to analyze how the different parameters influence the breakdown time t_M . Here the parameters $C_1(\rho_0)$ and τ are considered separately.

First, we study the influence of the parameter $C_1(\rho_0)$. The other parameters are fixed as $\tau = \frac{\gamma_2}{\gamma_1 + \gamma_2} = \frac{0.1}{0.1+0.1} = 0.5$ and $\langle \delta_z^{(1)} \rangle_{\rho_0} = -0.5$. $C_1(\rho_0)$ is equal to 0.5, 0.6, and 0.7, respectively, and the corresponding initial states are $\rho_{0,1}$, $\rho_{0,2}$, and $\rho_{0,3}$, respectively, where

$$\rho_{0,1} = \begin{pmatrix} 0.2 & 0.25 & 0 \\ 0.25 & 0.7 & 0 \\ 0 & 0 & 0.1 \end{pmatrix}, \rho_{0,2} = \begin{pmatrix} 0.2 & 0.3 & 0 \\ 0.3 & 0.7 & 0 \\ 0 & 0 & 0.1 \end{pmatrix}, \rho_{0,3} = \begin{pmatrix} 0.2 & 0.35 & 0 \\ 0.35 & 0.7 & 0 \\ 0 & 0 & 0.1 \end{pmatrix}$$

Obviously, the three initial states do not reside in S_0 , in addition $\rho_{0,1}$ is nearest to S_0 , and $\rho_{0,2}$ is nearer to S_0 than $\rho_{0,3}$ in the $\langle \delta_z^{(1)} \rangle_{\rho^I} - \rho_{ee}^I$ phase plane. The simulation results are shown in Figure 12.3, from which one can see that the breakdown time is inversely proportional to the desired constant initial coherence value. This indicates that the nearer the initial state is to S_0 , the longer the breakdown time is.

Second, to study the parameter τ , the other parameters are fixed as $C_1(\rho_0) = 0.4$ and $\langle \delta_z^{(1)} \rangle_{\rho_0} = -0.5$. The initial state is assumed to be

$$\rho_0 = \begin{pmatrix} 0.2 & 0.3 & 0 \\ 0.3 & 0.7 & 0 \\ 0 & 0 & 0.1 \end{pmatrix}$$

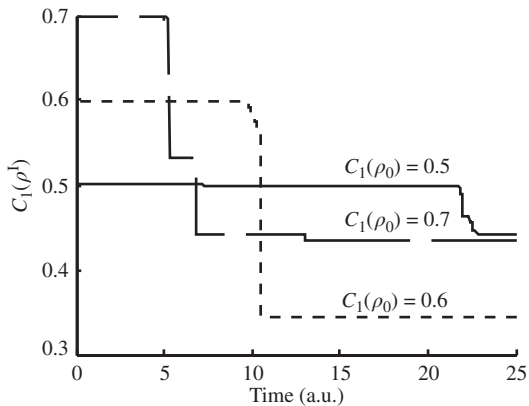


Figure 12.3 Coherence function $C_1(\rho^I)$ for different $C_1(\rho_0)$. The solid line, the dotted line, and the dashed line correspond to $C_1(\rho_0) = 0.5, 0.6$, and 0.7 respectively

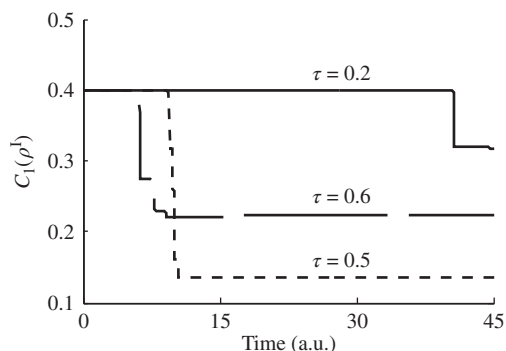


Figure 12.4 Coherence function $C_1(\rho^I)$ for different τ . The solid line, the dotted line, and the dashed line correspond to $\tau = 0.2, 0.5$, and 0.6 respectively

One can see from Equation 12.24 that different τ values determine whether the initial state resides in S_0 , and the initial state becomes closer to S_0 as τ increases. Let τ be equal to 0.2, 0.5, and 0.6, respectively. The simulation results are displayed in Figure 12.4, from which one can see that the breakdown time becomes longer as τ increases. In other words, the closer the initial state is to S_0 , the longer the breakdown time is.

12.2 Purity Preservation of Quantum Systems by a Resonant Field

At present, quantum decoherence control is still an unsolved problem for open quantum systems. A common way to describe an open quantum system is by a Markov master equation, in which the environmental information is eliminated. However, this also ignores the influences of control fields on the interactions between the system and environment, which may play a

positive role in coherence inhibiting so the influences of the control fields on the interaction should be considered. To describe the state evolution precisely, accurate information on the environment is needed, which is of course not usually available, so some generalized conditions for control fields should be used to instruct the designing of the control fields that can inhibit the decoherence effect.

The issue of inhibiting the decoherence effect ties up with the preservation of state purity in some situations, for example phase decoherence. In fact, the coherence of a state can be regarded as a projection of the state purity to some subspace from the point of view of algebraic geometry. For a spin-1/2 particle, its state coherence is the projection of its purity denoted by the Bloch vector to the x - y plane in the Bloch sphere. In this section purity evolution is therefore studied for a system interacting with the environment. The interaction should be non-Markovian if the purity can be controlled. A simple situation is that both the particles and the environment have a few degrees of freedom so the environment could be included and composes a closed system with the particles together. This is true in some cases of quantum information and the computation process, in which the concerned particles of a closed system are regarded as the controlled system and the others as the environment. For simplification a closed complex quantum system involving two interacting particles is discussed in this section, in which one particle is regarded as the controlled system and interacts with the other acting as the environment. We study the decoupling effect of the external control field to get some instructions in principle when designing control fields in quantum system manipulations. As will be shown in our work, control fields should be large enough and resonant with the controlled particle to effectively preserve the state purity, otherwise the purity reduction may be accelerated.

12.2.1 Problem Description

In order to simplify the discussion, two spin-1/2 quantum particles with Ising interaction are considered, where which particle 1 is regarded as the controlled system and the other as its environment. The two particles therefore comprise a closed quantum system with Hamiltonian:

$$H = H_0 + H_c \\ = -\frac{\hbar}{2} (\omega_1 \sigma^z \otimes I + \omega_2 I \otimes \sigma^z + J \sigma^z \otimes \sigma^z + \Omega_1 (e^{i\omega t} |0\rangle\langle 1| + e^{-i\omega t} |1\rangle\langle 0|) \otimes I) \quad (12.27)$$

where J is the interaction intensity between two particles, ω_j is the eigenfrequency of particle j , Ω_1 is the Rabi frequency of particle 1 and it is related to the intensity of the control field, ω is the frequency of the control field, and σ^z is the Pauli matrix σ_3 , which denotes rotation of the Bloch vector around the z -axis.

The density matrix of the closed system is $\rho = |\phi\rangle\langle\phi|$, in which $|\phi\rangle$ is denoted by

$$|\phi\rangle = a_1(t)|00\rangle + a_2(t)|01\rangle + a_3(t)|10\rangle + a_4(t)|11\rangle \quad (12.28)$$

For such two interaction particles, the density matrix can also be expressed as the form of coherent vector (Altafini, 2004):

$$\rho = \sum_{j=0}^{15} Tr(4\rho X_j) X_j = \sum_{j=0}^{15} x_j X_j \quad (12.29)$$

where x_j are components of the coherent vector and X_j are the generators of the unitary group. These are defined as follows:

$$X_j = \frac{1}{4} \left\{ I \otimes I, \sigma_x \otimes I, \sigma_y \otimes I, \sigma_z \otimes I, I \otimes \sigma_x, I \otimes \sigma_y, I \otimes \sigma_z, \sigma_x \otimes \sigma_x, \sigma_x \otimes \sigma_y, \sigma_x \otimes \sigma_z, \sigma_y \otimes \sigma_x, \sigma_y \otimes \sigma_y, \sigma_y \otimes \sigma_z, \sigma_z \otimes \sigma_x, \sigma_z \otimes \sigma_y, \sigma_z \otimes \sigma_z \right\} \quad (12.30)$$

Therefore x_j can be expressed by the elements of ρ , for example:

$$\begin{cases} x_1 = \rho_{31} + \rho_{42} + \rho_{13} + \rho_{24} \\ x_2 = (\rho_{31} + \rho_{42} - \rho_{13} - \rho_{24}) / i \\ x_3 = \rho_{11} + \rho_{22} - \rho_{33} - \rho_{44} \end{cases} \quad (12.31)$$

In fact, $x_{i=1,2,3}$ are the components corresponding to the three axes in the Bloch sphere, which compose the Bloch vector. The Bloch vector is zero when the state is maximum mixed and its module is 1 when the state is pure. The states purity of the controlled particle p_1 can therefore be defined by the module of the Bloch vector:

$$p_1 = \sqrt{x_1^2 + x_2^2 + x_3^2} \quad (12.32)$$

This definition is directly proportional to the usual form of purity $tr(\rho^2)$, in fact $p_1 = 2tr(\rho^2) - 1$ so the two definitions of purity are equivalent, and the form in Equation 12.32 is chosen in this section for convenience.

Our goal is to decouple the two particles by an external control field so that the controlled particle will be maintained in almost pure states, viz. to preserve purity p_1 at its maximum value, and to find out how the parameters such as the initial states of the particles, frequency, and intensity of the control field affect the decoupling process. For convenience, the initial state of the closed system is assumed to be separable, viz. it can be written as a tensor product of the two particles' states.

12.2.2 Purity Property Preservation

At first we consider the purity evolution without the external control field. In such a case, the purity of the two particles will change due to their interactions, and their dynamics are dependent on the two initial states of the particles. To begin a detailed analysis, an accurate expression of purity evolution for particle 1 is given:

$$p_1^2(t) = x_3^2(0) + (x_1^2(0) + x_2^2(0)) (\cos^2 Jt + x_6^2(0) \sin^2 Jt) \quad (12.33)$$

in which x_3 denotes a component along rotation axis z that is invariant through the whole process of evolution. $\sqrt{x_1^2 + x_2^2}$ is a component in the $x-y$ plane, which is changed by the factor $\sqrt{\cos^2 Jt + x_6^2(0) \sin^2 Jt}$. This means that the larger the $x-y$ component is, the more fiercely the purity fluctuates. For example, the purity motion equation of the controlled particle is $p_1(t) = |\cos(Jt)|$ when the initial state of the closed system is $\rho(0) = (|00\rangle + |01\rangle + |10\rangle + |11\rangle)(\langle 00| + \langle 01| + \langle 10| + \langle 11|)/4$, and it becomes $p_1(t) = 1$ when the initial state is $\rho(0) = |00\rangle\langle 00|$. It is also noted that only the $x-y$ component of

the state is affected by the interaction and it should be reduced to weaken the effect of the interaction.

Now consider the effect of the external control field. In order to get the analytic solution we consider the problem in the interaction picture, that is, we change the density matrix ρ into $\rho = e^{-iH_0 t/\hbar} \tilde{\rho} e^{iH_0 t/\hbar}$. Thus the system Hamiltonian becomes Equation 12.34, in which $\Delta = \omega - \omega_1$ is the detuning between the controlled particle and the control field:

$$\tilde{H}(t) = -\frac{\hbar}{2} \begin{pmatrix} 0 & 0 & \Omega_1 e^{i(\Delta-J)t} & 0 \\ 0 & 0 & 0 & \Omega_1 e^{i(\Delta+J)t} \\ \Omega_1 e^{-i(\Delta-J)t} & 0 & 0 & 0 \\ 0 & \Omega_1 e^{-i(\Delta+J)t} & 0 & 0 \end{pmatrix} \quad (12.34)$$

$$\begin{cases} \tilde{a}_1(t) = (\tilde{a}_1(0) - c_1) e^{i(\sqrt{\Omega_1^2 + (\Delta-J)^2} + (\Delta-J))t/2} + c_1 e^{-i(\sqrt{\Omega_1^2 + (\Delta-J)^2} - (\Delta-J))t/2} \\ \tilde{a}_2(t) = (\tilde{a}_4(0) - c_2) \frac{\sqrt{\Omega_1^2 + (\Delta+J)^2} - (\Delta+J)}{\Omega_1} e^{i(\sqrt{\Omega_1^2 + (\Delta+J)^2} + (\Delta+J))t/2} - c_2 \frac{\sqrt{\Omega_1^2 + (\Delta+J)^2} + (\Delta+J)}{\Omega_1} e^{-i(\sqrt{\Omega_1^2 + J^2} - (\Delta+J))t/2} \\ \tilde{a}_3(t) = (\tilde{a}_1(0) - c_1) \frac{\sqrt{\Omega_1^2 + (\Delta-J)^2} + (\Delta-J)}{\Omega_1} e^{i(\sqrt{\Omega_1^2 + (\Delta-J)^2} - (\Delta-J))t/2} - c_1 \frac{\sqrt{\Omega_1^2 + (\Delta-J)^2} - (\Delta-J)}{\Omega_1} e^{-i(\sqrt{\Omega_1^2 + (\Delta-J)^2} + (\Delta-J))t/2} \\ \tilde{a}_4(t) = (\tilde{a}_4(0) - c_2) e^{i(\sqrt{\Omega_1^2 + (\Delta+J)^2} - (\Delta+J))t/2} + c_2 e^{-i(\sqrt{\Omega_1^2 + (\Delta+J)^2} + (\Delta+J))t/2} \end{cases} \quad (12.35a)$$

Solving the Schrödinger equation in the interaction picture gives Equation 12.35a, in which

$$\begin{cases} c_1 = \frac{\tilde{a}_1(0) \sqrt{\Omega_1^2 + (\Delta-J)^2} + \tilde{a}_1(0)(\Delta-J) - \tilde{a}_3(0)\Omega_1}{2\sqrt{\Omega_1^2 + (\Delta-J)^2}} \\ c_2 = \frac{\tilde{a}_4(0) \sqrt{\Omega_1^2 + (\Delta+J)^2} - \tilde{a}_4(0)(\Delta+J) - \tilde{a}_2(0)\Omega_1}{2\sqrt{\Omega_1^2 + (\Delta+J)^2}} \end{cases} \quad (12.35b)$$

Then purity p_1 can be calculated according to Equations 12.31, 12.32, 12.35a, and 12.35b, but the generalized expression is too expatiatory to be presented here. Notice that the transform $\rho = e^{-iH_0 t/\hbar} \tilde{\rho} e^{iH_0 t/\hbar}$ would change the value of p_1 , so we should make an inverse transform before calculating.

The effect of detuning is investigated through numerical simulation. Figure 12.5 shows the minimum purity curves on detuning with the initial state $\rho(0) = (|00\rangle + |01\rangle + |10\rangle + |11\rangle) \langle (00| + \langle 01| + \langle 10| + \langle 11|)/4$ and the parameters $\Omega_1 = 10$ and $J = 1$, in which the y-axis denotes the minimum value of the purity during the system evolution. In Figure 12.5a the minimum purity achieves its peak value 0.98 when the detuning is zero, and in Figure 12.5b it is not zero only when the detuning tends to zero. From Figure 12.5 one can see that only when the detuning tends to zero, viz. the control field is resonant with the controlled particle, do the two particles become decoupled. Otherwise, although the purity of the controlled particle could be preserved to a certain extent, the purity of the other particle still has a minimum value close to zero.

The phenomenon that the two particles become decoupled only when the detuning tends to zero could be understood as follows. Because the Ising interaction denotes interaction of rotation around the z -axis, when there is no control field, only the component in the $x-y$ plane has a rotation with an angular speed ω_1 around the z -axis, so it varies during the state evolution, while the component along the z -axis is invariant. Now we consider the problem in rotary coordinates at angular speed ω_1 . The existence of the control field adds another rotation axis \vec{r} that is rotating around the z -axis in the $x-y$ plane with angular speed Δ . If detuning

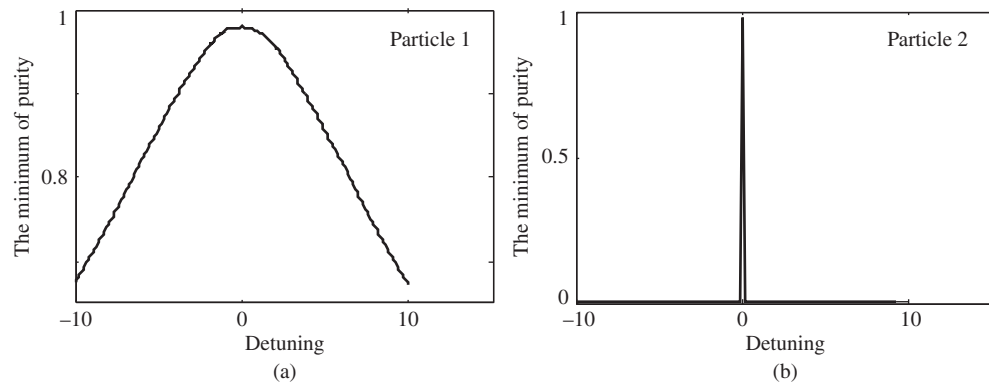


Figure 12.5 Minimum purity curves of two particles upon detuning: (a) the minimum purity curve of particle 1 and (b) the minimum purity curve of particle 2

$\Delta = 0$, viz. the rotation of axis \vec{r} is synchronous with the rotary coordinates, then the Bloch vector of the controlled particle will rotate around \vec{r} with angular speed Ω_1 . In this case, the instantaneous rotation component around the z -axis is small, and the larger Ω_1 is, the smaller it becomes. Because the rotation axis \vec{r} is static in rotary coordinates, the time average of the instantaneous rotation component around the z -axis is zero, thus the purity is almost preserved and the two particles become decoupled. However, when detuning $\Delta \neq 0$, the time average of the instantaneous rotation component around the z -axis is no longer zero, which is associated with the detuning. When the detuning is large enough, the purity of the controlled particle can achieve zero at times and the interaction between the two particles can be enhanced instead of weakened.

Now consider the purity motion when the detuning is zero and the initial state is

$$\rho(0) = (|00\rangle + |01\rangle + |10\rangle + |11\rangle)(\langle 00| + \langle 01| + \langle 10| + \langle 11|)/4 \quad (12.36)$$

According to Equations 12.35a and 12.35b the purity can be calculated as

$$p_1(t) = |P_a + P_f \cos(\omega_f t)| \quad (12.37)$$

where the frequency is $\omega_f = \sqrt{\Omega_1^2 + J^2}$, the average purity is $P_a = \Omega_1^2 / (\Omega_1^2 + J^2)$, and the fluctuating magnitude is $P_f = J^2 / (\Omega_1^2 + J^2)$. Figure 12.6 shows the track of the Bloch vector of the controlled particle (Figure 12.6a) and the purity curve (Figure 12.6b) with the parameters $\Omega_1 = 10$ and $J = 1$. Figure 12.6b shows that the purity fluctuation under constant control can be restricted in a range of (0.98, 1), and the fluctuating frequency is about 3π .

One can see from Equation 12.37 that the frequency ω_f is a vector sum of the angular speed Ω_1 and the interacting intensity J . In order to get a small purity fluctuating magnitude, Ω_1 should be much bigger than J , for example $\Omega_1 = 10J$ in Figure 12.6. Therefore the purity can be controlled in a certain range in resonant conditions. When $\Omega_1 = J = 1$, we can get $p_1(t) = \cos^2(\sqrt{2}t)$ and the purity fluctuates between 0 and 1. $\Omega_1/J = 0$ is the situation without the control field. The purity fluctuating frequency ω_f increases as Ω_1 increases so if Ω_1 is not big enough to restrain the purity fluctuating magnitude, the reduction of purity can be accelerated,

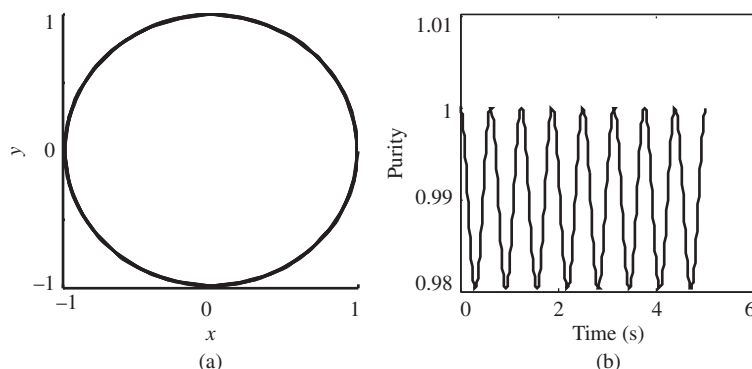


Figure 12.6 The track of the Bloch vector of the controlled particle and the purity curve: (a) the track of state evolution in the Bloch sphere and (b) the purity curve of the controlled particle

for example when $\Omega_1 = J$, purity p_1 achieves its minimum value zero at time $t = \sqrt{2\pi}/4J$, but when $\Omega_1/J = 0$ this is achieved at time $t = \pi/2J$.

The purity also relates to the initial states of the two particles. No precise analysis will be given here because an accurate expression of the purity for a general initial state is not only inconvenient to discuss, but also unnecessary as the state of particle 2 may be unknown. Qualitatively speaking, large x - y components of the two initial Bloch vectors determine a large purity fluctuating magnitude. In particular, if one of the Bloch vectors has no component in the x - y plane the purity of the two particles would be unchanged. The local phase of the controlled particle (or the phase of the control field) also affects the purity. When it gets closer to $\pi/2$ or $3\pi/2$, the purity fluctuating magnitude is more reduced. This means that one should adjust the phase difference between the control field and the initial state to $\pi/2$ in order to reduce the purity fluctuating. Of course initial states with different local phases also lead to different state evolution tracks. Take as an example initial states with no z component: when the local phase is zero, the state of the controlled particle would have no z component during the evolution, illustrated by Figure 12.6a. When the local phase is $\pi/2$, one can get $x_3 = -\Omega_1 \sin(\omega_f t)/\omega_f$ and $\sqrt{x_1^2 + x_2^2} = |\cos(\omega_f t)|$. If $\Omega_1 t \approx \omega_f t = \pi$, the controlled system is in its initial state again (if the local phase can be ignored).

12.2.3 Discussion

The state purity varies due to the interaction between the system and its environment. When the interaction is non-Markovian, such as the case in which the environment has finite degrees of freedom, so that it could be included and composes a closed system along with the controlled system, the state purity can be preserved by some active control field, for instance a resonant and constant control field. This is very important to controlling quantum systems with decoherence and it indicates that a resonant control field has a decoupling effect, which can prevent the purity from decreasing. Of course the field intensity and the phase should also be adjusted in order to achieve an expected evolution track for the system state: the field intensity determines the range of purity fluctuation and the phase impact on the population distribution.

To preserve the state purity (or coherence) only, one should adjust the field to have the same phase as the initial state, and if the population distribution needs to be changed, the phase difference of the field and the initial state should be $\pi/2$ or $3\pi/2$. In general situations, constant (continuous-wave) control is enough to achieve this, and it is easy to adjust the time to complete an expected rotation around the x -axis, thus the expected population distribution is accomplished.

12.3 Coherence Preservation in Markovian Open Quantum Systems

A central issue in the quantum computation and quantum information technique (QIT) is dealing with quantum coherence (Giulini *et al.*, 1996). Any realistic quantum system interacts with its surrounding environment, which can lead to the loss of coherence (Breuer and Petruccione, 2002). Understanding and suppressing decoherence are major issues in quantum information science. From a theoretical viewpoint, there are many system-environment models based on the theory of open quantum systems (Breuer and Petruccione, 2002). There is a broad range of systems of practical interest, mostly in quantum optics and solid state physics. In some cases, it is possible to describe the dynamics of an open system's density matrix by the so-called Markovian master equation under the conditions of trace preservation and satisfaction of complete positivity (Rivas *et al.*, 2010). Hence we study decoherence control in the context of the Markovian master equation.

A number of interesting schemes have been proposed to counter Markovian decoherence, including QEC codes (Viola and Lloyd, 1998; Cirac and Pellizzari, 1996) and error-avoiding codes (Zanardi and Rasetti, 1997; Chuang and Yamamoto, 1995), which encode quantum states onto carefully selected subspaces that are isolated from the decoherence channels. Such subspaces are in general DFSs in which the states do not undergo decoherence (Lidar and Whaley, 2003; Lidar, Chuang, and Whaley, 1998). Several DFS-based decoherence-suppressing strategies were proposed (Patra and Brooke, 2008; Cappellaro, Hodges, and Havel, 2006; Karasik *et al.*, 2008), and such methods aim at encoding and steering the quantum within such a subspace. Bang-bang control (Du *et al.*, 2009; Uhrig, 2008; Viola and Lloyd, 1998) is another early proposed strategy using high-frequency pulses to average out the decoherence effect, but it requires the bath correlation time to be finite, which is generally invalid for Markovian decoherence. Optimization techniques have also been used to reduce decoherence effects by minimizing a certain class of cost functionals, for example by optimally tracking desired unitary evolving trajectories (Zhang *et al.*, 2005; Sugny, Kontz, and Jauslin, 2007). A class of decoherence control strategies is based on algebra decomposition (Zhang *et al.*, 2007; Oreshkov and Calsamiglia, 2010). Feedback control is another method to manage decoherence, where the dynamics of a system are manipulated using information obtained about the system through measurements.

Although various strategies have been proposed, there is a need for additional techniques to suppress decoherence for N -level Markovian open quantum systems. The QEC and error-avoiding code schemes require a number of ancillary/redundant bits scaling rapidly with the size of the original system. The open-loop optimal control strategy has no analytical solution, and can only partially suppress amplitude and phase damping even in a two-level system. The DFS-based scheme is a passive strategy and does not admit arbitrary control Hamiltonians, as any transition out of the subspace would subject the state to decoherence and hence loss of information. We therefore investigated decoherence suppression in N -level

Markovian open quantum systems in this section, with the goal of designing an active controller to fight against decoherence. Based on the work by Lidar and Schneider (2005), where open-loop coherent control is applied to decoherence suppression for single-qubit Markovian systems and the coherence of the quantum state can be well preserved, we have extended decoherence control to N -level Markovian systems.

N -level systems can have different types of level structure. We first of all focus on the case of ladder-type coupling and only the coherence between adjacent levels is taken into account. The coherence is embodied by suitable coherence functions. In the rotating wave approximation (RWA), each component of the control field is designed to independently keep the corresponding coherence function constant over time. We also discuss circumstances where the control field has singular character.

12.3.1 Problem Formulation

In this section, we first explain the general control model for a Markovian open quantum system and then introduce a special N -level ladder-type model subject to Markovian decoherence. Finally, we formulate the control problem to be investigated.

1) Models of decoherence under control

The dynamics of a Markovian open quantum system can be described by the master equation:

$$\dot{\rho} = -i [H_0 + H_C(t), \rho] + \mathcal{L}(\rho) \quad (12.38)$$

where Planck's constant \hbar has been set to 1. The quantum state is represented by the reduced density matrix ρ , which is a positive semi-definite Hermitian operator in the system dynamical space and satisfies $\text{tr}\rho = 1$. H_0 refers to the field-free Hamiltonian and H_C is the control Hamiltonian, which usually takes the form $H_C(t) = -\vec{\mu}E(t)$, with $\vec{\mu}$ being the dipole operator. The Lie bracket on the operator space is defined as $[A, B] = AB - BA$. The Lindblad term $\mathcal{L}(\rho)$ can be written as

$$\mathcal{L}(\rho) = \sum_j \Gamma_j \mathcal{D}[L_j] \rho = \frac{1}{2} \sum_{j=1}^{N^2-1} \Gamma_j \left\{ [L_j, \rho L_j^\dagger] + [L_j \rho, L_j^\dagger] \right\} \quad (12.39)$$

with the system operators L_j and damping rates Γ_j representing different decoherence channels.

In this section, we consider an N -level ladder-type system (e.g., an atom), as shown in Figure 12.7, where the levels are denoted as $|1\rangle, |2\rangle, \dots, |N\rangle$ in sequence from low energy to high energy, respectively. The corresponding energy eigenvalues are labeled as E_1, E_2, \dots, E_N , respectively, with $E_1 < E_2 < \dots < E_N$.

It is convenient to introduce the following notation:

$$\begin{aligned} \sigma_z^{(m,n)} &= |m\rangle\langle m| - |n\rangle\langle n| & \sigma_x^{(m,n)} &= |m\rangle\langle n| + |n\rangle\langle m| & \sigma_y^{(m,n)} &= -i|m\rangle\langle n| + i|n\rangle\langle m| \\ \sigma_-^{(m,n)} &= |n\rangle\langle m| & \sigma_+^{(m,n)} &= |m\rangle\langle n| \end{aligned} \quad (12.40)$$

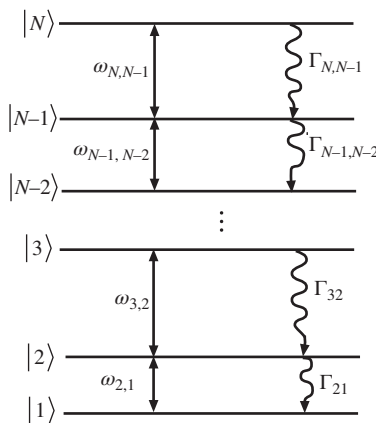


Figure 12.7 *N*-level atom in the ladder-configuration

where $i = \sqrt{-1}$. With the above notation, the field-free Hamiltonian of the system can be written as

$$H_0 = \frac{1}{N} \sum_{m>n=1}^N \omega_{m,n} \sigma_z^{(m,n)} \quad (12.41)$$

where $\omega_{m,n} = (E_m - E_n) / \hbar$ is the transition frequency between $|m\rangle$ and $|n\rangle$, and the constant energy term $\sum_{n=1}^N E_n / N$ has been ignored.

Suppose that $\Gamma_{m,n}$ represents the decay rate from state $|m\rangle$ to $|n\rangle$, and there is only decay between adjacent levels, that is, $m - n = 1$. Then the Lindblad item in Equation 12.39 can be rewritten as

$$\begin{aligned} \mathcal{L}(\rho) &= \sum_{j=2}^N \Gamma_{j,j-1} \mathcal{D}[\sigma_-^{(j,j-1)}] \rho \\ &= \sum_{j=2}^N \frac{1}{2} \Gamma_{j,j-1} \left\{ \left[\sigma_-^{(j,j-1)}, \rho \sigma_+^{(j,j-1)} \right] + \left[\sigma_-^{(j,j-1)} \rho, \sigma_+^{(j,j-1)} \right] \right\} \end{aligned} \quad (12.42)$$

The components of the density matrix satisfy the following equations:

$$\begin{aligned} \dot{\rho}_{kn}(t) &= -\frac{i}{\hbar} ([H, \rho(t)])_{kn}, k \neq n+1 \\ \dot{\rho}_{n+1,n}(t) &= -\frac{i}{\hbar} ([H, \rho(t)])_{n+1,n} - \Gamma_{n+1,n} \rho_{n+1,n} \\ \dot{\rho}_{nn}(t) &= -\frac{i}{\hbar} ([H, \rho(t)])_{nn} - \Gamma_{n,n-1} \rho_{nn} + \Gamma_{n+1,n} \rho_{n+1,n+1} \end{aligned}$$

Obviously, the Lindblad term not only decreases the coherence, but also contributes to the change in the population.

2) Coherence functions and control problems

Any qubit state can be expressed as $\psi = a|0\rangle + b|1\rangle$, with $|a|^2 + |b|^2 = 1, a, b \in \mathbb{C}$. Its density matrix is

$$\rho = |\psi\rangle\langle\psi| = |a|^2|0\rangle\langle 0| + |b|^2|1\rangle\langle 1| + ab^*|0\rangle\langle 1| + a^*b|1\rangle\langle 0|$$

The cross term $ab^*|0\rangle\langle 1| + a^*b|1\rangle\langle 0|$ can be thought of as reflecting coherence between the different states $|0\rangle$ and $|1\rangle$. Under decoherence, due to dephasing the evolution of the density matrix is $\rho(t) = \begin{pmatrix} |a|^2 & e^{-\gamma t}ab^* \\ e^{-\gamma t}a^*b & |b|^2 \end{pmatrix}$, with the coherence decaying with time.

Similarly, suppose $\{|n\rangle\}$ is a complete basis of the system. In the Hilbert space spanned by $\{|n\rangle\}$, the reduced density operator ρ is represented by its matrix elements given by

$$\rho_{m,n}(t) = \langle m|\rho(t)|n\rangle \quad (12.43)$$

The diagonal matrix element $\rho_{m,m}$ and off-diagonal matrix element $\rho_{m,n}$ ($m \neq n$) are the population of state $|m\rangle$ and coherence of states $|m\rangle$ and $|n\rangle$, respectively. The effect of decoherence on density matrices is reflected in the decay of the off-diagonal elements (Zurek, 2003).

The goal of this section is to protect the off-diagonal elements, which characterize the coherence of quantum state. Here we define the function

$$C_{m,n}(\rho) = \sqrt{\left\langle \sigma_x^{(m,n)} \right\rangle_\rho^2 + \left\langle \sigma_y^{(m,n)} \right\rangle_\rho^2} \quad (12.44)$$

which represents the coherence between levels $|m\rangle$ and $|n\rangle$, where $\langle A \rangle_\rho = \text{Tr}(A\rho)$. We may show that $\left\langle \sigma_x^{(m,n)} \right\rangle_\rho = 2\text{Re}(\rho_{m,n})$ and $\left\langle \sigma_y^{(m,n)} \right\rangle_\rho = 2\text{Im}(\rho_{mn})$. Hence for an N -level system, all the off-diagonal elements reflect the total coherence of the system. Here, we only consider the coherence between adjacent levels.

The control problem can be stated as follows: consider the N -level ladder-type atom in Figure 12.7 and define $M = [N/2]$ coherence functions:

$$C_{2,1}(\rho), C_{4,3}(\rho), \dots, C_{2M,2M-1}(\rho) \quad (12.45)$$

where $[A]$ represents the maximal integer less than A and $C_{2j,2j-1}(\rho)$ represents the coherence between $|2j\rangle$ and $|2j-1\rangle$. Then we seek to design $E(t)$ to ensure that all the coherence functions in Equation 12.45 remain constant during the evolution.

Then let the control field $E(t)$ have M components with frequencies $\omega_{21}, \omega_{43}, \dots, \omega_{2M,2M-1}$, that is,

$$E(t) = \sum_{j=1}^M \epsilon_j(t) \cos(\omega_{2j,2j-1}t + \phi_j) \quad (12.46)$$

where the amplitudes $\epsilon_j(t)$ and phases ϕ_j are the control variables that need to be designed.

Assuming all the transition frequencies are distinct, that is,

$$\omega_{jk} \neq \omega_{pq} (j, k) \neq (p, q) \quad (12.47)$$

the control Hamiltonian in the RWA approximation can be expressed as (see Appendix 12.A)

$$H_C = \sum_{j=1}^M \epsilon_j(t) e^{-i(\omega_{2j,2j-1}t + \phi_j)} |2j\rangle\langle 2j-1| + h.c. \quad (12.48)$$

where we have set $\vec{\mu}_{ij} = 1, \forall (i,j)$ without losing generality. It is convenient to analyze the system dynamics in the interaction picture, where an operator X in the Hilbert space is transformed into

$$X^I = e^{iH_0 t} X e^{-iH_0 t} \quad (12.49)$$

Then we can derive

$$H_C^I = e^{iH_0 t} H_C e^{-iH_0 t} = \sum_{j=1}^M \varepsilon_j(t) \left(\cos \phi_j \sigma_x^{(2j,2j-1)} + \sin \phi_j \sigma_y^{(2j,2j-1)} \right) \quad (12.50)$$

$$\sigma_-^{(n,n-1)I} = e^{-i\omega_{n,n-1} t} \sigma_-^{(n,n-1)I}, n = 2, 3, \dots, N \quad (12.51)$$

In the interaction representation, Equation 12.38 becomes

$$\dot{\rho}^I = -i [H_C^I, \rho^I] + \sum_{j=2}^N \frac{1}{2} \Gamma_{j,j-1} \left\{ \left[\sigma_-^{(j,j-1)}, \rho^I \sigma_+^{(j,j-1)} \right] + \left[\sigma_-^{(j,j-1)} \rho^I, \sigma_+^{(j,j-1)} \right] \right\} \quad (12.52)$$

The control problem can now be reformulated to design the control variables $\{\varepsilon_j, \phi_j, j = 1, 2, \dots, M\}$ to keep all the coherence functions in Equation 12.45 constant during the evolution.

12.3.2 Design of Control Variables

To protect the coherence functions in Equation 12.44, that is, $C_{2j,2j-1}(\rho) = C_{2j,2j-1}(\rho_0), j = 1, 2, \dots, M$, the first derivative of the coherence functions must be zero, that is, $\dot{C}_{2j,2j-1}(\rho^I) = 0$.

To find a solution for this problem, we start from the following equations for $\langle \sigma_x^{(2j,2j-1)} \rangle_{\rho^I}$

and $\langle \sigma_y^{(2j,2j-1)} \rangle_{\rho^I}$ respectively,

$$\begin{aligned} \frac{d \langle \sigma_x^{(2j,2j-1)} \rangle_{\rho^I}}{dt} &= \text{Tr} \left(\sigma_x^{(2j,2j-1)} \dot{\rho}^I \right) \\ &= \text{Tr} \left(\sigma_x^{(2j,2j-1)} \left(-i [H_C^I, \rho^I] + \sum_{n=2}^N \Gamma_{n,n-1} D [\sigma_-^{(n,n-1)}] \rho^I \right) \right) \\ &= \text{Tr} \left(\left[\sigma_x^{(2j,2j-1)}, -i H_C^I \right] \rho^I \right) + \sum_{j=2}^N \Gamma_{j,j-1} \text{Tr} \left(\sigma_x^{(2j,2j-1)} D [\sigma_x^{(j,j-1)}] \rho^I \right) \\ &= \varepsilon_n(t) \sin \phi_n \text{Tr} \left(\left[\sigma_x^{(2j,2j-1)}, -i \sigma_y^{(2j,2j-1)} \right] \rho^I \right) \\ &\quad + \frac{1}{2} \sum_{n=2}^N \Gamma_{n,n-1} \left(\text{Tr} \left(\left[\sigma_x^{(2j,2j-1)}, \sigma_-^{(n,n-1)} \right] \rho^I \sigma_+^{n,n-1} \right) \right) \\ &\quad + \text{Tr} \left(\sigma_-^{(n,n-1)} \rho^I \left[\sigma_+^{(n,n-1)}, \sigma_x^{(2j,2j-1)} \right] \right) \\ &= 2\varepsilon_j(t) \sin \phi_j \left\langle \sigma_z^{(2j,2j-1)} \right\rangle_{\rho^I} - \frac{\Gamma_{2j,2j-1} + \Gamma_{2j-1,2j-2}}{2} \left\langle \sigma_x^{(2j,2j-1)} \right\rangle_{\rho^I} \end{aligned} \quad (12.53)$$

Likewise, we can get

$$\begin{aligned} \frac{d \langle \sigma_y^{(2j,2j-1)} \rangle_{\rho^I}}{dt} &= \text{Tr} \left(\sigma_x^{(2j,2j-1)} \dot{\rho}^I \right) \\ &= -2\varepsilon_j(t) \cos \phi_j \langle \sigma_z^{(2j,2j-1)} \rangle_{\rho^I} - \frac{\Gamma_{2j,2j-1} + \Gamma_{2j-1,2j-2}}{2} \langle \sigma_y^{(2j,2j-1)} \rangle_{\rho^I} \quad (12.54) \end{aligned}$$

Combining Equations 12.53 and 12.54 with the condition $\dot{C}_{2j,2j-1}(\rho^I) = 0$ yields the required control variables:

$$\varepsilon_j(t) \frac{(\Gamma_{2j,2j-1} + \Gamma_{2j-1,2j-2}) C_{2j,2j-1}(\rho_0)}{4 \langle \sigma_z^{(2j,2j-1)} \rangle_{\rho^I}} \quad (12.55)$$

$$\phi_n = \begin{cases} \arctan \left(-\langle \sigma_x^{(2j,2j-1)} \rangle_{\rho_0} / \langle \sigma_y^{(2j,2j-1)} \rangle_{\rho_0} \right), & \langle \sigma_y^{(2j,2j-1)} \rangle_{\rho_0} < 0 \\ \pi/2, & \langle \sigma_y^{(2j,2j-1)} \rangle_{\rho_0} = 0 \\ \pi + \arctan \left(-\langle \sigma_x^{(2j,2j-1)} \rangle_{\rho_0} / \langle \sigma_y^{(2j,2j-1)} \rangle_{\rho_0} \right), & \langle \sigma_y^{(2j,2j-1)} \rangle_{\rho_0} > 0 \end{cases} \quad (12.56)$$

It is easy to verify that the control field with variables in Equations 12.55 and 12.56 satisfies $d \langle \sigma_y^{(2j,2j-1)} \rangle_{\rho^I} / dt = 0$ and $d \langle \sigma_x^{(2j,2j-1)} \rangle_{\rho^I} / dt = 0$, which naturally leads to $C_{2j,2j-1}(\rho^I(t)) = C_{2j,2j-1}(\rho_0)$, that is, the coherence between $|2j\rangle$ and $|2j-1\rangle$ is preserved with the control variables given in Equations 12.55 and 12.56.

The above derivation indicates that the design of each pair of variables $\{\varepsilon_j, \phi_j\}$ in the control field is independent. Henceforth, we can draw the following conclusion: for an N -level system described by Equation 12.52, the coherence functions in Equation 12.45 can be preserved by the control field $E(t)$ whose M control components have the variables $\{\varepsilon_j, \phi_j, j = 1, 2, \dots, M\}$ expressed by Equations 12.55 and 12.56.

Although we have demonstrated that the control field with the variables in Equations 12.55 and 12.56 can ensure that all the coherence functions are constant, this procedure may suffer from the field diverging at a breakdown time t_b , that is, at singularities.

We can derive

$$\begin{aligned} \frac{d \langle \sigma_z^{(n,n-1)} \rangle_{\rho^I}}{dt} &= \frac{-(\Gamma_{n,n-1} + \Gamma_{n-1,n-2}) C_{n,n-1}^2(\rho_0)}{2 \langle \sigma_z^{(n,n-1)} \rangle_{\rho^I}} \\ &\quad - \left(2\Gamma_{n,n-1}\rho_{nn}^I + \Gamma_{n-1,n-2}\rho_{n-1,n-1}^I - \Gamma_{n+1,n}\rho_{n+1,n+1}^I \right) \quad (12.57) \end{aligned}$$

$$\dot{\rho}_{n,n}^I(t) = \frac{-(\Gamma_{n,n-1} + \Gamma_{n-1,n-2}) C_{n,n-1}^2(\rho_0)}{2 \langle \sigma_z^{(n,n-1)} \rangle_{\rho^I}} - \Gamma_{n,n-1}\rho_{nn}^I + \Gamma_{n+1,n}\rho_{n+1,n+1}^I \quad (12.58)$$

Obviously, Equations 12.57 and 12.58 are not analytically solvable, so the analytical solution of the breakdown time t_b cannot be derived. However, $\left\langle \sigma_z^{(n,n-1)} \right\rangle_{\rho^I}$ is related to $C_{n,n-1}^2(\rho_0)$, $\rho_{n+1,n+1}^I$, ρ_{nn}^I , and $\rho_{n-1,n-1}^I$, therefore the breakdown time depends on the initial coherence, decay rates, and the population of three levels, which are the two levels associated with the coherence function and the higher adjacent level. We identified a region that is described by these parameters to judge the length of the breakdown time in a three-level system where only one coherence function is considered in Section 11.1. The closer the initial state is to the region, the longer the breakdown time is. However, how the parameters affect the breakdown time is not clear for the N -level case since the dynamical equations are more complicated and there are more coherence functions.

In 1999 Zhu and Rabitz studied the control field singularities and distinguished between several types: (i) a trivial singularity occurs when the denominators of the field are zero over a continuous time domain and (ii) a non-trivial singularity arises when the denominators are zero only at isolated points. In our case the singularities can possibly arise due to the denominator becoming zero at isolated points of time in Equation 12.57. For this situation, there are two sub-cases: (i) the singularity is of the form $f_j(t_b) = \alpha/0$ with $\alpha \neq 0$ and (ii) the singularity is of the form $f_j(t_b) = 0/0$. In case (ii) one can apply l'Hospital's rule, and overcome the singularity. In our case, the designed control law is of the form

$$f_n(t) = \frac{\left(\Gamma_{i_n,i_{n-1}} + \Gamma_{i_{n-1},i_{n-2}} \right) C_{i_n,i_{n-1}}(\rho_0) \cos(\omega_n t + \phi_n)}{4 \left\langle \sigma_z^{(i_n,i_{n-1})} \right\rangle_{\rho^I}}$$

It is difficult to derive an analytical solution for the breakdown time. Thus one cannot ensure that when $\left\langle \sigma_z^{(n,n-1)} \right\rangle_{\rho^I} = 0$ it also happens that $t_b = ((k + 0.5)\pi - \phi_n)/\omega_n$. Thus the singularities for our case can be regarded as case (i) where there is no solution for the field and the system is uncontrollable at singular points. This behavior will be observed in the simulations, which show that an open system is never strongly controllable and it is usually impossible to preserve the entire unitary dynamics (e.g., the purity) under coherent control. In other words, one cannot control the variation of diagonal elements and the coherence simultaneously. It follows that the proposed method cannot ensure $\left\langle \sigma_z^{(n,n-1)} \right\rangle_{\rho^I} = 0$ at any time as the coherence is kept constant so singularities may occur.

12.3.3 Numerical Simulations

To demonstrate the effectiveness of our strategy, we present some numerical examples. The propagation of the dynamical equation in Equation 12.52 was carried out by fourth-order Runge–Kutta integration.

An example of a four-level ladder-type atom is labeled as $|1\rangle$, $|2\rangle$, $|3\rangle$, and $|4\rangle$, respectively. The objective is to preserve the coherence between $|4\rangle$ and $|3\rangle$, and between $|2\rangle$ and $|1\rangle$ simultaneously. So we define two coherence functions $C_{21}(\rho^I)$ and $C_{43}(\rho^I)$ according to Equation 12.45. In all the following simulation examples, we let $|4\rangle = [0 \ 0 \ 0 \ 1]^T$, $|3\rangle =$

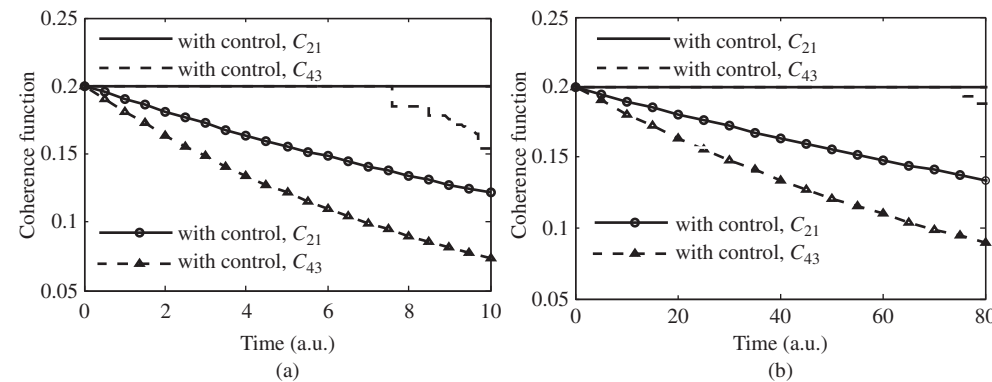


Figure 12.8 The evolution of coherence functions C_{21} and C_{43} for different decay rates: (a) comparison of the evolution of the coherence functions C_{21} and C_{43} both with and without the control field for $\Gamma_{4,3} = \Gamma_{3,2} = \Gamma_{2,1} = 0.1$ and (b) comparison of the evolution of the coherence functions C_{21} and C_{43} , both with and without the control field for $\Gamma_{4,3} = \Gamma_{3,2} = \Gamma_{2,1} = 0.01$

$[0\ 0\ 1\ 0]^T$, $|2\rangle = [0\ 1\ 0\ 0]^T$, and $|1\rangle = [1\ 0\ 0\ 0]^T$. The decay rates $\Gamma_{4,3}$, $\Gamma_{3,2}$, and $\Gamma_{2,1}$ are chosen as either 0.01 or 0.1, and the initial state is assumed to be

$$\rho_0 = \begin{pmatrix} 0.4 & 0.1 & 0 & 0 \\ 0.1 & 0.1 & 0 & 0 \\ 0 & 0 & 0.4 & 0.1 \\ 0 & 0 & 0.1 & 0.1 \end{pmatrix}$$

In other words, the initial coherence functions are $C_{21}(\rho_0) = 0.2$ and $C_{43}(\rho_0) = 0.2$, and the initial populations distributed on the levels $|4\rangle$, $|3\rangle$, $|2\rangle$, and $|1\rangle$ are 0.1, 0.4, 0.1, and 0.4, respectively.

The simulations are performed to verify the effectiveness of the proposed method. The corresponding control variables $\{\epsilon_1, \phi_1\}$ and $\{\epsilon_1, \phi_2\}$ are obtained according to Equations 12.55 and 12.56. Figure 12.8 compares the time evolution of the coherence functions $C_{21}(\rho^I)$ and $C_{43}(\rho^I)$ for cases both with and without the control field being present. The cases of $\Gamma_{4,3} = \Gamma_{3,2} = \Gamma_{2,1} = 0.1$ and 0.01 are shown in Figure 12.8a and Figure 12.8b, respectively. Figure 12.8a,b shows that the coherence functions C_{21} and C_{43} are lost quickly in the absence of control, and that the coherence functions can be maintained with the control field. Additionally, one can also see from Figure 12.8a,b that C_{43} decreases abruptly at breakdown time. This phenomenon is due to singularities of control fields. This behavior has been explained in Section 12.3.2. In addition, by comparing Figure 12.8a with Figure 12.8b, the larger the decay rate is, the shorter the time of the coherence as a constant is.

Although the proposed method theoretically is ineffective only at a breakdown time in a continuous time domain when the control field trends to infinite, it becomes ineffective once the field becomes large enough to approach the breakdown time. The simulation error $\delta(t_k)$ in $\langle \sigma_z(t_k) \rangle = \langle \sigma_z(t) \rangle + \delta(t_k)$ will produce $\dot{C}(t_{k+1}) = \epsilon(t_k) C(t_k) \delta(t_k)$, giving $C(t_{k+1}) = C(t_k) + O(\epsilon(t_k) \delta(t_k))$. If the envelope $\epsilon(t_k)$ is sufficiently small, $C(t_{k+1}) \approx C(t_k)$ is satisfied and we can conclude that the coherence is preserved. If $\epsilon(t_k)$ is large enough, it will make $C(t_k)$ jump to $C(t_{k+1})$. Then from Equations 12.55 and 12.56 we have $\dot{C}(t) = \frac{C^2(0) - C^2(t)}{C^2(t)}$, and

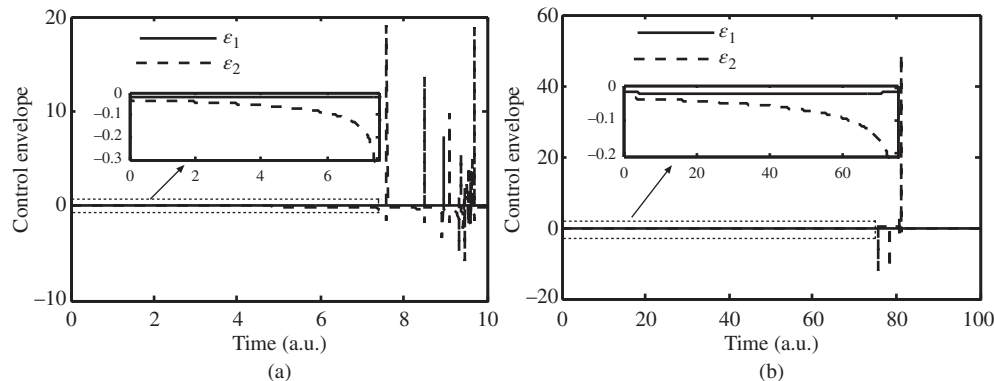


Figure 12.9 The envelopes of the control field ϵ_1 and ϵ_2 for different decay rates: (a) the envelope of the control field for $\Gamma_{4,3} = \Gamma_{3,2} = \Gamma_{2,1} = 0.1$ and (b) the envelope of the control field for $\Gamma_{4,3} = \Gamma_{3,2} = \Gamma_{2,1} = 0.01$

$\{\epsilon(t_{k+1}), \phi(t_{k+1})\}$ cannot satisfy $\dot{C} = 0$, implying that the coherence cannot be preserved. Therefore, the proposed method becomes ineffective when the modulus of $\epsilon(t_k)$ becomes large enough that the coherence function behaves in an unstable way at some point before breakdown time.

The envelopes of the control fields ϵ_1 and ϵ_2 are displayed in Figure 12.9a and Figure 12.9b correspond to the cases where the decay rates are 0.1 and 0.01, respectively. The embedded panel in Figure 12.9b displays the time evolution curve of the envelopes ϵ_2 and ϵ_1 for the time interval [0 72]. It clearly indicates that ϵ_2 slowly increases monotonically and its value is small in this time interval. Thus the control fields are deemed satisfactory. However, Figure 12.9b shows that ϵ_2 jumped abruptly to -15 at about the time 78 a.u., which is strong enough to make the coherence function hop and it is thought to diverge. We find that the control field f_2 is invalid after about 78 a.u. These results correspond to an abrupt decrease in C_{43} in Figure 12.8b. For $\Gamma_{4,3} = \Gamma_{3,2} = \Gamma_{2,1} = 0.1$, parallel results are observed in Figure 12.9a.

In summary, the simulations indicate that the control fields with the parameters expressed by Equations 12.57 and 12.58 can keep the coherence functions constant, although the control fields will diverge at some time. The divergence time becomes shorter as the decay rates increase. The divergence of the control field comes from the fact that the diagonal elements are not controllable, as discussed in Section 12.3.2. It should be noted that we have only focused on the situation where the off-diagonal elements to be preserved are in different rows and columns of the density matrix. For other cases, we cannot easily derive an expression for the control fields.

12.3.4 Discussion

In this section we considered the problem of coherence preservation of an N -level atom in Ξ configuration subject to Markovian decoherence. For the sake of simplicity, we assume that the system is ladder-type, and only atomic decay between two adjacent levels is allowed. The two

levels associated with each coherence function are distinct from all others. We have derived the variables of the control fields to satisfy the object of constant coherence functions. This is possible up to a finite time that depends on the initial coherence and population distribution, at which point the control field diverges.

There are several open questions suggested by these results.

- (i) Singularities are a well-known feature of tracking control, and how to remove or avoid them is still an open question. There are two possibilities: keeping the coherent functions in a small interval $C(0) - e < C(t) < C(0) + e$ with e a small positive constant and formulating an optimal control problem with the objective being the time integral of the coherence functions.
- (ii) While our original goal was to keep the coherence $C = \sqrt{\langle \sigma_x \rangle^2 + \langle \sigma_y \rangle^2}$ constant, we in fact solved the more restrictive problem of separately controlling $\langle \sigma_x \rangle$ and $\langle \sigma_y \rangle$. It would be interesting to consider the case where the two components are allowed to vary while truly trying to fix only C , and even the case where $\frac{dC}{dt} = \frac{2\epsilon(t)\langle \sigma_z \rangle (\sin \phi \langle \sigma_x \rangle - \cos \phi \langle \sigma_y \rangle)}{C} - \frac{\Gamma}{2}C \geq 0$, to see if this enables the extension of the breakdown time.

Appendix 12.A Derivation of H_C

Any electric field with frequency ω_L , given by $f(t) = \epsilon(t) \cos(\omega_L t + \phi)$, acts on the system leading to the interaction Hamiltonian (Scully and Zubairy, 1997)

$$H_I = \vec{\mu} \cdot f(t) = \sum_{m>n}^N \vec{\mu}_{mn} \epsilon(t) e^{-i(\omega_L t + \phi)} |p\rangle\langle q| + h.c. \quad (\text{A1})$$

The condition that the dipole operator has zero diagonal elements, that is, $\vec{\mu}_{m,m} = 0$, is used here. The next stage is to find the Hamiltonian in the interaction picture \bar{H} :

$$\begin{aligned} \bar{H} &= e^{iH_0 t} H_I e^{-iH_0 t} = \sum_{m>n}^N \vec{\mu}_{m,n} \epsilon(t) e^{-i[(\omega_{mn} - \omega_L)t + \phi]} |m\rangle\langle n| + h.c \\ &= \sum_{m>n}^N \Omega e^{-i\Delta_{mn}t} |m\rangle\langle n| + \Omega^* e^{i\Delta_{mn}t} |n\rangle\langle m| \end{aligned} \quad (\text{A2})$$

where $\Omega = \vec{\mu}_{m,n} \epsilon(t) e^{-i\phi}$ and $\Delta_{mn} = \omega_{mn} - \omega_L$.

If the electric field is near resonant with the atomic transition between $|i\rangle$ and $|j\rangle$, that is, $\omega_{ij} \approx \omega_L$, this means that $\Delta_{ij} \ll \Delta_{mn}$, $(m, n) \neq (i, j)$. Then the complex exponentials multiplying Ω and Ω^* can be considered to be rapidly oscillating. Hence on an appreciable time scale the oscillations will quickly average to 0. The RWA thus claims that these terms are negligible and the Hamiltonian can be written in the interaction picture as

$$\bar{H}_{RWA} = \vec{\mu}_{i,j} \epsilon(t) e^{-i(\Delta_{ij}t + \phi)} |i\rangle\langle j| + \vec{\mu}_{i,j}^* \epsilon^*(t) e^{i(\Delta_{ij}t + \phi)} |j\rangle\langle i| \quad (\text{A3})$$

Transforming the approximate Hamiltonian back to the Schrödinger picture gives

$$H_{I,RWA} = e^{-iH_0 t} \bar{H} e^{iH_0 t} = \vec{\mu}_{i,j} \epsilon(t) e^{-i(\omega_L t + \phi)} |i\rangle\langle j| + \vec{\mu}_{i,j}^* \epsilon^*(t) e^{i(\omega_L t + \phi)} |j\rangle\langle i| \quad (\text{A4})$$

The effect of $\hat{\mu}_{ij}$ can be adjusted by altering $\varepsilon(t)$, assuming $\hat{\mu}_{ij} = 1$ without lose any generality. Equation A4 is used to describe the interaction between one field and the system. Based on this, we can obtain the total control Hamiltonian and Equation 12.47 is formulated.

References

- Ai, Q., Li, Y.S. and Long, G.L. (2006) Influences of gate operation errors in the quantum counting algorithm. *Journal of Computer Science and Technology*, **21** (6), 927–932.
- Altafini, C. (2004) Coherent control of open quantum dynamical systems. *Physical Review A*, **70** (6), 062321.
- Bacon, D., Kempe, J., Lidar, D.A. et al. (2000) Universal fault-tolerant quantum computation on decoherence-free subspaces. *Physical Review Letters*, **85** (8), 1758–1761.
- Breuer, H.P. and Petruccione, F. (2002) *The Theory of Open Quantum Systems*, Oxford University Press, Oxford.
- Byrd, M.S., Wu, L.A. and Lidar, D.A. (2004) Overview of quantum error prevention and leakage elimination. *Journal of Modern Optics*, **51** (16–18), 2449–2460.
- Calderbank, A.R. and Shor, P.W. (1996) Good quantum error-correcting codes exist. *Physical Review A*, **54** (2), 1098–1105.
- Cappellaro, P., Hodges, J.S. and Havel, T.F. (2006) Principles of control for decoherence-free subsystems. *Journal of Chemical Physics*, **125** (4), 044514.
- Chuang, I.L. and Yamamoto, Y. (1995) Simple quantum computer. *Physical Review A*, **52** (5), 3489–3496.
- Cirac, J.I. and Pellizzari, T. (1996) Enforcing coherent evolution in dissipative quantum dynamics. *Science*, **273**, 1207–1210.
- Du, J., Rong, X., Zhao, N. et al. (2009) Preserving electron spin coherence in solids by optimal dynamical decoupling. *Nature*, **461**, 1235–1268.
- Duan, L.M. and Guo, G.C. (1998) Prevention of dissipation with two particles. *Physical Review A*, **57** (4), 2399–2402.
- Facchi, P., Tasaki, S., Pascazio, S. et al. (2005) Control of decoherence: analysis and comparison of three different strategies. *Physical Review A*, **2005** (71), 2.
- Giulini, D., Joos, E., Kiefer, C. et al. (1996) *Decoherence and the Appearance of a Classical World in Quantum Theory*, Springer, Berlin.
- Hao, L., Huo, W.Y. and Long, G.L. (2008) Dynamical decoupling method for the suppression of decoherence of the Δ -type three-level atom with finite control pulse length. *Journal of Physics B: Atomic, Molecular and Optical Physics*, **41** (12), 125501.
- Huang, C., Tang, L., Kong, F. et al. (2006) Entropy evolution of field interacting with V-type three-level atom via intensity-dependent coupling. *Physica A: Statistical Mechanics and its Applications*, **368** (1), 25–30.
- Karasik, R.I., Marzlin, K.P., Sanders, B.C. et al. (2008) Criteria for dynamically stable decoherence-free subspace and incoherently generated coherences. *Physical Review A*, **77** (5), 052301.
- Kern, O. and Alber, G. (2005) Controlling quantum systems by embedded dynamical decoupling schemes. *Physical Review Letters*, **95** (25), 250501.
- Khodjasteh, K. and Lidar, D.A. (2005) Fault-tolerant quantum dynamical decoupling. *Physical Review Letters*, **95** (18), 180501.
- Khodjasteh, K. and Lidar, D.A. (2007) Performance of deterministic dynamical decoupling schemes: concatenated and periodic pulse sequences. *Physical Review A*, **75** (6), 062310.
- Kiffner, M., Evers, J. and Keitel, C.H. (2007) Coherent control in a decoherence-free subspace of a collective multilevel system. *Physical Review A*, **75** (3), 032313.

- Knill, E. and Laflamme, R. (1997) Theory of quantum error-correcting codes. *Physical Review A*, **55** (2), 900–911.
- Laflamme, R., Miquel, C., Paz, J.P. et al. (1996) Perfect quantum error correcting code. *Physical Review Letters*, **77** (1), 198–201.
- Lidar, D.A., Bacon, D., Kempe, J. et al. (2001) Decoherence-free subspaces for multiple-qubit errors. II. Universal, fault-tolerant quantum computation. *Physical Review A*, **63** (2), 022307.
- Lidar, D.A., Bacon, D. and Whaley, K.B. (1999) Concatenating decoherence-free subspaces with quantum error correcting codes. *Physical Review Letters*, **82** (22), 4556–4559.
- Lidar, D.A., Chuang, I.L. and Whaley, K.B. (1998) Decoherence-free subspaces for quantum computation. *Physical Review Letters*, **81** (12), 2594–2597.
- Lidar, D.A. and Schneider, S. (2005) Stabilizing qubit coherence via tracking-control. *Quantum Information and Computation*, **5** (415), 350–363.
- Lidar, D.A. and Whaley, K.B. (2003) Decoherence-free subspaces and subsystems, in *Irreversible Quantum Dynamics*, Lecture Notes in Physics, vol. **622** pp. 83–120.
- Nielsen, M.A. and Chuang, I.L. (2010) *Quantum Computation and Quantum Information*, Cambridge University Press, Cambridge.
- Niwa, J., Matsumoto, K. and Imai, H. (2002) General-purpose parallel simulator for quantum computing, in *Unconventional Models of Computation*, Lecture Notes in Computer Science, Springer, New York, p. 2509.
- Oreshkov, O. and Calsamiglia, J. (2010) Adiabatic Markovian dynamics. *Physical Review Letters*, **105** (5), 050503.
- Patra, M.K. and Brooke, P.G. (2008) Decoherence-free quantum information in Markovian systems. *Physical Review A*, **78** (1), 010308R.
- Rivas, Á., Plato, A.D.K., Huelga, S.F. et al. (2010) Markovian master equations: a critical study. *New Journal of Physics*, **12**, 113032.
- Santos, L.F. and Viola, L. (2006) Enhanced convergence and robust performance of randomized dynamical decoupling. *Physical Review Letters*, **97** (15), 150501.
- Scully, M.O. and Zubairy, M.S. (1997) *Quantum Optics*, Cambridge University Press, Cambridge.
- Shor, P.W. (1995) Scheme for reducing decoherence in quantum computer memory. *Physical Review A*, **52** (4), R2493–R2496.
- Sugny, D., Kontz, C. and Jauslin, H. (2007) Time-optimal control of a two-level dissipative quantum system. *Physical Review A*, **76** (2), 023419.
- Tasaki, S., Tokuse, A., Facchi, P. et al. (2004) Control of decoherence: dynamical decoupling versus quantum Zeno effect: a case study for trapped ions. *International Journal of Quantum Chemistry*, **98**, 160–322.
- Ticozzi, F. and Viola, L. (2008) Quantum Markovian subsystems: invariance, attractivity and control. *IEEE Transaction on Automatic Control*, **53** (9), 2048–2063.
- Uhrig, G.S. (2008) Exact results on dynamical decoupling by π pulses in quantum information processes. *New Journal of Physics*, **10**, 083024.
- Viola, L. and Knill, E. (2005) Random decoupling schemes for quantum dynamical control and error suppression. *Physical Review Letters*, **94** (6), 060502.
- Viola, L., Knill, E. and Lloyd, S. (1999) Dynamical decoupling of open quantum systems. *Physical Review Letters*, **82** (12), 2417–2421.
- Viola, L. and Lloyd, S. (1998) Dynamical suppression of decoherence in two-state quantum systems. *Physical Review A*, **58** (4), 2733–2744.
- Wang, Z.C. and Tan, L. (2003) Dissipative force and laser cooling of a ladder-type three-level atom. *Journal of the Physical Society of Japan*, **72**, 2213–2218.
- Zanardi, P. and Rasetti, M. (1997) Error avoiding quantum codes. *Modern Physics Letters B*, **11** (25), 1085–1093.
- Zhang, J., Li, C., Wu, R.B. et al. (2005) Maximal suppression of decoherence in Markovian quantum systems. *Journal of Physics A: Mathematical and General*, **38** (29), 6587–6601.

- Zhang, J., Wu, R.B., Li, C.W. *et al.* (2007) Asymptotically noise decoupling for Markovian open quantum systems. *Physical Review A*, **75** (2), 022324.
- Zhang, J., Wu, R., Li, C. and Tarn, T. J. (2010) *Protecting coherence and entanglement by quantum feedback controls*. IEEE Transactions on Automation and Control, **55** (3), 619–633.
- Zurek, W.H. (2003) Decoherence, einselection, and the quantum origins of the classical. *Reviews of Modern Physics*, **75** (3), 715–775.

13

State Manipulation in Decoherence-Free Subspace

13.1 State Transfer and Coherence Maintenance Based on DFS for a Four-Level Energy Open Quantum System

Because of the impact of the environment, the information of states in open quantum systems is leaked to the environment. The coherence of quantum states is destroyed, which turns quantum states into classical states. This phenomena is called the decoherence effect. In fact, most practical quantum systems are open and how to keep their coherence is worthy of study. To begin with, active correction (Shor, 1995) and passive correction (Duan and Guo, 1998) were proposed to deal with decoherence, which require a large number of redundant qubits although the idea is straightforward. Viola and Lloyd (1998) proposed a bang-bang control strategy to suppress decoherence, which is an effective method but needs ultra-high frequency pulses. So far, the decoherence-free space (DFS) (Wei *et al.*, 2007) is an interesting method for solving this problem.

The DFS is an unchanged Hilbert subspace under non-unitary dynamics. In DFS, the system is decoupled from the environment, dynamical evolution of which is completely unitary. The DFS protects quantum information from the destruction caused by the interaction with the environment, the state that can be stably used in quantum computing (Beige *et al.*, 2000). Among the existing research, Yi and others (Yi *et al.*, 2009; Wang, Wang, and Yi, 2010) derived that when the DFS is known, a convergent Lyapunov control law can be designed to transfer an arbitrary initial state to the eigenstate in DFS for a four-level energy open quantum system, but this program will fail if the target state is not in DFS. For this reason, we will study a more general Λ -type four-level energy open quantum system in this section, where the DFS included the desired target state is constructed and the invariant set is deduced by designing control Hamiltonian. Finally, we transfer the excited state to the superposition state in DFS by Lyapunov-based control. The concrete idea is to firstly construct a DFS including the target state, then design a convergent control law to steer the system state to the target state in DFS. This involves two steps: we design an external laser field I to change the original DFS of the open system into the one including the target state and then a Lyapunov control field II is designed to steer the system initial state out of DFS to the target state.

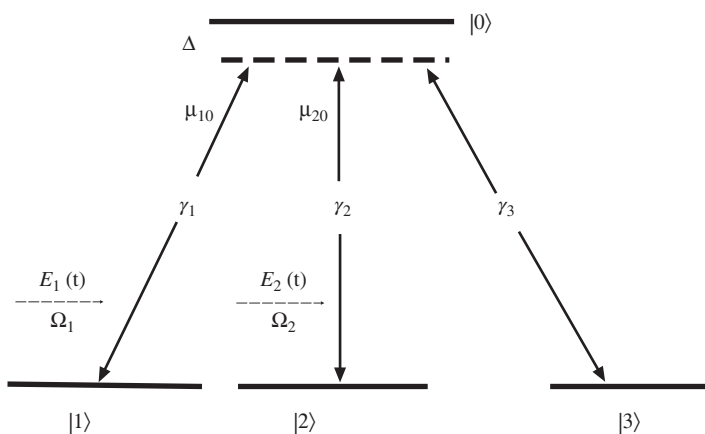


Figure 13.1 A four level atomic system under an external laser field

13.1.1 Construction of DFS and the Desired Target State

To maintain coherence in the problem of state transfer for open quantum systems, the target state is expected to be included in DFS, which means that under the action of control field II, the system state is decoupled from the environment after being transferred to its target state since decoherence then no longer occurs. In the case of the system controlled being given, we firstly determine whether the target state is in DFS. If it is not, a new DFS-included target state should be constructed before transferring the state.

Figure 13.1 shows the four-level open-atom system under external laser field I. The excited state $|0\rangle$ is coupled to the two degenerate ground states by two laser fields I, where $E_j(j = 1, 2)$ is the intensity of the laser field I, $\Omega_j(j = 1, 2)$ is its Rabi frequency, $\mu_{j0}(j = 1, 2)$ represents the electric dipole moment, and Δ describes detuning between the carrier frequency and the transition frequency. Excited state $|0\rangle$ spontaneously decays to the three ground states with rates of $\gamma_j(j = 1, 2, 3)$, respectively. The laser field I we will design is the control field I to construct the DFS.

We assume the process of attenuation is Markovian and the master equation of the system is of general Lindblad form:

$$\frac{d\rho(t)}{dt} = -\frac{i}{\hbar} [\mathbf{H}_0, \rho(t)] + \mathbf{L}(\rho(t)) \quad (13.1)$$

$$\mathbf{H}_0 = \Delta \mathbf{A}_{00} + \frac{1}{2} (\Omega_1 \mathbf{A}_{10} + \Omega_2 \mathbf{A}_{20} + h.c.) \quad (13.2)$$

$$\mathbf{L}(\rho(t)) = \frac{1}{2} \sum_{j=1}^3 \gamma_j (2 \mathbf{F}_j \rho(t) \mathbf{F}_j^\dagger - \mathbf{F}_j^\dagger \mathbf{F}_j \rho(t) - \rho(t) \mathbf{F}_j^\dagger \mathbf{F}_j) \quad (13.3)$$

where, *h.c.* denotes the Hermitian conjugate, \mathbf{A}_{ij} represents $|i\rangle\langle j|$, $\mathbf{L}(\rho(t))$ is the dissipation of the system, which contains all factors that may produce decoherence, the decay rate

$\gamma_j (j = 1, 2, 3)$ is a non-negative constant, F_i indicates Lindblad operators, and $\Omega_j (j = 1, 2)$ is the Rabi frequency of laser field I.

Only spontaneous emission coherence deduced by a vacuum-mode electromagnetic field is considered here, namely, the interaction between the atom and the quantized vacuum-mode field. By introducing external coherent optical field I one can regulate the Rabi frequency of the coupled laser field to weaken cross-coupled spontaneous emission coherence. In this way, the control goal is to decompose the coupling between the system and the environment to prepare the DFS for four-level atom systems.

From the analysis above, the decoherence-free target state is constructed using the following two steps:

First, under the action of control field I, one can get the master equation and the decoherence description of the system according to the characteristics of the four-level atom system.

Second, according to the conditions of decoherence-free subspace, the parameters of control field I and its relationship with the decoherence-free state are obtained to derive the control law of coherent optical field I.

Assuming Θ , the description of DFS is spanned by $\{|\psi_\alpha\rangle\} (\alpha = 1, \dots, n)$ and the reduced density matrix defined in Θ is expressed as

$$\rho = \sum_{\alpha, \beta=1}^n \rho_{\alpha, \beta} |\psi_\alpha\rangle\langle\psi_\beta| \quad (13.4)$$

According to the definition of a state in DFS (Karasik *et al.*, 2008), $F_j |\varphi_\alpha\rangle = \lambda_j \langle\varphi_\alpha| (j = 1, \dots, M)$ and Lidar theorem (Lidar, Chuang, and Whaley, 1998), one can get two determining conditions of DFS Θ (Lidar and Whaley, 2003):

$$H_0 |\psi_\alpha\rangle\langle\psi_\beta| \in S \quad (13.5)$$

$$L |\psi_\alpha\rangle\langle\psi_\beta| = 0, \alpha, \beta = 1, \dots, n \quad (13.6)$$

where S denotes a subspace of DFS. Equation 13.5 guarantees the completeness of space; Equation 13.6 makes sure evolution of the system is unitary under operators bases $\{|\psi_\alpha\rangle\}$.

Suppose states in subspace Θ satisfy eigenequation

$$F_j |\psi_\alpha\rangle = \lambda_j |\psi_\alpha\rangle, j = 1, \dots, M \quad (13.7)$$

where $|\psi_\alpha\rangle$ is the degenerate eigenstate of all operators F_j . Equation 13.6 is obtained by substituting Equations 13.4 and 13.7 into Equation 13.3, viz. if elements in subspace Θ satisfy Equation 13.7, subspace Θ meets the second determining equation (Equation 13.6) of DFS.

Consider the DFS states expression that satisfies Equation 13.5. Expanding bases of DFS for four-level atom systems is derived from decoherence produced spontaneously, which results in the states expression.

Assuming transition dipole moment vectors of states are mutually perpendicular, then the Rabi frequency of the external optical field remains unchanged, which is the prerequisite of continuous action of the external field. The control task is to eliminate the decoherent item in

the master equation. The concrete expression of the decoherent item is

$$\begin{aligned} L(\rho(t)) = & \frac{1}{2}\gamma_{10}(2\mathbf{A}_{10}\rho\mathbf{A}_{01} - \mathbf{A}_{01}\mathbf{A}_{10}\rho - \rho\mathbf{A}_{01}\mathbf{A}_{10}) \\ & + \frac{1}{2}\gamma_{20}(2\mathbf{A}_{20}\rho\mathbf{A}_{02} - \mathbf{A}_{02}\mathbf{A}_{20}\rho - \rho\mathbf{A}_{02}\mathbf{A}_{20}) \\ & + \frac{1}{2}\gamma_{30}(2\mathbf{A}_{30}\rho\mathbf{A}_{03} - \mathbf{A}_{03}\mathbf{A}_{30}\rho - \rho\mathbf{A}_{03}\mathbf{A}_{30}) \end{aligned} \quad (13.8)$$

In view of the forbidden dipole, the expression of operators \mathbf{F}_j is

$$\mathbf{F}_1 = \mathbf{A}_{10}, \mathbf{F}_2 = \mathbf{A}_{20}, \mathbf{F}_3 = \mathbf{A}_{30} \quad (13.9)$$

According to the definition of DFS, finding DFS in a system is equivalent to finding eigenvalues λ_j independent of parameter α and satisfying the solution of Equation 13.7.

Taking the conjugate on both sides of Equation 13.7 gives

$$\langle \psi_\alpha | \lambda_j^* = \langle \psi_\alpha | \mathbf{F}_j^\dagger \quad (13.10)$$

Then

$$\lambda_2^* \lambda_1 = \langle \psi_\alpha | \mathbf{A}_{02} \mathbf{A}_{10} | \psi_\alpha \rangle = 0 \quad (13.11)$$

Suppose $\lambda_1 = 0$. Combining this with $\mathbf{F}_1 |\psi_\alpha\rangle = \lambda_1 |\psi_\alpha\rangle$ one gets $\mathbf{F}_1 |\psi_\alpha\rangle = 0$, viz.

$$\mathbf{A}_{10} |\psi_\alpha\rangle = 0 \quad (13.12)$$

$|\psi_\alpha\rangle$ is spanned by bases of subspace Θ as

$$|\psi_\alpha\rangle = c_0|0\rangle + c_1|1\rangle + c_2|2\rangle + c_3|3\rangle \quad (13.13)$$

where coefficients satisfy $|c_0|^2 + |c_1|^2 + |c_2|^2 + |c_3|^2 = 1$. Substituting Equation 13.14 into Equation 13.12 gives $c_0 = 0$. Thus, states in subspace Θ can be described as

$$|\psi_\alpha\rangle = c_1|1\rangle + c_2|2\rangle + c_3|3\rangle \quad (13.14)$$

Putting Equation 13.13 into $\mathbf{F}_2 |\psi_\alpha\rangle = \lambda_2 |\psi_\alpha\rangle$ and $\mathbf{F}_3 |\psi_\alpha\rangle = \lambda_3 |\psi_\alpha\rangle$, one has $\lambda_2 = \lambda_3 = 0$.

In such a way, subspace Θ will be spanned linearly by three lower energy states, which is to say the subspace Θ that satisfies Equation 13.6 degenerates to $\mathbf{Z} = \{|1\rangle, |2\rangle, |3\rangle\}$. To meet Equation 13.5, the following condition must hold: if $|\psi_\alpha\rangle$ belongs to subspace \mathbf{Z} , so does $\mathbf{H}_0 |\psi_\alpha\rangle$, which requires that no high-energy state $|0\rangle$ is contained in $\mathbf{H}_0 |\psi_\alpha\rangle$. We get

$$\mathbf{A}_{10} \mathbf{H}_0 |\psi_\alpha\rangle = 0 \quad (13.15)$$

According to Equations 13.12 and 13.15

$$(\mathbf{A}_{10} \mathbf{H}_0 - \mathbf{H}_0 \mathbf{A}_{10}) |\psi_\alpha\rangle = 0 \quad (13.16)$$

Substituting Equation 13.2 into Equation 13.16 gives $|1\rangle (\Omega_1 (1|\psi_\alpha\rangle + \Omega_2 (2|\psi_\alpha\rangle)) = 0$. The expression of wave function $|\psi_\alpha\rangle$ is

$$\begin{aligned} |\psi_\alpha\rangle &= c_1|1\rangle + c_2|2\rangle + c_3|3\rangle \\ \Omega_1 c_1 + \Omega_2 c_2 &= 0 \\ c_1^2 + c_2^2 + c_3^2 &= 1 \end{aligned} \quad (13.17)$$

States $|\psi_a\rangle$ satisfying Equation 13.17 will meet Equations 13.5 and 13.6 of DFS simultaneously, which indicates complete decoupling from the environment. It can also be seen from Equation 13.17 that decoherence-free states only depend on the Rabi frequency $\Omega_j(j = 1, 2)$ of the external optical field. Under the premise that the electric dipole moment is assured, the Rabi frequency Ω of the external optical field only relates to field intensity E and electric dipole moment μ , viz. $\Omega_j = 2\mu_{j0}E_j/\hbar(j = 1, 2)$. Therefore, if the laser is regulated continuously, the decoherence-free states expected can be obtained by modulating the external field and then preparing the DFS of the system.

For the construction of DFS, if the desired target state of the four-level atom system in Figure 13.1 is

$$|\psi_D\rangle = c'|1\rangle + c''|2\rangle + c'''|3\rangle \quad (13.18)$$

where $c'^2 + c''^2 + c'''^2 = 1$, according to the conditions of DFS we only need to regulate the Rabi frequency $\Omega_j(j = 1, 2)$ of the external field I to satisfy $\Omega_1c' + \Omega_2c'' = 0$ and the target state $|\psi_D\rangle$ is a decoherence-free state in DFS.

13.1.2 Design of the Lyapunov-Based Control Law for State Transfer

After constructing DFS including the target state, the control goal of state transfer becomes the design of a series of control fields $\{f_n(t), n = 1, 2, \dots, F\}$ as control field II, which makes system state $\rho(t)$ evolve to its target state $\rho_D = |\psi_D\rangle\langle\psi_D|$ in DFS. The coherence of the system state will remain in DFS. The control Hamiltonian under the action of control field II becomes

$$\mathbf{H} = \mathbf{H}_0 + \sum_{n=1}^F f_n(t) \mathbf{H}_n \quad (13.19)$$

where the free Hamiltonian \mathbf{H}_0 is expressed as Equation 13.2, $\mathbf{H}_n(n = 1, 2, \dots, F)$ is the control Hamiltonian, and $f_n(t)(n = 1, 2, \dots, F)$ represents control field II.

To design control field II $\{f_n(t)\}$ based on the Lyapunov stability theorem, a proper Lyapunov function $V(\rho_D, \rho)$ is first selected as

$$V = 1 - Tr(\rho_D \rho) \quad (13.20)$$

where the physical meaning of $Tr(\rho_D \rho)$ is the probability of system state $\rho(t)$ in target state ρ_D . The Lyapunov function can make sure target state ρ_D is a stable point. Conditions for V as a Lyapunov function are $V \geq 0$ and $\dot{V} \leq 0$. From Equation 13.20 we know $V \geq 0$, the first time order derivation of which is

$$\dot{V} = -Tr \left\{ \rho_D (-i [\mathbf{H}_0, \rho] + L(\rho)) \right\} - \sum_{n=1}^F f_n(t) Tr \left\{ \rho_D [-i\mathbf{H}_n, \rho] \right\} \quad (13.21)$$

Choose n_0 to satisfy $Tr \left\{ \rho_D [-i\mathbf{H}_{n_0}, \rho] \right\} \neq 0$ and let

$$f_{n_0}(t) = \frac{-Tr \left\{ \rho_D (-i [\mathbf{H}_0, \rho] + L(\rho)) \right\}}{Tr \left\{ \rho_D [-i\mathbf{H}_{n_0}, \rho] \right\}} \quad (13.22)$$

where $f_{n_0}(t)$ balances out the action of the free Hamiltonian \mathbf{H}_0 and passion item $L(\rho)$. Let the other parts of control field II be

$$f_n(t) = K_n \left(\text{Tr} \left\{ \rho_D \left[-i\mathbf{H}_n, \rho \right] \right\} \right)^* K_n > 0, \text{ for } n \neq n_0 \quad (13.23)$$

Equations 13.22 and 13.23 are the control laws satisfying Lyapunov conditions, which hold for $\dot{V} \leq 0$.

The open quantum system under the action of Lyapunov control laws (Equations 13.22 and 13.23) evolves according to a non-linear equation as

$$\frac{d\rho(t)}{dt} = -\frac{i}{\hbar} \left[\mathbf{H}_0 + \sum_n f_n(t) \mathbf{H}_n, \rho(t) \right] + \mathbf{L}(\rho(t)) \quad (13.24)$$

where $f_n(t)$ depends on Equations 13.22 and 13.23.

As we know from the LaSalle invariant set (LaSalle and Lefschetz, 1961), the dynamical system described by Equation 13.24 finally evolves to the invariant set $\epsilon = \{\dot{V} = 0\}$, which contains the target state and some other states. From Equation 13.21, the invariant set is a set of states satisfying

$$\text{Tr} \left\{ \rho_D \left[-i\mathbf{H}_n, \rho \right] \right\} = 0, n \neq n_0 \quad (13.25)$$

It can be seen from Equation 13.25 that the size of invariant set ϵ depends on \mathbf{H}_n . Control field II will be zero as soon as states evolve into the invariant set, which leads to no control action on state transfer. One therefore expects to design \mathbf{H}_n to get an invariant set as small as possible that satisfies Equation 13.25. We want to construct a set of \mathbf{H}_n to decrease eligible states, which will reduce invariant set ϵ and increase the probability of the system state evolving to the target state. Detailed analysis about these three conditions follow, from which we can design the control Hamiltonian \mathbf{H}_n and invariant set ϵ .

First, for any n , the necessary and sufficient condition for $[\rho_D, \mathbf{H}_n] = 0$ is ρ_D and \mathbf{H}_n have identical eigenvectors. To meet $[\rho_D, \mathbf{H}_n] \neq 0$, we design a set of control Hamiltonians \mathbf{H}_n ($n = 1, 2, 3$) with different eigenvectors. Then $[\rho_D, \mathbf{H}_n] = 0$ holds for any n if and only if $\rho_D = \frac{I}{N}$. Because DFS is a set of pure states, only ρ_D is selected as a pure state, not $\rho_D = \frac{I}{N}$, which establishes $[\rho_D, \mathbf{H}_n] \neq 0$.

Second, because different eigenvectors of the control Hamiltonian \mathbf{H}_n are designed in Equation 13.1, the condition $[\rho, \mathbf{H}_n] = 0$ cannot be satisfied simultaneously for $n = 1, 2, 3$ except for $\rho = \frac{I}{N}$, which is not a stable state and does not belong to the invariant set ϵ . So $[\rho, \mathbf{H}_n] \neq 0$ is obtained.

Third, states ρ satisfying $[\rho_D, \rho] = 0$ are those which have identical eigenvectors with ρ_D . Because states in the invariant set ϵ are stable, ρ may be a superposition state or a mixed state of ground states $|1\rangle$, $|2\rangle$, and $|3\rangle$, which contain the target state ρ_D . So far, we have narrowed the scope of the invariant set ϵ by designing the control Hamiltonian \mathbf{H}_n .

In the following context, we will illustrate how to construct DFS around the target state in a specific example and transfer the system state to the target state.

13.1.3 Numerical Simulations

Consider a four-level energy open quantum system in which we assume the target state is a superposition state: $|\psi_D\rangle = -0.5257|1\rangle + 0.7236|2\rangle - 0.4472|3\rangle$, where $c' = -0.5257$, $c'' =$

0.7236, and $c''' = -0.4472$. According to Equation 13.18, a laser field I satisfying $c'\Omega_1 + c''\Omega_2 = 0$ is implemented to change the target state $|\psi_D\rangle$ into a decoherence-free state. It is acceptable to choose the Rabi frequencies of the laser field I as $\Omega_1 = 4.0451$ and $\Omega_2 = 2.9389$. The DFS is made up of degenerate dark states of the free Hamiltonian \mathbf{H}_0 :

$$\begin{aligned} |D_1\rangle &= -\frac{\Omega_2}{\sqrt{\Omega_1^2 + \Omega_2^2}}|1\rangle + \frac{\Omega_1}{\sqrt{\Omega_1^2 + \Omega_2^2}}|2\rangle \\ |D_2\rangle &= |3\rangle \end{aligned} \quad (13.26)$$

To shrink the invariant set, we construct the control Hamiltonian as

$$\mathbf{H}_c = \sum_{n=1}^3 f_n(t) \mathbf{H}_n \quad (13.27)$$

where $\mathbf{H}_n = |0\rangle\langle n| + |n\rangle\langle 0|$ ($n = 1, 2, 3$) have different eigenvectors, which will achieve the goal of shrinking the invariant set according to analysis in Section 13.1.3.

Other parameters are set as follows: the initial state is selected as the excited state $|0\rangle$, the detuning factor is $\Delta = 3$, the decay rate is $\gamma_1 = \gamma_2 = \gamma_3 = 0.1$, the proportional coefficient of the control field is $K_n = 110$, and the sampling period is $\Delta t = 0.01$.

The result of system state transfer under control fields I and II is shown in Figure 13.2, in which the solid line in Figure 13.2a denotes probability evolution to target state $|\psi_D\rangle$ with control field II, and the dashed line is the case without control field II. The solid line in Figure 13.2b is the probability of the system state evolving to DFS with control field II and the dashed line is the case without control field II.

It can be seen from Figure 13.2 under the action of control field II that the open quantum system state is transferred from its original excited state $|0\rangle$ to the desired target superposition

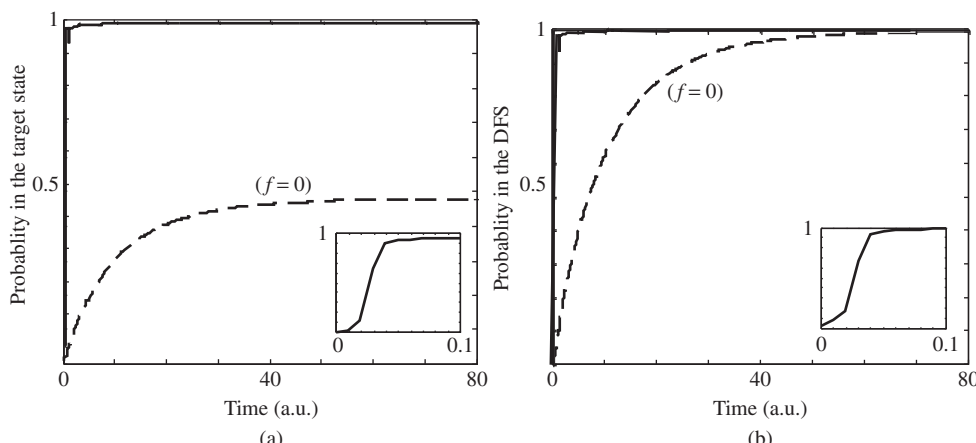


Figure 13.2 The result of system state transfer under control fields I and II: (a) the probability of the system state transferring to the target state $|\psi_D\rangle$ and (b) the probability of the system state transferring to the DFS

state $|\psi_D\rangle = -0.5257|1\rangle + 0.7236|2\rangle - 0.4472|3\rangle$, from which one can see that the transition probability reaches 99%. At the same time, the system state remained in target state $|\psi_D\rangle$, which shows that the laser field I we designed can change the target state $|\psi_D\rangle$ into a decoherence-free state and retain coherence after the state has achieved its target state. The proportional coefficient of control field K_n is related to decay rate γ . The larger γ is the more intense the decay, which results in a stronger control field intensity.

The dashed line in Figure 13.2 is the evolution of the system state without control field II. The open quantum system affected by the environment decays to one of the stable states at the rate of γ , viz. a maximum mixed state of $|D_1\rangle$ and $|D_2\rangle$, which is also the least energy stable state. We can conclude that the open quantum system affected by the environment is sure to evolve to a stable state, but control field II not only reaches a stable state at a much faster rate than the free-evolution one and also transfers to the target state with a higher probability.

13.2 State Transfer Based on a Decoherence-Free Target State for a Λ -Type N -Level Atomic System

In this section we not only steer the initial state into DFS, but also construct a DFS containing an expected target state, and transfer the initial state to the expected target. The system state can therefore stay in the expected target state and be decoupled from the environment. In order to achieve this goal, two steps are required. First, an external laser field I is designed to construct a decoherence-free subspace around the expected target state. In this way the target state will become a decoherence-free state and be decoupled from the environment with no further decoherence process. With the decoherence-free target state we design a Lyapunov-based control field II to transfer a given initial state of the open quantum system to the expected target state in the DFS as completely as possible.

13.2.1 Construction of the Decoherence-Free Target State

Quantum coherence can be easily damaged when the quantum state is subjected to factors such as spontaneous emission. We will design an external laser control field, called control I, in this subsection to construct a subspace free from the decoherence effect, which contains the expected target state $\rho_D = |\psi_D\rangle\langle\psi_D|$.

A Λ -type N level atomic system (Arimondo, 1996) is shown in Figure 13.3, in which $N - 1$ degenerate ground stable states are coupled to an excited state $|e\rangle$ by $N - 1$ separate external lasers with coupling constants g_i ($i = 1, \dots, N - 1$). Ω_i ($i = 1, \dots, N - 1$) denote the Rabi frequencies of the laser fields, Δ denotes the detuning, μ_{ie} ($i = 1, \dots, N - 1$) denote electric dipole moments, and E_i ($i = 1, \dots, N - 1$) denote the intensity of the laser fields. The dynamics of such a system obey the Lindblad-type Markovian master equation ($\hbar = 1$):

$$\begin{aligned} \dot{\rho} &= -i[H, \rho] + L(\rho) \\ L(\rho) &= \frac{1}{2} \sum_{i,j=1}^{N-1} \gamma_{ij} \left(2F_i \rho(t) F_j^\dagger - F_j^\dagger F_i \rho(t) - \rho(t) F_j^\dagger F_i \right) \end{aligned} \quad (13.28)$$

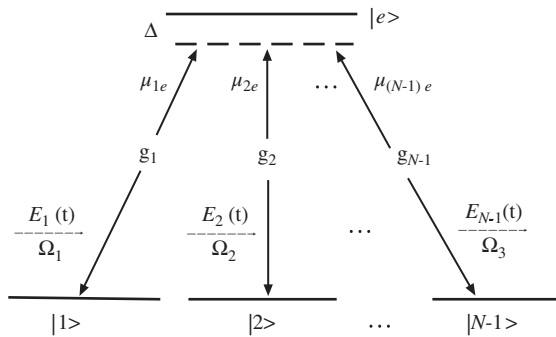


Figure 13.3 A Λ -type N -level atomic system under an external laser field

where H is the Hamiltonian of the system, L is the dissipation term, γ_{ij} ($i, j = 1, \dots, N - 1$) are decay rates, and $F_i = |i\rangle\langle e|$ ($i = 1, \dots, N - 1$) are the Lindblad operators, which denote the decay channel between states $|i\rangle$ and $|e\rangle$.

The main idea of the construction is as follows. Consider a Λ -type N -level atomic system (Equation 13.28) with spontaneous emission coherence induced by a vacuum-mode electromagnetic field, namely interaction between an atom and a quantized vacuum-mode field. The purpose of the control scheme is to introduce the external coherent field I in order to weaken the decoherence caused by the cross-coupled spontaneous emission coherence by adjusting the Rabi frequency of the coupling laser field to decouple the system state from the environment and prepare a decoherent-free subspace of the N -level atomic system.

The construction procedure of the decoherence-free target state ρ_D based on this idea can be implemented in the following order:

- According to the feature of the N -level atomic system after control field I is introduced, the master equation and the decoherence expression of the system are used to analyze the parameters of control field I.
- According to the decoherence expression and the condition of decoherence-free subspace, the relationship between the parameters of control field I and the decoherence-free state gives the control law of the coherent laser field I.

Assuming the $N - 1$ detunings between the carrier frequency of the $N - 1$ laser fields and their corresponding transition frequencies are equal, namely, $\Delta_i = \Delta$ ($i = 1, \dots, N - 1$), then the Hamiltonian of the system will be

$$H = \Delta|e\rangle\langle e| + \left(\sum_{j=1}^{N-1} \Omega_j |e\rangle\langle j| + H.c. \right) \quad (13.29)$$

where $H.c.$ is the Hermitian conjugate.

According to the definition of DFS (Lidar, Chuang, and Whaley, 1998; Ficek and Swain, 2005; Karasik *et al.*, 2008), the two determination conditions of DFS are

$$H|\psi_\alpha\rangle\langle\psi_\beta| = S, \alpha, \beta = 1, \dots, m \quad (13.30)$$

$$L|\psi_\alpha\rangle\langle\psi_\beta| = 0, \alpha, \beta = 1, \dots, m \quad (13.31)$$

where S is the DFS spanned by $\{|\psi_\alpha\rangle\langle\psi_\beta|\}$ ($\alpha, \beta = 1, \dots, n$) and m is the dimension of S . Equation 13.30 guarantees the completeness of the space, while Equation 13.31 guarantees that the system evolution under the operator bases $\{|\psi_\alpha\rangle\}$ is unitary.

Theorem 13.1 The open quantum system described in Equation 13.28 has the formulation of a decoherence-free state

$$|\psi_\alpha\rangle = \sum_{i=1}^N c_i |i\rangle \quad (13.32)$$

where the coefficients c_i ($i = 1, \dots, N - 1$) satisfy two conditions

$$\sum_{i=1}^{N-1} \Omega_i c_i = 0, \sum_{i=1}^{N-1} c_i^2 = 1 \quad (13.33)$$

where Ω_i ($i = 1, \dots, N - 1$) are the Rabi frequencies of the monochromatic laser field I.

Proof According to the definition of a state in DFS $F_j|\psi_\alpha\rangle = \lambda_j|\psi_\alpha\rangle$ ($j = 1, \dots, N - 1$), one can get

$$\lambda_2^* \lambda_1 = \langle\psi_\alpha|e\rangle\langle 2|1\rangle\langle e|\psi_\alpha\rangle = 0 \quad (13.34)$$

Assuming $\lambda_1 = 0$, then one can get $F_1|\psi_\alpha\rangle = 0$ from $F_1|\psi_\alpha\rangle = \lambda_1|\psi_\alpha\rangle$, which means that

$$|1\rangle\langle e|\psi_\alpha\rangle = 0 \quad (13.35)$$

Then one can substitute the expansion form $|\psi_\alpha\rangle = \sum_{i=1}^{N-1} c_i |i\rangle + c_N |e\rangle \left(\sum_{i=1}^{N-1} c_i^2 = 1 \right)$ of a state $|\psi_\alpha\rangle$ in the DFS into Equation 13.35. Let $c_N|1\rangle\langle e|e\rangle = 0$ make Equation 13.35 be true, therefore $c_N = 0$, and a state in the DFS can be formulated as

$$|\psi_\alpha\rangle = \sum_{i=1}^{N-1} c_i |i\rangle \quad (13.36)$$

Then, according to $\lambda_2|\psi_\alpha\rangle = F_2|\psi_\alpha\rangle = |2\rangle\langle e| \left(\sum_{i=1}^{N-1} c_i |i\rangle \right) = 0$, one can obtain $\lambda_2 = 0$. For the same reason, one can obtain $\lambda_i = 0$ ($i = 1, \dots, N - 1$).

The DFS is therefore linearly spanned by the $N - 1$ ground states $\{|1\rangle, \dots, |N - 1\rangle\}$. Because the DFS contains the states $|\psi_\alpha\rangle$ and $H|\psi_\alpha\rangle$, one has

$$|1\rangle\langle e|H|\psi_\alpha\rangle = 0 \quad (13.37)$$

From Equations 13.35 and 13.37, one can obtain

$$(|1\langle\langle e|H-H|1\rangle e|)|\psi_\alpha\rangle=0 \quad (13.38)$$

Substituting the Hamiltonian H shown in Equation 13.29 into Equation 13.38, one can obtain

$$|1\rangle\left(\sum_{i=1}^{N-1}\Omega_i\langle i|\psi_\alpha\rangle\right)=0 \quad (13.39)$$

Then, substituting the state form in DFS as Equation 13.36 into Equation 13.39, one can obtain the formulation of a decoherence-free state as Equation 13.32.

The proof is finished. ■

Remark 13.1 States in form of Equation 13.32 meet the two determining conditions of DFS in Equations 13.30 and 13.31, and are decoupled from the environment. From Equations 13.32 and 13.33 one can see that the decoherence-free states depend only on the Rabi frequency Ω_i ($i = 1, \dots, N - 1$) of the external laser field I, which only relates to the intensity E_i ($i = 1, \dots, N - 1$) and the direction of the field when the electric dipole moment μ_{ie} ($i = 1, \dots, N - 1$) is constant:

$$E_i = \frac{\Omega_i \hbar}{2\mu_{ie}}, i = 1, \dots, N - 1 \quad (13.40)$$

Therefore, if the laser is continuously adjustable, the decoherence-free state needed can be obtained by regulating laser field I, and the decoherence-free subspace can be built up. That state is free from decoherence caused by spontaneous emission and is set to be the expected target state ρ_D .

13.2.2 Design of the Lyapunov-Based Control Law for State Transfer

Comparing the form of a decoherence-free state in Equation 13.32, the expected target state ρ_D can be constructed to be a decoherence-free state through an external laser field I in Equation 13.40. Thus, the control task will be designing a set of control field II $\{f_n(t), n = 1, 2, \dots, F\}$ to make the system state evolve to the expected target state ρ_D in DFS and stay there. At this point, the Hamiltonian of the system is

$$H = H_0 + \sum_{n=1}^F f_n(t) H_n \quad (13.41)$$

where the free Hamiltonian H_0 has the form in Equation 13.29, H_n ($n = 1, 2, \dots, F$) are control Hamiltonians, and $f_n(t)$, $n = 1, 2, \dots, F$ are the control fields denoted as control field II.

The control field II $\{f_n(t)\}$ can be established by the Lyapunov function $V(\rho_D, \rho)$, which is selected as the form

$$V = 1 - \text{Tr}(\rho_D \rho) \quad (13.42)$$

where the physical meaning of $V(\rho_D, \rho)$ is the probability of system state $\rho(t)$ being the expected target state ρ_D . In order to make the control system stable, V should meet $V \geq 0$

and $\dot{V} \leq 0$. From Equation 13.42, one can see that $V \geq 0$ and its first-order time derivative is

$$\dot{V} = -\text{Tr} \{ \rho_D (-i [H_0, \rho] + L(\rho)) \} - \sum_{n=1}^F f_n(t) \text{Tr} \{ \rho_D [-iH_n, \rho] \} \quad (13.43)$$

One can choose n_0 satisfied with $\text{Tr} \{ \rho_D [-iH_{n_0}, \rho] \} \neq 0$, and set

$$f_{n_0}(t) = \frac{-\text{Tr} \{ \rho_D (-i [H_0, \rho] + L(\rho)) \}}{\text{Tr} \{ \rho_D [-iH_{n_0}, \rho] \}} \quad (13.44)$$

in which $f_{n_0}(t)$ offsets the effect of the free Hamiltonian H_0 and the dissipation term $L(\rho)$.

Then the other components of control field II can be set as

$$f_n(t) = K \text{Tr} \{ \rho_D [-iH_n, \rho] \}, K > 0, \text{ for } n \neq n_0 \quad (13.45)$$

Equations 13.44 and 13.45 can make $\dot{V} \leq 0$. These two equations are control laws meeting the conditions of the Lyapunov stability theorem.

From LaSalle's invariant principle (LaSalle and Lefschetz, 1961), the system will stop evolving when the value of the control field becomes zero. In other words, the closed-loop control system will converge to the largest state invariant set $e = \{\dot{V} = 0\}$, which can make the first derivative of the Lyapunov function \dot{V} zero. According to the expanded form of \dot{V} in Equation 13.43, the invariant set of the controlled system is the same set of states that satisfied $f_n(t) = 0$ ($n \neq n_0$) in Equation 13.45. Namely, states that meet the condition

$$\text{Tr} \{ \rho_D \rho H_n \} = \text{Tr} \{ \rho_D H_n \rho \}, \text{ or } n \neq n_0 \quad (13.46)$$

compose the LaSalle's invariant set.

Remark 13.2 According to the construction of DFS, the expected target state ρ_D is definitely in the largest invariant set. The largest invariant set we expected will only contain the expected target state ρ_D , or the system may evolve to the other states in the largest invariant set with a certain probability. Specific results and analysis are given in the next section.

13.2.3 Numerical Simulations and Results Analyses

In order to verify the effectiveness of the control laws proposed in Equations 13.44 and 13.45, we will do some numerical simulation experiments by taking a Λ -type four-level atomic system as an example, whose Hamiltonian has the form

$$H = H_0 + \sum_{n=1}^3 f_n(t) H_n \quad (13.47)$$

where the free Hamiltonian H_0 has the form in Equation 13.29. The control Hamiltonians are $H_n = |e\rangle\langle n| + |n\rangle\langle e|$ ($n = 1, 2, 3$).

Without loss of generality, the coupling constants g_i ($i = 1, \dots, N-1$) are parameterized as $g_1 = g \sin \theta \cos \phi$, $g_2 = g \sin \theta \sin \phi$, and $g_3 = g \cos \theta$, with $g = \sqrt{g_1^2 + g_2^2 + g_3^2}$. The excited

state $|e\rangle$ decays to the three degenerate ground states with rates γ_1 , γ_2 , and γ_3 , respectively. The two degenerate dark states of the free Hamiltonian H_0 are

$$\begin{aligned}|D_1\rangle &= \cos\phi|2\rangle - \sin\phi|1\rangle \\ |D_2\rangle &= \cos\theta(\cos\phi|1\rangle + \sin\phi|2\rangle) - \sin\theta|3\rangle\end{aligned}\quad (13.48)$$

The DFS is spanned by $\{|D_1\rangle, |D_2\rangle\}$. State $|\psi_D\rangle = \sqrt{p_1}|D_1\rangle + \sqrt{1-p_1}|D_2\rangle$ in DFS is a decoherence-free state that can be treated as the expected target state $|\psi_D\rangle$.

In order to demonstrate the effect of the control law we designed, the initial state $|\psi_0\rangle$ of the state transfer control is set to be the excited state $|\psi_0\rangle = |e\rangle$. The three decay rates are set to be equivalent, $\gamma_1 = \gamma_2 = \gamma_3 = \gamma$. The other parameters are chosen to be $\Delta = 3$, $g = 5$, $\phi = \pi/4$, $\theta = \pi/3$, $f_n(0) = 0.01$, and $\Delta t = 10^{-2}$ a.u., respectively. The experimental time is $t_f = 300$ a.u.

First, we simulate the transfer process from the initial state $|\psi_0\rangle = |e\rangle$ to the expected target state $|\psi_D\rangle = \sqrt{p_1}|D_1\rangle + \sqrt{1-p_1}|D_2\rangle$ ($p_1 = 0.1$). We set the decay rates $\gamma_1 = \gamma_2 = \gamma_3 = 0.1$ and the proportional coefficient $K = 1$. $Tr\left\{\rho_D\left[-iH_{n_0}, \rho\right]\right\} \neq 0$ is tenable when $n_0 = 1, 2, 3$. Figure 13.4 shows the experimental results of the state transfer, where Figure 13.4a is the curve of the Lyapunov function V , Figure 13.4b is the probability of the system state transferring to the DFS with $n_0 = 1$, Figure 13.4c is the probability of the system state transferring to the expected target state ρ_D with $n_0 = 1$, and Figure 13.4d displays the probability of the system state transferring to the expected target state ρ_D with $n_0 = 2$. In order to show the effect of the Lyapunov-based control method, the result of a comparative experiment is displayed in Figure 13.4e, where the system makes a free evolution without the control field we designed.

From Figure 13.4 one can see that the probabilities of the system state terminally evolving to the DFS and the expected target state ρ_D are 100% (see Figure 13.4b) and 98% (see Figure 13.4c) with $n_0 = 1$, respectively. Comparing Figure 13.4a–e, one can see that the Lyapunov-based control law we designed can transfer the initial state to the expected target state and keep it there. When $n_0 = 2$, the probability for the system state evolving to ρ_D is only 50% (see Figure 13.4d), therefore the result of transition probability depends on the choice of n_0 . We will derive the best option of n_0 later.

We already know that $f_{n_0}(t)$ offsets the effect of the free Hamiltonian H_0 and the dissipation term $L(\rho)$, while $f_n(t)$ ($n \neq n_0$) transfers the population from state $|e\rangle$ to state $|n\rangle$. The system state evolves into a superposition of states $|2\rangle$ and $|3\rangle$ when $n_0 = 1$, it evolves into a superposition of states $|1\rangle$ and $|3\rangle$ when $n_0 = 2$, and it evolves into a superposition of states $|1\rangle$ and $|2\rangle$ when $n_0 = 3$. The best choice of n_0 therefore corresponds to the smallest probability distribution of $|\psi_D\rangle$ among $|1\rangle$, $|2\rangle$, and $|3\rangle$. The expected target state $|\psi_D\rangle$ in Figure 13.4 is $|\psi_D\rangle = 0.1118|1\rangle + 0.5590|2\rangle - 0.8216|3\rangle$, in which the smallest probability distribution among $|1\rangle$, $|2\rangle$, and $|3\rangle$ is $|1\rangle$. Consequently, the transition probability of 98% with $n_0 = 1$ (see Figure 13.4c) is much better than 50% with $n_0 = 2$ (see Figure 13.4d), namely, $n_0 = 1$ effectively improves the state transition probability.

Substituting the expected target state $|\psi_D\rangle = \sqrt{p_1}|D_1\rangle + \sqrt{1-p_1}|D_2\rangle$ into Equation 13.46 gives

$$p_1\langle D_1 | [-iH_n, \rho] | D_1 \rangle + (1-p_1)\langle D_2 | [-iH_n, \rho] | D_2 \rangle = 0, \text{ for } n \neq n_0 \quad (13.49)$$

Clearly, Equation 13.46 is valid when the system state is $\rho = |D_1\rangle\langle D_1|$ or $\rho = |D_2\rangle\langle D_2|$. Accordingly, $\{|D_1\rangle, |D_2\rangle\}$ spans LaSalle's invariant set, namely DFS. The control laws we

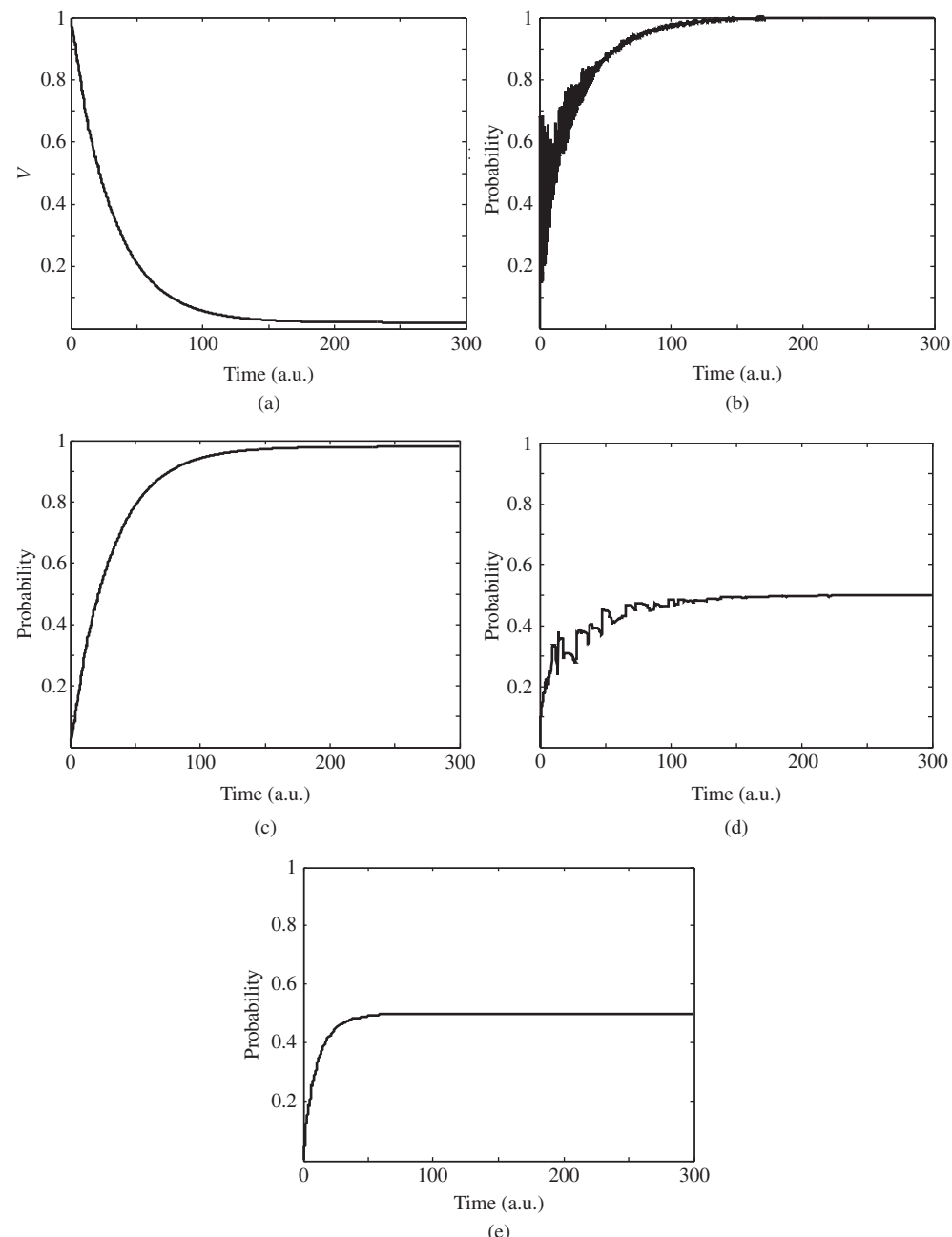


Figure 13.4 The experimental results of open quantum state transfer: (a) Lyapunov function V with $n_0 = 1$, (b) the probability of the system state transferring to the DFS with $n_0 = 1$, (c) the probability of the system state transferring to the ρ_D with $n_0 = 1$, (d) the probability of the system state transferring to the ρ_D with $n_0 = 2$, and (e) free evolution without control fields

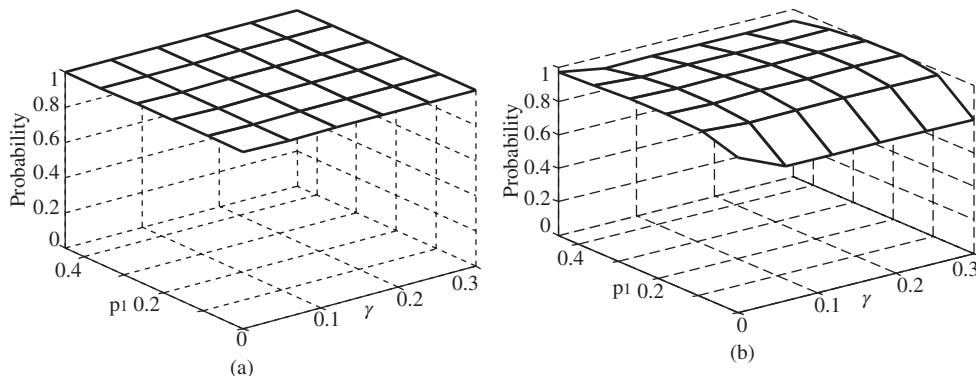


Figure 13.5 The experimental results of open quantum state transfer regulated by p_1 and γ : (a) the probability of the system state transferring to the DFS and (b) the probability of the system state transferring to the ρ_D

designed in Equations 13.44 and 13.45 drive the system state $\rho(t)$ into the DFS close to the point of the decoherence-free target state ρ_D .

Then, we change the value of p_1 in the expected target state $|\psi_D\rangle = \sqrt{p_1}|D_1\rangle + \sqrt{1-p_1}|D_2\rangle$ and the decay rate γ with the experimental time $t_f = 300\text{a.u.}$. n_0 is chosen to correspond to the smallest probability distribution of $|\psi_D\rangle$ among $|1\rangle$, $|2\rangle$, and $|3\rangle$. Figure 13.5 shows the experimental results of transfer progress regulated by p_1 and γ , where Figure 13.5a shows the probabilities for the DFS and Figure 13.5b shows the probabilities for the expected target state ρ_D . From Figure 13.5 one can see that the system states almost evolve into DFS after the experimental time $t_f = 300\text{a.u.}$, while the probabilities for the expected target state ρ_D range from 80 to 100%. The probabilities for the DFS will achieve 100% if the experimental time t_f extended enough. The transfer probability of the expected target state ρ_D is relevant to the value of p_1 and γ . When $\gamma = 0$, there is no spontaneous decay and the state transfer is completely manipulated by the control laws we designed. Therefore, the effect of state transfer is better than the results when $\gamma \neq 0$. For most cases with $\gamma \neq 0$, $f_{n_0}(t)$ is used to offset the effect of the free Hamiltonian H_0 and the dissipation term $L(\rho)$, without inducing state transfer on its direction. Thus, the probability of the expected target state ρ_D cannot achieve 100% as long as the smallest probability distribution of $|\psi_D\rangle$ among $|1\rangle$, $|2\rangle$, and $|3\rangle$ is non-zero. Substituting Equation 13.48 into the expected target state $|\psi_D\rangle = \sqrt{p_1}|D_1\rangle \pm \sqrt{1-p_1}|D_2\rangle$, one can get

$$|\psi_D\rangle = \left(\pm \sqrt{1-p_1} \cos \theta \cos \phi - \sqrt{p_1} \sin \phi \right) |1\rangle + \left(\pm \sqrt{1-p_1} \cos \theta \sin \phi + \sqrt{p_1} \cos \phi \right) |2\rangle \pm \sqrt{1-p_1} \sin \theta |3\rangle \quad (13.50)$$

It can be derived from Equation 13.50 that ρ_1 in form of

$$p_1 = 1 \text{ or } \frac{\cos^2 \theta \cos^2 \phi}{\sin^2 \phi + \cos^2 \theta \cos^2 \phi} \text{ or } \frac{\cos^2 \theta \sin^2 \phi}{\cos^2 \phi + \cos^2 \theta \sin^2 \phi} \quad (13.51)$$

can make the smallest probability distribution of $|\varphi_D\rangle$ among $|1\rangle$, $|2\rangle$, and $|3\rangle$ be zero. Then, the control field designed plays the role completely, and the largest transition the transfer probability of the expected target state ρ_D achieves 100%.

13.3 Control of Quantum States Based on the Lyapunov Method in Decoherence-Free Subspaces

In this section, we aim to design a controller by the Lyapunov method to steer the open quantum system to any desired pure target state in DFS.

The open quantum system is described by the Lindblad master equations (LMEs), and DFS has frequently been defined as a collection of states for which the dissipative or decoherence part of the Markovian master equation is zero. In the scheme, we first choose the Lyapunov function as the average of an observable operator, then derive the control laws in the interaction picture. In contrast to the closed system, we design a special control field to cancel decoherence terms in the first derivative of the Lyapunov function. In order to study the convergence of the control system transformed into the interaction picture, which is a non-autonomous system, Barbalat's lemma is introduced to analyze the largest invariant set, which relies on the structure of the observable operator. To give the target state asymptotic stability, we give a sufficient condition about the observable operator to achieve the convergence of any target state. In light of this condition, we provide a method to construct the observable operator via Schmidt orthogonalization.

13.3.1 Problem Description

The state of a quantum system defined on an N -dimensional Hilbert space can be represented by a density operator ρ , that is, an $n \times n$ positive Hermitian operator with unit trace. Under certain conditions the evolution of the density operator under the interaction with the environment can be described by a quantum dynamical semigroup and satisfies an LME ($\hbar = 1$) (Lindblad, 1976):

$$\dot{\rho}(t) = -i[H, \rho] + \mathcal{L}(\rho) \quad (13.52a)$$

$$\mathcal{L}(\rho) = \frac{1}{2} \sum_{m=1}^M \lambda_m \left([L_m, \rho L_m^\dagger] + [L_m \rho, L_m^\dagger] \right) \quad (13.52b)$$

$$H = H_0 + \sum_{n=1}^F f_n(t) H_n \quad (13.52c)$$

where H_0 is a field-free Hamiltonian, which is a Hermitian diagonal matrix, H_n is a control Hamiltonian, and $f_n(t)$ is a control field. $\mathcal{L}(\rho)$ is the decoherence term, characterizing the interaction between the system and the environment. The quantities λ_m are positive and time-independent parameters that characterize the intensity of the decoherence effect. The quantities L_m are the Lindblad operators. Equations 13.52a–c have all the required properties of a physical density matrix at all times (Baumgartner, Narnhofer, and Thirring, 2008).

Throughout this section, we work in an orthonormal basis of energy eigenvectors, that is, H_0 is diagonal and can be expressed as $H_0 = \sum_{j=1}^N E_j |j\rangle\langle j|$, where $|j\rangle, j = 1, 2, \dots, N$ are the energy levels, and the eigenvalues E_j represent the energy values associated with the $|j\rangle$ values of the system, while $\omega_{jl} = E_j - E_l$ represents the Bohr frequency (transition frequency) between the energy levels $|j\rangle$ and $|l\rangle$. Furthermore, we give the following definition.

Definition 13.1 System Equations 13.52a–c are called strongly regular if all the transition frequencies (differences of pairs of energy levels) are different, viz. $\omega_{jk} \neq \omega_{pq}$, $(j, k) \neq (p, q)$, where $\omega_{jk} = E_j - E_k$ and E_j is an eigenvalue of H_0 .

In the context of LMEs, the DFS has frequently been defined as a collection of states for which dissipative (decoherence) part of the Markovian master equation is zero, that is, $\mathcal{L}(\rho) = 0$, leading to the following conditions for the DFS (Karasik *et al.*, 2008).

Definition 13.2 For the system in Equations 13.52a–c, a subspace

$$\mathcal{H}_{DFS} = \text{span} \{|\psi_1\rangle, |\psi_2\rangle, \dots, |\psi_D\rangle\} \quad (13.53)$$

is a DFS for all time t if and only if (i) \mathcal{H}_{DFS} is invariant under H_0 and (ii) $L_m |\psi_k\rangle = c_m |\psi_k\rangle$ and $\Gamma |\psi_k\rangle = g |\psi_k\rangle$ for all $m = 1, 2, \dots, M$ and $k = 1, 2, \dots, D$ with $g = \sum_{m=1}^M \lambda_m |c_m|^2$ and $\Gamma = \sum_{m=1}^M \lambda_m L_m^\dagger L_m$.

Remark 13.3 In the work, we assume DFS is non-trivial, that is, the DFS (Equation 13.53) is spanned by at least two bases. Definition 13.2 gives the sufficient and necessary condition to judge whether a given subspace is DFS, rather than guide us to construct the DFS. Nonetheless, one can obtain the DFS by intuition for some simple system. An example is a three-level Λ -type system with the excited state $|3\rangle$ decaying to two ground states $|1\rangle$ and $|2\rangle$. The Lindblad operator can be expressed as $L_1 = |1\rangle\langle 3|, L_2 = |2\rangle\langle 3|$. Then it is easy to verify that the DFS is $\mathcal{H}_{DFS} = \text{span} \{|1\rangle, |2\rangle\}$. We do not focus on how to construct the DFS and assume the DFS does exist and is known in our work.

Then the target state is the superposition of basic vectors in DFS, that is,

$$\phi_f = \sum_{d=1}^D c_d |\psi_d\rangle, \sum_{d=1}^D |c_d|^2 = 1 \quad (13.54)$$

Our control problem could be stated as follows: for the system in Equations 13.52a–c with subspace as in Equation 13.53 as its DFS, design control laws $f_n(t), n = 1, 2, \dots, F$ to steer the system from an arbitrary initial state ψ_0 to a desired target state shown in Equation 13.54.

Remark 13.4 The target states in Equation 13.54 represent all the pure states in DFS. The initial state being arbitrary means the target state is globally attractive, which require us to analyze the convergence of the system. The control laws are designed based on the Lyapunov theory.

13.3.2 Control Design in the Interaction Picture

In this subsection we mainly derive the control laws. To reduce the difficulty and complexity of the control design, the system will be transformed into an interaction picture.

By transforming the system (Equations 13.52a–c) into the interaction picture, viz. setting $\rho' = e^{iH_0 t} \rho e^{-iH_0 t}$, the LME (Equations 13.52a–c) can be written as

$$\dot{\rho}' = \left[\sum_{j=1}^F A_j(t) f_j(t), \rho' \right] + \mathcal{L}'(\rho') \quad (13.55a)$$

$$\mathcal{L}'(\rho') = \frac{1}{2} \sum_{m=1}^M \lambda_m \left([L'_m, \rho' L'_m^\dagger] + [L'_m \rho', L'_m^\dagger] \right) \quad (13.55b)$$

where $A_j(t) = -ie^{iH_0 t} H_j e^{-iH_0 t}$ and $L'_m = e^{iH_0 t} L_m e^{-iH_0 t}$ are the control Hamiltonian and the Lindblad operator, respectively, in the interaction picture. It can be verified that such a transformation does not change the population distribution of the system state, therefore ρ is equivalent to ρ' and we will omit the label “‘” in the following text for convenience.

Consider the Lyapunov function as the average quality of an observable operator P

$$V(\rho) = \text{tr}(P\rho) \quad (13.56)$$

where P is a positive definite Hermitian operator to be constructed. The basic idea of the Lyapunov control is to design the control functions such that a suitably chosen Lyapunov function is monotonically decreasing, that is, the first derivative of the Lyapunov function is negative semi-definite. Then we can establish the control fields. The derivation of the Lyapunov function is

$$\dot{V}(\rho(t)) = \sum_{j=1}^F f_j \text{tr}([\rho(t), P] A_j) + \text{tr}(P \mathcal{L}(\rho)) \quad (13.57)$$

To make $\dot{V}(\rho) \leq 0$, the following control laws can be derived:

$$f_{j_0}(t) = -\frac{\text{tr}(\mathcal{L}(\rho) P)}{\text{tr}([\rho(t), P] A_{j_0})}, j_0 \in \{1, 2, \dots, F\} \quad (13.58)$$

$$f_j(t) = -\kappa_j(t) \text{tr}([\rho(t), P] A_j(t)), \kappa_j(t) > 0, j \neq j_0 \quad (13.59)$$

where $\kappa_j(t)$ is a control gain that is used to adjust the convergent speed of the system. It is usually chosen as a constant.

Remark 13.5 The control field $f_{j_0}(t)$ is specified to cancel $\text{tr}(P \mathcal{L}(\rho))$ in \dot{V} , and it contributes to the dynamics of the open system. Additionally, this special field must always exist before the system reaches the target state otherwise one cannot ensure \dot{V} is negative semi-definite. Thus the stability may not be guaranteed. To find $f_{j_0}(t)$, $\text{tr}([\rho(t), P] A_{j_0}) \neq 0$ is required. This can be done by construction of the observable operator P and control Hamiltonians.

Remark 13.6 One can verify that all the designed fields are real. The definition of $\mathcal{L}(\rho)$ shows that it is Hermitian, so $\text{tr}(\mathcal{L}(\rho) P)$ is real since P is also a Hermitian operator. Note that $\rho(t)$

and A_{j_0} are Hermitian, so $\text{tr}([\rho(t), P]A_{j_0})$ is also real. Thus, $f_{j_0}(t)$ is real. By the same reasoning, we can show that all the control fields are real as long as the control Hamiltonians are Hermitian.

Generally, control laws (Equations 13.58 and 13.59) only guarantee the controlled system stabilized, rather than convergent. In other words, the control laws could steer the system to some local extreme point of some evolution trajectories and stay on it, instead of to the minimum point that usually is the target state. In order to solve such a problem, the observable operator P will be designed and conditions on control Hamiltonians will be proposed in the next section under certain assumptions.

13.3.3 Construction of P and Convergence Analysis

In this subsection, we first derive the largest invariant set of the system. Then we give a sufficient condition that makes the target state be global asymptotic stable. Finally, according to this condition we provide a method to construct the operator P via Schmidt orthogonalization.

1) Largest Invariant Set

In the following, we analyze the convergence of the system. By LaSalle's invariant principle, the autonomous dynamical system converges to an invariant set defined by $\mathcal{R} = \{\rho : \dot{V}(\rho) = 0\}$. However, in the present situation the controlled system becomes non-autonomous in the interaction picture, rendering the application of the invariance principle problematic. One can derive the largest invariant set by Barbalat's lemma (Lemma 7.2).

Note that the operators ρ and P are both of finite dimensions, and the Lyapunov function $V(\rho) = \text{tr}(P\rho)$ is lower bounded. It is evident that $\dot{V}(\rho, t)$ is negative semi-definite under the control laws. The second derivative of the Lyapunov function can be derived as

$$\ddot{V}(\rho, t) = \sum_j \{f_j \text{tr}([\dot{\rho}(t), P]A_j(t)) + f_j \text{tr}([\rho(t), P]\dot{A}_j(t))\} + \text{tr}(P\mathcal{L}(\dot{\rho})) \quad (13.60)$$

Equation 13.60 is bounded when the inputs are bounded. Thus, $\dot{V}(\rho, t)$ is uniformly continuous in time. According to Lemma 7.2, the first derivative of the Lyapunov function converges to zero, viz., $\dot{V}(\rho(\infty), \infty) = 0$. This indicates that the control system will converge to some state that makes $\dot{V} = 0$.

Let \mathcal{R} be the set of critical points on any dynamic trajectory, viz.,

$$\mathcal{R} \equiv \{\rho : \text{tr}([\rho, P]A_j(t)) = 0, \forall j \neq j_0, t\} \quad (13.61)$$

Then the system state converges to the largest invariant set in \mathcal{R} . In the following, we deduce the largest invariant set \mathcal{E} in \mathcal{R} .

Assume the system evolves under control laws (Equations 13.58 and 13.59) from an initial state ρ_0 and reaches a critical point in \mathcal{R} at time t_1 , that is, $\rho(t_1) \in \mathcal{R}$. At this time

$$f_j(t_1) = -\kappa_j(t_1) \text{tr}([\rho(t_1), P]A_j(t_1)) = 0 \quad (13.62)$$

and the evolution equation of the state turns to

$$\dot{\rho}(t_1) = [f_{j0}(t_1), \rho(t_1)] + \mathcal{L}(\rho(t_1)) \quad (13.63)$$

If $\rho(t_1)$ is a point of \mathcal{E} , then $\forall t \geq t_1$, $\rho(t) \in \mathcal{R}$ holds, which implies $\dot{\rho}(t_1) = 0$ based on Equations 13.62 and 13.63. This requires $\mathcal{L}(\rho(t_1)) = 0$. As a result, the largest invariant set \mathcal{E} in \mathcal{R} is

$$\mathcal{E} = \{\rho(t_1) : \text{tr}([\rho(t_1), P] A_j(t_1)) = 0, \mathcal{L}(\rho(t_1)) = 0, \forall j \neq j_0, \forall t_1\}$$

It is easy to verify the largest invariance of \mathcal{E} (D'Alessandro, 2008). Then the following theorem is established.

Theorem 13.2 The system in Equation 13.53 with the control laws in Equations 13.58 and 13.59 converges to the set \mathcal{E} given by

$$\mathcal{E} = \mathcal{E}_1 \cap \mathcal{E}_2, \mathcal{E}_1 = \{\rho : \text{tr}([\rho, P] A_j(t)) = 0, \forall j \neq j_0, t\}, \mathcal{E}_2 = \{\rho : \mathcal{L}(\rho) = 0\} \quad (13.64)$$

Remark 13.7 Obviously, if the system is closed, that is, the decoherence term $\mathcal{L}(\rho)$ vanishes, the largest invariant set is reduced to \mathcal{E}_1 . This set is the same as the largest invariant set in the Schrödinger picture. This implies that considering the problem in the interaction picture is equivalent to that in the Schrödinger picture.

2) A Sufficient Condition for Convergence

The target state being globally asymptotic stable means the largest invariant set \mathcal{E} written by Equation 13.64 only includes the target state. However, the set \mathcal{E} is, in general, not empty and of finite dimension, indicating that it is difficult to control it from an arbitrary initial state to a given target state. To reduce \mathcal{E} , we give some assumptions on control Hamiltonians and Lindblad terms. Then we give a sufficient condition about the operator P to make the system converge to the target state.

Assumption 13.1 The system in Equations 13.52a–c is strongly regular.

Assumption 13.2 For $\forall j, k, \exists l \in \{1, 2, \dots, F\}$, such that $(H_l)_{jk} \neq 0$ holds.

Environmentally induced decoherence (e.g., spontaneous emission, dephasing, relaxation processes, etc.) can have a significant impact on system dynamics (e.g., desired excitations, product selectivity, etc). The Lindblad operators in Equation 13.52b can be expressed phenomenologically as (Zhu and Rabitz, 2003)

$$L_{jk} = |j\rangle\langle k| \quad (13.65)$$

This it is transformed to $L'_{jk} = e^{-i\omega_{jk}t} L_{jk}$ in the interaction picture. It can be verified that $\mathcal{L}'(\rho') = \mathcal{L}(\rho')$, therefore the bases of the DFS are invariant under the transformation of the interaction picture, showing that the DFS is invariant.

Assumption 13.3 The DFS of the system in Equations 13.52a–c is known and spanned by D orthonormal eigenstates of H_0 , that is

$$\mathcal{H}_{DFS} = \text{span} \{ |d_1\rangle, |d_2\rangle, \dots, |d_D\rangle \}, D < N, \text{ and } |d_j\rangle \in \{|1\rangle, |2\rangle, \dots, |N\rangle\}, \text{ for } j = 1, 2, \dots, D \quad (13.66)$$

Remark 13.8 Assumption 13.1 says that the transition energies between two different levels are clearly identified. In principle, it is possible to use tailored radio-frequency pulses to selectively transfer population between two levels. Assumption 13.2 says that all the levels are directly coupled. Assumption 13.3 is possible if the Lindblad operators are of the form in Equation 13.65. Under the condition of Assumption 13.3, the target state is the superposition of eigenstates of the free Hamiltonian, that is,

$$\phi_f = \sum_{j=1}^D c_j |d_j\rangle, \sum_{j=1}^D |c_j|^2 = 1.$$

Lemma 13.1 Suppose Assumptions 13.1 and 13.2 are met. Then the set \mathcal{E}_1 in Theorem 13.2 can be redefined as

$$\mathcal{E}_1 = \{\rho : [\rho, P] = 0\} \quad (13.67)$$

Proof First we prove that the state ρ in \mathcal{E}_1 makes $[\rho, P]$ be diagonal.

Applying $e^A B e^{-A} = \sum_{n=0}^{\infty} \frac{[A^{(n)}, B]}{n!}$ to Equation 13.64 yields

$$\begin{aligned} \text{tr}([\rho, P] A_j(t)) &= \text{tr}([\rho, P] e^{iH_0 t} H_j e^{-iH_0 t}) = 0 \iff \text{tr}\left(\sum_{n=0}^{\infty} \frac{1}{n!} [(iH_0 t)^{(n)}, H_j] [\rho, P]\right) = 0 \\ &\iff \sum_{n=0}^{\infty} \frac{i^n t^n}{n!} \text{tr}([H_0^{(n)}, H_j] [\rho, P]) = 0 \end{aligned} \quad (13.68)$$

where $[H_0^{(n)}, H_j] = \underbrace{[H_0, [H_0, \dots, [H_0, H_j]]]}_{n \text{ times}}$ and in particular $[H_0^{(0)}, H_j] = H_j$.

Considering the linear independence of time sequences $1, t, t^2, \dots$, Equation 13.68 can be written as

$$\text{tr}([H_0^{(n)}, H_j] [\rho, P]) = 0, n = 0, 1, 2, \dots \text{ and } j = 1, 2, \dots, F, j \neq j_0 \quad (13.69)$$

Let us denote the (j, k) th element of matrix A by A_{jk} . Noting that H_0 is diagonal, one can calculate $[H_0^{(n)}, H_j]$ as

$$[H_0^{(n)}, H_j] = ((E_r - E_l)^n (H_j)_{rl}) = (\omega_{rl}^n (H_j)_{rl}), r, l = 1, 2, \dots, N \quad (13.70)$$

Let $T = [\rho, P]$. Substituting Equation 13.70 into Equation 13.69 yields

$$\sum_{r,l=1}^N \omega_{rl}^n (H_j)_{rl} T_{lr} = 0, n = 0, 1, 2, \dots, j = 1, 2, \dots, F, j \neq j_0 \quad (13.71)$$

Considering the Hermitian property of H_j and T , Equation 13.71 can be further written as

$$\sum_{r < l} \left(\omega_{rl}^n (H_j)_{rl} T_{lr} - \omega_{lr}^n (H_j)_{rl}^* T_{lr}^* \right) = 0 \quad (13.72)$$

When n is even, Equation 13.72 can be reduced to

$$\sum_{r < l} \operatorname{Im} \left(\omega_{rl}^n (H_j)_{rl} T_{lr} \right) = 0, n = 0, 2, \dots, j = 1, 2, \dots, F, j \neq j_0 \quad (13.73)$$

When n is odd, Equation 13.72 can be reduced to

$$\sum_{r < l} \operatorname{Re} \left(\omega_{rl}^n (H_j)_{rl} T_{lr} \right) = 0, n = 1, 3, \dots, j = 1, 2, \dots, F, j \neq j_0 \quad (13.74)$$

Denote

$$\xi_j = \begin{bmatrix} (H_j)_{12} T_{21} \\ \vdots \\ (H_j)_{1N} T_{N1} \\ (H_j)_{23} T_{32} \\ \vdots \\ (H_j)_{2N} T_{N2} \\ \vdots \\ (H_j)_{N-1,N} T_{N,N-1} \end{bmatrix}, \Lambda = \operatorname{diag} \{ \omega_{12}, \dots, \omega_{1N}, \omega_{23}, \dots, \omega_{2N}, \dots, \omega_{N-1,N} \}$$

$$\Gamma = \begin{bmatrix} 1 & \cdots & 1 & 1 & \cdots & 1 & \cdots & 1 \\ \omega_{12}^2 & \cdots & \omega_{1N}^2 & \omega_{23}^2 & \cdots & \omega_{2N}^2 & \cdots & \omega_{N-1,N}^2 \\ \omega_{12}^4 & \cdots & \omega_{1N}^4 & \omega_{23}^4 & \cdots & \omega_{2N}^4 & \cdots & \omega_{N-1,N}^4 \\ \vdots & \ddots & \vdots & \vdots & \ddots & \vdots & \ddots & \vdots \\ \omega_{12}^{N(N-1)-2} & \cdots & \omega_{1N}^{N(N-1)-2} & \omega_{23}^{N(N-1)-2} & \cdots & \omega_{2N}^{N(N-1)-2} & \cdots & \omega_{N-1,N}^{N(N-1)-2} \end{bmatrix}$$

Then, Equations 13.73 and 13.74 are equivalent to

$$\Gamma \operatorname{Im} (\xi_j) = 0, j = 1, 2, \dots, F, j \neq j_0 \quad (13.75)$$

and

$$\Gamma \Lambda \operatorname{Re} (\xi_j) = 0, j = 1, 2, \dots, F, j \neq j_0 \quad (13.76)$$

respectively. According to Assumption 13.1, both Λ and Γ are non-singular square matrices of order $[N(N-1)]/2$. Thus, Equations 13.75 and 13.76 imply

$$\xi_j = 0, j = 1, 2, \dots, F, j \neq j_0 \quad (13.77)$$

that is,

$$(H_j)_{rl} T_{lr} = 0, r, l = 1, 2, \dots, N, l < r, j = 1, 2, \dots, F, j \neq j_0 \quad (13.78)$$

According to Assumption 13.2, $T_{lr} = 0$, $l < r$ holds. In other words, $[\rho, P] = D$, where D is a diagonal matrix with $(D)_{jj} = d_j$.

P is then transformed to a diagonal matrix D_f by a unitary transformation U , that is, $[U\rho U^+, D_f] = UDU^+$. Consider the diagonal elements:

$$\sum_k d_k |(U)_{jk}|^2 = 0 \quad (13.79)$$

Then, $d_k = 0$, viz., $[\rho, P] = 0$.

The proof is finished. ■

Remark 13.9 In a closed quantum system, the initial state and the target state have the same spectrum because this is a necessary condition for the target state to be reachable under unitary evolution. By contrast, in the open quantum system this condition needs not be satisfied, which leads to the complexity of largest invariant set. For example, in Section 5.1 the largest invariant set comprises $N!$ discrete states, whereas \mathcal{E}_1 in Equation 13.67 represents a continuous convex set.

Lemma 13.2 Suppose A and B are Hermitian matrices of order N . They commute, that is, $[A, B] = 0$, if and only if A and B have the same eigenstates (Zeng, 2007), that is,

$$A = \sum_{j=1}^N A_j |\mu_j\rangle\langle\mu_j|, B = \sum_{j=1}^N B_j |\mu_j\rangle\langle\mu_j| \quad (13.80)$$

In 2010 Wang *et al.* proved the following lemma via variational calculus.

Lemma 13.3 With the constraint condition $\text{tr}(\rho) = 1$ and $\rho \geq 0$, the set of critical points of the Lyapunov function $V = \text{tr}(\rho P)$ is given by the normalized eigenvectors of P . The eigenvectors with the largest eigenvalue are the maxima of V , the eigenvectors with the smallest eigenvalue are the minima, and all others are saddle points.

This lemma is of importance in theory. According to this lemma, if we set the eigenvector with the smallest eigenvalue as the target state, then the system is likely to be steered to the target state because the Lyapunov function monotonically decreases. On the other hand, the target state is stable because the target state is the minima. This idea will be used to construct P .

An Hermitian operator P has a unique spectral decomposition $P = \sum_{k=1}^N p_k |\phi_k\rangle\langle\phi_k|$, where p_k is the eigenvalue of P and $|\phi_k\rangle$ is the corresponding eigenstate. To determine P , the key is to design its eigenstates and eigenvalues. According to Lemma 13.3, we can set one eigenstate of P to be the target state and the corresponding eigenvalue is the minimum. The other eigenstates and eigenvalues can be constructed as follows.

Theorem 13.3 Suppose all the three assumptions are satisfied if the operator P has the following structure

$$P = \sum_{j=1}^{N-1} p_j |\psi_j\rangle\langle\psi_j| + p_0 |\psi_f\rangle\langle\psi_f|, \text{ for } \langle\psi_j|\psi_f\rangle = \delta_{jk} \text{ and } 0 < p_0 < p_j, p_j \neq p_k \text{ for } j \neq k \quad (13.81)$$

where the target state $|\psi_f\rangle \in \mathcal{H}_{DFS}$ and the other eigenstates $|\psi_j\rangle \notin \mathcal{H}_{DFS}$. The system in Equation 13.53 converges to $\mathcal{E} = \left\{ \rho : \rho = |\psi_f\rangle\langle\psi_f| \right\}$ under the control laws (Equations 13.58 and 13.59).

Proof It is equivalent to prove that the largest invariant set is $\mathcal{E} = \left\{ \rho : \rho = |\psi_f\rangle\langle\psi_f| \right\}$.

On the one hand, based on Lemmas 13.1 and 13.2, and Equation 13.81, any state of \mathcal{E}_1 has the structure

$$\mathcal{E}_1 = \left\{ \rho : \sum_{j=1}^{N-1} \alpha_j |\psi_j\rangle\langle\psi_j| + \alpha_0 |\psi_f\rangle\langle\psi_f|, \sum_{k=0}^{N-1} \alpha_k = 1 \right\} \quad (13.82)$$

On the other hand, the state of \mathcal{E}_2 can be expressed as

$$\rho = \sum_j c_j |\varphi_j\rangle\langle\varphi_j|, \text{ where } |\varphi_j\rangle = \sum_{k=1}^D d_{jk} |d_k\rangle \quad (13.83)$$

because $|\psi_j\rangle \notin \mathcal{H}_{DFS}$ and $\langle\psi_j|\psi_f\rangle = \delta_{jk}$, thus $\mathcal{E}_1 \cap \mathcal{E}_2 = \left\{ \rho : \rho = |\psi_f\rangle\langle\psi_f| \right\}$. Theorem 13.3 is proven. ■

Remark 13.10 Theorem 13.3 suggests how to construct operator P to make the target state be a globally asymptotically stable state. However, it just gives a construction principle of P and apart from $|\psi_f\rangle$, the other $N - 1$ eigenstates of P are still unclear.

3) Construction of P via Schmidt Orthogonalization

From Theorem 13.3, all the eigenstates of P are orthogonal. Schmidt orthogonalization provides us with a powerful tool to obtain orthogonal states. Utilizing it, the steps of the construction of P are as follows:

1. Select N linearly independent vectors as $\phi_0, \phi_1, \dots, \phi_{N-1}$, where $\phi_0 = |\psi_f\rangle$ and $\phi_1, \dots, \phi_{N-1} \notin \mathcal{H}_{DFS}$. For instance, we can choose

$$\phi_j = \sqrt{N-D+1} \left(|d_j\rangle + \sum_{|k\rangle \notin \mathcal{H}_{DFS}} |k\rangle \right), j = 1, 2, \dots, D \quad (13.84)$$

$$\phi_j = |k\rangle, |k\rangle \notin \mathcal{H}_{DFS}, j = D+1, D+2, \dots, N-1 \quad (13.85)$$

It is evident that $\phi_1, \dots, \phi_{N-1} \notin \mathcal{H}_{DFS}$ and we can verify $\text{rank}(\phi_0, \phi_1, \dots, \phi_{N-1}) = N$, that is, the N vectors are linearly independent.

2. Orthogonalize the N vectors via Schmidt methods and the orthonormal bases $\eta_0, \eta_1, \dots, \eta_{N-1}$ are obtained, that is,

$$\begin{aligned}\beta_0 &= \phi_0 = \psi_f, \eta_0 = \psi_f \\ \beta_1 &= \phi_1 - \langle \phi_1 | \eta_0 \rangle \eta_0, \eta_1 = \beta_1 / \| \beta_1 \| \\ \beta_2 &= \phi_2 - \langle \phi_2 | \eta_0 \rangle \eta_0 - \langle \phi_2 | \eta_1 \rangle \eta_1, \eta_2 = \beta_2 / \| \beta_2 \| \\ &\vdots \\ \beta_{N-1} &= \phi_{N-1} - \sum_{i=0}^{N-2} \langle \phi_{N-1} | \eta_i \rangle \eta_i, \eta_{N-1} = \beta_{N-1} / \| \beta_{N-1} \| \end{aligned} \quad (13.86)$$

3. Utilize the N orthonormal basis to construct P

$$P = \sum_{j=1}^{N-1} p_j |\eta_j\rangle\langle\eta_j| + p_0 |\eta_0\rangle\langle\eta_0|, \quad 0 < p_0 < p_j, p_j \neq p_k \text{ for } j \neq k \quad (13.87)$$

Remark 13.11 Here, because the eigenstates of P to be constructed are orthogonal, we employ the Schmidt orthogonalization to obtain the orthonormal basis. Obviously, such orthonormal bases are infinite. We just give one of the methods. The key point is to select N linearly independent vectors in step 1, where two conditions need to be met: one is that the target $|\psi_f\rangle$ must be included, the other is that $\phi_1, \dots, \phi_{N-1}$ cannot be completely expressed as a linear combination of bases in DFS.

13.3.4 Numerical Simulation Examples and Discussion

To verify the effectiveness of the proposed control strategy, numerical examples are simulated on a three-level Λ -type quantum system, as shown in Figure 13.6, in this subsection.

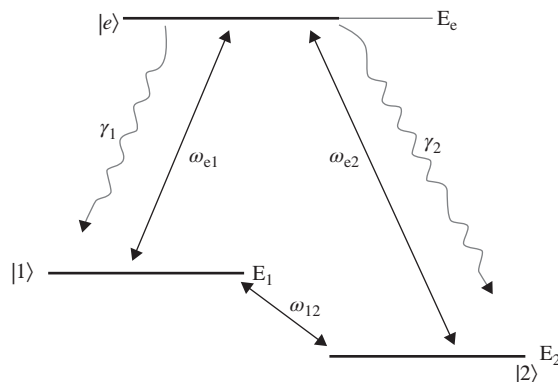


Figure 13.6 Schematic energy diagram: a three-level system with two stable states $|1\rangle$ and $|2\rangle$ and an excited state $|e\rangle$. The excited state decays to $|j\rangle$ ($j=1,2$) with decay rate γ_j .

In the following simulation we denote $|e\rangle = [1 \ 0 \ 0]^T$, $|1\rangle = [0 \ 1 \ 0]^T$, and $|2\rangle = [0 \ 0 \ 1]^T$. The free Hamiltonian of such a system has the form

$$H_0 = E_e |e\rangle\langle e| + E_1 |1\rangle\langle 1| + E_2 |2\rangle\langle 2| \quad (13.88)$$

where $E_e = 0.8$, $E_1 = 0.5$ and $\omega_2 = 0.4$. Their energy-level differences are: $\omega_{e1} = 0.3$, $\omega_{e2} = 0.4$, and $\omega_{12} = 0.1$, respectively. They are mutually distinct so that Assumption 13.1 is satisfied. Assume the decay process is Markovian and can be described by the Lindblad term

$$\mathcal{L}(\rho) = \frac{1}{2} \sum_{k=1}^2 \gamma_k \left\{ \left[\sigma_-^{(k)}, \rho \sigma_+^{(k)} \right] + \left[\sigma_-^{(k)} \rho, \sigma_+^{(k)} \right] \right\} \quad (13.89)$$

where $\sigma_k^- = |k\rangle\langle e|$, $\sigma_k^+ = (\sigma_k^-)^\dagger$. It is not difficult to find that the two stable states form the DFS, that is, $\mathcal{H}_{DFS} = \text{span}\{|1\rangle, |2\rangle\}$. Thus Assumption 13.3 is satisfied. According to

Assumption 13.2, we choose the control Hamiltonian $\sum_{n=1}^4 f_n(t) H_n$, where

$$H_1 = |1\rangle\langle e| + |e\rangle\langle 1|; H_2 = |e\rangle\langle 2| + |2\rangle\langle e|, H_3 = |2\rangle\langle 1| + |1\rangle\langle 2|; H_4 = \begin{pmatrix} 1 & 1 & 1 \\ 1 & 1 & 1 \\ 1 & 1 & 1 \end{pmatrix} \quad (13.90)$$

The control laws are designed based on Equations 13.58 and 13.59, in which the observable operator is constructed according to Equations 13.84–13.86, and 13.87. The process of designing P is as follows: (i) select three linearly independent vectors as $\phi_0 = |\psi_f\rangle$, $\phi_1 = \sqrt{2}/2(|e\rangle + |1\rangle)$, $\phi_2 = \sqrt{2}/2(|e\rangle + |2\rangle)$, (ii) orthogonalize the three vectors via Schmidt methods and three orthonormal bases η_0, η_1, η_2 are obtained, where $\eta_0 = |\psi_f\rangle$, and (iii) construct the observation operator

$$P = p_1 |\eta_1\rangle\langle\eta_1| + p_2 |\eta_2\rangle\langle\eta_2| + p_0 |\eta_0\rangle\langle\eta_0|, 0 < p_0 < p_1, p_2$$

Assume $|\psi_0\rangle = |e\rangle$ to be the initial state, that is, the system stays on the excited state. We hope our scheme is effective for any pure state in DFS, so the target state is written as

$$|\psi_f\rangle = \sin \beta |1\rangle + \cos \beta |2\rangle, \beta \in [0, 2\pi) \quad (13.91)$$

The target state written in Equation 13.91 omits the relative phases between the states $|1\rangle$ and $|2\rangle$. The eigenvalues of the observation operator P are selected as $p_1 = 3$, $p_2 = 2$ and $p_0 = 1$. By taking values in domain of $[0, 2\pi)$ with a step of 0.1, we obtain 63 target states in DFS. The numerical results are presented in Figure 13.7. The fidelity is defined as $F(\rho, \rho_f) = \text{tr} \sqrt{\sqrt{\rho} \rho_f \sqrt{\rho}}$. It is equal to one only when the system reaches the target state. As illustrated in Figure 13.7, all the fidelities would converge to one. The embedded figure in Figure 13.7 clearly indicates that all the curves ascend very quickly at the time interval $[0, 1]$, and later slowly evolve toward one. Additionally, it shows that the fidelities have not reached but would tend to one, which means the control laws can steer the open system from the initial state to any pure target state in DFS. In particular, the red and green curves correspond to the cases of $|\psi_f\rangle = |2\rangle$ and $|\psi_f\rangle = [0, 0.8415, 0.5403]^T$, respectively. The corresponding control laws are displayed in Figures 13.8 and 13.9, respectively.

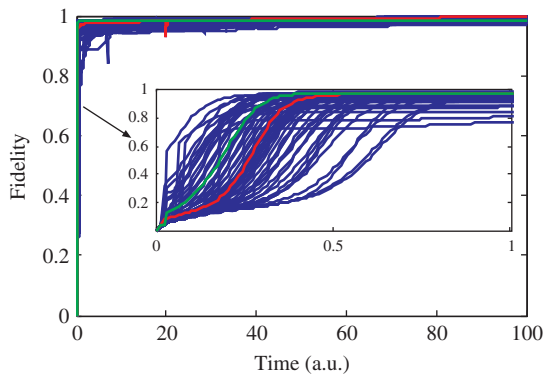


Figure 13.7 Evolution curves of fidelity of the system in the target state. The parameters are $\gamma_1 = \gamma_2 = 0.1$, the red line and green line correspond to $\beta = 0$ and 1, respectively

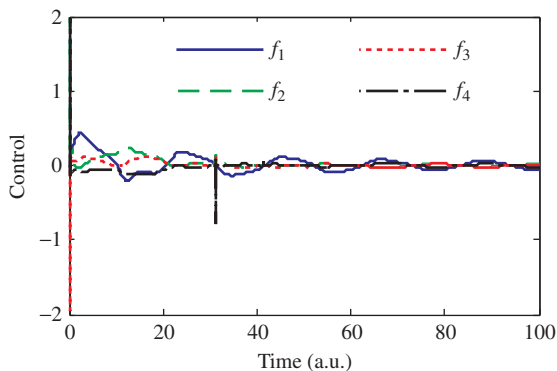


Figure 13.8 Control curves for the target state $|\psi_f\rangle = [0, 0.8415, 0.5403]^T$. The control gain is $\kappa_j(t) = 5, j = 1, 2, 3$

One can see from Figures 13.8 and 13.9 that the control functions decrease in an oscillatory manner. At the beginning of the time axes, the controls are intense enough to quickly steer the open system to the target state. As the system states close to the target states, the controls gradually decrease and tend to zero. In addition, the special control field f_4 always exists during the evolution. It is the premise of the feasibility of the proposed scheme.

This scheme works well not only for pure initial states but also for mixed initial states. Figure 13.10 shows the fidelity of the control as a function of time for 100 initial states randomly chosen from the state space. The initial states are randomly chosen from the state space. The target state is $|2\rangle$ and the other parameters are the same as for Figure 13.7, from which we find that all the curves converge to one.

The above numerical results suggest that the proposed method is feasible not only for initial pure states but also for initial mixed states. In other words, we can drive the mixed states to

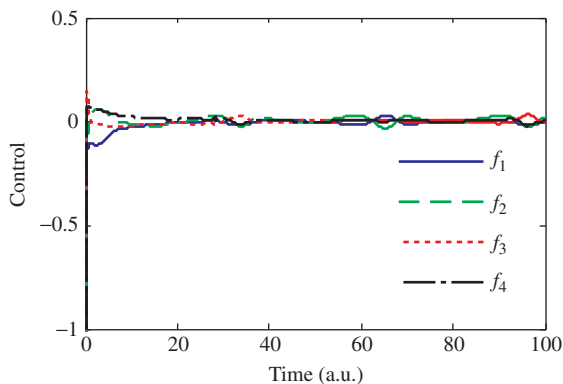


Figure 13.9 Control curves for the target state $|\psi_f\rangle = |2\rangle$. The control gain is $\kappa_j(t) = 5, j = 1, 2, 3$

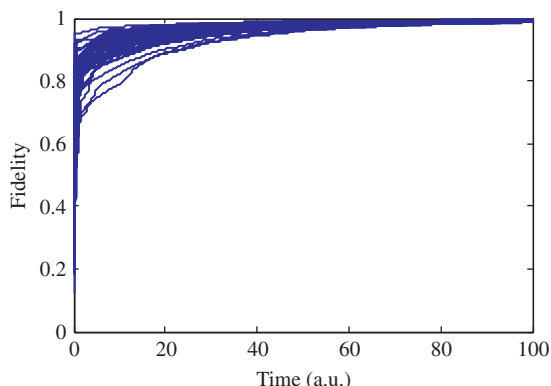


Figure 13.10 Fidelity of the system in the target state

the pure states and preserve it. Hence our method can also be used to purify the mixed state that is contaminated by the environment.

References

- Arimondo, E. (1996) Coherent population trapping in laser spectroscopy. *Progress in Optics*, **35**, 257–353.
- Baumgartner, B., Narnhofer, H. and Thirring, W. (2008) Analysis of quantum semigroups with GKS–Lindblad generators: I. Simple generators. *Journal of Physics A: Mathematical and Theoretical*, **41**(6), 065201.
- Beige, A., Braun, D., Tregenna, B. et al. (2000) Quantum computing using dissipation to remain in a decoherence-free subspace. *Physical Review Letters*, **85**(8), 1762–1765.
- D’Alessandro, D. (2008) *Introduction to Quantum Control and Dynamics*, Taylor & Francis Group, LLC, FL.

- Duan, L.M. and Guo, G.C. (1998) Prevention of dissipation with two particles. *Physical Review A*, **57**(4), 2399–2402.
- Ficek, Z. and Swain, S. (2005) *Quantum Interference and Coherence-Theory and Experiments*, Springer, New York.
- Karasik, R.I., Marzlin, K.P., Sanders, B.C. et al. (2008) Criteria for dynamically stable decoherence-free subspace and incoherently generated coherences. *Physical Review A*, **77**(5), 052301.
- LaSalle, J. and Lefschetz, S. (1961) *Stability By Liapunov's Direct Method With Applications*, Academic Press, New York.
- Lidar, D.A., Chuang, I.L. and Whaley, K.B. (1998) Decoherence-free subspaces for quantum computation. *Physical Review Letters*, **81**(12), 2594–2597.
- Lidar, D.A. and Whaley, K.B. (2003) in *Decoherence-Free Subspaces and Subsystems*, Lecture Notes in Physics, vol. **622**(eds F. Benatti and R. Floreanini), Springer, Berlin, pp. 83–120.
- Lindblad, G. (1976) On the generators of quantum dynamical semigroups. *Communications in Mathematical Physics*, **48**(2), 119–130.
- Shor, P.W. (1995) Scheme for reducing decoherence in quantum computer memory. *Physical Review A*, **52**(4), R2493–R2496.
- Viola, L. and Lloyd, S. (1998) Dynamical suppression of decoherence in two-state quantum systems. *Physical Review A*, **58**(4), 2733–2744.
- Wang, W., Wang, L.C. and Yi, X.X. (2010) Lyapunov control on quantum open systems in decoherence-free subspaces. *Physical Review A*, **82**(3), 034308.
- Wei, H., Deng, Z.J., Zhang, X.L. et al. (2007) Transfer and teleportation of quantum states encoded in decoherence-free subspace. *Physical Review A*, **76**(5), 054304.
- Wu, L.A. and Lidar, D.A. (2002) Creating decoherence-free subspaces using strong and fast pulses. *Physical Review Letters*, **88**(20), 207902.
- Yi, X.X., Huang, X.L., Wu, C. et al. (2009) Driving quantum systems into decoherence-free subspaces by Lyapunov control. *Physical Review A*, **80**(5), 052316.
- Zeng, J.Y. (2007) *Quantum Mechanics*, Science Press, Beijing.
- Zhu, W.S. and Rabitz, H. (2003) Closed loop learning control to suppress the effects of quantum decoherence. *Journal of Chemical Physics*, **118**(15), 6751–6758.

14

Dynamic Decoupling Quantum Control Methods

14.1 Phase Decoherence Suppression of an n -Level Atom in Ξ -Configuration with Bang-Bang Controls

Since the birth of quantum mechanics in the twentieth century, it has achieved great success in many ways as a fundamental theory of natural sciences. With the development of science, the combination of quantum mechanics, classical information theory, and computing technology led to the emergence of quantum information theory and quantum theory of computation. A series of topics based on quantum information technology have been proposed, and the realization of quantum computers (Feynman, 1982) is one of the important research areas. Coherence and entanglement are essential for quantum computation and quantum information processing, but decoherence destroys the coherence of the quantum superposition states in the process of evolution and results in the reduction or even the erosion of the entanglement between subsystems. In order to maintain quantum coherence, quantum error-correcting codes (Calderbank and Shor, 1996; Laflamme *et al.*, 1996), quantum error-avoiding codes (Zanardi and Rasetti, 1997; Duan and Guo, 1997, 1998, 1999), and a dynamic coupling scheme (Viola and Lloyd, 1998) (originally known as quantum bang-bang (BB) control) were proposed. Quantum error-correcting codes and quantum error-avoiding codes need to introduce a lot of redundant information, and also add a certain symmetry assumptions between the system and the environment. Compared with these two methods, BB control does not require the introduction of redundant qubits. The BB control scheme makes use of coherent averaging effects (Haeberlen and Waugh, 1968) and uses twin-born tailored powerful pulses to average out the effect of the unwanted Hamiltonian. After the quantum dynamical decoupling scheme was proposed by Viola and Lloyd in 1998, it was used to suppress the decoherence for one qubit. In recent years, the BB control schemes for phase decoherence in the \wedge -, V -, and Ξ -configurations in three-level atoms have been studied (Liu *et al.*, 2005a,b), and the BB control scheme for amplitude decoherence was designed by Cao, Liu, and Bai (2008). The BB control scheme to suppress phase decoherence in a four-level atom system in the Ξ -configuration is discussed in

Wang *et al.* (2008), and the general decoherence suppression with BB controls in a three-level atom system in the V- and Ξ-configurations is studied in Wang *et al.* (2008).

In this section, we will develop a new BB decoupling scheme to suppress phase decoherence in an arbitrary n -level atom in Ξ-configuration. To achieve this goal, we first give a derivation of the dynamical decoupling conditions in an arbitrary n -level atom in Ξ-configuration in different cases. On this basis, we propose our BB decoupling scheme under phase decoherence in an arbitrary n -level atom in Ξ-configuration, and derive the corresponding decoupling operators explicitly. Then, taking a six-level atom system in Ξ-configuration as an example, we use the BB decoupling scheme to design the corresponding decoupling operators. Meanwhile, we consider the BB decoupling operators from the physical implementation and design sequences of periodic twin-born pulses to suppress phase decoherence in the system. Most notably, taking into account the situation of phase decoherence, the proposed BB decoupling scheme is suitable for an arbitrary n -level atom in Ξ-configuration, so it is more general than the previous studies in Liu *et al.* (2005a,b) and Wang *et al.* (2008).

14.1.1 Dynamical Decoupling Mechanism

1) Hamiltonian of a n -level atom in Ξ-configuration

Consider an arbitrary n -level atom in Ξ-configuration. Let $|j\rangle$ ($j = 0, 1, \dots, n - 1$) be the energy level of an n -level Ξ-configuration atom. E_j is the eigen-energy of the level $|j\rangle$. Each lower level $|j-1\rangle$ couples with its upper level $|j\rangle$ via a laser at resonant frequency $\omega_{j,j-1}$. We have $\omega_{j,j-1} = (E_j - E_{j-1})/\hbar$. Similarly, we define frequencies $\omega_{j,j-2}$ ($j-2 \geq 0$), \dots , $\omega_{j,j-n}$ ($j-n \geq 0$) as the resonant frequencies of the atom and the laser field.

In the Hilbert space the state is defined by

$$|j\rangle = \underbrace{(00 \cdots 01)}^j \underbrace{0 \cdots 0}_{n-j-1}' (j = 0, 1, \dots, n - 1) \quad (14.1a)$$

Define the following operators:

$$\begin{aligned} \sigma_x^{(a,b)} &= |a\rangle\langle b| + |b\rangle\langle a|, \sigma_z^{(a,b)} = |a\rangle\langle a| - |b\rangle\langle b| \\ \sigma_y^{(a,b)} &= (|a\rangle\langle b| - |b\rangle\langle a|) * i \\ \sigma_+^{(a,b)} &= |a\rangle\langle b|, \sigma_-^{(a,b)} = |b\rangle\langle a| \end{aligned} \quad (14.1b)$$

where i is the imaginary unit and $a, b = 0, 1, \dots, n - 1$, respectively.

Then the total Hamiltonian for the whole system can be expressed as

$$H = H_S + H_B + H_{R.F.} + H_{SB} \quad (14.2)$$

in which H_S represents the Hamiltonian of the quantum system, H_B represents the Hamiltonian of the bath, $H_{R.F.}$ is the interaction Hamiltonian between the atom and the radio frequency (R.F.) fields, and H_{SB} represents the interaction Hamiltonian between the bath and the quantum system, respectively.

The Hamiltonian for the n -level atom H_S is

$$H_S = \sum_{i>j=0}^{n-1} \frac{\hbar\omega_{ij}}{n} \sigma_z^{(i,j)} \quad (14.3)$$

where the constant energy term $\sum_{i=0}^{n-1} E_i/n$ is ignored.

When the atom is exposed to reservoirs, one can describe reservoirs by a large number of uncoupled bosonic modes, that is, a reservoir of simple harmonic oscillators, and write its Hamiltonian as

$$H_B = \sum_{i=0}^{n-2} \sum_{ki} \hbar\omega_{ki} a_{ki}^+ a_{ki} \quad (14.4)$$

where a_{ki} and a_{ki}^+ are the bosonic annihilation and creation operators of the baths.

We assume that the transition dipole moment for the linearly polarized electric fields are real, namely $l_{i,i-1} = l_{i-1,i}^T$ for simplicity, and let ϵ_i be the amplitude for the electric moment. The decoupling fields can be written as

$$H_{R.F.} = - \sum_{i=1}^{n-1} \left(l_{i,i-1} |i\rangle \langle i-1| + l_{i-1,i}^\dagger |i-1\rangle \langle i| \right) \epsilon_i \cos(\omega_{i,i-1} t) \quad (14.5)$$

The coupling interaction Hamiltonian which leads to the quantum decoherence is

$$H_{SB} = \hbar \sum_{i=0}^{n-2} \sum_{ki} \left(c_{ki} \sigma_z^{(i+1,i)} + b_{ki} \sigma_x^{(i+1,i)} \right) \left(j_{ki} a_{ki}^+ + j_{ki}^\dagger a_{ki} \right) \quad (14.6)$$

where c_{ki} and b_{ki} are the coefficients of the relative magnitude of phase decoherence and amplitude decoherence, respectively, and $\{j_{ki}\}$ are the coupling constants for virtual exchanges of excitations with thermal reservoirs. As c_{ki} and b_{ki} are different values, one can get several decoherence cases in which we can conclude that:

1. when $c_{ki} = 0, b_{ki} \neq 0$, the reservoir is an adiabatic reservoir, which results in amplitude damping;
2. when $c_{ki} \neq 0, b_{ki} = 0$, the reservoir is a thermal reservoir, which results in phase damping;
3. when $c_{ki} \neq 0, b_{ki} \neq 0$, the reservoir is a general reservoir, which results in general decoherence.

Therefore the total Hamiltonian for the whole system H is

$$\begin{aligned} H = & \sum_{i>j=0}^{n-1} \frac{\hbar\omega_{ij}}{n} \sigma_z^{(i,j)} + \sum_{i=0}^{n-2} \sum_{ki} \hbar\omega_{ki} a_{ki}^+ a_{ki} \\ & + \left(- \sum_{i=1}^{n-1} \left(l_{i,i-1} |i\rangle \langle i-1| + l_{i-1,i}^\dagger |i-1\rangle \langle i| \right) \epsilon_i \cos(\omega_{i,i-1} t) \right) \\ & + \hbar \sum_{i=0}^{n-2} \sum_{ki} \left(c_{ki} \sigma_z^{(i+1,i)} + b_{ki} \sigma_x^{(i+1,i)} \right) \left(j_{ki} a_{ki}^+ + j_{ki}^\dagger a_{ki} \right) \end{aligned} \quad (14.7)$$

We will then derive the conditions for maintaining quantum coherence based on the decoupling principle of BB control.

2) Dynamic decoupling conditions of an n -level atom in Ξ -configuration

The core ideology of quantum BB control is to eliminate the unwanted Hamiltonian H_{SB} in Equation 14.6 from the total Hamiltonian H in Equation 14.2. It uses the twin-born tailored powerful pulses to average out the interaction Hamiltonian H_{SB} between the atom and the bath, which results in the decoherence. The key for designing the BB decoupling scheme is therefore to find the decoupling group G , which is defined as a finite group of BB decoupling operations $G = \{g_m\} (m = 0, 1, \dots, |G| - 1)$ where $|G|$ represents the number of operations, and determine the order of pulse sequences.

In order to find a suitable BB operations group, we first need to get the dynamic decoupling condition. Suppose a given system has evolution time T divided into N cycles, and each cycle length of time is T_c . In every cycle, the time T_c divides into $|G|$ pieces and Δt is the inter-operation period, so one has $T_c = |G| * \Delta t$. Set τ_p is every pulse time. Because τ_p is negligible ($\tau_p < \Delta t$), we can get

$$T = N * T_c = N * |G| * \Delta t \quad (14.8)$$

Now consider a cycle, according to BB operations group, in which we apply the pulses on the system in each Δt . For $t \in [j * \Delta t, (j + 1) * \Delta t]$, the total Hamiltonian therefore reads

$$\tilde{H}(t) = g_j^+ H g_j \quad (14.9)$$

in which $j * \Delta t \leq t \leq (j + 1) * \Delta t$ and g_j^+ is the adjoint matrix of g_j .

On the other hand, the transfer matrix $\tilde{U}(t)$ in open quantum system can be conveniently expanded in Magnus series (Ticozzi and Ferrante, 2006), according to which one has for $t = T_c$

$$\tilde{U}(T_c) = e^{-i(H^{(0)} + H^{(1)} + \dots)T_c} \quad (14.10)$$

where we set $\hbar = 1$ and

$$H^{(0)} = \frac{1}{T_c} \int_0^{T_c} \tilde{H}(t) dt = \frac{\Delta t}{T_c} \sum_{i=0}^{|G|-1} g_i^+ H g_i = \frac{1}{|G|} \sum_{m=0}^{|G|-1} g_m^+ H g_m \quad (14.11)$$

where $H^{(1)}$ and $H^{(2)} \dots$ are the higher-order integrated terms. With the increasing number of cycles N , T_c in Equation 14.8 becomes smaller, and the role of higher-order terms becomes smaller and smaller (Magnus, 1954). We consider the ideal situation $N \rightarrow \infty$ and $T_c \rightarrow 0$. Under these assumptions, it can be shown that the higher-order terms in Equation 14.10 are negligible in a suitable norm since they are of order T_c or higher, and we are left with

$$\begin{aligned} \tilde{U}(T_c) &\approx e^{-iH^{(0)}T_c} = e^{-i\frac{1}{|G|} \sum_{m=0}^{|G|-1} g_m^+ H g_m T_c} \\ &= e^{-i\frac{1}{|G|} \sum_{m=0}^{|G|-1} g_m^+ (H_S + H_B + H_{R.F.} + H_{SB}) g_m T_c} \end{aligned} \quad (14.12)$$

To achieve the purpose of decoupling, we should eliminate the unwanted Hamiltonian H_{SB} in Equation 14.12. The dynamic decoupling condition can therefore be expressed as

$$\sum_{i=0}^{|G|-1} g_i^+ H_{SB} g_i = 0 \quad (14.13)$$

Combined with Equations 14.6 and 14.13, we will discuss the dynamic decoupling condition when the system exhibits amplitude decoherence, phase decoherence, and general decoherence, respectively.

- When the system only exhibits amplitude decoherence, that is, $c_{ki} = 0, b_{ki} \neq 0$, the dynamic decoupling condition can be expressed as

$$\sum_{i=0}^{n-2} \sum_{m=0}^{|G|-1} g_m^+ \sigma_x^{(i+1,i)} g_m = 0 \quad (14.14)$$

- When the system only exhibits phase decoherence, that is, $c_{ki} \neq 0, b_{ki} = 0$, the dynamic decoupling condition can be expressed as

$$\sum_{i=0}^{n-2} \sum_{m=0}^{|G|-1} g_m^+ \sigma_z^{(i+1,i)} g_m = 0 \quad (14.15)$$

- When the system exhibits general decoherence, that is, $c_{ki} \neq 0, b_{ki} = 0$, the dynamic decoupling condition can be expressed as

$$\begin{aligned} & \sum_{i=0}^{n-2} \sum_{m=0}^{|G|-1} \left(g_m^+ \sigma_x^{(i+1,i)} g_m + g_m^+ \sigma_z^{(i+1,i)} g_m \right) \\ &= \sum_{i=0}^{n-2} \sum_{m=0}^{|G|-1} g_m^+ \sigma_x^{(i+1,i)} g_m + \sum_{i=0}^{n-2} \sum_{m=0}^{|G|-1} g_m^+ \sigma_z^{(i+1,i)} g_m = 0 \end{aligned}$$

It is obvious that general decoherence can be suppressed when the system meets the conditions in Equations 14.14 and 14.15 simultaneously.

14.1.2 Design of the Bang–Bang Operations Group in Phase Decoherence

When the system only exhibits phase decoherence, according to the dynamic decoupling condition in Equation 14.15, we can derive an order n ($n = |G|$) BB operations group that meets the decoupling condition, which can be expressed as $G = \{I, g_1, g_2, \dots, g_{n-1}\}$ where I represents an order n unit matrix and g_1, g_2, \dots, g_{n-1} can be expressed as

$$g_1 = \begin{cases} \begin{bmatrix} 0 & 0 & 0 & \cdots & 0 & i \\ i & 0 & 0 & \cdots & 0 & 0 \\ 0 & i & 0 & \cdots & 0 & 0 \\ \cdots & \cdots & \cdots & \cdots & \cdots & \cdots \\ 0 & 0 & 0 & \cdots & i & 0 \\ 0 & 0 & 0 & \cdots & 0 & -1 \\ i & 0 & 0 & \cdots & 0 & 0 \\ 0 & i & 0 & \cdots & 0 & 0 \\ \cdots & \cdots & \cdots & \cdots & \cdots & \cdots \\ 0 & 0 & 0 & \cdots & i & 0 \\ 0 & 0 & 0 & \cdots & 0 & -i \\ i & 0 & 0 & \cdots & 0 & 0 \\ 0 & i & 0 & \cdots & 0 & 0 \\ \cdots & \cdots & \cdots & \cdots & \cdots & \cdots \\ 0 & 0 & 0 & \cdots & i & 0 \\ 0 & 0 & 0 & \cdots & 0 & 1 \\ i & 0 & 0 & \cdots & 0 & 0 \\ 0 & i & 0 & \cdots & 0 & 0 \\ \cdots & \cdots & \cdots & \cdots & \cdots & \cdots \\ 0 & 0 & 0 & \cdots & i & 0 \end{bmatrix} & \text{for } n = 4k + 2 \quad (k = 0, 1, 2, \dots) \\ \begin{bmatrix} 0 & 0 & 0 & \cdots & 0 & i \\ i & 0 & 0 & \cdots & 0 & 0 \\ 0 & i & 0 & \cdots & 0 & 0 \\ \cdots & \cdots & \cdots & \cdots & \cdots & \cdots \\ 0 & 0 & 0 & \cdots & i & 0 \\ 0 & 0 & 0 & \cdots & 0 & -i \\ i & 0 & 0 & \cdots & 0 & 0 \\ 0 & i & 0 & \cdots & 0 & 0 \\ \cdots & \cdots & \cdots & \cdots & \cdots & \cdots \\ 0 & 0 & 0 & \cdots & i & 0 \\ 0 & 0 & 0 & \cdots & 0 & 1 \\ i & 0 & 0 & \cdots & 0 & 0 \\ 0 & i & 0 & \cdots & 0 & 0 \\ \cdots & \cdots & \cdots & \cdots & \cdots & \cdots \\ 0 & 0 & 0 & \cdots & i & 0 \end{bmatrix} & \text{for } n = 4k + 3 \quad (k = 0, 1, 2, \dots) \\ \begin{bmatrix} 0 & 0 & 0 & \cdots & 0 & i \\ i & 0 & 0 & \cdots & 0 & 0 \\ 0 & i & 0 & \cdots & 0 & 0 \\ \cdots & \cdots & \cdots & \cdots & \cdots & \cdots \\ 0 & 0 & 0 & \cdots & i & 0 \\ 0 & 0 & 0 & \cdots & 0 & -i \\ i & 0 & 0 & \cdots & 0 & 0 \\ 0 & i & 0 & \cdots & 0 & 0 \\ \cdots & \cdots & \cdots & \cdots & \cdots & \cdots \\ 0 & 0 & 0 & \cdots & i & 0 \\ 0 & 0 & 0 & \cdots & 0 & 1 \\ i & 0 & 0 & \cdots & 0 & 0 \\ 0 & i & 0 & \cdots & 0 & 0 \\ \cdots & \cdots & \cdots & \cdots & \cdots & \cdots \\ 0 & 0 & 0 & \cdots & i & 0 \end{bmatrix} & \text{for } n = 4k + 4 \quad (k = 0, 1, 2, \dots) \\ \begin{bmatrix} 0 & 0 & 0 & \cdots & 0 & i \\ i & 0 & 0 & \cdots & 0 & 0 \\ 0 & i & 0 & \cdots & 0 & 0 \\ \cdots & \cdots & \cdots & \cdots & \cdots & \cdots \\ 0 & 0 & 0 & \cdots & i & 0 \\ 0 & 0 & 0 & \cdots & 0 & -i \\ i & 0 & 0 & \cdots & 0 & 0 \\ 0 & i & 0 & \cdots & 0 & 0 \\ \cdots & \cdots & \cdots & \cdots & \cdots & \cdots \\ 0 & 0 & 0 & \cdots & i & 0 \\ 0 & 0 & 0 & \cdots & 0 & 1 \\ i & 0 & 0 & \cdots & 0 & 0 \\ 0 & i & 0 & \cdots & 0 & 0 \\ \cdots & \cdots & \cdots & \cdots & \cdots & \cdots \\ 0 & 0 & 0 & \cdots & i & 0 \end{bmatrix} & \text{for } n = 4k + 5 \quad (k = 0, 1, 2, \dots) \end{cases} \quad (14.16a)$$

$$g_2 = (g_1)^2, \dots, g_{n-1} = (g_1)^{n-1} \quad (14.16b)$$

Now, we will incorporate the BB operations group above into the decoupling condition to verify its correctness.

First, given the arbitrary order n diagonal matrix $Z = \text{diag}\{q_1, q_2, \dots, q_n\}$ that meets the condition of $\sum_{i=1}^n q_i = 0$, according to Equations 14.16a and 14.16b one can get

$$\begin{aligned} Z + g_1^+ Z g_1 + \cdots + g_{n-1}^+ Z g_{n-1} &= \text{diag}\{q_1, q_2, \dots, q_{n-1}, q_n\} + \\ &\quad \text{diag}\{q_n, q_1, \dots, q_{n-2}, q_{n-1}\} + \cdots + \text{diag}\{q_2, q_3, \dots, q_n, q_1\} \\ &= \text{diag}\left\{\sum_{i=1}^n q_i, \sum_{i=1}^n q_i, \dots, \sum_{i=1}^n q_i, \sum_{i=1}^n q_i\right\} = 0 \end{aligned} \quad (14.17)$$

According to the decoupling condition (Equations 14.15 and 14.1), one can know that $\sigma_z^{(i,j)}$ is a diagonal matrix of which the sum of principal diagonal elements is 0. Thus, one can know

from Equation 14.17 that the system can meet the decoupling condition by the BB operations group above. Furthermore, considering the BB operators from the physical implementation, we can get

$$g_1 = \exp\left(i * \sigma_x^{(1,0)} * \pi/2\right) * \dots * \exp\left(i * \sigma_x^{(k+1,k)} * \pi/2\right) * \exp\left(i * \sigma_x^{(k+2,k+1)} * \pi/2\right) * \dots * \exp\left(i * \sigma_x^{(n-1,n-2)} * \pi/2\right) \quad (14.18)$$

In fact, the order n BB operations group that meets the decoupling condition is not just one kind because the BB operations group can be realized by various pulses: some by x -rotation operation, some by y - and z -rotation operation. Thus the operation groups can be designed in several ways. However, we can design it generally using the following means:

$$g_0 = I, g_2 = (g_1)^2, \dots, g_{n-1} = (g_1)^{n-1} \quad (14.19)$$

Insert Equation 14.18 into Equation 14.15, then all BB operations groups we get meet the decoupling purpose. For example, let

$$g_1 = \begin{bmatrix} 0 & 0 & 0 & \dots & 0 & 1 \\ 1 & 0 & 0 & \dots & 0 & 0 \\ 0 & 1 & 0 & \dots & 0 & 0 \\ \dots & \dots & \dots & \dots & \dots & \dots \\ 0 & 0 & 0 & \dots & 1 & 0 \end{bmatrix}, g_2 = (g_1)^2, \dots, g_{n-1} = (g_1)^{n-1}$$

then the BB operations group we obtain also meets the decoupling condition. In addition, the BB operations group is unitary so it can be realized by pulses physically.

14.1.3 Examples of Design

Consider a six-level atom in Ξ -configuration as shown in Figure 14.1, in which the six levels are labeled $|0\rangle$, $|1\rangle$, $|2\rangle$, $|3\rangle$, $|4\rangle$, and $|5\rangle$, respectively, and their energies are E_0 , E_1 , E_2 , E_3 , E_4 , and E_5 . The level $|k\rangle$ is coupled to the level $|k+1\rangle$ via the fields of resonance frequencies $\omega_{k+1,k}$, ($k = 0, 1, \dots, 4$), respectively. We place the atom under the driving of five fields with frequencies of $\omega_{10} = (E_1 - E_0)/\hbar$, $\omega_{21} = (E_2 - E_1)/\hbar$, $\omega_{32} = (E_3 - E_2)/\hbar$, $\omega_{43} = (E_4 - E_3)/\hbar$, and $\omega_{54} = (E_5 - E_4)/\hbar$, respectively. Similarly, the frequencies can be defined as $\omega_{j,j-2}$ ($j-2 \geq 0$), \dots , $\omega_{j,j-n}$ ($j-5 \geq 0$), ($j = 2, 3, \dots, 5$).

The total Hamiltonian of the system can be expressed as

$$H = H_S + H_B + H_{R.F.} + H_{SB} \quad (14.20)$$

where

$$H_S = \sum_{i>j=0}^5 \frac{\hbar\omega_{ij}}{6} \sigma_z^{(i,j)} + \sum_{i=0}^5 \frac{E_i}{6} \quad (14.21)$$

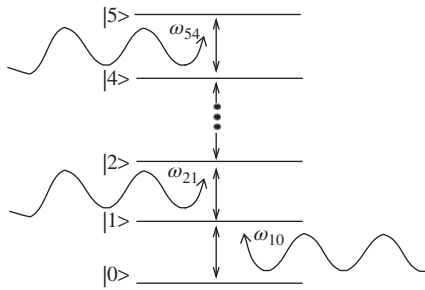


Figure 14.1 A six-level atom in Ξ -configuration under five driving fields with frequencies ω_{10} , ω_{21} , ω_{32} , ω_{43} , and ω_{54}

and the constant term $\sum_{i=0}^5 E_i/6$ can be ignored as usual. The reservoirs Hamiltonian is

$$H_B = \sum_{i=0}^4 \sum_{ki} \hbar \omega_{ki} a_{ki}^\dagger a_{ki} \quad (14.22)$$

The driving fields Hamiltonian is

$$H_{R.F.} = - \sum_{i=0}^4 \left(l_{i+1,i} |i+1\rangle\langle i| + l_{i,i+1}^\dagger |i\rangle\langle i+1| \right) e_i \cos(\omega_{i+1,i} t) \quad (14.23)$$

The interaction between the atom and its environment under phase decoherence is

$$H_{SB} = \hbar \sum_{i=0}^4 \sum_{pi} \sigma_z^{(i+1,i)} \left(j_{pi} a_{pi}^\dagger + j_{pi}^\dagger a_{pi} \right) \quad (14.24)$$

Now we can follow the method in Section 14.1.2 to design the BB operations group under phase decoherence in the six-level atom system in Ξ -configuration. The BB operations group for this type of atom is an order 6 cyclic group $G = \{I, g_1, g_2, g_3, g_4, g_5\}$. According to Equations 14.16a and 14.16b we can get the generators g_1, g_2, g_3, g_4, g_5 as

$$g_1 = \begin{bmatrix} 0 & 0 & 0 & 0 & 0 & i \\ i & 0 & 0 & 0 & 0 & 0 \\ 0 & i & 0 & 0 & 0 & 0 \\ 0 & 0 & i & 0 & 0 & 0 \\ 0 & 0 & 0 & i & 0 & 0 \\ 0 & 0 & 0 & 0 & i & 0 \end{bmatrix} = \begin{cases} \exp(i\pi/2\sigma_x^{(1,0)}) \\ * \exp(i\pi/2\sigma_x^{(2,1)}) \\ * \exp(i\pi/2\sigma_x^{(3,2)}) \\ * \exp(i\pi/2\sigma_x^{(4,3)}) \\ * \exp(i\pi/2\sigma_x^{(5,4)}) \end{cases} \quad (14.25a)$$

$$g_2 = (g_1)^2 = \begin{bmatrix} 0 & 0 & 0 & 0 & -1 & 0 \\ 0 & 0 & 0 & 0 & 0 & -1 \\ -1 & 0 & 0 & 0 & 0 & 0 \\ 0 & -1 & 0 & 0 & 0 & 0 \\ 0 & 0 & -1 & 0 & 0 & 0 \\ 0 & 0 & 0 & -1 & 0 & 0 \end{bmatrix} = \begin{cases} \exp(i\pi/2\sigma_x^{(1,0)}) \\ * \exp(i\pi/2\sigma_x^{(2,1)}) \\ * \exp(i\pi/2\sigma_x^{(3,2)}) \\ * \exp(i\pi/2\sigma_x^{(4,3)}) \\ * \exp(i\pi/2\sigma_x^{(5,4)}) \end{cases}^2 \quad (14.25b)$$

$$g_3 = (g_1)^3 = \begin{bmatrix} 0 & 0 & 0 & -i & 0 & 0 \\ 0 & 0 & 0 & 0 & -i & 0 \\ 0 & 0 & 0 & 0 & 0 & -i \\ -i & 0 & 0 & 0 & 0 & 0 \\ 0 & -i & 0 & 0 & 0 & 0 \\ 0 & 0 & -i & 0 & 0 & 0 \end{bmatrix} = \left\{ \begin{array}{l} \exp(i\pi/2\sigma_x^{(1,0)}) \\ * \exp(i\pi/2\sigma_x^{(2,1)}) \\ * \exp(i\pi/2\sigma_x^{(3,2)}) \\ * \exp(i\pi/2\sigma_x^{(4,3)}) \\ * \exp(i\pi/2\sigma_x^{(5,4)}) \end{array} \right\}^3 \quad (14.25c)$$

$$g_4 = (g_1)^4 = \begin{bmatrix} 0 & 0 & 1 & 0 & 0 & 0 \\ 0 & 0 & 0 & 1 & 0 & 0 \\ 0 & 0 & 0 & 0 & 1 & 0 \\ 0 & 0 & 0 & 0 & 0 & 1 \\ 1 & 0 & 0 & 0 & 0 & 0 \\ 0 & 1 & 0 & 0 & 0 & 0 \end{bmatrix} = \left\{ \begin{array}{l} \exp(i\pi/2\sigma_x^{(1,0)}) \\ * \exp(i\pi/2\sigma_x^{(2,1)}) \\ * \exp(i\pi/2\sigma_x^{(3,2)}) \\ * \exp(i\pi/2\sigma_x^{(4,3)}) \\ * \exp(i\pi/2\sigma_x^{(5,4)}) \end{array} \right\}^4 \quad (14.25d)$$

$$g_5 = (g_1)^5 = \begin{bmatrix} 0 & i & 0 & 0 & 0 & 0 \\ 0 & 0 & i & 0 & 0 & 0 \\ 0 & 0 & 0 & i & 0 & 0 \\ 0 & 0 & 0 & 0 & i & 0 \\ 0 & 0 & 0 & 0 & 0 & i \\ i & 0 & 0 & 0 & 0 & 0 \end{bmatrix} = \left\{ \begin{array}{l} \exp(i\pi/2\sigma_x^{(1,0)}) \\ * \exp(i\pi/2\sigma_x^{(2,1)}) \\ * \exp(i\pi/2\sigma_x^{(3,2)}) \\ * \exp(i\pi/2\sigma_x^{(4,3)}) \\ * \exp(i\pi/2\sigma_x^{(5,4)}) \end{array} \right\}^5 \quad (14.25e)$$

where $\sigma_x^{(1,0)} = |1\rangle\langle 0| + |0\rangle\langle 1|$, $\sigma_x^{(2,1)} = |2\rangle\langle 1| + |1\rangle\langle 2|$, $\sigma_x^{(3,2)} = |3\rangle\langle 2| + |2\rangle\langle 3|$, $\sigma_x^{(4,3)} = |4\rangle\langle 3| + |3\rangle\langle 4|$, and $\sigma_x^{(5,4)} = |5\rangle\langle 4| + |4\rangle\langle 5|$.

If we put the BB operations group G into the dynamic decoupling condition of phase decoherence, it is easy to verify that the above-designed BB operations group G satisfies the decoupling condition in Equation 14.15 under phase decoherence.

Now we consider the BB operations group G from the physical implementation. According to Equation 14.25, we can realize the BB control operators g_1, g_2, g_3, g_4 , and g_5 by twin-born pulses. For example, g_1 can be realized by a $\pi/2$ pulse at frequency ω_{54} , which is followed by a $\pi/2$ pulse at frequency ω_{43} , a $\pi/2$ pulse at frequency ω_{32} , a $\pi/2$ pulse at frequency ω_{21} , and a $\pi/2$ pulse at frequency ω_{10} . The other decoupling elements in G can be constructed likewise.

With the full expressions for these operators $\{g_k\}$ and the knowledge of their physical realization, we obtain the exact sequences of operations in a cycle. We program the pulse sequences in a cycle T_c as

$$\{g'_1, g'_1^+, g'_2, g'_2^+, g'_3, g'_3^+, g'_4, g'_4^+, g'_5, g'_5^+\} \quad (14.26)$$

which is shown in Figure 14.2, in which the t -axis denotes the passage of time. Among the bars above the t -axis there is one kind of column that is divided into five parts. From top to bottom, the column with the first part black indicates the $\pi/2$ pulse with frequency ω_{54} , the column with the second part black indicates the $\pi/2$ pulse with frequency ω_{43} , the column with the third part black indicates the $\pi/2$ pulse with frequency ω_{32} , the column with the fourth part black indicates the $\pi/2$ pulse with frequency ω_{21} , and the column with the fifth part black indicates the $\pi/2$ pulse with frequency ω_{10} . Their adjoint pulses are drawn upside down under the t -axis. In Figure 14.2 we use the column with the top half black to denote the generator g_1 and use the one with the bottom half black to denote the generator g_1^+ .

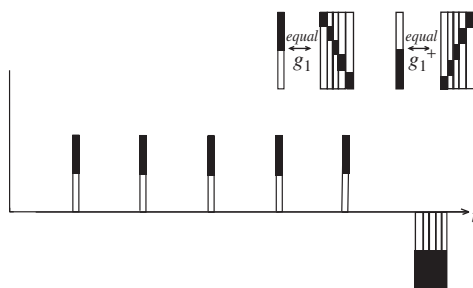


Figure 14.2 The twin-born pulse sequences in a cycle for a six-level atom in Ξ -configuration under phase decoherence

A full cycle of the evolution of the system can be described as the following sequences of operators:

$$\begin{aligned} & g_5^+ U(t_p^{(5)} + 5\tau_p, t_p^{(6)}) g_5 g_4^+ U(t_p^{(4)} + 5\tau_p, t_p^{(5)}) g_4 g_3^+ U(t_p^{(3)} + 5\tau_p, t_p^{(4)}) \\ & g_3 g_2^+ U(t_p^{(2)} + 5\tau_p, t_p^{(3)}) g_2 g_1^+ U(t_p^{(1)} + 5\tau_p, t_p^{(2)}) g_1 U(t_p^{(0)} + \tau_p, t_p^{(1)}) \\ & = (g_1)^5 U(t_p^{(5)} + 5\tau_p, t_p^{(6)}) g_1 U(t_p^{(4)} + 5\tau_p, t_p^{(5)}) g_1 U(t_p^{(3)} + 5\tau_p, t_p^{(4)}) \\ & g_1 U(t_p^{(2)} + 5\tau_p, t_p^{(3)}) g_1 U(t_p^{(1)} + 5\tau_p, t_p^{(2)}) g_1 U(t_p^{(0)} + \tau_p, t_p^{(1)}) \end{aligned}$$

Here, we assume that the duration for every pulse is τ_p and we use $U(t_i, t_j)$ to denote the free evolution of the system under the Hamiltonian H in Equation 14.20 within the time intervals between t_i and t_j . If we repeatedly perform such pulse sequences in a given period of time rapidly, phase decoherence will be averaged out.

14.2 Optimized Dynamical Decoupling in Ξ -Type n -Level Atom

In the quantum world, coherence and entanglement are the sources of power that make quantum computation (Feynman, 1982) surpass classical computation. However, quantum systems always interact with their surrounding environment realistically to some extent. No matter how weak the coupling is, the evolution of the quantum system is eventually plagued by non-unitary features like decoherence and dissipation (Gardiner, 1991). In recent years, many strategies have been proposed to counteract the effects of environmental couplings successfully in open-system evolutions (Viola and Lloyd, 1998; Haeberlen and Waugh, 1968), but up to now the dynamical decoupling pulse sequences have been designed based on dividing the total evolution time into equidistant time periods. It has been further shown that in principle it is possible to use optimized pulse sequences (Uhlig, 2007; Khodjasteh and Lidar, 2005). In Uhlig (2007), the Uhlig dynamical decoupling (UDD) was discussed in the spin-boson model and the potential of non-equidistant pulse sequences was demonstrated by concatenated pulse sequences in Khodjasteh and Lidar (2005). However, high-dimensional systems have attracted much interest for their applications in quantum control and quantum computation (Unruh, 1995) so the related research in high-dimensional systems needs to be studied.

In this section, we will demonstrate the effectiveness of the optimized dynamical decoupling scheme UDD in an arbitrary n -level atom in Ξ -configuration. The key point is to put on the

comparison of the effectiveness of suppressing the decoherence between the standard periodic dynamical decoupling scheme (PDD) (Viola and Lloyd, 1998) and UDD. Toward this goal, we first study the dynamics of a decoherence Ξ -type n -level atom driven by dynamical decoupling, and design the corresponding BB operation group of the dynamical decoupling scheme. Then according to different time intervals between the adjacent BB pulses, two decoupling schemes, PDD and UDD, are designed, and the non-diagonal element of the density matrix (Viola and Lloyd, 1998), (Wang *et al.*, 2008) is selected as a reference index to investigate the behavior of the quantum coherence of the Ξ -type n -level atom under dynamical decoupling schemes. Finally, a Ξ -type six-level atom is taken as an example. The numerical simulation is carried out and the analysis is given.

From the analysis in Section 14.1.1, one can see that there are $N * |G|$ BB operators (pluses) in the evolution time T . Let t_i ($i = 1, 2, \dots, N * |G|$) represent the moments when the BB operators are produced, so although there is a operator at $t_{N*|G|} = T$, in the time interval $(0, T)$ the number of pulses M is

$$M = |G| * N - 1 \quad (14.27)$$

According to different choices of t_i , one can obtain many kinds of dynamical decoupling schemes. Next we will introduce the PDD and the UDD.

14.2.1 Periodic Dynamical Decoupling

PDD is the basic dynamical decoupling scheme. It uses the twin-born tailored powerful pulses periodically to average out the effect of the unwanted Hamiltonian H_{SB} and achieves the purpose of decoupling with the environment. The BB operation group G is designed to satisfy the dynamic decoupling condition (Equation 14.13). We set $t_i = \delta_i T$ ($i = 1, 2, \dots, M; 0 < \delta_1 < \delta_2 < \dots < \delta_{M-1} < \delta_M < 1$), where the time of M pulses t_i can be written as

$$t_i = T * \delta_{i-PDD} = T * i / (M + 1) \quad (14.28)$$

$$\delta_{i-PDD} = i / (M + 1) \quad i = 1, 2, \dots, M \quad (14.29)$$

14.2.2 Uhrig Dynamical Decoupling

The UDD (Uhrig, 2007) is an optimized dynamical decoupling scheme proposed by Uhrig. It also uses twin-born tailored powerful pulses to average out the effect of the unwanted Hamiltonian H_{SB} and achieves the purpose of decoupling with the environment. The BB operation group G in UDD is also designed to completely cancel errors up to the first order in the Magnus expansion and should satisfy the dynamic decoupling condition Equation 14.13. This is just the same as PDD, but the difference from PDD is that UDD optimizes the time intervals between adjacent pulses, and in UDD the time of M pulses t_i can be expressed as (Uhrig, 2007)

$$t_i = T * \delta_{i-UDD} \quad (14.30)$$

$$\delta_{i-UDD} = \sin^2 [i * \pi / (2M + 2)] \quad i = 1, 2, \dots, M \quad (14.31)$$

14.2.3 Behaviors of Quantum Coherence under Various Dynamical Decoupling Schemes

In order to investigate the performance of suppressing the decoherence of these dynamical decoupling schemes, we first derive the trend of the non-diagonal element of the density matrix to observe the evolution of the Ξ -type n -level atom under dynamical decoupling schemes. We then choose an Ξ -type six-level atom as a model for the controlled system and derive the trends of the non-diagonal element of the density matrix while PDD and UDD are applied respectively, finally making a comparison and analysis of the results.

In order to analyze easily the impact of the decoupling pulse sequence, we transform the system into the interaction picture. Then the interaction Hamiltonian in Equation 14.2 can be expressed as

$$\tilde{H}_{SB} = \hbar \sum_{i=0}^{n-2} \sum_{ki} \sigma_z^{(i+1,i)} \left(j_{ki} a_{ki}^+ e^{i\omega_{ki} t} + j_{ki}^\dagger a_{ki} e^{-i\omega_{ki} t} \right) \quad (14.32)$$

and the evolution propagator of the whole system can be expressed as

$$\tilde{U}(t_s, t_o) = \exp \left\{ \sum_{i=0}^{n-2} \sum_{ki} \sigma_z^{(i+1,i)} (a_{ki}^+ e^{i\omega_{ki} t_o} \zeta_{ki} (t_o - t_s) - h.c.) \right\} \quad (14.33)$$

where t_s and t_o represent the start and end moments of this evolution process, $\zeta_{ki} (t_o - t_s) = \frac{j(\omega_{ki})}{\omega_{ki}} (1 - e^{i\omega_{ki} (t_o - t_s)})$.

Now consider the situation in the j th ($j = 1, 2, \dots, N$) decoupling cycle. According to the full expressions for the BB operators $\{g_k\}$ in Equation 14.19, we can program a cycle of pulse sequences as $\{g_1, g_1^+, g_2, g_2^+, \dots, g_{n-2}, g_{n-2}^+, g_{n-1}, g_{n-1}^+\}$ so we get a cycle of the unitary evolution of the atom system under the BB operations as the form of

$$\tilde{U}(t_j^s, t_j^o) = g_{n-1}^+ \tilde{U}(t_j^{(n-1)}, t_j^{(n)}) g_{n-1} g_{n-2}^+ \cdots g_2 g_1^+ \tilde{U}(t_j^{(1)}, t_j^{(2)}) g_1 \tilde{U}(t_j^{(0)}, t_j^{(1)}) \quad (14.34)$$

where t_j^s and t_j^o are the start and end moments in the j th decoupling cycle, where $t_j^s = t_j^{(0)}$ and $t_j^o = t_j^{(n)}$.

Let $T_{c,j}$ represent the length of the j th decoupling cycle, then one can get $T_{c,j} = t_j^o - t_j^s$. Let $t_j^{(i)}$ and $\Delta t_j(i)$ ($i = 1, 2, \dots, n$) represent the moments of the pulse $g_i g_{i-1}^+$ and the i th time interval of the adjacent two pluses in the j th decoupling cycle, Then one can have $\Delta t_j(i) = t_j^{(i)} - t_j^{(i-1)}$.

Consider the total evolution time T . After applying periodically the decoupling operations $\{g_k\}$ in Equation 14.19 in N decoupling cycles, the evolution propagator of the whole system is

$$\tilde{U}(0, T) = \tilde{U}(t_N^s, T) \tilde{U}(t_{N-1}^s, t_{N-1}^o) \cdots \tilde{U}(t_2^s, t_2^o) \tilde{U}(0, t_1^o) \quad (14.35)$$

As is well known, if the atom is not affected by the environment, the relevant quantity is the qubit coherence $\tilde{\rho}_S^{ij}(T)$ ($i \neq j$) and, of course, $\tilde{\rho}_S^{ii}(T) = \tilde{\rho}_S^{ii}(0)$. To observe the suppression effect of the BB decoupling pulse sequences on the atom of the adiabatic decoherence, we are interested in calculating the reduced density matrix of the atom. In this work, we choose and calculate the non-diagonal element $\tilde{\rho}_S^{01}(T)$ for simplicity. The other non-diagonal elements $\tilde{\rho}_S^{ij}(T)$ ($i \neq j$) can also be chosen, but they are not discussed here.

We assume that the atom and environment are initially uncorrelated, that is,

$$\tilde{\rho}(0) = \tilde{\rho}_S(0) \otimes \tilde{\rho}_B(0) \quad (14.36)$$

where $\tilde{\rho}_B(0)$ is a kind of thermal equilibrium state at temperature T' , that is,

$$\tilde{\rho}_B(0) = \prod_k (1 - e^{\beta \hbar \omega_k}) * e^{-\beta \hbar \omega_k a_k^\dagger a_k}$$

where $\beta = 1 / (k_B * T')$, k_B is the Boltzmann constant, and T' is the temperature of the bath. One can choose henceforth units such that $\hbar = k_B = 1$ for simplicity. Then combined with Equations 14.33–14.36, one obtains

$$\begin{aligned} \tilde{\rho}_s^{01}(T) &= \langle 0 | \text{Tr}_B \left\{ \tilde{U}(0, T) \tilde{\rho}(0) \tilde{U}^\dagger(0, T) \right\} | 1 \rangle \\ &= \tilde{\rho}_s^{01}(0) * \exp \left\{ - \sum_{m=1}^{n-1} \Gamma_m(\Delta t_j(i), T_{c,j}, T) \right\} \end{aligned} \quad (14.37)$$

where $i = 1, 2, \dots, n$, $j = 1, 2, \dots, N$,

$$\Gamma_m(\Delta t_j(i), T_{c,j}, T) = \frac{1}{2} \sum_{ki} |\chi_m(\Delta t_j(i), T_{c,j}, T)|^2 \coth \frac{\omega_{ki}}{2T}, \quad (14.38)$$

where $m = 1, 2, \dots, n-1$. $\chi_m(\Delta t_j(i), T_{c,j}, T)$ in Equation 14.38 can be expressed as

$$\begin{aligned} \chi_1(\Delta t_j(i), T_{c,j}, T) &= -2 * \eta_1(\Delta t_j(i), T_{c,j}, T) \\ &\quad + \eta_2(\Delta t_j(i), T_{c,j}, T) + \eta_n(\Delta t_j(i), T_{c,j}, T) \end{aligned} \quad (14.39a)$$

$$\begin{aligned} \chi_2(\Delta t_j(i), T_{c,j}, T) &= -2 * \eta_2(\Delta t_j(i), T_{c,j}, T) \\ &\quad + \eta_1(\Delta t_j(i), T_{c,j}, T) + \eta_{n-1}(\Delta t_j(i), T_{c,j}, T) \end{aligned} \quad (14.39b)$$

and when $m = 3, 4, \dots, n-1$,

$$\begin{aligned} \chi_m(\Delta t_j(i), T_{c,j}, T) &= -2 * \eta_{n-m+2}(\Delta t_j(i), T_{c,j}, T) \\ &\quad + \eta_{n-m+1}(\Delta t_j(i), T_{c,j}, T) \\ &\quad + \eta_{n-m+3}(\Delta t_j(i), T_{c,j}, T) \end{aligned} \quad (14.39c)$$

where

$$\begin{aligned} \eta_l(\Delta t_j(i), T_{c,j}, T) &= \zeta_{ki}(\Delta t_1(l)) * e^{i\omega_{ki} \sum_{i=1}^{l-1} \Delta t_1(i)} \\ &\quad + \zeta_{ki}(\Delta t_2(l)) * e^{i\omega_{ki} \sum_{i=1}^{l-1} \Delta t_2(i)} * e^{i\omega_{ki} T_{c,1}} + \dots \\ &\quad + \zeta_{ki}(\Delta t_N(l)) * e^{i\omega_{ki} \sum_{i=1}^{l-1} \Delta t_N(i)} * e^{i\omega_{ki} \sum_{j=1}^{N-1} T_{c,j}} \end{aligned} \quad (14.40)$$

where $l = 1, 2, \dots, n$.

Now according to different moments to generate the decoupling pulse sequence in the PDD and the UDD, we get different $\Delta t_j(i)$ and $T_{c,j}$.

1. When the PDD is applied, one has

$$\delta_{0-PDD} = 0, \delta_{(n*N)-PDD} = 1 \quad (14.41a)$$

$$\Delta t_j(i) = (\delta_{m-PDD} - \delta_{(m-1)-PDD}) * T \quad (14.41b)$$

where

$$m = (j-1) * n + i, i = 1, 2, \dots, n, j = 1, 2, \dots, N$$

$$T_{c,j} = \Delta t_j(1) + \Delta t_j(2) + \dots + \Delta t_j(n) \quad (14.41c)$$

2. When the UDD is applied, one has

$$\delta_{0-UDD} = 0, \delta_{(n*N)-UDD} = 1 \quad (14.42a)$$

$$\Delta t_j(i) = (\delta_{m-UDD} - \delta_{(m-1)-UDD}) * T \quad (14.42b)$$

where

$$m = (j-1) * 3 + i, i = 1, 2, \dots, n, j = 1, 2, \dots, N$$

$$T_{c,j} = \Delta t_j(1) + \Delta t_j(2) + \dots + \Delta t_j(n) \quad (14.42c)$$

We know that the spectral density $I(\omega) \rightarrow 0$ when the frequency ω is greater than the finite cut-off frequency of each mode of the environment ω_c , that is, $\omega > \omega_c$ (Viola and Lloyd, 1998). When the bath is generally considered to be an Ohmic bath, we can have the spectral density for each mode of the bath to be $I(\omega) = \frac{\alpha}{4} \omega^r e^{-\omega/\omega_c}$, where α measures the strength of the system-environment interaction and $r = 1$ (Viola and Lloyd, 1998), (Mozyrsky and Provman, 1998; Leggett *et al.*, 1987; Palma, Suominen, and Ekert, 1996). The following transformation (Viola and Lloyd, 1998; Hu, Paz, and Zhang, 1992) can be taken in the continuum limit of the bath mode:

$$\sum_{ki} \rightarrow \int_0^{\omega_c} d\omega_{ki} I(\omega_{ki}) \frac{1}{|j(\omega_{ki})|^2}$$

Then Equation 14.38 changes into

$$\Gamma_m(\Delta t_j(i), T_{c,j}, T) = \frac{1}{2} \int_0^{\omega_c} d\omega_{ki} I(\omega_{ki}) \coth \frac{\omega_{ki}}{2T} \left| \frac{\chi_m(\Delta t_j(i), T_{c,j}, T)}{j(\omega_{ki})} \right|^2 \quad (14.43)$$

Set

$$P(T) = \exp \left\{ - \sum_{m=1}^{n-1} \Gamma_m(\Delta t_j(i), T_{c,j}, T) \right\} \quad (14.44)$$

where $\Gamma_m(\Delta t_j(i), T_{c,j}, T)$ is derived from Equation 14.43.

So Equation 14.37 is changed into

$$\tilde{\rho}_S^{01}(T) = \tilde{\rho}_S^{01}(0) * \exp \left\{ - \sum_{m=1}^{n-1} \Gamma_m(\Delta t_j(i), T_{c,j}, T) \right\} = \tilde{\rho}_S^{01}(0) * P(T) \quad (14.45)$$

From Equation 14.45 one can see that $P(T)$ represents the attenuation rate of the non-diagonal element $\tilde{\rho}_S^{01}(0)$ at the moment T under dynamical decoupling schemes and

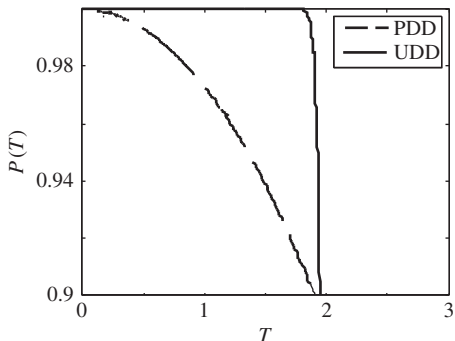


Figure 14.3 The curves of $P(T)$ while applying PDD and UDD

no control schemes, respectively. It is easy to see that when $P(T)$ is closer to 1, the better suppression of decoherence will be obtained. Thus we can observe the curves of the function $P(T)$ to understand the loss of the quantum coherence when the PDD and the UDD are applied, respectively.

14.2.4 Examples

Consider the six-level atom in Ξ -configuration shown in Figure 14.1. The six levels are labeled $|0\rangle$, $|1\rangle$, $|2\rangle$, $|3\rangle$, $|4\rangle$, and $|5\rangle$, respectively, and their energies are E_0 , E_1 , E_2 , E_3 , E_4 , and E_5 . The level $|k\rangle$ is coupled to the level $|k+1\rangle$ via the fields of resonance frequencies $\omega_{k+1,k}$, ($k = 0, 1, \dots, 4$), respectively. We place the atom under the driving of five fields with frequencies of $\omega_{j,j-1} = (E_j - E_{j-1})/\hbar$, ($1 \leq j \leq 5$), respectively. Similarly we define frequencies $\omega_{j,j-2}$ ($j-2 \geq 0$), \dots , $\omega_{j,j-n}$ ($j-5 \geq 0$), ($j = 2, 3, \dots, 5$).

According to Section 14.1.2, one can have $n = 6$. Thus from Equation 14.44 one can obtain

$$P(T) = \exp \left\{ - \sum_{m=1}^5 \Gamma_m (\Delta t_j(i), T_{c,j}, T) \right\} \quad (14.46)$$

Now insert Equations 14.41a–c and 14.42a–c in Equation 14.46. We do the numerical simulation experiments of the function $P(T)$ under the PDD and the UDD with the same other simulation parameters. The results are shown in Figure 14.3.

In Figure 14.3, the dotted line represents the evolution of $P(T)$ while the PDD is applied and the solid line represents the evolution of $P(T)$ while the UDD is applied. The correlated parameters are $\alpha = 0.25$, $T' = 150$ K, $N = 50$, and $\omega_c = 100$ Hz.

From Figure 14.3 one can see that under the same parameters, UDD is better at suppressing decoherence than PDD. The results reveal that UDD is optimized. This means that the UDD enhances the possible storage time by up to several times below a certain threshold of the loss of the quantum coherence. The number of pulses required to obtain a certain prolongation of the storage time of the UDD can be much smaller than the number for the standard scheme in PDD.

14.2.5 Discussion

We have investigated the suppression of decoherence of an n -level atom in Ξ -configuration by means of the dynamic decoupling methods in this section. Through comparison simulation experiments, it has been shown that UDD offers superior performance to PDD over a range of experimentally relevant parameters, such as the temperature of the bath T' , the cycle number N , the cut-off frequency ω_c , and the strength of the system–environment interaction α . This means that the optimized scheme in UDD can obtain more storage time than the standard one in PDD below a certain threshold of the loss of the quantum coherence when the same number of pulses is applied. This is very helpful in practical implementations of quantum computation. By selecting the non-diagonal element of the density matrix as a reference indicator, the comparison of the results also reveals that UDD enhances the possible storage time by up to several times below a certain threshold of the loss of quantum coherence. Alternatively, the number of pulses required to obtain a certain prolongation of the storage time can be much smaller than the number for the standard scheme in PDD. Compared to the standard equidistant pulse sequences, it is easy to see that the optimized dynamical decoupling scheme (UDD) is a good way to optimize the time intervals between the adjacent BB pulses.

14.3 An Optimized Dynamical Decoupling Strategy to Suppress Decoherence

In order to fight decoherence, many effective schemes have been proposed during the last few years. Dynamical decoupling (DD) (Viola and Lloyd, 1998; Viola, Knill, and Lloyd, 1999), based on a universal dynamical decoupling pulse sequence, is one of these promising techniques. The key ingredient of DD is the design of a classical control field to eliminate interaction with the environment as much as possible to achieve the purposes of decoupling with the environment and maintaining quantum coherence. The BB control method (Viola and Lloyd, 1998; Viola, Knill, and Lloyd, 1999; Duan and Guo, 1999; Zanardi, 1999; Viola, Lloyd, and Knill, 1999; Vitali and Tombesi, 1999) is the most typical control field which makes use of the coherent averaging effects (Haeberlen and Waugh, 1968) and applies frequent (unitary) interruptions during the evolution of the system to average out the effect of the unwanted Hamiltonian. According to different time intervals between adjacent pulses, the sequences can be divided into two categories: equidistant and non-equidistant sequences. In the first category are PDD (Viola, Knill, and Lloyd, 1998; Viola *et al.*, 1999) and the iterated Carr–Purcell–Meiboom–Gill (CPMG) sequence (Carr and Purcell, 1954; Meiboom and Gill, 1958), where the pulses are regularly divided (apart from the very first and the very last ones). The second category includes the universal UDD sequence (Uhrig, 2007), locally optimized dynamical decoupling (LODD) (Biercuk *et al.*, 2009), optimized noise filtration by dynamical decoupling (OFDD) (Uys *et al.*, 2009), and bandwidth-adapted dynamical decoupling (BADD) (Khodjasteh, Erd’elyi, and Viola, 2011) for pure dephasing models and concatenated dynamical decoupling (CDD) (Khodjasteh and Lidar, 2005) or concatenated UDD (CUDD) (Uhrig, 2009), quadratic DD (QDD) (West, Fong, and Lidar, 2010), or nested Uhrig dynamical decoupling (NUDD) (West, Fong, and Lidar, 2010; Mukhtar *et al.*, 2010) for models with dephasing and relaxation. So far, of all control sequences in the literature, UDD is the best.

In this section we will develop a new optimized DD scheme to suppress decoherence. Compared with established DD approaches, the highlight of our proposed approach is the novel method, which is a normal distribution, to determine the time intervals between successive pulses. Toward this goal, we first briefly derive the DD condition from group theoretical considerations (Viola and Lloyd, 1998), in which a short sequence of unitary decoupling operators is designed to completely cancel errors up to the first order in the Magnus expansion (Magnus, 1954). Then according to different time intervals between adjacent pulses, two important DD schemes, PDD and UDD, are analyzed and on this basis we propose our DD scheme, where the time intervals between adjacent pulses follow a normal distribution. In order to investigate the efficiency of our proposed decoupling scheme, we consider a Ξ -type three-level atom and select the non-diagonal element of the density matrix as a reference indicator to provide an analytic study of the performance of these three DD strategies. Through the comparison of the results, we analytically prove that our proposed decoupling strategy offers superior performance to PDD and UDD in the low error range of the non-diagonal element of the density matrix. This indicates that our optimized scheme can obtain more hold time than PDD or UDD under some low range of the loss of quantum coherence when the same number of pulses are applied, in other words, the pulses needed to reach a reasonable level of fidelity to the initial state in our proposed approach are smaller than the pulses in PDD and UDD.

14.3.1 Universal Dynamical Decoupling for a Qubit

It is known that because of the system–bath interaction Hamiltonian H_{SB} , the system results in decoherence. The core ideology of the UDD scheme, which is termed quantum BB control, is to design a BB control field and eliminate the unwanted Hamiltonian H_{SB} from the total Hamiltonian H for the whole system under the BB control field. The BB control field is implemented with the twin-born tailored powerful pulse sequence chosen deterministically, for example periodically (Viola and Lloyd, 1998; Byrd and Lidar, 2003; Pryadko and Sengupta, 2006), or randomly (Facchi, Lidar, and Pascazio, 2004; Viola and Knill, 2005). Each pulse in the pulse sequence represents a unitary BB operator, and the pulse sequence represents a BB operation group. Thus, the key to designing the BB control field is to design the BB operation group, and the operators in the BB operation group should be the smallest.

Suppose a quantum system has the evolution time T , and T is divided into N cycles equally, thus each cycle time length T_c is

$$T_c = T/N \quad (14.47)$$

Repeating the pulse sequences of the cycle time T_c N times forms the pulse sequences of the total time T , and this is shown in Figure 14.4.

Assume that the BB operation group is expressed as $G = \{g_m\} m = 0, 1, \dots, |G| - 1$, where $|G|$ represents the number of the operations and g_m is a constant pulse matrix. According to the BB operation group G , we can get the corresponding decoupling pulse sequence $\{D_j\}$ ($j = 1, 2, \dots, |G|$), where D_j can be written as (Viola, Lloyd, and Knill, 1999)

$$D_j = g_j g_{j-1}^+ \quad (14.48)$$

In every cycle T_c , one applies the pulse sequences $\{D_j\}$ on the system and divides the time T_c into $|G|$ pieces. Set Δt and τ_p^j are the inter-operation period and every pulse time, respectively, and the pulse sequences of the time T_c are shown in Figure 14.5.

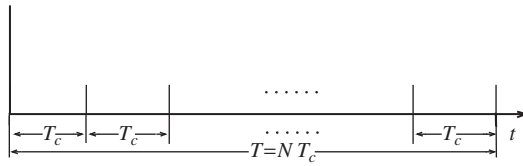


Figure 14.4 The pulse sequence of the total time T

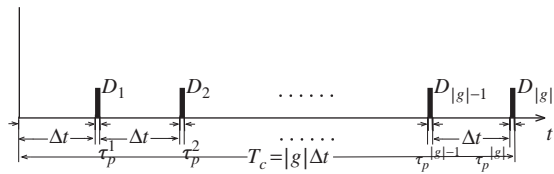


Figure 14.5 The pulse sequences of every cycle time T_c

Because τ_p^j is negligible ($\tau_p^j \ll \Delta t$), one can get

$$\Delta t = T_c / |g| = T / (N * |g|) \quad (14.49)$$

PDD is the basic DD scheme. When the designed BB operation group G satisfies the DD condition (Equation 14.13) and the time interval Δt between adjacent pulses is chosen equally, the designed pulse sequence in the total time T is called periodic dynamical decoupling.

From the analysis in Section 14.2 one can see that the periodic pulse sequences divide T into $N * |G|$ parts equally, and produce a pulse at the last moment t_i ($i = 1, 2, \dots, N * |G|$) of every part, so apart from the pulse at $t_{N*|G|} = T$, in the time interval $(0, T)$ the number of pulses M in Equation 14.27 is:

$$M = |G| * N - 1 \quad (14.50)$$

Set $t_i = \delta_i T$ ($i = 1, 2, \dots, M; 0 < \delta_1 < \delta_2 < \dots < \delta_{M-1} < \delta_M < 1$) and according to the principle of PDD, the M pulses moments t_i can be written as Equations 14.28 and 14.29:

$$t_i = T * \delta_{i-PDD} = T * i / (M + 1) \quad (14.51)$$

$$\delta_{i-PDD} = i / (M + 1), i = 1, 2, \dots, M \quad (14.52)$$

The difference with PDD is that UDD optimizes the time intervals between adjacent pulses, and the M pulses moments t_i of the UDD can be expressed as Equations 14.30 and 14.31:

$$t_i = T * \delta_{i-UDD} \quad (14.53)$$

$$\delta_{i-UDD} = \sin^2 [i * \pi / (2M + 2)], i = 1, 2, \dots, M \quad (14.54)$$

For example, take $M = 1, 2, 3, 4, 5, 6$, and 7 , respectively, and use UDD1, UDD2, UDD3, UDD4, UDD5, UDD6, and UDD7 to represent the corresponding UDD. The UDD pulse sequence of the total time T is shown in Figure 14.6.

14.3.2 An Optimized Dynamical Decoupling Scheme

Now we propose an alternative optimized DD scheme, which we call Cong-Chan-Dynamical Decoupling (CCDD). It also uses twin-born tailored powerful pulses to average out the effect of the unwanted Hamiltonian H_{SB} , and achieves the purpose of decoupling with the environment in which the BB operation group G is also designed to completely cancel errors up to the first order in the Magnus expansion, which should satisfy the DD condition (Equation 14.13). This is the same as for UDD, but the difference with UDD is that the time intervals between adjacent CCDD pulses follow a normal distribution, and the M moments t_i in the UDD pulses are fixed as

$$t_i = T * \delta_{i-CCDD} \quad (14.55)$$

$$\delta_{i-CCDD} = F(i, \mu, \sigma) = \frac{1}{\sqrt{2\pi}} \int_{-\infty}^i \exp\left(-\frac{(x - \mu)^2}{2\sigma^2}\right) dx, i = 1, 2, \dots, M \quad (14.56)$$

where μ and σ are the mean and variance of the normal distribution function $F(i, \mu, \sigma)$, respectively.

We set $\mu = (M + 1)/2$, but the variance σ can be selected arbitrarily. When a fixed variance σ is chosen, the corresponding pulse sequence is one kind of CCDD pulse sequence. For example, take $\sigma = (M - \mu)/2.5$, $M = 1, 2, 3, 4, 5, 6$, and 7 , respectively, and use CCDD1, CCDD2, CCDD3, CCDD4, CCDD5, CCDD6, and CCDD7 to represent the corresponding CCDD. Thus the CCDD pulse sequence of the total time T is shown in Figure 14.7.

14.3.3 Simulation and Comparison

In this section we will present the numerical simulation experiments to illustrate the effectiveness of the proposed CCDD in suppressing decoherence. We choose a Ξ -type three-level atom as the model for the simulation.

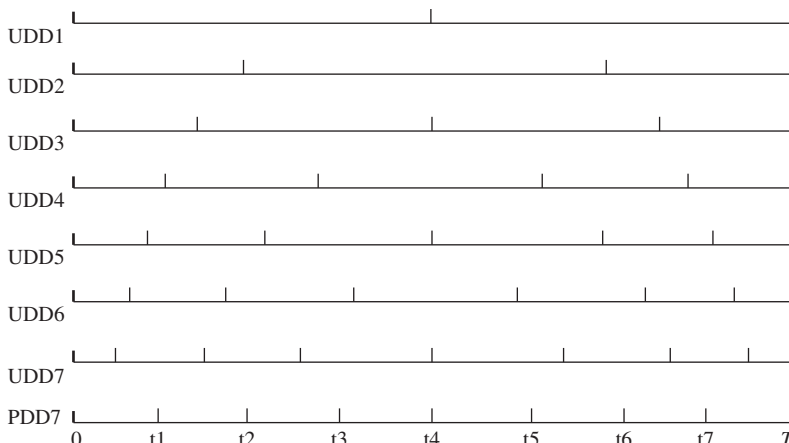


Figure 14.6 The UDD pulse sequence of the total time T

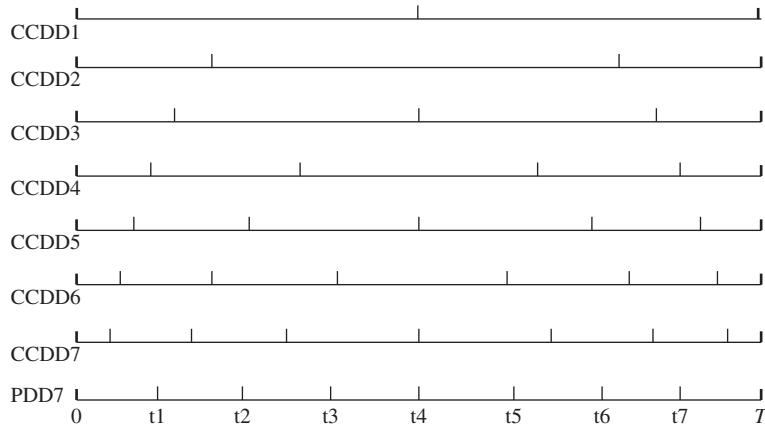


Figure 14.7 The CCDD pulse sequence of the total time T

1) Design of bang-bang operators

The total Hamiltonian of a Ξ -type three-level atom interacted with the environment can be expressed as (Wang *et al.*, 2008)

$$H = H_S + H_B + H_{SB} = \sum_{i>j=0}^2 \frac{\hbar\omega_{ij}}{3} \sigma_z^{(i,j)} + \sum_{i=0}^1 \sum_{ki} \hbar\omega_{ki} a_{ki}^\dagger a_{ki} + \hbar \sum_{i=0}^1 \sum_{ki} \sigma_z^{(i+1,i)} (j_{ki} a_{ki}^\dagger + j_{ki}^\dagger a_{ki}) \quad (14.57)$$

where the first part $\sum_{i>j=0}^2 \frac{\hbar\omega_{ij}}{3} \sigma_z^{(i,j)}$ represents the Hamiltonian H_S for the three-level atom, ω_{ij} is the resonant frequency between $|i\rangle$ and $|j\rangle$, σ_x , σ_y , and σ_z are the Pauli matrices, the second part $\sum_{i=0}^1 \sum_{ki} \hbar\omega_{ki} a_{ki}^\dagger a_{ki}$ represents the Hamiltonian H_B for the bath, a_{ki} and a_{ki}^\dagger are the bosonic annihilation and creation operators of the bath, the third part $\hbar \sum_{i=0}^1 \sum_{ki} \sigma_z^{(i+1,i)} (j_{ki} a_{ki}^\dagger + j_{ki}^\dagger a_{ki})$ represents the interaction Hamiltonian H_{SB} , which leads to the phase decoherence, and $\{j_{ki}\}$ are the coupling constants for virtual exchanges of excitations with the thermal bath.

According to Equation 14.50, combined with Equation 14.57, the decoupling dynamical condition can be written as

$$\sum_{m=0}^{|G|-1} g_m^\dagger \sigma_z^{(1,0)} g_m = 0 \text{ and } \sum_{m=0}^{|G|-1} g_m^\dagger \sigma_z^{(2,1)} g_m = 0 \quad (14.58)$$

from which we can find that a BB operation group $G = \{g_0, g_1, g_2\}$, where $|G| = 3$, $g_0 = I$, where I represents a unit matrix, $g_1 = \exp(i * \sigma_x^{(1,0)} * \pi/2) * \exp(i * \sigma_x^{(2,1)} * \pi/2)$, $g_2 = (g_1)^2 = g_1^\dagger = \exp(-i * \sigma_x^{(2,1)} * \pi/2) * \exp(-i * \sigma_x^{(1,0)} * \pi/2)$. Put the BB operation group G into Equation 14.58 and satisfy the dynamic decoupling condition. Thus according to Equation 14.48, the pulse sequence $\{D_i\}$ ($i = 1, 2, 3$) of every cycle time

can be expressed as $D_1 = g_1 g_0^+ = g_1$, $D_2 = g_2 g_1^+ = g_1$, and $D_3 = g_0 g_2^+ = g_1$, and $g_1 = \exp(i * \sigma_x^{(1,0)} * \pi/2) * \exp(i * \sigma_x^{(2,1)} * \pi/2)$ can be realized by a $\pi/2$ -pulse at frequency ω_{21} , which is followed by a $\pi/2$ -pulse at frequency ω_{10} .

2) Evolution of Ξ -type three-level atom

In order to analyze easily the impact of the pulse sequence, we transform the system into the interaction picture. The interaction Hamiltonian \tilde{H}_{SB} can be written as

$$\tilde{H}_{SB} = \hbar \sum_{i=0}^1 \sum_{ki} \sigma_z^{(i+1,i)} \left(j_{ki} a_{ki}^+ e^{i\omega_{ki} t} + j_{ki}^\dagger a_{ki} e^{-i\omega_{ki} t} \right) \quad (14.59)$$

and the evolution propagator of the whole system can be expressed as

$$\tilde{U}(t_s, t_o) = \exp \left\{ \sum_{i=0}^1 \sum_{ki} \sigma_z^{(i+1,i)} (a_{ki}^+ e^{i\omega_{ki} t_o} \zeta_{ki} (t_o - t_s) - h.c.) \right\} \quad (14.60)$$

where t_s and t_o represent the start and end moments of the evolution process, $\zeta_{ki} (t_o - t_s) = \frac{j(\omega_{ki})}{\omega_{ki}} (1 - e^{i\omega_{ki} (t_o - t_s)})$, respectively.

Consider the j th ($j = 1, 2, \dots, N$) decoupling cycle. After applying the pulse sequence $\{D_i\}$ ($i = 1, 2, 3$), the evolution propagator of the whole system during this process is

$$\tilde{U}(t_j^s, t_j^o) = D_3 \tilde{U}(t_j^{(2)}, t_j^{(3)}) D_2 \tilde{U}(t_j^{(1)}, t_j^{(2)}) D_1 \tilde{U}(t_j^{(0)}, t_j^{(1)}) \quad (14.61)$$

where t_j^s and t_j^o are the start and end moments of the j th decoupling cycle, with $t_j^s = t_j^{(0)}$ and $t_j^o = t_j^{(3)}$. Let $T_{c,j}$ represent the length of the j th decoupling cycle, then one can get $T_{c,j} = t_j^o - t_j^s$. Let $t_j^{(i)}$ and $\Delta t_j(i)$ ($i = 1, 2, 3$) represent the moment of the pulse D_i and the i th time interval of the pulses in the j th decoupling cycle. One can therefore have $\Delta t_j(i) = t_j^{(i)} - t_j^{(i-1)}$.

Then consider the total evolution time T . After applying periodically the pulse sequence $\{D_i\}$ ($i = 1, 2, 3$) in N decoupling cycles, the evolution propagator of the whole system is

$$\tilde{U}(0, T) = \tilde{U}(t_N^s, T) \tilde{U}(t_{N-1}^s, t_{N-1}^o) \cdots \tilde{U}(t_2^s, t_2^o) \tilde{U}(0, t_1^o) \quad (14.62)$$

3) Numerical simulation and comparison

In quantum information, the realization of a physically tractable quantum information system will be facilitated if qubit (quantum bit) error rates are far below the so-called fault-tolerance error threshold (Biercuk *et al.*, 2009). The greater the loss of quantum coherence is, the greater the qubit (quantum bit) error rates become. In DD schemes we can evaluate the loss of quantum coherence through the attenuation of the non-diagonal elements of the density matrix (Viola and Lloyd, 1998; Wang *et al.*, 2008). After applying the decoupling pulse sequences, we calculate the non-diagonal element $\rho_S^{ij}(T)$ ($j \neq i$) of the density matrix at the moment T and find the error $K^{ij}(t)$ with the non-diagonal element $\rho_S^{ij}(0)$ of the density matrix at the initial moment to give

$$K^{ij}(T) = \rho_S^{ij}(0) - \rho_S^{ij}(T) \quad (14.63)$$

In this work, we choose the non-diagonal element $\rho_S^{01}(T)$ and calculate $K^{01}(T)$. The other non-diagonal elements $\rho_S^{02}(T)$ and $\rho_S^{12}(T)$ can also be calculated, but they are not discussed here.

We assume that the atom and environment are initially uncorrelated, that is,

$$\rho_{total}(0) = \rho_S(0) \otimes \rho_B(0) \quad (14.64)$$

where $\rho_B(0)$ is a kind of thermal equilibrium state at temperature T' , that is,

$$\rho_B(0) = \prod_k (1 - e^{\beta \hbar \omega_k}) * e^{-\beta \hbar \omega_k a_k^\dagger a_k}$$

where $\beta = 1 / (k_B * T')$, k_B is the Boltzman constant, and T' is the temperature of the bath.

One can choose henceforth units such that $\hbar = k_B = 1$ for simplicity. Combining with Equations 14.58–14.62 and 14.64, one can obtain

$$\begin{aligned} \rho_S^{01}(T) &= \langle 0 | \text{Tr}_B \left\{ \tilde{U}(0, T) \rho_{total}(0) \tilde{U}^\dagger(0, T) \right\} | 1 \rangle \\ &= \rho_S^{01}(0) * \exp \left\{ -\Gamma_1(\Delta t_j(i), T_{c,j}, T) - \Gamma_2(\Delta t_j(i), T_{c,j}, T) \right\} \end{aligned} \quad (14.65)$$

where $i = 1, 2, 3, j = 1, 2, \dots, N$,

$$\Gamma_1(\Delta t_j(i), T_{c,j}, T) = \frac{1}{2} \sum_{ki} |\chi_1(\Delta t_j(i), T_{c,j}, T)|^2 \coth \frac{\omega_{ki}}{2T} \quad (14.66a)$$

$$\Gamma_2(\Delta t_j(i), T_{c,j}, T) = \frac{1}{2} \sum_{ki} |\chi_2(\Delta t_j(i), T_{c,j}, T)|^2 \coth \frac{\omega_{ki}}{2T} \quad (14.66b)$$

$\chi_1(\Delta t_j(i), T_{c,j}, T)$ and $\chi_2(\Delta t_j(i), T_{c,j}, T)$ in Equations 14.66a and 14.66b can be expressed as

$$\chi_1(\Delta t_j(i), T_{c,j}, T) = -2 * \eta_1(\Delta t_j(i), T_{c,j}, T) + \eta_2(\Delta t_j(i), T_{c,j}, T) + \eta_3(\Delta t_j(i), T_{c,j}, T) \quad (14.67a)$$

$$\chi_2(\Delta t_j(i), T_{c,j}, T) = -2 * \eta_3(\Delta t_j(i), T_{c,j}, T) + \eta_1(\Delta t_j(i), T_{c,j}, T) + \eta_2(\Delta t_j(i), T_{c,j}, T) \quad (14.67b)$$

where

$$\begin{aligned} \eta_1(\Delta t_j(i), T_{c,j}, T) &= \zeta_{ki}(\Delta t_1(1)) + \zeta_{ki}(\Delta t_2(1)) * e^{i\omega_{ki}T_{c,1}} + \dots \\ &\quad + \zeta_{ki}(\Delta t_n(1)) * e^{i\omega_{ki} \sum_{j=1}^{N-1} T_{c,j}} \end{aligned} \quad (14.68a)$$

$$\begin{aligned} \eta_2(\Delta t_j(i), T_{c,j}, T) &= \zeta_{ki}(\Delta t_1(2)) * e^{i\omega_{ki}\Delta t_1(1)} + \zeta_{ki}(\Delta t_2(2)) * e^{i\omega_{ki}\Delta t_2(1)} * e^{i\omega_{ki}T_{c,1}} \\ &\quad \dots + \zeta_{ki}(\Delta t_N(2)) * e^{i\omega_{ki}\Delta t_N(1)} * e^{i\omega_{ki} \sum_{j=1}^{N-1} T_{c,j}} \end{aligned} \quad (14.68b)$$

$$\eta_3(\Delta t_j(i), T_{c,j}, T) = \zeta_{ki}(\Delta t_1(3)) * e^{i\omega_{ki}(\Delta t_1(1)+\Delta t_1(2))}$$

$$\begin{aligned}
& + \zeta_{ki} (\Delta t_2 (3)) * e^{i\omega_{ki}(\Delta t_2(1)+\Delta t_2(2))} * e^{i\omega_{ki}T_{c,1}} \\
& + \dots + \zeta_{ki} (\Delta t_N (3)) * e^{i\omega_{ki}(\Delta t_N(1)+\Delta t_N(2))} * e^{i\omega_{ki}\sum_{j=1}^{N-1} T_{c,j}}
\end{aligned} \quad (14.68c)$$

It is known that the spectral density $I(\omega) \rightarrow 0$ when the frequency ω is greater than the finite cut-off frequency of each mode of the environment ω_c , that is, $\omega > \omega_c$ (Viola and Lloyd, 1998). Assume a spectral density with the following functional form:

$$I(\omega) = \frac{\alpha}{4} \omega^r e^{-\omega/\omega_c} \quad (14.69)$$

where the parameter $\alpha > 0$ measures the strength of the system–environment interaction and the index $r > 0$ classifies different environment behaviors. Here the bath we considered is the general Ohmic bath, and $r = 1$ (Leggett *et al.*, 1987; Palma, Suominen, and Ekert, 1996; Hu, Paz, and Zhang, 1992; Mozyrsky and Provman, 1998).

By considering the continuum limit of the bath mode, Equations 14.66a and 14.66b can become (Viola and Lloyd, 1998; Hu, Paz, and Zhang, 1992)

$$\Gamma_1 (\Delta t_j(i), T_{c,j}, T) = \frac{1}{2} \int_0^{\omega_c} d\omega_{ki} I(\omega_{ki}) \coth \frac{\omega_{ki}}{2T} \left| \frac{\chi_1 (\Delta t_j(i), T_{c,j}, T)}{j(\omega_{ki})} \right|^2 \quad (14.70a)$$

$$\Gamma_2 (\Delta t_j(i), T_{c,j}, T) = \frac{1}{2} \int_0^{\omega_c} d\omega_{ki} I(\omega_{ki}) \coth \frac{\omega_{ki}}{2T} \left| \frac{\chi_2 (\Delta t_j(i), T_{c,j}, T)}{j(\omega_{ki})} \right|^2 \quad (14.70b)$$

Combined with Equations 14.65, 14.67a and 14.67b, 14.68a and 14.68b, and 14.70a and 14.70b, Equation 14.63 can be changed into

$$K^{01}(T) = \rho_S^{01}(0) - \rho_S^{01}(T) = \rho_S^{01}(0) * (1 - \exp \{-\Gamma_1 (\Delta t_j(i), T_{c,j}) - \Gamma_2 (\Delta t_j(i), T_{c,j})\}) \quad (14.71)$$

Setting $P^{01}(T) = 1 - \exp \{-\Gamma_1 (\Delta t_j(i), T_{c,j}, T) - \Gamma_2 (\Delta t_j(i), T_{c,j}, T)\}$, one can have $K^{01}(T) = \rho_S^{01}(0) - \rho_S^{01}(T) = \rho_S^{01}(0) * P^{01}(T)$, in which $P^{01}(T)$ represents the attenuation ratio of the non-diagonal element $\rho_S^{01}(0)$ at the moment T . Thus we can observe the curve of the function $P^{01}(T)$ as a tolerate error to understand the loss of quantum coherence.

According to the decoupling pulse sequences in PDD, UDD, and CCDD, we get individual $\Delta t_j(i)$ and $T_{c,j}$ as follows.

1. When PDD is applied, one has

$$\delta_{0-PDD} = 0, \delta_{(3*N)-PDD} = 1 \quad (14.72a)$$

$$\Delta t_j(i) = (\delta_{m-PDD} - \delta_{(m-1)-PDD}) * T, m = (j-1) * 3 + i, i = 1, 2, 3, j = 1, 2, \dots, N, \quad (14.72b)$$

$$T_{c,j} = \Delta t_j(1) + \Delta t_j(2) + \Delta t_j(3) \quad (14.72c)$$

2. When UDD is applied, one has

$$\delta_{0-UDD} = 0, \delta_{(3*N)-UDD} = 1 \quad (14.73a)$$

$$\Delta t_j(i) = (\delta_{m-UDD} - \delta_{(m-1)-UDD}) * T, m = (j-1) * 3 + i, i = 1, 2, 3, j = 1, 2, \dots, N, \quad (14.73b)$$

$$T_{c,j} = \Delta t_j(1) + \Delta t_j(2) + \Delta t_j(3) \quad (14.73c)$$

3. When CCDD is applied, one has

$$\delta_{0-CCDD} = 0, \delta_{(3*N)-CCDD} = 1 \quad (14.74a)$$

$$\Delta t_j(i) = (\delta_{m-CCDD} - \delta_{(m-1)-CCDD}) * T, m = (j-1) * 3 + i, i = 1, 2, 3, j = 1, 2, \dots, N, \quad (14.74b)$$

$$T_{c,j} = \Delta t_j(1) + \Delta t_j(2) + \Delta t_j(3) \quad (14.74c)$$

Now we numerically simulate the function $P^{01}(T)$ under PDD, UDD, and CCDD with the same simulation parameters, respectively. The results are shown in Figure 14.8.

In Figure 14.8, the horizontal axis $\omega_c * T$ represents time and the vertical axis is $P^{01}(T)$. The chain dotted line represents the $P^{01}(T)$ of PDD, the dotted line represents the evolution of $P^{01}(T)$ in UDD, and the three solid lines represent the evolution of $P^{01}(T)$ for three kinds of CCDD pulse sequences with different variances σ : from top to bottom the variances σ of the three CCDD pulse sequences are fixed as $\sigma = (M - \mu)/3$, $\sigma = (M - \mu)/3.5$, and $\sigma = (M - \mu)/4.5$, respectively. The other correlated parameters are $\alpha = 0.25$, $T' = 1$, $\omega_c = 100$ Hz, and $N = 20$.

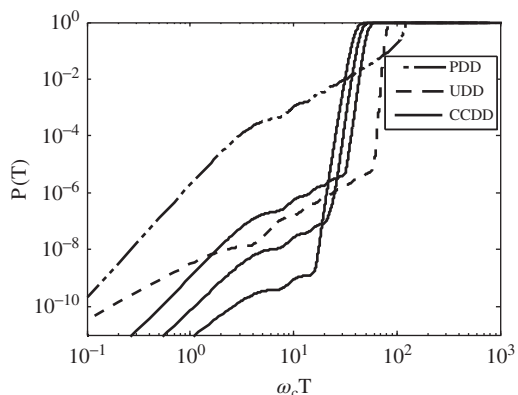


Figure 14.8 The curves of $P^{01}(T)$ under PDD, UDD, and CCDD

Table 14.1 Comparison of the hold times of the qubit at some tolerate error levels

Approach	Hold time	Error level	PDD (seconds)	UDD (seconds)	CCDD (seconds)
	$P^{01}(T) = 10^{-7}$		0.0050	0.0730	$0.2069 \text{ s } (\sigma = (M - \mu) / 3.5)$
	$P^{01}(T) = 10^{-9}$		0.0020	0.0060	$0.1080 \text{ s } (\sigma = (M - \mu) / 4.5)$

14.3.4 Discussion

From the comparison of the results in Figure 14.8, one can see that

1. CCDD pulse sequences are related to variance σ . One can get many kinds of CCDD pulse sequences with different values of σ . Smaller variances are better at suppressing the decoherence of CCDD effects.
2. The loss of the quantum coherence under UDD is much slower than that of under PDD, and the loss of quantum coherence under CCDD is the slowest during the initial stage.
3. We can always find an appropriate small variance σ . One can see from Figure 14.8 that when the variance σ is fixed as $\sigma = (M - \mu) / 3.5$ and $\sigma = (M - \mu) / 4.5$, respectively, the corresponding CCDD gets the longest lasting time of all three cases. For example, with a tolerance error of $P^{01}(T) = 10^{-7}$ and variance $\sigma = (M - \mu) / 3.5$, the hold times for PDD, UDD, and CCDD are 0.0050, 0.0730, and 0.2069 a.u., respectively. The hold time for CCDD is 0.2019 seconds longer than that of PDD, and 0.1339 seconds longer than that of UDD. With a tolerance error of $P^{01}(T) = 10^{-9}$ and variance $\sigma = (M - \mu) / 4.5$, the hold times of PDD, UDD, and CCDD are 0.0020, 0.0060, and 0.1080 a.u., respectively. The hold time of CCDD is 0.1060 a.u. longer than that of PDD and 0.1020 a.u. longer than that of UDD. Table 14.1 compares the hold times of qubits at some error levels for PDD, UDD, and CCDD.

Another important aspect for the efficiency of the proposed approach is how many pulses are needed to reach a reasonable level of fidelity to the initial state. It is well known that at a reasonable error level in the same length of time, the smaller the pulses needed to keep the qubit the better the approach will be. In order to analyze the effectiveness of the number of pulses, we plot the curves of $P^{01}(T)$ under the action of CCDD and UDD, as shown in Figure 14.9, in which the solid lines represent the $P^{01}(T)$ of CCDD. The CCDD sequences are, from the top to bottom, for variances σ fixed as $\sigma = (M - \mu) / 3.5$ and $\sigma = (M - \mu) / 4$, respectively. The other parameters are $N = 20$, $\alpha = 0.25$, $T' = 1$, and $\omega_c = 100 \text{ Hz}$. The dotted lines represent the $P^{01}(T)$ while UDD is applied, from the top to bottom, the number of the cycles N are 20, 30, and 70. The other parameters are $\alpha = 0.25$, $T' = 1$, and $\omega_c = 100 \text{ Hz}$. From Figure 14.9 it is easy to see that when we choose the number of cycles to be 20, that is, the number of pulses is $60 = N * 3 = 20 * 3$, with $\sigma = (M - \mu) / 3.5$ for both UDD and CCDD, the CCDD sequence gives better performance if the error level is selected as $P^{01}(T) \leq 10^{-6}$. For example, with a tolerate error of $P^{01}(T) = 10^{-7}$ with $\sigma = (M - \mu) / 3.5$, in order to maintain the same length of time, one can calculate that the number of pulses needed to reach this tolerate error level under

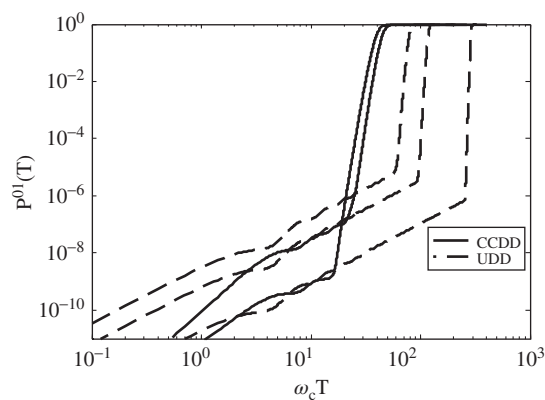


Figure 14.9 The curves of $P^{01}(T)$ under CCDD and UDD

Table 14.2 Comparison of the number of pulses needed to keep some error levels under the actions of UDD and CCDD

Approach	Number of pulses	Error level	UDD	CCDD
$P^{01}(T) = 10^{-7}$			90	60 (with $\sigma = (M - \mu)/3.5$)
$P^{01}(T) = 10^{-9}$			210	60 (with $\sigma = (M - \mu)/4$)

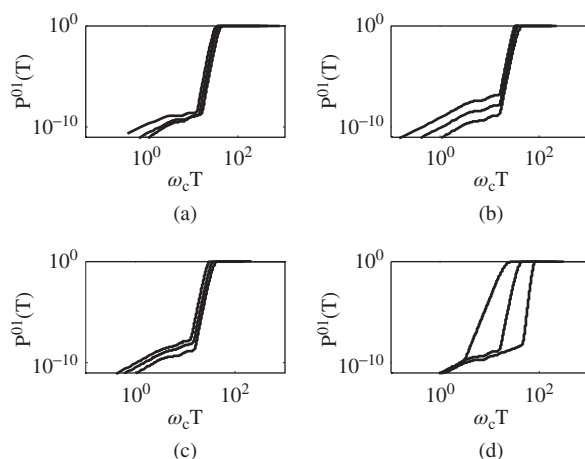


Figure 14.10 The curves of $P^{01}(T)$ under the action of CCDD with different parameters: (a) $P^{01}(T)$ for $\alpha = 0.25$, $T' = 1$, $N = 20$, and cut-off frequency $\omega_c = 50$, 200 , and 500 Hz, (b) for $T' = 1$, $N = 20$, and $\omega_c = 100$ Hz, and $\alpha = 0.25$, 2.5 , and 25 , (c) for $\alpha = 0.25$, $N = 20$, $\omega_c = 100$ Hz, and $T' = 1$, 100 , 200 , and (d) for $\alpha = 0.25$, $T' = 1$, $\omega_c = 100$ Hz, and $N = 10$, 20 , 30

the action of UDD is $90(14.71^*3)$, while the pulse number of CCDD is $60 = 20^*3$, which is 30 less than that of UDD. In addition, with a tolerate error of $P^{01}(T) = 10^{-9}$, in order to maintain the same length of time, the number of pulses needed in UDD is $210 = 70^*3$, but the number of pulses needed in CCDD with variance $\sigma = (M - \mu)/4.5$ is $60 = 20^*3$, which is 150 less than for UDD. Table 14.2 gives the comparison of the number of pulses needed to keep some tolerate error levels under the actions of UDD and CCDD.

Now we analyze the effects of the parameters. Figure 14.10 gives the curves of $P^{01}(T)$ under the action of CCDD with different parameters and fixed $\sigma = (M - \mu)/4$. From top to bottom, Figure 14.10a shows $P^{01}(T)$ in the case of $\alpha = 0.25$, $T' = 1$, $N = 20$, and the cut-off frequencies $\omega_c = 50, 200$, and 500 Hz, respectively, Figure 14.10b is for $T' = 1$, $N = 20$, and $\omega_c = 100$ Hz, and $\alpha = 0.25, 2.5$, and 25 , respectively. Figure 14.10c is for $\alpha = 0.25$, $N = 20$, $\omega_c = 100$ Hz, and $T' = 1, 100$, and 200 , respectively. Figure 14.10d is for $\alpha = 0.25$, $T' = 1$, $\omega_c = 100$ Hz, and $N = 10, 20$, and 30 , respectively.

We can conclude the following from Figure 14.10:

1. The $P^{01}(T)$ declines faster as ω_c increases. This means that the ability to suppress decoherence decreases when the cut-off frequency ω_c increases.
2. Since α measures the strength of the system–environment interaction, it is seen that $P^{01}(T)$ declines faster as α increases, and one needs to use more sequences to obtain the same suppression decoherence effect.
3. The higher temperature T' , the worse the decoupling effect becomes.
4. $P^{01}(T)$ declines slower as N increases, indicating that the more pulses we apply, the better the performance of decoupling decoherence will be.

The effects of the variations of parameters in the CCDD sequence with $\sigma = (M - \mu)/4$ are given in Table 14.3.

Table 14.3 The effects of the variations of parameters in CCDD sequence with $\sigma = (M - \mu)/4$

Changing parameters	Fixed parameters	Variation values of parameters	Value of $P^{01}(T)$ at $T = 0.5$	Effects
The cut-off frequency ω_c	$\alpha = 0.25$	50 Hz	$7.22 * 10^{-5}$	ω_c increases, the performance
	$T' = 1$	200 Hz	0.999 632	decreases
	$N = 20$	500 Hz	0.999 999	
The strength of system-environment interaction α	$T' = 1$	0.25	0.932 612	α increases, the performance
	$N = 20$	2.5	0.999 324	decreases
	$\omega_c = 100$ Hz	25	0.999 999	
The environment temperature T'	$\alpha = 0.25$	1	0.932 612	T' increases, the performance
	$N = 20$	100	0.998 793	decreases
	$\omega_c = 100$ Hz	200	0.999 997	
The cycles of the sequence N	$\alpha = 0.25$	10	0.981 746	N increases, the performance
	$T' = 1$	20	0.932 612	increases
	$\omega_c = 100$ Hz	40	$4.74 * 10^{-8}$	

References

- Biercuk, M.J., Uys, H., VanDevender, A.P. *et al.* (2009) Optimized dynamical decoupling in a model quantum memory. *Nature*, **458**, 996–1000.
- Byrd, M.S. and Lidar, D.A. (2003) Empirical determination of dynamical decoupling operations. *Physical Review A*, **67**(1), 012324.
- Calderbank, A.R. and Shor, P.W. (1996) Good quantum error-correcting codes exist. *Physical Review A*, **54**(2), 1098–1105.
- Cao, W.C., Liu, X.S. and Bai, H.B. (2008) Bang-bang control suppression of amplitude damping in a three-level atom. *Science in China Series G-Physics Mechanics Astron*, **51**(1), 29–37.
- Carr, H.Y. and Purcell, E.M. (1954) Effects of diffusion on free precession in nuclear magnetic resonance experiments. *Physical Review*, **94**(3), 630–638.
- Duan, L.M. and Guo, G.C. (1997) Preserving coherence in quantum computation by pairing quantum bits. *Physical Review Letters*, **79**(10), 1953–1956.
- Duan, L.M. and Guo, G.C. (1998) Prevention of dissipation with two particles. *Physical Review A*, **57**(4), 2399–2402.
- Duan, L.M. and Guo, G.C. (1999) Suppressing environmental noise in quantum computation through pulse control. *Physics Letters A*, **261**(3–4), 139–144.
- Facchi, P., Lidar, D.A. and Pascazio, S. (2004) Unification of dynamical decoupling and the quantum Zeno effect. *Physical Review A*, **69**(3), 032314.
- Feynman, R. (1982) Simulating physics with computers. *International Journal of Theoretical Physics*, **21**, 467–488.
- Gardiner, C.W. (1991) *Quantum Noise*, Springer, Berlin.
- Haeberlen, U. and Waugh, J.S. (1968) Coherent averaging effects in magnetic resonance. *Physical Review*, **175**, 453–467.
- Hu, B.L., Paz, J.P. and Zhang, Y. (1992) Quantum Brownian motion in a general environment: exact master equation with nonlocal dissipation and colored noise. *Physical Review D*, **45**(8), 2843–2861.
- Khodjasteh, K., Erd'elyi, T. and Viola, L. (2011) Limits on preserving quantum coherence using multi-pulse control. *Physical Review A*, **83**(2), 020305(R).
- Khodjasteh, K. and Lidar, D.A. (2005) Fault-tolerant quantum dynamical decoupling. *Physical Review Letters*, **95**(18), 180501.
- Laflamme, R., Miquel, C., Paz, J.P. *et al.* (1996) Perfect quantum error correcting code. *Physical Review Letters*, **77**(1), 198–201.
- Leggett, A., Chakravarty, S., Dorsey, A. *et al.* (1987) Dynamics of the dissipative two-state system. *Reviews of Modern Physics*, **59**(1), 1–85.
- Liu, X.S., Wu, R.B., Liu, Y. *et al.* (2005a) Decoupling bang-bang group for adiabatic decoherence control in a three-level atom. *Communications in Theoretical Physics*, **44**(5), 810–816.
- Liu, X.S., Wu, R.B., Liu, Y. *et al.* (2005b) Dynamical control of adiabatic decoherence in the single three-level atom. *Journal of Optics B: Quantum and Semiclassical Optics*, **7**(9), 268–275.
- Magnus, W. (1954) On the exponential solution of differential equations for a linear operator. *Communications on Pure and Applied Mathematics*, **7**(4), 649–673.
- Meiboom, S. and Gill, D. (1958) Modified spin-echo method for measuring nuclear relaxation times. *Review of Scientific Instruments*, **29**(8), 688–691.
- Mozyrsky, D. and Provman, V. (1998) Adiabatic decoherence. *Journal of Statistical Physics*, **91**(3–4), 787–799.
- Mukhtar, M., Soh, W.T., Saw, T.B. *et al.* (2010) Protecting unknown two-qubit entangled states by nesting Uhrig's dynamical decoupling sequences. *Physical Review A*, **82**(5), 052338.
- Palma, G.M., Suominen, K.A. and Ekert, A.K. (1996) Quantum computers and dissipation. *Proceedings of the Royal Society London A*, **452**(1946), 567–584.
- Pryadko, L.P. and Sengupta, P. (2006) Quantum kinetics of an open system in the presence of periodic refocusing fields. *Physical Review B*, **73**(8), 085321.

- Ticozzi, F. and Ferrante, A. (2006) Dynamical decoupling in quantum control: a system theoretic approach. *Systems & Control Letters*, **55**(7), 578–584.
- Uhrig, G.S. (2007) Keeping a quantum bit alive by optimized π -pulse sequences. *Physical Review Letters*, **98**(10), 100504.
- Uhrig, G.S. (2009) Concatenated control sequences based on optimized dynamic decoupling. *Physical Review letters*, **102**, 120502.
- Unruh, W.G. (1995) Maintaining coherence in quantum computers. *Physical Review A*, **51**(2), 992–997.
- Uys, H., Biercuk, M.J. and Bollinger, J.J. (2009) Optimized noise filtration through dynamical decoupling. *Physical Review Letters*, **103**(4), 040501.
- Viola, L. and Knill, E. (2005) Random decoupling schemes for quantum dynamical control and error suppression. *Physical Review Letters*, **94**(6), 060502.
- Viola, L., Knill, E. and Lloyd, S. (1999) Dynamical decoupling of open quantum systems. *Physical Review Letters*, **82**(12), 2417–2421.
- Viola, L. and Lloyd, S. (1998) Dynamical suppression of decoherence in two-state quantum systems. *Physical Review A*, **58**(4), 2733–2744.
- Viola, L., Lloyd, S. and Knill, E. (1999) Universal control of decoupled quantum systems. *Physical Review letters*, **83**(23), 4888–4891.
- Vitali, D. and Tombesi, P. (1999) Using parity kicks for decoherence control. *Physical Review A*, **59**(6), 4178–4186.
- Wang, Y.-H., Hao, L., Zhou, X. et al. (2008) Behavior of quantum coherence of Ξ -type four-level atom under bang–bang control. *Optics Communications*, **281**(18), 4793–4799.
- West, J.R., Fong, B.H. and Lidar, D.A. (2010) Near-optimal dynamical decoupling of a qubit. *Physical Review Letters*, **104**(13), 130501.
- Zanardi, P. (1999) Symmetrizing evolutions. *Physics Letters A*, **258**(2–3), 77–82.
- Zanardi, P. and Rasetti, M. (1997) Noiseless quantum codes. *Physical Review Letters*, **79**(17), 3306–3309.

15

Trajectory Tracking of Quantum Systems

Over the last few decades, a series of research results has been widely used in chemical reactions (Shapiro and Brumer, 1997), molecular motion (Chen *et al.*, 1995), quantum teleportation (Wang, 2001), and so on. After intensive study for half a century, many methods in classical control theory have been introduced into microscopic systems, such as optimal control (D'Alessandro and Dahleh, 2001; Cong and Zhang, 2011; Sugawara, 2003; Salomon and Turinici, 2006; Zhang and Chen, 2008; Chen *et al.*, 2008), adaptive control (Zhu and Rabitz, 1999; Abhinav *et al.*, 2009; Rothman, Ho, and Rabitz, 2005), and Lyapunov-based control (Wang and Schirmer, 2010a,b; Liu and Cong, 2011; Karasik *et al.*, 2008; Mirrahimi, Rouchon, and Turinici, 2005a; Mirrahimi, Turinici, and Rouchon, 2005b; Beaucharda *et al.*, 2007; Liu, Cong, and Zhu, 2012). Depending on whether a system is isolated or interacts with the environment, a quantum system can be divided into a closed or an open system. In a closed quantum system, the system is in unitary evolution. In an open quantum system, the leakage of information from system to environment leads to un-unitary evolution. The commonly used master equation for an open quantum system is in the Lindblad style, $\dot{\rho} = -\frac{i}{\hbar}[H_0, \rho] + L_D(\rho)$, which consists of a closed system $\dot{\rho} = -\frac{i}{\hbar}[H_0, \rho]$ with a dissipation item $L_D(\rho)$. Obviously, the analysis of a closed quantum system is easier. In fact, the study of closed quantum systems is the basis of open quantum system research. Currently, there are still many unresolved problems of control and methods in closed quantum systems that require further study.

From the system control perspective, two types of control problems can be classified in quantum systems. One is state transfer or state preparation, which involves the transfer of an arbitrary initial state to a desired target state under the action of control law designed by means of a suitable kind of system control theory. The other is tracking control, which consists of orbit tracking and trajectory tracking. Orbit tracking refers to the tracking of a free-evolutionary system of the target system, where the target system has the same free Hamiltonian H_0 as the system controlled. Orbit tracking is a unique phenomenon in quantum systems because there is always free-evolution even without the control. There are two types of trajectory tracking.

The first tracks another target quantum system $i\hbar \frac{\partial}{\partial t} \hat{\rho}_f(t) = \left[H_{0f} + \sum_r f_r H_r, \hat{\rho}_f(t) \right]$, which may

possess the same free Hamiltonian as the system controlled or a different one. This is just orbit tracking when $H_{0f} = H_0$ and $f_r = 0$, therefore orbit tracking is a special case of trajectory tracking. This problem will be discussed in Sections 15.1 and 15.2. The second type tracks an arbitrary time-dependent function, such as ramp function, step function, and so on. This is discussed in Section 15.3.

15.1 Orbit Tracking of Quantum States Based on the Lyapunov Method

For a quantum system described by the Liouville equation, the density matrix ρ is used to represent the system state. Here we would like to introduce an error $\hat{e}(t)$ as a new state of the control system, which is defined as the difference between the target state $\hat{\rho}_f(t)$ and the controlled state $\hat{\rho}(t)$, that is, $\hat{e}(t) = \hat{\rho}_f(t) - \hat{\rho}(t)$. In the control system with the error as the controlled state, the control goal becomes to steer an arbitrary initial error state to zero, which results in the same control goal of making the controlled state $\hat{\rho}(t)$ track the target state $\hat{\rho}_f(t)$, that is, $\hat{\rho}(t)$ follows $\hat{\rho}_f(t)$. In this way we can change the quantum state trajectory tracking problem into a state regulation problem. A unitary transformation is performed in the quantum system in order to facilitate control law design. The control law is designed based on the Lyapunov stability theorem. So far the studies of trajectory tracking have only involved pure state tracking (Mirrahimi and Rouchon, 2004; Mirrahimi, Turinici, and Rouchon, 2005b) because state tracking in these studies depends on the error defined by the Lyapunov function. Because of the defined error state, the control strategy proposed in this section will be available to different kinds of quantum state transfer, including pure state, superposition state, and mixed state.

15.1.1 Description of the System Model

The state of a quantum mechanical system can be described in various ways. A pure state system not entangled with the environment can be represented by wave functions that evolve according to the Schrödinger equation. In another formation, one can describe the system state by a density operator $\hat{\rho}(t)$ that evolves with time in terms of quantum Liouville equation acting on the system's Hilbert space:

$$i\hbar \frac{\partial}{\partial t} \hat{\rho}(t) = \left[H_0 + \sum_{m=1}^M f_m(t) H_m, \hat{\rho}(t) \right], \hat{\rho}(0) = \hat{\rho}_0 \quad (15.1)$$

$$i\hbar \frac{\partial}{\partial t} \hat{\rho}_f(t) = [H_0, \hat{\rho}_f(t)], \hat{\rho}_f(0) = \hat{\rho}_{f0} \quad (15.2)$$

where H_0 and H_m represent the system's internal (or free) and external (or control) Hamiltonian, respectively, and these will be assumed to be time-independent. $f_m(t)$ are time-dependent external control fields. We choose the Planck constant $\hbar = 1$ for convenience.

Here the error $\hat{e}(t)$ is defined as

$$\hat{e}(t) = \hat{\rho}_f(t) - \hat{\rho}(t) \quad (15.3)$$

The control system with this state error can be derived by subtracting Equation 15.1 from Equation 15.2:

$$i\frac{\partial}{\partial t}\hat{e}(t) = \left[H_0 + \sum_{m=1}^M f_m(t)H_m, \hat{e}(t) \right] - \left[\sum_{m=1}^M f_m(t)H_m, \hat{\rho}_f(t) \right], \quad \hat{e}(0) = \hat{\rho}_{f0} - \hat{\rho}_0 \quad (15.4)$$

Unitary transformation plays an important role in quantum systems. Just as linear transformation is always used to simplify calculations in the macroscopic systems, here unitary transformation is needed for the quantum system (Equation 15.4) to simplify the Lyapunov-based control law design. We employ a unitary transformation $U(t) = \exp(-iH_0t)$, and $e(t) = U^\dagger(t)\hat{e}(t)U(t)$, where “ \dagger ” denotes the conjugate and “ \wedge ” denotes the state before the unitary transformation.

Equation 15.4 can be written after the unitary transformation as

$$i\frac{\partial}{\partial t}e(t) = \left[\sum_{m=1}^M f_m(t)H_m(t), e(t) \right] - \left[\sum_{m=1}^M f_m(t)H_m(t), \rho_f(t) \right] \quad (15.5a)$$

$$\rho_f(t) = U^\dagger(t)\hat{\rho}_f(t)U(t) \quad (15.5b)$$

where $H_m(t) = U^\dagger(t)H_mU(t)$.

According to Equation 15.5b and $e(t) = U^\dagger(t)\hat{e}(t)U(t)$, one can get $e(t) = \rho_f(t) - \rho(t)$ and $\rho(t) = U^\dagger(t)\hat{\rho}(t)U(t)$. The same transformation is used for the initial error $\hat{e}(0)$. As a result of the unitary transformation $U(0) = U^\dagger(0) = 1$ ($t = 0$) one has $e(0) = \hat{e}(0) = \hat{\rho}_{f0} - \hat{\rho}_0$.

On the other hand, the solution of Equation 15.2 is $\hat{\rho}_f(t) = U(t)\hat{\rho}_f(0)U^\dagger(t)$, where $U(t) = \exp(-iH_0t)$. By substituting this solution into Equation 15.5b, the target state $\rho_f(t)$ becomes

$$\rho_f(t) = U^\dagger(t)U(t)\hat{\rho}_f(0)U^\dagger(t)U(t) = \hat{\rho}_f(0) = \hat{\rho}_{f0} \quad (15.6)$$

so one can replace $\rho_f(t)$ with $\hat{\rho}_{f0}$ in Equation 15.5a and obtain

$$i\frac{\partial}{\partial t}e(t) = \left[\sum_{m=1}^M f_m(t)H_m(t), e(t) \right] - \left[\sum_{m=1}^M f_m(t)H_m(t), \hat{\rho}_{f0} \right] \quad (15.7a)$$

$$e(0) = \hat{e}(0) = \hat{\rho}_{f0} - \hat{\rho}_0 \quad (15.7b)$$

Equations 15.7a and 15.7b are the new transformed control system.

From the procedure above one can see the following:

First, the target state $\hat{\rho}_f(t)$ in Equation 15.2 is time-dependent and non-stationary. After the unitary transformation, $\rho_f(t)$ becomes time-independent and stationary, with a constant value that is equal to the initial value of target state $\hat{\rho}_f(0)$.

Second, after the transformation, the control Hamiltonian H_m , which is time-independent, becomes $H_m(t)$, which is time-dependent.

After introducing the error state equation (Equation 15.3) and the unitary transformation $U(t) = \exp(-iH_0t)$, the problem of state $\hat{\rho}(t)$ tracking $\hat{\rho}_f(t)$ is changed into a regulation problem of error $e(t)$ in Equations 15.7a and b. Error $e(t)$ is the new controlled state, and the new control goal becomes to regulate an arbitrary initial error state e_0 to $e_f = 0$. The control task now is to design an effective control law $f_m(t)$ such that the new state $e(t)$

will be zero, which is equivalent to controlling the system state $\hat{\rho}(t)$ to track the target state $\hat{\rho}_f(t)$.

15.1.2 Design of Control Law

Of the many control methods, the Lyapunov method is the simplest and easiest to design. The basic idea of the Lyapunov method is to select $V(x)$ as the Lyapunov function, which must satisfy the following three conditions: (a) $V(x)$ is positive semi-definite, that is, $V(x) \geq 0$, (b) $V(x)$ equals zero only when the system is in the target state (the system is able to remain in the target state from then on because of the zero value of the control), and (c) the first-order time derivative of the Lyapunov function is negative semi-definite, that is, $\dot{V}(x) \leq 0$, and the target state will be stable in the Lyapunov sense.

Generally, there are three kinds of Lyapunov function forms for the Schrödinger equation. Here we choose the one for the Liouville equation as

$$V = \frac{1}{2} \text{tr}(e^2) \quad (15.8)$$

It can be seen from Equation 15.8 that for every e , $V \geq 0$ and $V = 0$ only when $e \rightarrow 0$. Condition (a) holds.

According to condition (c):

$$\dot{V} = \sum_{m=1}^M f_m(t) \text{tr}(iH_m(t)[\hat{\rho}_f, e(t)]) \quad (15.9)$$

For the sake of simplicity and availability, we let each item on the right-hand side of Equation 15.9 with a summation sign be non-positive in order to ensure $\dot{V} \leq 0$. The control laws can be derived as

$$f_m(t) = -k_m(\text{tr}(iH_m(t)[\hat{\rho}_f, e(t)])), k_m > 0 \quad (15.10)$$

where $k_m > 0$ is the gain of control, which is used to adjust the convergence speed of the system state.

Remark 15.1 In fact, control fields $f_m(t)$ act on the original system in Equation 15.1, in which the control Hamiltonian H_m is time-independent and determined by the system's inherent construction. The unitary transformation used in this section results in a time-dependent $H_m(t)$, which is a part of the design of the process of control strategy.

Remark 15.2 Because $\dot{V} \leq 0$, the Lyapunov function $V(x)$ is monotonically decreased. A control law (Equation 15.10) will make the target state $e_f = 0$ be the minimum point of the function $V(x)$. We have chosen the Lyapunov function as Equation 15.8, $\forall e, V(x) \geq 0$, so any non-zero state e makes Equation 15.8 greater than zero. Only our target state $e_f = 0$ makes Equation 15.8 have its minimum value. The proper Lyapunov function therefore ensures that the control law in Equation 15.10 is not only stable but also convergent.

15.1.3 Numerical Simulation Experiments and Results Analysis

To demonstrate the effectiveness of the methods proposed in this section, numerical quantum system simulations are done and experimental results are analyzed here.

Consider a four-level system. The free Hamiltonian of the controlled system is

$$H_0 = \sum_{j=1}^4 E_j |j\rangle\langle j| \quad (15.11)$$

where $E_1 = 0.4948$, $E_2 = 1.4529$, $E_3 = 2.3691$, and $E_4 = 3.2434$. Thus the free Hamiltonian of the system becomes $H_0 = \text{diag}(0.4948, 1.4529, 2.3691, 3.2434)$, where $\text{diag}(\cdot)$ denotes a diagonal matrix. For convenience a ladder-level system is considered, which permits energy transitions between level 1 and level 2, level 2 and level 3, and level 3 and level 4. Thus the control Hamiltonian is $H_1 = [0, 1, 0, 0; 1, 0, 1, 0; 0, 1, 0, 1; 0, 0, 1, 0]$. Suppose this system is controlled by a single control field $f(t)$. The total Hamiltonian of the system can be written as $H = H_0 + f(t)H_1$. Time step length is chosen as $\Delta t = 0.01$ for all the experiments. The eigenvalues of the system are $\lambda_1 = 0.4948$, $\lambda_2 = 1.4592$, $\lambda_3 = 2.3691$, and $\lambda_4 = 3.2434$. The corresponding eigenstates are $|\lambda_1\rangle = [1, 0, 0, 0]^T$, $|\lambda_2\rangle = [0, 1, 0, 0]^T$, $|\lambda_3\rangle = [0, 0, 1, 0]^T$, and $|\lambda_4\rangle = [0, 0, 0, 1]^T$.

Two experiments are performed. Experiment A is the trajectory tracking control between pure states, including tracking (i) from eigenstate to eigenstate, (ii) from superposition state to superposition state, (iii) from eigenstate to superposition state, and (iv) from superposition state to eigenstate. Experiment B is the trajectory tracking between mixed states.

For a given quantum system, state vector $|\psi\rangle$ contains all possible information and $|\psi\rangle = \sum_n c_n |n\rangle$, where $\{|n\rangle\}$ is a set of basic vectors of Hilbert space and $|c_n|^2$ is the probability that the system is in the state $|n\rangle$. The density operator ρ is denoted by a Hermit matrix $\rho = \sum_k p_k |\psi_k\rangle\langle\psi_k|$. The matrix element is calculated by $\rho^{(np)} = \langle n|\rho|p\rangle$. The diagonal elements of ρ can therefore be written as $\rho^{(nn)} = \sum_k p_k |c_n^{(k)}|^2$, which indicates the average probability that the system is in the state $|n\rangle$ and is called the population of state $|n\rangle$. The off-diagonal elements $\rho^{(np)} = \sum_k p_k c_n^{(k)} c_p^{(k)*}$ describe quantum interference between states $|n\rangle$ and $|p\rangle$, and always appears in superposition states.

In the particular case in which all p_k are zero except the one for state $|\psi_0\rangle$, then $\rho = |\psi_0\rangle\langle\psi_0|$ and this state is a pure state.

1) Tracking control between eigenstates

The initial state of the system controlled is chosen as an eigenstate $|\lambda_1\rangle$, viz. $\hat{\rho}_0 = |\lambda_1\rangle\langle\lambda_1| = \text{diag}(1, 0, 0, 0)$. The target initial state $\hat{\rho}_{f0}$ of Equation 15.2 is another eigenstate $|\lambda_2\rangle$, viz. $\hat{\rho}_{f0} = |\lambda_2\rangle\langle\lambda_2| = \text{diag}(0, 1, 0, 0)$. According to Equations 15.7a and 15.7b, one can get $e(0) = \hat{\rho}_{f0} - \hat{\rho}_0 = \text{diag}(-1, 1, 0, 0)$. Because $e(t) = \rho_f(t) - \rho(t)$, the diagonal elements imply population error $P_n = \rho_f^{(nn)} - \rho^{(nn)}$. According to Equation 15.10, the control law $f(t)$ can be obtained as $f(t) = -k(\text{tr}(iH_1(t)[\hat{\rho}_{f0}, e(t)]))$, in which $f_0 = 0.015$, $k = 0.05$, and $H_1(t) = U^\dagger(t)H_1U(t)$. The numerical simulation results are shown in Figure 15.1, where

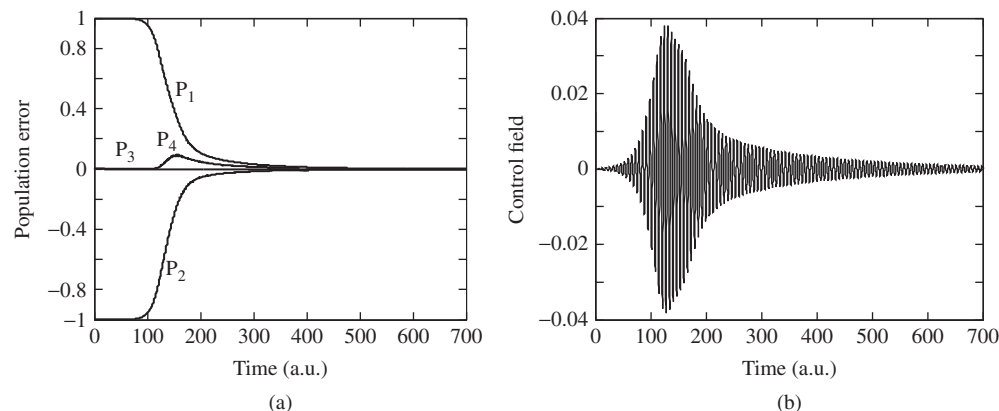


Figure 15.1 Numerical simulation results: (a) evolution result of diagonal element P_n in $e(t)$ and (b) control field $f(t)$

Figure 15.1a is the evolution of $e(t)$ with diagonal elements P_n where $n = 1, 2, 3, 4$ represents four energy levels and Figure 15.1b is the control filed $f(t)$.

To demonstrate the control effectiveness quantitatively, we define a performance index

$$v = \text{tr}(e^2(t)) = \|\rho_f(t) - \rho(t)\|^2 \quad (15.12)$$

which refers to state distance between the states of the systems in Equation 15.1 and Equation 15.2. The final value v in this experiment is 0.0016.

2) Tracking control between superposition states

Assume the initial state of the system in Equation 15.1 is the probability superposition of $|\lambda_1\rangle$ and $|\lambda_2\rangle$, viz. $|\psi_0\rangle = (1/\sqrt{2})|\lambda_1\rangle + (1/\sqrt{2})|\lambda_2\rangle$. Its density matrix form is $\hat{\rho}_0 = |\psi_0\rangle\langle\psi_0|$. The target initial state is $|\psi_f\rangle = \sqrt{1/8}|\lambda_1\rangle + 1/2|\lambda_2\rangle + 1/2|\lambda_3\rangle + \sqrt{3/8}|\lambda_4\rangle$ and $\hat{\rho}_{f0} = |\psi_f\rangle\langle\psi_f|$. According to Equations 15.7a and 15.7b, one can obtain a new system with $e(0) = \hat{\rho}_{f0} - \hat{\rho}_0$. We select parameters $k = 0.1$ and $f_0 = 0.015$ for the control law $f(t) = -k(\text{tr}(iH_1(t)[\hat{\rho}_{f0}, e(t)]))$ in Equation 15.10. System numerical experimental results are shown in Figure 15.2, where Figure 15.2a is the result of the performance index (Equation 15.12) and Figure 15.2b is the control field $f(t)$.

It can be seen from Figure 15.2a that when $t = 700$ a.u., v tends to zero. The final experimental value of v is $v = \text{tr}(e^2(t)) = 0.0012$.

To show that the control strategy proposed in this section can achieve the control object, we will do the experiments for the state of the original system. Consider Equations 15.1 and 15.2. After introducing the unitary transformation $U(t) = \exp(-iH_0t)$, one has: $\rho(t) = U^\dagger(t)\hat{\rho}(t)U(t)$ and $\rho_f(t) = U^\dagger(t)\hat{\rho}_f(t)U(t)$. Because of the invariability of the probability distributions of eigenstates before and after the unitary transformation, the original systems will be

$$i\frac{\partial}{\partial t}\rho(t) = [f(t)H_1(t), \rho(t)], \quad \rho(0) = \hat{\rho}_0 \quad (15.13)$$

$$i\frac{\partial}{\partial t}\rho_f(t) = 0, \quad \rho_f(0) = \hat{\rho}_{f0} \quad (15.14)$$

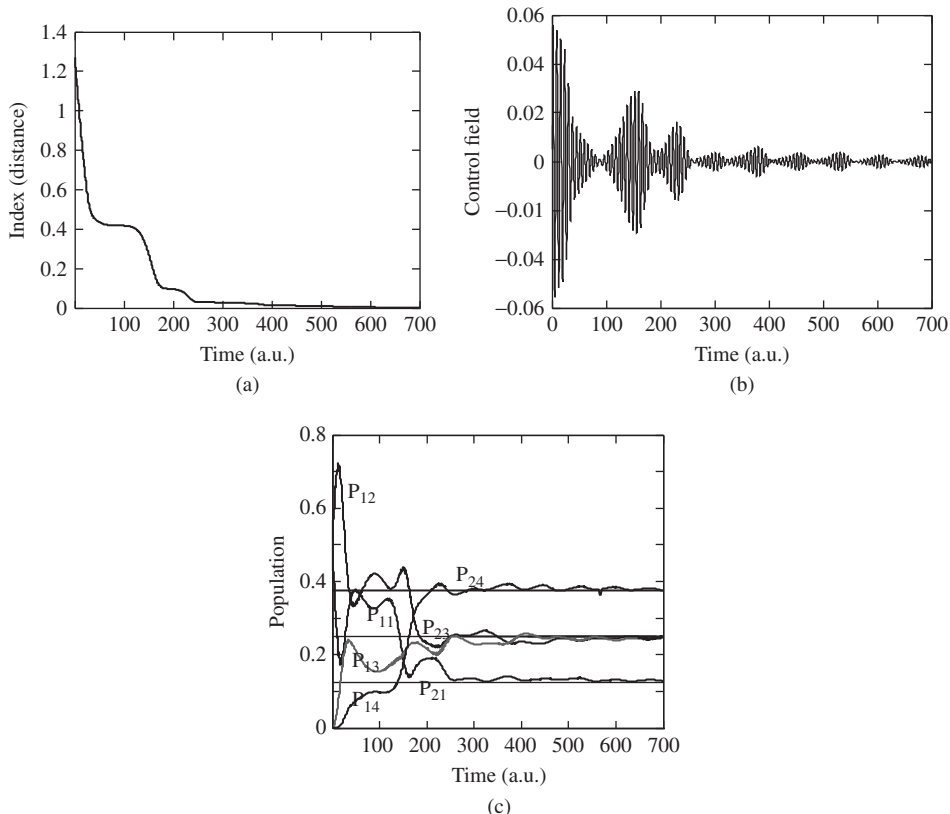


Figure 15.2 System numerical experimental results: (a) result of the index $v = \text{tr}(e^2(t))$, (b) control field $f(t)$, and (c) population tracking between Equation 15.1 and Equation 15.2

The control law is designed in the same way as Equation 15.8:

$$V = \frac{1}{2} \text{tr}(e^2) = \frac{1}{2} \text{tr}[(\rho_f - \rho)^2] \quad (15.15)$$

The control law can then be obtained:

$$f(t) = -k(\text{tr}(iH_1(t)[\hat{\rho}_f, \rho(t)])), k > 0 \quad (15.16)$$

We select the same parameters as for Equation 15.10, that is, $k = 0.1$ and $f_0 = 0.015$. The final tracking experiment result is shown in Figure 15.2c, where P_{ij} is the population where the first index i indicates the system and the second one j is the energy level, for example P_{13} refers to the third energy level of state $\rho(t)$ in Equation 15.1. Notice that P_{ij} is different from population error P_n in Figure 15.1a. In this experiment, we have $P_{23} = P_{22}$ of $\rho_f(t)$. In Figure 15.2c, the dashed line is the population evolution of the target state $\rho_f(t)$. The results also demonstrate that Equation 15.1 follows the target system in Equation 15.2 completely at 700 a.u., which has the same time as in Figure 15.2a.

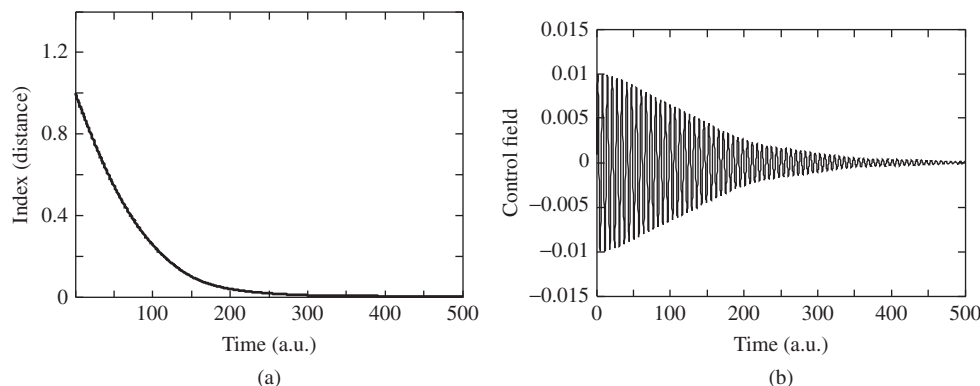


Figure 15.3 Simulation results: (a) result of the index $v = \text{tr}(e^2(t))$ and (b) control field $f(t)$

3) Tracking control between eigenstates and superposition states

Assume the initial state in Equation 15.1 is $\hat{\rho}_0 = \text{diag}(1, 0, 0, 0)$ and $\hat{\rho}_{f0} = |\psi\rangle\langle\psi| = [0.5, 0.5, 0, 0; 0.5, 0.5, 0, 0; 0, 0, 0, 0; 0, 0, 0, 0]$ in Equation 15.2. According to Equation 15.7a and 15.7b, $e(0) = \hat{\rho}_{f0} - \hat{\rho}_0$. According to Equation 15.10 the control law is designed as $f(t) = -k(\text{tr}(iH_1(t)[\hat{\rho}_{f0}, e(t)]))$, in which $k = 0.01$ and $f_0 = 0.005$. Simulation results are shown in Figure 15.3, in which Figure 15.3a shows $v = \text{tr}(e^2(t)) \rightarrow 0$ at 350 a.u. The control accuracy is $v = 0.0033$ at $t = 500$ a.u.

4) Tracking control between superposition states and eigenstates

In this experiment, we select $\hat{\rho}_0 = [1/3, 0, \sqrt{2}/3, 0; 0, 0, 0, 0; \sqrt{2}/3, 0, 2/3, 0; 0, 0, 0, 0]$ as the initial state of Equation 15.1 and $\hat{\rho}_{f0} = \text{diag}(0, 1, 0, 0)$ for Equation 15.2. The control law is designed as $f(t) = -k(\text{tr}(iH_1(t)[\hat{\rho}_{f0}, e(t)]))$ according to Equation 15.10, where $k = 0.01$ and $f_0 = 0.005$. Simulation results are displayed in Figure 15.4, where Figure 15.4a is the evolution of state distance and Figure 15.4b is the control field. The control accuracy is $v = 5.1901e - 004$ at $t = 1200$ a.u.

In case (iv) of experiment A, if we have $f_0 = 0.01$ and keep the same values for the other parameters, then the response time will be 1000 a.u. and $v = 0.0024$. Generally speaking, the convergence speed of a system and its control value are always contradictory. Increasing the initial control value properly will maintain the convergence speed and the value can be adjusted according to actual application.

5) Tracking between mixed states

In quantum systems there are two reasons for a mixed-state: one is quantum dissipation due to quantum system entanglement with the environment. In such a situation, the system will be open. The quantum state will become a mixed state even though it is a pure state at the beginning. Here, the evolution of the density matrix in the open system will not be unitary. Second, the amounts of the same particles in different pure states are incoherently mixed, which would be a quantum ensemble. Particles in different pure states are in this ensemble with some probability, viz. average statistically. In this section, we only consider closed systems

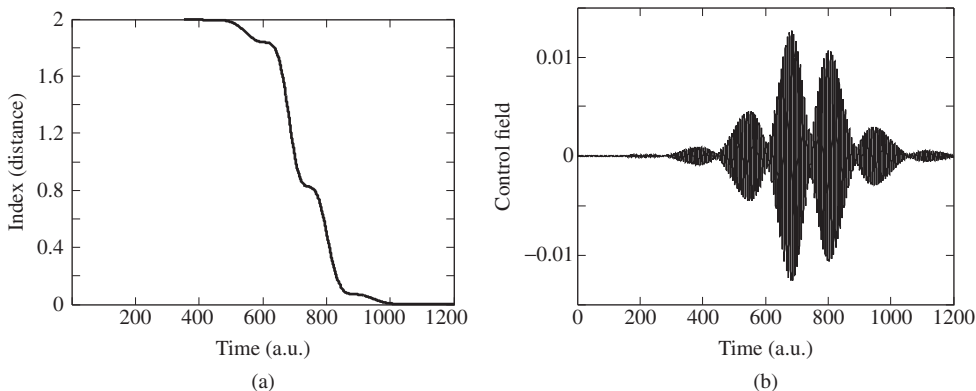


Figure 15.4 Simulation results: (a) result of the index $v = \text{tr}(e^2(t))$ and (b) control field $f(t)$

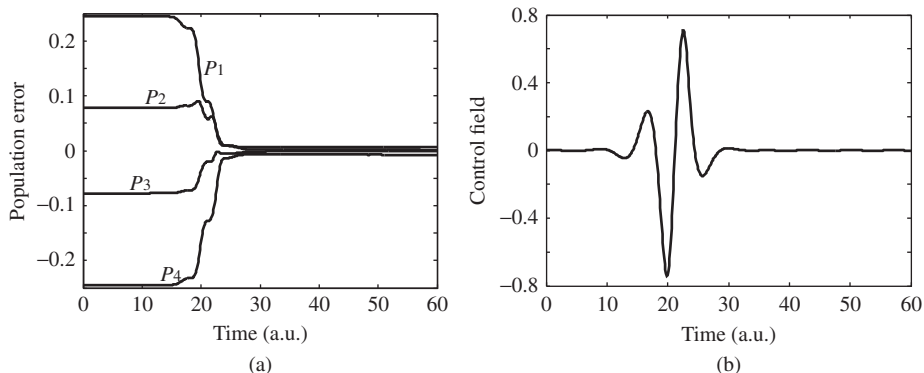


Figure 15.5 (a) Diagonal elements P_n of error $e(t)$ and (b) evolution of control field $f(t)$

that do not interact with the environment, so mixed state here refers to the mixed state in the ensemble.

Assume that the initial state of Equation 15.1 is $\hat{\rho}_0 = \text{diag}(0.3877, 0.2736, 0.1961, 0.1426)$ and $\hat{\rho}_{f0} = \text{diag}(0.1426, 0.1961, 0.2736, 0.3877)$ for Equation 15.2. Both are mixed states. According to Equation 15.10, the control law is $f(t) = -k(\text{tr}(iH_1(t)[\hat{\rho}_{f0}, e(t)]))$, where $k = 25$ and $f_0 = 0.002$. Simulation results are shown in Figure 15.5, where Figure 15.5a is the diagonal element P_n of error $e(t)$ and Figure 15.5b is the control field. The control accuracy is $v = 0.0037$ at $t = 60$ a.u.

15.2 Orbit Tracking Control of Quantum Systems

In Section 15.1, with the help of some concepts of system control, we studied trajectory tracking of the quantum state, introducing an error state $e(t)$ by defining the difference between the target state $\hat{\rho}_f(t)$ and the system state $\hat{\rho}(t)$. We changed the tracking control goal of $\hat{\rho}(t)$ following $\hat{\rho}_f(t)$ into a regulation problem of error state $e(t)$ from the arbitrary initial error state

$e(0)$ to its stable state $e(t_f)$, which is a zero matrix. To design a proper control law, we also introduced a unitary transformation $U(t) = \exp(-itH_0)$ to remove the drift item in H_0 , which made it difficult to determine the sign of the first-order derivative of the Lyapunov function.

We find that the unitary transformation introduced in Section 15.1 can not only eliminate the drift item in H_0 but also turn the time-dependent target state $\hat{\rho}_f(t)$ of the original system into a stationary state $\hat{\rho}_{f0}$. In other words, with the help of unitary transformation the system state $\hat{\rho}(t)$ tracking the target state $\hat{\rho}_f(t)$ simultaneously becomes the steering problem of the system state toward a target initial state $\hat{\rho}_{f0}$. Because of this we think the procedure of introducing the error state $e(t)$ is not necessary in quantum tracking control, and this forms the basis of the content of this section.

In this section, unitary transformation will be applied to the original system, which changes the free-evolutionary target system $\hat{\rho}_f(t)$ into a time-independent state $\hat{\rho}_{f0}$. We achieve the tracking goal by steering the system initial state from $\hat{\rho}_0$ to $\hat{\rho}_{f0}$. In such a case, the stable target state $\hat{\rho}_{f0}$ of the steering problem is no longer a zero matrix, which is different from the case in Section 15.1.

15.2.1 System Model and Control Law Design

In this section, the system model in Equations 15.1 and 15.2 in Section 15.1 is used, where Equation 15.1 is the controlled system and Equation 15.2 describes the target system, which is time-dependent and free-evolutionary.

For Equations 15.1 and 15.2, the expected control goal is as follows. For an arbitrary initial state of Equation 15.2, the state $\hat{\rho}(t)$ in Equation 15.1 will follow the target system in Equation 15.2. Since the evolution of a closed quantum systems is unitary, the spectrum of $\hat{\rho}(t)$ is time-invariant, viz. $\text{Tr}[\hat{\rho}^n(t)] = \text{Tr}[\hat{\rho}^n(0)]$.

The transformation deduced by a linear unitary operator is called unitary transformation. Here we introduce the unitary transformation $U(t) = \exp(-itH_0)$ to the original systems in Equations 15.1 and 15.2. The controlled state $\hat{\rho}(t)$ and the target state $\hat{\rho}_f(t)$ become

$$\begin{aligned}\rho(t) &= U^\dagger(t)\hat{\rho}(t)U(t) \\ \rho_f(t) &= U^\dagger(t)\hat{\rho}_f(t)U(t)\end{aligned}\quad (15.17)$$

where “ \dagger ” denotes a conjugate, and $\hat{\rho}(t)$ and $\hat{\rho}_f(t)$ are the system state and target state before the unitary transformation, respectively. Because $U(0) = U^\dagger(0) = 1$ ($t = 0$), one has $\rho(0) = \hat{\rho}(0) = \hat{\rho}_0$ and $\rho_f(0) = \hat{\rho}_f(0) = \hat{\rho}_{f0}$ after the transformation. Moreover, the target system in Equation 15.2 is free-evolutionary under the free Hamiltonian H_0 . The solution of Equation 15.2 is $\hat{\rho}_f(t) = U(t)\hat{\rho}_f(0)U^\dagger(t)$, where $U(t)$ is the evolution matrix and $U(t) = \exp(-itH_0)$. Substituting this solution into Equation 15.3, the transformed target state $\rho_f(t)$ becomes

$$\rho_f(t) = U^\dagger(t)U(t)\hat{\rho}_f(0)U^\dagger(t)U(t) = \hat{\rho}_f(0) = \hat{\rho}_{f0} \quad (15.18)$$

The original Equations 15.1 and 15.2 after the unitary transformation will therefore be

$$i\hbar \frac{\partial}{\partial t} \rho(t) = \left[\sum_m f_m(t) H_m(t), \rho(t) \right], \rho(0) = \hat{\rho}_0 \quad (15.19a)$$

$$\rho_f(t) = \hat{\rho}_{f0} \quad (15.19b)$$

Equation 15.19 is the new controlled and target systems from which one can see that:

Remark 15.3 State $\hat{\rho}_f(t)$ in the original target system (Equation 15.2) evolves according to the Liouville equation, which is time-dependent and non-stationary. After the unitary transformation the trajectory of the target system in Equation 15.19 becomes time-independent and stationary, with a constant value and equal to the initial state $\hat{\rho}_{f0}$ of the target system.

Remark 15.4 After the transformation the control Hamiltonian H_m , which is time-independent, becomes $H_m(t)$, which is time-dependent and determines the evolution of states in the interaction picture.

The unitary transformation in this section has two meanings, one of which is the rotation of the basic vectors in Hilbert space. We say a unitary operator leads to the rotation of the Hilbert space. New state operators $\rho(t)$ and $\rho_f(t)$ are used to describe the transformed quantum system in Equation 15.19. Under unitary transformation all physical properties are unchanged. The other meaning of unitary transformation is that only the control Hamiltonian remains in the new system (Equation 15.19a) makes every item in the first-order derivation of the Lyapunov function is controllable, which is convenient for design control law.

By introducing the unitary transformation, the original trajectory tracking problem of system state $\hat{\rho}(t)$ following the free-evolutionary target state $\hat{\rho}_f(t)$ becomes the steering problem of state $\rho(t)$ being regulated to $\hat{\rho}_f(0)$ in Equation 15.19.

Similarly, the Lyapunov stability theorem can be applied to design control law. The average value of an observable quantity is selected as the Lyapunov function:

$$V = \text{tr}(P\rho) + C \quad (15.20)$$

where P is the observable operator, which is not necessarily positive definite as it does not always correspond to an actual observable quantity. P is also called a virtual mechanical quantity operator. C is a constant used to adjust the value of the Lyapunov function.

According to the third condition of the Lyapunov function and system (Equation 15.19), one can obtain

$$\dot{V} = - \sum_m f_m(t) \text{tr}(iH_m(t)[\rho(t), P]) \quad (15.21)$$

For the sake of simplicity and availability we let each item on the right-hand side of Equation 15.21 with a summation sign be non-positive in order to ensure $\dot{V} \leq 0$. The control law can be derived as

$$f_m(t) = k_m \text{tr}(iH_m(t)[\rho(t), P]), k_m > 0 \quad (15.22)$$

where $k_m > 0$ is the control gain, which is used to adjust the convergence speed of the system state.

15.2.2 Numerical Simulation Experiments

In order to demonstrate the effectiveness and advantage of the method proposed in this section, two examples and results analysis will be given.

A five-level energy quantum system is selected, where the free Hamiltonian is

$$H_0 = \begin{pmatrix} 1 & 0 & 0 & 0 & 0 \\ 0 & 1.2 & 0 & 0 & 0 \\ 0 & 0 & 1.3 & 0 & 0 \\ 0 & 0 & 0 & 2 & 0 \\ 0 & 0 & 0 & 0 & 2.15 \end{pmatrix}.$$

The eigenvalues of H_0 are $\lambda_1 = 1$, $\lambda_2 = 1.2$, $\lambda_3 = 1.3$, $\lambda_4 = 2$ and $\lambda_5 = 2.15$. The corresponding eigenstates are

$$|\lambda_1\rangle = \begin{bmatrix} 1 \\ 0 \\ 0 \\ 0 \\ 0 \end{bmatrix}, |\lambda_2\rangle = \begin{bmatrix} 0 \\ 1 \\ 0 \\ 0 \\ 0 \end{bmatrix}, |\lambda_3\rangle = \begin{bmatrix} 0 \\ 0 \\ 1 \\ 0 \\ 0 \end{bmatrix}, |\lambda_4\rangle = \begin{bmatrix} 0 \\ 0 \\ 0 \\ 1 \\ 0 \end{bmatrix} \text{ and } |\lambda_5\rangle = \begin{bmatrix} 0 \\ 0 \\ 0 \\ 0 \\ 1 \end{bmatrix}$$

It is assumed that the initial state of Equation 15.1 is $\hat{\rho}_0$. The free-evolutionary target system in Equation 15.2 has an initial value $\hat{\rho}_{f0}$.

According to the conditions above, after unitary transformation the new system (Equation 15.19) replaces the original systems (Equations 15.1 and 15.2). The tracking problem has become a state steering one, with the new state $\rho(t)$ in Equation 15.19 being driven from its initial state $\hat{\rho}_0$ to a stationary target state $\hat{\rho}_{f0}$.

In this system all the transition frequencies are different, viz. $\omega_{jk} \neq \omega_{pq}$, $(j, k) \neq (p, q)$, where $\omega_{jk} = \lambda_j - \lambda_k$, which satisfies Assumption 7.3 of convergence conditions in Section 7.2.2. According to Assumption 7.4, control Hamiltonians must be full connected, which means ten control Hamiltonians are needed for this system. In most cases, however, we do not need as many control Hamiltonians, and their number is determined by the concrete structure of $\hat{\rho}_0$ and $\hat{\rho}_{f0}$.

Example A The initial state of Equation 15.1 is an eigenstate $|\lambda_1\rangle = [1 \ 0 \ 0 \ 0 \ 0]^T$ of H_0 . Then

$$\hat{\rho}_0 = \begin{pmatrix} 1 & 0 & 0 & 0 & 0 \\ 0 & 0 & 0 & 0 & 0 \\ 0 & 0 & 0 & 0 & 0 \\ 0 & 0 & 0 & 0 & 0 \\ 0 & 0 & 0 & 0 & 0 \end{pmatrix}.$$

The probability superposition of eigenstates $|\lambda_2\rangle$ and $|\lambda_3\rangle$ is the initial state of the free-evolutionary target system in Equation 15.2, viz. $|\psi_{f0}\rangle = (1/\sqrt{2})|\lambda_2\rangle + (1/\sqrt{2})|\lambda_3\rangle$

$$\hat{\rho}_{f0} = |\psi_{f0}\rangle\langle\psi_{f0}| = 0.5 * \begin{pmatrix} 0 & 0 & 0 & 0 & 0 \\ 0 & 1 & 1 & 0 & 0 \\ 0 & 1 & 1 & 0 & 0 \\ 0 & 0 & 0 & 0 & 0 \\ 0 & 0 & 0 & 0 & 0 \end{pmatrix}$$

Considering the specific forms of $\hat{\rho}_0$ and $\hat{\rho}_{f0}$, the density matrices of the initial and target states only have differences in the population of energies 1–3 and the interference item of

energies 2 and 3. The designed control law is therefore aimed at these different items, that is to say, interaction only exists between energies 1 and 3. Three control Hamiltonians are enough to deal with the problem in this section, shown in Equation 15.23:

$$H_1 = \begin{pmatrix} 0 & 1 & 0 & 0 & 0 \\ 1 & 0 & 0 & 0 & 0 \\ 0 & 0 & 0 & 0 & 0 \\ 0 & 0 & 0 & 0 & 0 \\ 0 & 0 & 0 & 0 & 0 \end{pmatrix}, H_2 = \begin{pmatrix} 0 & 0 & 1 & 0 & 0 \\ 0 & 0 & 0 & 0 & 0 \\ 1 & 0 & 0 & 0 & 0 \\ 0 & 0 & 0 & 0 & 0 \\ 0 & 0 & 0 & 0 & 0 \end{pmatrix}, H_3 = \begin{pmatrix} 0 & 0 & 0 & 0 & 0 \\ 0 & 0 & 1 & 0 & 0 \\ 0 & 1 & 0 & 0 & 0 \\ 0 & 0 & 0 & 0 & 0 \\ 0 & 0 & 0 & 0 & 0 \end{pmatrix} \quad (15.23)$$

Next, we consider the diagonal elements ρ_{nn} ($n = 1, 2 \dots 5$) of the density matrix, which is for population of state, and the off-diagonal elements ρ_{23} , which represents the interference item. Here we mainly observe the tracking of interference item ρ_{23} .

According to Equation 15.23, the control fields corresponding to each Hamiltonian are f_1, f_2 , and f_3 . The control law can be obtained from Equation 15.22, where $k = 0.5$ and $f_0 = 0.015$.

To demonstrate the tracking of Equation 15.1 to Equation 15.2 we keep the data for the control function $f_m(t)$, $m = 1, 2, 3$, at all times and apply them to the original system in Equation 15.1. As we know that the population of the target system in Equation 15.2 is unchanged under unitary evolution. Figure 15.6 displays the effectiveness of the state steering of $\rho(t)$ from its initial state $\hat{\rho}_0$ to final state $\hat{\rho}_{f0}$ of Equation 15.19, where Figure 15.6a is the evolution of diagonal items $\rho_{nn}, n = 1, 2, 3$ and interference item ρ_{23} of state $\rho(t)$.

From Figure 15.6a one can see that both states evolve toward relevant items of the target state $\hat{\rho}_{f0}$. Figure 15.6b tracks the interference item. The dotted line is the free-evolutionary trajectory of $\hat{\rho}_{f23}$ of the target system state $\hat{\rho}_f(t)$ and the solid line is the tracking curve of $\hat{\rho}_{23}$ of the controlled system state $\hat{\rho}(t)$. Figure 15.6c shows the control fields $f_m(t)$. The performance index Equation 15.12 is used, and here $v = \|\rho_f(t) - \rho(t)\|^2 = 1.4125e-006(t=30\text{ au})$.

Example B The initial state of Equation 15.1 is a superposition state $|\psi_0\rangle = (1/\sqrt{3})|\lambda_1\rangle + (\sqrt{2}/\sqrt{3})|\lambda_4\rangle$. The initial target state of Equation 15.2 is an eigenstate $|\lambda_3\rangle = [0, 0, 1, 0, 0]^T$.

Here we choose the same parameters $k = 0.15$ and $P = \text{diag}(0.8, 1.1, 0.4, 1.2, 0.6)$, and the

control Hamilton is selected to have the form $H_c = \begin{pmatrix} 0 & 0 & 1 & 0 & 0 \\ 0 & 0 & 0 & 0 & 0 \\ 1 & 0 & 0 & 1 & 0 \\ 0 & 0 & 1 & 0 & 0 \\ 0 & 0 & 0 & 0 & 0 \end{pmatrix}$, where interactions exist between energies 1 and 3 and between energies 4 and 3.

The simulation experiment results are shown in Figure 15.7, which demonstrates the effectiveness of state steering of $\rho(t)$ from its initial state $\hat{\rho}_0$ to its final state $\hat{\rho}_{f0}$. Figure 15.7a shows population evolution, Figure 15.7b is control law and Figure 15.7c shows the interference item ρ_{14} , where the dashed line indicates the item of the target state and the solid line indicates the corresponding item of $\rho(t)$.

In experiment B we can divide the control Hamiltonian into two parts, as in experiment A. If we set

$$H_1 = \begin{pmatrix} 0 & 0 & 1 & 0 & 0 \\ 0 & 0 & 0 & 0 & 0 \\ 1 & 0 & 0 & 0 & 0 \\ 0 & 0 & 0 & 0 & 0 \\ 0 & 0 & 0 & 0 & 0 \end{pmatrix}, H_2 = \begin{pmatrix} 0 & 0 & 0 & 0 & 0 \\ 0 & 0 & 0 & 0 & 0 \\ 0 & 0 & 0 & 1 & 0 \\ 0 & 0 & 1 & 0 & 0 \\ 0 & 0 & 0 & 0 & 0 \end{pmatrix} \quad (15.24)$$

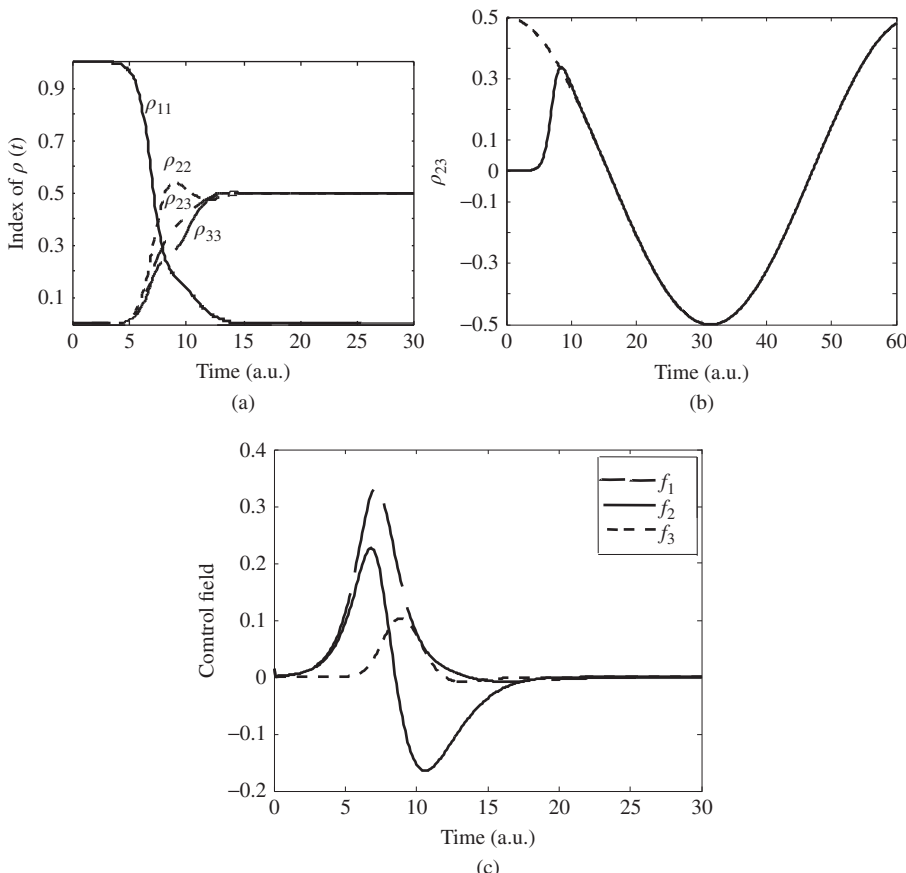


Figure 15.6 Simulation results: (a) population of state $\rho(t)$ in Equation 15.19, (b) tracking of ρ_{23} for original Equations 15.1 and 15.2, and (c) control fields $f_m(t)$

where $H_c = H_1 + H_2$ then two control fields will be needed.

The results are shown in Figure 15.8, where the three part of the figure correspond to those in Figure 15.7.

We can see from Figure 15.8 that the time required to complete the control task is shorter than in Figure 15.7, and is less than 100 a.u. In Figure 15.7 there is only one control Hamiltonian including all energy transformations, so control action on all energy is the same, which brings restrictions to control fields and lengthens the time required to complete control task, sometimes even causing a larger error.

15.3 Adaptive Trajectory Tracking of Quantum Systems

As we know, if the target state is stationary, the problem mentioned above is known as state regulation or state-transfer control of quantum systems, and has been researched widely in

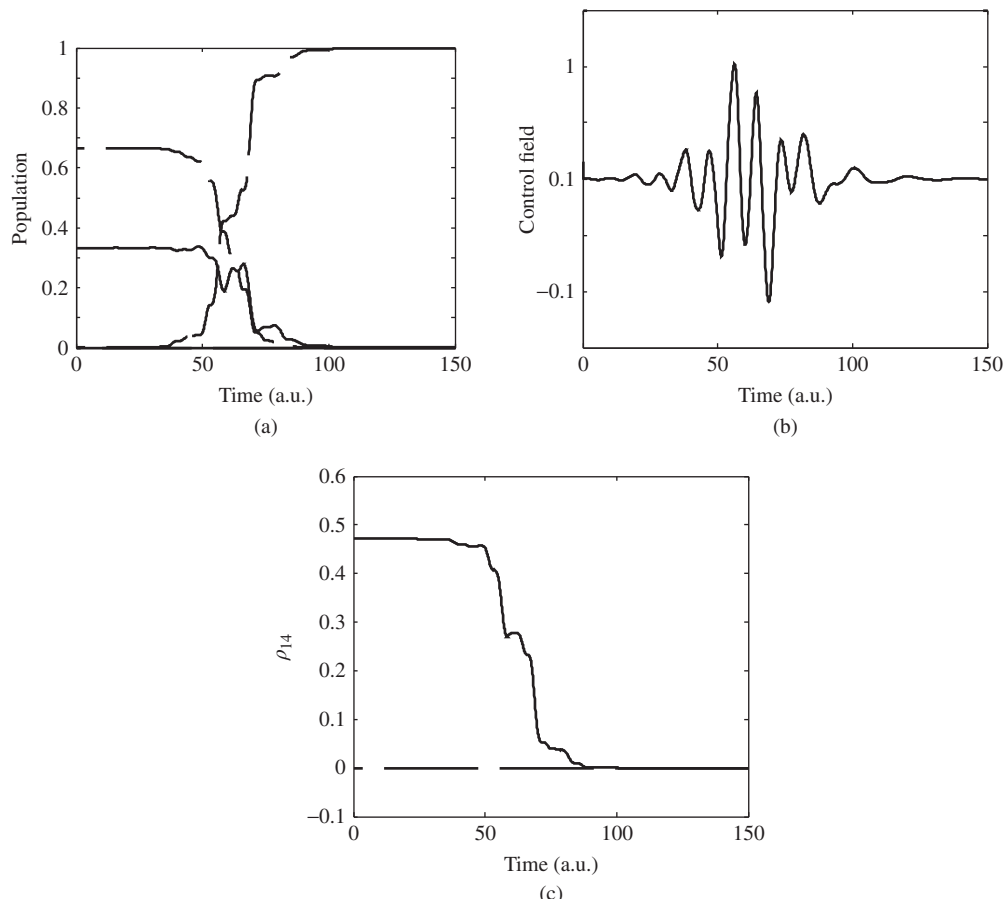


Figure 15.7 Simulation experimental results: (a) population of state $\rho(t)$ in Equation 15.19, (b) control fields $f_1(t)$, and (c) tracking of interference item ρ_{14}

recent years. If the target state is a time-dependent function, then it becomes a tracking problem from the control system perspective. Because of its complexity, the trajectory tracking control of quantum systems has been studied less. In quantum systems there are several kinds of states, for example superposition states, mixed states, entangled states, and so on, which are very different from the situation in classical control systems. These differences and the particular qualities of quantum systems mean it is not as easy to track a given trajectory as it is in classical engineering. In this section we will study trajectory tracking for a closed quantum system to a time-dependent function. The control law is designed based on the Lyapunov stability theorem. An adaptive algorithm is also used to settle the problem of singularities or bigger control values. Another advantage of our proposed method is that we do not require that the initial states of the controlled system and target system have to be the same. The control strategy proposed here can adaptively track a time-dependent function from an arbitrary initial state for the controlled system.

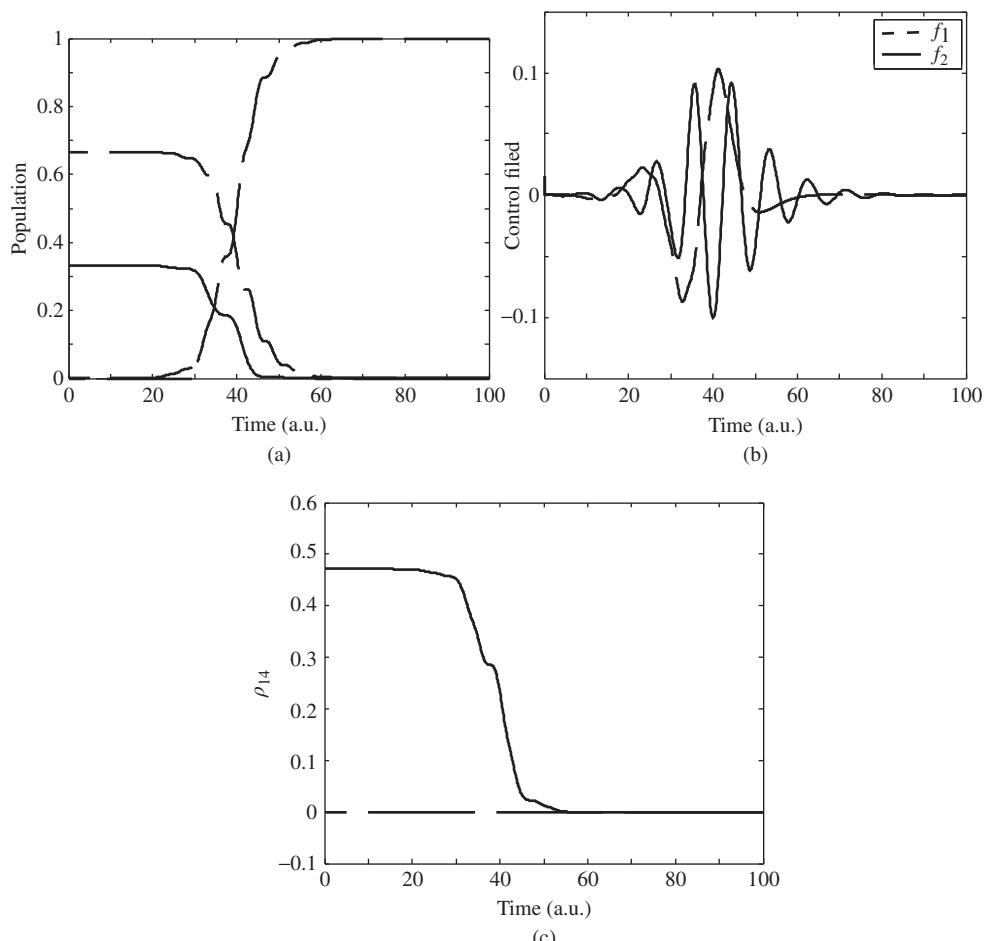


Figure 15.8 Simulation results: (a) population of state $\rho(t)$ in Equation 15.19, (b) control fields $f(t)$, and (c) tracking of interference item ρ_{14}

15.3.1 Description of the System Model

The main task of this work will focus on the pure-states trajectory tracking of closed quantum systems. A quantum system with wave function $\psi(t)$ is described by the Schrödinger equation

$$i\hbar \frac{\partial}{\partial t} \psi(t) = H\psi(t), \psi(0) = \psi_0 \quad (15.25)$$

where $H = H_0 + \sum_{m=1}^M u_m(t)H_m$, H_0 is the internal (free) Hamiltonian of the system, and H_m is the external (control) one, both of which are Hermitian and assumed to be independent of time. We choose the Plank constant $\hbar = 1$ for convenience.

For a closed quantum system, the measurable quantities or observables are represented by the linear, self-adjoint operator $P(t)$ in the Hilbert space. If $P(t)$ is measured, the outcome is an eigenvalue of $P(t)$. Let S be a measurable subset of the spectrum of $P(t)$. If the state at the moment of the measurement is $|\psi\rangle$, the probability of obtaining a value γ in S as the result of the measurement is given by $p_\gamma(\gamma \in S) = \langle\psi|P_j|\psi\rangle = \|P_j|\psi\rangle\|^2$, where P_j is the projector of $P(t)$, viz. $P(t) = \sum_j \gamma_j P_j$ in the discrete spectrum case. When the system is in the state $|\psi\rangle$, the expectation of the measurable operator $P(t)$, denoted $Y(t)$, is represented by

$$Y(t) = \langle P(t) \rangle_{\psi(t)} = \sum_j \gamma_j \langle\psi(t)|P_j|\psi(t)\rangle = \langle\psi(t)|P(t)|\psi(t)\rangle \quad (15.26)$$

Equation 15.25 is the controlled system and Equation 15.26 is the controlled variable, which is also the output of the controlled system (Equation 15.25).

In this work, let $|\lambda_j\rangle$ denote the j th eigenstate of the free Hamiltonian H_0 . It is convenient to assign the projective operator of the first eigenstate $|\lambda_1\rangle$ as the observable operator $P(t)$, which is time-independent, viz. $P = |\lambda_1\rangle\langle\lambda_1|$. As a matter of fact, the tracking is the evolution of population: $Y(t) = \langle\psi(t)|\lambda_1\lambda_1|\psi(t)\rangle = |\langle\psi(t)|\lambda_1|^2$. Because of the probability characteristic, $Y(t)$ is a real value ranging from 0 to 1.

The desired target system can take different forms but it should be a time-dependent function. As we have studied the tracking problem of the free-evolutionary Liouville equation, here we will study a desired target function $S(t)$ of a step response, which is a typical function often used to test the performance of control systems in engineering:

$$S(t) = 1 - e^{-t^2/2\tau^2}, t \geq 0 \quad (15.27)$$

where τ determines the change rate of the target output.

In fact, the output of the desired target system (Equation 15.27) corresponds to the range of Equation 15.26. Our control objective is to track the output of desired target system (Equation 15.27) at every moment. The control task is to make the controlled variable Equation 15.26 track the output of Equation 15.27, viz. let $Y(t)$ follow the output $S(t)$. The error $e(t)$ between $S(t)$ and $Y(t)$ is a performance index used to measure the tracking effectiveness.

The control idea based on model reference adaptive control and error regulation control is used to deal with the trajectory tracking problem in this section. The target system $S(t)$ is regarded as the reference model, and the control goal then becomes that the output of an adjustable system, which really just consists of a controlled system and controller, is in accordance with that of the reference model in Equation 15.27. An adaptive control law can therefore be designed based on the idea mentioned above that will adjust automatically the output of the adjustable system to track the target function.

The error function $e(t)$ is defined as

$$e(t) = S(t) - Y(t) \quad (15.28)$$

Subtracting Equation 15.26 from Equation 15.27 one can obtain

$$e(t) = 1 - e^{-t^2/2\tau^2} - \langle\psi(t)|P(t)|\psi(t)\rangle \quad (15.29)$$

The first-order time derivation of $e(t)$ is

$$\dot{e}(t) = \frac{t}{\tau^2} e^{-t^2/2\tau^2} - \langle \dot{\psi}(t) | P(t) | \psi(t) \rangle - \langle \psi(t) | \dot{P}(t) | \psi(t) \rangle - \langle \psi(t) | P(t) | \dot{\psi}(t) \rangle \quad (15.30)$$

Putting Equation 15.25 into Equation 15.30 gives

$$\dot{e}(t) = \frac{t}{\tau^2} e^{-t^2/2\tau^2} - \langle \psi(t) | i[H, P(t)] + \dot{P}(t) | \psi(t) \rangle \quad (15.31)$$

The control law is designed based on the Lyapunov stability theory according to the error state $e(t)$ and the first-order time derivation of $e(t)$ obtained in Equations 15.29 and 15.30. The control goal will be achieved by gradually decreasing the error $e(t)$ to zero under the action of the designed control law.

15.3.2 Control System Design and Characteristic Analysis

1) Design of control law

We will design the control law based on the Lyapunov method as described in Section 15.1.2. The Lyapunov function based on the error is chosen here as

$$V(x) = \frac{1}{2} e^2(t) \quad (15.32)$$

where Equation 15.32 meets the required conditions of the Lyapunov function. The first-order time derivation of Equation 15.32 is

$$\dot{V}(x) = e(t) \cdot \dot{e}(t) \quad (15.33)$$

Subtracting Equation 15.31 into Equation 15.33, one obtains

$$\dot{V}(t) = e(t) \cdot \left(\frac{t}{\tau^2} e^{-t^2/2\tau^2} - 2\text{Im} \langle \psi(t) | P \cdot H_0 | \psi(t) \rangle - 2 \sum_{m=1}^M u_m(t) \text{Im} \langle \psi(t) | P \cdot H_m | \psi(t) \rangle \right) \quad (15.34)$$

It can be seen from Equation 15.34 that the right-hand side of the equation contains the drifting item $\frac{t}{\tau^2} e^{-t^2/2\tau^2} - 2\text{Im} \langle \psi(t) | P \cdot H_0 | \psi(t) \rangle$, which makes it difficult to determine whether $\dot{V}(x) \leq 0$ holds. To solve this problem, we divide Equation 15.34 into two parts:

$$\begin{aligned} \dot{V}(t) = & e(t) \cdot \left(\frac{t}{\tau^2} e^{-t^2/2\tau^2} - 2\text{Im} \langle \psi(t) | P \cdot H_0 | \psi(t) \rangle \right. \\ & \left. - 2u_1(t) \text{Im} \langle \psi(t) | P \cdot H_1 | \psi(t) \rangle - 2 \sum_{m=2}^M u_m(t) \text{Im} \langle \psi(t) | P \cdot H_m | \psi(t) \rangle \right) \end{aligned} \quad (15.35)$$

First, we let

$$e(t) \cdot \left(\frac{t}{\tau^2} e^{-t^2/2\tau^2} - 2\text{Im} \langle \psi(t) | P \cdot H_0 | \psi(t) \rangle - 2u_1(t) \cdot \text{Im} \langle \psi(t) | P \cdot H_1 | \psi(t) \rangle \right) = 0 \quad (15.36)$$

The control law u_1 is derived as

$$u_1(t) = \frac{\frac{t}{\tau^2} e^{-t^2/2\tau^2} - 2\text{Im} \langle \psi(t) | P \cdot H_0 | \psi(t) \rangle}{2\text{Im} \langle \psi(t) | P \cdot H_1 | \psi(t) \rangle} \quad (15.37)$$

Second, we let

$$-2e(t) \cdot \sum_{m=2}^M u_m(t) \text{Im}\langle \psi(t) | P \cdot H_m | \psi(t) \rangle \leq 0 \quad (15.38)$$

The control law u_m is derived as

$$u_m(t) = k_m e(t) \cdot \text{Im}\langle \psi(t) | P \cdot H_m | \psi(t) \rangle, (m = 2, 3, \dots, M) \quad (15.39)$$

where $k_m > 0 (m = 2, 3, \dots, M)$ is control gain.

From the above derivation process one can see that the drifting item comes from H_0 . In order to get rid off the effect of the drifting item and at the same time obtain a good tracking performance, one needs to design at least two component control laws u_1 and $u_m(t) (m \geq 2)$ in which u_1 is used to remove the drifting item while $u_m(t) (m \geq 2)$ is the main control law used to track the target function. However, the functions of these two component control laws are not well-defined. In the following, the interaction relation between them will be analyzed.

2) Analysis of control performance

According to the expression of $u_1(t)$ obtained in Equation 15.37, $u_1(t)$ is a fractional and its denominator is related to system state, which may result in a denominator of zero. This situation implies that during the tracking progress the control law $u_1(t)$ may be infinite and singular for some states because of a zero denominator. Such a control law might trigger the following two issues: (i) singularity and (ii) control values that are too large.

In fact, in the process of trajectory tracking singularity can be divided into two categories: removable and intrinsic, which take the forms $0/0$ and $\alpha/0 (\alpha \neq 0)$ (Zhu and Rabitz, 1999), respectively. For the first case, the removable singularities only appear at certain moments of the whole tracking process and can be deleted by some effective method for low-order systems. For four-order or higher-order system, however, it is difficult to solve directly the singular points. In such a case, l'Hospital's rule can be used, where one changes the control law $0/0$ into $\alpha/\beta (\alpha, \beta \neq 0)$ and then no singularity exists. Moreover, an alternative method, a small modification of target trajectory, is suitable to avoid the first type of singularity. In fact this kind of singularity brings few troubles for tracking control. There are intrinsic singularities in the second case in which the denominator will be zero at all times. The system in this case is not controllable and no control law is applicable. All singular points in this section are mathematical but not physical by simple analysis, so the system is controllable.

However, even if there is no singularity or all singularities have been removed, there remain some problems. In fact, $u_1(t)$ not only removes drifting items, but also plays a control role. For example, a smaller denominator in $u_1(t)$ will lead to a control value that is too large, which makes stable tracking impossible. For the most cases, however, the error is permitted within a range. The important thing is to reach the control goal. We can therefore give a limitation of control amplitude and permit a tolerance of the error in the tracking performance. When control amplitude exceeds the given limited value, an appropriate modification of target trajectory is added. The concrete process for adjusting target trajectory is as follows.

It is supposed that $u_1(t)$ or $u_m(t)$ is bigger than the boundary value at $t = t_0$. The target function $S(t_1)$ at $t = t_1$ then becomes (Zhu and Rabitz, 2003b)

$$S(t_1) = S(t_0) + (1 - S(t_0))(1 - e^{-(t-t_0)/2\tau^2}) \quad (15.40)$$

$S(t_1) = S(t_0)$ holds at $t_1 = t_0$ and $S(t_1) \rightarrow 1$ when $t_1 \rightarrow \infty$, so the adjusted trajectory $S(t_1)$ displays the same trend as the former one. $S(t_1) = S(t_0)$ is almost correct on the condition that the time interval is small enough, but it may slightly decrease the control accuracy of the tracking performance, so we also need to give the permitted error tolerance. Similarly, the general amended expression for tracking trajectory is

$$S_{k+1}(t) = S_{t_k}(t_k) + (1 - S_k(t_k))(1 - e^{-(t-t_k)/2\tau^2}) \quad (15.41)$$

In other words, the trajectory amendment is applied when any one of the control amplitudes exceeds the given boundary value. Furthermore, the control gain of $u_m(t)$ is reduced at the same time to avoid a large control value.

15.3.3 Numerical Simulation and Result Analysis

In order to verify the effectiveness of the method proposed, numerical simulation will be performed in this section for a four-level quantum system with a free control Hamiltonian:

$$H_0 = \sum_{i=1}^4 E_i = |j\rangle\langle j| \quad (15.42)$$

where $E_1 = 0.4948$, $E_2 = 1.4529$, $E_3 = 2.3691$, and $E_4 = 3.2434$, and

$$H_0 = \text{diag}(0.4948, 1.4529, 2.3691, 3.2434) \quad (15.43)$$

For this four-level system, a full-connected control Hamiltonian is given for convenience, which means that interactions between any two levels are allowable, so the control Hamiltonian is $[0, 1, 1, 1; 1, 0, 0, 0; 1, 1, 0, 1; 1, 1, 1, 0]$. Based on the discussion in Section 15.3.2, two control laws are needed at least, and therefore two control Hamiltonians. We assume $H_1 = [0, 1, 1, 0; 1, 0, 0, 1; 1, 0, 0, 1; 0, 1, 1, 0]$ and $H_2 = [0, 1, 0, 1; 1, 0, 1, 0; 0, 1, 0, 1; 1, 0, 1, 0]$, and the total Hamiltonian of the system is $H = H_0 + u_1(t)H_1 + u_2(t)H_2$.

The eigenvalues of the matrix H_0 are denoted by $\lambda_i (i = 1, 2, 3, 4)$, with $\lambda_1 = 0.4948$, $\lambda_2 = 1.4529$, $\lambda_3 = 2.3691$, and $\lambda_4 = 3.2434$, and the corresponding eigenvectors are $|\lambda_1\rangle = [1, 0, 0, 0]^T$, $|\lambda_2\rangle = [0, 1, 0, 0]^T$, $|\lambda_3\rangle = [0, 0, 1, 0]^T$, and $|\lambda_4\rangle = [0, 0, 0, 1]^T$. In this experiment, the observable operator is $P = |\lambda_1\rangle\langle\lambda_1| = [1, 0, 0, 0; 0, 0, 0, 0; 0, 0, 0, 0; 0, 0, 0, 0]$. The time step is chosen as $\Delta t = 0.01$ and $\tau = 20$.

For the controlled system (Equation 15.25), the initial state is the superposition of $|\lambda_1\rangle$, $|\lambda_2\rangle$, $|\lambda_3\rangle$, and $|\lambda_4\rangle$, i.e., $|\psi_0\rangle = (1/2)|\lambda_1\rangle + (1/2)|\lambda_2\rangle + (1/2)|\lambda_3\rangle + (1/2)|\lambda_4\rangle$.

The initial output variable becomes $Y(0) = \langle\psi_0|P|\psi_0\rangle = 0.25$. For the target system (Equation 15.27), at $t = 0$, the initial state is $S(0) = 0$. Then the initial error is $e(0) = S(0) - Y(0) = -0.25$, which is put into Equations 15.37 and 15.39 to get the control laws. We choose control gain $k_2 = 220$ for the second control law $u_2(t)$. If the control value exceeds a boundary value, the control gain will be changed to $k'_2 = 40$. The initial control value is $u_1(0) = u_2(0) = 0.005$. The boundary values are $u_1(t) = 2$ and $u_2(t) = 5$.

The simulation results are as follows. Figure 15.9 shows the output evolution of the controlled system and the target system. Figure 15.10 is the record of error. Figure 15.11 depicts control law $u_1(t)$ and $u_2(t)$ is shown in Figure 15.12.

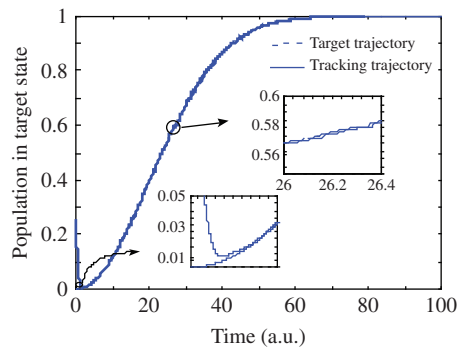


Figure 15.9 Output evolutions of the controlled system (solid line) and the target system (dashed line)

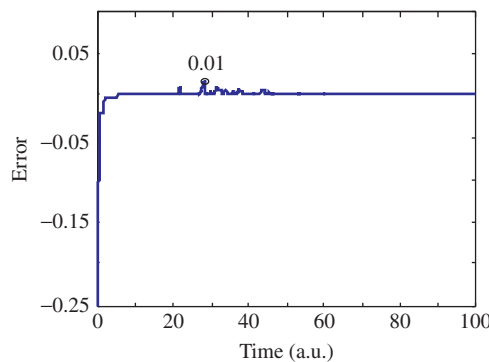


Figure 15.10 Record of error $e(t)$

From Figure 15.9 one can see that tracking procedures happen after state transferring, where the initial value 0.25 of the controlled system is transferred to the target system during the first 5 a.u. After that, the system output tracks the target output over time. Between 26 and 26.4 a.u. the controlled state produces a too low a value of $\text{Im}\langle\psi(t)|P \cdot H_1|\psi(t)\rangle$, which leads to a larger control value of $u_1(t)$ than its boundary value. At this point, a slight modification of target trajectory and control law $u_2(t)$ with control gain 40 is carried on simultaneously. The two control amplitudes are limited in their upper boundary values 2 and 5 in Figures 15.11 and 15.12, respectively. From Figure 15.10 one can see that over the first 5 a.u. the error decreases quickly from its initial value of 0.25 to 0, which indicates that the system is able to track the target system from its initial state under the action of the control law proposed. An enlarged error of 0.01 appears around 26 a.u., denoting a control value that is too big. During the whole tracking process the error remains within 0.01 and tends to 0 after 40 a.u. The control accuracy of the control system reaches 99%. The output of the system can track the given time-variant objective trajectory fairly well. Figure 15.13 is the error surface of the control system under the relation between control gain k_2 and the boundary of control u_1 , in which k_2 is in the range [5, 100] with a step increase of 5 and u_1 is in the range [0.5, 8] with a step increase of 0.5.

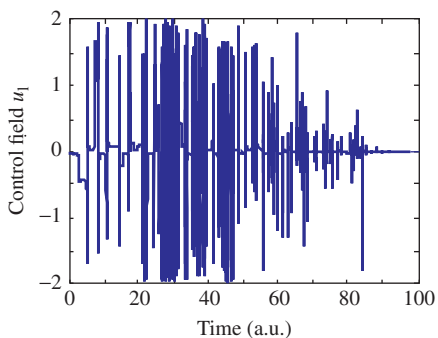


Figure 15.11 Control law $u_1(t)$

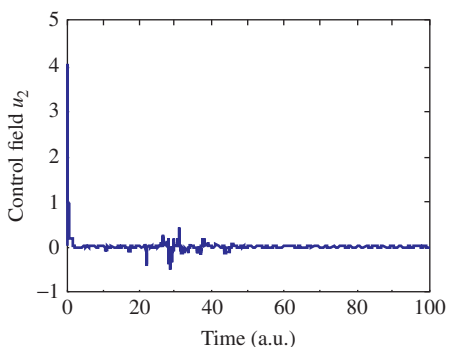


Figure 15.12 Control law $u_2(t)$

From Figure 15.13 one can see that the situation is complicated and there is no simple law to follow for the relationship between the error and the parameters, but Figure 15.13 can still provide us with some knowledge about the effects of control parameters on the error of the control system.

15.4 Convergence of Orbit Tracking for Quantum Systems

The convergence of the orbit tracking of the free-evolutionary target system in quantum systems is studied based on the Lyapunov method in this section. After changing the tracking problem into a state transfer problem, we focus on the convergence problem of state transferring. Two objectives are expected: (i) a convergent control law is derived for complete state transfer between arbitrary states and (ii) a control method for tracking a free-evolutionary target system is proposed based on (i).

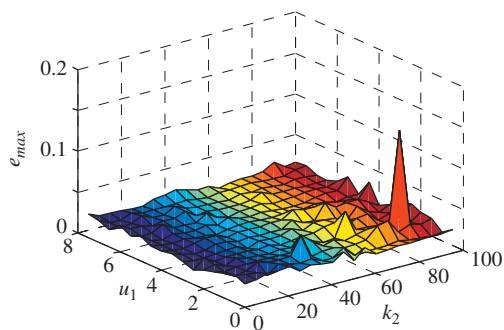


Figure 15.13 Error surface of the control system under the relation between control gain k_2 and the boundary of control u_1

15.4.1 Description of the Control System Model

The control system model studied in this section is also described in Equations 15.1 and 15.2. For the orbit tracking problem in Equation 15.1, the target system in Equation 15.2 is a time-dependent quantum system. To deal with the problem, a unitary transformation $U(t) = \exp(-itH_0)$ is introduced, and the states in Equation 15.1 become $\rho(t) = U^\dagger(t)\hat{\rho}(t)U(t)$ and $\rho_f(t) = U^\dagger(t)\hat{\rho}_f(t)U(t)$, where “ \dagger ” denotes a conjugate and “ $\hat{\cdot}$ ” denotes states before unitary transformation. After this transformation the system in Equation 15.1 is represented by

$$i\frac{\partial}{\partial t}\rho(t) = \left[\sum_{m=1}^M f_m(t) H_m(t), \rho(t) \right], \quad \rho(0) = \hat{\rho}_0 \quad (15.44a)$$

$$i\frac{\partial}{\partial t}\rho_f(t) = 0, \quad \rho_f(0) = \hat{\rho}_{f0} \quad (15.44b)$$

where $H_m(t) = U^\dagger(t)H_mU(t)$.

It can be seen that the dynamic system (Equation 15.44a) is governed by the new Hamiltonian $H_m(t) = e^{iH_0 t}H_m e^{-iH_0 t}$ after the transformation. The control systems are changed from the Schrodinger picture into the interaction picture, and the target system (Equation 15.2) becomes Equation 15.44b, which means the target state $\rho_f(t)$ is equal to a constant. Because of $\rho_f(0) = \hat{\rho}_{f0}$, we have

$$\rho_f(t) = \hat{\rho}_{f0} \quad (15.45)$$

Equation 15.45 means that the target state (Equation 15.45) in Equation 15.44b is the initial state $\hat{\rho}_{f0}$ of the original target system (Equation 15.2), and the tracking problem is changed into the state $\rho(t)$ transfer problem after the transformation. In the remainder of this section we replace the initial state of the target system with the target state for convenience.

Comparing Equation 15.1 with Equations 15.44a and 15.45, one can see the following:

1. The system in Equation 15.1 is autonomous but Equation 15.44a is not.
2. After unitary transformation, the control Hamiltonian H_m in Equation 15.1, which is time-independent, becomes $H_m(t) = e^{iH_0 t}H_m e^{-iH_0 t}$ in Equation 15.44a, which is time-dependent.

3. The time-dependent target state $\rho_f(t)$ in Equation 15.2 becomes a stationary state $\hat{\rho}_{f0}$ in Equation 15.45.

The control objective now becomes to design a convergent control law to steer the state $\rho(t)$ of Equation 15.44a to the target state $\hat{\rho}_f(0)$ of Equation 15.45. Since the evolution of a closed quantum system is unitary, the spectrum of $\rho(t)$ is time-invariant during the whole evolution, viz. $\text{Tr}[\rho^n(t)] = \text{Tr}[\rho_f^n(t)]$.

15.4.2 Control Law Derivation

Here the Lyapunov function based on the virtual physical quantity P is chosen:

$$V(\rho) = \text{tr}(P\rho) \quad (15.46)$$

where P is the observable operator.

To obtain a stable control law, the first-order time derivation of function (Equation 15.46) is obtained as

$$\dot{V} = - \sum_{m=1}^M f_m(t) \text{tr}(iH_m(t)[\rho(t), P]) \quad (15.47)$$

For the sake of simplicity and availability, we let each item on the right-hand side of Equation 15.47 with a summation sign be non-positive in order to ensure $\dot{V} \leq 0$. The control law can be derived as

$$f_m(t) = -k_m \text{tr}(iH_m(t)([\rho(t), P])), k_m > 0 \quad (15.48)$$

where $k_m > 0$ is the control gain to adjust the convergence speed of the system state.

The control law (Equation 15.48) designed by the Lyapunov function (Equation 15.46) will realize the orbit tracking of a free-evolutionary target system (Equation 15.2). However, the control law (Equation 15.48) is only a stable control, which cannot guarantee that the system will converge to the target state. For this reason, we need to study the convergence conditions further, which will guide the design of a convergent control law. Next, we deal with this problem in detail.

15.4.3 Convergence Analysis

In Section 15.4.1 we complete the task of changing orbit tracking into state transferring by means of unitary transformation, and the desired target becomes a time-invariant state $\hat{\rho}_{f0}$. In fact the variety of quantum states, such as eigenstate, superposition state, and mixed state, produces different forms of target state. Generally, the target states in a density matrix can be divided into two kinds. The first one is diagonal target states, including eigenstates and some mixed states, which can be represented by a diagonal density matrix. So far, the convergence analysis of eigenstates has been dealt with well (Wang and Schirmer, 2010a; Kuang and Cong, 2010). Some research results have also been obtained for diagonal mixed states. The second kind of target state is non-diagonal target states, including superposition states and some mixed states. This is so far unresolved fully.

In the existing research, for an autonomous system (1), LaSalle's invariant principle can be used to analyze convergence, where two assumptions are needed (LaSalle and Lefschetz, 1961). Assumption 1 is that H_0 is strongly regular, that is, all the transition frequencies (differences of pairs of energy levels) are different, viz. $\Delta_{jk} \neq \Delta_{pq}$, $(j, k) \neq (p, q)$, where $\Delta_{jk} = \lambda_j - \lambda_k$ and λ_j is an eigenvalues of H_0 . Assumption 2 is that the control Hamiltonian H_m is fully connected: $H_m \in \{\hbar h_{jk} | h_{jk} = |j\rangle\langle k| + |k\rangle\langle j|, j > k\}$, where $|j\rangle$ is the eigenstate associated with λ_j . Because of the unitary evolution of closed quantum systems, if the target state is reachable, which must be unitarily equivalent to the initial state, that is, there exists a unitary transformation U such that $\hat{\rho}_0 = U\hat{\rho}_{f0}U^\dagger$. We take $\hat{\rho}_0 = U\hat{\rho}_{f0}U^\dagger$ as Assumption 3. However, LaSalle's invariant principle fails to deal with the situation in this section because the system in Equation 15.44a is a non-autonomous system. On the other hand, based on the above three assumptions, the "Lyapunov-like lemma," which is also called the improved Barbalat lemma, can be applied to the non-autonomous system with the following contents (Slotine and Li, 1991). If scalar function $V(x, t)$ satisfies (i) $V(x, t)$ is lower bounded, (ii) $\dot{V}(x, t)$ is negative semi-definite, and (iii) $\dot{V}(x, t)$ is uniformly continuous in time, then $\dot{V}(x, t) \rightarrow 0$ as $t \rightarrow \infty$. By selecting the Lyapunov function (Equation 15.46) here all three conditions of the Lyapunov-like lemma mentioned above are satisfied: (i) $V = \text{tr}(P\rho) \geq 0$ is lower bounded for a positive P , (ii) the first-order derivative of $V(x, t)$ is negative semi-definite under control law (Equation 15.48), and (iii) the third condition can be replaced by the existence and continuity of the second derivation of $V(x, t)$. In this section,

$$\ddot{V}(\rho, t) = - \sum_{m=1}^M f_m(t) \{ \text{tr}(i\dot{H}_m(t)[\rho, P]) + \text{tr}(iH_m(t)[\dot{\rho}, P]) \} \text{ is bounded for a bounded input.}$$

According to the Lyapunov-like lemma, the first derivation of the Lyapunov function (Equation 15.46) converges to zero for $t \rightarrow \infty$, viz., $\dot{V}(\rho(\infty), \infty) = 0$. The trajectory of the controlled system (Equation 15.44a) under the Lyapunov function (Equation 15.46) will converge to the limit set at $t \rightarrow \infty$, which is denoted \mathcal{R}_1 . The states that make Equation 15.47 be zero make up the set \mathcal{R}_1 :

$$\mathcal{R}_1 \equiv \{\rho_s : \dot{\nu} = 0\} = \{\rho_s : \text{tr}(iH_m(t)[\rho_s, P]) = 0, \forall m, t\} \quad (15.49)$$

where ρ_s denotes critical stable points of Equation 15.44a and $\rho_f \in \mathcal{R}_1$.

According to the formula of the control law (Equation 15.48), the states in \mathcal{R}_1 satisfy $f_m = 0$, $m = 1, 2, \dots, M$. For the non-autonomous system in Equation 15.44a, if $\rho \in \mathcal{R}_1$, then $\dot{\rho} = 0$ holds for $f_m = 0$, $m = 1, 2, \dots, M$. To increase the convergence probability of the target state, the limit set \mathcal{R}_1 can be reduced and then Proposition 15.1 is obtained:

Proposition 15.1 According to Assumptions 1 and 2, the limit set \mathcal{R}_1 in Equation 15.49 can be redefined as $\mathcal{R}_1 \equiv \{\rho_s : [\rho_s, P] = D\}$, where D is a diagonal matrix.

Proof The control Hamiltonian H_m can be written as $H_m = H_{kl} = |k\rangle\langle l| + |l\rangle\langle k|$. Then $H_{mt} = e^{iH_0t}(|k\rangle\langle l| + |l\rangle\langle k|)e^{-iH_0t} = e^{iw_{kl}t}|k\rangle\langle l| + e^{-iw_{kl}t}|l\rangle\langle k|$, where $\omega_{kl} = \lambda_k - \lambda_l$, λ_i ($i = 0, \dots, n$) is the eigenvalue of H_0 . Because H_0 is non-degenerate, $\omega_{kl} \neq 0$ holds.

The Equation 15.49 becomes

$$\text{tr}(H_m(t)[\rho_s, P]) = e^{iw_{kl}t}\langle l|[\rho_s, P]|k\rangle + e^{-iw_{kl}t}\langle k|[\rho_s, P]|l\rangle = 0$$

Then $\langle l | [\rho_s, P] | k \rangle = 0$, viz. $([\rho_s, P])_{kl} = 0$ holds. Let $A = [\rho_s, P]$, because of the hermiticity and positivity of P , where A is a skew Hermit matrix. The control Hamiltonian H_m is fully connected, so $([\rho_s, P])_{kl} = 0$ holds for all $k \neq l$. Then $[\rho_s, P] = D$, where D is a diagonal matrix.

Proposition 15.1 is proved. ■

There are two significant points:

1. If P is chosen as a diagonal matrix, the limit set is reduced to $\mathcal{R}_1 \equiv \{\rho_s : [\rho_s, P] = 0\}$.
2. If the case (i) is not true, one denotes $[\rho, P] = Ad_p(\vec{P})$, where Ad_p is a linear map from Hermitian or anti-Hermitian matrices into $su(n)$. Let $A(\vec{P})$ be the real $(n^2 - 1) * (n^2 - 1)$ matrix corresponding to the Bloch representation of Ad_p . Denote $su(n) = T \oplus C$ and $R^{n^2-1} = S_T \oplus S_C$, where S_C and S_T are real subspaces corresponding to the Cartan and non-Cartan subspaces, C and T , respectively. Let $\tilde{A}(\vec{P})$ be the first $n^2 - n$ rows of $A(\vec{P})$. Then we can obtain the following Lemma 15.1:

Lemma 15.1 Given a generic P , if $\text{rank}\tilde{A}(\vec{P}) = n^2 - n$ holds, then the limit set \mathcal{R}_1 is regular, viz. $\mathcal{R}_1 \equiv \{\rho_s : [\rho_s, P] = 0\}$.

Based on the above analysis, we choose P with different eigenvalues and satisfy the condition of Lemma 15.1. This means that the critical points ρ_s of Equation 15.44a and P are commutative, and the limit set \mathcal{R}_1 is reduced to

$$\mathcal{R}_2 \equiv \{\rho_s : [\rho_s, P] = 0\} \quad (15.50)$$

In the following content, it is shown that there cannot be only one option for P . We can always choose a suitable P to get a limit set, as in Equation 15.50.

Equation 15.44a will converge to the limit set in Equation 15.50. Whether or not the system converges to the target state depends on the relative positions of the target state, the controlled initial state, and the other stable states. To make the system converge to the target state, the following condition is needed:

$$v(\rho_f) < v(\rho_0) < v(\rho_s) \quad (15.51)$$

Three things are required according to Equation 15.51: (i) the target state ρ_f must make the Lyapunov function (Equation 15.46) take its minimum value, (ii) the initial state ρ_0 makes the value of Equation 15.46 be sub-minimum, and (iii) the Lyapunov function values of states in \mathcal{R}_2 except the target one are larger than that of ρ_0 . Now the control law (Equation 15.48) holds, which means $\dot{v} \leq 0$, so the monotonically decreasing function (Equation 15.46) evolves toward a smaller value. For this reason, if the condition in Equation 15.51 is satisfied, Equation 15.44a with initial state ρ_0 will uniquely converge to the target state.

Equation 15.51 is the condition that ensures the convergence of the controlled system. How to realize Equation 15.51 is studied in the following subsection. We will concentrate on how to construct P to meet Equation 15.51, and the instruction of the structure of P which is satisfied Equation 15.51 for the diagonal and non-diagonal target states, respectively.

1) The case of diagonal target states

The states with diagonal density matrices include eigenstates and mixed states. Suppose the target state ρ_f is a diagonal mixed state and $\{\lambda_i, i = 1, 2 \dots n\}$ is the eigen-spectrum of ρ_0 .

The target state ρ_f should be a permutation of $\{\lambda_i, i = 1, 2 \dots n\}$, viz. $\rho_f = \text{diag}(\lambda_1, \lambda_2 \dots \lambda_n)$. According to the set $\mathcal{R}_2 \equiv \{\rho_s : [\rho_s, P] = 0\}$ in Equation 15.50, a diagonal P is the simplest choice. The other states ρ_s in \mathcal{R}_2 are the different permutations of the eigen-spectrum. In order to construct a P satisfies Equation 15.51, three steps need to be performed.

First, P is constructed to make ρ_f be the point corresponding to the minimum of the Lyapunov function (Equation 15.46), which is realized by Lemma 15.2:

Lemma 15.2 If the diagonal target state is $\rho_f = \text{diag}(\lambda_1, \lambda_2 \dots \lambda_n)$, the matrix P corresponding to ρ_f is $P = \text{diag}(p_1, p_2, \dots, p_n)$. Then ρ_f is the point where the Lyapunov function (Equation 15.46) is a minimum if the diagonal element p_i of P meets $(\lambda_i - \lambda_j)(p_i - p_j) < 0, \forall i \neq j$.

Proof P is a diagonal matrix and one can get $\dot{v}(\rho_f) = 0$ from Equation 15.47:

$$\begin{aligned}\ddot{v}(\rho) &= -i * \sum_m f_m \{ \text{tr}(\dot{H}_{mt}[\rho, P]) + \text{tr}(H_{mt}[\dot{\rho}, P]) \} \\ \ddot{v}(\rho_f) &= - \sum_m f_m^2 \text{tr}([H_{mt}, \rho_f] * [P, H_{mt}]) = \sum_m f_m^2 \text{tr}([H_{mt}, \rho_f] * [H_{mt}, P])\end{aligned}$$

Let $A = [H_{mt}, \rho_f], B = [H_{mt}, P]$, then $(A)_{ij} = (\lambda_j - \lambda_i)(H_{mt})_{ij}, (B)_{ij} = (p_j - p_i)(H_{mt})_{ij}$, so

$$\text{tr}(AB) = \sum_{i=1}^n \sum_{j=1}^n A_{ij} B_{ji} = \sum_{i=1}^n \sum_{j=1}^n (\lambda_j - \lambda_i)(p_i - p_j)(H_{mt})_{ij}^2 = - \sum_{i=1}^n \sum_{j=1}^n (\lambda_j - \lambda_i)(p_j - p_i)(H_{mt})_{ij}^2.$$

If ρ_f is a stable state, then $\ddot{v}(\rho_f) > 0$ and one gets $(\lambda_i - \lambda_j)(p_i - p_j) < 0, \forall i \neq j$.

Let $\{\mu_1, \mu_2 \dots \mu_n\}$ be the spectrum of ρ_f with μ_i arranged in a non-increasing order, viz $\mu_1 < \mu_2 < \dots < \mu_n$. Then the corresponding P is $P = \text{diag}(p_1, p_2, \dots, p_n)$ and $p_1 > p_2 > \dots > p_n$ is obtained by the above method. One of the P values is $P = -\rho_f$. For any other states ρ_s in the limit set \mathcal{R} can be obtained by swapping two arbitrary elements of $\{\mu_1, \mu_2 \dots \mu_n\}$ m times. Let $\text{bool} = \text{tr}(P\rho_f) - \text{tr}(P\rho_s)$.

Suppose the spectrum from the smallest to the largest target state is $\{\mu_1, \mu_2, \dots, \mu_i, \dots, \mu_j, \dots, \mu_k, \dots, \mu_n\}$, then

$$\begin{aligned}i \leftrightarrow j : \text{bool} &= p_i(\mu_i - \mu_j) + p_j(\mu_j - \mu_i) = (p_i - p_j)(\mu_i - \mu_j) < 0 \\ i \leftrightarrow j, j \leftrightarrow k : \text{bool} &= p_i(\mu_i - \mu_j) + p_j(\mu_j - \mu_k) + p_k(\mu_k - \mu_i) \\ &= p_i(\mu_i - \mu_j) + p_j(\mu_j - \mu_i + \mu_i - \mu_k) + p_k(\mu_k - \mu_i) \\ &= (p_i - p_j)(\mu_i - \mu_j) + (p_j - p_k)(\mu_i - \mu_k) < 0 \\ i \leftrightarrow j, j \leftrightarrow k, k \leftrightarrow l : \text{bool} &= p_i(\mu_i - \mu_j) + p_j(\mu_j - \mu_k) + p_k(\mu_k - \mu_l) + p_l(\mu_l - \mu_i) \\ &= p_i(\mu_i - \mu_j) + p_j(\mu_j - \mu_i + \mu_i - \mu_k) + p_k(\mu_k - \mu_i + \mu_i - \mu_l) \\ &\quad + p_l(\mu_l - \mu_i) \\ &= (p_i - p_j)(\mu_i - \mu_j) + (p_j - p_k)(\mu_i - \mu_k) + (p_k - p_l)(\mu_i - \mu_l) < 0\end{aligned}$$

and so on. Finally, we get $v(\rho_f) < v(\rho_s)$. Lemma 15.2 is proved. ■

Second, Equation 15.51 is divided into two parts:

1. $v(\rho_f) < v(\rho_0)$. The condition $v(\rho_f) < v(\rho_0)$ indicates that the value of value of Equation 15.46 of the initial state is larger than that for the target state. Otherwise, it is inconsistent with the monotonically decreasing Equation 15.46, and the target state will be unreachable. It is easy to obtain $v(\rho_f) - v(\rho_0) = \sum_{i=1}^n (P)_{ii}(\lambda_i - (\rho_0)_{ii})$. Based on the relationship between eigenvalues and matrix diagonal elements, the expression $\sum_{i=1}^n \lambda_i = \sum_{i=1}^n \mu_i = \sum_{i=1}^n (\rho_0)_{ii} = 1$ holds, where $(\rho_0)_{ii}$ is the i th diagonal element of initial state ρ_0 . There must therefore be at least one k to make $\lambda_k < (\rho_0)_{kk}$ hold. If one wants to make $v(\rho_f) - v(\rho_0) = (P)_{kk}(\lambda_k - (\rho_0)_{kk}) + \sum_{i=1, i \neq k}^n (P)_{ii}(\lambda_i - (\rho_0)_{ii}) < 0$ hold, where $(P)_{kk}$ is the k th diagonal element of P , then $(P)_{kk} > \sum_{i=1, i \neq k}^n (P)_{ii}(\lambda_i - (\rho_0)_{ii}) / ((\rho_0)_{kk} - \lambda_k)$ is obtained, viz. a certain k satisfying $\lambda_k < (\rho_0)_{kk}$ is chosen, giving

$$(P)_{kk} > \sum_{i=1, i \neq k}^n (P)_{ii}(\lambda_i - (\rho_0)_{ii}) / ((\rho_0)_{kk} - \lambda_k) \quad (15.52)$$

There may be more than one k to satisfy $\lambda_k < (\rho_0)_{kk}$, but usually we choose the $(P)_{kk}$ corresponding to a larger value to determine $v(\rho_f) < v(\rho_0)$, otherwise slight regulation of $(P)_{kk}$ is performed.

2. $v(\rho_0) < v(\rho_s)$. ρ_s should be one of the permutations of the eigen-spectrum. It gives $v(\rho_0) - v(\rho_s) = \text{tr}(P\rho_0) - \text{tr}(P\rho_s)$. According to Assumption 3, $\rho_0 = U\rho_f U^\dagger$, so

$$\text{tr}(P\rho_0) = \text{tr}(PU\rho_f U^\dagger) = \text{tr}(U^\dagger PU\rho_f) = \sum_{i=1}^n (P)_{ii} \sum_{j=1}^n (\rho_f)_{jj} (U_{ij})^2, \text{tr}(P\rho_s) = \sum_{i=1}^n (P)_{ii} (\rho_s)_{ii},$$

and

$$\text{tr}(P\rho_0) - \text{tr}(P\rho_s) = \sum_{i=1}^n (P)_{ii} \left(\sum_{j=1}^n (\rho_f)_{jj} (U_{ij})^2 - (\rho_s)_{ii} \right).$$

Both ρ_s and ρ_f have the same spectrum so $(\rho_f)_{kk} = (\rho_s)_{ii}$. Because of the unitary matrix U , $UU^\dagger = U^\dagger U = I$ and $\sum_{j=1}^n (U_{ij})^2 = 1$. One gets:

$$\begin{aligned} \text{tr}(P\rho_0) - \text{tr}(P\rho_s) &= \sum_{i=1}^n (P)_{ii} \left(\sum_{j \neq k}^n (\rho_f)_{jj} (U_{ij})^2 + (\rho_f)_{kk} ((U_{ik})^2 - 1) \right) \\ &= \sum_{i=1}^n (P)_{ii} \left(\sum_{j \neq k}^n (\rho_f)_{jj} (U_{ij})^2 - (\rho_f)_{kk} \sum_{j \neq k}^n (U_{ij})^2 \right) \\ &= \sum_{i=1}^n (P)_{ii} \sum_{j \neq k}^n ((\rho_f)_{jj} - (\rho_f)_{kk}) (U_{ij})^2 \end{aligned}$$

For the above equation, there is at least one l to make $(\rho_f)_{ll} - (\rho_f)_{kk} < 0$ hold. If $\text{tr}(P\rho_0) - \text{tr}(P\rho_s) < 0$ is expected to hold, then the following expression is workable:

$$(P)_{ll} > \left(\sum_{i \neq l}^n (P)_{ii} \sum_{j \neq k}^n ((\rho_f)_{jj} - (\rho_f)_{kk})(U_{ij})^2 + (P)_{ll} \sum_{j \neq k, j \neq l}^n ((\rho_f)_{jj} - (\rho_f)_{kk})(U_{lj})^2 \right) / ((\rho_f)_{kk} - (\rho_f)_{ll}) \quad (15.53)$$

The above process constructs P for mixed states with a diagonal density matrix. We conclude that if the target state is diagonal, a Hermitian and positive diagonal matrix P is selected. To ensure convergence, the diagonal elements of P must satisfy Lemma 15.2 and Equations 15.52 and 15.53 simultaneously. In addition to this, we choose non-negative diagonal elements for P to ensure its positivity.

2) The case of a non-diagonal target density matrix

It is more complicated to analyze the convergence for the case of a non-diagonal target state. The idea is as follows: the non-diagonal target state is changed into a diagonal matrix, and then P is designed by using the method proposed in case 1 in Section 15.4.3. However, one needs notice that the superposition state is a kind of pure state, which can be represented by wave functions as $\rho_f = |\psi_f\rangle\langle\psi_f|$. As a result, a diagonal state conversion is not necessary for a superposition state. What one only needs to design a proper P . Next, we go on to the analysis of a non-diagonal superposition state and a mixed state in detail.

1. For a target superposition state Before the analysis in depth, Lemma 15.3 needs to be introduced.

Lemma 15.3 For the n -level Hermitian matrices A and B , if they are commutative, viz. $[A, B] = 0$, then both A and B own the same eigenstates (Karasik *et al.*, 2008).

We rewrite P according to its eigen-decomposition as $P = \sum_k p_k |\psi_k\rangle\langle\psi_k|$, where $|\psi_k\rangle$ is its eigenstate and p_k is its eigenvalue. It is known that the target state ρ_f can be described as $\rho_f = |\psi_f\rangle\langle\psi_f|$. According to $\rho_f \in \mathcal{R}_2$ and Lemma 15.3, P can be described as

$$P = p_1 |\psi_f\rangle\langle\psi_f| + \sum_{k=2}^n p_k |\psi_k\rangle\langle\psi_k|, \text{ where } |\psi_1\rangle = |\psi_f\rangle. \text{ And } \psi_i|\psi_j\rangle = 0, \text{ for } i \neq j \quad (15.54)$$

and ρ_s should be

$$\rho_s = \lambda_1 |\psi_f\rangle\langle\psi_f| + \sum_{k=2}^n \lambda_k |\psi_k\rangle\langle\psi_k|, \quad \sum_{k=1}^n \lambda_k = 1 \quad (15.55)$$

It is known that the states ρ_0 and ρ_s have the same spectrum under unitary evolution, therefore ρ_s has the same eigenvalues as ρ_0 and so does the target state ρ_f .

Substituting $\rho_f = |\psi_f\rangle\langle\psi_f|$ into Equation 15.55, the eigen-spectrum of ρ_f is $\{1, 0, \dots, 0\}$, so for ρ_s there is only one eigenvalue λ_i to be non-zero, viz. $\rho_s = \lambda_i |\psi_i\rangle\langle\psi_i|$ ($\lambda_i = 1$).

To make the system asymptotically stable, Equation 15.51 is needed. If $\rho_j = |\psi_j\rangle\langle\psi_j|$ are as denoted in Equation 15.54, then:

$$\begin{cases} v(\rho_f) = \text{tr}(P\rho_f) = p_1 \\ v(\rho_0) = p_1 \text{tr}(\rho_f\rho_0) + \sum_{k=2}^n p_k \text{tr}(\rho_k\rho_0) \\ v(\rho_s) = p_j (j \neq 1) \end{cases} \quad (15.56)$$

Combining Equation 15.56 with Equation 15.51, a suitable P can be constructed to satisfy

$$0 < p_1 < p_1 \text{tr}(\rho_f\rho_0) + \sum_{k=2}^n p_k \text{tr}(\rho_k\rho_0) < p_j (j \neq 1) \quad (15.57)$$

It can be seen from Equation 15.57 that P may not be a diagonal matrix for a non-diagonal target superposition state. The P constructed based on Equations 15.54 and 15.57 guarantees the convergence of non-diagonal target superposition state, where Equation 15.54 describes how to construct the eigenstate and Equation 15.57 determines the eigenvalue. Moreover, the eigenvalue p_1 of P , whose corresponding eigenstate is the target state, is the smallest one. One then obtains $(1 - \text{tr}(\rho_f\rho_0))p_1 < \sum_{k=2}^n p_k \text{tr}(\rho_k\rho_0) \& p_1 < p_k, \forall k \neq 1$. Let $\frac{(1 - \text{tr}(\rho_f\rho_0))}{\text{tr}(\rho_k\rho_0)}p_1 < p_k \& p_1 < p_k, \forall k \neq 1$, then one has

$$g_k > \max \left\{ \frac{(1 - \text{tr}(\rho_f\rho_0))}{\text{tr}(\rho_k\rho_0)}, 1 \right\}, p_k = g_k p_1 \quad (15.58)$$

where g_k is the weight coefficient corresponding to p_k . Equation 15.58 means that p_k is proportional to the smallest eigenvalue p_1 . It is obvious that Equation 15.58 is not the only one for P . It is selected carefully to also satisfy the condition of Lemma 15.1.

2. For a non-diagonal mixed state

For the system in Equation 15.1, suppose the initial target state $\hat{\rho}_{f0}$ is a non-diagonal mixed state. The solution of Equation 15.2 is $\hat{\rho}_f(t) = e^{-iH_0t}\hat{\rho}_{f0}e^{iH_0t}$. In this case, a unitary transformation has been used to transform the tracking problem of Equation 15.1 into the state transferring one of Equation 15.44a. We follow the idea of changing the non-diagonal $\hat{\rho}_{f0}$ into a diagonal by another unitary transformation and then a convergent control law can be designed based on case 1 in Section 15.4.3.

As mentioned in Section 15.4.1, the unitary transformation $U = \exp(i * H_0 t)$ is applied to change the tracking of the free-evolutionary target quantum system in Equation 15.2 into the transferring one of a stationary target state $\hat{\rho}_{f0}$. $\hat{\rho}_{f0}$ is a Hermitian matrix, so there exists another unitary transformation U_f to meet $U_f \hat{\rho}_{f0} U_f^\dagger = D_f$. After this transformation, The target state $\hat{\rho}_{f0}$ of Equation 15.44b becomes the diagonal matrix D_f . In other words, two unitary transformations are performed on Equation 15.1 and then the target system tracking with non-diagonal initial state is changed into the state transferring of diagonal target state D_f . In fact, in the case of orbit tracking with a non-diagonal mixed target state, the problem can be solved by a two-in-one unitary transformation U_T .

Let $U_T = U_f e^{iH_0 t}$. This is performed on Equation 15.1, viz., $\rho = U_T \hat{\rho} U_T^\dagger$ and $\rho_f = U_T \hat{\rho}_f U_T^\dagger = U_T U_f^\dagger D_f U_T U_f^\dagger = D_f$. Then Equation 15.1 becomes

$$i\hbar \frac{\partial}{\partial t} \rho(t) = \left[\sum_{m=1}^M f_m(t) H_{mt}, \rho(t) \right], \quad \rho(0) = U_f \hat{\rho}_0 U_f^\dagger \quad (15.59a)$$

$$i\hbar \frac{\partial}{\partial t} \rho_f(t) = 0, \quad \rho_f(0) = D_f \quad (15.59b)$$

where $H_{mt} = U_T H_m U_T^\dagger$.

After the unitary transformation U_T , the tracking of the target system with non-diagonal initial state $\hat{\rho}_f(0)$ in Equation 15.1 can be changed into the state transferring of a diagonal stationary state in Equation 15.59a. According to Proposition 15.1, the critical points set of Equation 15.59a is still $\mathcal{R}_2 \equiv \{\rho_s : [\rho_s, P] = 0\}$. The convergence analysis is the same as that in case 1 in Section 15.4.3. We do not repeat it here.

15.4.4 Applications and Experimental Results Analyses

The trajectory of a quantum state in a two-level system can be described by the point's trajectory in the Bloch sphere, so in this section a two-level atom system controlled by a single control field is considered. The effectiveness of the proposed method will be illustrated.

The free Hamiltonian of the controlled system (Equation 15.1) is $H_0 = \omega \sigma_z$ and the control Hamiltonian is $H_1 = \omega \sigma_x$, where $\sigma_i (i = x, y, z)$ denotes the Pauli matrix, $\sigma_x = [0 \ 1; 1 \ 0]$ and $\sigma_z = [1 \ 0; 0 \ -1]$.

For this two-level system, we denote $e_1 = |0\rangle$ and $e_2 = |1\rangle$ as the basic vectors of H_0 . According to Equation 15.48, the control law is $f_1(t) = -k_1 \text{tr}(iH_1(t)[\rho(t), P])$. This example satisfies the three conditions in Section 15.4.3.

1) For a non-diagonal target superposition state

The initial state of Equation 15.1 is $|\psi_0\rangle = \frac{1}{\sqrt{3}}|0\rangle + \sqrt{\frac{2}{3}}|1\rangle$ and the initial target state of Equation 15.2 is $|\psi_f\rangle = \frac{1}{\sqrt{8}}|0\rangle + \sqrt{\frac{7}{8}}|1\rangle$. These are both non-diagonal superposition states. The design process of a convergent control law is as follows:

1. Construction of P

To construct P , a set of linearly independent vectors $|\psi_k\rangle (k = 1, 2)$ is prepared. In this example, we choose $|\psi_1\rangle = |\psi_f\rangle$, $|\psi_2\rangle = e_1$. The Schmidt orthogonalization is then performed. Suppose the orthogonalized vectors are $|s_1\rangle$ and $|s_2\rangle$, where $|s_1\rangle = |\psi_f\rangle$. According to Equation 15.54, $P = p_1|s_1\rangle\langle s_1| + p_2|s_2\rangle\langle s_2|$ holds. The state, apart from the target state, in \mathcal{R}_2 is $\rho_s = |s_2\rangle\langle s_2|$. To ensure the convergence, Equation 15.51 is satisfied: $p_1 < p_1 \text{tr}(\rho_f \rho_0) + p_2 \text{tr}(\rho_s \rho_0) < p_2$. It then obtains $p_2 > \max\{p_1 * (1 - \text{tr}(\rho_f \rho_0)) / \text{tr}(\rho_2 \rho_0), p_1\}$.

According to Equation 15.58, one obtains $p_2 = g_2 * p_1$, where $g_2 > \max\left\{\frac{1 - \text{tr}(\rho_f \rho_0)}{\text{tr}(\rho_2 \rho_0)}, 1\right\}$.

If $p_1 = 0.2$, $g_2 = 10$ is selected and $P = \begin{bmatrix} 1.775 & -0.595 \\ -0.595 & 0.425 \end{bmatrix}$. We denote P with its Bloch

vector as $\vec{P} = (x_1, x_2, x_3) = (-1.19, 0, 1.35)$. In fact, if P is chosen as a real Hermitian matrix, one always gets $x_2 = 0$. According to Lemma 15.1, ρ is expressed with the Bloch

vector as $\rho = \frac{1}{2}I + \sum_{i=1}^3 \lambda_i \sigma_i$. One then gets $A(\vec{P}) = \begin{pmatrix} 0 & -x_3 & 0 \\ x_3 & 0 & -x_1 \\ 0 & x_1 & 0 \end{pmatrix}$ and $\text{rank } A(\vec{P}) = 2$, which

satisfies the condition of Lemma 15.1.

2. Illustrations of system simulation experiments

The control gain in Equation 15.48 is selected as $k = 0.1$. The control law (Equation 15.48) with the P designed in Section 15.4.3 is applied to Equations 15.44a and 15.44b. Simulation experimental results are shown in Figure 15.14, where Figure 15.14a shows the state transferring process during time $t \in [0, 50]$. Figure 15.14b is the control field. The open circle denotes the initial state of the controlled system and the solid circle is the target state, the line is the trajectory of the controlled state from its initial point to its final point, and the arrow indicates its transferring direction.

To illustrate better the effectiveness of the control strategy proposed, the control field Figure 15.14b is applied to the original system (Equation 15.1). The tracking results are shown in Figure 15.15, where the dashed line is the evolution curve of the controlled state in Equation 15.1 and the solid line is one of the target states in the target system (Equation 15.2), the open circle and solid circle indicate the initial location at the current period of the controlled state and the target state, respectively, and the arrow indicates the direction. The evolution trajectory during the time $t \in [0, 8]$ a.u. is shown in Figure 15.15a. One can see that the controlled system is asymptotically convergent to the target system on the Bloch sphere. Figure 15.15b is the state trajectory during time $t \in [8, 30]$ a.u. and Figure 15.15c is the magnified bottom view of Figure 15.15b. The different locations are labelled with black boxes. It can be seen from Figure 15.15c that the open circle overlaps the solid one at $t = 30$ (the upper right box), so the tracking is achieved at this point. After that the controlled system will follow the target state in the target orbit. All three figures demonstrate integrally how the system in Equation 15.1 tracks Equation 15.2. If the performance index $v = \|\hat{\rho}(t) - \hat{\rho}_f(t)\|^2 = \text{tr}((\hat{\rho} - \hat{\rho}_f)^\dagger (\hat{\rho} - \hat{\rho}_f))$ is used to measure the tracking accuracy, then $v = 9.41 * 10^{-5}$ is reached at $t = 50$ a.u.

3. Analysis of tracking properties

According to the weight coefficient g_k defined in Equation 15.58, the relationship between the two eigenvalues of P is proportional. The experiment is used to demonstrate the effects of performance index produced by different coefficients g_k when other parameters remain unchanged. In the experiments, g_2 was selected as 3, 6, and 12, respectively. The performance index is $v = \|\hat{\rho}(t) - \hat{\rho}_f(t)\|^2$. Figure 15.3 shows the influence of different g_2 on performance index, where the solid line is for $g_2 = 3$ and the dotted line and the dashed line are for $g_2 = 6$ and $g_2 = 12$, respectively. We also drawn the performance index in $100 < t < 150$ in Figure 15.16.

From Figure 15.16 one can see that the performance index $v = 9.26 \times 10^{-5}$ was achieved at $t = 15.1$ a.u. for $g_2 = 12$, $v = 9.46 \times 10^{-5}$ was reached at $t = 39.6$ a.u. for $g_2 = 6$, and $v = 9.48 \times 10^{-5}$ was achieved at $t = 123.9$ a.u. for $g_2 = 3$. It is found that coefficient g_2 determines the convergent rate. The larger the value of g_2 , the faster the rate.

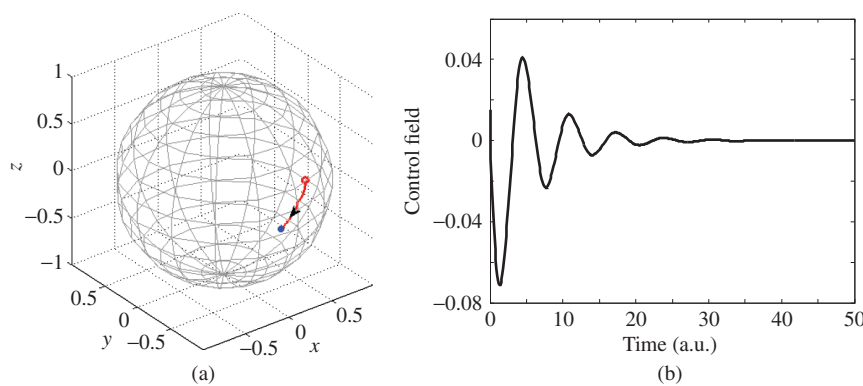


Figure 15.14 Simulation experimental results: (a) state transferring process and (b) control field

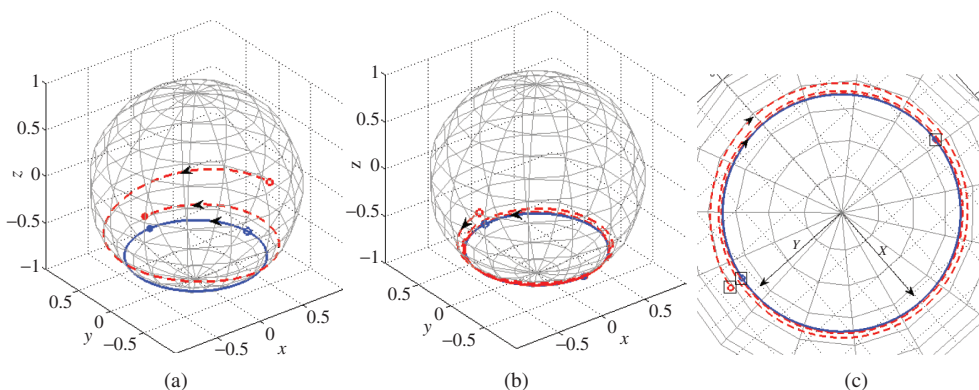


Figure 15.15 The trajectory tracking process of a non-diagonal superposition target state: (a) $t \in [0, 8]$, (b) $t \in [8, 30]$, and (c) the bottom view of magnified (b)

2) For a non-stationary target mixed state

The initial states of Equations 15.1 and 15.2 are $\hat{\rho}_0 = [0.45\ 0.274; 0.274\ 0.55]$ and $\hat{\rho}_{f0} = [0.762\ -0.094; -0.094\ 0.238]$, respectively, which are both non-diagonal mixed states. Because the purity of the mixed state is less than 1 and the initial state is unitary equivalently to the target state, the evolution of the mixed state is on a certain sphere inside the Bloch sphere. According to Equation 15.44a and 15.44b, a unitary transformation $U_T = U_f e^{iH_0 t}$ is first applied to Equation 15.1, where $U_f = [0.985\ -0.171; 0.171\ 0.985]$. Equation 15.59a and 15.59b is then obtained, where $\rho_f(0) = D_f = \text{diag}([0.778, 0.222])$ and $\rho(0) = [0.361\ 0.241; 0.241\ 0.639]$. Then $P = \text{diag}([p_1, p_2])$ is constructed to meet Equation 15.51 and as $p_1(D_f)_{11} + p_2(D_f)_{22} < p_1(\rho_0)_{22} + p_2(\rho_0)_{22} < p_1(D_f)_{22} + p_2(D_f)_{11}$, one gets $p_1 < p_2$. If we choose $p_1 = 0.1$ and $g_2 = 2$, then $P = \text{diag}([0.1, 0.2])$ holds. The

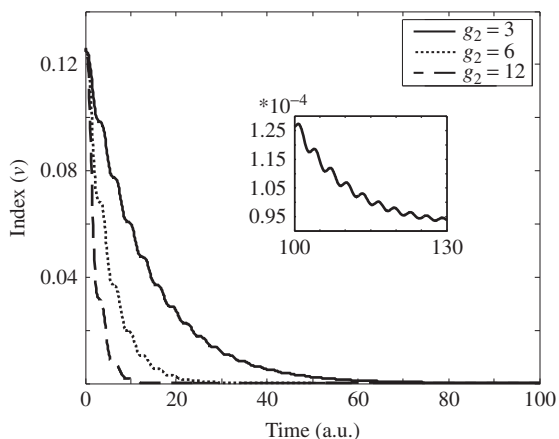


Figure 15.16 Influence of different g_2 on performance index $v = \|\hat{\rho}(t) - \hat{\rho}_f(t)\|^2$

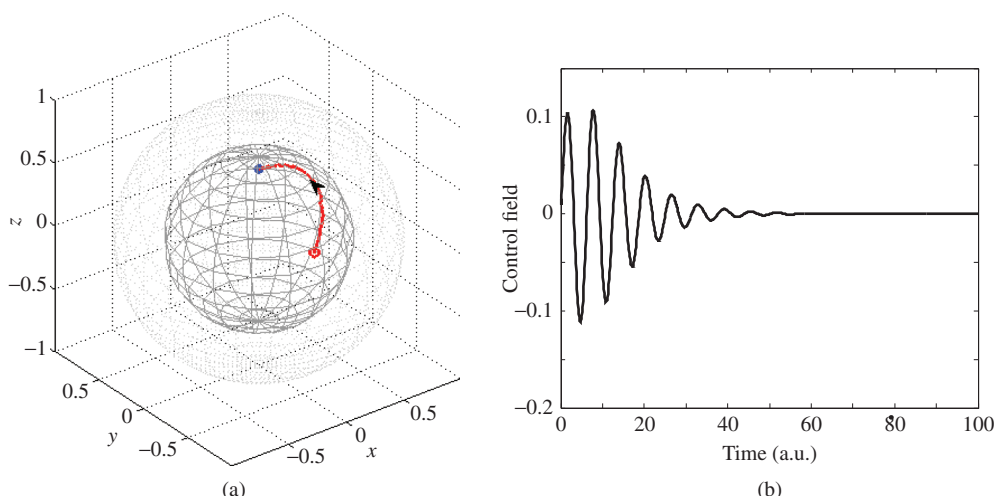


Figure 15.17 The state transferring process of a non-diagonal mixed target state: (a) state evolution and (b) control field

control gain in Equation 15.48 is $k = 2$. Figure 15.17 is the state transferring process of the non-diagonal mixed target state in which Figure 15.17a is the evolutionary trajectory, the open circle denotes the initial state of the controlled system, the solid circle is the target state, the line is the trajectory of the controlled state from its initial point to its final point, and the arrow indicates its direction. Figure 15.17b is the control field.

Similarly, the control field is applied to the original system (Equation 15.1). The trajectory tracking results are shown in Figure 15.18, where the red dashed line denotes the trajectory of the controlled state and the solid line denotes that of target state. The two open circles are the starting points of the controlled system and the target system, respectively, and two

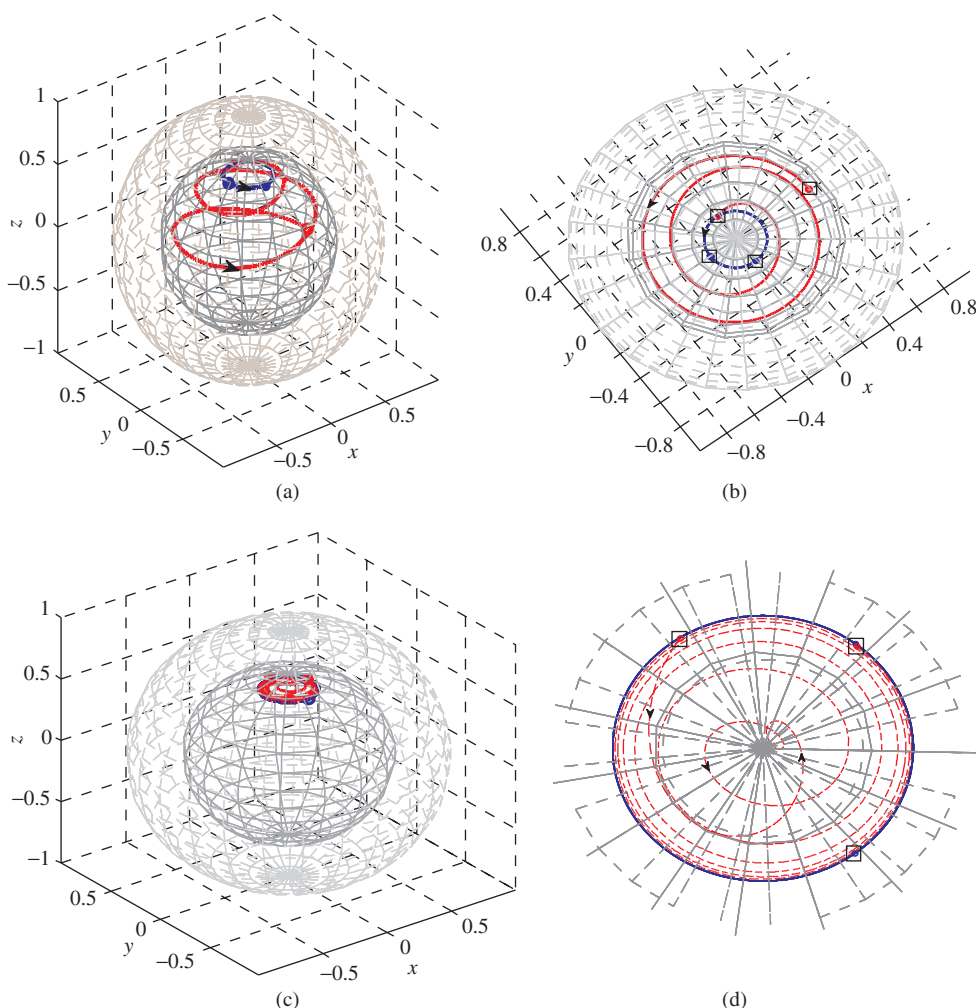


Figure 15.18 The trajectory tracking process of a non-diagonal mixed-state: (a) trajectory tracking, (b) plan view of magnified (a), (c) trajectory tracking, and (d) plan view of magnified (c)

solid circles indicate the final points. The black arrow indicates the tracking direction and the black boxes label the locations of states. Figure 15.18a shows the trajectory tracking process at $t \in [0, 14.2]$. Figure 15.18b is the magnified plane view of Figure 15.18a. From Figure 15.18 it can be seen that the controlled state is asymptotically convergent with respect to the target orbit from outside to inside. It enters the target orbit at $t = 14.2$ a.u. At this time, however, because the target state (the solid circle on solid line in Figure 15.18b) is far from the controlled state (the solid circle on dashed line in Figure 15.18b), the control law is non-zero. The system keeps the evolution. During time $t \in [14.2, 60]$, the trajectory tracking is shown in Figure 15.18c,d is the plan view of Figure 15.18c. In Figure 15.18d, the upper left box and the bottom right box label the locations of the controlled state and the target state at $t = 14.2$ a.u. After this time the

controlled state goes away from the target orbit. Under control law, it gradually comes back to the target orbit from inside to outside and overlaps the target state at the upper right-hand location at $t = 60$ a.u. Both the controlled state and the target state then stay in the target orbit and have the same evolution. The performance $v = 6.5 \times 10^{-5}$ at $t = 100$ a.u.

In summary, for a diagonal or a non-diagonal target initial state, the controlled system will converge to its target system under the action of the control law in Equation 15.48 with P designed as proposed in Section 15.4.3.

References

- Abhinav, J., Beltrani, V., Rosenthal, C. and Rabitz, H. multiple solutions in the tracking control of quantum systems. *Journal of Physical Chemistry A*, **113**(26), 7667–7670.
- Beaucharda, K., Coronb, J.M., Mirrahimic, M. et al. (2007) Implicit Lyapunov control of finite dimensional Schrödinger equations. *Systems and Control Letters*, **56**(5), 388–395.
- Chen, B.S., Chen, W.H., Hsu, F. et al. (2008) Optimal tracking control design of quantum systems via tensor formal power series method. *Open Automation and Control System Journal*, **1**, 50–64.
- Chen, Y., Gross, P., Ramakrishna, V. et al. (1995) Competitive tracking of molecular objectives described by quantum mechanics. *Journal of Chemical Physics*, **102**(20), 8001–8010.
- Cong, S. and Zhang, Y.Y. (2011) *Optimal Control of Mixed-State Quantum Systems Based on Lyapunov Method*, BIOSIGNALS, Rome, pp. 22–30.
- D'Alessandro, D. and Dahleh, M. (2001) Optimal control of two-level quantum systems. *IEEE Transaction on Automatic Control*, **46**(6), 866–876.
- Jha, A., Beltrani, V., Rosenthal, C. et al. (2009) Multiple solutions in the tracking control of quantum systems. *Journal of Physical Chemistry A*, **113**, 7667–7670.
- Karasik, R.I., Marzlin, K.P., Sanders, B.C. et al. (2008) Criteria for dynamically stable decoherence-free subspace and incoherently generated coherences. *Physical Review A*, **77**(5), 052301.
- Kuang, S. and Cong, S. (2010) Population control on equilibrium states of quantum systems via Lyapunov method. *Acta Automatica Sinica*, **36**(9), 1257–1263.
- LaSalle, J. and Lefschetz, S. (1961) *Stability By Liapunov's Direct Method With Applications*, Academic Press, New York.
- Liu, J.X. and Cong, S. (2011) Trajectory tracking of quantum states based on Lyapunov method. 9th IEEE International Conference on Control and Automation (ICCA), Santiago, Chile, pp. 318–323.
- Liu, J.X., Cong, S., and Zhu, Y. (2012) Adaptive trajectory tracking of quantum systems. 12th International Conference on Control, Automation and Systems, Jeju Island, Korea, pp. 322–327.
- Mirrahimi, M. and Rouchon, P. (2004) Trajectory tracking for quantum systems: a Lyapunov approach. Proceedings of the International Symposium MTNS, Belgium.
- Mirrahimi, M., Rouchon, P. and Turinici, G. (2005a) Lyapunov control of bilinear Schrödinger equations. *Automatica*, **41**(11), 1987–1994.
- Mirrahimi, M., Turinici, G. and Rouchon, P. (2005b) Reference trajectory tracking for locally designed coherent quantum controls. *Journal of Physical Chemistry A*, **109**(11), 2631–2637.
- Rothman, A., Ho, T. and Rabitz, H. (2005) Quantum observable homotopy tracking control. *Journal of Chemical Physics*, **123**(13), 134104.
- Salomon, J. and Turinici, G. (2006) On the relationship between the local tracking procedures and monotonic schemes in quantum optimal control. *Journal of Chemical Physics*, **124**(7), 074102.
- Shapiro, M. and Brumer, P. (1997) Quantum control of chemical reactions. *Journal of the Chemical Society, Faraday Transactions*, **93**, 1263–1277.
- Slotine, J.J.E. and Li, W.P. (1991) *Applied Nonlinear Control*, Prentice-Hall, Inc, Mexico.
- Sugawara, M. (2003) General formulation of locally designed coherent control theory for quantum system. *Journal of Chemical Physics*, **118**(15), 6784–6801.

- Wang, X. (2001) Quantum teleportation of entangled coherent states. *Physical Review A*, **64**(2), 022302.
- Wang, X. and Schirmer, S. (2010a) Analysis of Lyapunov method for control of quantum states. *IEEE Transactions on Automatic Control*, **55**(10), 2259–2270.
- Wang, X. and Schirmer, S. (2010b) Analysis of effectiveness of Lyapunov control for non-generic quantum states. *IEEE Transactions on Automation Control*, **55**(6), 1406–1411.
- Zhang, W. and Chen, B.-S. (2008) Stochastic affine quadratic regulator with applications to tracking control of quantum systems. *Automatica*, **44**(11), 2869–2875.
- Zhu, W.S. and Rabitz, H. (1999) Managing singular behavior in the tracking control of quantum dynamical observables. *Journal of Chemical Physics*, **10**(4), 1905–1915.
- Zhu, W.S. and Rabitz, H. (2003a) Closed loop learning control to suppress the effects of quantum decoherence. *Journal of Chemical Physics*, **118**(15), 6751–6758.
- Zhu, W.S. and Rabitz, H. (2003b) Quantum control design via adaptive tracking. *Journal of Chemical Physics*, **119**(7), 3619–3625.

Index

- adaptive trajectory tracking, 394
- adiabatic reservoir, 353
- auxiliary system, 147
- arbitrary pure state, 145
- atom system, 291
 - Λ -type three-level, 291
 - n -level, 352
 - four-level open, 322
 - Ξ -configuration, 352
 - n -level Ξ -configuration, 352
- asymptotic stability, 78, 168
- Barbalat lemma, 168
- bath-induced decoherence dynamics, 237
- bang-bang control, 61
- bang-bang operations group, 355
- Bell states, 221
- bilinear models, 3
- bilinear system, 82
- Bloch sphere, 21, 244
- Block vector, 22, 102, 214, 218, 244, 298
- Boltzmann distribution, 143
- bra, 2
- bra-ket, 2, 22
- breakdown time, 297, 314
- characteristic analysis, 398
- classical control theory, 7
- closed-loop, 6
- closed quantum systems, 3, 48
- coherence, 248
- coherence maintainance, 321
- coherence preservation, 291
- coherence superposition, 48
- coherent vector, 225
- commutation, 4
- commutation operator, 4
- compensation, 246
 - coherence, 247
- complex conjugate, 220
- complex vector space, 2
- complex Hilbert space, 2
- completely positive map, 270
- condition, 340
 - convergence, 196
 - dynamic decoupling, 354
 - stability, 75
- Cong-Chan-dynamical decoupling, 369
- conjugate transpose, 3, 8, 126
- control, 125
 - amplitude of, 3
 - bang-bang, 14, 351
 - closed-loop, 7
 - decoherence, 278
 - feedback, 7
 - general state, 125
 - geometry, 14
 - law design, 2
 - implicit lyapunov, 187
 - interaction, 147, 232
 - open loop, 7
 - orbit tracking, 389
 - population, 99

- constant magnetic field, 3
constrained minimization, 41
control actions, 30
 trajectories of, 30
control engineering, 2
control field, 30
 design of, 294
 minimum, 30
 single, 237
control goal, 8
 desired, 8
control law, 13, 238
 feedback, 77
 design of, 384, 398
control laws design, 13
control magnetic field, 28
control methods, 39
 dynamic decoupling quantum, 351
control objectives, 8
control performance, 399
 analysis of, 399
control strategy, 178
 a path programming, 178
control theory and methods, 2
control trajectory, 31
control system, 1
 analysis, 2
 closed-loop, 7
 design, 1
 invariant set of, 157
 open-loop, 7
 simulation experiment of, 2
control systems analysis, 2
control system design, 241
control system engineering, 2
control task, 8
control techniques, 2
controllability, 2, 9
convergence, 2, 10, 340, 402
convergence analysis, 155, 205, 339,
 404
convergent state set, 102
convergence condition, 157, 192
convergence proof, 192
cost function, 39
criteria, 277
 non-linear separability, 277
computable cross norm, 270
generalized partial transpose, 271
Peres, 269
damping, 353
 amplitude, 353
 phase, 353
decoherence, 252, 291
 dephasing, 298
 equation, 294
 phase, 355
 pure dephasing, 254
decoherence-free subspace, 321
degenerate cases, 187
description, 22
 Bloch sphere, 22
density matrix, 3, 237, 270
density matrix space, 102
density operator, 3
design methods, 7
 feedback, 7
diagonal element, 159, 343, 408
diagonal Lyapunov function, 158
diagonal matrix, 156, 406
diagonal target state, 208, 406
Dirac representation, 2
dissipation, 26
dissipative model, 238
distance, 75
 state, 75
Bures, 76
Hilbert Schmidt, 149, 193
von Neumann, 231
disturbance, 77
dynamic condition, 79
dynamic decoupling, 13, 354
dynamical decoupling mechanism,
 352
dynamical equation, 238
dynamical model, 237
eigen-equation, 83, 126
eigenstate, 25, 73, 80, 126, 385
 manipulation of, 73

- ensembles, 4, 25
 - quantum, 4
- entangled state, 3, 213
- entanglement, 53, 269
 - relative entropy of, 274
- entanglement cost, 274
- entanglement degree, 215
- entanglement detection, 268
- entanglement measures, 268
 - estimation of, 276
- entanglement preparation, 53
- entanglement state, 3, 53, 213, 269
 - preparation of, 220
- entanglement witnesses, 271
- entropy, 214
 - von Neumann, 214, 275
- equilibrium point, 75
- equilibrium states, 99, 243
- error function, 382
- error tolerance, 400
- estimation, 2, 261
 - Bayesian, 265
 - least variance, 266
 - state, 261
- estimation method, 261
 - Bayesian, 265
 - least variance, 266
 - state, 261
 - maximum entropy, 264
 - maximum likelihood, 265
- external control, 237
- external control field, 244
- external environment, 3
- extra disturbance, 77
- Euclidean space, 22
- fidelity, 12, 228
- field, 301
 - decoupling, 353
 - single control, 237
- filter, 2
- frequency, 13, 29
 - eigen-, 29, 32
 - Rabi, 29, 52, 325
 - cut-off, 377
- frequency spectrum, 13
- function, 13
 - control, 13
 - convex, 274
 - Lagrange, 41
 - Lyapunov-like, 7
 - implicit, 7
- gate, 9
 - quantum logical, 26
 - Hadamard, 88
- gate control, 15
- general reservoir, 353
- general damping, 353
- general state, 125, 213
- general state control, 125
- geometric analysis, 213
- geometric control, 15, 59
- geometric measure, 276
- global optimization, 15
- global phase, 126
- global phase factor, 127
- Greenberger-Horne-Zeilinger, 272
- group, 27
 - semi-, 27
- bang–bang operations, 355
- gyromagnetic ratios, 222
- half counterintuitive sequence, 55
- half intuitive sequence, 53
- Hamiltonian, 4
 - control, 1, 58, 294
 - free, 4, 58
 - inner, 125
 - interaction, 125
 - multi-control, 187
 - system and control, 2
 - total, 4, 58
- harmonic oscillator model, 143
- Hilbert space, 2, 213, 352
- homodyne tomography, 263
- Hypergeometric function, 6
- identical copy, 262
- identification, 2
- imagine part, 44, 126
- imaginary mechanical quantity, 195

- implicit Lyapunov control approach, 187
improved quantum optimal control
 method, 42
interaction control, 232
Interaction model, 248
interaction picture, 165, 220, 295, 338
interaction transformation, 165 12
intuitive sequence, 53
invariant set, 157, 7, 200
 mathematical expression of, 157
isolated and non-isolated target eigenstates, 219
Krotov-based method, 43
LaSalle's invariance principle, 157, 192
largest invariant set, 101, 339
largest eigenvalue, 343
l'Hospital's rule, 241, 313
Lie algebra, 28, 100, 224
Lie bracket, 308
Lie group, 58
Lie group decomposition, 179
Lindblad form, 5
Lindblad operator, 238, 329
Lindblad semigroup form, 238
Lindblad-type Markovian master equation, 328
linear transformation, 127, 133
Liouville equation, 4, 177
Liouville operator, 6, 137
Liouville space, 102, 150
Liouville super-operator, 5
local operate and classical communication, 269, 273
local phase, 306
Lyapunov-based control methods, 15, 74, 156
Lyapunov function, 75, 126, 156, 189, 232
Lyapunov method, 382
Lyapunov stability theorem, 74, 155, 166
Lyapunov sense, 75
macroscopic control system, 351
macroscopic world, 14
manipulation, 125
pure state, 125
mixed state, 145
state, 321
superposition state, 131
amplitude decoherence, 353
Markovian master equations, 5
Markovian system, 5
matrix, 24
 covariance, 11
density, 24, 165
non-singular square, 342
trace-free Pauli, 22
 reduced-density, 215
Markovian approximation, 5
Markovian characteristics, 5
Mathematical model, 82, 125
maximum entropy estimation method, 264
maximum entropy reconstruction, 264
maximum likelihood estimation method, 265
maximal mixed state, 218
minimum time, 57
measure, 275
 multipartite entanglement, 275
measurement, 261
 local von Neumann, 273
method, 261
 Bayesian, 265
 Krotov, 40
minimum variance estimation, 266
quantum state reconstruction, 267
state tomography, 263
microscopic world, 14
mixed state, 3, 24, 135, 201, 243, 270, 388
 purification of, 230
model, 237
 four-level Morse oscillator, 142
 Harmonic oscillator, 143
 Ising, 50
 Ising interaction, 50
 N-level ladder-type, 308
 system, 390
molecular systems, 3
modeling, 2
multipartite states, 276

- non-Markovian system, 5
nano-material, 2
non-degenerate cases, 187
non-degenerate system, 158
non-diagonal elements, 283
non-diagonal target state, 404
non-diagonal target density matrix, 409
non-diagonal target superposition state, 411
non-diagonal mixed state, 410
non-linear system, 75
non-linear separation criterion, 277
non-Markovian characteristics, 5
non-Markovian master equation, 5
non-stationary target state, 141
non-unital decoherence, 300
nuclear magnetic resonance, 3
numerical simulation, 2, 134, 299, 345
nuclear magnetic resonance, 278
- observable operator, 166, 225
observability, 2, 10
ohmic environment, 6
off-diagonal elements, 25, 146
operation, 24
 bang-bang, 354
 imaginary part, 6
 Hadamard, 88
 rotate-, 94
open quantum systems, 3, 237, 291, 321
operator, 4
 atomic creation and annihilation, 5
 bit flip, 22
 density, 24
orbit tracking, 3, 382
 convergence of, 402
optimality, 40, 85, 139
optimal control, 1, 15, 40, 85
optimal control law, 238
optimized dynamical decoupling, 360
optical homodyne tomography, 264
orthonormal basis, 345
orthogonal vector, 218
orthogonalization, 344
 Schmidt, 344
- particle, 222
 gyromagnetic ratios of, 222, 12
passage, 14
 Chirped Adiabatic, 14
 Stimulated Raman Adiabatic, 15
path programming control strategy, 176
Pauli vector, 22
performance, 11, 138
performance index, 138, 238
permutation, 207
perturbation, 192
 implicit function, 190
periodic dynamical decoupling, 361
phase factor, 92
phase decoherence, 351
phase decoherence suppression, 351
phase plane, 299
phase relaxation rate, 241
Planck's constant, 4
point, 157
 critical, 157
 extreme, 100
 minimum, 157
 measurement, 279
pole, 35, 61
 north, 35, 61
 south, 35, 61
populations, 45
population transfer, 48
population control, 94, 105
population distribution, 134, 160, 295
population evolution, 48, 194
positive-operator valued measurement, 278
preservation, 291
 state, 291
 coherence, 291, 307
probability, 3, 12, 94, 263
probability completeness, 22
probability distribution, 128, 263, 335
inner product, 102
projection, 279
projective measurement, 282
pulses, 52
 control sequence of, 52
 radio-frequency, 158
pulse sequences, 14

- pure state, 3, 21, 125, 248
pure state manipulation, 125
purity, 12, 225, 246
purity compensation, 246
purity evolution, 303
purity-leaking rate, 253
purity preservation, 296, 301
purification, 230
- quantum chemistry, 1
quantum computation, 1
quantum control, 1
 methods and technologies of, 1
quantum control theory and methods 13
quantum control systems, 1
quantum electro-dynamics, 1
quantum ensemble, 3
quantum entanglement, 1
quantum error correction, 1
quantum feedback control, 7
quantum Hadamard gate, 88
 realization of, 88
quantum information, 1
 corruption of, 1
quantum information processor, 1
quantum information sciences, 1
quantum Liouville equation, 3, 26
quantum mechanics, 1
quantum mechanical systems, 1
quantum phenomena, 1
quantum physics, 1
quantum state, 2
 global phase of a, 2
 spectrum of, 2
 superposition principle of, 22
quantum systems, 1, 237
 bilinear, 4
 composite, 3
 finite dimensional, 4
 high-dimensional spin-1/2, 48
 two-level (two-state), 2, 21
 two-level open, 241
quantum systems control, 13
quantum systems control methods, 3
quantum technologies, 1
qubit, 21, 14
- reachability, 2, 9
reduced density matrix, 217
regulation problem, 383
relative entropy, 274
representation, 21
 adjoint, 21
 Bloch sphere, 21
resonant condition, 50
resonant field, 301
resonant frequency, 50
robustness, 10
reflect-operation, 89
rotate-operation, 89
route extension strategy, 7
- Schrödinger equation, 4, 26, 77, 195
Schmidt decomposition, 214, 272
Schmidt orthogonalization, 336
separable state, 3
largest invariant, 24
 orthogonal basis, 24
simulation experiment, 47
simulation experiment results, 47, 4
single qubit, 21, 28
single spin-1/2 particle, 28
singularity, 297, 15
singularities Issues, 297
spectral decomposition, 343
 unique, 343
spin, 28
spin 1/2 quantum systems, 27, 114
spin particle, 28
spin qubits, 80
state, 213
 equilibrium, 99
state control, 125, 237
state manipulation, 125
state estimation, 261
state error, 187
state estimation methods, 261
state preparation, 9
state preservation, 9, 291
state space, 3, 58
state topography, 263
state-to-state transition, 9
state transfer, 13, 27, 80

- stationary condition, 79
stationary target state, 138
stochastic noise, 26
subspaces, 321
 decoherence-free, 321
sufficient condition, 340
sufficient and necessary condition, 165
super-operator, 5, 26
superposition state, 15, 22, 131, 386
superposition principle, 221
system, 4
 composite, 231
 three-level Λ -type, 345
 4-level multi-control Hamiltonians, 8
 four-Level energy open quantum, 321
 Λ -Type N -Level Atomic, 328
 five-level, 161
 free Hamiltonian of, 4
 Markovian open quantum, 307
multi-control Hamiltonians, 187
 multi-qubit, 278
open quantum, 237, 291
 single-spin, 9
 spin-1/2 particle, 241
synthesis, 2
 two-level, 2, 21
 two-qubit, 3
- target states, 84
 stability of, 84
tensor product, 3
thermal reservoir, 353
time-convolution-less master equation, 5
time-dependent function, 13, 141, 395
time-dependent operator, 13, 134, 216
time-optimal control, 57
time-dependent purity, 231
tomography, 263
two-qubit local gate, 216
tracking control, 385
tracking properties, 412
 analysis of, 412
tracking problem, 383
trajectory tracking, 13, 141, 394
trajectory programming, 173
transfer, 48
 population, 48
 coherent population, 48
 half population, 54
 mixed-state, 149
 state, 61, 325
transform, 90
 Hadamard, 90
transition frequency, 15
- unit orthogonal vector, 215
unit vector, 15, 89
unitary evolution, 3, 13
unitary matrix, 127
unitary operation, 22
unitary operator, 216
unitary propagator, 148
unitary transformation, 127, 133, 222
universal dynamical decoupling, 367
Uhrig dynamical decoupling, 361
unconstrained minimization, 41
- vector, 22
 Pauli, 22
- wave function, 4
weak measurement, 278
weak measurement operator, 279
 construction of a, 279